

Adaptations, chemical communication and chemotaxis in *Rhodobacteraceae* associated with surfaces in coastal habitats

Anpassungen, chemische Kommunikation und Chemotaxis von oberflächenassoziierten *Rhodobacteraceae* in Küstengebieten

Angenommene

Dissertation

zur Erlangung des akademischen Grades und Titels einer

Doktorin der Naturwissenschaften

– Dr. rer. nat. –

der Fakultät für Mathematik und Naturwissenschaften

der Carl von Ossietzky Universität Oldenburg

von Frau

Laura Amanda Wolter

geboren am 16. November 1987 in Braunschweig, Deutschland

Tag der Disputation, 29. März 2019



Die vorliegende Arbeit wurde am Institut für Chemie und Biologie des Meeres (ICBM) an der Carl von Ossietzky Universität Oldenburg in der Arbeitsgruppe „Biologie Geologischer Prozesse“ angefertigt.

Diese Arbeit wurde von der Deutschen Forschungsgemeinschaft (DFG) im Rahmen des Sonderforschungsbereichs TRR 51 „Ecology, Physiology and Molecular Biology of the *Roseobacter* clade: Towards a System Biology Understanding of a Globally Important Clade of Marine Bacteria“ gefördert.

Erster Gutachter: apl. Prof. Dr. Thorsten Brinkhoff

Zweiter Gutachter: Prof. Dr. Tilmann Harder

Für alle meine Lieben

Table of contents

Summary	iii
Zusammenfassung	iv
List of publications	vi
Presentations at national and international symposia	viii
List of abbreviations.....	ix
Background and scope of this thesis.....	1
Adaptations of marine bacteria to surfaces and coastal habitats and the influence of secondary metabolites	1
Population-shaping dynamics of quorum sensing and chemotaxis	3
Ecological importance of the <i>Roseobacter</i> group	5
Ecology and secondary metabolite production in <i>Phaeobacter</i> spp.	7
Aims of this thesis.....	9
Manuscript 1	10
<i>Pseudoceanicola algae</i> sp. nov., isolated from the marine macroalga <i>Fucus spiralis</i> shows genomic and physiological adaptations for an algae-associated lifestyle.....	10
Figures and Tables.....	23
Manuscript 2	28
<i>Rhodobacteraceae</i> on the marine brown alga <i>Fucus spiralis</i> are abundant and show physiological adaptation to an epiphytic lifestyle	28
Figures and Tables.....	43
Manuscript 3	51
Smalltalk in the ocean - signaling molecules and DNA elicit chemotactic and regulatory effects in surface-associated <i>Rhodobacteraceae</i>	51
Figures and Tables.....	63
Manuscript 4	67
Different AHL-based quorum sensing systems in <i>Phaeobacter inhibens</i> T5 ^T regulate distinct traits for association or horizontal gene transfer	67
Figures and Tables.....	77
Discussion	81
Short summary of the results	81
Adaptations of a <i>Roseobacter</i> to surface-associated life includes mutual and detrimental traits	81
Chemotaxis and chemical crosstalk in surface-associated bacteria.....	83
Secondary metabolite production varies among closely related species.....	85
Influence of secondary metabolites on bacterial transcriptomes reveal known but also yet unknown patterns with implications on surface attachment	86
Outlook	89
References	90
Curriculum vitae.....	105
Erklärung	106

Supplementary Material for Manuscript 1.....	107
Supplementary Figures and Tables	108
Supplementary Material for Manuscript 2.....	149
Supplementary Figures and Tables	154
Supplementary Material for Manuscript 3.....	170
Supplementary Figures and Tables	173
Supplementary Material for Manuscript 4.....	200
Supplementary Figures and Tables	202
Manuscript 5	211
Supplementary Material for Manuscript 5	225
Manuscript 6	227
Supplementary Material for Manuscript 6	241
Manuscript 7	245
Supplementary Material for Manuscript 7	255

Supplementary Tables with complete gene lists can be found in the digital supplementary material attached to the printed version of this dissertation.

Summary

Bacteria of the *Roseobacter* group (α -*Proteobacteria*), part of the *Rhodobacteraceae*, are ubiquitously distributed in the marine environment and thus are an important ecological component of many bacterial communities, which is supported by their broad metabolic capacities and secondary metabolism. Especially surface-associated roseobacters show a great potential to produce and communicate through secondary metabolites, although the ecological significance of these compounds and how they contribute to habitat adaptation and species differentiation remain largely unknown.

Within this thesis, unique genomic features including secondary metabolite production were investigated for a specific *Roseobacter* strain, *Pseudoceanicola algae* sp. nov., isolated from a marine macroalga, regarding adaptations to abiotic habitat conditions as well as biotic host interactions. Genomic and physiological adaptations for macroalgal surface-association and tidal areas supported discrimination of this species from pelagic or sediment-related *Pseudoceanicola* spp., specifically attributed to high salt, antibiotic and heavy metal tolerance, degradation of algal-derived oligosaccharides, the potential to counteract eukaryotic defense systems and the production of secondary metabolites including communication molecules. Together with the shown potential for provision of iron-scavenging siderophores and vitamins, the results support molecular evidence that related *Rhodobacteraceae* constitute a predominant part of the bacterial communities on common brown macroalgae.

A second focus of this thesis addressed the influence of *Roseobacter*-derived secondary metabolites and biofilm-related molecules for surface colonization and how these might connect population-shaping dynamics of chemotaxis and quorum sensing (QS). Secondary metabolites addressed in these investigations were *N*-acyl-homoserine lactones (AHLs) and the antibiotic tropodithietic acid (TDA) as well as extracellular DNA (eDNA). Since all tested compounds had an influence on the chemotactic behavior of bacteria, we postulate that QS-related effects not only originate from passive diffusion but might be mediated by “active” sensing and movement towards the production site, facilitating the establishment of biofilms and subsequent QS-mediated actions.

A more detailed understanding of the regulatory mechanisms mediated by communication- and biofilm-related metabolites was provided by analyzing selected strains of *Phaeobacter inhibens* using high-resolution RNA-sequencing. First, own and foreign AHLs, TDA and eDNA were added to the *P. inhibens* DSM 17395 wild type and second, mutant strains of single AHL synthases were produced for the *P. inhibens* T5^T type strain. Strain T5 has four *luxIR* gene clusters for AHL-mediated QS, of which three could be knocked out. This enabled matching produced AHLs to their respective synthases and illuminating subsequent gene regulatory effects of QS circuits. Both approaches showed similar albeit

at times opposed regulatory features relating to motility, nutrient conversion, potential pathogenicity and genetic exchange, all important aspects within dense bacterial assemblages.

Further collaborative contributions to chemical elucidation of secondary metabolites from surface-associated *Rhodobacteraceae*, underlined the substantial molecular diversity of produced molecules by detection of AHLs with uncommon side chains (C12:2, 5-C12:1, 3OH-C12:1 and 9-C17:1-HSL) and yet unknown *N*-acetylated amino acid methyl esters (NAMEs).

In conclusion, this thesis adds knowledge to how adaptations and communication in surface-associated *Rhodobacteraceae* is performed and illuminates interconnection of QS and chemotaxis, providing detailed insights into concurring gene regulatory effects in such habitats. These insights are a fundamental advance towards elucidating the microbiological and chemical complexity within surface-associated habitats and how marine roseobacters contribute to these processes.

Zusammenfassung

Bakterien der *Roseobacter*-Gruppe (α -*Proteobakterien*) sind in marinen Habitaten weitverbreitet und stellen einen zentralen Bestandteil vieler bakterieller Gemeinschaften dar, was durch vielseitige metabolische Kapazitäten und ausgeprägten Sekundärmetabolismus unterstützt wird. Insbesondere oberflächenassoziierte Mitglieder besitzen ein großes Potenzial zur Produktion von und Kommunikation durch Sekundärmetaboliten, obgleich die ökologische Bedeutung dieser Verbindungen und ihre Rolle in der Anpassung an verschiedene Lebensräume und zur Artendifferenzierung, noch weitgehend unbekannt ist.

In dieser Arbeit wurden genomische Merkmale, einschließlich der Produktion von Sekundärmetaboliten, im von einer Makroalge isolierten und neu beschriebenen *Roseobacter*-Vertreter, *Pseudoceanicola algae* sp. nov., beschrieben und inwieweit diese die Anpassung an abiotische Lebensraumbedingungen sowie biotische Wirtswechselwirkungen vermitteln. Die gefundenen genomischen und physiologischen Anpassungen an Oberflächen von Makroalgen und Gezeitengebiete unterstützten die Diskriminierung von *P. algae* von pelagischen oder aus Sediment isolierten *Pseudoceanicola* spp., charakterisiert durch hohe Salz-, Antibiotika- und Schwermetalltoleranz, den Abbau von Algen-Oligosacchariden, das Potenzial eukaryotischen Abwehrsystemen entgegenzuwirken sowie Sekundärmetabolitproduktion einschließlich Molekülen zur Kommunikation. Zusammen mit bereits bekannten Fähigkeiten zur Bereitstellung eisenbindender Siderophore oder Vitaminen, unterstützten diese Ergebnisse den molekularen Nachweis, dass verwandte *Rhodobacteraceae* einen großen Anteil der Bakteriengemeinschaften auf weitverbreiteten Braunalgen ausmachen.

Ein weiterer Fokus dieser Arbeit untersuchte den Einfluss von *Roseobacter*-Sekundärmetaboliten oder in Biofilmen vorkommenden Molekülen auf bakterielle Oberflächenbesiedlung und wie diese die Dominanz von Roseobactern unterstützen könnten, indem sie populationsbildende Prozesse wie Chemotaxis und Quorum Sensing (QS) verbinden. Untersuchte Sekundärmetabolite, beinhalteten *N*-Acyl-Homoserinlactone (AHLs) und das Antibiotikum Tropodithiolsäure (TDA) sowie in Biofilm vorkommende extrazelluläre DNA (eDNA). Wir konnten zeigen, dass die getesteten Verbindungen einen Einfluss auf das chemotaktische Verhalten von Bakterien hatten, und postulieren, dass QS-bedingte Wirkungen nicht nur von passiver Diffusion herrühren, sondern durch "aktives" Wahrnehmen und Bewegung zur Produktionsstätte vermittelt werden können, was die Etablierung von Biofilmen und nachfolgende QS-vermittelte Aktionen erleichtert.

Ein detaillierteres Verständnis der Regulationsmechanismen dieser Moleküle wurde für ausgewählte Stämme der Gattung *Phaeobacter inhibens* unter Verwendung hochauflösender RNA-Sequenzierung analysiert. Zum einen wurden eigene und fremde AHLs, TDA und eDNA zum Wildtyp von *P. inhibens* DSM 17395 hinzugefügt, und zum anderen Mutanten einzelner AHL-Synthasen für den Typstamm *P. inhibens* T5^T generiert. Der Stamm T5 hat vier *luxIR* Gencluster für AHL-basiertes QS, von denen drei ausgeknockt werden konnten. Dies ermöglichte die Zuordnung produzierter AHLs zu ihren jeweiligen Synthasen und die nachfolgende Beleuchtung der genregulatorischen Effekte verschiedener QS Systeme innerhalb eines Bakterienstammes. Beide Ansätze zeigten meist ähnliche, jedoch auch teilweise widersprüchliche regulatorische Merkmale, die Motilität, Nährstoff-Umwandlung, potenzielle Pathogenität und genetischen Austausch umfassen, welche wichtige Aspekte in dichten bakteriellen Gemeinschaften darstellen.

Weitere Beiträge zu chemischen Untersuchungen an Sekundärmetaboliten von oberflächenassoziierten *Rhodobacteraceae* unterstrichen die große molekulare Diversität der erzeugten Moleküle durch den Nachweis von AHLs mit ungewöhnlichen Seitenketten (C12:2, 5-C12:1, 3OH-C12:1 und 9-C17:1-HSL) und bisher unbekannte *N*-acetylierte Aminosäuremethylester (NAMEs).

Zusammenfassend trägt diese Arbeit zum tieferen Verständnis von Anpassungen und Kommunikation von oberflächenassoziierten *Rhodobacteraceae* bei und beleuchtet die Verknüpfung von QS und Chemotaxis mit detaillierten Einsichten in für diese Habitate wichtige Genregulationseffekte. Diese Einblicke stellen fundamentale Fortschritte hinsichtlich der mikrobiologischen und chemischen Komplexität in oberflächenassoziierten Habitaten dar und in welcher Weise marine *Roseobacter* zu diesen Prozessen beitragen.

List of publications

This thesis includes four main manuscripts and contributions to three further papers, of which four are published and three are close to submission to peer-reviewed scientific journals. My contributions to the manuscripts are listed below.

The whole manuscript text for Manuscripts 5 - 7 are not listed in this thesis but can be accessed from the CD enclosed in the printed version or the attached supplementary files of the electronic version.

Manuscript 1

Wolter L. A. Wietz M. Ziesche L. Picard A. Breider S. Leinberger J. Poehlein A. Daniel R. Schulz S. Brinkhoff T. (to be submitted to *Systematics and Applied Microbiology*) *Pseudoceanicola algae* sp. nov., isolated from the marine macroalga *Fucus spiralis* shows genomic and physiological adaptations for an algae-associated lifestyle

LAW: Preparation of original draft, concept of the study, sample collection and preparation, isolation and maintenance of the bacterial strain, taxonomic classification, analysis of genomic data, physiological experiments and analysis.

Manuscript 2

Dogs M. Wemheuer B. **Wolter L. A.** Bergen N. Daniel R. Simon M. Brinkhoff T. (2017) *Rhodobacteraceae* on the marine brown alga *Fucus spiralis* are predominant and show physiological adaptation to an epiphytic lifestyle. *Systematic and Applied Microbiology*, 40 (6), 370-382

LAW: Isolation of bacteria and taxonomic analysis, physiological experiments and analysis, revision of the manuscript.

Manuscript 3

Wolter L. A. Srinivas S. Tomasch J. Wietz M. Nivia Torres D. N. Scharfe M. Wagner-Döbler I. Brinkhoff T. (to be submitted to *ISME Journal*) Smalltalk in the ocean – signaling molecules and DNA elicit chemotactic and regulatory effects in surface-associated *Rhodobacteraceae*

LAW: Concept of the study, preparation of original draft, sequence analyses and complementation of the mutant strain, development of the chemotaxis chamber (with DNT) and chemotaxis experiments (with SS) and analysis, total RNA preparation and analysis of genome and transcriptome data, physiological experiments, data evaluation.

Manuscript 4

Wolter L. A. Ziesche L. Berger M. Poehlein A. Schulz S. Brinkhoff, T (to be submitted to *Journal of Bacteriology*) Different AHL-based quorum sensing systems in *Phaeobacter inhibens* T5^T regulate distinct traits for host-association or horizontal gene transfer

LAW: Concept of the study, preparation of original draft, mutant construction, total RNA isolation and analysis of genome and transcriptome data, gene comparison analysis, physiological experiments, data evaluation.

Manuscript 5

Ziesche L. Bruns H. Dogs M. **Wolter L.** Mann F. Wagner-Döbler I. Brinkhoff T. Schulz S. (2015) Homoserine lactones, methyl oligohydroxy-butyrate, and other extracellular metabolites of macroalgae-associated bacteria of the *Roseobacter* clade: Identification and functions. *ChemBioChem* 16, 2094-2107

LAW: Provision of bacterial isolates and phylogenetic analysis, interpretation of the data, contribution to the first draft and revision of the manuscript.

Manuscript 6

Ziesche L. **Wolter L.** Wang H. Brinkhoff T. Pohlner M. Engelen B. Wagner-Döbler I. Schulz S. (2019) An unprecedented medium-chain diunsaturated *N*-acylhomoserine lactone from marine *Roseobacter* group bacteria. *Marine Drugs*, 17 (1), 20

LAW: Provision of bacterial isolates and phylogenetic analysis, interpretation of the data, contribution to the first draft and revision of the manuscript.

Manuscript 7

Bruns H. Ziesche L. Taniwal N.K. **Wolter L.** Brinkhoff T. Herrmann J. Mueller R. Schulz S. (2018) *N*-acylated amino acid methyl esters from marine *Roseobacter* group bacteria. *Beilstein Journal of Organic Chemistry*, 14, 2964-2973

LAW: Provision of bacterial isolates and phylogenetic analysis, interpretation of the data, contribution to the first draft and revision of the manuscript.

Presentations at national and international symposia

Wolter L. A. Srinivas S. Tomasch J. Brinkhoff T. (2017) Let's talk – Chemotaxis of marine *Rhodobacteraceae* towards own and foreign secondary metabolites: a complex chemical crosstalk. SAME15, Zagreb, Croatia. **Poster presentation**

Wolter L. A. Srinivas S. Ziesche L. Schulz S. Brinkhoff T. (2016) Interplay between *Phaeobacter inhibens* TDA production, quorum sensing and chemotaxis. ISME16, Montreal, Canada. **Poster presentation**

Wolter L. A. Nivia Torres D. Ziesche L. Berger M. Schulz S. Brinkhoff T. (2015) The influence of the AHL systems of *Phaeobacter inhibens* T5 on gene expression. Symposium of TRR-51, Oldenburg, Germany. **Oral and poster presentation**

Wolter L. A. Nivia Torres D. Ziesche L. Berger M. Schulz S. Brinkhoff T. (2015) The AHL systems of *Phaeobacter inhibens* T5 and chemotaxis behavior of *Phaeobacter* spp. Symposium of TRR 51, Oldenburg, Germany. **Poster presentation**

Wolter L. A. Ziesche L. Berger M. Schulz S. Brinkhoff T. (2015) The influence of various AHL systems on the gene expression of *Phaeobacter inhibens* T5. VAAM, Marburg, Germany. **Poster presentation**

Wolter L. A. Berger M. Brinkhoff T. (2014) Genetics, regulation and ecological significance of secondary metabolite production of *Roseobacter* clade bacteria. Symposium of TRR-51, Oldenburg, Germany. **Oral presentation**

List of abbreviations

AHL	<i>N</i> -acyl homoserine lactone
AI	Autoinducer
ALA	5- aminolevulinic acid
BLAST	Basic Local Alignment Search Tool
CM	Chemotaxis medium
CPM	Counts per million
DMSO	Dimethyl sulfoxide
DMSP	Dimethylsulfoniopropionate
DSMZ	German Collection of Microorganisms and Cell Cultures
FC	Fold change expressed as log ₂ -fold change
GC-MS	Gas chromatography – mass spectrometry
GGDH	Genome-to-Genome Distance Calculator
GI	Genomic island
GTA	Gene transfer agent
HSL	Homoserine lactone (acyl-side chain is specified)
MB	Marine broth modified from Difco 2216
MCP	Methyl-accepting chemotaxis protein
MIC	Minimal inhibitory concentration
NAME	<i>N</i> -acylated amino acid methyl ester
QS	Quorum sensing
ROS	Reactive oxygen species
SIC	Sub-inhibitory concentration
TDA	Tropodithetic acid

Background and scope of this thesis

The present PhD thesis is focused on how bacteria of the *Roseobacter* group adapt to life in coastal areas as well as host-association and how secondary metabolites mediate intra- and interspecific as well as interkingdom interactions. Therefore, *Roseobacter* representatives isolated from marine surfaces, including macroalgae, were used as model organisms to study how bacterial traits mediate habitat adaptation, biofilm formation and organismal interactions.

Adaptations of marine bacteria to surfaces and coastal habitats and the influence of secondary metabolites

Surface-associated bacteria possess specific adaptations that facilitate their establishment in such habitats. For instance, life in coastal environments is considerably shaped by abiotic components as tidal areas undergo regular desiccation and rewetting events. These require distinct adaptations to swiftly changing environmental conditions, e.g. the production of compatible solutes such as ectoin to deal with osmotic stress (Zhang et al. 2012). Furthermore, coastal habitats are characterized by terrestrial input of heavy metals and antibiotics that can accumulate in algal biomass (Hamdy 2000), and microorganisms possess different mechanisms to cope with these substances (Vignaroli et al. 2018). In view of biological parameters, secondary metabolite production is a common feature of surface-associated bacteria (Long et al. 2001, Grossart et al. 2004), as biosynthetic capacities are prevalent in nutrient-rich habitats with high bacterial densities such as biofilms on eukaryote surfaces. Macroalgae in tidal zones harbor diverse and abundant bacterial communities often dominated by α -*Proteobacteria* including *Roseobacter* group members, especially in temperate coastal waters (Antunes et al. 2018). Other common taxa include *Sphingomonadaceae* (α -*Proteobacteria*), *Alteromonadaceae* (γ -*Proteobacteria*) as well as *Bacteroidetes* (Antunes et al. 2018). The common production of diverse secondary metabolites by *Rhodobacteraceae* (Ziesche et al. 2015) contributes to biofilm formation and metabolic interdependencies (Rao et al. 2006). Coastal and macroalgae-associated habitats therefore display promising potential to study adaptations to abiotic factors and interactions with algal hosts.

Interactions between bacteria and algae (interkingdom) as well as between bacteria from the same (intra-) or different (inter-) species (Fig. 1) are influenced by both partners and shaped by mechanisms of commensalism, mutualism or parasitism (Egan et al. 2013). Mutual interactions rely on communication (Fig. 2) and secondary metabolite production, e.g. via the provision of bacterially-produced vitamins for auxotrophic algae (Fig. 3) (Croft et al. 2005) or siderophores to access insoluble Fe^{3+} (Soria-Dengg et al. 2001). Algal polysaccharides in return can be utilized by associated bacteria with specialization for high- or low-molecular-weight compounds (Hehemann et al. 2016). Stimulatory mechanisms include the promotion of algal growth by bacterial phytohormones (Segev et al. 2016). On

the contrary, antagonistic interactions include macroalgal defense systems to actively shape their epibiotic community e.g. by growth inhibition via antifouling compounds (Rao et al. 2007) or destabilization of quorum sensing (QS) systems (Goecke et al. 2010), whereas algal morphogenesis can in turn also be affected by QS molecules (Joint et al. 2002, Weinberger et al. 2007). However, iron scavenging, toxin synthesis and antibiotic resistance can be relevant for both mutualistic and antagonistic interactions under changing conditions (Cárdenas et al. 2017). Notably, these interactions can resemble terrestrial plant-bacteria interactions, a conceivable scenario as macroalgae are the marine equivalent of land plants. For instance, bacteria can produce volatile secondary metabolites (Piccoli et al. 2013) linked to defensive mechanisms of algae (Jerković et al. 2018) or terpenes with ecological implications as feeding deterrent, membrane stabilizer, anti-oxidant, signaling and antagonistic molecule (Gershenzon et al. 2007, Piccoli et al. 2013).

The establishment of bacteria on marine surfaces, including macroalgae, is often accompanied by secretion of extracellular polymeric substances, which constitute a protective matrix for bacterial communities and reduce diffusion of excreted substances (Decho et al. 2017) and contribute to the high resilience of biofilms against environmental changes (Flemming et al. 2016). Another important compound class in such assemblages is extracellular DNA (eDNA) originating from passive release of lysing cells (Torti et al. 2015) or active secretion (Gloag et al. 2013). DNA in biofilms can provide structural stability (Vorkapic et al. 2016) but also constitutes a source of carbon, nitrogen and phosphorous or potentially favorable DNA sequences (Pinchuk et al. 2008, Ellison et al. 2018).

Taken together, the interactions between algae and bacteria and among surface-associated bacterial consortia is to a large extent mediated by various secondary metabolites. One bacterial group with high metabolic diversity and a prevalence for secondary metabolite production is the marine *Roseobacter* group of the family *Rhodobacteraceae*, constituting one of the most abundant families e.g. on the marine brown macroalgae *Fucus spiralis* (Dogs et al. 2017), inhabiting the shore lines of North American and European coasts. Adaptations and secondary metabolism within this widespread and ecologically relevant bacterial group represents the focus of the present thesis.

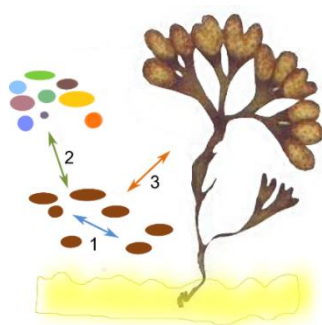


Fig. 1: Schematic representation of interactions in surface-associated communities (e.g. the macroalgae *Fucus spiralis*). Communication can occur on intra-specific (1), inter-specific (2) or interkingdom (3) levels, mediated by the provision and exchange of chemical compounds (depicted by arrows in both directions).

Population-shaping dynamics of quorum sensing and chemotaxis

Surface attachment and interactions with the surrounding bacterial community or the eukaryotic host are supported by communication molecules, which regulate concerted actions when bacterial cells reach a specific population density (termed a quorum). Drivers of such interactions are small diffusible molecules called autoinducers (AI), which are produced by specific synthases and sensed by regulatory proteins (Fig. 2). There are several well-defined classes of chemical signals used for quorum sensing (Decho et al. 2011), of which two are of interest in the present thesis: *N*-acyl homoserine lactones (AHL) and furanosyl diesters (AI-2) (Fig. 2).

The mechanism of AHL-based quorum sensing (QS) relies on a *luxI*-type AHL-synthase and a *luxR*-type transcriptional regulator, often encoded in direct proximity (Fig. 2A). AHLs are the main communication molecules of *Rhodobacteraceae* and other Gram-negative bacteria and the ability for AHL-based QS is widespread among the *Roseobacter* group (Cude et al. 2013, Zan et al. 2014). However, the encoding genes are not phylogenetically conserved and can show different arrangements or presence/absence in closely related species (Slightom et al. 2009). As several roseobacters harbor extra *luxR*-type genes without encoding a respective synthase, they may be able to sense and respond to foreign AHL molecules in a process called eavesdropping (Case et al. 2008), a possibly important process for cross-species interactions during biofilm formation (Chandler et al. 2012). Although AI production is more prevalent in surface-associated bacteria, AHLs were recently detected in a pelagic *Rhodobacteraceae* from oligotrophic waters under nutrient-rich conditions, suggesting that external conditions may trigger AHL production (Doberva et al. 2017). AHL production is a density-dependent process enhanced in a feedback loop by the corresponding AHL (Fuqua et al. 2002, Waters et al. 2005), but also co-regulatory effects of other QS systems in the same bacterium can activate or repress synthases (McDougald et al. 2006, Patzelt et al. 2013), illustrating a balance between costs and benefits of regulated features (Gupta et al. 2013). In contrast, the mechanism for AI-2 sensing is more complex and includes several proteins that differ between bacterial species (Fig. 2B). While recognition of AI-2 by *luxP* is restricted to *Vibrio* spp., sensing of AI-2 by *IsrB* binding receptor and subsequent transport through *IsrACD* is more widespread and also occurs in roseobacters (Pereira et al. 2009). AI-2 is considered as universal signal for interspecies communication, as its production is widespread in Gram-negative and Gram-positive bacteria via AI-2 synthase LuxS (Asad et al. 2008). QS-regulated features include motility, biofilm formation (including exopolysaccharide production), production of (antibiotic) secondary metabolites, influence of important metabolic traits (e.g. nitrogen-fixation) but also features related to virulence, conjugation and transformation, e.g. lysogenic-lytic switch of bacteriophages (Whitehead et al. 2001, Brinkhoff et al. 2004, DeAngelis et al. 2008, Berger et al. 2011, Patzelt et al. 2013, Zan et al. 2014, Silpe et al. 2019).

attachment. One relevant consideration is that concentrations of signaling molecules in the environment are probably low and compounds with antibiotic effects in laboratory tests may have different functions at *in situ* concentrations. Given the prevalence of several roseobacters to produce a specific sulfur-containing antibiotic, TDA, we investigated the potential ecological role of sub-inhibitory TDA concentrations, addressing a completely new role of such substances in biofilms.

Ecological importance of the *Roseobacter* group

Members of the *Roseobacter* group (often called roseobacters) are heterotrophic bacteria, frequently occurring on macro- and microalgal surfaces (Alavi et al. 2001, Buchan et al. 2005, Wagner-Döbler et al. 2006, Rao et al. 2007), where they can constitute up to 23% of associated bacterial communities (Dogs et al. 2017). In addition, roseobacters are broadly distributed in the marine environment and were detected e.g. in open and coastal oceans, sea ice, deep sea sediments or associated to animals (Moran et al. 2007, Brinkhoff et al. 2008, Wietz et al. 2010). Their broad distribution and spatiotemporal abundance is connected with a versatile metabolism and the ability to switch lifestyles according to environmental conditions (Newton et al. 2010, Luo et al. 2014). Metabolic features expressed by members of the roseobacters include aerobic and anaerobic respiration, aerobic anoxygenic photosynthesis and CO oxidation (Fig. 3) (Luo et al. 2014). But of major interest for this thesis is the potential of many roseobacters to produce various secondary metabolites especially within Clade 1 (Fig. 3, brownish color), including antimicrobials like indigoidine or tropodithietic acid (TDA) (Bruhn et al. 2005, Martens et al. 2007). The metabolic versatility is enhanced by an enlarged accessory genome, as roseobacters incorporate up to twelve extrachromosomal elements including chromids (resembling genome characteristics) and plasmids (Petersen et al. 2013) that can be transferred across genus boundaries through type IV secretion systems in pure cultures and natural settings (Patzelt et al. 2016, Petersen et al. 2017). Therefore, the success of roseobacters in marine habitats is also attributed to their genomic plasticity and mechanisms for the horizontal transfer of genes (Newton et al. 2010), underlined by the fact that some genomes comprise up to 5% prophage-related genes (Chen et al. 2006). In this context, an exclusive feature of *Rhodobacteraceae* is the presence of phage-like gene transfer agents (GTAs; Fig. 3) (Lang et al. 2017) that contain only a few kilobases of DNA and can laterally transfer defined sets of host DNA (Tomasch et al. 2018). The patchy distribution of ecologically relevant genes, spread within the genomes of *Roseobacter* group members (Fig. 3), support the importance of horizontal gene transfer within this bacterial group (Newton et al. 2010, Luo et al. 2014). The transfer of adaptive plasmid-encoded traits like aerobic photosynthesis, antibiotic or siderophore production likely represents one important mechanism of fast adaptation of roseobacters to changing habitats. Further, roseobacters can impact global nutrient cycles e.g. by degradation of the common algal constituent dimethylsulfoniopropionate (DMSP) to the climatically relevant gas DMS (Fig. 3)

(Wagner-Döbler et al. 2006, Reisch et al. 2011). Moreover, single *Roseobacter* spp. were investigated for potential functions in applied sciences, relating to the potential to degrade oil products (Klotz et al. 2018) or the use as probiotic in aquaculture (Planas et al. 2006, D'Alvise et al. 2012, Porsby et al. 2016).

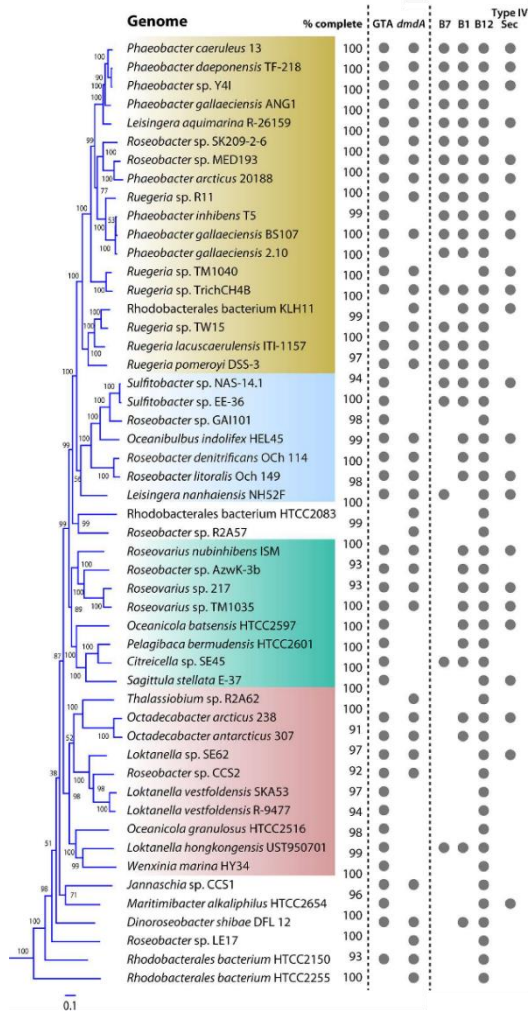


Fig. 3: Phylogeny of *Roseobacter* group bacteria and traits that influence eukaryote-association and biogeochemical cycling. Survey of select genes and metabolic pathways in 52 *Roseobacter* genomes. % complete, estimate of genome completeness; GTA, gene transfer agent; *dmdA*, dimethylsulfoniopropionate demethylase (forming DMS from DMSP); B7, biotin synthase; B1, thiamine synthase; B12, cobalamin synthase; Type IV Sec, type IV secretion system. Colors indicate four major clades of isolate genomes (Adapted from Luo et al. 2014).

Among this array of relevant functions, the present thesis focused on the ecological roles of secondary metabolite production by surface-associated roseobacters. To date, the role of secondary metabolites in mediating associations and interactions with biological surfaces remains poorly understood. Mutual interactions are e.g. known from *Pseudovibrio* sp. FO-BEG1, maintaining close association to sulfur-oxidizing *Beggiatoa* through specific genomic features including the production of bioactive chemicals (Bondarev et al. 2013). *Ruegeria* sp. TM1040 isolated from the dinoflagellate *Pfisteria piscicida* supports growth of the microalgae as demonstrated by “add-back” experiments of the microbial community to axenic dinoflagellate (Alavi et al. 2001). However, close associations of roseobacters with eukaryotic hosts can also be characterized by pathogenic behavior, e.g. *Nautella italica* R11 (the type strain currently reclassified as *Phaeobacter italicus* (Wirth et al. 2018)) and the red macroalga *Delisea pulchra* (Case et al. 2011) or *Sulfitobacter* sp. D7 with the microalgae *Emiliania huxleyi* (Barak-Gavish et al. 2018).

A special interaction between *Phaeobacter inhibens* and the diatom *E. huxleyi* is characterized by a shift from mutual interaction to pathogenic behavior during algal senescence, featured by the infochemicals DMSP and p-coumaric acid excreted from the alga, which “report” its current life stage and mediate *Phaeobacter* to exert respective behavior (Seyedsayamdost et al. 2011) (Fig. 4). The production and importance of various secondary metabolites with potential ecological implications

among roseobacters underlines the focus of the present PhD thesis, with special emphasis on *P. inhibens* considering its importance as model organism for roseobacters.

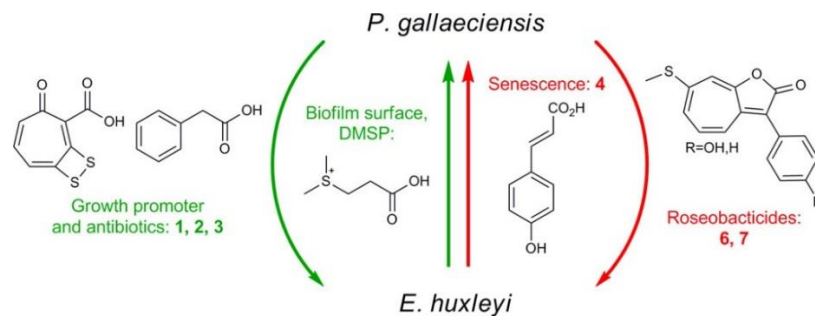


Fig. 4: Proposed working model for the interaction between *E. huxleyi* and *P. inhibens*, showing mutualistic (green) characteristics upon microalgal growth, changing to pathogenic (red) behavior as *E. huxleyi* senesces. Infochemicals for this behavior are DMSP from the algae, growth promoters and TDA from the bacterium (1,2,3) and for the switch, algal breakdown products (4), that stimulate *P. inhibens* to produce roseobactericides (6,7) (Seyedsayamdost et al. 2011).

Ecology and secondary metabolite production in *Phaeobacter* spp.

Phaeobacter bacteria are proficient colonizers of marine surfaces and able to invade established epiphytic communities, corroborated by frequently observed aggregated growth and unique genomic features for biofilm formation (Thole et al. 2012), largely encoded on a „biofilm-plasmid“ (Frank et al. 2015). *P. inhibens* represents one key species of *Phaeobacter*, including the model strain DSM 17395 isolated from aquaculture seawater of the scallop *Pecten maximus* (Ruiz-Ponte et al. 1998). The related species *Phaeobacter gallaeciensis*, *Phaeobacter porticola* and *Phaeobacter piscinae* have been predominately reported from anthropogenically influenced habitats like aquacultures or harbor environments (Hjelm et al. 2004, Porsby et al. 2008, Balcazar et al. 2010, Gram et al. 2015, Breider et al. 2017) or associated to marine animals (Grigioni et al. 2000, Barbieri et al. 2001, Bruhn et al. 2005, Freese et al. 2017). However, few isolates were obtained from macroalgae or tidal habitats, which can also be affected by anthropogenic influence (Rao et al. 2005, Martens et al. 2006).

The surface-adapted lifestyle of *Phaeobacter* is often linked to the production of TDA, mediating antagonistic effects against other epibionts with simultaneous beneficial antifouling effects for the host (Rao et al. 2005, Rao et al. 2007). TDA production was first reported from the *P. inhibens* type strain T5^T (Brinkhoff et al. 2004) and *P. piscinae* 27-4 (Bruhn et al. 2005) and results in a typical brown coloration of pure cultures. TDA production is restricted to a small subgroup within the *Rhodobacteraceae* including *Phaeobacter* and *Ruegeria* of the *Roseobacter* group (Clade 1, Fig. 3), and *Pseudovibrio* (Brinkhoff et al. 2004, Bruhn et al. 2005, Porsby et al. 2008, Penesyan et al. 2011, Sonnenschein et al. 2017). Production of TDA is regulated by AHL-based QS in *Phaeobacter* spp, and

autoinduced in *Phaeobacter* and *Ruegeria* (Geng et al. 2010, Berger et al. 2011), while being independent from AHL and TDA in *Pseudovibrio* spp. (Harrington et al. 2014). Likewise, produced concentrations of TDA vary between 10 – 400 μM in pure cultures under different growth conditions (Geng et al. 2010, Berger et al. 2011, Bondarev et al. 2013). Due to its antibiotic and antialgal effects (Porsby et al. 2011, Ziesche et al. 2015), TDA production by *Phaeobacter* is investigated for beneficial effects as probiotic in aquaculture (Planas et al. 2006, D'Alvise et al. 2012, Karim et al. 2013, Porsby et al. 2016). Nonetheless, in natural environments, production of minimal inhibiting concentration of 180 μM (Porsby et al. 2011) was recently questioned, due to iron-dependent production, while native habitats are normally iron-limited (D'Alvise et al. 2016). The notion is underlined by frequent observation that TDA is produced in nutrient and iron-rich, but not in defined mineral medium (Berger et al. 2012, D'Alvise et al. 2016).

The ecological function of TDA thus remains unclear also since TDA production imposes a high metabolic burden for the producing organism (Trautwein et al. 2016). Part of an explanation might be that the TDA biosynthesis genes are similarly important for producing roseobactinoids (Wang et al. 2016), another class of secondary metabolites specific for *Phaeobacter* with implications on the *P. inhibens* – *E. huxleyi* interaction (Fig. 4). The genes involved in biosynthesis of TDA and roseobactinoids are encoded on a 262 kb chromid, conserved in all TDA-producing strains (Petersen et al. 2013), which also encodes TDA resistance genes in close proximity (Wilson et al. 2016). The proposed working mechanism of TDA is an exchange of extracellular protons for cytoplasmic monovalent cations causing the proton motive force to collapse, while resistance is mediated by pumping back protons via the γ -glutamyl cycle (Wilson et al. 2016), explaining the high metabolic burden of TDA production (Will et al. 2017).

Given the metabolic disadvantage of TDA production, this molecule should provide a significant advantage to *P. inhibens* in competition for nutrients to compensate energetic costs, corroborated by the fact that naturally isolated *Phaeobacter* contain the TDA plasmid, while it is lost with high frequency in laboratory cultures (D'Alvise 2013). TDA may thus fulfill other functions in natural settings, for instance facilitating the prevalence of *Phaeobacter* spp. on surfaces. Hence, this thesis also investigated if TDA might function as communication molecule at sub-inhibitory concentrations and may influence biofilm formation through chemotactic attraction (Beyersmann et al. 2017).

Aims of this thesis

This thesis aimed to investigate strain-specific adaptations to tidal flat environments, surface-associated growth and macroalgae hosts, with special emphasis on the function of secondary metabolites in these processes. Therefore, a *Roseobacter* isolated from a macroalgae-surface was analyzed on genomic, chemical and physiological level to identify unique traits for a surface-associated life in coastal habitats. Another focus of this thesis was to illuminate the influence of biofilm-related secondary metabolites on communication and behavior of surface-associated *Rhodobacteraceae* that might in turn influence the succession of colonization in such habitats. An in-depth analysis of gene regulations upon sensing of biofilm-related and signaling compounds should provide deeper insights into the mechanisms resulting from chemical crosstalk.

Manuscripts 1 & 2 address specific patterns enabling *Rhodobacteraceae* to adapt to surfaces in tidal areas. A comprehensive elucidation of unique traits in *Pseudoceanicola algae* sp. nov., the first *Pseudoceanicola* species associated to macroalgae illuminated genomic and phenotypic adaptations to surface-association and tidal flats in comparison with other genome-sequenced *Pseudoceanicola* from different habitats. The environmental relevance of these aspects was analyzed by molecular characterization of bacterial communities on the common brown alga *Fucus spiralis* and to what extent culturable bacterial associates harbor mutual traits such as vitamin and iron provision for algae.

Manuscripts 3 & 4 elucidate secondary metabolite-mediated communication and behavior of *Rhodobacteraceae* that might be prevalent in surface-associated assemblages. Combined functions of chemotaxis and quorum sensing molecules were determined under special consideration how these dynamics may influence surface colonization and gene regulation of selected *Rhodobacteraceae* (*Phaeobacter*, *Ruegeria*, *Pseudovibrio* and *Loktanella*). The analyses of available isolates as well as AHL mutants generated in the present thesis enabled to determine phenotypic and regulatory features during chemical crosstalk.

Manuscripts 5-7 include contributions for elucidating further communication molecules in selected roseobacters, enriching the understanding of physiological, chemical, metabolic and transcriptomic dynamics during secondary metabolite-mediated interactions.

The illumination of multiple perspectives of how *Rhodobacteraceae* adapt to surface-associated life in coastal habitats and on macroalgae and the potential influence of chemical crosstalk therein, contribute to the understanding of traits that influence the widespread distribution and biogeochemical importance of this major marine bacterial group.

Manuscript 1

***Pseudoceanicola algae* sp. nov., isolated from the marine macroalga *Fucus spiralis* shows genomic and physiological adaptations for an algae-associated lifestyle**

Laura A. Wolter¹, Matthias Wietz¹, Lisa Ziesche², Agnès Picard¹, Sven Breider¹, Janina Leinberger¹,
Anja Poehlein³, Rolf Daniel³, Stefan Schulz², Thorsten Brinkhoff^{1,*}

¹ Institute for Chemistry and Biology of the Marine Environment (ICBM), University of Oldenburg, Oldenburg, Germany

² Institute of Organic Chemistry, University of Braunschweig, Braunschweig, Germany

³ Genomic and Applied Microbiology and Göttingen Genomics Laboratory, Institute of Microbiology and Genetics, University of Göttingen, Göttingen, Germany

* corresponding author

T. Brinkhoff, Institute for Chemistry and Biology of the Marine Environment (ICBM), University of Oldenburg, PO Box 2503, D-26111 Oldenburg, Germany

Email: t.brinkhoff@icbm.de; phone: +49-(0)441-798-3269; fax: +49-(0)441-798-3438

Contribution of Wolter, L. A.: Preparation of original draft, concept of the study, sample collection and preparation, isolation and maintenance of the bacterial strain, taxonomic classification, analysis of genomic data, physiological experiments and analysis.

Abstract

The genus *Pseudoceanicola* belongs to the alphaproteobacterial *Roseobacter* group (*Rhodobacteraceae*) and currently comprises eight validated species originating from seawater or marine sediments. We herein describe the first *Pseudoceanicola* strain, Lw-13e^T, isolated from the epibiotic bacterial community of the common brown alga *Fucus spiralis*. The closest described relative of Lw-13e^T is *Pseudoceanicola antarcticus* Ar-45^T, isolated from Southern Ocean seawater with 97% 16S rRNA gene sequence similarity. Physiological characterization and pangenome analyses showed adaptive characteristics of Lw-13e^T including the potential to grow in a broad salinity range, degrade oligomeric alginate and other macroalgal-derived substrates (mannitol, mannose, proline), as well as multidrug and heavy metal tolerance. Of high interest is the natural tolerance of Lw-13e^T against 0.6 mM of the broad spectrum antibiotic tropodithietic acid (TDA) which was not reported from non-TDA producing strains to date. Furthermore, Lw-13e^T shows features found in terrestrial plant-bacteria associations, i.e. biosynthesis of siderophores, terpenes and volatiles, which may contribute to mutual algae-bacteria interaction. Based on 16S rRNA gene and whole-genome phylogenies in combination with (chemo)taxonomic distinctions, we propose strain Lw-13e^T (= DSM 29013^T = LMG 30557^T) as a novel species with the name *Pseudoceanicola algae*.

Keywords: *Pseudoceanicola* / *Roseobacter* group / algae-associated lifestyle / tidal flat / comparative genomics / secondary metabolites

Introduction

The genus *Pseudoceanicola* of the alphaproteobacterial *Roseobacter* group (*Rhodobacteraceae*) currently comprises eight validated species of aerobic or facultatively anaerobic, Gram-negative, non-motile rods. Whereas all so-far described *Pseudoceanicola* spp. originate from seawater or marine sediment, we herein describe the first *Pseudoceanicola* strain designated Lw-13e^T, isolated from the surface of the marine brown alga, *Fucus spiralis*. This alga has a broad distribution in tidal areas along the European and North American Atlantic coast and *Rhodobacteraceae* can constitute almost a quarter of the epibacterial community on *F. spiralis* (Stratil et al. 2013). Physiological properties of bacterial strains obtained from the algal surface indicated adaptation of the *Rhodobacteraceae* strains to an epiphytic lifestyle (Dogs et al. 2017).

Organisms inhabiting tidal areas or being associated with coastal macroalgae encounter regular desiccation and rewetting events that require distinct adaptations to swiftly changing environmental conditions. Bacteria produce compatible solutes to deal with osmotic stress (Zhang et al. 2012), and coastal macroalgae-associates are potentially enriched in such features. In addition, the terrestrial input

of heavy metals and antibiotics can accumulate in algal biomass (Hamdy 2000), and microorganisms are found to adapt to these substances (Vignaroli et al. 2018). Furthermore, the lifestyle of organisms from such habitats is likely shaped by biological interactions, including mechanisms of commensalism, mutualism or parasitism between bacteria and algae (Egan et al. 2013). One relevant aspect is the utilization of algal constituents by associated bacteria, with specialization for high- or low-molecular-weight compounds (Hehemann et al. 2016). Furthermore, bacteria-algae interactions can rely on chemical communication and secondary metabolites, e.g. via the bacterial production of siderophores to access insoluble Fe^{3+} (Soria-Dengg et al. 2001) and vitamins for auxotrophic algae (Croft et al. 2005), known for *Roseobacter* bacteria and their microalgal hosts (Alavi et al. 2001). Stimulatory mechanisms include the promotion of algal growth by bacterial phytohormones (Segev et al. 2016), however, both bacteria and algae can also exert inhibitory mechanisms like production of antifouling compounds, shaping the epibiotic community (Rao et al. 2007). Production of iron-scavenging molecules as well as toxins and antibiotic resistances were shown to be relevant for both mutualistic and antagonistic relationships between bacteria and algae (Cárdenas et al. 2017).

Here, we provide a detailed characterization of Lw-13e^T in comparison with *Pseudoceanicola* strains from seawater and sediment, to identify traits mediating a coastal macroalgae-associated lifestyle. Preliminary studies with epibiotic isolates, including Lw-13e^T, already indicated degradation of algae-derived compounds as well as production of siderophores and vitamin B₁₂ (Dogs et al. 2017). Here, we extended the characterization of this strain by a comprehensive analysis of genomic and physiological features that show similarities to terrestrial plant-bacteria interactions. The characteristics of Lw-13e^T in combination with detection of a closely related phylotype in amplicon sequencing data from a *Fucus*-associated bacterial community (Dogs et al. 2017) further supports the association of Lw-13e^T with macroalgae. The specific adaptations of strain Lw-13e^T to life on macroalgae in tidal areas distinguish it from other seawater- or sediment-derived *Pseudoceanicola* spp. Thus, supported by (chemo)taxonomic distinctions and genomic analyses we consider that strain Lw-13e^T is a representative of a novel species within the genus *Pseudoceanicola*.

Materials and methods

Sample collection and bacterial isolation

Specimens of the brown macroalga *F. spiralis* were collected at the German North Sea coast in Neuuharlingersiel (53°42'17.0"N 7°42'16.1"E) on June 27th 2013 during low tide. Algal specimens were brought to the lab at 4°C within two hours and washed three times with sterile seawater to remove loosely attached bacteria. Subsequently, surfaces of algal receptacles were swept over agar plates with marine broth (MB, Difco 2216) medium prepared with slight modifications, referred to as MB in the whole

paper. Plates were incubated at 20°C in the dark for three days and single colonies re-streaked four times on fresh plates for purification, resulting in the isolation of strain Lw-13e^T (Dogs et al. 2017).

Morphological and physiological characterization

Cell morphology and motility were examined by light microscopy (Axio Lab A1; Zeiss, Germany) in exponential and stationary phase, in MB as well as in artificial seawater (ASW) (Zech et al. 2009) supplemented with MB and single carbon sources. For transmission electron microscopy, 50 µl of a culture grown in MB were placed on a copper grid (200 mesh; Plano, Germany), negatively stained using uranyl acetate, and analyzed with an EM 902A electron microscope (Zeiss, Germany). Gram-staining, cytochrome oxidase and catalase activity as well as production of bacteriochlorophyll *a* were assayed as described elsewhere (Klotz et al. 2018). Presence of a photosynthetic operon was tested by specific PCR (Giebel et al. 2013). Analyses of respiratory quinones, lipoquinones and cellular fatty acids were carried out by the German Collection of Cell Cultures and Microorganisms (DSMZ, Braunschweig, Germany) (Supplementary Methods).

Growth experiments

Unless stated otherwise, all growth experiments were carried out at 20°C in the dark. Tests with liquid cultures were performed in triplicates in test tubes containing each 5 ml medium, shaken at 150 rpm. Each tube was inoculated to a starting OD₆₀₀ of 0.001 with cells from a pre-culture grown for 24 h. Growth was followed daily by OD₆₀₀ measurements, including media and substrate controls. Range for growth at different pH values was tested between pH 4 and 10.5, in increments of 0.5 and determined in artificial seawater (ASW) with 5 mM proline and 3% MB (3% MB was found to be obligate for growth of strain Lw-13e^T in ASW). The pH values were adjusted for pH 4 - 8 with 1 M NaOH, and for 8.5 - 10.5 with glycine-NaOH, followed by sterile-filtration of the adjusted medium. Salinity range was tested in NaCl-free ASW with 5 mM proline and 3% MB, adjusted to 0, 0.5, 1 - 10 (in 1% increments), 12.5, 15, 17.5 and 20% NaCl using sterile 30% NaCl solution. Before inoculation, cells from a pre-culture were washed twice in NaCl-free ASW. Temperature range was analyzed in MB at 4, 7, 9, 15, 20, 24, 26, 28, 30, 34, 36 and 40°C. Maximal growth rate (μ_{\max}) and doubling time ($t_d = \ln 2 / \mu_{\max}$) were determined under optimal growth conditions: inoculation to a starting OD₆₀₀ of 0.001 in 100 ml MB incubated in a 500 ml baffled Erlenmeyer flasks at 28°C, pH 7.6 and 150 rpm in the dark. Growth rate and doubling time were determined based on OD₆₀₀ measurements every two hours, using linear regression of a semi-logarithmic plot of mean optical density (from three replicates) versus time.

Utilization of different carbon sources (dissolved in water and sterile-filtered) was determined at final concentrations of 10 mM or 0.1% (w/v) for alginate substrates (polymeric and oligomeric alginate, oligomeric β -D-mannuronate and *Fucus* powder [dried and shredded algal material]) after five days of incubation. The pre-culture was washed twice in pure ASW prior to inoculation. Cells grown in ASW+MB

without further addition of carbon source were used as negative control. Growth was scored as negative when equal to or less than in the negative control and scored as positive after two transfers and repeated growth in the same medium. Cells grown with sterile *Fucus* powder or in co-culture with an axenic *Thalassiosira rotula* culture were analyzed for potentially triggered motility by light microscopy. Reduction of nitrate and nitrite was tested in anoxic ASW+MB containing 0.5 g/L resazurin (Cypionka et al. 1986) (Supplementary Methods).

Antibiotic and heavy metal susceptibility

Antibiotic susceptibility was tested in triplicates using an antibiotic flake assay (Brinkhoff et al. 2004) with penicillin G, tetracycline, streptomycin sulfate, chloramphenicol, kanamycin sulfate, spectinomycin, gentamicin and ampicillin (final concentrations 1 mM) and the marine broad-spectrum antibiotic tropodithietic acid (0.1, 0.3, 0.5, 0.6 and 1 mM). Plates were inspected daily for inhibition zones. Controls included solvents of the antibiotics (water and ethanol) as well as MB. Heavy metal tolerance was tested in modified liquid and solid MB with 0.04, 0.075 and 0.1 mM CuCl₂ and 1 mM of arsenate/arsenite (Supplementary methods). Tests were done in triplicates and agar plates or tubes containing no heavy metals served as controls.

Production of secondary metabolites

Production and excretion of hemolysins was tested using a plate-based blood hemolysis test. Cell culture was grown for 48 h in MB at 20°C and 100 rpm. 50 µL cell suspension was inoculated in a pierced whole in the Columbia blood agar plates (Merck Millipore, Germany, No. 146559) and occurrence of a yellow, clear ring around the well within two weeks was scored as β-hemolysis. Production of volatile organic compounds and acyl-homoserine lactones was analyzed by GC/MS of CLSA and XAD culture extracts (Supplementary Methods).

Chemotactic triggering of motility

Chemotaxis was tested on soft (0.25 %) agar slides with 10% MB as carbon source. 10 µL of 24 h-grown bacteria in MB were inoculated on one side of the plate and 10 µL of the tested substances opposite and bacteria move towards or away from the substance, depending on the chemotaxis response. *Fucus* powder (preparation described above); 1 M of sodium-acetate, glucose, proline; 500 µM of *N*-acetyl glucosamine, maltose, mannose, arabinose, fructose and DMSP; B-vitamin solution (Balch et al. 1979); 1% of polymeric alginate and polymeric β-D-mannuronate were analyzed. Furthermore, the bacteria were inoculated without substance as control for motility on these plates.

Genome sequencing and functional analysis

Chromosomal DNA of Lw-13e^T was isolated using the innuPREP DNA Mini kit (Analytik Jena, Germany). The extracted DNA was used to generate Illumina paired-end sequencing libraries with the

Nextera XT sample preparation kit (Illumina, San Diego, CA). Generated libraries were sequenced with a MiSeq instrument and reagent kit v3, as recommended by the manufacturer. Quality-filtering using Trimmomatic v0.36 (Bolger et al. 2014) resulted in 2,392,874 paired-end reads, which were assembled to 63 contigs (>500 bp) with an average coverage of 120-fold using SPAdes v3.11.1 (Bankevich et al. 2012). The assembly was validated and read coverage determined with QualiMap v2.1 (Garcia-Alcalde et al. 2012). Automatic gene prediction of the draft genome sequence was performed using Prokka (Seemann 2014). Putative biosynthetic gene clusters were predicted using AntiSMASH v4.1.0 (Blin et al. 2017), genomic islands using Islandviewer 4 (Bertelli et al. 2017), prophages using PHASTER (Arndt et al. 2016), and carbohydrate-active enzymes using dbCAN2 (Zhang et al. 2018). Core, accessory and unique genes were identified in Lw-13e^T and a range of related strains (Table S1) using BPGA (Chaudhari et al. 2016) with a 30% amino acid identity threshold. The genome of *Pseudoceanicola lipolyticus* (PGTB00000000) was excluded from further analyses due to high fragmentation (442 contigs with a medium size of 11 kb including many truncated genes). Hypothetical and Domain of Unknown Function (DUF) proteins were excluded in subsequent analyses. Accessory and unique genes were functionally annotated against the KEGG GENES database using KAAS (Moriya et al. 2007). Of the 35-50% of genes with functional annotation, 30-40% could be assigned to a specific KEGG category, meaning that 15-20% of all unique genes could be analyzed in more detail. Data were processed using R (R Core Team 2018) within RStudio (<https://www.rstudio.com>), including package pvclust (Suzuki et al. 2006) for hierarchical clustering. Gene annotations were checked by sequence searches against the Uniprot database (UniProt Consortium 2018). The completeness of the draft genome sequence was estimated using CheckM (Parks et al. 2015). Analysis of homologies of single genes or gene clusters was done using Geneious v11.0.2 (Biomatters Ltd., Auckland, New Zealand).

Phylogenetic analysis

Phylogenetic analysis based on the 16S rRNA gene was done in ARB (Ludwig et al. 2004) using database Silva132 (release Dec. 2017), including the *Pseudoceanicola* type species as well as related type strains with ≥96% sequence similarity. *Roseobacter litoralis* (X78312) served as outgroup. In addition, whole-genome phylogenies were performed in two ways: first, UBCG was used to identify and align nucleotide sequences of 92 core genes with in-built prodigal, hmmsearch and mafft algorithms (Na et al. 2018). The concatenated alignment was manually curated and the best substitution model (GTR+G) computed using jModelTest2 (Darriba et al. 2012). Second, amino acid sequences of 20 random core genes identified by BPGA were aligned with MUSCLE (Edgar 2004). The alignment was manually curated and the best substitution model (LG+G+F) computed using protest3 (Darriba et al. 2011). Alignments are included in Supplementary data file 1 and 2. For both alignments maximum-likelihood phylogenies with 100 (nucleotide) or 1,000 (protein) bootstrap replicates were calculated using RaxML (Stamatakis 2014) on the CIPRES Science Gateway (Miller et al. 2010) with *Roseobacter*

litoralis as outgroup. Digital DNA-DNA hybridization (dDDH) was calculated by the genome-to-genome distance calculator of the DSMZ with formula 2 (Auch et al. 2010, Meier-Kolthoff et al. 2013) and average amino acid identities (AAI) with the AAI matrix tool (Rodriguez-R et al. 2016).

Data availability

The GenBank/EMBL/DDBJ accession number for the 16S rRNA gene sequence of strain Lw-13e^T is KM268063. The Whole Genome Shotgun project has been deposited at DDBJ/ENA/GenBank under the accession QBBT00000000 and is the version described in this paper. Strain Lw-13e^T has been deposited under LMG 30557^T and DSM 29013^T. Supplementary materials for this Manuscript can be accessed from the CD enclosed in the printed version or the attached supplementary files of the electronic version.

Results and discussion

Morphological characterization of Lw-13e^T

Strain Lw-13e^T was isolated from the receptacle surface of the widely distributed brown macroalga *Fucus spiralis*, collected from the German North Sea coast in summer, when brown algae have their highest physiological activity and thus possibly pronounced interactions with bacterial associates occur (Egan et al. 1990, Dogs et al. 2017). Lw-13e^T was among the first organisms forming colonies on MB agar plates. After two days colonies appeared cream-colored, circular, convex, with a shiny surface and a diameter of up to 0.5 mm. After one week, colonies turned yellowish with fuzzy edges and diameters up to 3 mm. In liquid medium, Lw-13e^T grew creamy-yellowish, with cells clumping in sticky aggregates that are hard to disrupt and appear partly orange when concentrated by centrifugation (Fig. 1A). Single cells are irregularly elongated rods, 1.5–3 μm long and approximately 1 μm wide, displaying heterogeneous morphologies in liquid cultures. Cells propagate through both binary fission (Fig. 1B) as well as budding (arrows in Fig. 1C), which might be due to a specific CtrA-based phosphorelay (see below). Most cells were connected by pilus-like structures as observed by light microscopy, which were probably disrupted during preparation for transmission electron microscopy (arrows in Fig. 1D). Detection of several flagellum-like appendages (Fig. 1E) correspond to the presence of flagella-encoding genes (Table S2), however, cells were non-motile independent of culture media or growth phase and were not triggered by addition of algal material to the media. The genus *Pseudoceanicola* was previously described as non-motile, although polar or subpolar flagella were sporadically reported (Zheng et al. 2010, Huo et al. 2014), genomes generally harbor flagella-encoding genes and motility has been indicated for two strains (Bartling et al. 2018).

Genomic and phylogenetic analysis of Lw-13e^T

The draft genome of Lw-13e^T consists of a single chromosome (4,067,555 bp) on 63 contigs (529-501,116 bp) with an overall G+C content of 64.05 % and estimated completeness of 98.5% (Parks et al. 2015). The draft genome contains 3 rRNA genes, 40 tRNA genes, 2,898 genes encoding proteins with predicted functions, and 864 genes encoding hypothetical proteins. Phylogenetic analysis based on the 16S rRNA gene demonstrated that Lw-13e^T forms a monophyletic group with other *Pseudoceanicola* species (Fig. 2A). *Pseudoceanicola antarcticus* Ar-45^T is the closest relative with 97% 16S rRNA gene sequence similarity, which is in accordance with the value for species separation (Stackebrandt et al. 1994). This observation was consistent with nucleotide- and amino acid-based core genome phylogenies, grouping Lw-13e^T with *P. antarcticus* and *P. marinus* (Fig. 2B, Fig. S1). Species separation was supported by amino acid identity (AAI) values of ≤70.4% (Table S3) and <25% similarities in digital DNA-DNA hybridization (Table S4) in accordance with suggested thresholds (Wayne et al. 1987, Rodriguez-R et al. 2014). Association of Lw-13e^T with *F. spiralis* is supported by amplicon sequencing data of the epibacterial community of this brown alga, including a 16S rRNA gene phylotype showing 99% sequence similarity (Dogs et al. 2017).

Pan-genome comparison of Lw-13e^T and related species

We performed a comprehensive genomic analysis for strain Lw-13e^T and related genera (Fig. 2B) to identify features that may reflect adaptations of Lw-13e^T to the tidal habitat and algal association of Lw-13e^T. The core genome of the analyzed strains encompasses ca. 25% of protein-coding genes, but profound differences in accessory and unique genes were recorded (Table 1). Unique genes of strain Lw-13e^T (genes not detected in any strain with >30% amino acid identity) constituted 17.3% of its genome (Table S5), a similar fraction as in other *Pseudoceanicola* spp., whereas *Salipiger* strains (recently reclassified from *Citricella* (Wirth et al. 2018)) and distantly related roseobacters (Kalhoefer et al. 2011) possess higher fractions. Across all strains, the majority of unique genes was related to KEGG category 'Transporters' (Fig. 2C), providing further evidence that roseobacters feature a high diversity of transporters on strain level providing substrate adaptations (Brinkhoff et al. 2008). This diversity may correspond to the likewise considerable fraction of unique genes in KEGG category 'Transcription', as transport and metabolism of different substrates is probably associated with specific regulatory processes (Grkovic et al. 2001). The average of only 7% unique genes among *Phaeobacter* strains emphasized their uniformity in genome content (Buddhuhs et al. 2013). Predominance of phage-related genes among *Phaeobacter* (23% of uniques) suggests a high frequency of past phage encounters and possibly in turn unknown mechanisms of phage resistance in *Pseudoceanicola* and *Salipiger*.

Habitat-related adaptations

Tolerance to challenging environmental conditions

Most unique genes in Lw-13e^T encode for membrane transport proteins (Fig. 2C) that reflect adaptations to a life on macroalgae in terrestrially influenced coastal habitats (Tappin et al. 2015). A set of unique transporters is predicted to transport compatible solutes for salt tolerance, including an ABC-type glycine betaine/carnitine transport system and a TRAP-transporter with highest BLASTp similarity (30.5%) to clusters for ectoine recovery during osmotic stress (Grammann et al. 2002) (Table 2). The ability of strain Lw-13e^T to grow in a broad salinity range of 0.5-17.5% (Table 3) indicated that these systems are important to withstand osmotic stress as found in tidal flats.

Growth in presence of 1 mM arsenate and 0.1 mM copper corresponds to the presence of genes for heavy metal resistance (Table S2) and illustrates a specific feature of bacteria from coastal environments (Hamdy 2000, Vignaroli et al. 2018). Resistance or higher tolerance against antibiotics also distinguish Lw-13e^T from other *Pseudoceanicola* (Table 3) and is congruent with genomic data (Table S2). Furthermore, strain Lw-13e^T shows considerable tolerance against the broad-spectrum marine antibiotic tropodithietic acid (TDA) up to 0.6 mM of TDA without growth limitation. This tolerance is in the same range as found for TDA-producing *Phaeobacter* spp. (Brinkhoff et al. 2004), whereas sensitive strains are normally growth-inhibited by 0.1 mM (Porsby et al. 2011). Tolerance to TDA by non-TDA producing strains is seldom (Porsby et al. 2011) and relate to unknown mechanisms, as the proposed resistance-mediating genes *tdaR1-R3* (Wilson et al. 2016) are absent in Lw-13e^T. TDA production by *Phaeobacter* spp. from the same habitat (Brinkhoff et al. 2004) may have enabled Lw-13e^T to evolve a resistance mechanism. The predisposition of Lw-13e^T to withstand environmental stress is underlined by presence of genes for reactive oxygen species (ROS) defense, which can help counteracting algal defense mechanisms (Egan et al. 2014) (Table S2).

Oligo-alginate degradation

A specific adaptation of strain Lw-13e^T to macroalgae is the presence of a unique alginate lyase gene encoded in a polysaccharide utilization locus (PUL) (Fig. 3A) (Grondin et al. 2017). Alginate is a linear polysaccharide composed of α -L-guluronate (G) and β -D-mannuronate (M) and major component of the cell wall matrix in brown algae, constituting ~50% of the dry weight of *F. spiralis* (Mabeau et al. 1987). The alginate lyase of Lw-13e^T is predicted as a polysaccharide lyase (PL) from family PL15 of exolytic oligo-alginate lyases (Lombard et al. 2014), poorly characterized to date. Accordingly, strain Lw-13e^T grows on oligomeric but not on polymeric alginate or oligo-mannuronate (Fig. 3B), consistent with the shown specificity of a related PL15 from *Agrobacterium fabrum* C58 (63% nucleotide identity, Fig. 3A) for guluronate-rich oligo-alginate (Ochiai et al. 2010). The PUL contains the genes *kdgF*, *kdgK* and a *fabG*-annotated short chain dehydrogenase/reductase, probably functioning as DEH reductase,

comparable to the corresponding enzyme of *Flavobacterium* sp. UMI-01 (Inoue et al. 2015) required for further downstream processing. As the alginate lyase lacks a signal peptide, a probable scenario for oligo-alginate degradation is that substrate is taken up by the PUL-encoded putative sugar ABC transporter (type I) into the periplasm for exolytic cleavage.

The degradation of oligo-alginate suggests that Lw-13e^T is a secondary consumer on algal surfaces, utilizing oligomers released by other associates that encode lyases targeting complex alginate polymers. Such cross-feeding on algal cell wall constituents illustrates a partitioning of different taxa into pioneers and harvesters (Hehemann et al. 2016). The presence of a PUL in Lw-13e^T is noteworthy as roseobacters are rarely described as oligosaccharide degraders. The adaptation of Lw-13e^T to *F. spiralis* was underlined by its use of various other substrates reported to be present in brown algae (Dogs et al. 2017). Lw-13e^T showed growth, e.g. on *Fucus* powder, proline (Fig. 3B), mannose (Table S6) and mannitol (Dogs et al. 2017), which are enriched in brown algal biomass (Klindukh et al. 2011).

Production of volatile organic compounds, terpenes and siderophores

Bacterially produced volatile compounds can mediate interspecies and interkingdom communication (Schulz-Bohm et al. 2017) as well as plant development and defense in terrestrial habitats (Junker et al. 2013). Strain Lw-13e^T was shown to produce diverse volatiles, including dimethyl di- and trisulfides, acetoin derivatives, aromatic compounds including nitrogenous compounds such as pyrazines, and aliphatic ketones (Table S8, Fig. S2), some of which were detected in other associated roseobacters as well (Thiel et al. 2010, Harig et al. 2017), indicating a considerable potential for chemical communication. Dimethyl di- and trisulfides are described as growth promoters or defense against reactive oxygen species (ROS) in land plants (Meldau et al. 2013, Cardoso et al. 2017). Of further interest are the aromatic compounds 2-aminoacetophenone and phenol, not commonly described for roseobacters. In *Pseudomonas aeruginosa* 2-aminoacetophenone regulates antibiotic tolerance via quorum sensing (QS) (Que et al. 2013). Phenol production is known from enteric and lactic acid bacteria (Couto et al. 2006) and the red algal-associated *Pseudovibrio* sp. D323, and was postulated as precursor for phenolic-based defense compounds common in brown algae (Zubia et al. 2008) with e.g. fish-deterrent effects (Steinberg 1988). Thus, provision of phenol by Lw-13e^T could be another adaptive factor for macroalgal association by strengthening algal defenses. Detection of saturated and unsaturated do- and tridecanones as major volatiles of strain Lw-13e^T matches the frequent detection of aliphatic ketones and alcohols originating from fatty acid biosynthesis (Dickschat et al. 2005) in marine and other bacteria (Dickschat et al. 2005).

Detection of the volatile terpenes limonene, nerolidol and farnesol (Table S8) is unprecedented for roseobacters to date and consistent with genomic enrichment of Lw-13e^T in the KEGG category for terpenoid and polyketide synthesis (Fig. 2C). Terpene production of Lw-13e^T may have ecological

implications as feeding deterrent, membrane stabilizer, anti-oxidant, signaling and antagonistic molecule (Gershenzon et al. 2007, Piccoli et al. 2013). Production of limonene could provide antimicrobial defense for the algal host (Subramenium et al. 2015), while farnesol may influence bacterial communication within macroalgal epibiota due to its inhibitory effect on QS (Cugini et al. 2007). Terpene metabolism in Lw-13e^T furthermore includes a unique biosynthetic gene cluster (Table 2) with 40% amino acid identity to a squalene producing gene cluster in *Rhodopseudomonas palustris* strain ATCC BAA-98 of the order *Rhizobiales*. In Lw-13e^T, production of squalene/ lycopene as precursors for hopanoids/ carotenoids (Schaub et al. 2012, Pan et al. 2015), influencing cell wall rigidity (Bramkamp et al. 2015), might explain the orange pigmentation of the cell pellet (Fig. 1E). The rarity of terpene production among *Rhodobacteraceae*, so far only indicated for a single *Tateyamaria* isolate from bobtail squid (Collins et al. 2015), was corroborated by detecting homologs of the terpene-related gene cluster only in *Limimanicola hongkongensis* DSM 17492 from a coastal seven-day old biofilm (~50% sequence identity; e-value <10⁻⁵) among 75 genomes from 16 genera.

Polyketide synthesis in Lw-13e^T relates to a unique siderophore cluster (Table 2) with >42% amino acid identity to enterobactin synthesis genes in *E. coli* K12 (Crosa et al. 2002). Enterobactin is one of the strongest bacterial siderophores (Raymond et al. 2003) and explains the previously demonstrated high siderophore production by strain Lw-13e^T (Dogs et al. 2017), which may be beneficial for the bacterium and its algal host in the typically iron-limited marine environment (Soria-Dengg et al. 2001).

Potential pathogenicity

Putative pathogenic traits of Lw-13e^T include secretion of membrane-destructing hemolysins, corroborated by observed β -hemolysis on blood agar plates. This observation corresponds to unique genes encoding for hemolysin production contained in a type-1 secretion system. Hemolysin production was described to drive virulence in a macroalgae pathogen upon elevated temperatures (Gardiner et al. 2017) and indicates that Lw-13e^T might likewise express opportunistic pathogenicity under specific conditions. A comparable mechanism was demonstrated for *P. inhibens*, changing from mutual to pathogenic behavior upon sensing of infochemicals (Seyedsayamdost et al. 2011). A potential pathogenic behavior of Lw-13e^T is further supported by unique genes for entericidin toxin production, as well as transport of C9-sialic acids via *siaTP*-like transporters both important for pathogenic host colonization (North et al. 2018) or as antifouling compounds (Rao et al. 2007) (Table S2). Another unique gene cluster of Lw-13e^T shows 80% nucleotide identity to a *dppABCDF* related gene cluster in terrestrial nodule-forming *Rhizobium* spp. (Table 2), physiologically shown to mediate uptake of the heme precursor δ -aminolevulinate (Carter et al. 2002). However, *dppABCDF* dipeptide transporters are consistently reported to be important for virulence in bacterial pathogens (Garai et al. 2017). The

additional presence of genes within the cluster annotated as hydantoinases (cleaving non-peptide C-N bonds, preferentially in cyclic amides) and a 5-oxoprolinase (participating in the γ -glutamyl cycle of glutathione synthesis) as well as two peptidases, as in a homologous cluster in the *Rhizobium* representative *Agrobacterium tumefaciens* K84, suggests a role in peptide-dependent host interactions with possible connections to pathogenicity. The close homology of the described gene cluster, as well as another unique squalene/phytoene biosynthesis cluster (see above) to terrestrial plant-pathogenic genes suggests acquisition by horizontal gene transfer. This is especially interesting in view of the spatial proximity of the Lw-13e^T habitat to terrestrial environments and that these unique traits may enforce close association with macroalgae, comparable to processes in terrestrial rhizospheres.

Budding morphology and regulatory mechanisms of Lw-13e^T

As described above, cells of Lw-13e^T exhibit a heterogenic phenotype, propagating through binary fission as well as budding, the latter often being regulated via a QS-driven phosphorelay including the *ctrA-chpT-cckA* cascade (Laub et al. 2002, Wang et al. 2014). A comparable but simpler regulation cascade was found to be conserved among *Rhodobacteraceae* (Brilli et al. 2010). Lw-13e^T harbors all genes for the *ctrA-chpT-cckA* response cascade (Table S2) as well as additional copies (one unique) of *cckA*, *ctrA* and *chpT*, suggesting observed budding in Lw-13e^T (Fig. 1C) to be comparably regulated. The phosphorelay of Lw-13e^T is supposedly not regulated via *N*-acyl homoserine lactone-mediated QS, as no *luxI*-synthase gene was detected and AHLs were not observed using common XAD extraction (L. Ziesche, personal communication). However, Lw-13e^T harbors *luxR*-like regulators, possibly enabling response to foreign AHLs, a process known as eavesdropping (Chandler et al. 2012). Alternative regulations may occur via autoinducer-2 (AI-2)-mediating cellular communication, proliferation, and biofilm formation (Herzberg et al. 2006), reflected by the presence of unique or accessory AI-2 related genes (Table S2).

Conclusions

According to our comprehensive genomic and physiological analyses, strain Lw-13e^T possesses an array of pheno- and genotypic traits that represent specific adaptations to a life on macroalgae and tidal areas (Fig. 4). These include the ability to counteract osmotic stress, tolerate chemical stressor and utilize macroalgae-derived substrates. The synthesis and excretion of secondary metabolites, including potential signaling molecules, highlight the capability for chemical communication that might strengthen interactions with the host and within associated microbiota. Moreover, production of hemolysin suggests that strain Lw-13e^T might turn into an opportunistic pathogen under specific environmental conditions. These traits clearly separate Lw-13e^T from other *Pseudoceanicola* strains. Combining phylogenetic, physiological and genomic data, we propose Lw-13e^T as the type strain of new species within the genus

Pseudoceanicola, with the name *Pseudoceanicola algae* (al'gae. L. gen. n. algae, of alga, seaweed; referring to the isolation source from algae). Description of the new species is done according to the Digital Protologue standard with the taxonnumber TA00551 (Table S6).

Acknowledgements

We thank Edith Kieselhorst for technical assistance with transmission electron microscopy and Marion Pohlner for technical assistance with anaerobic cultivations.

Funding

This work was supported by the Transregional Collaborative Research Center 'Roseobacter' (TRR 51) and grant WI3888/1-2 (to MW), both from the German Research Foundation (DFG).

Figures and Tables

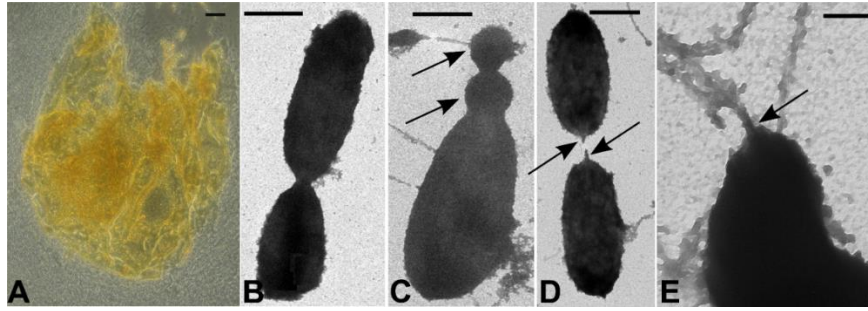


Fig. 1: Transmission electron and light microscopy of Lw-13e^T. Dense cell aggregates of Lw-13e^T are characterized by orange coloration, potentially through pigment production (A). Transmission electron photographs revealed heterogenic morphology of the cells, dividing via binary fission (B) and potential budding (arrows in C), often connected by pilus-like structures (arrows in D). Some cells display flagellum-like structures (arrow in E) and light microscopy suggested that two or more cells are connected, but these structures were destroyed during sample preparation for TEM (also note cell debris in the samples). Bars represent 20 μm (A), 1 μm (B, C, D) and 0.2 μm (E).

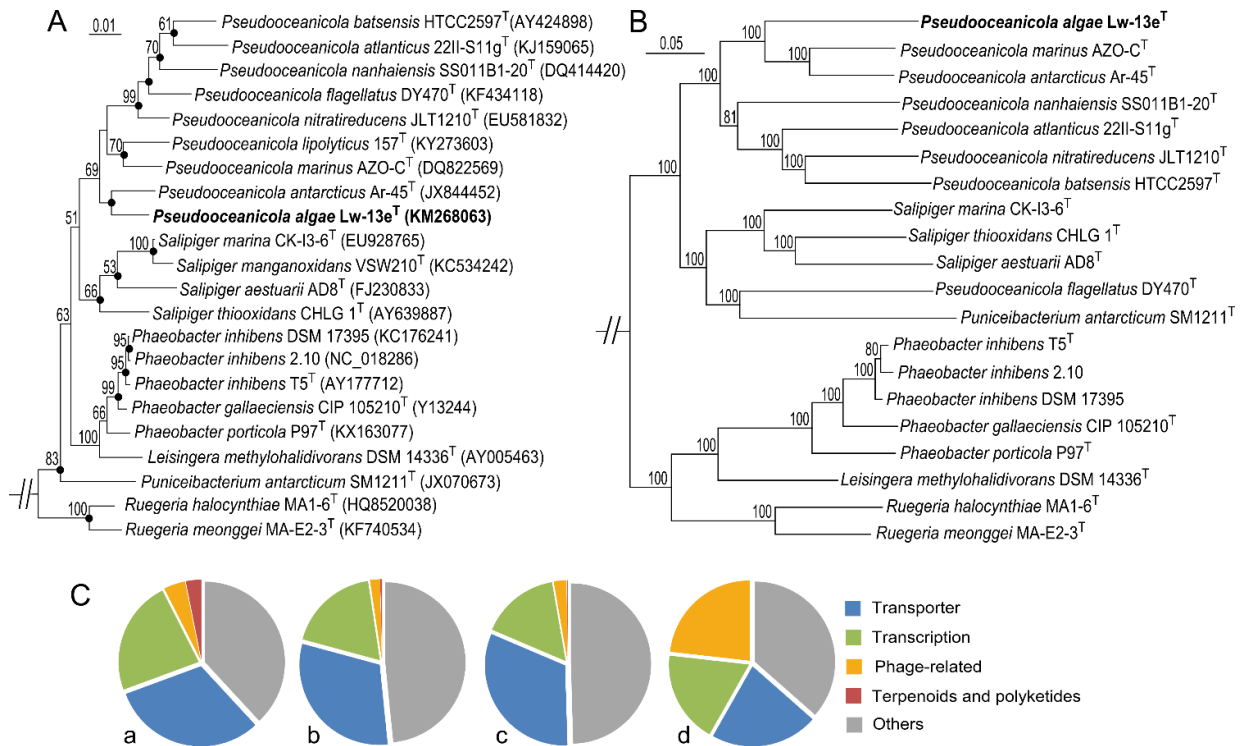


Fig. 2: Phylogenetic placement of strain Lw-13e^T and KEGG categorization of unique genes compared to related bacteria. (A) 16S rRNA gene tree calculated using neighbor-joining with 1000 bootstrap replicates (values >50% are shown); filled circles indicate nodes also recovered reproducibly with maximum likelihood (PHYML). Bar: 0.01 substitutions per nucleotide position. (B) Core genome phylogeny based on nucleotide sequence of 92 core genes identified using UBCG. Support values (based on 100 bootstrap replicates) are indicated. *Roseobacter litoralis* (not shown) served as outgroup. Bar: 0.05 substitutions per nucleotide position. (C) Fraction of unique genes associated with different KEGG categories for strain Lw-13e^T (a), mean of all other *Pseudoceanicola* (b), *Salipiger* spp. (including *P. flagellates* and *Puniceibacterium antarcticum*) (c) and *Phaeobacter* spp. (d). Transporter category includes 'Transport and Catabolism', 'Cellular processes and Signaling' and 'Membrane Transport'. Distinction of strain Lw-13e^T from other *Pseudoceanicola* spp. is demonstrated by unique genes for the metabolism of terpenoids and polyketides (red), whereas phage-related genes (yellow) are predominant among *Phaeobacter* strains.

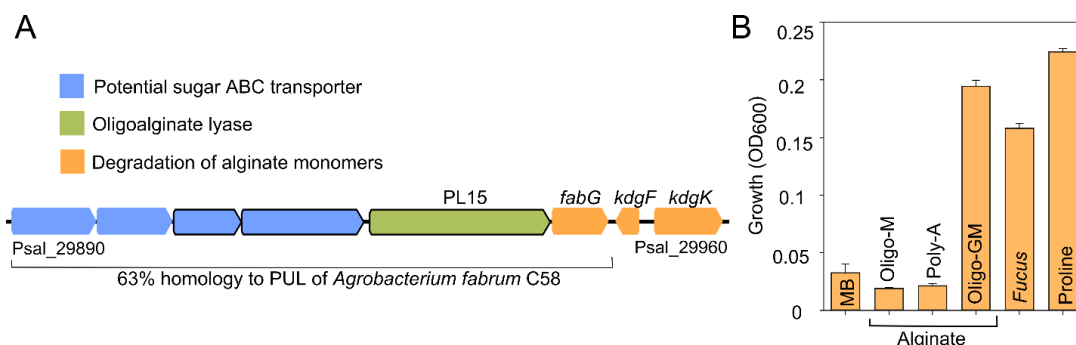


Fig. 3: Unique polysaccharide utilization locus (PUL) of strain Lw-13e^T enables growth on oligomeric alginate. (A) PUL containing PL15 oligo-alginase (green), a type-I sugar ABC transporter (blue) and genes for alginate monomers degradation (orange) with 63% homology to a PUL in *Agrobacterium fabrum* C58. Framed genes are not found in other *Pseudooceanicola* spp. (B) Results of growth experiments showing that the PUL of Lw-13e^T allows degradation of mixed guluronate-mannuronate oligomers (Oligo-GM) but not mannuronate-rich oligomers (Oligo-M) and polymeric alginate (Poly-A). In addition, Lw-13e^T was able to grow on *Fucus* powder.

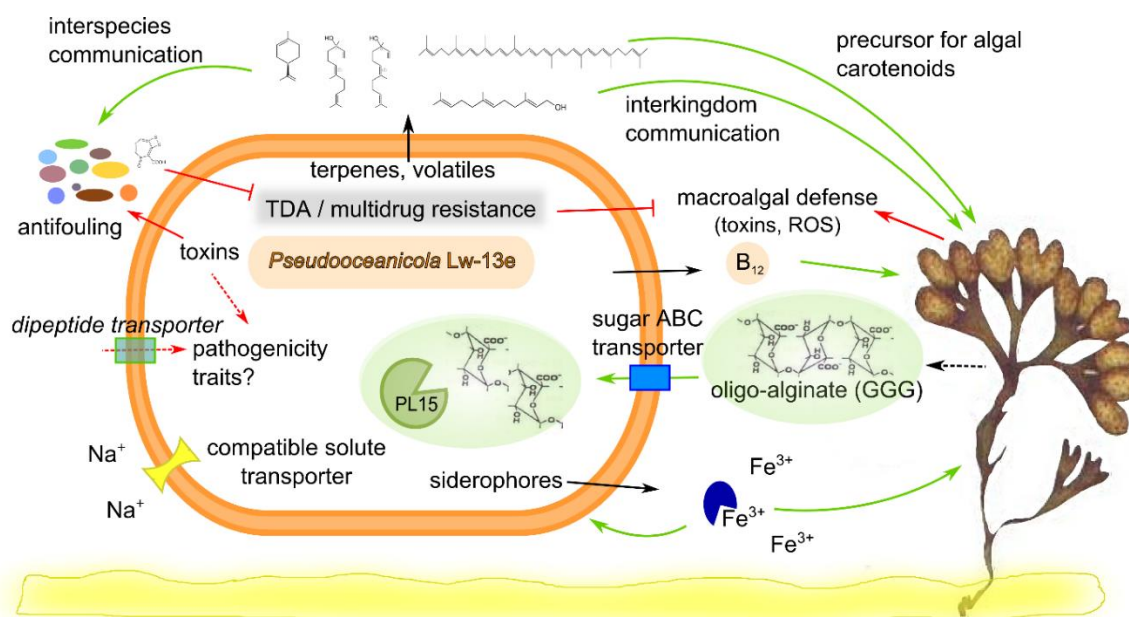


Fig. 4: Summary of traits that mediate adaptations of Lw-13e^T to macroalgae and tidal habitats. From lower left corner counterclockwise: Broad salinity tolerance based on transporters for compatible solutes (yellow); production of iron-chelating siderophores (blue circle); degradation of oligo-alginate by alginate lyase PL15; production and release of vitamin B₁₂; multidrug resistance; interspecies and interkingdom communication through production of terpenes and volatiles; toxin and dipeptide transporters as potential means of pathogenicity.

Table 1: Mean fractions of core, accessory and unique genes in the investigated bacterial groups.

	core (%)	accessory (%)	unique (%)
<i>Pseudoceanicola</i> spp.	27.2	54.5	13.6
<i>Salipiger</i> spp.	23.1	51.6	20.6
<i>Phaeobacter</i> spp.	27.8	61.3	7.0

Table 2: Unique genomic features of strain Lw-13e^T related to secondary metabolite production, alginate degradation, osmotic stress resistance and dipeptide transport.

Function	Gene annotation	Locus Tag
Terpene synthesis	amine oxidoreductase <i>hpnE</i> /squalene associated desaturase	Psal_11720
	dehydroxysqualene synthase <i>hpnD/crtB1</i> All-trans-phytoene synthase	Psal_11730
	squalene synthase <i>hpnC/crtB2</i> 15-cis-phytoene synthase	Psal_11740
Siderophore synthesis	<i>entA</i> ; 2,3-dihydro-2,3-dihydroxybenzoate dehydrogenase	Psal_20560
	<i>entB</i> , bifunctional isochorismatylase/aryl carrier protein	Psal_20570
	<i>entC</i> ; isochorismate synthase	Psal_20580
	<i>besA</i> : ferri-bacillibactin esterase	Psal_36980
Oligo-alginate degradation	potential sugar ABC transporter	Psal_29890-29920
	oligo-alginate lyase PL15	Psal_29930
	degradation of alginate monomers	Psal_29940-29960
Osmotic stress response	TRAP-transporter for uptake of hydroxy-/ectoine	Psal_26970-90
	ABC-type glycine betaine/carnitine transport system	Psal_08740-60
Peptide transport	<i>dppABCDF</i> related gene cluster	Psal_15940-16040

Table 3: Phenotypic characteristics of strain Lw-13e^T compared to related *Pseudoceanicola* type strains. Differences mostly relate to cell size, culture coloration, temperature and salinity ranges, and some variation in substrate use, Tween 80 hydrolysis, antibiotic resistance and fatty acid composition. 1: Lw-13e^T; 2: *P. antarcticus* Ar-45^T; 3: *P. marinus* LMG 23705^T; 4: *Pseudoceanicola atlanticus* 22II-S11g^T (type species). +, positive; -, negative; w, weak; ND, not determined; * Complete fatty acid compositions are shown in Table S7.

Characteristic	1	2	3	4
Isolation source	Surface of <i>Fucus spiralis</i>	seawater	seawater	surface seawater
Cell size (µm)	1 x 1.5 – 3	0.6 x 1	0.5 x 1	1 x 2.5
DNA G+C content (mol%)	64.1	62	70.9	64.1
Colony color	yellow cream	cream	cream white	faint yellow
Temperature range (°C)	4 – 34	4 – 40	4 – 42	10 – 41
Temperature optimum (°C)	20 – 28	35 – 37	28 – 35	25 – 28
Salinity range (% NaCl)	0.5 – 17.5	0.5 – 10	2 – 8	0.5 – 9
Salinity optimum (% NaCl)	0.5 – 7.5	0.5 – 3	3 – 5	1 – 7

Substrates used:

Alanine	+	-	+	ND
D-Mannose	+	+	-	-
<i>N</i> -acetyl-glucosamine	+	+	-	-

Hydrolysis of:

Tween 80	-	+	-	-
----------	---	---	---	---

Susceptibility to:

Gentamicin	w	+	+	+
Kanamycin	-	+	+	ND
Streptomycin	-	-	+	+
Major fatty acids (>10%) (in order of abundance)*	C18:1 ω6c/ω7c (84%)	C16:0 (34%), C19:0 cyclo ω8c (33%), C18:1 ω6c/ω7c (21%)	C18:1 ω6c/ω7c (49%), C19:0 cyclo ω8c (25%), C16:0 (15%)	C18:1 ω6c/ω7c (55%), C16:0 (16%), 11-methyl C18:1 ω7c (11%)

Manuscript 2

***Rhodobacteraceae* on the marine brown alga *Fucus spiralis* are abundant and show physiological adaptation to an epiphytic lifestyle**

Marco Dogs¹, Bernd Wemheuer², Laura Wolter¹, Nils Bergen¹, Rolf Daniel², Meinhard Simon¹,
Thorsten Brinkhoff¹

¹ Institute for Chemistry and Biology of the Marine Environment (ICBM), University of Oldenburg, Oldenburg, Germany

² Genomic and Applied Microbiology and Göttingen Genomics Laboratory, Institute of Microbiology and Genetics, University of Göttingen, Göttingen, Germany

Published in Systematic and Applied Microbiology

Contribution of Wolter L. A.: Isolation of bacteria and taxonomic analysis, physiological experiments and analysis, revision of the manuscript.

Abstract

Macroalgae harbor specific microbial communities on their surface with functions related to host health and defense. In this study, the bacterial biofilm of the marine brown alga *Fucus spiralis* was investigated using 16S rRNA gene amplicon-based analysis and isolation of bacteria. *Rhodobacteraceae* (*Alphaproteobacteria*) were the predominant family constituting 23% of the epibacterial community. At the genus level *Sulfitobacter*, *Loktanella*, *Octadecabacter* and a previously undescribed cluster were most abundant, and together they comprised 89% of the *Rhodobacteraceae*. Supported by a specific PCR approach, 23 different *Rhodobacteraceae*-affiliated strains were isolated from the surface of *F. spiralis* which belonged to 12 established and three new genera. For seven strains, closely related sequences were detected in the 16S rRNA gene dataset. Growth experiments with substrates known to be produced by *Fucus* spp. showed that all of them were consumed by at least three strains and vitamin B₁₂ was produced by 70% of the isolates. Since growth of *F. spiralis* depends on B₁₂ supplementation, bacteria may provide the alga with this vitamin. Most strains produced siderophores, which can enhance algal growth under iron-deficient conditions. Inhibiting properties against other bacteria were only observed when material of *F. spiralis* was present in the medium. Thus, the physiological properties of our isolates indicate adaptation to an epiphytic lifestyle.

Keywords: *Rhodobacteraceae* / *Roseobacter* group / *Fucus spiralis* / North Sea / vitamin B₁₂

Introduction

Bacteria of the family *Rhodobacteraceae* (*Alphaproteobacteria*) are widespread in natural environments, particularly in marine ecosystems. The family comprises a large variety of mainly aerobic photo- and chemoheterotrophs (Pujalte et al. 2014) and, for some representatives, high abundances up to 25% of the total bacterial community have been reported (Selje et al. 2004, Voget et al. 2015, Landa et al. 2016). Physiological and genomic characteristics of *Rhodobacteraceae* indicate that they are metabolically highly diverse (Buchan et al. 2005, Brinkhoff et al. 2008, Luo et al. 2014) and many of these bacteria live in symbiosis with eukaryotic micro- and macroorganisms (Buchan et al. 2005, Pujalte et al. 2014). Of approximately 100 genera currently assigned to the *Rhodobacteraceae*, 70 are affiliated to the *Roseobacter* group (Pujalte et al. 2014). Roseobacters are often found on marine algae and most metabolize algal osmolytes such as dimethylsulfoniopropionate (DMSP) (Moran et al. 2012) and harbor genes reflecting adaptation to a surface and algae-associated lifestyle (Wagner-Döbler et al. 2010, Kalhoefer et al. 2011, Thole et al. 2012, Penesyan et al. 2013, Luo et al. 2014).

Interactions between bacteria and algae are separated in three major categories: (i) close relationships between planktonic algae and bacterial cells, (ii) algae as components of highly structured benthic microbial mats, and (iii) macroalgal-bacterial partnerships (Graham et al. 1999). Microbial

biofilms on marine macroalgae harbor different types of bacteria with densities from 10^2 to 10^7 cells cm^{-2} , depending on the macroalgal host, external physical pressure, and the thallus section of the algae (Armstrong et al. 2000, Bengtsson et al. 2010). The common epiphytic bacterial community on marine green, red and brown algae comprises members of *Alphaproteobacteria*, *Gammaproteobacteria*, *Bacteroidetes* and *Cyanobacteria*; however, they vary in quantity and composition among different macroalgal species (Hollants et al. 2013). Marine macroalgae excrete a variety of organic compounds, including carbohydrates, lipopolysaccharides, organohalogens, amino acids and peptides, which can be used by the epiphytic bacteria but may also serve as deterrents for various pathogens. In return for algal exudates, the bacteria provide growth factors, vitamins, chelators and remineralized inorganic nutrients useful for the algae (Graham et al. 1999). Since many marine macroalgae harbor microbial surface communities that differ from their surrounding environment, algal host-derived control of the microbial epibiosis resulting in specific epimicrobial communities has been suggested (Wahl et al. 2012, Hollants et al. 2013).

Fucus spiralis is a brown macroalga living in the littoral zone of the Atlantic coast of Europe and North America, and the genus *Fucus* is often very abundant in rocky intertidal, temperate environments (Alongi 1997, Graham et al. 1999). *Fucus vesiculosus* and *F. spiralis* are the two most common species in the Atlantic biome, ranging along the European coast from northern Norway to southern Portugal (Ferreira et al. 2014). In addition to natural rocky undergrowths, solid artificial wave-breakers, stone walls and timber piles are often covered by dense mats of *Fucus* species (Graham et al. 1999). *F. spiralis* is well adapted to tidal areas because of its water-absorbing polysaccharides and effective photosynthetic rates in air at low tide (Madsen et al. 1990). In line with other brown algae, such as *Laminaria* and *Macrocystis*, *Fucus* spp. show high net primary production rates of $0.3\text{-}12.0$ g C m^{-2} d^{-1} based on photosynthetic activity, and their biomass can exceed 500 g dry weight m^{-2} (Alongi 1997).

The main compounds supplied by bacteria to their algal hosts are growth factors such as vitamins, because many algae, including macroalgae, lack biosynthetic pathways for vitamin production (Croft et al. 2005, Sañudo-Wilhelmy et al. 2014). For example, *F. spiralis* has been shown to depend on exogenous supply of vitamin B₁₂ (Fries 1993). Another relevant class of compounds supplied are siderophores under iron-limiting growth conditions (Keshtacher-Liebson et al. 1995, Soria-Dengg et al. 2001). Furthermore, antagonistic activities to inhibit the growth of pathogens on macroalgae is another trait shown by some epibiotic bacteria (Holmström et al. 1996, Singh et al. 2014).

The aim of this current study was to assess the composition of epibacterial communities on *F. spiralis* with special emphasis on vitamin- and siderophore-supplying bacteria and their antagonistic activities. The great majority of *Rhodobacteraceae* genomes encode the biosynthetic pathway for vitamin B₁₂ production (Sañudo-Wilhelmy et al. 2014), but reports concerning physiological tests for B₁₂

production are scarce and little is known about siderophore production by members of this family (Thole et al. 2012, Buddhuhs et al. 2013, Riedel et al. 2013). The study used 16S rRNA gene amplicon sequences to analyze the overall epibacterial community of *F. spiralis*, and the results showed a predominance of *Rhodobacteraceae*. Subsequently, strains affiliated to this family were isolated from algal surfaces and their physiological properties were investigated in order to elucidate the adaptation of *Rhodobacteraceae* to an epiphytic lifestyle on *F. spiralis*.

Material and methods

Study area and sampling

The epibacterial community associated with *F. spiralis* was investigated in a tidal flat area of the southern North Sea, Germany (53°42'14" N, 07°42'13" E). Samples were collected from a rocky site (i.e. an artificial wave-breaker) on June 8th, 2010 that was the isolation source for subsequent amplicon sequencing and denaturing gradient gel electrophoresis (DGGE), and samples from November 2011 to October 2012 in intervals of four to five weeks were used for DGGE analysis only (for details see Supplementary Table S1). To analyze the influence of the individual location on the epibacterial community structure of *F. spiralis*, samples were also collected on June 26th, 2012 for DGGE analyses at the nearby Neuharlingersiel village harbor, which is strongly influenced by freshwater input at low tide through a tide gate, as well as high sediment resuspension rates caused by shipping traffic (Supplementary Fig. S1). In each case, three specimens of the alga were collected. The samples were transported at 4°C to the laboratory within two hours and then washed three times with sterile filtered autoclaved artificial seawater (Zech et al. 2009) in order to remove loosely attached bacteria. Subsequently, the algae were used directly as the isolation source for bacterial strains (see below). For subsequent molecular biological analyses, approximately 2 cm² pieces of the receptacles (upper part), fronds (middle part) and stipes (lower part) of the algae were cut off and stored at -80°C until further use (Supplementary Fig. S2).

DNA extraction, PCR-DGGE and cluster analysis

DNA of bacterial biofilms attached to the algal surface was extracted from 2 cm long sections of the algal material, as described by Zhou et al. (Zhou et al. 1996), with the modifications provided by Giebel et al. (Giebel et al. 2009). Extracted DNA stock solutions were stored at -80°C and subsamples at -20°C until further analysis. Bacterial 16S rRNA gene fragments were amplified using primers GC-GM5f and 907RM (Muyzer et al. 1993, Muyzer et al. 1998) and the *Roseobacter* group-specific primer system GC-ROSE0536f and GRb735r (Rink et al. 2007), which also detects several other *Rhodobacteraceae*. DGGE was performed with an Ingeny U 2x2 system (INGENY, Leiden,

Netherlands) and DNA was loaded at 400–600 ng per lane. Cluster analysis of DGGE banding patterns was performed using Gel Compar II, Version 6.5 (Applied maths, Kortrijk).

Sequencing of 16S rRNA gene amplicons

To analyze the overall epibacterial community on *F. spiralis*, samples of the receptacles and fronds were merged. These data were also intended to serve as a reference for the isolation approach. Fragments of 16S rRNA genes, including the hypervariable regions V3–V5, were amplified as described by Wemheuer et al. (Wemheuer et al. 2014). Amplicon libraries were sequenced by the Göttingen Genomics Laboratory (Göttingen, Germany) with a Roche 454 pyrosequencer using Titanium chemistry. Processing and analysis of pyrosequencing-derived datasets were performed as described by Wemheuer et al. (Wemheuer et al. 2014). The 16S rRNA gene amplicon sequences were deposited in the National Center for Biotechnology Information Sequence Read Archive under accession number SRA198204. A consensus sequence for each operational taxonomic unit (OTU) used for phylogenetic analysis (see below) was calculated using Usearch (version 7.0.1090) (Edgar 2010). Sequences were deposited at GenBank under accession numbers KM359626–M359660 and KM516056–KM516059, and the details are presented in Supplementary Text S1.

Isolation of Rhodobacteraceae affiliated strains

Washed algal material was directly rubbed on agar plates with three different media: Difco Marine Broth (MB) 2216 agar (Becton Dickinson, MD, USA), MB 2216 agar supplemented with 0.1% (w/v) dried and pestled *F. spiralis* (*F. spiralis* material was first air-dried at 60°C for at least 12 hours), and artificial sea water agar according to Kisand et al. (Kisand et al. 2008) supplemented with 0.1% (w/v) dried and pestled *F. spiralis*. Incubation was carried out at 20°C over a period of three month in the dark, and then single colonies were transferred onto agar plates containing MB 2216. Affiliation to the *Rhodobacteraceae*/*Roseobacter* group was tested by using the PCR approach of Rink et al. (Rink et al. 2007). Single colonies of positively tested strains were transferred at least three times until they were considered pure. Purity of cultures was additionally checked by DGGE according to Rocker et al. (Rocker et al. 2012). Strains isolated in this study were identified by 16S rRNA gene sequencing and subsequent phylogenetic analysis (see below). Glycerol stocks of each isolate were prepared and stored at -80°C until further analysis.

Sequencing and phylogenetic analysis of 16S rRNA genes

The 16S rRNA genes of the isolates were amplified and sequenced according to Brinkhoff and Muyzer (Brinkhoff et al. 1997), and the sequences were deposited in GenBank under the accession numbers KC731427, KC731428, KJ786453–KJ786461 and KM268054–KM268074. Phylogenetic trees with 16S rRNA gene sequences obtained from the amplicon-based community analysis and the bacterial

isolates were constructed using the ARB software package (www.arb-home.de) (Ludwig et al. 2004). For details see Supplementary Text S1.

Growth experiments and physiological tests

For growth tests, isolates were cultivated in artificial sea-water medium according to Zech et al. (Zech et al. 2009), supplemented with various compounds reported to be present in brown algae and *F. spiralis* (i.e. betaine, L-proline, D(+)-sucrose, taurine, D(+)-melibiose, D(+)-trehalose, D-mannitol, L-serine, D(+)-glucose, laminarin, fucoidan, D(+)-fucose and the algal osmolyte sarcosine; Table 3). Growth of strains D12_1.68, B14, D4_47, E11, E4_2.2, D17, B14_27, E13 and E8, showing no or only weak growth in minimal medium on single substrates, was supported by adding 0.01% yeast extract, as described previously for other representatives of the *Rhodobacteraceae* (Wagner-Döbler et al. 2004).

Tests for inhibitory effects of the isolates were performed against various marine bacteria (Supplementary Table S2) and the axenic diatom *Skeletonema costatum* CCMP1332. To induce antagonism, isolates were grown on MB 2216, supplemented with pieces of *F. spiralis* or various compounds reported for brown algae and *F. spiralis* (see above). Siderophore production of the isolates was determined by Chrome Azurol S (CAS) assays according to (Shin et al. 2001), with slight modifications, and (Thole et al. 2012). The presence of bacteriochlorophyll *a* (Bchl *a*) in the isolates was analyzed spectrophotometrically, and genes encoding subunits of the photosynthetic reaction center complex (*pufL* and *pufM*) by a specific PCR approach (Beja et al. 2002). Vitamin B₁₂ biosynthesis of the isolates was tested by growing them in artificial seawater medium according to (Zech et al. 2009) but without B₁₂. Glucose and yeast extract were used as carbon sources. Extraction and quantification of B₁₂ was carried out with the ELISA test VitaFast® Vitamin B₁₂ – Kit. For further details of growth experiments and individual physiological tests see Supplementary Text S1.

Data availability

Supplementary material published with this Manuscript can be accessed from the CD enclosed in the printed version or the attached supplementary files of the electronic version.

Results

*Diversity and variability of the epibacterial community on *F. spiralis**

The composition of the total bacterial community and the *Rhodobacteraceae* subcommunity on *F. spiralis* from the inner harbour, differed markedly from that on the wave-breaker as shown by a cluster analysis of DGGE banding patterns, applying EUB- and *Rhodobacteraceae*/*Roseobacter* group-specific primer sets (Fig. 1A and B; images of the original DGGE banding patterns are provided in the supplement as Fig. S3A-C). This indicated that the sampling location had a strong influence on the epibacterial community of the *F. spiralis* specimens investigated in our study. Data obtained with the

specific PCR approach also demonstrated that *Rhodobacteraceae* were permanently present on *F. spiralis*. Diversity analysis based on the *Roseobacter* group-specific primer system resulted in two major subclusters, one with samples of the receptacles, and one with samples of stipes and fronds (Fig. 1B), but these differences were less pronounced for the total bacterial communities (Fig. 1A). For both analyses, samples from the wave-breaker show a much higher similarity among each other than those from the harbor site.

Cluster analysis of samples taken at the wave-breaker over the course of one year revealed that changes in the epibacterial community were influenced by different seasons (Fig. 1C). Samples taken in spring and summer (early March to late July) were grouped in a subcluster that also contained samples taken two years earlier (June 2010). The only exception in this subcluster is one subsample of one specimen collected in October. The samples collected in December and January, when the lowest air temperatures were measured (Supplementary Table S1), were also well separated in another subcluster. Overall, the similarity of the banding patterns, and thus stability of the epibacterial community, was higher for samples taken in spring and summer compared to autumn and winter (Fig. 1C).

In summary, these data showed that the epibacterial biofilm of *F. spiralis* was influenced by the location, season, and different parts of the alga. On the other hand, DGGE banding patterns of specimens collected in triplicates at the same date and location generally showed high similarities and clustered together (Fig. 1A-C), indicating that under the same conditions the biofilm develops similarly.

Epibacterial community composition on Fucus spiralis

Due to the fact that the bacterial biofilm differed between different algal parts, samples of the receptacles and fronds were merged for further molecular biological analysis to obtain the overall epibacterial community composition on *F. spiralis*. Amplicon pyrosequencing of the V3–V5 region of the 16S rRNA gene was performed and amplicons were generated by PCR based on the same primer system used for DGGE and subsequent cluster analysis (Fig. 1A and C). For detailed sequencing statistics, rarefaction and alpha diversity, see the supplementary Text S1.

Taxonomic classification of the 16S rRNA gene amplicons showed that the epibacterial community of the three individual *F. spiralis* specimens was dominated by *Proteobacteria* and *Bacteroidetes*, which on average constituted 73% and 26%, respectively (Supplementary Fig. S4A). *Gammaproteobacteria* (42%), *Alphaproteobacteria* (30%) and, within the *Bacteroidetes*, the *Flavobacteriia* (20%) and *Sphingobacteriia* (6%) were the dominant classes, with some variance between the three specimens (Supplementary Fig. S4B). *Rhodobacteraceae* (*Alphaproteobacteria*) represented 23% of the total epibacterial community and was the most abundant family, followed by *Halomonadaceae* (*Gammaproteobacteria*) with 19.5%, and *Flavobacteriaceae* (*Flavobacteriia*) with 19% (Fig. 2). OTUs of the *Rhodobacteraceae* were assigned to 40 different genera and four equivalent

taxa for which no organism was described yet (i.e. the unclassified isolate ANT9283, the NAC11-7 and AS-21 lineages, and the newly defined Marine Host-associated *Rhodobacteraceae* [MHR] cluster from this study [see below]) (Table 1). Furthermore, 3.31% of the OTUs of this family were combined in the category of “uncultured *Rhodobacteraceae*” because they were scattered within the family.

OTUs affiliated to the genera *Sulfitobacter*, *Loktanella* and *Octadecabacter* were present in high abundances on all three specimens, constituting 27, 24 and 12%, respectively, of the *Rhodobacteraceae* (Table 1), and 5.9, 5.6 and 2.8% of the total bacterial community (Supplementary Table S3). In addition, sequences from the genera *Roseobacter* and *Shimia* each comprised ~1% of the *Rhodobacteraceae* in all specimens, and sequences related to the sea ice isolate ANT9283 1.68%, whereas the genera *Litoreibacter*, *Jannaschia*, *Thalassobacter*, *Planktotalea* and the NAC11-7 lineage each comprised <1% (Table 1).

Seven consensus OTUs of the epibacterial community of *F. spiralis* were found to be associated with the new MHR cluster (Fig. 3A and B), comprising 25.7% of the *Rhodobacteraceae* (Table 1) and 6.4% of the total bacterial community (Supplementary Table S3). The sequences within this cluster exclusively represented uncultured organism and were obtained from marine surface samples, although the vast majority were from macroalgae and invertebrates (Fig. 3B). Sequences of the MHR cluster were only distantly related to those of currently described genera of the *Rhodobacteraceae*. The highest identity of the longest 16S rRNA gene sequence in the MHR cluster, clone REP5-5 (1453 bp, acc. no. JF769682), was 91% related to already described organisms (i.e. *Gemmobacter*, *Rhodobacter*, *Halovulum* and *Paracoccus* species).

Several genera affiliated to *Gammaproteobacteria* and the *Bacteroidetes* phylum were also found in high abundances on *F. spiralis*. All genera that made up at least 1% of the total bacterial community are listed in Supplementary Table S4. The most abundant genus detected was *Halomonas* (*Halomonadaceae*), which represented up to 19.5% of the total epibacterial community on *F. spiralis*. Other abundant genera of the *Gammaproteobacteria* were *Shewanella*, *Granulosicoccus* and *Glaciecola* with 7, 6.5 and 6%, respectively, of the total bacterial community. The second major phylum, the *Bacteroidetes*, was dominated by the genera *Zobellia*, *Nonlabens*, *Lacinutrix*, *Winogradskyella*, *Pibocella* and *Maribacter*, which were all affiliated to the family *Flavobacteriaceae*.

Isolation and phylogeny of new F. spiralis-associated Rhodobacteraceae strains

Overall, 23 different strains affiliated to the *Rhodobacteraceae* were isolated from the surface of *F. spiralis* (Table 2). Thirteen strains were isolated using MB 2216, and eight strains were obtained using MB 2216 with air-dried and pestled *F. spiralis* added to the medium. Only two strains, *Paracoccus* sp. C13 and *Loktanella* sp. D15_40, were isolated using a mineral medium containing pieces of *F. spiralis* as single substrate. Nine further strains were obtained that were closely related to the isolates *Loktanella*

sp. D3, *Dinoroseobacter* sp. Lw-35, *Citreicella* sp. Lw-41a, *Roseovarius* sp. D12_1.68 or *Octadecabacter* sp. E8, and they showed a 16S rRNA gene sequence identity of $\geq 99\%$. These strains were not included in subsequent phylogenetic and physiological analyses (Supplementary Table S5).

The strains obtained were widely distributed within the *Rhodobacteraceae*, as shown by their 16S rRNA gene sequence phylogenies (Fig. 3A). Twenty-two strains belonged to the *Roseobacter* group and the majority showed a clear affiliation to species of eleven established genera. In accordance with the abundant OTUs obtained, thirteen strains showed affiliation to species of the genera *Sulfitobacter* (including *Oceanibulbus*), *Loktanella* and *Octadecabacter*. Strain C13 was related to the genus *Paracoccus* and was thus the only isolate outside the *Roseobacter* group. Based on a difference of the 16S rRNA gene sequence to the closest described organism of $\geq 2-3\%$ and separate branching in the phylogenetic tree, nine strains (*Sulfitobacter* sp. A12, *Sulfitobacter* sp. B13, *Rhodobacteraceae* bacterium B14_27, *Paracoccus* sp. C13, *Rhodobacteraceae* bacterium D4_55, *Octadecabacter* sp. E8, *Rhodobacteraceae* bacterium E13, *Rhodobacteraceae* bacterium Lw-13e, *Loktanella* sp. Lw-55a) belonged to potentially new species or genera.

Overall, 32 consensus OTUs obtained from all three *F. spiralis* specimens were affiliated to the *Roseobacter* group (Fig. 3A). The seven strains *Sulfitobacter* sp. D4_47, *Sulfitobacter* sp. B15_G2_red, *Oceanibulbus* sp. E11, *Sulfitobacter* sp. E4-2.2, *Rhodobacteraceae* bacterium B14_27, *Litoreaibacter* sp. F3 and *Jannaschia* sp. B3 were very closely related to OTU consensus sequences (sequence identity of $\geq 99\%$), and an additional 12 strains showed a 16S rRNA gene identity $\geq 97\%$ to OTU consensus sequences. Only strains *Citreicella* sp. Lw-41a, *Roseovarius* sp. D12_1.68, *Dinoroseobacter* sp. Lw-35 and *Paracoccus* sp. C13 showed more than 3% sequence divergence to the calculated consensus OTUs, indicating low abundance of these organisms (Supplementary Table S6).

Physiological characteristics of the isolates

To elucidate the predominance of *Rhodobacteraceae* on *F. spiralis*, the specific physiological characteristics of the isolates useful for an epiphytic lifestyle were investigated. Thus, the new strains were tested for growth on substrates previously indicated as being produced by *F. spiralis* or other brown algae. Furthermore, the isolates were screened for inhibitory activity, vitamin B₁₂ biosynthesis, and production of siderophores and bacteriochlorophyll *a* (Bchl *a*).

All tested substrates were utilized by at least three of the isolates (Table 3). Glucose and mannitol were each used by 22 of the 23 strains. Growth on fucose was detected for eight strains, and the tested disaccharides sucrose, melibiose and trehalose were utilized by approximately half of the isolates. Growth on the polysaccharides laminarin and fucoidan, a sulphated compound, was detected for three and five strains, respectively. Twenty-two and 19 strains grew on the proteinogenic amino acids proline and serine, respectively, whereas 17, 12 and nine strains on betaine and the non-proteinogenic amino

acids taurine and sarcosine, respectively (Table 3). Strain *Litoreibacter* sp. F3 was the only isolate that showed growth on all 13 tested *Fucus*-related substrates. In contrast, strains *Sulfitobacter* sp. B15_G2_red and *Jannaschia* sp. B3 grew on four substrates each. Identical substrate spectra were observed only for the two *Loktanella*-affiliated strains D15_40 and Lw-55a.

Six strains that were scattered widely within the *Rhodobacteraceae* tested positive for *pufLM* genes via PCR screening and therefore had the potential to obtain additional energy by aerobic anoxygenic photosynthesis (Table 3, Fig. 3A). For five of these strains, production of Bchl a was confirmed by spectroscopic measurements (Supplementary Table S7).

Production of metabolites indicating possible interaction between the isolates and other microorganisms or the host was found for all the strains except one (*Rhodobacteraceae* bacterium D4_55) (Fig. 3A, Table 3). Seven strains showed antagonistic activity against one or two bacterial target strains or *S. costatum* (Fig. 3A, Table 3, Supplementary Table S7). Only two strains (*Roseovarius* sp. D12_1.68 and *Sulfitobacter* sp. E4_2.2) showed inhibition of two target strains, whereas all other strains inhibited one target organism. Inhibition of other bacteria was only observed when material from *F. spiralis* or *F. spiralis*-related substrates was present in the medium. In contrast, *S. costatum* was inhibited after growing the isolates on MB medium without *F. spiralis* material.

Siderophores were produced by 17 strains (Table 3). However, the production differed substantially among the various isolates. Strains *Paracoccus* sp. C13, *Rhodobacteraceae* bacterium Lw-13e and *Rhodobacteraceae* bacterium Lw-III1a produced the largest amounts of siderophores or siderophores with a strong iron chelating ability, as demonstrated by a relatively large bleaching zone (Supplementary Table S7). The CAS diffusion agar method yielded more positive and clear-cut results than the overlay method, suggesting that the former was more sensitive.

Growth of *F. spiralis* depends on vitamin B₁₂ supplementation (Fries 1993), and production of this vitamin was found in various extents for 16 strains. The most prolific strains were *Octadecabacter* sp. E8 and *Loktanella* sp. Lw-55a, which both produced approximately 60 ng B₁₂ per 100 ml, and *Sulfitobacter* sp. D4_47 for which approximately 30 ng B₁₂ per 100 ml were measured in the late exponential growth phase (Fig. 4). In cultures of seven isolates affiliated with different genera, the B₁₂ concentration decreased, indicating that these strains consumed the vitamin (traces of B₁₂ in the medium derived from yeast extract). For all seven strains of the *Sulfitobacter* cluster, vitamin B₁₂ production was observed (Figs. 3A and 4). Only the two strains *Rhodobacteraceae* bacterium D17 and *Rhodobacteraceae* bacterium D4_55, which were affiliated to the distantly related species *Sulfitobacter pseudonitzschiae*, did not produce B₁₂.

Even though the closely related strains *Sulfitobacter* sp. A12 and *Sulfitobacter* sp. B13 were obtained from the same habitat and host, they varied considerably in their physiological properties (Fig.

3A, Table 3). Only the strains *Sulfitobacter* sp. B13 and *Litoreibacter* sp. F3 were positive for antagonistic activity, production of siderophores and vitamin B₁₂.

Comparison of the physiological characteristics of the isolates with their phylogenetic affiliations revealed that none of the tested traits were present only in a specific cluster or genus (Fig. 3A, Table 3). Some characteristics (e.g. production of Bchl *a*) were found to be scattered, and the substrate spectra were also very diverse among the isolates. Characteristics likely to be important for the bacteria-alga interaction (i.e. production of vitamin B₁₂ and siderophores, as well as antagonism) were found for the majority of the isolates.

Discussion

Epibacterial community composition on F. spiralis

The analysis of the epibacterial community composition on *F. spiralis* showed that *Rhodobacteraceae* constituted the most abundant family with a high internal diversity. Within this family, four dominant taxa were identified, the genera *Sulfitobacter*, *Loktanella* and *Octadecabacter*, and the newly discovered MHR cluster of exclusively uncultured organisms. Presence of *Rhodobacteraceae* on marine macroalgae has previously been reported (Wahl et al. 2012) and this family was also found to be dominant on *F. vesiculosus* (Stratil et al. 2013). However, this is the first study that has combined a quantitative and seasonal assessment of *Rhodobacteraceae* on an abundant *Fucus* species with a detailed analysis of the potential functional role of individual family members based on physiological data.

DGGE banding patterns of *F. spiralis* samples taken over the course of one year indicated that some bacteria were present on all algal samples and were thus members of the core community (Supplementary Fig. S3C). Using the specific PCR approach, *Rhodobacteraceae* were detected in all samples collected and they also belonged to the core community. Bacterial communities on *F. spiralis* in winter/autumn differed to some extent from those in the spring/summer, indicating seasonal fluctuations (Fig. 1C). Recurrent seasonal patterns of epibacterial communities on macroalgae have previously been observed and were attributed to temporally variable algal exudates or abiotic factors such as seawater temperature (Bengtsson et al. 2010, Lachnit et al. 2011). Saha and Wahl (Saha et al. 2013) reported seasonal changes in the production of antifouling compounds by *F. vesiculosus*, which also appeared possible for *F. spiralis*.

Based on high stability of the epibacterial community between March and July (Fig. 1C), we chose to focus on samples taken in June 2010, which appeared appropriate for analyzing the representative natural community on *F. spiralis*. At this time of the year, macroalgae show their highest physiological activity (Lüning 1979, Egan et al. 1990) and probably have the most intense interaction with bacterial

biofilm. The distinct clusters obtained in the analysis of the DGGE banding patterns of the fronds/stipes and the receptacles indicated that different members of the *Rhodobacteraceae* were specialized for different sections of the alga (Fig. 1B). Different bacterial communities on distinct sections of macroalgae have been found before (Staufenberger et al. 2008) and are presumably a consequence of different interactions of the upper and lower part of the alga with the water column and the substratum.

Cluster analyses of the DGGE banding patterns demonstrated that samples from the wave-breaker were distinct from those of the harbor site and had a much higher similarity between each other (Fig. 1A, B). This indicated that the environment obviously had an impact on the epibacterial community of *F. spiralis* and probably also on the host's physiology. Salinity and water temperature at the wave-breaker were much less variable than at the harbor site, which was strongly influenced by freshwater input over a floodgate at low tide, resulting in salinity values as low as 4–5 psu (Beck et al. 2012). Salinity was identified as the most dominant factor affecting morphogenesis and thus the physiology of *F. spiralis* (Cairrao et al. 2009). This might explain the different epibacterial communities of *F. spiralis* at the wave-breaker and in the harbor.

Physiological capacities of Rhodobacteraceae isolates from F. spiralis

The collection of strains obtained during this study (Table 1–3) enabled the physiology and potential interactions of representative bacteria with their host to be analyzed. Adding dried and pestled *F. spiralis* material to our media resulted in isolation of a broader diversity of *Rhodobacteraceae* strains. However, for the strains obtained after addition of *F. spiralis*, no specific physiological characteristics were observed that would differentiate them from our other isolates. Mutualistic relationships between bacteria and their algal host are based on the capacity of the algae to produce organic compounds and oxygen, which are utilized by the bacteria. In return, bacteria can supply the algae with carbon dioxide, minerals and growth factors (Goecke et al. 2010). The results of the current study showed that all tested *Fucus*-related substrates were consumed by at least three of our isolates. Twenty-two isolates were able to grow on mannitol and proline, which are the most common low-molecular-weight organic osmolytes, previously also found in *Fucus* spp. (Klindukh et al. 2011). Mannitol is also a storage compound of brown algae that achieves its maximum content in summer (Imbs et al. 2009) and can constitute up to 20–30% of the dry weight (Reed et al. 1985). In contrast, laminarin, a storage glucan in brown algae, was used by only three isolates, which represented less than 1% of the *Rhodobacteraceae* (*Litoreibacter* sp. F3) or was not detected in the 16S rRNA gene amplicons (*Oceanibulbus* sp. E11, *Rhodobacteraceae* bacterium D4_55) (Table 1). Laminarin, like most polysaccharides, is an untypical substrate for most roseobacters and it cannot be used by pelagic members of this clade (Hahnke et al. 2013). However, laminarin is an important substrate for other marine bacteria such as *Zobellia galactanivorans* (Labourel et al. 2015), which belongs to the *Flavobacteriaceae*. *Flavobacteriaceae* were

the third-most abundant family on *F. spiralis*, and *Zobellia*, constituting 4.7 % of the total bacterial community (Supplementary Table S4), was the most abundant genus within this family. Fucoidan, a major sulfated structural polysaccharide of *F. spiralis*, was consumed by five strains (*Sulfitobacter* sp. D4_47, *Litoreibacter* sp. F3, *Roseobacter* sp. B14, *Rhodobacteraceae* bacteria D17, *Rhodobacteraceae* bacterium Lw-III1a) (Table 3). *Sulfitobacter* sp. D4_47 was closely related to OTU471, the most abundant consensus sequence which constituted more than 15% of the total *Rhodobacteraceae* on *F. spiralis* (Fig. 3A; Supplementary Table S6). However, polysaccharide degradation of, for example, structural elements, cell walls or storage materials can have a detrimental impact on the macroalgal host. Therefore, the dominant stable or long-term bacterial associates of macroalgae might either lack the capacity for initial polymer degradation, like most of the isolates, or have a need to control it tightly (Egan et al. 2013).

Macroalgae control bacterial epibionts by growth inhibition via antibiotics or destabilisation of quorum sensing (QS) systems (Goecke et al. 2010). Algal morphogenesis in turn is affected by QS molecules of Gram-negative bacteria (Joint et al. 2002, Weinberger et al. 2007). Recently, we investigated 25 *Rhodobacteraceae* strains isolated from macroalgae, including nine strains of the present study, for production of QS autoinducers (N-acylhomoserine lactones, AHLs) (Ziesche et al. 2015). Nineteen of these strains produced AHLs with acyl chains ranging between 10 to 18 carbon atoms (Ziesche et al. 2015). AHLs with acyl chains less than 10 carbon atoms are much more prone to hydrolysis by alkaline pH, as found on the algal thallus (Beer et al. 1990, Decho et al. 2009, Kalia et al. 2014). Thus, the QS systems of macroalgae-associated *Rhodobacteraceae* appeared well adapted to the pH values found on their hosts. Furthermore, we recently found that 22 of the *Rhodobacteraceae* strains produced indole (Ziesche et al. 2015), a known signalling compound (Benkendorff et al. 2001, Lee et al. 2007, Mueller et al. 2009). Indole negatively affects AHL-regulated bacterial phenotypes by inhibiting regulator-folding (Kim et al. 2013), leading to QS inhibition. Large amounts of indole were emitted by *Litoreibacter* sp. F3 (Ziesche et al. 2015), one of the physiologically most versatile strains of the present study. Widespread production of extracellular signalling compounds by macroalgae-associated *Rhodobacteraceae* suggested that these bacteria are strongly involved in controlling the physiological activities of epibacterial communities.

Production of vitamin B₁₂ and siderophores, as well as growth on some substrates (i.e. glucose, mannitol, proline and serine) were found for the majority of the strains, and thus seemed to represent generally important physiological features for the associated bacteria. Many algae have an obligate requirement for exogenous vitamin B₁₂ (cobalamin) in order to promote their growth (Martens et al. 2002, Croft et al. 2005, Sañudo-Wilhelmy et al. 2014). For *F. spiralis*, a cobalamin dependence has been reported and growth of the alga can be enhanced by cobalamin addition (Fries 1993). A mutualistic

relationship between *Dinoroseobacter shibae*, a member of the *Rhodobacteraceae* and close relative to one of the isolates in this study, and the dinoflagellate *Prorocentrum minimum* has been described (Wagner-Döbler et al. 2010). *D. shibae* provides *P. minimum* with essential vitamins (B₁ and B₁₂) and *P. minimum* in return provides *D. shibae* with carbon sources and vitamins (B₃ and 4-aminobenzoic acid) essential for growth of the bacterium. Most of the isolates in the current study excreted B₁₂ and thus may have been able to supply the alga with this particular vitamin. Since isolates of the most abundant genera, *Sulfitobacter*, *Octadecabacter* and *Loktanella*, exhibited the highest production potential (Fig. 4) it appears very likely that they played a key role in the B₁₂ supply to *F. spiralis*.

Halomonas spp., which accounted for approximately 20% of all bacteria on *F. spiralis* (Supplementary Table S4), have also been reported to provide various algae with vitamin B₁₂ (Croft et al. 2005). Furthermore, *Halomonas* spp. can enhance algal growth under iron-deficient conditions via the supply of siderophores. In a co-culture experiment, growth of the microalga *Dunaliella bardawil* was enhanced when precipitated Fe(OH)₃ was added and solubilized by siderophores excreted by a *Halomonas* sp. (Keshtacher-Liebson et al. 1995). The general significance of siderophores for enhancing phytoplankton growth has also been shown (Soria-Dengg et al. 2001). Hence, the *Halomonas* spp. on the biofilm of *F. spiralis* might play important roles in supplying the alga with B₁₂ and Fe. As more than 80% of our isolates were able to secrete siderophores, it was assumed that they, and thus *Rhodobacteraceae* in general, were also important in supplying *F. spiralis* with iron.

The fact that only two of the isolates showed identical substrate spectra and that all the strains differed when all the investigated parameters were taken into account (Table 3), indicated that these strains, which simultaneously share the same host, occupied different ecological micro-niches. This supported the theory that members of the *Rhodobacteraceae* use the “mix and match” strategy to adapt to specific conditions that they encounter in their various habitats (Moran et al. 2007). Antagonism also seemed to be specific in the interaction, since it was observed mainly when algal material was present and was only effective against specific target organisms (Supplementary Table S7). Antimicrobial compounds are useful tools not only for colonization by the producing strain but also as defence mechanisms for the algal host against pathogens, fungi and invertebrate larvae (Holmström et al. 1996, Singh et al. 2014). *F. spiralis*-associated *Rhodobacteraceae* might therefore be able to protect the algae against harmful bacteria and other microorganisms.

The combination of results from different approaches (i.e. molecular biological methods) for an overall bacterial community analysis, providing a reference for the parallel isolation of new strains, followed by their physiological characterization, demonstrated that members of the *Rhodobacteraceae* formed a diverse and important fraction of the epibacteria on *F. spiralis*. The phylogenetic analysis revealed the presence of a new MHR cluster within the *Rhodobacteraceae* (Fig. 3A and B). This cluster

was abundant on *F. spiralis* and exclusively contained sequences of an uncultured organism, since the approach adopted in this study failed to obtain an isolate. The fact that the vast majority of sequences within this cluster came from macroalgae and invertebrates, indicated that the respective organisms were well adapted to a surface-attached and host-associated life style. However, future studies will need to focus on more detailed aspects or specific organisms of the *Rhodobacteraceae* and interactions with their hosts.

Acknowledgements

We thank Bert Engelen for helpful instructions to the software package Gel Compar II, and Thomas Badewien for supply of physico-chemical data of the Spiekeroog time series station. This work was supported by the German Research Foundation (DFG) within the Transregional Collaborative Research Centre TRR 51 Roseobacter.

Appendix A. Supplementary data

Supplementary data associated with this article can be found, in the online version, at <http://dx.doi.org/10.1016/j.syapm.2017-05-006>.

Figures and Tables

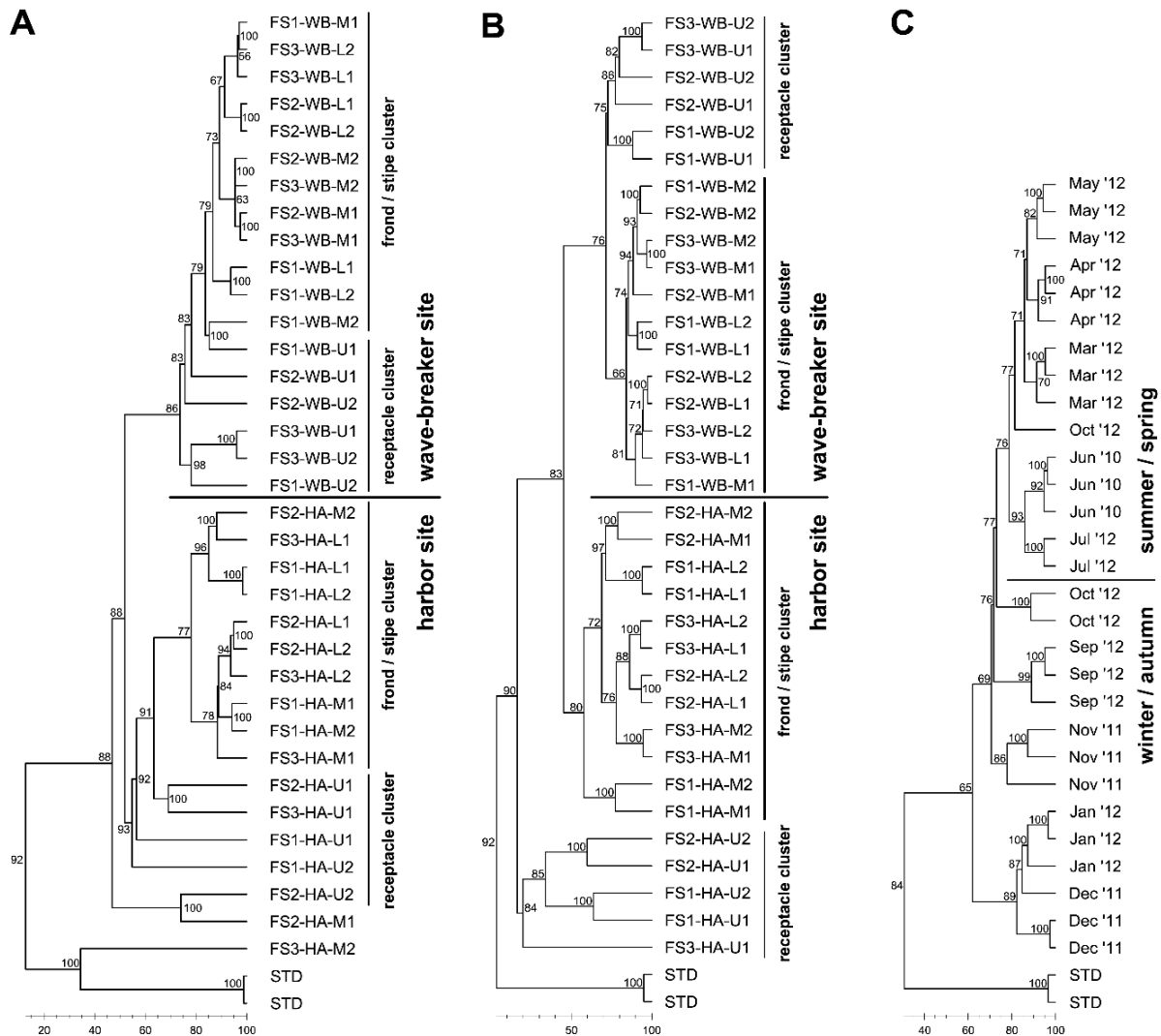


Fig. 1: Cluster analysis of DGGE banding patterns based on 16S rRNA gene amplicons obtained with DNA of *F. spiralis*-associated bacterial biofilms. (A) Analysis based on amplicons generated with a bacterial primer system and (B) a *Rhodobacteraceae* (*Roseobacter* group) specific primer system and DNA of three specimens, each collected at two different sites at the coast off Neuharlingersiel, southern North Sea. Individual alga samples are indicated by the first position of the sample designation [*Fucus spiralis* = FS1/2/3] and sample origin by the second position [i.e., WB = wave-breaker, HA = harbour (see Supplementary Fig. S1)]. The third position indicates two parallel subsamples of different parts [U = upper part (receptacles); M = middle part (fronds); L = lower part (stipes)] of each individual alga. Sample FS3-HA-U1 was excluded due to problems during the DNA extraction process. (C) Analysis based on amplicons generated with a bacterial primer system and samples taken over a period of one year in four to five-week intervals at the same wave-breaker mentioned above. Samples were taken in triplicates and receptacles and stipes were combined in order to analyze the overall epibacterial community on *F. spiralis*. Scale bars indicate Pearson correlation. Numbers at the nodes indicate the calculated cophenetic correlations of each branching. STD = standard.

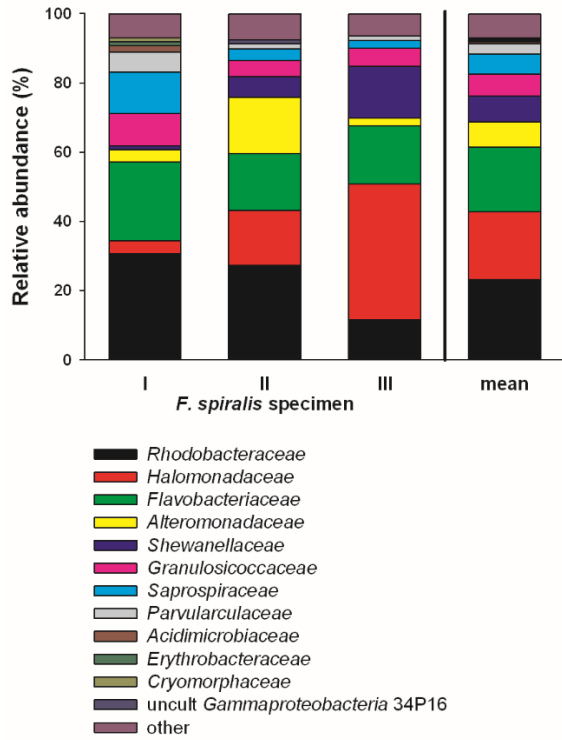
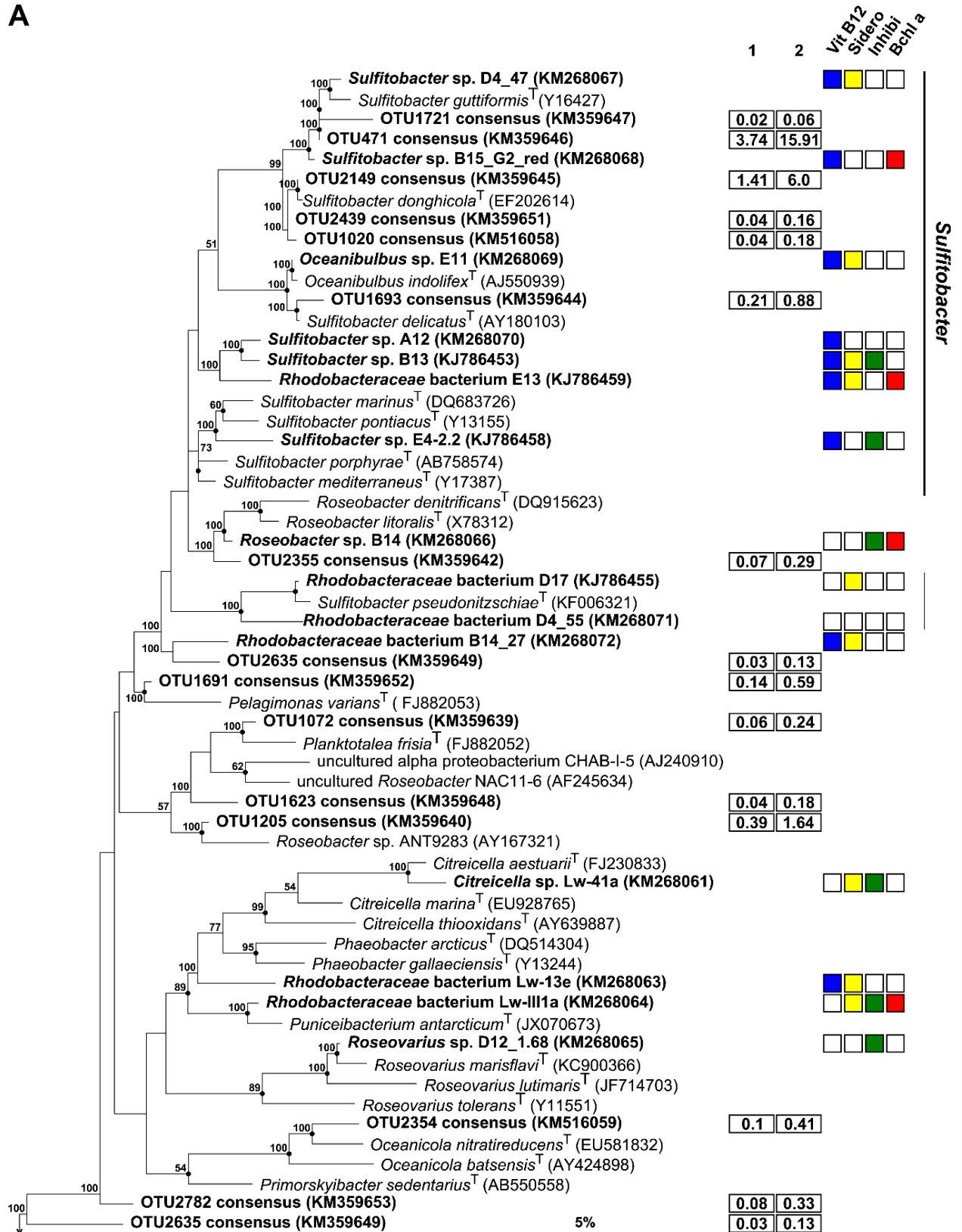
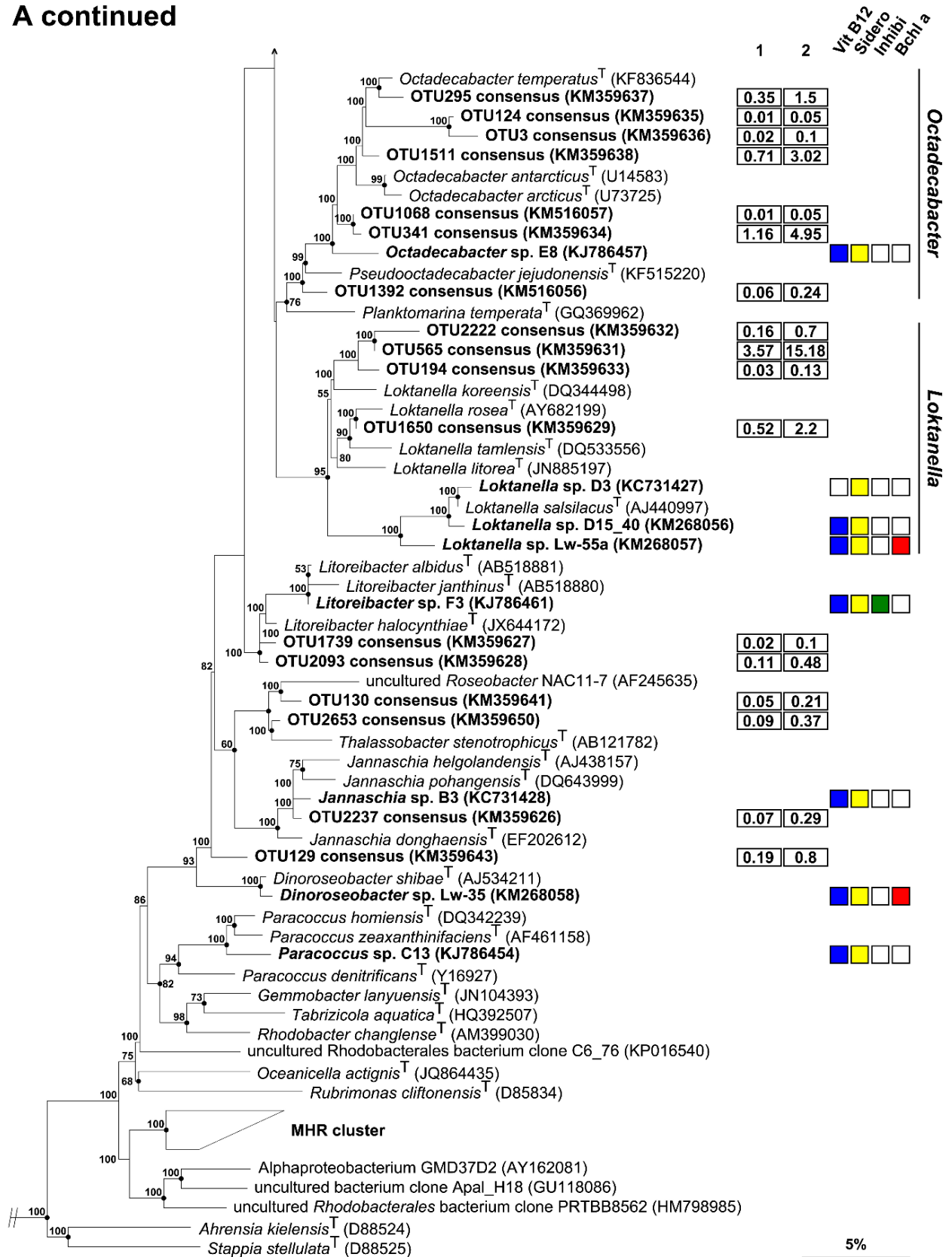


Fig. 2: Relative abundance and mean values of bacterial families within attached biofilms on three *F. spiralis* specimens. Only families with a relative abundance of $\geq 1\%$ are shown. The samples were collected at an artificial wave-breaker in the southern North Sea (for details see Material and methods). Parts of the receptacles and fronds were merged for the analysis in order to obtain the overall epibacterial community composition.

A



A continued



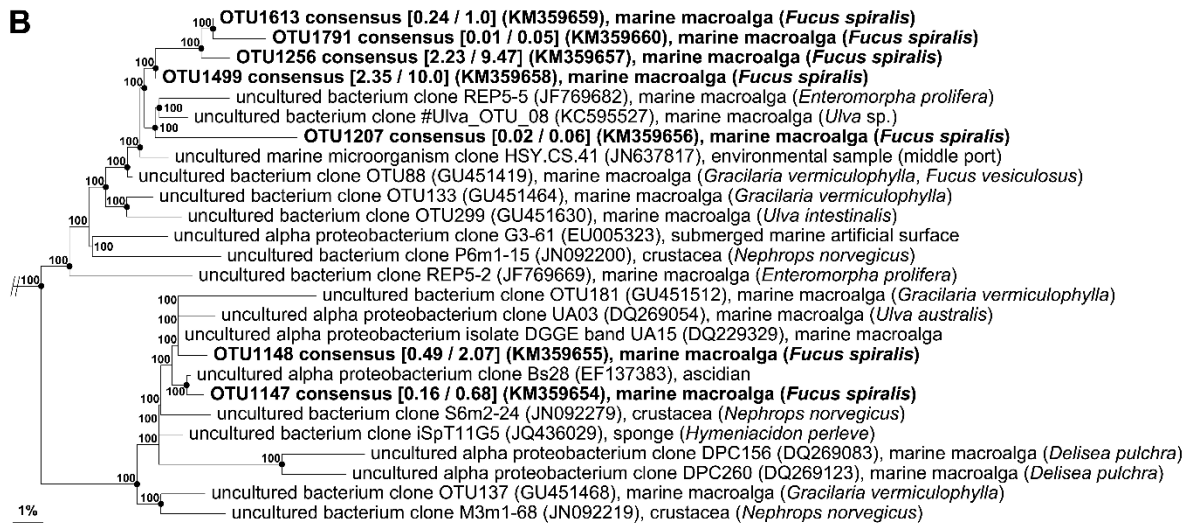


Fig. 3: Neighbor-joining tree based on 16S rRNA gene similarity showing the phylogenetic affiliation of isolates and OTU consensus sequences obtained in this study (bold) within the *Rhodobacteraceae* (A). Only bootstrap values $\geq 50\%$ (derived from 1500 replicates) are shown. Filled circles indicate nodes also recovered reproducibly with the maximum-likelihood calculation. Selected sequences related to *Gammaproteobacteria* were used as an outgroup in order to define the root of the tree (not shown). GenBank accession numbers are given in parentheses. Column 1 and 2: Relative abundance of OTU consensus sequences as a percentage of *Bacteria* and of *Rhodobacteraceae*, respectively; columns Vit B₁₂, Sidero, Inhibi, Bchl a: isolates detected positive for production of vitamin B₁₂ (blue), siderophores (yellow), inhibiting activity (green) and bacteriochlorophyll a synthesis/*pufLM* gene presence (red). (B) Uncompressed version of the Marine Host-associated *Rhodobacteraceae* (MHR) cluster shown in (A). The origin or hosts of bacteria of the MHR cluster are also given. Relative abundances of OTU consensus sequences within the *Bacteria* (first position) and the *Rhodobacteraceae* (second position) are given in square parentheses. Scale bars indicate the percentage sequence divergence.

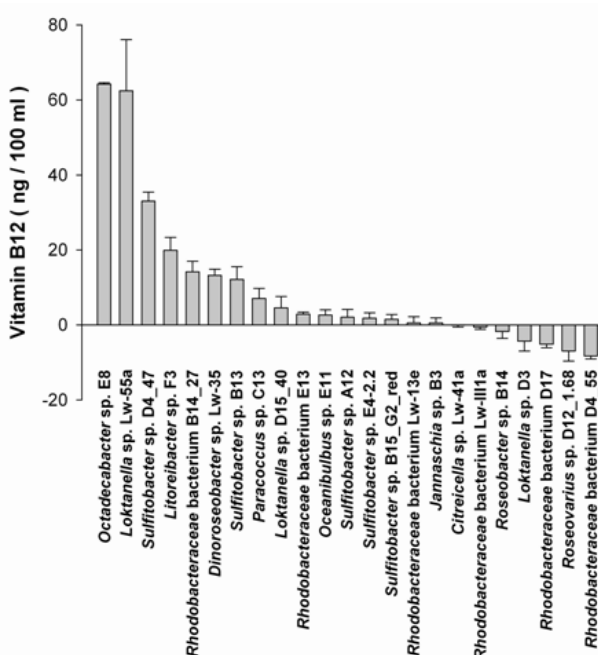


Fig. 4: Concentration of vitamin B₁₂ (ng 100 mL⁻¹) in the supernatants of cultures of isolates obtained in this study. The supernatants were obtained from cultures in the late exponential growth phase. Data were derived from triplicates and normalized against the medium. Traces of vitamin B₁₂ in the medium derived from yeast extract were necessary to support growth of some strains. Error bars indicate standard deviations.

Table 1: Relative abundance of genera or equivalent clusters affiliated to *Rhodobacteraceae* (percentage of 16S rRNA gene amplicons of total *Rhodobacteraceae* reads) found in the epibacterial biofilms of three *F. spiralis* specimens, mean + standard deviation (SD) and number of obtained isolates affiliated to the respective genera.

Genus or cluster	<i>F. spiralis</i>			Mean \pm SD	No. of isolates
	I	II	III		
<i>Sulfitobacter</i>	21.12	28.24	30.23	26.53 \pm 3.91	5
uncultured MHR Cluster	42.73	10.67	23.70	25.7 \pm 13.16	
<i>Loktanella</i>	17.00	31.95	24.14	24.36 \pm 6.11	3
<i>Octadecabacter</i>	7.59	16.98	12.64	12.40 \pm 3.84	1
<i>Roseobacter</i> sp. ANT9283 ^a	2.01	1.12	1.90	1.68 \pm 0.40	
<i>Roseobacter</i>	1.25	1.25	1.24	1.25 \pm 0.01	1
<i>Shimia</i>	0.63	0.54	2.00	1.05 \pm 0.67	
<i>Litoreibacter</i>	1.09	0.45	0.67	0.73 \pm 0.27	1
<i>Jannaschia</i>	0.53	0.94	0.48	0.65 \pm 0.21	1
<i>Thalassobacter</i>	0.26	0.76	0.29	0.44 \pm 0.23	
<i>Rhodobacter</i>	0.30	0.67	n.d.	0.32 \pm 0.27	
<i>Roseobacter</i> clade NAC11-7 lineage	0.03	0.49	0.38	0.30 \pm 0.20	
<i>Planktotalea</i>	0.13	0.45	0.19	0.26 \pm 0.14	
<i>Tateyamaria</i>	0.26	0.13	n.d.	0.13 \pm 0.11	
<i>Roseovarius</i>	0.20	0.13	n.d.	0.11 \pm 0.08	1
<i>Marinosulfonomonas</i>	0.10	0.13	n.d.	0.08 \pm 0.06	
<i>Rubellimicrobium</i>	0.07	n.d.	0.13	0.07 \pm 0.05	
<i>Celeribacter</i>	0.13	0.04	n.d.	0.06 \pm 0.05	
<i>Tropicimonas</i>	0.07	0.09	n.d.	0.05 \pm 0.04	
<i>Oceanicola</i>	n.d.	0.04	0.10	0.05 \pm 0.04	
<i>Sagittula</i>	0.03	0.09	n.d.	0.04 \pm 0.04	
<i>Dinoroseobacter</i>	0.07	0.04	n.d.	0.04 \pm 0.03	1
<i>Phaeobacter</i>	0.07	0.04	n.d.	0.04 \pm 0.03	
<i>Roseobacter</i> clade AS-21 lineage	0.07	0.04	n.d.	0.04 \pm 0.03	
<i>Thalassobius</i>	0.07	0.04	n.d.	0.04 \pm 0.03	
<i>Nereida</i>	0.03	0.04	n.d.	0.03 \pm 0.02	
<i>Pseudoruegeria</i>	0.03	0.04	n.d.	0.03 \pm 0.02	
<i>Albimonas</i>	n.d.	0.09	n.d.	0.03 \pm 0.04	
<i>Maribius</i>	0.07	n.d.	n.d.	0.02 \pm 0.03	
<i>Pacificibacter</i>	n.d.	0.04	n.d.	0.01 \pm 0.02	
<i>Paracoccus</i>	n.d.	0.04	n.d.	0.01 \pm 0.02	1
<i>Thalassococcus</i>	n.d.	0.04	n.d.	0.01 \pm 0.02	
<i>Wenxinia</i>	n.d.	0.04	n.d.	0.01 \pm 0.02	
<i>Citreicella</i>	0.03	n.d.	n.d.	0.01 \pm 0.02	1
<i>Citreimonas</i>	0.03	n.d.	n.d.	0.01 \pm 0.02	
<i>Leisingera</i>	0.03	n.d.	n.d.	0.01 \pm 0.02	
<i>Maritimibacter</i>	0.03	n.d.	n.d.	0.01 \pm 0.02	
<i>Oceaniovalibus</i>	0.03	n.d.	n.d.	0.01 \pm 0.02	
<i>Palleronia</i>	0.03	n.d.	n.d.	0.01 \pm 0.02	
<i>Pelagicola</i>	0.03	n.d.	n.d.	0.01 \pm 0.02	
<i>Ponticoccus</i>	0.03	n.d.	n.d.	0.01 \pm 0.02	
<i>Profundibacterium</i>	0.03	n.d.	n.d.	0.01 \pm 0.02	
<i>Pseudorhodobacter</i>	0.03	n.d.	n.d.	0.01 \pm 0.02	
<i>Planktomarina</i> ^b	0.03	n.d.	n.d.	0.01 \pm 0.02	
<i>Oceanibulbus</i>	n.d.	n.d.	n.d.	-	1
<i>Rhodobacteraceae</i> bacterium	n.d.	n.d.	n.d.	-	6
uncultured <i>Rhodobacteraceae</i>	3.71	4.16	2.06	3.31 \pm 0.9	

n.d. = not detected

^a Manual correction of the cluster *Roseobacter* CHAB-1-5 to *Roseobacter* ANT9283 based on phylogenetic analysis and incorrect designations in the SILVA database.

^b Manual correction of the *Roseobacter* DC5-80-3 lineage (Buchan et al., 2005) to *Planktomarina* (Giebel et al., 2013).

Table 2: Isolates obtained in this study, medium used for isolation, closest described relative (accession number of 16S rRNA gene) and similarity of the respective 16S rRNA gene.

Strain	Medium ^a	Closest described relative ^b (acc. no.)	16S rRNA similarity (%)
A12	MBF	<i>Sulfitobacter mediterraneus</i> (Y17387)	98
B3	MBF	<i>Jannaschia donghaensis</i> (EF202612)	98
B13	MBF	<i>Sulfitobacter marinus</i> (DQ683726)	99
B14	MBF	<i>Roseobacter litoralis</i> (X78312)	99
B14_27	MBF	<i>Sulfitobacter pacificus</i> (AB934383)	98
B15_G2_red	MBF	<i>Sulfitobacter guttiformis</i> (Y16427)	99
C13	ASWF	<i>Paracoccus homiensis</i> (DQ342239)	98
D3	MB	<i>Loktanella salsilacus</i> (AJ440997)	99
D4_47	MB	<i>Sulfitobacter guttiformis</i> (Y16427)	99
D4_55	MB	<i>Sulfitobacter pseudonitzschiae</i> (KF006321)	97
D12_1.68	MB	<i>Roseovarius marisflavi</i> (KC900366)	99
D15_40	ASWF	<i>Loktanella salsilacus</i> (AJ440997)	99
D17	MB	<i>Sulfitobacter pseudonitzschiae</i> (KF006321)	99
E4-2.2	MBF	<i>Sulfitobacter mediterraneus</i> (Y17387)	98
E8	MB	<i>Octadecabacter antarcticus</i> (U14583)	97
E11	MB	<i>Oceanibulbus indolifex</i> (AJ550939)	100
E13	MBF	<i>Sulfitobacter porphyrae</i> (AB758574)	98
F3	MB	<i>Litoreibacter albidus</i> (AB518881)	99
Lw-III1a	MB	<i>Puniceibacterium antarcticum</i> (JX070673)	99
Lw-13e	MB	<i>Phaeobacter gallaeciensis</i> (Y13244)	97
Lw-35	MB	<i>Dinoroseobacter shibae</i> (AJ534211)	99
Lw-41a	MB	<i>Citricella aestuarii</i> (FJ230833)	99
Lw-55a	MB	<i>Loktanella salsilacus</i> (AJ440997)	97

^a Medium abbreviation: MB = Marine Broth 2216; MBF = Marine Broth 2216 supplemented with air dried *F. spiralis*; ASWF = artificial sea water supplemented with air dried *F. spiralis*.

^b Affiliation identified by BLAST analysis (<http://blast.ncbi.nlm.nih.gov/Blast.cgi>).

Table 3: Physiological characteristics of investigated strains. Growth on substrates previously described as typical biomass components of *F. spiralis* or other brown algae.

Strain	Substrate												Sum	Antagonism	Bchl <i>a</i>	Vitamin B ₁₂	Siderophore	
	Glucose	Mannitol	Fucose	Sucrose	Melibiose	Trehalose	Laminarin	Fucoidan	Proline	Serine	Betaine	Sarcosine						Taurine
<i>Citricella</i> sp. Lw-41a	+	w	w	+	-	+	-	-	+	w	-	w	-	8	+	-	-	+
<i>Dinoroseobacter</i> sp. Lw-35	+	+	w	+	w	+	-	-	+	+	+	+	+	11	-	+	+	+
<i>Jannaschia</i> sp. B3	w	w	-	-	-	-	-	-	w	-	-	-	w	4	-	-	+	+
<i>Litoreibacter</i> sp. F3	+	+	+	+	+	+	+	+	+	+	+	w	+	13	+	-	+	+
<i>Loktanella</i> sp. D3	+	+	+	+	+	+	-	-	+	w	w	-	-	9	-	-	-	+
<i>Loktanella</i> sp. D15_40	+	+	-	+	+	+	-	-	+	-	+	-	-	7	-	-	+	+
<i>Loktanella</i> sp. Lw-55a	+	+	-	+	+	+	-	-	+	-	+	-	-	7	-	+	+	+
<i>Oceanibulbus</i> sp. E11	+	+	-	+	-	+	+	-	+	+	+	-	-	8	-	-	+	+
<i>Octadecabacter</i> sp. E8	+	+	+	w	+	-	-	-	+	-	-	-	-	6	-	-	+	+
<i>Paracoccus</i> sp. C13	+	+	-	+	-	+	-	-	+	+	+	-	-	7	-	-	+	+
<i>Rhodobacteraceae</i> bacterium B14_27	+	+	-	-	+	-	-	-	+	+	w	w	+	8	-	-	+	+
<i>Rhodobacteraceae</i> bacterium D4_55	-	+	-	-	-	-	+	-	+	+	-	w	+	6	-	-	-	-
<i>Rhodobacteraceae</i> bacterium D17	+	+	-	-	-	-	-	+	+	+	+	+	+	8	-	-	-	+
<i>Rhodobacteraceae</i> bacterium E13	+	+	-	-	-	w	-	-	+	+	+	-	w	7	-	+	+	+
<i>Rhodobacteraceae</i> bacterium Lw-III1a	+	+	+	+	+	+	-	+	+	+	+	-	-	10	+	+	-	+
<i>Rhodobacteraceae</i> bacterium Lw-13e	+	+	+	+	-	+	-	-	+	w	w	-	-	8	-	-	+	+
<i>Roseobacter</i> sp. B14	+	+	-	+	+	+	-	+	+	+	+	+	+	11	+	+	-	-
<i>Roseovarius</i> sp. D12_1.68	+	-	-	-	-	-	-	-	+	+	+	-	w	5	+	-	-	-
<i>Sulfitobacter</i> sp. A12	w	w	-	-	-	+	-	-	-	w	-	w	w	6	-	-	+	-
<i>Sulfitobacter</i> sp. B13	+	+	w	+	w	+	-	-	+	+	+	w	-	10	+	-	+	+
<i>Sulfitobacter</i> sp. B15_G2_red	w	+	-	-	-	-	-	-	w	+	-	-	-	4	-	+	+	-
<i>Sulfitobacter</i> sp. D4_47	+	+	-	-	-	-	-	+	+	+	+	-	+	7	-	-	+	+
<i>Sulfitobacter</i> sp. E4_2.2	+	+	-	w	-	-	-	-	+	+	+	-	+	7	+	-	+	-
Sum	22	22	8	14	10	14	3	5	22	19	17	9	12		7	6	16	17

+: growth; -: no growth; w: weak growth, sum of substrates used by individual strains, and results of tests for antagonism against bacteria or *Skeletonema costatum*, production of bacteriochlorophyll *a*, vitamin B₁₂ and siderophores (+: positive result, -: negative result).

Manuscript 3

Smalltalk in the ocean - signaling molecules and DNA elicit chemotactic and regulatory effects in surface-associated *Rhodobacteraceae*

Laura Wolter¹, Sujatha Srinivas¹, Jürgen Tomasch², Matthias Wietz^{1,+}, David Nivia Torres^{1,‡}, Maren Scharfe², Irene Wagner-Döbler³, Thorsten Brinkhoff^{1,*}

¹ Institute for Chemistry and Biology of the Marine Environment, University of Oldenburg, Germany

² Helmholtz Centre for Infection Research, Braunschweig, Germany

³ Technical University Braunschweig, Germany

* corresponding author

T. Brinkhoff, Institute for Chemistry and Biology of the Marine Environment, University of Oldenburg,
PO Box 2503, D-26111 Oldenburg, Germany

Email: t.brinkhoff@icbm.de; phone: +49-(0)441-798-3269; fax: +49-(0)441-798-3438

+ present address: Alfred Wegener Institute Helmholtz Centre for Polar and Marine Research;
Bremerhaven, Germany

‡ present address: Hannover Medical School, Germany

Contribution of Wolter L. A.: Concept of the study, preparation of original draft, sequence analyses and complementation of the mutant strain, development of the chemotaxis chamber (with DNT) and chemotaxis experiments (with SS) and analysis, total RNA preparation and analysis of genome and transcriptome data, physiological experiments, data evaluation.

Abstract

Rhodobacteraceae (*Alphaproteobacteria*) are prominent colonizers of marine surfaces, which is supported by chemotactic abilities and production of signaling molecules as well as antibiotics. Here we investigated chemotaxis effects of quorum sensing (QS) autoinducers and other biofilm-associated compounds on *Rhodobacteraceae* which may influence surface colonization. For this purpose, we analyzed chemotactic and gene regulatory effects in *Phaeobacter*, *Ruegeria*, *Pseudovibrio* and *Loktanella* spp. by various *N*-acyl-homoserine lactones (AHLs), the antibiotic tropodithietic acid (TDA) and extracted DNA from the strains. The tested strains all belong to the *Rhodobacteraceae* but differ in their production of AHLs and TDA. Our results show that AHLs induced chemotaxis and caused changes in the transcriptome, independent from the strains ability to produce the substance. However, TDA only attracted TDA-producing but repelled non-producing strains. Moreover, strains were rather attracted towards foreign than their own DNA. Differentially regulated features on transcriptome level included upregulation of traits for host association (with TDA), upregulation of genetic exchange (with AHLs), and downregulation of nitrogen metabolism (with TDA, AHLs and DNA). Together with differential regulation of functional hemolysins that might mediate virulence, the observed specific responses, including processes of “eavesdropping”, suggest different strategies of surface colonization and chemical crosstalk with surface-associated microbiota.

Introduction

Members of the *Rhodobacteraceae* (*Alphaproteobacteria*) are proficient colonizers of marine surfaces (Dang et al. 2008), supported by their ability to recognize and move towards (favorable) attachment sites (Miller et al. 2004). This behavior is generally facilitated by cellular signaling and chemotaxis towards ecologically relevant molecules (Stocker 2012, Antunes et al. 2018). For instance, bacterial sensing and responses to host-released products, dimethylsulfoniopropionate (DMSP) produced by marine phytoplankton (Seymour et al. 2010), supports the establishment of biofilms and strengthens biological interactions (DeLoney-Marino et al. 2003).

Surface colonization and biofilm formation by bacteria is commonly accompanied by changes in gene expression (Kuchma et al. 2000) including increased production of secondary metabolites (Yan et al. 2002, Wilson et al. 2011) with roles in cellular communication and organismal interactions (Dittmann et al. 2018). In a natural biofilm, metabolite secretion by *Rhodobacteraceae* and other bacteria results in a complex chemical microenvironment, influencing nearby attached and swimming bacteria that may in turn secrete chemical cues themselves (Lutz et al. 2016, Seymour et al. 2017). One important route of communication in roseobacters and other Gram-negative bacteria is density-dependent quorum sensing (QS) via *N*-acyl-homoserine lactones (AHLs), regulating population-wide processes involved in

cooperation and competition, such as biofilm formation, antibiotic production or genetic exchange (Abisado et al. 2018, Silpe et al. 2019). These mechanisms are facilitated within enclosed biofilm matrices comprising exopolymers and extracellular DNA (eDNA) (Decho et al. 2017). One relevant QS-controlled process in surface-associated roseobacter is the production of tropodithietic acid (TDA), a broad spectrum antibiotic with minimal inhibitory concentrations (MIC) of 180 μ M (Porsby et al. 2011). However, at subinhibitory concentration (SIC), TDA shows gene regulatory effects comparable to AHLs by influencing 10% of protein coding genes (Beyersmann et al. 2017), supported by the general perception that antibiotics in SIC function as inter-microbial signals (Linares et al. 2006, Romero et al. 2011).

An important question in the context of biofilm formation is whether QS molecules and other compounds can cause chemotactic effects to selectively attract other bacteria to the surface and how these dynamics vary depending on the taxonomic and chemical properties of producing and sensing organisms. Nagy et al. (2015) showed that quorum sensing signaling molecules of *Pseudomonas aeruginosa* are attractants for *Escherichia coli*. Common signaling compounds such as autoinducer 2 (AI-2) and AHLs can have chemotactic effects on bacteria of the same but also different species (Englert et al. 2009, Nagy et al. 2015) indicating a connection between chemotaxis and QS with influence on biofilm formation or dispersal (Anderson et al. 2015, Laganenka et al. 2016). AI-2 is predominantly involved in interspecies communication, also used by roseobacters (Pereira et al. 2009), and bacteria can discriminate chemical languages and “eavesdrop” on foreign AHLs (Case et al. 2008, Chandler et al. 2012) with probable implications for gene regulation. However, a thorough understanding of regulatory effects in marine settings and chemosensory behavior towards molecules released from biofilms is missing to date.

Studying chemotactic responses to AHLs is relevant, as these are the main type of signaling molecules in *Rhodobacteraceae* and other Gram-negative bacteria (Slightom and Buchan 2009) and can influence biofilm formation (Zan et al. 2014, Beyersmann et al. 2017). TDA is relevant considering its role in efficient surface colonization (Rao et al. 2007), production through AHL-mediated QS (Berger et al. 2011) and regulatory effects as a signaling molecule at sub-inhibitory concentrations (Beyersmann et al. 2017). DNA is abundant in biofilms in the form of extracellular DNA (eDNA) originating from passive release from dying cells (Torti et al. 2015) or active excretion (Gloag et al. 2013), supporting biofilm structure and genetic exchange (Flemming et al. 2016), however also perturbs settlement of α -*Proteobacteria* including *Phaeobacter* (Berne et al. 2010, Segev et al. 2015).

Here we investigate the complexity of chemical communication among surface-associated *Rhodobacteraceae* by studying AHLs, the antibiotic tropodithietic acid (TDA) as well as DNA (extracted from the analyzed strains) for their potential as chemotaxis and communication agents, with special

emphasis on possible discrimination between self and foreign compounds. For this purpose, we compared chemotactic response of four bacterial strains with different biosynthetic potentials. *Phaeobacter inhibens* DSM 17395 producing four AHLs as well as TDA, *Ruegeria* sp. TM1040 and *Pseudovibrio* sp. FO-BEG1 producing TDA but no AHLs (however encoding extra *luxR* genes) and *Loktanella* sp. I 8.24 producing C14:1-HSL but no TDA. Furthermore, we investigated gene regulatory effects by transcriptome analysis in *P. inhibens* DSM 17395 in presence of AHLs, TDA and DNA. The linkages of cellular communication, secondary metabolism, chemotaxis and gene regulation provide insights into the dynamic chemical landscape of marine biofilms that encompass bacteria with different potentials to produce and respond to signaling molecules.

Materials and methods

Bacterial strains and growth conditions

All growth experiments were carried out in defined mineral medium (Zech et al. 2009) supplemented with 1 mM sodium acetate and 50 μ M D-glucose (referred to as chemotaxis medium CM), since nutrient starvation increases chemotaxis (Miller et al. 2004). Four bacterial strains, *Phaeobacter inhibens* DSM 17395, *Ruegeria* sp. TM1040, *Pseudovibrio* sp. FO-BEG1 and *Loktanella* sp. I 8.24 were investigated in this study and their motility confirmed previous to the performed experiments (Supplementary Methods).

Chemotaxis capillary test

Bacterial chemotactic responses to different substances was analyzed quantitatively in a modified capillary assay (Fröstl et al. 1998) with cells grown to mid-exponential phase in CM (Supplementary Methods). Tested substances included AHLs dissolved in dimethylsulfoxide (DMSO) at 0.01, 0.1, 1 and 10 μ M, TDA at 1, 10, 100, 250 and 500 μ M (covering sub-inhibitory and inhibitory concentrations) dissolved in DMSO, as well as DNA (5 μ g/mL) dissolved in water. DNA was extracted using the PowerSoil™ DNA Isolation Kit (MO BIO Laboratories Inc., Carlsbad, CA) or NucleoSpin® Tissue (Macherey-Nagel, Germany) (*Loktanella* sp. I 8.24). Controls were 500 μ M aqueous solution of dimethylsulfoniopropionate (DMSP) (positive chemotaxis); 270 μ M (100 μ g/ml) aqueous solution of ampicillin (negative chemotaxis) as well as 14 mM DMSO (solvent control) and CM (medium control). For each strain tested, 150 mL culture grown in CM until late exponential phase (Supplementary methods) were filled into the chemotaxis chamber (Fig. S2), 10 μ L of the tested substances were loaded into each capillary and the capillaries subsequently inserted into the chamber, submerged in the medium (n = 4). After two hours, the liquid from the capillaries containing chemotactically attracted bacteria was removed and mixed with 40 μ L CM. Samples were treated with 25 mM (v/v) ethylene diamine tetra acetic acid (EDTA) for 10 min and vortexed for 1 min to disrupt cell aggregates before fixation with

formaldehyde (1% v/v at 4°C for 4 h). Fixed samples were filtered onto black polycarbonate filters (0.22 µm pore size, 25 mm diameter; cat. no. GTBP02500, Merck, Germany), dried for 10 minutes, stained with freshly prepared staining solution (Moviol +2.5% SYBR Green I + 2% ascorbic acid) and cell numbers were enumerated by epifluorescence microscopy (Axio Scope.A1, Zeiss, Germany). Accuracy of the chemotaxis results was confirmed by generating growth curves (n = 3) for each strain (Supplementary Methods). Doubling times of five hours for *P. inhibens* DSM 17395 and *Loktanella* sp. I 8.24 or 7-9 hours for *Ruegeria* sp. TM1040 and *Pseudovibrio* sp. FO-BEG1 confirmed that increasing cell numbers in capillaries resulted from chemotactic behavior and not cell division. Furthermore, results were validated by showing absence of chemotaxis in a chemotaxis-deficient mutant *cheA::Tn5* (Tm400; provided by the DSMZ; Braunschweig, Germany) with an insertion mutation in the *cheA* gene (PGA1_262p02120; position 229,676) (Supplementary Methods; Fig. S1).

Statistical evaluation of chemotaxis effects and visualization by response factor (F_R)

Statistical analyses were carried out using SigmaPlot v12.0 (Systat, Germany) including Kruskal-Wallis One Way Analysis of Variance on Ranks and Shapiro-Wilk Normality test on raw cell counts. Pairwise multiple comparison to the control was done using the Dunn's Method. For visualization, a response factor (F_R) was calculated by dividing cell numbers for each treatment by cell numbers in control capillaries subtracted by one (control response). Data are presented as mean ± standard error, with F_R > 0 indicating attracting and F_R < 0 indicating repelling effects.

RNA isolation, sequencing and analysis

Transcriptomic changes were analyzed in *P. inhibens* DSM 17395. A culture grown in CM until late exponential phase (28°C, 100 rpm, 20 h) was split in 20 ml aliquots and transferred into Erlenmeyer flasks and the following substances added: 1 µM for AHLs, 10 µM for TDA and 5 ng/ml for eDNA (final concentrations). For each compound, cultures were grown in triplicates. After 2 h, cultures were centrifuged (4°C, 6,000 x g, 10 min) for subsequent RNA extraction. All reagents were kept on ice and procedures were done as quickly as possible to minimize RNA degradation. Cell pellets were dissolved in 2 ml RNA protect (Qiagen, Germany), vortexed for 2 sec, incubated for 5 min at RT, centrifuged (10 min, 6,000 x g), flash-frozen in liquid nitrogen, and stored at -80°C until further processing. RNA was extracted using the RNeasy Mini kit (Qiagen) according to the manufacturer's instructions using mechanical (0.1 mm zirconia/silica beads; Biospec, Bartlesville, OK) and chemical (15 mg/ml lysozyme) disruption of cells. An on-column DNA digestion step was performed for 15 min at RT and RNA eluted with RNase-free water. Complete DNA digestion was verified by PCR with standard primers Gm3/Gm4 (Muyzer et al. 1995) followed by RNA quantification using a Qubit 3.0 fluorometer (Thermo Fisher Scientific, Waltham, MA). Samples still containing DNA were treated with DNase I (Qiagen) for 30 min at 37°C. DNA-free total RNA was treated with RiboZero (Bacteria) kit (Illumina, San Diego, CA) following

the manufacturer's protocol to remove ribosomal RNA from the samples. RNA sequencing was done on a HiSeq 2500 instrument followed by quality control and mapping using bowtie2 (Supplementary Methods). Raw read counts were analyzed with R (R Core Team 2018) and package edgeR (Robinson et al. 2010), implemented in RStudio. Differential expression was calculated compared to the DMSO control (for AHL and TDA-treated samples) and the untreated control (for DMSP and eDNA-treated samples). Only genes with a false discovery rate < 0.05 and an absolute log₂-fold change (FC) > 2 compared to the control were considered as differentially expressed. Multidimensional scaling was performed using the plotMDS function of edgeR, which calculates Euclidian distances between samples based on the 500 genes with the highest log₂FC between the samples. Raw and processed sequencing data have been deposited at the Gene Expression Omnibus database under the accession number GSE126034.

Data availability

Supplementary materials for this Manuscript can be accessed from the CD enclosed in the printed version or the attached supplementary files of the electronic version.

Results and Discussion

We tested chemotactic responses of four surface-associated *Rhodobacteraceae* towards own and foreign communication molecules (AHLs), DNA and TDA to identify linkages of chemotaxis and chemical communication possibly relevant for the formation of marine biofilms. Tested strains included *Phaeobacter inhibens* DSM 17395, *Ruegeria* sp. TM1040, *Pseudovibrio* sp. FO-BEG1 and *Loktanella* sp. I 8.24, differing in their ability to produce TDA and/ or AHLs (Table S1). Responses were compared to DMSP, an algae-derived metabolite with chemotactic and regulatory influence in many roseobacters (Seymour et al. 2010, Seyedsayamdost et al. 2011, Barak-Gavish et al. 2018) serving as "baseline" to compare responses to other ecologically relevant metabolites.

Studying these four strains is of ecological relevance, as all have been isolated from marine surfaces and thus are able to form surface-attachment. *P. inhibens* DSM 17395 originates from scallop aquacultures (Ruiz-Ponte et al. 1998), *Ruegeria* sp. TM1040 is associated with the dinoflagellate *Pfisteria piscicida* (Alavi et al. 2001) and TDA increases TDA production in presence of TDA (Geng et al. 2010). *Pseudovibrio* sp. FO-BEG1 has been isolated from a coral off Florida (Brock et al. 2011, Schwedt 2011) and *Loktanella* sp. I 8.24 from the macroalga *Sargassum muticum* (Ziesche et al. 2015). The importance for AI-binding proteins to transmit chemotaxis signals was shown with AI-2 in *E. coli* (Hegde et al. 2011, Rader et al. 2011). A comparable genetic set-up for the tested strains suggest chemotactic abilities are likely. All genomes encode for methyl-accepting chemotaxis proteins (MCPs)

as well as *luxR*-like regulators with adjacent AHL-synthase (DSM 17395; I 8.24) or orphan *luxR* (TM1040, FO-BEG1).

P. inhibens DSM 17395 shows concentration-dependent chemotaxis towards AHLs and TDA

Functionality of our assay was demonstrated by chemotactic responses of the wild type *P. inhibens* DSM 17395 towards different AHLs, TDA, DMSP (chemoattracting control) and ampicillin (negative chemotaxis control), whereas chemotactic responses were completely missing in a chemotaxis-deficient mutant. Further, no strain showed a chemotactic response towards the solvent control DMSO (Fig. 1A). This permitted detailed analyses of chemotactic behavior towards different concentrations of AHLs and TDA, showing attraction to own (3-OH-C10) and foreign AHLs (C14:1 from *Loktanella* sp. I 8.24) as well as TDA in a concentration-dependent manner (Figs. 1B and C). The observation of threshold, peak and saturating concentrations over three orders of magnitude illustrated that chemotactic responses in marine roseobacters follow similar principles as in *E. coli* (Mesibov et al. 1973). Saturating TDA concentration for a positive response was 250 μ M, which corresponds to minimal inhibitory concentrations for TDA-sensitive strains (Porsby et al. 2011), whereas a peak response was towards sub-inhibitory concentrations of 10 μ M. Together with the notion that TDA likely occurs at sub-inhibitory concentrations in the environment and may hence not elicit antibiosis (D'Alvise et al. 2016), it may indeed function as signaling molecule (Beyersmann et al. 2017) despite the fact that TDA production is a high metabolic burden (Trautwein et al. 2016, Will et al. 2017).

Generally, chemotactic attraction to signaling molecules like AHLs represents a largely undescribed feature for the formation of marine biofilms, although AHLs are known to influence these dynamics after settlement (Huang et al. 2009). Higher attraction of DSM 17395 to foreign C14:1 AHL ($P = 0.005$) demonstrates that chemoattraction towards AHLs is independent from the ability to produce the substance, comparable to observations with AI-2 in *E. coli* (Anderson et al. 2015, Laganenka et al. 2016). Hence, eavesdropping on foreign communication via *luxR*-related genes (Case et al. 2008) may be an important process during biofilm formation with probable influence on cross-species interactions and competition (Chandler et al. 2012). Responses to foreign AHLs may facilitate surface colonization, as exogenous AHLs can strongly influence behavior (Dulla et al. 2009) and sensing the presence of already attached strains may indicate favorable surfaces (Rao et al. 2006). Colonization may then be followed by attracting other phaeobacters through TDA and AHL production until a certain threshold value is reached that is not attracting swimming cells anymore. These interlinked factors provide a window into chemical communication during biofilm formation; processes likely to be amplified in natural settings where other strains with different chemosensory potentials are present.

Chemotaxis towards AHLs and TDA in other Rhodobacteraceae

We broadened the ecological perspective by testing chemotactic responses to AHLs and TDA in three other surface-associated *Rhodobacteraceae* with varying abilities to produce these substances. Comparable to DSM 17395, chemotaxis towards AHLs was independent from own production (Fig. 2A). *Ruegeria* sp. TM1040 and *Pseudovibrio* sp. FO-BEG1 do not produce AHLs but responded significantly and to different extent to foreign AHLs (Fig. 2A), strengthening the role of eavesdropping in biofilm formation. Notably, *Pseudovibrio* sp. FO-BEG1 was the only strain being repelled by an AHL (3OH-C10-HSL; Fig. 2A), potentially related to greater taxonomic distance (Simon et al. 2017) and different TDA regulation (see below). *Loktanella* sp. I 8.24 was attracted by all three AHLs, with strongest response to own C14:1-HSL ($P < 0.01$), which might relate to a lower preference for eavesdropping.

Opposed to AHLs, chemotaxis of the tested strains towards TDA was dependent on the ability to produce this secondary metabolite, with TDA-producers being significantly attracted and non-producing *Loktanella* sp. I 8.24 being repelled (Fig. 2B). All TDA producers were attracted by 10 and 100 μM TDA ($P = 0.005$), whereas 1 μM only attracted *Phaeobacter* and *Ruegeria*, potentially related to higher production of TDA (Geng et al. 2010, Berger et al. 2011) compared to *Pseudovibrio* (Bondarev et al. 2013). The repellent response for non-TDA producing *Loktanella* was underlined by susceptibility towards TDA $\geq 100 \mu\text{M}$ in a plate-based inhibition test (data not shown). The shown responses are interesting in view of present knowledge in AHL and TDA-regulated TDA production. Contrasting responses to 3OH-C10-HSL in *Ruegeria* sp. TM1040 and *P. inhibens* DSM 17395 (attracted) vs. *Pseudovibrio* sp. FO-BEG1 (repelled) are consistent with prior evidence that TDA production in *Ruegeria* and *Phaeobacter* is autoregulated by TDA and 3OH-C10-HSL for the latter (Geng et al. 2010, Berger et al. 2011), whereas production is independent from TDA and 3OH-C10-HSL in *Pseudovibrio* (Harrington et al. 2014). Demonstrating that TDA in SIC (10 μM) influences chemotactic behavior of several *Rhodobacteraceae* is in accordance with previously reported effects of such TDA concentrations in bacterial signaling (Beyersmann et al. 2017). This notion adds another dimension to concentration-dependent interconnectivity of chemical communication by linking chemotaxis, signaling and antibiosis.

Rhodobacteraceae show differential chemotaxis towards own and foreign DNA

Extracellular DNA (eDNA) represents an important component in biofilms (Vorkapic et al. 2016), suggesting specific responses of bacteria. Indeed, DNA elicited chemotactic responses in all tested *Rhodobacteraceae*; with all but I 8.24 being repelled by their own DNA ($P = 0.005$) (Fig. 2C) supporting previous observations that own DNA perturbs bacterial surface attachment (Berne et al. 2010, Segev et al. 2015). Albeit this appears counterintuitive to the role of DNA for biofilm stability, we used extracted DNA in our assay, which may transmit signals relating to lysis through bacterivory, virus encounter or nutrient limitation (Vorkapic et al. 2016). Tested concentrations of 5 $\mu\text{g/ml}$ could resemble DNA amounts

released by dense bacterial assemblages as might occur on surfaces, considering the quantification of up to 33 µg/mL eDNA in late exponential phase in pure cultures (Tang et al. 2013). Higher chemotactic attraction to foreign DNA may facilitate the gain of novel traits (Ellison et al. 2018) or serving as source for carbon, nitrogen and phosphate (Pinchuk et al. 2008). Substantial attraction of strain I 8.24 towards DNA of TDA-producing bacteria may signify a scenario when populations of TDA producers diminish and safe attachment for I 8.24 becomes possible, considering that I 8.24 is susceptible to TDA. Overall, this indicated different strategies of *Rhodobacteraceae* during biofilm formation relating to chemosensory and biosynthetic potential. *Loktanella* sp. I 8.24 may favor a strategy to avoid contact with antibiotic producers (strong attraction to DNA of TDA producers and own AHL, repellence by TDA) in contrast to mutualistic competitive behavior (strong attraction to TDA, foreign AHL and DNA). Different strategies of biofilm formers can promote the stability of oral biofilms (Palmer et al. 2001) and may hence also influence related processes in the oceans.

The discrimination between own and foreign DNA may relate to different methylation patterns, which also enables discrimination of viral vs. self-DNA for specific cleavage by restriction modification systems (Vasu et al. 2013). Supporting this hypothesis, DSM 17395 was repelled by DNA of the closely related *P. inhibens* T5 ($P = 0.007$) (data not shown) which features 87.7% genome-to-genome distance and hence possibly comparable methylation patterns.

Influence of AHLs, TDA and DNA on the transcriptome of P. inhibens DSM 17395

The described interplay of chemotaxis and cellular communication has probable consequences for gene expression and regulation. Hence, we analyzed the transcriptome of *P. inhibens* DSM 17395 in presence of AHLs, TDA and DNA in comparison to DMSP, known as chemotactic attractant and to subsequently influence bacterial behavior, revealing specific transcriptomic responses (Fig. 3A). Highest responses were observed with TDA and the chemotaxis control DMSP (Table 1), and differential regulation of 17% of all genes corroborated the regulatory function of TDA at sub-inhibitory concentrations (Beyersmann et al. 2017). Between 0.3 and 5% of the genes were differentially expressed in presence of own (3-OH-C10 and C18:1) and foreign AHL (C14:1) as well as DNA (Table 1). To the best of our knowledge, this is the first description of global gene regulation in wildtype roseobacters in presence of infochemicals, whereas prior work investigated AHL mutants (Venturi 2006, Patzelt et al. 2013, Beyersmann et al. 2017). Notably, own AHL resulted in higher fraction of upregulated genes than foreign C14:1-HSL, although DSM 17395 showed stronger chemotaxis towards C14:1-HSL, suggesting fine-tuned responses on multiple levels.

On COG level, TDA and DMSP showed opposite regulatory effects compared to AHLs and DNA (Fig. 3B). Specifically, genes related to growth and metabolic activity (e.g. translation, ribosomal proteins) were upregulated by TDA and DMSP, but downregulated by C14:1 and 3OH-C10 AHLs as

well as DNA. Induction of genes signifying elevated metabolic activity by TDA was noteworthy, as TDA is not used as growth substrate. However, similarities to DMSP responses indicate that both compounds serve as signal for comparable environmental conditions, potentially reflecting that interactions with phytoplankton include both DMSP and TDA (Wang et al. 2016) and coincide with high metabolic activity (Teeling et al. 2012). Only features related to amino acid transport and metabolism were comparably regulated with TDA and AHLs/DNA (Figure 3B, Table S2), mostly to nitrogenous amino acids (further discussed below). Chemotaxis-related genes overall lacked transcriptomic responses, probably since substances were homogeneously distributed in the cell culture and not present in gradients as in chemotaxis assays.

TDA and own 3OH-C10-HSL regulate genes for host attachment and genetic exchange

In addition to elevated metabolic status, TDA modulated gene expression towards host interaction by upregulation of protein synthesis and export, siderophore transport (PGA1_78p00360-390) and terpenoid production (Table 2), beneficial e.g. for algal hosts (Soria-Dengg et al. 2001, Piccoli et al. 2013), similar to other surface-associated roseobacters upon sensing of infochemicals (Johnson et al. 2016). This switch was supported by downregulation of motility while upregulating exopolysaccharide production (e.g. *exoD*), comparable to previous studies (Beyersmann et al. 2017) and host attachment (e.g. PGA1_c19730; log₂FC > 9) (Table S2), which may facilitate settlement on surfaces. Indeed, we microscopically observed enhanced attachment in the capillaries filled with TDA (Fig. S3), consistent with increased biofilm formation in presence of antibiotics (Oliveira et al. 2015). Interactions may further benefit from concurrent downregulation of hemolysins and the tad secretion system, i.e. putative pathogenic traits (Moran et al. 2007, Nykyri et al. 2013, Gardiner et al. 2017). Comparable effects were seen with DMSP, which triggers other roseobacters to increase pathogenicity (Barak-Gavish et al. 2018), supporting the notion that *Phaeobacter* participates in mutual interactions with eukaryotes under such conditions (Seyedsayamdost et al. 2011).

In contrast, 3-OH-C10-HSL caused upregulation of motility and hence might initiate dispersal from surfaces. Further upregulated genes encoding genetic exchange via GTAs, including GTA-regulating *ctrA* (PGA1_14360) (Westbye et al. 2017), were downregulated by TDA (Table S2). Contrasting effects were underlined by the fact that AHL addition did not induce traits related to metabolic activity opposed to TDA and DMSP (Fig. 3B). Although this does not completely correspond to chemotactic attraction, TDA and 3OH-C10-HSL hence induce different phenotypes geared towards growth/host attachment vs. dispersal/genetic exchange.

Hemolysins and teichoic acid

The presence of multiple hemolysin genes and their different regulation under the changing conditions warrants special consideration. DSM 17395 encodes 20 RTX-like hemolysins, of which 12

were differentially expressed in presence of AHLs and DNA ($\log_2\text{-CPM} > 6$) (Table S2). The notion of hemolysins as important characteristic of *Phaeobacter* (Fig. 3C) is supported by the fact that most other roseobacters encode fewer RTX-like toxins (Christie-Oleza et al. 2012). One hemolysin (PGA1_65p00350) represented the highest expressed gene in the transcriptome and the gene product also dominated the DSM 17395 proteome in another study (Durighello et al. 2014). Another hemolysin (PGA1_65p00040) with adjacent type I secretion system (T1SS) and *luxR*-type regulator were highly upregulated upon addition of foreign C14:1-HSL (Fig 3C; Table S2), suggesting potential excretion and cytotoxic functions as seen in different pathogens (Thomas et al. 2014). This functionality was confirmed by showing increased β -hemolysis upon C14:1-HSL addition *in vitro* using a blood agar test (Fig. 3C), potentially contributing to pathogenic interaction of *Phaeobacter* with micro- or macroorganisms, that might also include iron-acquisition through cell lysis (Li et al. 2008, Gardiner et al. 2017). Concurrent with hemolysin induction, foreign C14:1-HSL upregulated genes predicted to encode the synthesis of teichoic acids, typical cell wall components in Gram-positive bacteria (Neuhaus et al. 2003), to date only reported once in Gram-negative (Gorshkova et al. 2007). The corresponding gene cluster (PGA1_c13610-13830) is unique for *Phaeobacter* strains (Thole et al. 2012) and its proposed function as carrier for hemolysins might explain the co-regulatory effect (Tsaihong et al. 1983). At the same time, this cluster was downregulated by own DNA, indicating that concurrent growth of other species (transmitted via elevated C14:1-HSL levels) and death of own populations (transmitted via elevated DNA) influences outer membrane composition with putative functions in attachment and interactions.

Nitrogen-related features

AHLs, TDA and DNA influenced several features related to nitrogen metabolism, including enhanced degradation of histidine (own 3OH-C10-HSL and DNA) and arginine (all AHLs and DNA) for nitrogen recycling with simultaneous downregulation of glutamine synthesis, nitrogen regulatory proteins and an ABC-type amino acid transporter (Table S2, Fig. 3C). These patterns were consistent with tight regulation of nitrogen pathways by AHLs (DeAngelis et al. 2008, Gao et al. 2019), suggesting that nitrogen fluxes are central factors in biofilms and potentially involve eavesdropping (Gao et al. 2015). Particular upregulation of genes for the turnover of nitrite to nitrous oxide and hence incomplete denitrification was induced by own 3OH-C10, foreign C14:1-HSL, TDA and DNA (Fig. 3C). Differential regulation of this gene cluster may indicate facultative anaerobic traits as in the closely related *P. inhibens* T5 (Dogs et al. 2013), despite missing nitrous oxide reductase, influence detoxification strategies (Thole et al. 2012, Trautwein et al. 2016) and taxis to denitrification intermediates (Bartnikas et al. 2002) or mediate interkingdom interactions considering the role of nitrous oxide as eukaryotic infochemical (Wang et al. 2011).

Ecological conclusions – indication of complex chemical crosstalk

The shown complex responses of surface-associated *Rhodobacteraceae* towards biofilm-related compounds, indicate dynamic chemical processes prior to the formation of marine biofilms, mediated through different AHLs, antibiotics as well as DNA. The combination of chemotactic and regulatory effects by AHLs, TDA and DNA provide first insights into the complexity and interdependencies of chemical processes that influence biological interactions. Sensing of own and eavesdropping on foreign metabolites can be conceived as mediators of population-wide dynamics, with specific attracting or repelling effects, influencing biofilm formation but also regulating density-dependent actions on transcriptome level. The finding that different environmental compounds are mediators of specific gene regulation, advises subsequent studies to elucidate the complexity of chemical ecology in marine biofilms.

Acknowledgements

We thank Claire Ellebrandt, Pascal Bartling and Jörn Petersen (DSMZ Braunschweig) and Heide Schulz-Vogt (IOW Warnemünde) for providing the chemotaxis deficient mutant (*cheA::Tn5*; Tm400) and *Pseudovibrio* sp. FO-BEG1, respectively. This work was supported by German Research Foundation (DFG) through the Transregional Collaborative Research Centre 'Roseobacter' (TRR 51) and grant WI3888/1-2 (to MW).

Figures and Tables

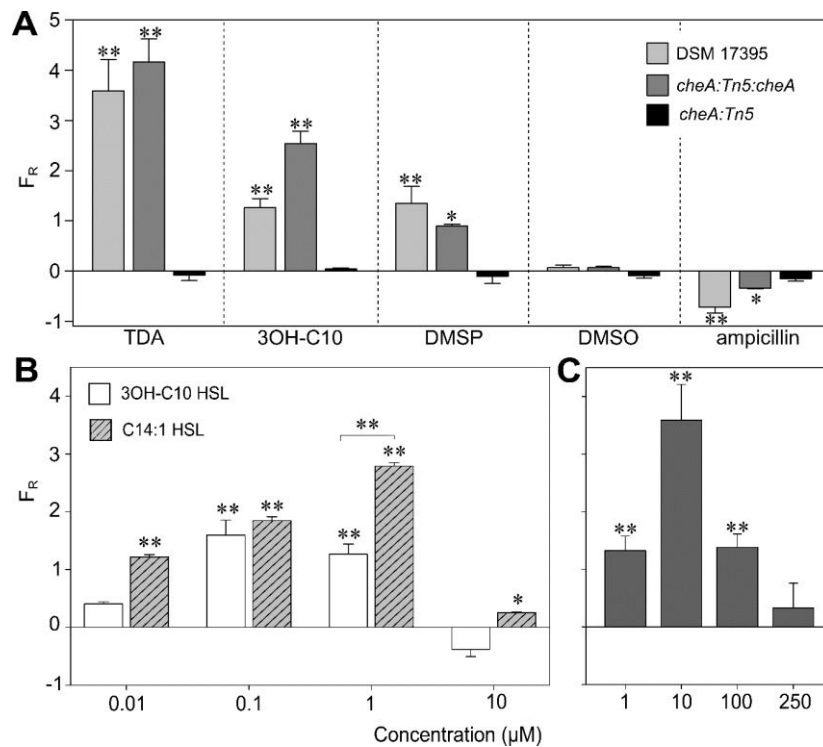


Fig. 1: Chemotactic response of DSM 17395 to different substances in comparison to a chemotaxis-negative mutant (*cheA::Tn5*) and the genetically complemented strain (*cheA::Tn5::cheA*). (A) Chemotactic response of DSM 17395 wildtype (grey), the chemotaxis-deficient mutant (black) and the complemented mutant with restored wildtype phenotype (dark grey). Tested concentrations were 10 μM TDA, 1 μM 3OH-C10 AHL, 500 μM DMSP (positive control), 14 mM DMSO (solvent control) and 270 μM ampicillin (repellent control). (B) Concentration-dependent chemotactic response of wildtype DSM 17395 to own 3OH-C10-HSL (white) and foreign C14:1-HSL (grey, shaded). (C) Concentration-dependent chemotactic response to TDA. F_R : response factor; * $P < 0.05$, ** $P < 0.01$.

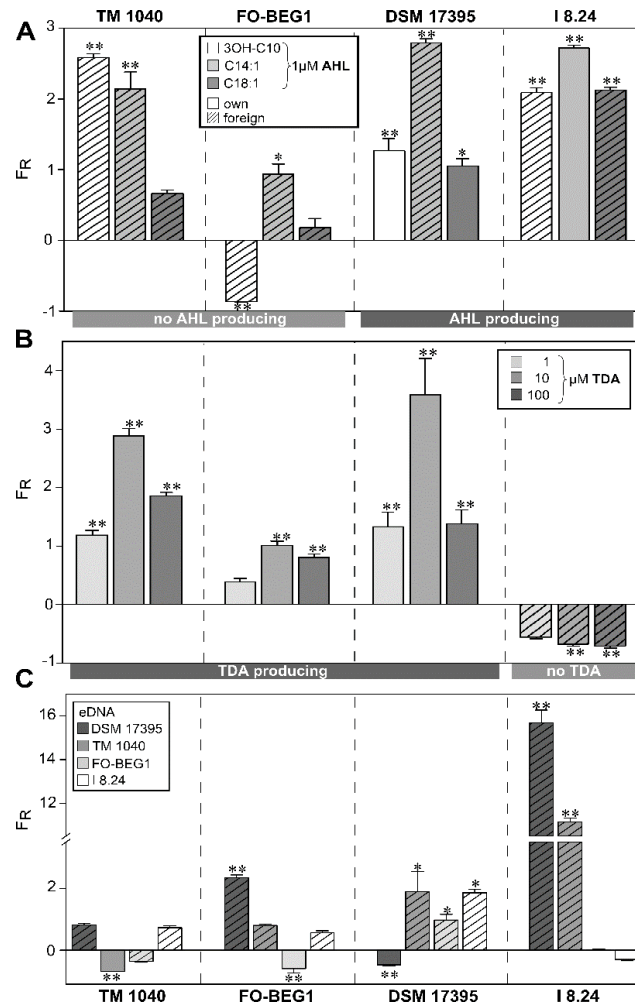


Fig. 2: Chemotactic response of surface-attached *Rhodobacteraceae* (*Ruegeria* sp. TM1040, *Pseudovibrio* sp. FO-BEG1, *Phaeobacter inhibens* DSM 17395, *Loktanella* sp. I 8.24) with different biosynthetic potentials towards AHLs (A), TDA (B) and DNA (C). (A) Responses towards 1 μ M of own (empty) and foreign (hatched) AHLs. (B) Responses to TDA (1, 10 and 100 μ M) in TD-producing (empty) and non-producing (hatched) bacteria. (C) Responses towards own DNA (empty) and foreign (hatched) DNA. FR: response factor, * $P < 0.05$, ** $P < 0.01$.

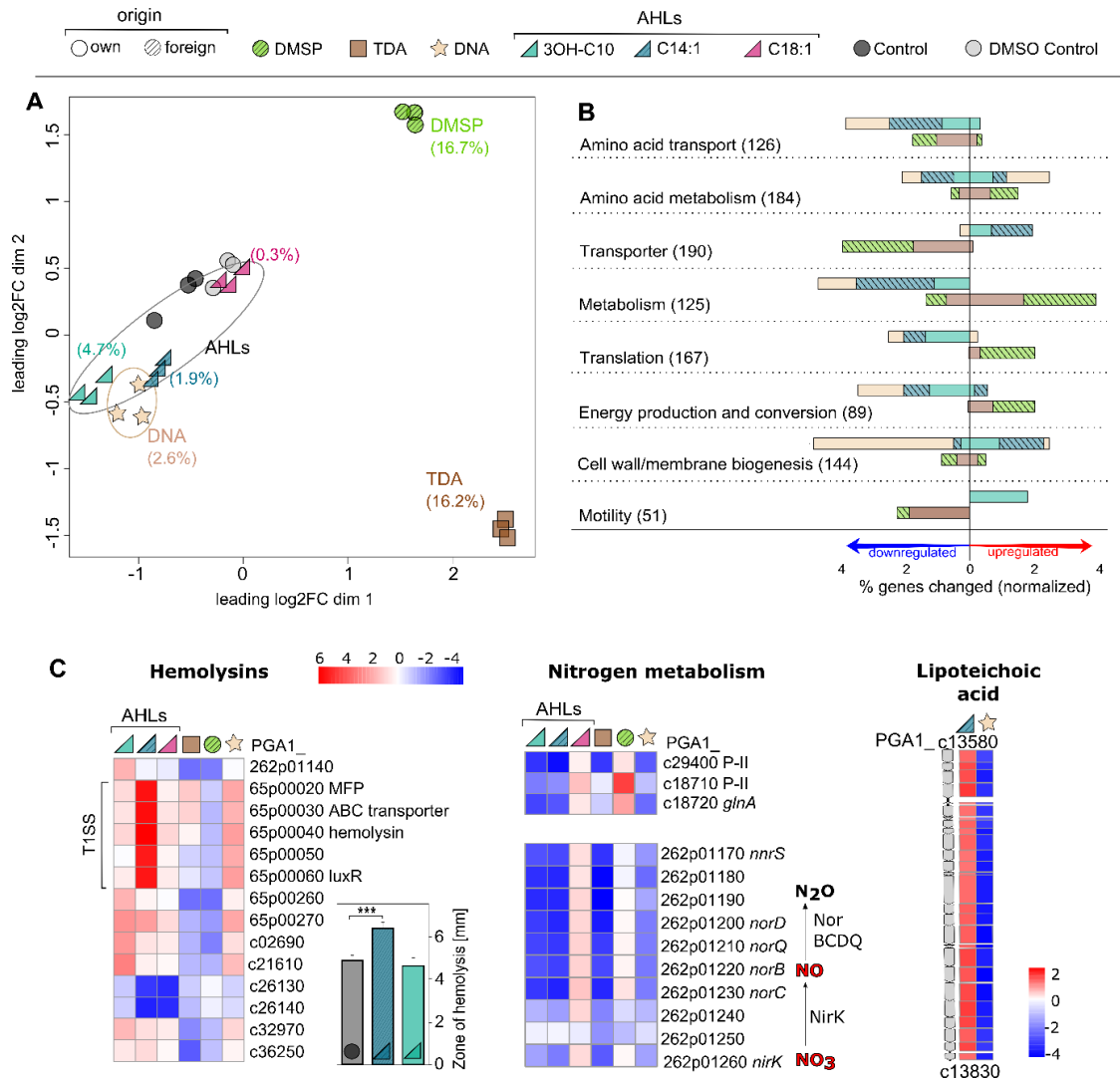


Fig. 3: Transcriptomic responses of *Phaeobacter inhibens* DSM 17395 to own (empty) and foreign (hatched) AHLs, TDA and DNA in relation to the chemotaxis control DMSP. (A) Multidimensional scaling demonstrates variances between transcriptomic data ($n = 3$); Values indicate percent fraction of differentially expressed genes ($\log_2\text{-FC} > 2$) upon substance addition (triangle: AHLs, rectangle: TDA, dot: controls, star: DNA). (B) Major transcriptional changes among different COG categories. Values indicate percent change in relation to total numbers of differentially expressed genes per substance and COG category (in parentheses), comparing effects with TDA and DMSP vs. AHLs and DNA using stacked bars. (C) Differential gene expression ($\log_2\text{-FC} > 2$) of genes encoding hemolysins (upregulation of a type-I secretion system encoded hemolysin with C14:1-HSL is supported by enhanced *in vitro* β -hemolysis; right insert; *** $P < 0.001$), nitrogen metabolism, and lipoteichoic acid.

Table 1: Absolute numbers and relative fractions of differentially expressed genes in *Phaeobacter inhibens* DSM 17395 in presence of own and foreign compounds.

	TDA	DMSP	AHLs			DNA
			3OH-C10	C14:1	C18:1	
Absolute changed genes	629	648	183	73	10	101
Relative changed genes (%)	16.2	16.7	4.7	1.9	0.3	2.6
Upregulated (%)	47	60	62	37	67	35
Downregulated (%)	53	40	38	63	33	65

Manuscript 4

Different AHL-based quorum sensing systems in *Phaeobacter inhibens* T5^T regulate distinct traits for association or horizontal gene transfer

Laura Wolter¹, Lisa Ziesche², Martine Berger¹, Anja Poehlein³, Stefan Schulz², Thorsten Brinkhoff^{1*}

¹ Institute for Chemistry and Biology of the Marine Environment, University of Oldenburg, Germany

² Institute of Organic Chemistry, University of Braunschweig, Germany

³ Genomic and Applied Microbiology and Göttingen Genomics Laboratory, Institute of Microbiology and Genetics, University of Göttingen, Germany

* corresponding author

T. Brinkhoff, Institute for Chemistry and Biology of the Marine Environment (ICBM), University of Oldenburg, PO Box 2503, D-26111 Oldenburg, Germany

Email: t.brinkhoff@icbm.de; phone: +49-(0)441-798-3269; fax: +49-(0)441-798-3438

Contribution of Wolter L. A.: Concept of the study, preparation of-original draft, mutant construction, total RNA isolation and analysis of genome and transcriptome data, gene comparison analysis, physiological experiments, data evaluation.

Abstract

Bacteria of the *Roseobacter* group are ubiquitous in the marine environment, which is attributed to a versatile lifestyle and frequent horizontal gene transfer. Bacteria of the genus *Phaeobacter* are model organisms of the *Roseobacter* group due to associations to various higher organisms, connected with production of *N*-acyl-homoserine lactones (AHLs) for quorum sensing (QS) and the antibiotic and signaling compound tropodithietic acid (TDA). Here, we report an in-depth analysis of QS circuits in *Phaeobacter inhibens* T5 with implications for surface colonization and strain divergence. We detected four QS systems in *P. inhibens* T5^T and generated AHL synthase-deficient strains by site-directed mutagenesis for three of the QS systems. GC-MS analysis enabled to assign the different synthase genes to the different AHLs produced by strain T5. Transcriptomic analysis showed distinct effects on gene regulation after QS disruption, with the major AHL being 3OH-C10-HSL, regulating 12% of genes in strain T5, comparable to a closely related strain. The low regulatory effects of the second major AHL, C18:1-HSL with no distinct pattern, questioned the ecological significance of this AHL. The regulation of genes of a bacteriophage by the newly described C12:2 indicates transfer of single QS systems, underlining the ecological and evolutionary implications of AHL production and the exchange of such systems across genus boundaries.

Introduction

Bacteria of the *Roseobacter* group (*Alphaproteobacteria*) are ubiquitously distributed in the marine environment and reach abundances of up to 23% of bacterial communities associated to macroalgal surfaces (Dogs et al. 2017). This abundance is attributed to a versatile heterotrophic metabolism and utilization of diverse substrates, the potential for mutual host interaction, and ability to produce secondary metabolites (Brinkhoff et al. 2008, Luo et al. 2014). These adaptations are enhanced by frequent horizontal gene transfer, corroborated by a patchy distribution of adaptive traits in *Roseobacter* genomes (Newton et al. 2010). The high genome plasticity of roseobacters is supported by a considerable number of mobile genetic elements such as plasmids and chromids, which constitute up to one third of the genome (Petersen et al. 2013). In addition, the commonness of prophages and gene transfer agents (GTAs) enable the transfer of distinct genetic material between roseobacters (Tomasch et al. 2018). This flexible genomic repertoire also facilitates colonization of surfaces, one important niche of many roseobacters (Frank et al. 2015).

The genus *Phaeobacter* is an important model organism of the *Roseobacter* group to study genome plasticity and surface colonization, attaching tightly to biotic or abiotic surfaces and invading established biofilms (Rao et al. 2006) via genes encoded on a “biofilm-plasmid” (Frank et al. 2015). These abilities are potentially facilitated by the production of the antimicrobial tropodithietic acid (TDA)

(Rao et al. 2006) and pronounced regulatory mechanisms, including bacterial communication using *N*-acyl-homoserine lactones (AHLs) (Slightom et al. 2009). AHL-mediated quorum sensing (QS) is widespread in *Roseobacter* spp. and genomes harbor varying numbers of AHL synthase or regulator genes (Cude et al. 2013). Some members only encode sole regulators, enabling them to eavesdrop on foreign QS molecules and hence respond to the activity of other bacterial taxa (Case et al. 2008, Cude et al. 2013). AHL-mediated functions in *Phaeobacter* include the regulation of motility or production of exopolymeric substances facilitating surface attachment (Beyersmann et al. 2017), and the production of TDA (Berger et al. 2011). Furthermore, QS influences genomic plasticity by modulating the expression of GTAs or inducing prophages (Schaefer et al. 2002, Ghosh et al. 2009, Silpe et al. 2019).

Prior analyses in *Dinoroseobacter shibae* have shown that expression of AHLs relies on the signal produced by one master AHL synthase influencing a heterogenic morphology, while in *P. inhibens* DSM 17395, *N*-3-hydroxydecanoyl homoserine lactone (3OH-C10-HSL) regulates TDA production (Berger et al. 2011). However, more detailed studies addressing different QS systems in *Phaeobacter* spp. are missing to date. For instance, the *Phaeobacter inhibens* type strain T5^T was described to harbor three synthase genes (Dogs et al. 2013) and produce six different AHLs (Ziesche et al. 2018) while the associated regulatory effects remain unknown to date, motivating a detailed study on the AHL-based regulations in this strain. Here, we report a complete inventory of encoded QS circuits, analyzed the produced AHLs via site-directed insertion mutants and GC-MS, and elucidated functional roles and regulatory effects by transcriptome analysis. Although there are several studies on QS-systems of roseobacters (Patzelt et al. 2013, Hudson et al. 2018) and genomic potential and relatedness of QS circuits encoded in *Roseobacter* genomes (Case et al. 2008, Cude et al. 2013), this study provides a first comprehensive overview of AHL-based QS systems among closely related roseobacters with implications for adaptation and concerted communication in natural habitats.

Materials and Methods

Bacterial strains and growth conditions

For this study we used *Phaeobacter inhibens* T5 (DSM 16374) and constructed three mutants of strain T5 each lacking one of the *phinI* genes encoding the AHL-synthase genes of T5 (see below). All strains were routinely grown aerobically at 28°C and 100 rpm in liquid or on solid media based on marine broth (MB), modified after Difco 2216 [(L⁻¹): 12.6 g MgCl₂*6H₂O and 2.38 g CaCl₂*2H₂O used instead of 8.8 g and 1.8 g, respectively and for trace element solution (L-1): 7 mg Na-Silicat*5 H₂O and 21.2 mg boric acid added compared to 4 and 2.2 mg, respectively].

Genome analyses

Comparative genomics to identify homologies of the AHL synthases was performed with finished genomes of *Phaeobacter inhibens* DSM 17395 (GCA_000154765.2), *Phaeobacter inhibens* 2.10 (GCA_000154745.2), *Phaeobacter inhibens* T5^T (GCA_000473105.1) and *Leisingera methylohalidivorans* MB2 (GCA_000511355.1) and the permanent draft genome of *Leisingera caerulea* DSM 24564 (GCA_000473325.1). Genomic islands were predicted using Island Viewer v4 (Bertelli et al. 2017) and gene transfer agents (GTAs) as well as prophages using PHASTER (Arndt et al. 2016). Homologies of single genes or gene clusters were analyzed using Geneious v11.0.2 (Biomatters Ltd., Auckland, New Zealand).

Site-directed mutagenesis of AHL synthase genes

We constructed three AHL-synthase-deficient mutants of strain T5, i.e. *phin1::Km*, *phin3::Km* and *phin2::Gm* insertion mutants. Therefore, the AHL synthase genes including 1.5 kb flanking regions were amplified from chromosomal DNA of the *P. inhibens* T5 wild type via PCR using the respective primer pairs (*phin1-3* f and r; Table S4) with blunt ends by Phusion polymerase (Thermo Fisher Scientific, Waltham, MA). The resulting PCR product was ligated into EcoICRI-digested pEX18Ap to yield pEX18Ap *phin1-3*. Ligation was performed according to (Legerski et al. 1985). The kanamycin and gentamicin resistance cassettes were amplified with specific primer pairs including a restriction site generating overlapping ends for further cloning (Table S4) from pBBR1MCS-2 and pBBR1MCS-5 respectively (Table S3). For *phin1::Km* construction, pEX18Ap *phin1* and amplified kanamycin resistance cassette were cut with BspEI, resulting in a disrupted *phin1* gene, purified and ligated together resulting in pEX18Ap *phin1* Km. Accordingly, for the other mutants, the resistance cassettes were amplified and cut with the primers and restriction enzymes specified in Table S4, resulting in pEX18Ap *phin2* Gm and pEX18Ap *phin3* Km. Cloning steps were performed in *E. coli* DH5 α or ST18 and conjugation of *P. inhibens* wild type cells with *E. coli* ST18 incorporating the final cloning plasmids was performed (Supplementary material). Evaluation of successful disruption of the AHL synthase gene was confirmed by PCR with primers (Test *phin1-3* f and r) binding within the genome sequence of wild type *P. inhibens* T5 next to the cloning site and subsequent sequencing at GATC (now Eurofins, Ebersberg, Germany).

Chemical analysis of AHL production

Bacterial cultures were grown in 100 mL MB for five days at 28°C and 160 rpm containing 2 g Amberlite XAD-16 resin (precleaned using Soxhlet extraction with acetonitrile, methanol and diethyl ether). The adsorbent was separated from the culture by filtration and extracted three times with CH₂Cl₂/H₂O (10:1) (Neumann et al. 2013). The combined organic phases were dried with MgSO₄, and the solvent was removed under reduced pressure. The extract was dissolved in CH₂Cl₂ (50 μ L) and

analyzed by GC/MS on a GC 7890A gas chromatograph connected to a 5975C mass-selective detector (Agilent) fitted with a HP-5 MS fused-silica capillary column (30 m x 0.25 mm i.d., 0.22 μ m film; Hewlett-Packard). Conditions were as follows: carrier gas (He): 1.2 mL min⁻¹; injection volume: 1 mL; injector: 250 °C; transfer line: 300 °C, EI 70 eV. The gas chromatograph was programmed as follows: 50 °C (5 min isothermal), increasing with 5 °C min⁻¹ to 320 °C, and operated in splitless mode. Gas chromatographic retention indices, *I*, were determined from a homologous series of *n*-alkanes.

Transcriptomic analysis

Transcriptomic analysis was performed for *phin1::Km*, *phin3::Km* and *phin2::Gm* compared to the wildtype. Therefore, bacterial cultures of 20 ml were grown in MB as specified above (n = 3), pelleted by centrifugation (10 min, 6,000 x g, 4°C), followed by RNA isolation and sequencing, performed at the Göttingen Genomics Lab (Supplementary Methods). Genes with absolute log₂-fold change > 1, a likelihood value of ≥ 0.9 , and an adjusted *P* value of ≤ 0.05 were considered differentially expressed.

Data availability

Supplementary materials for this Manuscript can be accessed from the CD enclosed in the printed version or the attached supplementary files of the electronic version.

Results and discussion

Genome mining revealed four complete QS systems (*luxIR* pairs) encoded in the genome of *P. inhibens* T5 that share < 31% amino acid sequence identity among each other (Fig. 1A), expanding previous insight into the strain's considerable potential for chemical communication (Dogs et al. 2013). Interestingly, two of these systems are encoded in genomic islands (GIs) including prophages (Fig. 2). The four QS systems and the respective AHL synthase genes are herein referred to as I-IV and *phin1*-4, respectively, to underline their origin from *Phaeobacter inhibens* and to distinguish them from *pgaI* genes of the closely related *P. inhibens* DSM 17395 (87% genome-to-genome relatedness) (Table 1).

We identified homologs of the four AHL synthases of *P. inhibens* T5^T in other roseobacters, showing that the two GI-encoded synthases *phin3* and *phin4* share 62 and 76% amino acid identity to *Leisingera*-related synthases, while the other two are almost identical ($\geq 98.5\%$) to synthases encoded in other *P. inhibens* strains (Table 1). Chemical analysis showed that strain T5 produces six AHLs: 3OH-C10, C18:1, C12:2, C16:1, 3-oxo-C10 and C16-HSL (in decreasing concentration detected), and the discrepancy between synthase count and AHL diversity may reflect unspecific action of AHL synthases dependent on ambient precursor molecules corresponding with recent evidence for unspecific production of recombinant *pgaI2* from DSM 17395 in feeding experiments with various fatty acid precursors (Ziesche et al. 2018). Elevated concentration of 3OH-C10-HSL underlines its importance for *P. inhibens*, including DSM 17395, T5^T and 2.10 (Ziesche et al. 2018). The C12:2-HSL

was only recently described in different surface-associated *Roseobacters* (Ziesche et al. 2018), suggesting a functional role in biofilm settings. To gain further insights into the potential regulatory and ecological roles of the different AHLs and to match produced AHLs to the corresponding synthases, we constructed AHL synthase-deficient mutants through site-directed mutagenesis of synthase genes *phin1-3*. Furthermore, we chemically quantified the produced AHLs, and analyzed the effects of lacking AHL production on transcriptomic level. A mutant for *phin4* could not be derived despite careful attempts, potentially relating to its localization within a genomic island. Nonetheless, fundamental insights into linkages between AHL production and gene regulation could still be derived from the three mutants tested (see below).

AHL analysis and assignment to synthase genes

The AHLs produced by the *phin1-3* insertion mutants were chemically determined via GC-MS, demonstrating lack of 3OH-C10, C18:1 and C12:2-HSL in *phin1::Km*, *phin2::Gm* and *phin3::Km*, respectively. Hence, we could reliably assign the three major AHLs 3OH-C10, C18:1 and C12:2 (37; 27 and 16% respectively of all produced AHLs) to their corresponding synthases. Hence, C16:1 HSL might derive from *phin4*, although this needs further investigation.

The production of 3OH-C10-HSL by *phin1* is consistent with 100% protein sequence identity of *phin1* and *pga1* in DSM 17395 (Table 1), known to result in production of this AHL (Berger et al. 2011). Production of C18:1 by *phin2* is consistent with 98.5% amino acid sequence identity to *pga2* in *P. inhibens* DSM 17395 (Cude et al. 2013) that was confirmed to produce long-chain AHLs as well (Ziesche et al. 2018). Lack of production of C12:2 in *phin3::Km* corresponds to 76% amino acid identity to an AHL synthase of *L. caerulea* (PhacaeDRAFT_0324), particularly producing C12 carbon chain AHLs (Ziesche, personal communication). *Leisingera* and *Phaeobacter* are closely related genera and lately several *Phaeobacter* spp. were transferred to the genus *Leisingera* (Breider et al. 2014) and both genera share a high degree of genetic material. Finally, potential production of C16 carbon chain AHLs by *phin4* is consistent with 94% amino acid sequence identity to a synthase in *P. inhibens* 2.10 (Table 1), that produces C16:1-HSL with a relative amount of 13% compared to 10% in strain T5, whereas in 17395 not encoding a related synthase only 3% were measured most likely through unspecific production (Ziesche et al. 2018).

Of specific interest was the detection of two QS systems, *phinIR3* and *phinIR4* within genomic islands (GIs) containing intact prophages (Fig. 2, Table 2). As mentioned above, the encoded *phinIR3* system has orthologs in a genomic island region of *L. caerulea* DSM 24564, however, the adjacent prophage does not share a high synteny to *L. caerulea* but to a prophage of DSM 17395 (70% nucleotide identity) without adjacent QS system (Fig. 2). This suggests that either the prophage integrated in both species independently into this “hot spot” of genetic transfer after the *luxIR* homolog had integrated into

the T5 genome, or that the *luxIR* homolog of *Leisingera* was inserted into the present prophage in the T5 genome sequence, corresponding to mobile QS systems detected in *Serratia* spp. (Wei et al. 2006). Whatever scenario might have happened, the different arrangement of genes underlines genetic plasticity in such hot spots (Juhas et al. 2009) and the exchange of *luxIR* type regulators by horizontal gene transfer (Gray et al. 2001). In this context, the *phinIR4* system has high nucleotide identity (94%) to a QS system of *P. inhibens* 2.10, although no prophage is present in the latter, while the prophage has 47% nucleotide sequence identity to a GI in *L. methylhalidivorans*, although encoded *luxIR* homologs are less related (61.5%) (Fig. 2, Table 1 and 2). The exchange of communication systems with potential influence on eukaryotic or prokaryotic interactions might be especially important for roseobacters as their broad and abundant distribution has been linked to their potential for genetic exchange (Newton et al. 2010).

Functional investigation of AHLs

First linkages between AHLs and the phenotype of T5 were established by physiological comparison of the mutants and wild type, showing a less dark brown coloration of *phin1::Km* related to threefold less pigmentation (OD₃₉₈) and fourfold lower TDA production (Fig. 3A and B). Hence, 3OH-C10-HSL possibly has a similar function on TDA regulation as in DSM 17395 (Berger et al. 2011) or even in *Phaeobacter* as a whole, considering generally high production of 3OH-C10-HSL in this genus (Ziesche et al. 2018). On the contrary, *phin2::Gm* and *phin3::Km* showed no obvious difference in growth, or TDA production, however, enhanced pigmentation was observed for *phin2* (Fig. 3B).

For a deeper insight into the regulatory effects of the described AHLs and potential ecological implications, we analyzed the transcriptomes of *phin1-3* mutants compared to the wild type. Overall, 14% of protein-coding genes were differentially expressed in the mutant transcriptomes, with specific responses in each mutant (Fig. 4A) and only a low overlap of regulated genes (Fig. 4B). The 40 genes that were shared differentially expressed in *phin1::Km* and *phin2::Gm* transcriptomes, assigned as flagella, transporter or hypothetical genes, showed the same regulation pattern (Table S1), indicating some overlap in regulated traits by these two widely present AHLs. Regulated genes in *phin1::Km* account for three quarter of all differentially expressed genes (12.5% of all genes), while *phin2::Gm* and *phin3::Km* had an influence on 15 and 10% (both 2% of all genes) respectively (Fig 4A), with specific responses (Fig. 4C).

Assignment of differentially expressed genes to Clusters of Orthologous Groups (COG) showed that the majority of genes differentially upregulated by *phin1::Km* are involved in cell motility and chemotaxis, amino acid transport and metabolism as well as cell wall, membrane and envelope biogenesis (Figure 5A). Notable was also the upregulation of genes relating to a high metabolic status of *phin1::Km* including genes for energy production and conversion, translation and ribosomal proteins

as well as signal transduction mechanisms, suggesting that metabolic functions are downregulated once a quorum is reached. This is corresponding to the common stableness of biofilms including maintenance metabolism (Flemming et al. 2016). In contrast, genes from COG categories for translation and ribosomal structure were downregulated in *phin2::Gm*, suggesting an upregulation of biosynthesis-related genes upon sensing of this AHL, however overall a low impact of C18:1 on the transcriptome of strain T5 was observed under the tested conditions (Fig. 4A, Fig. S1). Notable in this context is also that for differentially regulated genes a threshold of log₂-fold change > 1 was analyzed, as the generally assumed fold change of 2, revealed only 3 differentially expressed genes in *phin2::Gm* (Table S2), however, differentially regulated genes for the other two mutants were more pronounced (Fig. 4A). A specific regulation pattern was determined for *phin3* as most downregulated genes in its transcriptome (Fig. 4C) are specifically related to prophages and transposons (>8% of all genes) (Fig. 5A). This includes the whole gene cluster assigned to the predicted prophage surrounding *phinR3* (Table 2, Fig. 2) and suggests that the newly discovered C12:2-HSL, regulates expression of the whole GI including the intact prophage 1 as further discussed below.

Analysis of the expression of single *phinI* and *phinR* genes in the wildtype demonstrated *phinR1* to be highest expressed, followed by *phin2* (Fig. 1B), corresponding to the detected ratios of the produced 3OH-C10 and C18:1-HSLs. Notably the *phin2* associated regulator *phinR2* was fivefold lower expressed than the synthase, which might be an explanation for the overall low difference of regulated genes in *phin2::Gm* and suggest that activation of this regulator might require additional traits, e.g. elevated water temperatures (Gardiner et al. 2017, Hudson et al. 2018).

C12:2 potentially induces prophage expression

The specific downregulation of genes assigned to prophage 1 surrounding *phinR3* (Table 2, Fig. 2) suggests that production of C12:2-HSL regulates the expression of the whole GI including induction of the predicted prophage 1, a phenomenon described for soil and groundwater bacteria (Ghosh et al. 2009). Comparable effects were shown for *Vibrio cholerae* autoinducers that are sensed by a phage-encoded regulator, illustrating tight interconnections in the decision between lysis and lysogeny (Silpe et al. 2019). Gene sequences associated with prophages are one major driver of horizontal gene transfer (HGT) and the induction of prophage gene expression by AHLs might contribute to species differentiation and evolution with potential implications for habitat adaptations (Antonova et al. 2011) and bacterial diversity (Paul 2008), and especially roseobacters were suggested to have acquired a high amount of ecologically relevant genes by HGT (Newton et al. 2010).

Gene regulation by 3OH-C10-HSL in *P. inhibens* T5 compared to DSM 17395

Physiological changes of TDA production, motility and attachment

Corresponding to lower TDA production in *phin1::Km*, compared to the wild type (Fig. 3A and B), plasmid-encoded *paa* and *tda* genes involved in TDA production were downregulated (Table S1, Fig. 5B). Regulation of TDA production by AHL-based quorum sensing in T5 was consistent with that in the closely related strain DSM 17395 (Berger et al. 2011) and the commonly described QS-mediated production of antimicrobial compounds (Cude et al. 2013). These mechanisms probably balance costs and benefits of production, as high antibiotic concentrations of TDA imposes a high metabolic burden on the producing organism (Trautwein et al. 2016, Will et al. 2017).

However, the highest fraction of genes differentially upregulated by *phin1::Km* relate to cell motility, chemotaxis and cell wall/ membrane biogenesis (Fig. 5A). Hence, when a quorum is reached, motility and simultaneous biofilm formation are downregulated, supporting the previously suggested “swim-and-attach” lifestyle in *Phaeobacter* upon quorum sensing (Beyersmann et al. 2017). Most regulated genes for cell wall, membrane and envelope biogenesis are contained in a single 26 gene cluster, annotated to produce lipoteichoic acids (Phain_01352-01377, Table S1). Teichoic acids are typical cell wall constituents in Gram-positive bacteria (Neuhaus et al. 2003) to date only reported once in Gram-negative bacteria (Gorshkova et al. 2007) and unique in *Phaeobacter* compared to other *Roseobacter* genomes (Thole et al. 2012), potentially conferring resistance against antimicrobial peptides (Percy et al. 2014) or might be carriers for hemolysins (Tsaihong et al. 1983). Regulation of a homologous gene cluster in *P. inhibens* DSM 17395 upon addition of exogenous foreign AHL (Wolter et al. 2019; Manuscript 3) and the uniqueness of the cluster in genomes of *Phaeobacter* spp. indicate consistent functionality as important cell wall components with putative functions for biofilm formation and attachment.

Gene transfer and type I secretion system

Other differentially regulated features in strain T5 relate to gene or protein transfer. Absence of 3OH-C10-HSL upregulates a gene cluster assigned to a gene transfer agent (GTA), common in *Roseobacter* genomes (Luo et al. 2014). AHL-mediated regulation of GTAs corresponds to regulatory cascades in *Rhodobacter capsulatus* SB1003, however, in this strain increase of long-chain AHLs activate the production (Schaefer et al. 2002, Fogg 2019). In *P. inhibens* T5, expression of GTAs seems to be repressed by 3OH-C10-HSL (Table 1), while in another study with the closely related *P. inhibens* DSM 17395 (Wolter et al 2019, Manuscript 3), the GTA was expressed by exogenous addition of 3OH-C10-HSL similar to *R. capsulatus*. AHL-mediated regulation of GTAs in *Roseobacter* group bacteria might contribute to their genome plasticity and metabolic versatility. Another upregulated feature in *phin1::Km* relates to an RTX-like hemolysin with an adjacent type I secretion system (Fig. 5B),

potentially mediating excretion and cytotoxic functions as seen in different pathogens (Thomas et al. 2014). Further differential expression by AHL-based quorum sensing of manifold RTX-like hemolysin genes encoded in the T5 genome (Fig. 5B), stress these genes might have an important function in *Phaeobacter* spp., supported by abundance (60%) of an RTX-like hemolysin in the exoproteome of *P. inhibens* DSM 17395 (Durighello et al. 2014). Hence, expression of these genes by AHL-based QS (this study) or temperature-induced in the closely related macroalgal pathogen *P. italicus* R11 (Gardiner et al. 2017) suggest an important ecological function for *Phaeobacter* spp., potentially involved in direct capture of organic matter from eukaryotic cells through the RTX toxin pore (Moran et al. 2007).

Ecological implications of quorum sensing in P. inhibens T5

According high regulatory effects by the main 3OH-C10-HSL of both strains DSM 17395 and T5, indicate that respective QS system in these closely related strains share a high analogy (supported by 100% amino acid identity), corroborated by similarly regulated traits of motility and TDA production. However, the presence and AHL-mediated regulation of QS systems in GIs encoding predicted intact prophages only in strain T5 demonstrate also considerable difference in other quorum sensing systems. The connection of regulated traits to horizontal gene transfer indicate another level of genome dynamics among roseobacters, enabling closely related strains to horizontally acquire QS systems (Gray et al. 2001). Such features may be especially relevant in dense microbial biofilms, as exchanged genes have a high probability to encounter appropriate recipient cells (Westbye et al. 2017), amplifying the acquisition of beneficial genomic features (Newton et al. 2010). Hence, in dense mixed-species biofilms, harboring a wealth of closely related strains e.g. of *Phaeobacter* spp. (Gram et al. 2015), the induction of GTAs or prophages by AHLs might contribute to *Roseobacter* species differentiation and evolution, facilitating further habitat adaptations.

Acknowledgements

This work was supported by German Research Foundation (DFG) through the Transregional Collaborative Research Centre 'Roseobacter' (TRR 51)

Figures and Tables

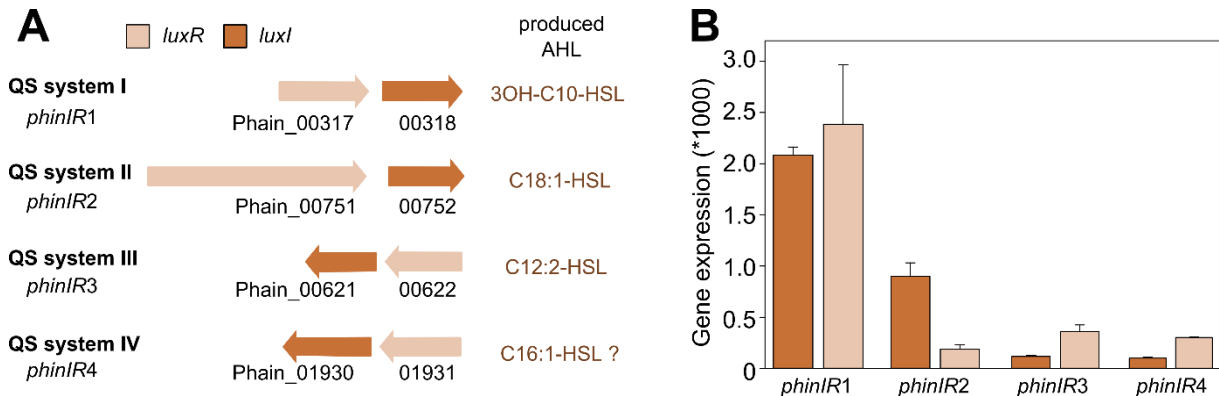


Fig. 1: QS systems in *P. inhibens* T5 with gene arrangement, produced AHLs as confirmed by GC-MS and expression data of the *luxIR* homologs, derived from transcriptomic analysis. For *phinIR4* produced AHL could not be determined chemically and it is only assumed to produce C16:1-HSL from exclusion analysis, specified by the question mark. The *luxIR* systems in *P. inhibens* T5 share < 31% protein sequence identity among each other.

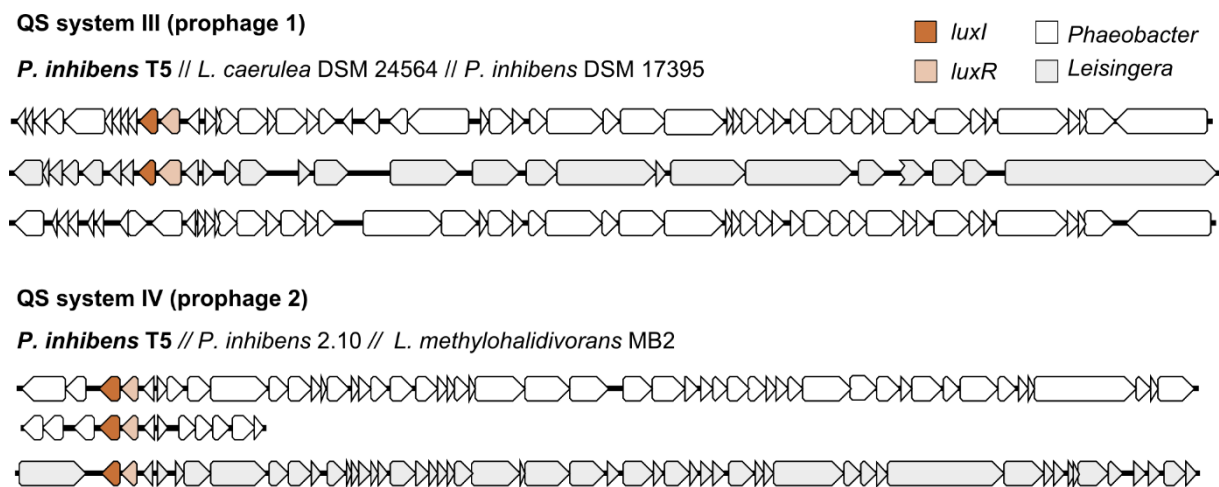


Fig. 2: Prophage regions including *luxIR* homologs (light brown = *luxR*, dark brown = *luxI*) of *P. inhibens* T5 with homologies (Table 1 and 2) to related *Phaeobacter* (white) and *Leisingera* strains (grey). Gene with serrated edge demonstrate an assembly gap in the permanent draft genome sequence of *L. caerulea* DSM 24564.

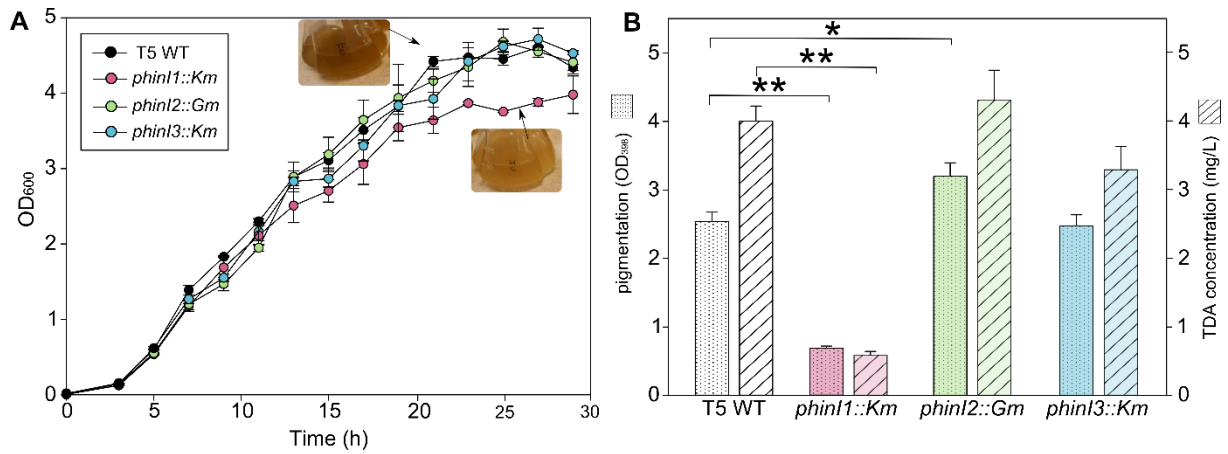


Fig. 3: Growth curves for T5 wild type and mutants as well as TDA production measured by pigmentation and chemical analysis in late exponential growth phase (20 h, OD₆₀₀ ~4). A: Growth curves of T5 wild type (black), *phin1::Km* (red), *phin2::Gm* (green) and *phin3::Km* (blue). B: pigmentation measured at OD₃₉₈ (dotted bars) and TDA concentrations (g/L) (shaded bars) measured for the strains. * $P < 0.05$, ** $P < 0.01$.

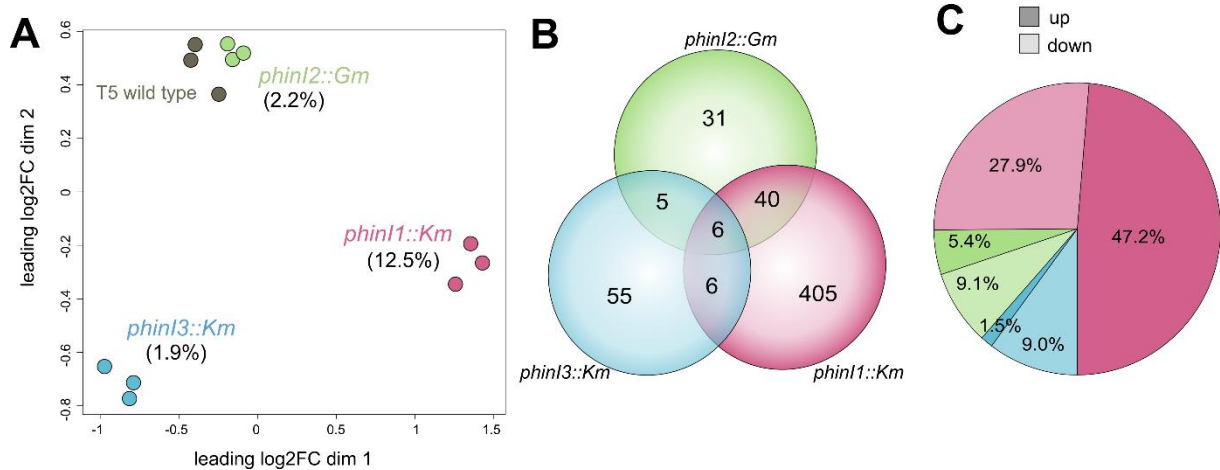


Fig. 4: Transcriptomic responses of *P. inhibens* T5 in comparison to the mutants *phin1::Km* (red), *phin2::Gm* (green) and *phin3::Km* (blue). A: Multidimensional scaling showing variances between transcriptomic data ($n = 3$). Values indicate percent fraction of differentially expressed genes in the mutants ($\log_2\text{-FC} > 1$). B: VENN diagram of differentially expressed genes unique or shared regulated in the corresponding mutant strains. C: Fraction of differentially up-(dark colors) or downregulated (bright colors) genes, revealing different transcriptional patterns in response to lack of AHLs.

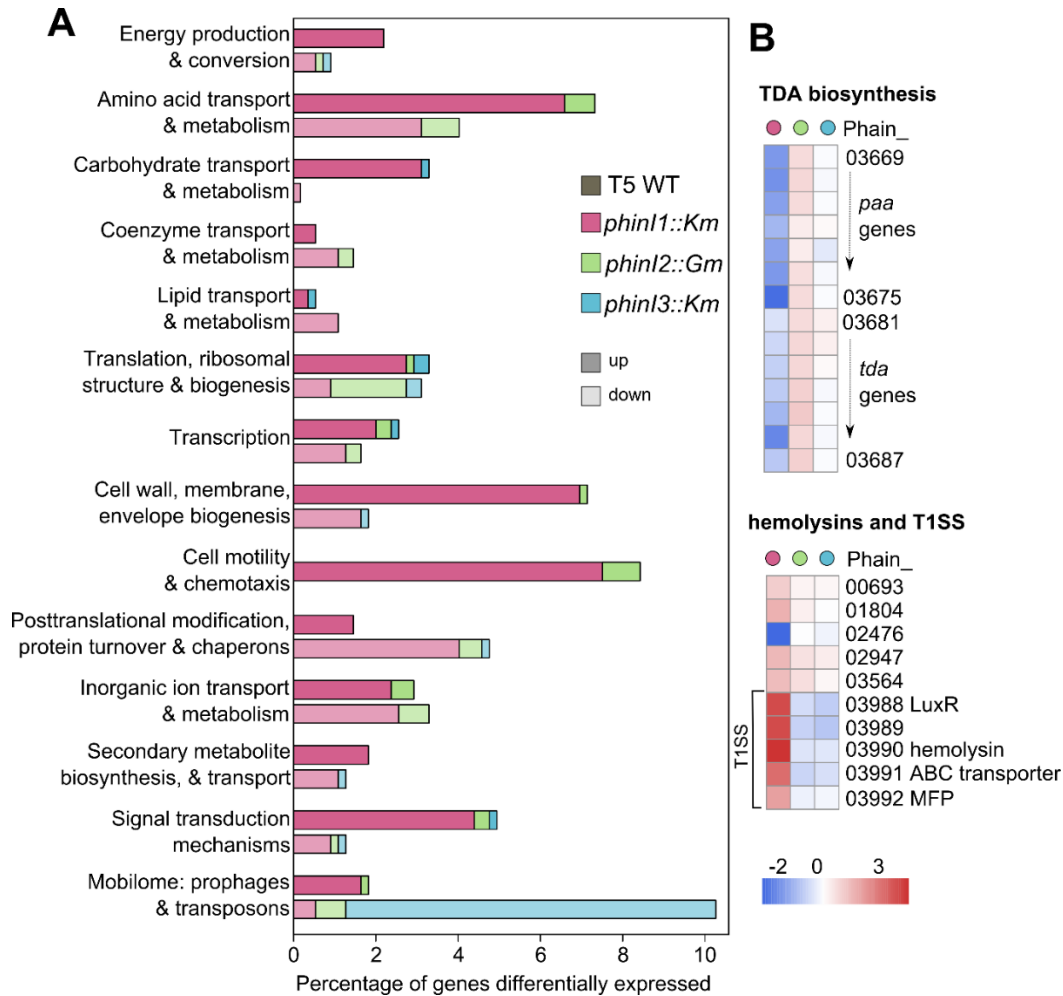


Fig. 5: Specific transcriptomic responses of *phin1::Km* (red), *phin2::Gm* (green) and *phin3::Km* (blue) in comparison to wild type cells. A: Major transcriptional changes among different Cluster of Orthologous Group (COG) categories, distinguishing up- (dark colors) and downregulated (light colors) features. Values are given as percentage of all differentially regulated genes in all mutant strains, comparing effects using stacked bars. B: Differential gene expression ($\log_2\text{-FC} > 1$) of genes encoding TDA biosynthesis, hemolysins and type-I secretion system.

Table 1: QS systems (QS S) I-IV of *P. inhibens* T5 with the closest homologs of *luxIR* genes in related strains of the *Phaeobacter - Leisingera* cluster (% BLASTp identity).

QS S	<i>luxIR</i> homolog	Locus tag (Phain_)	% ID	Strain	IMG Locus Tag	NCBI Locus Tag
I	<i>phinIR1</i>	00317/18	100	<i>P. inhibens</i> DSM 17395	PGA1_c03890/80	PGA1_RS01920/15
			99.5	<i>P. inhibens</i> 2.10	PGA2_c03440/30	PGA2_c03440/30
II	<i>phinIR2</i>	00751/52	99.5	<i>P. inhibens</i> 2.10	PGA2_c07460/50	PGA2_c07460/50
			98.5	<i>P. inhibens</i> DSM 17395	PGA1_c07680/70	PGA1_RS03815/10
III	<i>phinIR3</i>	00621/22	76.0	<i>L. caerulea</i> DSM 24564	PhacaeDRAFT_0324/23	CAER_RS28505/_RS0124580
IV	<i>phinIR4</i>	01930/31	94.0	<i>P. inhibens</i> 2.10	PGA2_c18960/70	PGA2_c18960/70
			61.5	<i>L. methylohalidivorans</i> DSM 14336	Leime_2648/49	METH_RS10640/45

Table 2: Predicted genomic islands containing prophage genes within the *Phaeobacter-Leisingera* cluster with homologs to the two *luxIR* systems *phinIR3* and *phinIR4* of *P. inhibens* T5. Gene designations in bold correspond to a related QS gene cluster encoded in the genomic island. * no analysis of the phage region is possible due to the incomplete sequence information. Locus tags relate to the genome sequence stored in IMG.

Strains	Locus tag start	Locus tag end	Specific encoded genes
<i>P. inhibens</i> T5	Phain_00617	Phain_00663	<i>luxIR (III)</i> ; complete prophage 1 (Phain_00629 - 663)
<i>L. caerulea</i> DSM 24564	PhacaeDRAFT_0307	PhacaeDRAFT_0334	<i>luxIR (III)</i> ; phage-related*
<i>P. inhibens</i> 17395	PGA1_c18060	PGA1_c18680	Prophage (PGA1_c18210 - 470)
<i>P. inhibens</i> T5	Phain_01886	Phain_01980	<i>luxIR (IV)</i> ; complete prophage 2 (Phain_01935 - 01978) Mu-like
<i>P. inhibens</i> 2.10	PGA2_c18780	PGA2_c19010	<i>luxIR (IV)</i> ; putrescine/spermidine transporter; transposase
<i>L. methylohalidivorans</i> MB2	Leime_2639	Leime_2693	<i>luxIR (IV)</i> ; complete prophage (Leime_2644 – 86), Mu-like

Discussion

Short summary of the results

In this thesis, roseobacters from surface-associated habitats in coastal environments were investigated for adaptations to hosts in tidal areas and the role of secondary metabolism for biological interactions and surface colonization. The study included a general assessment of adaptations to coastal habitats and specific association with macroalgae by analyzing a novel species isolated and genome-sequenced herein, *Pseudoceanicola algae* Lw-13e^T sp. nov. (Manuscript 1). Furthermore, it was investigated how related strains establish in macroalgae-associated microbiota, supported by molecular evidence that *Rhodobacteraceae* constitute a predominant part of bacterial communities on the brown alga *Fucus spiralis* (Manuscript 2). Manuscripts 3 and 4 show that this dominant occurrence is supported by secondary metabolism and the ability for chemotaxis and communication through quorum sensing (QS). First evidence was given that AHLs and other biofilm-associated compounds (TDA, eDNA) enabled chemical communication and exerted chemotactic effects, being influenced by whether compounds originated from members of the same or another species. Subsequent analysis of the gene regulatory effects of these molecules revealed the importance of chemical communication in mediating surface-association, metabolite turnover and genetic exchange with other species. Finally, the thesis contributed to three papers on the chemical diversity of secondary metabolites from surface-associated *Rhodobacteraceae* that further illustrate the molecular diversity behind chemical communication (Manuscripts 5-7), including hitherto unknown molecules.

Adaptations of a *Roseobacter* to surface-associated life includes mutual and detrimental traits

Metagenomic and physiological investigations of *Rhodobacteraceae*, including the *Roseobacter* group as their largest subgroup, revealed proficient colonization of various marine eukaryotes, including micro- and macroalgal surfaces (Wagner-Döbler et al. 2006, Brinkhoff et al. 2008). For instance, roseobacters can constitute up to 23% of the epibacterial communities on *Fucus* spp., brown algae with broad distribution on European and North American shores (Dogs et al. 2017). Specific bacterial members, even if low in abundance, can have major impacts on the interactions occurring in surface-associated communities (Rao et al. 2007), amplified by physiological habitat adaptations and presence of biological interactions encompassing commensalism, mutualism or parasitism (Egan et al. 2013). Such patterns, as found in *Pseudoceanicola algae* Lw-13e^T sp. nov. (Manuscript 1), may also explain the prevalence of the roseobacters *Sulfitobacter*, *Loktanella*, *Octadecabacter*, as well as the newly described Marine Host-associated *Rhodobacteraceae* (MHR) cluster in epibacterial communities of *Fucus spiralis* (Dogs et al. 2017/ Manuscript 2).

The investigation of *P. algae* Lw-13e^T provided detailed insights into such specific habitat adaptations. Lw-13e^T was isolated in summertime when macroalgae show their highest physiological activity (Egan et al. 1990), probably fostering intense interactions within bacterial biofilms. Unique features of Lw-13e^T that drive habitat and host adaptations and distinguish it from pelagic and sediment-associated *Pseudoceanicola* spp., elucidated by pangenome analyses, include high salt tolerance to counteract osmotic stress during tidal cycles as well as a broad tolerance of antibiotics and heavy metals, corresponding to previously shown adaptation strategies of bacteria from coastal environments with terrestrial input (Grammann et al. 2002, Zhang et al. 2012, Vignaroli et al. 2018). Demonstrated production of siderophores to access insoluble Fe³⁺ and vitamins for auxotrophic algae coincided with general processes observed in bacteria-algae interactions (Soria-Dengg et al. 2001, Croft et al. 2005, Dogs et al. 2017) (Manuscript 2). Detected production of volatiles including terpenes, which can provide membrane stabilization or confer feeding deterrence and defense against pathogens for the macroalgal host (Gershenson et al. 2007, Singh et al. 2014, Jerković et al. 2018), underlined mutual interactions of Lw-13e^T with algae. Further functions of volatiles in interspecies and interkingdom communication (Schulz-Bohm et al. 2017) and the potential of Lw-13e^T to produce AI-2, a frequent communication molecule of Gram-negative and -positive bacteria, underlined its potential to interact with surrounding bacteria and eukaryotes.

However, interactions also included potentially detrimental features, demonstrated by the degradation of oligomeric alginate by Lw-13e^T through a unique PL15 alginate lyase, which is noteworthy as roseobacters are generally not considered as polysaccharide degraders. Degradation of oligo- but not polymeric alginate of Lw-13e^T indicated that it may be a secondary consumer benefiting from hydrolytic strains cleaving algal polymers to oligomers and hence to constitute a “harvester” in mixed-species assemblages (Hehemann et al. 2016). The required previous action of primary consumers such as *Zobellia galactanivorans* of the phylum *Bacteroidetes* equipped with a broad diversity of different lyases for degradation of various polymeric compounds (Thomas et al. 2017, Zhu et al. 2017), suggests niche separation in *Fucus*-associated communities and might explain why Lw-13e^T was not among abundantly detected bacterial species on healthy algal surfaces. The detection of unique genes for hemolysin and entericidin toxin production as well as transporters known from terrestrial pathogens, indicates that Lw-13e^T may opportunistically harm the algal host under certain conditions. Additionally, it is likely that Lw-13e^T may be especially prevalent in settings where the algal host is damaged or decaying. Terrestrially known systems for instance include a potential heme/peptide permease or sialic acid transport, facilitating uptake of released compounds from decaying algae (Carter et al. 2002, Garai et al. 2017, North et al. 2018). The prevalent detection of homologs in terrestrial bacteria raise the intriguing possibility that Lw-13e^T might have acquired genes from terrestrial relatives through horizontal gene transfer (HGT) that equipped it with traits seldom detected for roseobacters,

such as observed oligomeric sugar degradation or the production of terpenes. This suggests a potential “genetic connectivity” between land and sea and moreover corresponds to the origin from a *Fucus* sp. as macroalgae are the marine equivalents of land plants and algae-associated bacteria may employ similar supportive features known from the rhizosphere (Philippot et al. 2013).

The demonstrated broad tolerance of Lw-13e^T against toxic compounds may mediate to withstand macroalgal defense systems like reactive oxygen species (Egan et al. 2014) but also bacterially produced antibiotic compounds such as tropodithietic acid (TDA), previously suggested to outcompete other bacteria in macroalgal assemblages (Rao et al. 2006). The tolerated concentration of Lw-13e^T was comparable to TDA-producing *Phaeobacter* spp. (Brinkhoff et al. 2004), and although tolerance cannot be explained at the moment as Lw-13e^T lacks the γ -glutamyl cycle for TDA tolerance (Wilson et al. 2016), this could be of special interest for further studies. The demonstrated adaptive traits enabled clear discrimination of Lw-13e^T from other relatives of the same genus isolated from pelagic waters and sediments. The study also highlights the importance of pangenome analysis to identify strain-specific adaptations, as only the analysis of multiple genomes from related strains can illustrate specific acquisition of additional gene cassettes by HGT. By analyzing a single bacterial species, the thesis hence highlighted the overall importance of secondary metabolites and other adaptive traits for roseobacters.

It needs to be noted, though, that biofilm communities harbor a wealth of different species with varying potentials for secondary metabolism and communication. A second focus of this thesis was therefore potential crosstalk in surface-associated communities by analyzing effects of own and foreign secondary metabolites on selected *Rhodobacteraceae* with potential implications on surface colonization.

Chemotaxis and chemical crosstalk in surface-associated bacteria

Biofilms are complex microhabitats harboring diverse bacterial members and chemical processes. Biological and chemical interactions influence communication and bacterial phenotypes, and surface colonization is likely facilitated by the ability to recognize favorable attachment sites. Such traits are found in several roseobacters, and we herein investigated specific responses to chemical signals. Chemotactic movement towards AHLs, TDA and other molecules abundant in biofilms (e.g. eDNA) of four surface-associated bacterial strains affiliated with the genera *Phaeobacter*, *Ruegeria*, *Pseudovibrio* and *Loktanella* suggested an “active” shaping of surface dynamics by secondary metabolites in guiding bacteria via gradient-dependent chemotaxis towards the surfaces where the respective compounds are produced (Manuscript 3), which was in line with recent observations in *Escherichia coli* (Englert et al. 2009, Anderson et al. 2015, Nagy et al. 2015, Laganenka et al. 2016).

Chemotactic effects caused by DNA were, to the best of our knowledge, not shown before for roseobacters and may represent a relevant ecological aspect in microbial biofilms that contain similar amounts of extracellular DNA (eDNA) (Tang et al. 2013) as tested in the present thesis (5 µg/mL). Repellence by own DNA was in accordance with prior studies, demonstrating perturbed surface attachment by own DNA (Berne et al. 2010, Segev et al. 2015). The herein used DNA (obtained by extraction) might transmit signals of damaged DNA after cell lysis (Vorkapic et al. 2016), however, this needs further investigation. Chemoattraction to foreign DNA could enable bacteria to gain favorable genomic information (Ellison et al. 2018) such as antibiotic resistance, new nutrient transporters or algal biomass-degrading enzymes (Manuscript 1) and might directly support the uptake of DNA by type IV secretion systems (Vorkapic et al. 2016), requiring direct cell-cell contact. This is also supported by the prevalence of such systems in *Roseobacter* genomes (Introduction, Fig. 3). Studies in Gram-positive bacteria revealed that QS enhanced DNA uptake (Li et al. 2001), further stressing the complexity of interactions in mixed-species biofilms. Another potential benefit for movement towards foreign DNA might relate to recycling of nutrients such as carbon, nitrogen or phosphate in nutrient limited environments (Pinchuk et al. 2008), indicative for resilience in biofilm settings characterized by internal turnover of nutrients (Flemming et al. 2016). Discrimination between own and foreign DNA may relate to different methylation patterns that also ensure correct function of type I restriction modification systems (Vasu et al. 2013), which was corroborated by the simultaneous repellence of the tested *Phaeobacter* strain (DSM 17395) from a close relative (T5T) with 87.7% genome-to-genome distance. Observed chemotactic response to TDA represented additional insights into the potential ecological role at subinhibitory concentrations, where it has been suggested as communication molecule (Beyersmann et al. 2017). Dependence of chemotaxis on own TDA production, suggested a targeted population-shaping function by selectively attracting TDA-producers which might strengthen surface colonization and antifouling capacity of *Phaeobacter* spp. (Rao et al. 2007).

The finding that QS molecules and other compounds within the biofilm matrix can exert chemotactic effects to selectively attract bacteria is especially interesting in light of wide occurrence of *luxR*-type autoinducer binding proteins in roseobacters (Slightom et al. 2009), enabling eavesdropping on foreign AHL molecules. Discrimination between own and foreign secondary metabolites might be mediated through a concerted action by the autoinducer binding protein LuxR and chemotaxis-mediating methyl-accepting chemotaxis proteins as suggested for *E. coli* (Hegde et al. 2011). The fact that related processes were shown for marine *Rhodobacteraceae* within the context of this study suggest functionality within and across species boundaries and concurrent effects on gene expression suggest distinct influence on the ecology of strains.

However, interactions in dense mixed biofilms rely on the potential of several different microbial classes to produce various secondary metabolites. Even among *Rhodobacteraceae* bacteria, production of secondary metabolites is vastly different and results in the constant identification of compounds, as exemplified by chemical studies performed within the context of this thesis (Manuscripts 5-7). Altogether, the results underline the complexity of secondary metabolism in roseobacters and how these traits support establishment in surface-associated habitats.

Secondary metabolite production varies among closely related species

The finding that 80% of analyzed macroalgae-associated *Rhodobacteraceae* produced different *N*-acyl homoserine lactones (AHLs) (Ziesche et al. 2015) (Manuscript 5) underlined the importance of such compounds for surface-associated roseobacters to perform chemical crosstalk (Atkinson et al. 2009, Amin et al. 2015), Especially interesting was the detection of C14:1-HSL as a cosmopolitan autoinducer of macroalgae-associated *Rhodobacteraceae*, corroborated by its influence on chemotactic behavior and genetic regulation of cell wall constituents and potential pathogenic compounds. However, also previously undetected chemical molecules were identified, such as AHLs with uncommon chain length or modifications (e.g. C12:2-HSL) and yet unknown *N*-acetylated amino acid methyl esters (NAMEs) (Manuscripts 6 and 7), adding to the chemical complexity of secondary metabolites of *Rhodobacteraceae*.

The finding that closely related strains differ in the amounts of encoded QS-systems and produced AHLs (including substantial variation in produced AHL concentrations) underlines the versatile potential of surface-associated marine bacteria to interact through QS, and how these dynamics vary even among closely related strains (Cude et al. 2013). For instance, the *Phaeobacter inhibens* type strain T5^T produced two additional AHLs compared to closely related DSM 17395, including the previously unknown C12:2-HSL, which motivated us to perform an in-depth analysis on the complete QS circuits encoded in this strain (Manuscript 4). Site-directed mutagenesis of single AHL synthases, allowed matching produced AHLs to the respective synthases as well as subsequent investigation on the regulatory effects of the different AHLs. Considering the production of diverse AHLs in *P. inhibens* DSM 17395 and T5^T, gene expression was compared upon exogenous addition of biofilm-related substances in *P. inhibens* DSM 17395 wild type (Manuscript 3) with synthase-deficient mutants of *P. inhibens* T5^T with intrinsic lack of AHL production (Manuscript 4). As both approaches showed comparable regulated features they will be discussed together, broadening the understanding of functional roles of these secondary metabolites.

Influence of secondary metabolites on bacterial transcriptomes reveal known but also yet unknown patterns with implications on surface attachment

In contrast to previous studies using microarrays (Beyersmann et al. 2017), the herein applied high-resolution RNA sequencing, enabled more detailed insights into regulatory effects of secondary metabolites in closely related strains. The finding that up to 17% of the *Phaeobacter* genes were differentially expressed upon exogenous addition of TDA corroborated the ecological and regulatory roles of TDA at sub-inhibitory concentrations (Beyersmann et al. 2017). The comparable upregulation of genes for growth and metabolic activity (e.g. energy production, translation, ribosomal proteins) as well as beneficial interaction with algal hosts (e.g. terpene production and concurrent protein synthesis and export) by both TDA and the algal osmolyte DMSP was concurrent with DMSP-mediated effects in other surface-associated roseobacters (Johnson et al. 2016) but represented a new functional role of TDA. The three percent of differentially expressed genes in presence of own DNA represent, to the best of our knowledge, the first example of regulatory effects of this important biofilm-related compound and adds to its role in mixed-species habitats, recommending future studies to understand the ecological roles of DNA for *Rhodobacteraceae*. The observed downregulation of genes involved in growth and metabolic activity was directly opposite to effects regulated by TDA, but concurred with observed regulations of AHLs in both strains, signifying important processes in established biofilm communities accompanied by efficient resource utilization and maintenance metabolism (Flemming et al. 2016). Overlapping regulatory features might indicate important functions for bacterial ecology during biofilm-associated lifestyle.

The observed different regulations by own or foreign AHLs corresponded to differential chemotactic responses, being supported by individual effects of AHLs in another *Roseobacter* member (Patzelt et al. 2016) and underlining the potential for eavesdropping (Case et al. 2008, Cude et al. 2013). Minor effects of the second major AHL in *Phaeobacter* spp. (C18:1-HSL) on gene regulation as well as chemotaxis of *P. inhibens* potentially resulted from fivefold lower expression of the relevant *luxR* homolog, however querying the ecological importance of this AHL under the tested conditions. Speculating that the AHL is produced for eavesdropping purpose is tempting in view of demonstrated chemotactic attraction by other *Rhodobacteraceae*. Alternatively, regulator activation might depend on additional triggers, e.g. elevated water temperatures as in other roseobacters (Gardiner et al. 2017, Hudson et al. 2018).

Highest regulatory effects by 3OH-C10-HSL in both *P. inhibens* DSM 17395 and T5 corresponded with the frequent production of this AHL in *Phaeobacter* spp. (Ziesche et al. 2018), demonstrating it might be a major regulatory element in these bacteria. Observed gene regulations by 3OH-C10-HSL on TDA production, motility and attachment were in accordance with previous

regulations of this AHL in *P. inhibens* DSM 17395 including a suggested “swim-and-attach” lifestyle, facilitating settlement on surfaces (Berger et al. 2011, Beyersmann et al. 2017). We speculate that opposed regulation of motility upon exogenous addition of 3OH-C10-HSL might derive from simultaneously high repression of motility genes by TDA (not present in the 3OH-C10-HSL-deficient mutant). Hence, studies with mutant strains could yield false results relating to co-occurring regulatory cascade effects, which should be considered carefully. Instead, exogenous addition of substances to wild type cells could represent a more suitable approach for the understanding of single regulatory traits. The overlapping effects of TDA and 3OH-C10-HSL indicates a substantial role of TDA for surface-association or be explained by the different concentrations exogenously added (10 μ M TDA vs 1 μ M AHL). Another important consideration when comparing gene expression patterns is the type of media used, or that exogenously added concentrations might not resemble indigenously produced concentrations. Furthermore, due to varying abilities for diverse (additional) AHL production, closely related strains could express different potential for secondary metabolite-mediated crosstalk, which adds another aspect of genomic plasticity for roseobacters relying on the previously observed influence of HGT on the transfer of such regulatory traits (Newton et al. 2010).

Potential pathogenicity

We identified a number of regulated traits that have not been described to be regulated by QS in *Phaeobacter* before. Encoded 20 RTX-like hemolysins in both *Phaeobacter* spp. and differential expression of >50% by various own and foreign AHLs, corroborated by the detection of generally less such genes in related roseobacters (Christie-Oleza et al. 2012), suggested a potential importance of hemolysins for the ecology of *Phaeobacter* spp. The finding that one RTX-like hemolysin constituted the highest expressed gene in both transcriptomes together with considerable high (60%) detection of the respective gene product in a previous exoproteome analysis of *P. inhibens* DSM 17395 (Durighello et al. 2014), indicate a major role of this protein under various growth conditions reflected by high expression in different media. Upregulation of another hemolysin (encoded adjacent to a type I secretion system) upon exogenous C14:1-HSL addition, coincident with physiological data for enhanced β -hemolysis under the same conditions, further strengthened this importance. Given the known disruption of animal cell membranes by hemolysins (Williams et al. 1991), this may support postulated occurrence of *P. inhibens* in association with marine animals (Freese et al. 2017), underlined by QS-dependent control of virulence via hemolysin production in human pathogenic bacteria (Wang et al. 2013, Guo et al. 2018). Hemolysins were also postulated to mediate virulence in a macroalgae-pathogenic *Phaeobacter* (Gardiner et al. 2017) and might support direct capture of organic matter from eukaryotic cells (Moran et al. 2007), potentially including iron-acquisition through cell lysis (Li et al. 2008). Simultaneous upregulation of a unique cell wall constituent of *Phaeobacter* spp., lipoteichoic acid

(Thole et al. 2012) might relate to the function of this compound as carrier of hemolysins to host cells (Theodore et al. 1981, Tsaihong et al. 1983). Although the functional role of hemolysins in *Phaeobacter* spp. remains elusive, we propose hemolysins have a yet overlooked importance for *Phaeobacter* and should be studied in the future. The co-regulation of a homologous hemolysin and the lipoteichoic acid cluster was corroborated by simultaneous upregulation of both traits in the mutant *phin11::Km* of *P. inhibens* T5^T. Conversely, in dense populations where signaling compounds can accumulate, both traits are downregulated upon sensing of own AHL. The opposed upregulation upon foreign C14:1-HSL sensing has implications on the potential shift in virulence mediated by complex mixtures of signaling molecules excreted by host-associated bacterial consortia.

Genetic exchange

The regulation of the expression for a gene transfer agent (GTA), widely encoded in *Roseobacter* genomes (Luo et al. 2014) and also regulated by QS in *Rhodobacter capsulatus* (Schaefer et al. 2002), constituted another yet undescribed regulated aspect of roseobacters. Together with the regulation of a prophage by the newly detected C12:2 in *P. inhibens* T5^T these observations have implications for HGT in mixed-species biofilms, supported by described AHL-induced induction of the lytic cycle of prophages (Ghosh et al. 2009, Silpe et al. 2019). Localization of the C12:2-producing synthase within the genomic island harboring the predicted intact prophage suggests horizontal transfer of QS systems in roseobacters (Gray et al. 2001, Wei et al. 2006). Such AHL-mediated genetic exchange might support genetic plasticity of roseobacters (Petersen et al. 2013) with potential implications for their adaptative success in various environments (Newton et al. 2010).

Overall, the present thesis illuminated multiple perspectives of adaptations and crosstalk in surface-associated *Rhodobacteraceae*, providing detailed insights but also underlining the complexity of these dynamics. The thesis underlines how secondary metabolites contribute to different processes with ecological relevance for surface association. These results substantially enrich prior knowledge on the importance of secondary metabolism in roseobacters and that produced compounds have diverse ecological roles. These insights are especially valuable as studies were done in an ecological framework, e.g. by using sub-inhibitory concentrations as possibly found in nature. To date, still little is known about chemical crosstalk *in situ* and how secondary metabolites may function under environmental scenarios. The thesis hence raises exciting perspectives on future studies on secondary metabolism that drive colonization and interaction on marine surfaces, productive and biologically rich habitats with ecological importance.

Outlook

The present thesis illustrated strain-specific adaptations and chemotactic abilities of different *Rhodobacteraceae* providing important insights into processes occurring in tidal habitats, on macroalgae and in mixed-species biofilms. However, the study relied on single substrates and single bacteria, while natural bacterial assemblages harbor diverse taxa of different classes with varying physiological abilities and secondary metabolite production. Further studies should therefore focus on the effect of mixtures of AHLs or own and foreign DNA to resemble more natural scenarios, e.g. by employing devices such as microfluidic chambers that allow microscopic observation of bacterial behavior within microspatial gradients. Such approaches will probably further illuminate the ecological effects of various compounds.

Measuring secondary metabolite concentrations in natural settings would help to understand the ecological importance of the tested concentrations and further elucidate the interconnection of population-shaping by QS and chemotaxis. This could be performed by chemical imaging studies, however previous approaches for TDA concerning this aspect failed (T. Brinkhoff, personal communication). Nevertheless, the knowledge of natural concentrations of specific AHLs and TDA produced in epibiotic communities would be an essential part to relate observed findings for tested concentrations to their ecological relevance. High resolution sequencing allowed detection of previously overlooked regulated features in *Phaeobacter* spp. with presumable importance for surface-attached lifestyle. Subsequent studies could focus on potentially exported hemolysins and co-regulated lipoteichoic acids in order to test potential involvement in virulence, which may be essential to identify potential pathogenic behavior of *Phaeobacter* spp. upon specific conditions.

Newly discovered secondary metabolites add a further dimension to the chemical diversity of roseobacters and offer exciting perspectives on so-far unknown roles in communication with other bacteria or eukaryotes. The newly discovered C12:2-HSL was assigned a function in this thesis and NAMEs are currently under investigation in a follow-up PhD project. Detection of opposing regulations e.g. for motility, GTA expression as well as the great variance of hemolysin regulations, suggests a careful consideration of growth conditions, concentrations of analyzed molecules, co-regulatory effects or different capacities for eavesdropping of the strains when evaluating future experiments. Although general conclusions on regulatory processes of specific AHLs are difficult, consistent regulation of the same metabolic features by different AHLs suggest a true ecological role for surface-attached roseobacters. The finding that some of these traits are unique for certain strains indicates considerable influence of horizontal gene transfer in such assemblages. To detect co-regulatory effects and minimize false-positive results, future studies should employ a combination of mutants and wild type strains to identify effects of single genes, but also more complex regulatory dependencies in multispecies settings.

References

- Abisado, R. G., Benomar, S., Klaus, J. R., Dandekar, A. A. and Chandler, J. R. (2018). "Bacterial quorum sensing and microbial community interactions." *Mbio* 9(5).
- Alavi, M., Miller, T., Erlandson, K., Schneider, R. and Belas, R. (2001). "Bacterial community associated with *Pfiesteria*-like dinoflagellate cultures." *Environ Microbiol* 3(6): 380-396.
- Alongi, D. M. (1997). Coastal ecosystem processes. Boca Raton, CRC Press.
- Amin, S. A., Hmelo, L. R., van Tol, H. M., Durham, B. P., Carlson, L. T., Heal, K. R., Morales, R. L., Berthiaume, C. T., Parker, M. S., Djunaedi, B., Ingalls, A. E., Parsek, M. R., Moran, M. A. and Armbrust, E. V. (2015). "Interaction and signalling between a cosmopolitan phytoplankton and associated bacteria." *Nature* 522: 98.
- Anderson, J. K., Huang, J. Y., Wreden, C., Sweeney, E. G., Goers, J., Remington, S. J. and Guillemin, K. (2015). "Chemorepulsion from the quorum signal autoinducer-2 promotes *Helicobacter pylori* biofilm dispersal." *mBio* 6(4): e00379-00315.
- Antonova, E. S. and Hammer, B. K. (2011). "Quorum-sensing autoinducer molecules produced by members of a multispecies biofilm promote horizontal gene transfer to *Vibrio cholerae*." *Fems Microbiol Lett* 322(1): 68-76.
- Antunes, J., Leão, P. and Vasconcelos, V. (2018). "Marine biofilms: diversity of communities and of chemical cues." *Environ Microbiol Rep* 0(0): 0-19.
- Armstrong, E., Rogerson, A. and Leftley, J. W. (2000). "The abundance of heterotrophic protists associated with intertidal seaweeds." *Estuar Coast Shelf Sci* 50(3): 415-424.
- Arndt, D., Grant, J. R., Marcu, A., Sajed, T., Pon, A., Liang, Y. J. and Wishart, D. S. (2016). "PHASTER: a better, faster version of the PHAST phage search tool." *Nucleic Acids Res* 44(W1): 16-21.
- Asad, S. and Opal, S. M. (2008). "Bench-to-bedside review: Quorum sensing and the role of cell-to-cell communication during invasive bacterial infection." *Crit Care* 12(6): 236.
- Atkinson, S. and Williams, P. (2009). "Quorum sensing and social networking in the microbial world." *J R Soc Interface* 6(40): 959-978.
- Auch, A. F., von Jan, M., Klenk, H. P. and Göker, M. (2010). "Digital DNA-DNA hybridization for microbial species delineation by means of genome-to-genome sequence comparison." *Stand Genomic Sci* 2(1): 117-134.
- Balcazar, J. L., Lee, N. M., Pintado, J. and Planas, M. (2010). "Phylogenetic characterization and in situ detection of bacterial communities associated with seahorses (*Hippocampus guttulatus*) in captivity." *Syst Appl Microbiol* 33(2): 71-77.
- Balch, W. E., Fox, G. E., Magrum, L. J., Woese, C. R. and Wolfe, R. S. (1979). "Methanogens - re-evaluation of a unique biological group." *Microbiol Rev* 43(2): 260-296.
- Bankevich, A., Nurk, S., Antipov, D., Gurevich, A. A., Dvorkin, M., Kulikov, A. S., Lesin, V. M., Nikolenko, S. I., Pham, S., Pribelski, A. D., Pyshkin, A. V., Sirotkin, A. V., Vyahhi, N., Tesler, G., Alekseyev, M. A. and Pevzner, P. A. (2012). "SPAdes: A new genome assembly algorithm and its applications to single-cell sequencing." *J Comput Biol* 19(5): 455-477.
- Barak-Gavish, N., Frada, M. J., Ku, C., Lee, P. A., DiTullio, G. R., Malitsky, S., Aharoni, A., Green, S. J., Rotkopf, R., Kartvelishvili, E., Sheyn, U., Schatz, D. and Vardi, A. (2018). "Bacterial virulence against an oceanic bloom-forming phytoplankton is mediated by algal DMSP." *Sci Adv* 4(10): eaau5716.
- Barbieri, E., Paster, B. J., Hughes, D., Zurek, L., Moser, D. P., Teske, A. and Sogin, M. L. (2001). "Phylogenetic characterization of epibiotic bacteria in the accessory nidamental gland and egg capsules of the squid *Loligo pealei* (Cephalopoda: Loliginidae)." *Environ Microbiol* 3(3): 151-167.
- Bartling, P., Vollmers, J. and Petersen, J. (2018). "The first world swimming championships of roseobacters - phylogenomic insights into an exceptional motility phenotype." *Syst Appl Microbiol* 41(6): 544-554.
- Bartnikas, T. B., Wang, Y. S., Bobo, T., Veselov, A., Scholes, C. P. and Shapleigh, J. P. (2002). "Characterization of a member of the NnrR regulon in *Rhodobacter sphaeroides* 2.4.3 encoding a haem-copper protein." *Microbiol-Sgm* 148: 825-833.
- Bauer, A. W., Kirby, W. M., Sherris, J. C. and Turck, M. (1966). "Antibiotic susceptibility testing by a standardized single disk method." *Am J Clin Pathol* 45(4): 493-496.
- Beck, M., Dellwig, O., Fischer, S., Schnetger, B. and Brumsack, H.-J. (2012). "Trace metal geochemistry of organic carbon-rich watercourses draining the NW German coast." *Estuar Coast Shelf Sci* 104-105: 66-79.
- Beer, S., Israel, A., Drechsler, Z. and Cohen, Y. (1990). "Photosynthesis in *Ulva fasciata*: V. Evidence for an inorganic carbon concentrating system, and ribulose-1,5-bisphosphate carboxylase/oxygenase CO(2) kinetics." *Plant Physiol* 94(4): 1542-1546.
- Beja, O., Suzuki, M. T., Heidelberg, J. F., Nelson, W. C., Preston, C. M., Hamada, T., Eisen, J. A., Fraser, C. M. and DeLong, E. F. (2002). "Unsuspected diversity among marine aerobic anoxygenic phototrophs." *Nature* 415(6872): 630-633.
- Bengtsson, M. M., Sjutun, K. and Ovreas, L. (2010). "Seasonal dynamics of bacterial biofilms on the kelp *Laminaria hyperborea*." *Aquat Microb Ecol* 60(1): 71-83.
- Benkendorff, K., Bremner, J. and Davis, A. (2001). "Indole derivatives from the egg masses of muricid molluscs." *Molecules* 6(2): 70-78.
- Berger, M., Brock, N. L., Liesegang, H., Dogs, M., Preuth, I. and Simon, M. (2012). "Genetic analysis of the upper phenylacetate catabolic pathway in the production of tropodithietic acid by *Phaeobacter gallaeciensis*." *Appl Environ Microbiol* 78(10): 3539-3551.

- Berger, M., Neumann, A., Schulz, S., Simon, M. and Brinkhoff, T. (2011). "Tropodithietic acid production in *Phaeobacter gallaeciensis* is regulated by *N*-acyl homoserine lactone-mediated quorum sensing." J Bacteriol 193(23): 6576-6585.
- Berne, C., Kysela, D. T. and Brun, Y. V. (2010). "A bacterial extracellular DNA inhibits settling of motile progeny cells within a biofilm." Mol Microbiol 77(4): 815-829.
- Bertelli, C., Laird, M. R., Williams, K. P., Lau, B. Y., Hoad, G., Winsor, G. L., Brinkman, F. S. L. and Grp, S. F. U. R. C. (2017). "IslandViewer 4: expanded prediction of genomic islands for larger-scale datasets." Nucleic Acids Res 45(W1): 30-35.
- Beyersmann, P. G., Tomasch, J., Son, K., Stocker, R., Göker, M., Wagner-Döbler, I., Simon, M. and Brinkhoff, T. (2017). "Dual function of tropodithietic acid as antibiotic and signaling molecule in global gene regulation of the probiotic bacterium *Phaeobacter inhibens*." Sci Rep 7.
- Beyersmann, P. G., Tomasch, J., Son, K., Stocker, R., Göker, M., Wagner-Döbler, I., Simon, M. and Brinkhoff, T. (2017). "Dual function of tropodithietic acid as antibiotic and signaling molecule in global gene regulation of the probiotic bacterium *Phaeobacter inhibens*." Sci Rep 7(1): 730.
- Blin, K., Wolf, T., Chevrette, M. G., Lu, X. W., Schwalen, C. J., Kautsar, S. A., Duran, H. G. S., Santos, E. L. C. D. L., Kim, H. U., Nave, M., Dickschat, J. S., Mitchell, D. A., Shelest, E., Breitling, R., Takano, E., Lee, S. Y., Weber, T. and Medema, M. H. (2017). "AntiSMASH 4.0-improvements in chemistry prediction and gene cluster boundary identification." Nucleic Acids Res 45(W1): 36-41.
- Bolger, A. M., Lohse, M. and Usadel, B. (2014). "Trimmomatic: a flexible trimmer for Illumina sequence data." Bioinformatics 30(15): 2114-2120.
- Bondarev, V., Richter, M., Romano, S., Piel, J., Schwedt, A. and Schulz-Vogt, H. N. (2013). "The genus *Pseudovibrio* contains metabolically versatile bacteria adapted for symbiosis." Environ Microbiol 15(7): 2095-2113.
- Bragg, L., Stone, G., Imelfort, M., Philip, H. and Tyson, G. (2012). "Fast, accurate error-correction of amplicon pyrosequences using Acacia." Nat Methods 9: 425-426.
- Bramkamp, M. and Lopez, D. (2015). "Exploring the existence of lipid rafts in bacteria." Microbiol Mol Biol Rev 79(1): 81-100.
- Breider, S., Freese, H. M., Sproer, C., Simon, M., Overmann, J. and Brinkhoff, T. (2017). "*Phaeobacter porticola* sp nov., an antibiotic-producing bacterium isolated from a sea harbour." Int J Syst Evol Microbiol 67(7): 2153-2159.
- Breider, S., Scheuner, C., Schumann, P., Fiebig, A., Petersen, J., Pradella, S., Klenk, H. P., Brinkhoff, T. and Goker, M. (2014). "Genome-scale data suggest reclassifications in the *Leisingera-Phaeobacter* cluster including proposals for *Sedimentitalea* gen. nov. and *Pseudophaeobacter* gen. nov." Front Microbiol 5: 416.
- Brilli, M., Fondi, M., Fani, R., Mengoni, A., Ferri, L., Bazzicalupo, M. and Biondi, E. G. (2010). "The diversity and evolution of cell cycle regulation in *alpha*-proteobacteria: a comparative genomic analysis." Bmc Syst Biol 4: 52.
- Brinkhoff, T., Bach, G., Heidorn, T., Liang, L. F., Schlingloff, A. and Simon, M. (2004). "Antibiotic production by a *Roseobacter* clade-affiliated species from the German Wadden Sea and its antagonistic effects on indigenous isolates." Appl Environ Microbiol 70(4): 2560-2565.
- Brinkhoff, T., Giebel, H. A. and Simon, M. (2008). "Diversity, ecology, and genomics of the *Roseobacter* clade: a short overview." Arch Microbiol 189(6): 531-539.
- Brinkhoff, T. and Muyzer, G. (1997). "Increased species diversity and extended habitat range of sulfur-oxidizing *Thiomicrospira* spp." Appl Environ Microbiol 63(10): 3789-3796.
- Brock, J. and Schulz-Vogt, H. N. (2011). "Sulfide induces phosphate release from polyphosphate in cultures of a marine *Beggiatoa* strain." ISME J 5(3): 497-506.
- Bruhn, J. B., Nielsen, K. F., Hjelm, M., Hansen, M., Bresciani, J. and Schulz, S. (2005). "Ecology, inhibitory activity, and morphogenesis of a marine antagonistic bacterium belonging to the *Roseobacter* clade." Appl Environ Microbiol 71(11): 7263-7270.
- Buchan, A., González, J. M. and Moran, M. A. (2005). "Overview of the marine *roseobacter* lineage." Appl Environ Microbiol 71(10): 5665-5677.
- Buddruhs, N., Chertkov, O., Petersen, J., Fiebig, A., Chen, A., Pati, A., Ivanova, N., Lapidus, A., Goodwin, L. A., Chain, P., Detter, J. C., Gronow, S., Kyrpides, N. C., Woyke, T., Goker, M., Brinkhoff, T. and Klenk, H. P. (2013). "Complete genome sequence of the marine methyl-halide oxidizing *Leisingera methylhalidivorans* type strain (DSM 14336(T)), a representative of the *Roseobacter* clade." Stand Genomic Sci 9(1): 128-141.
- Buddruhs, N., Pradella, S., Goker, M., Pauker, O., Pukall, R., Sproer, C., Schumann, P., Petersen, J. and Brinkhoff, T. (2013). "Molecular and phenotypic analyses reveal the non-identity of the *Phaeobacter gallaeciensis* type strain deposits CIP 105210(T) and DSM 17395." Int J Syst Evol Microbiol 63: 4340-4349.
- Cairrao, E., J. Pereira, M., Morgado, F., Nogueira, A., Guilhermino, L. and Soares, A. (2009). "Phenotypic variation of *Fucus ceranoides*, *F. spiralis* and *F. vesiculosus* in a temperate coast (NW Portugal)." Bot Stud 50: 205-215.
- Caporaso, J. G., Kuczynski, J., Stombaugh, J., Bittinger, K., Bushman, F. D., Costello, E. K., Fierer, N., Pena, A. G., Goodrich, J. K., Gordon, J. I., Huttley, G. A., Kelley, S. T., Knights, D., Koenig, J. E., Ley, R. E., Lozupone, C. A., McDonald, D., Muegge, B. D., Pirrung, M., Reeder, J., Sevinsky, J. R., Turnbaugh, P. J., Walters, W. A., Widmann, J., Yatsunencko, T., Zaneveld, J. and Knight, R. (2010). "QIIME allows analysis of high-throughput community sequencing data." Nat Methods 7(5): 335-336.

- Cárdenas, A., Neave, M. J., Haroon, M. F., Pogoreutz, C., Rådecker, N., Wild, C., Gärdes, A. and Voolstra, C. R. (2017). "Excess labile carbon promotes the expression of virulence factors in coral reef bacterioplankton." *ISME J* 12(1): 59-76.
- Cardoso, P., Santos, M., Freitas, R., Rocha, S. M. and Figueira, E. (2017). "Response of *Rhizobium* to Cd exposure: A volatile perspective." *Environ Pollut* 231: 802-811.
- Carter, R. A., Yeoman, K. H., Klein, A., Hosie, A. H. F., Sawers, G., Poole, P. S. and Johnston, A. W. B. (2002). "Dpp genes of *Rhizobium leguminosarum* specify uptake of delta-aminolevulinic acid." *Mol Plant Microbe Interact* 15(1): 69-74.
- Case, R. J., Labbate, M. and Kjelleberg, S. (2008). "AHL-driven quorum-sensing circuits: their frequency and function among the *Proteobacteria*." *ISME J* 2(4): 345-349.
- Case, R. J., Longford, S. R., Campbell, A. H., Low, A., Tujula, N., Steinberg, P. D. and Kjelleberg, S. (2011). "Temperature induced bacterial virulence and bleaching disease in a chemically defended marine macroalga." *Environ Microbiol* 13(2): 529-537.
- Chandler, J. R., Heilmann, S., Mittler, J. E. and Greenberg, E. P. (2012). "Acyl-homoserine lactone-dependent eavesdropping promotes competition in a laboratory co-culture model." *ISME J* 6(12): 2219-2228.
- Chao, A. and Bunge, J. (2002). "Estimating the Number of Species in a Stochastic Abundance Model." *Biometrics* 58(3): 531-539.
- Chaudhari, N. M., Gupta, V. K. and Dutta, C. (2016). "BPGA- an ultra-fast pan-genome analysis pipeline." *Sci Rep* 6: 24373.
- Chen, F., Wang, K., Stewart, J. and Belas, R. (2006). "Induction of multiple prophages from a marine bacterium: a genomic approach." *Appl Environ Microbiol* 72(7): 4995-5001.
- Christie-Oleza, J. A., Pina-Villalonga, J. M., Bosch, R., Nogales, B. and Armengaud, J. (2012). "Comparative proteogenomics of twelve *Roseobacter* exoproteomes reveals different adaptive strategies among these marine bacteria." *Mol Cell Proteomics* 11(2).
- Collins, A. J., Fullmer, M. S., Gogarten, J. P. and Nyholm, S. V. (2015). "Comparative genomics of *Roseobacter* clade bacteria isolated from the accessory nidamental gland of *Euprymna scolopes*." *Front Microbiol* 6: 123.
- Couto, J. A., Campos, F. M., Figueiredo, A. R. and Hogg, T. A. (2006). "Ability of lactic acid bacteria to produce volatile phenols." *Am J Enol Vitic* 57(2): 166-171.
- Croft, M. T., Lawrence, A. D., Raux-Deery, E., Warren, M. J. and Smith, A. G. (2005). "Algae acquire vitamin B₁₂ through a symbiotic relationship with bacteria." *Nature* 438(7064): 90-93.
- Crosa, J. H. and Walsh, C. T. (2002). "Genetics and assembly line enzymology of siderophore biosynthesis in bacteria." *Microbiol Mol Biol Rev* 66(2): 223-249.
- Cude, W. N. and Buchan, A. (2013). "Acyl-homoserine lactone-based quorum sensing in the *Roseobacter* clade: complex cell-to-cell communication controls multiple physiologies." *Front Microbiol* 4: 336.
- Cugini, C., Calfee, M. W., Farrow, J. M., Morales, D. K., Pesci, E. C. and Hogan, D. A. (2007). "Farnesol, a common sesquiterpene, inhibits PQS production in *Pseudomonas aeruginosa*." *Mol Microbiol* 65(4): 896-906.
- Cypionka, H. and Pfennig, N. (1986). "Growth yields of *Desulfotomaculum orientis* with hydrogen in chemostat culture." *Arch Microbiol* 143(4): 396-399.
- D'Alvise, P. W. (2013). "Aquaculture application and ecophysiology of marine bacteria from the *Roseobacter* clade." PhD Thesis, Technical University of Denmark, Denmark.
- D'Alvise, P. W., Phippen, C. B. W., Nielsen, K. F. and Gram, L. (2016). "Influence of iron on production of the antibacterial compound tropodithietic acid and its noninhibitory analog in *Phaeobacter inhibens*." *Appl Environ Microbiol* 82(2): 502-509.
- D'Alvise, P. W., Lillebo, S., Prol-Garcia, M. J., Wergeland, H. I., Nielsen, K. F. and Bergh, O. (2012). "*Phaeobacter gallaeciensis* reduces *Vibrio anguillarum* in cultures of microalgae and rotifers, and prevents vibriosis in cod larvae." *PLoS One* 7(8): e43996.
- Dang, H. Y., Li, T. G., Chen, M. N. and Huang, G. Q. (2008). "Cross-ocean distribution of *Rhodobacterales* bacteria as primary surface colonizers in temperate coastal marine waters." *Appl Environ Microbiol* 74(1): 52-60.
- Darriba, D., Taboada, G. L., Doallo, R. and Posada, D. (2011). "ProtTest 3: fast selection of best-fit models of protein evolution." *Bioinformatics* 27(8): 1164-1165.
- Darriba, D., Taboada, G. L., Doallo, R. and Posada, D. (2012). "jModelTest 2: more models, new heuristics and parallel computing." *Nat Methods* 9(8): 772-772.
- DeAngelis, K. M., Lindow, S. E. and Firestone, M. K. (2008). "Bacterial quorum sensing and nitrogen cycling in rhizosphere soil." *FEMS Microbiol Ecol* 66(2): 197-207.
- Decho, A. W., Frey, R. L. and Ferry, J. L. (2011). "Chemical challenges to bacterial AHL signaling in the environment." *Chem Rev* 111(1): 86-99.
- Decho, A. W. and Gutierrez, T. (2017). "Microbial extracellular polymeric substances (EPSs) in ocean systems." *Front Microbiol* 8: 922.
- Decho, A. W., Visscher, P. T., Ferry, J., Kawaguchi, T., He, L., Przekop, K. M., Norman, R. S. and Reid, R. P. (2009). "Autoinducers extracted from microbial mats reveal a surprising diversity of *N*-acylhomoserine lactones (AHLs) and abundance changes that may relate to diel pH." *Environ Microbiol* 11(2): 409-420.
- DeLoney-Marino, C. R., Wolfe, A. J. and Visick, K. L. (2003). "Chemoattraction of *Vibrio fischeri* to serine, nucleosides, and *N*-acetylneuraminic acid, a component of squid light-organ mucus." *Appl Environ Microbiol* 69(12): 7527-7530.
- Dickschat, J. S., Bode, H. B., Wenzel, S. C., Müller, R. and Schulz, S. (2005). "Biosynthesis and identification of volatiles released by the myxobacterium *Stigmatella aurantiaca*." *Chembiochem* 6(11): 2023-2033.

- Dickschat, J. S., Helmke, E. and Schulz, S. (2005). "Volatile organic compounds from arctic bacteria of the *Cytophaga-Flavobacterium-Bacteroides* group: A retrobiosynthetic approach in chemotaxonomic investigations." Chem Biodivers 2(3): 318-353.
- Dittmann, K. K., Sonnenschein, E. C., Egan, S., Gram, L. and Bentzon-Tilia, M. (2018). "Impact of *Phaeobacter inhibens* on marine eukaryote-associated microbial communities." Environ Microbiol Rep 0(0).
- Doberva, M., Stien, D., Sorres, J., Hue, N., Sanchez-Ferandin, S., Eparvier, V., Ferandin, Y., Lebaron, P. and Lami, R. (2017). "Large diversity and original structures of acyl-homoserine lactones in strain MOLA 401, a marine *Rhodobacteraceae* bacterium." Front Microbiol 8: 1-10.
- Dogs, M., Voget, S., Teshima, H., Petersen, J., Davenport, K., Dalingault, H., Chen, A., Pati, A., Ivanova, N., Goodwin, L. A., Chain, P., Detter, J. C., Standfest, S., Rohde, M., Gronow, S., Kyrpides, N. C., Woyke, T., Simon, M., Klenk, H. P., Göker, M. and Brinkhoff, T. (2013). "Genome sequence of *Phaeobacter inhibens* type strain (T5(T)), a secondary metabolite producing representative of the marine *Roseobacter* clade, and emendation of the species description of *Phaeobacter inhibens*." Stand Genomic Sci 9(2): 334-350.
- Dogs, M., Wemheuer, B., Wolter, L., Bergen, N., Daniel, R., Simon, M. and Brinkhoff, T. (2017). "*Rhodobacteraceae* on the marine brown alga *Fucus spiralis* are abundant and show physiological adaptation to an epiphytic lifestyle." Syst Appl Microbiol 40(6): 370-382.
- Dulla, G. F. and Lindow, S. E. (2009). "Acyl-homoserine lactone-mediated cross talk among epiphytic bacteria modulates behavior of *Pseudomonas syringae* on leaves." ISME J 3(7): 825-834.
- Durighello, E., Christie-Oleza, J. A. and Armengaud, J. (2014). "Assessing the exoproteome of marine bacteria, lesson from a RTX-toxin abundantly secreted by *Phaeobacter* strain DSM 17395." PLoS One 9(2).
- Edgar, R. C. (2004). "MUSCLE: multiple sequence alignment with high accuracy and high throughput." Nucleic Acids Res 32(5): 1792-1797.
- Edgar, R. C. (2010). "Search and clustering orders of magnitude faster than BLAST." Bioinformatics 26(19): 2460-2461.
- Edgar, R. C., Haas, B., Clemente, J. C., Quince, C. and Knight, R. (2011). "UCHIIME improves sensitivity and speed of chimera detection." Bioinformatics 27: 2194-2200.
- Egan, B. and Yarish, C. (1990). "Productivity and life history of *Laminaria longicuris* at its southern limit in the Western Atlantic Ocean." Mar Ecol Prog Ser 67(3): 263-273.
- Egan, S., Fernandes, N. D., Kumar, V., Gardiner, M. and Thomas, T. (2014). "Bacterial pathogens, virulence mechanism and host defence in marine macroalgae." Environ Microbiol 16(4): 925-938.
- Egan, S., Harder, T., Burke, C., Steinberg, P., Kjelleberg, S. and Thomas, T. (2013). "The seaweed holobiont: understanding seaweed-bacteria interactions." FEMS Microbiology Reviews 37(3): 462-476.
- Ellison, C. K., Dalia, T. N., Ceballos, A. V., Wang, J. C. Y., Biais, N., Brun, Y. V. and Dalia, A. B. (2018). "Retraction of DNA-bound type IV competence pili initiates DNA uptake during natural transformation in *Vibrio cholerae*." Nat Microbiol 3(7): 773-780.
- Englert, D. L., Manson, M. D. and Jayaraman, A. (2009). "Flow-based microfluidic device for quantifying bacterial chemotaxis in stable, competing gradients." Appl Environ Microbiol 75(13): 4557-4564.
- Ferreira, J. G., Arenas, F., Martinez, B., Hawkins, S. J. and Jenkins, S. R. (2014). "Physiological response of fucoid algae to environmental stress: comparing range centre and southern populations." New Phytol 202(4): 1157-1172.
- Flemming, H. C., Wingender, J., Szewzyk, U., Steinberg, P., Rice, S. A. and Kjelleberg, S. (2016). "Biofilms: an emergent form of bacterial life." Nat Rev Microbiol 14(9): 563-575.
- Fogg, P. C. M. (2019). "Identification and characterization of a direct activator of a gene transfer agent." Nat Commun 10(1): 595.
- Frank, O., Michael, V., Pauker, O., Boedeker, C., Jogler, C., Rohde, M. and Petersen, J. (2015). "Plasmid curing and the loss of grip - The 65-kb replicon of *Phaeobacter inhibens* DSM 17395 is required for biofilm formation, motility and the colonization of marine algae." Syst Appl Microbiol 38(2): 120-127.
- Freese, H. M., Methner, A. and Overmann, J. (2017). "Adaptation of surface-associated bacteria to the open ocean: a genomically distinct subpopulation of *Phaeobacter gallaeciensis* colonizes pacific mesozooplankton." Front Microbiol 8: 1659.
- Freese, H. M., Sikorski, J., Bunk, B., Scheuner, C., Meier-Kolthoff, J. P., Sproer, C., Gram, L. and Overmann, J. (2017). "Trajectories and drivers of genome evolution in surface-associated marine *Phaeobacter*." Genome Biol Evol 9(12): 3297-3311.
- Fries, L. (1993). "Vitamin-B₁₂ heterotrophy in *Fucus spiralis* and *Ascophyllum nodosum* (*Fucales*, *Phaeophyta*) in axenic cultures." Bot Mar 36(1): 5-7.
- Fröstl, J. M. and Overmann, J. (1998). "Physiology and tactic response of the phototrophic consortium "*Chlorochromatium aggregatum*"." Arch Microbiol.(1432-072X (Electronic)).
- Fuqua, C. and Greenberg, E. P. (2002). "Listening in on bacteria: Acyl-homoserine lactone signalling." Nat Rev Mol Cell Bio 3(9): 685-695.
- Gao, J., Duan, Y., Liu, Y., Zhuang, X., Liu, Y., Bai, Z., Ma, W. and Zhuang, G. (2019). "Long- and short-chain AHLs affect AOA and AOB microbial community composition and ammonia oxidation rate in activated sludge." J Environ Sci 78: 53-62.
- Gao, J., Ma, A., Zhuang, X. and Zhuang, G. (2015). Quorum sensing in nitrogen fixation. Quorum Sensing vs Quorum Quenching: A Battle with No End in Sight. V. C. Kalia. New Delhi, Springer India: 51-60.
- Garai, P., Chandra, K. and Chakravorty, D. (2017). "Bacterial peptide transporters: Messengers of nutrition to virulence." Virulence 8(3): 297-309.

- Garcia-Alcalde, F., Okonechnikov, K., Carbonell, J., Cruz, L. M., Gotz, S., Tarazona, S., Dopazo, J., Meyer, T. F. and Conesa, A. (2012). "Qualimap: evaluating next-generation sequencing alignment data." Bioinformatics 28(20): 2678-2679.
- Gardiner, M., Bournazos, A. M., Maturana-Martinez, C., Zhong, L. and Egan, S. (2017). "Exoproteome analysis of the seaweed pathogen *Nautella italica* R11 reveals temperature-dependent regulation of RTX-like proteins." Front Microbiol 8: 1203.
- Geng, H. and Belas, R. (2010). "Expression of tropodithetic acid biosynthesis is controlled by a novel autoinducer." J Bacteriol 192(17): 4377-4387.
- Gershenzon, J. and Dudareva, N. (2007). "The function of terpene natural products in the natural world." Nat Chem Biol 3(7): 408-414.
- Ghosh, D., Roy, K., Williamson, K. E., Srinivasiah, S., Wommack, K. E. and Radosevich, M. (2009). "Acyl-homoserine lactones can induce virus production in lysogenic bacteria: an alternative paradigm for prophage induction." Appl Environ Microbiol 75(22): 7142-7152.
- Giebel, H. A., Brinkhoff, T., Zwisler, W., Selje, N. and Simon, M. (2009). "Distribution of *Roseobacter* RCA and SAR11 lineages and distinct bacterial communities from the subtropics to the Southern Ocean." Environ Microbiol 11(8): 2164-2178.
- Giebel, H. A., Kahlhoefer, D., Gahl-Janssen, R., Choo, Y. J., Lee, K., Cho, J. C., Tindall, B. J., Rhiel, E., Beardsley, C., Aydogmus, O. O., Voget, S., Daniel, R., Simon, M. and Brinkhoff, T. (2013). "*Planktomarina temperata* gen. nov., sp nov., belonging to the globally distributed RCA cluster of the marine *Roseobacter* clade, isolated from the German Wadden Sea." Int J Syst Evol Microbiol 63: 4207-4217.
- Gloag, E. S., Turnbull, L., Huang, A., Vallotton, P., Wang, H., Nolan, L. M., Mililli, L., Hunt, C., Lu, J., Osvath, S. R., Monahan, L. G., Cavaliere, R., Charles, I. G., Wand, M. P., Gee, M. L., Prabhakar, R. and Whitchurch, C. B. (2013). "Self-organization of bacterial biofilms is facilitated by extracellular DNA." Proc Natl Acad Sci USA 110(28): 11541-11546.
- Goecke, F., Labes, A., Wiese, J. and Imhoff, J. F. (2010). "Chemical interactions between marine macroalgae and bacteria." Mar Ecol Prog Ser 409: 267-299.
- Gorshkova, R. P., Isakov, V. V., Shevchenko, L. S., Ivanova, E. P., Denisenko, V. A. and Nazarenko, E. L. (2007). "Structure of teichoic acid from the marine proteobacterium *Sulfitobacter brevis* KMM 6006." Chem Nat Compd 43(6): 643-647.
- Graham, L. and Wilcox, L. (1999). *Algae*. Upper Saddle River, NJ, Pearson Education (US).
- Gram, L., Rasmussen, B. B., Wemheuer, B., Bernborg, N., Ng, Y. Y., Porsby, C. H., Breider, S. and Brinkhoff, T. (2015). "*Phaeobacter inhibens* from the Roseobacter clade has an environmental niche as a surface colonizer in harbors." Syst Appl Microbiol 38(7): 483-493.
- Grammann, K., Volke, A. and Kunte, H. J. (2002). "New type of osmoregulated solute transporter identified in halophilic members of the bacteria domain: TRAP transporter TeaABC mediates uptake of ectoine and hydroxyectoine in *Halomonas elongata* DSM 2581(T)." J Bacteriol 184(11): 3078-3085.
- Gray, K. M. and Garey, J. R. (2001). "The evolution of bacterial LuxI and LuxR quorum sensing regulators." Microbiology 147(Pt 8): 2379-2387.
- Grigioni, S., Boucher-Rodoni, R., Demarta, A., Tonolla, M. and Peduzzi, R. (2000). "Phylogenetic characterisation of bacterial symbionts in the accessory nidamental glands of the sepoid *Sepia officinalis* (*Cephalopoda*: *Decapoda*)." Mar Biol 136(2): 217-222.
- Grkovic, S., Brown, M. H. and Skurray, R. A. (2001). "Transcriptional regulation of multidrug efflux pumps in bacteria." Semin Cell Dev Biol 12(3): 225-237.
- Grondin, J. M., Tamura, K., Dejean, G., Abbott, D. W. and Brumer, H. (2017). "Polysaccharide utilization loci: fueling microbial communities." J Bacteriol 199(15).
- Grossart, H. P., Schlingloff, A., Bernhard, M., Simon, M. and Brinkhoff, T. (2004). "Antagonistic activity of bacteria isolated from organic aggregates of the German Wadden Sea." FEMS Microbiol Ecol 47(3): 387-396.
- Guo, M. H., Fang, Z. J., Sun, L. J., Sun, D. F., Wang, Y. L., Li, C., Wang, R. D., Liu, Y., Hu, H. Q., Liu, Y., Xu, D. F. and Gooneratne, R. (2018). "Regulation of thermostable direct hemolysin and biofilm formation of *Vibrio parahaemolyticus* by quorum-sensing genes *luxM* and *luxS*." Curr Microbiol 75(9): 1190-1197.
- Gupta, R. and Schuster, M. (2013). "Negative regulation of bacterial quorum sensing tunes public goods cooperation." ISME J 7(11): 2159-2168.
- Hahnke, S., Brock, N. L., Zell, C., Simon, M., Dickschat, J. S. and Brinkhoff, T. (2013). "Physiological diversity of *Roseobacter* clade bacteria co-occurring during a phytoplankton bloom in the North Sea." Syst Appl Microbiol 36(1): 39-48.
- Hamdy, A. A. (2000). "Biosorption of heavy metals by marine algae." Curr Microbiol 41(4): 232-238.
- Hanahan, D. (1983). "Studies on transformation of *Escherichia coli* with plasmids." J Mol Biol 166(4): 557-580.
- Harig, T., Schlawis, C., Ziesche, L., Pohlner, M., Engelen, B. and Schulz, S. (2017). "Nitrogen-containing volatiles from marine *Salinispora pacifica* and *Roseobacter* group bacteria." J Nat Prod 80(12): 3290-3296.
- Harrington, C., Reen, F. J., Mooij, M. J., Stewart, F. A., Chabot, J.-B., Guerra, A. F., Glöckner, F. O., Nielsen, K. F., Gram, L., Dobson, A. D. W., Adams, C. and O'Gara, F. (2014). "Characterisation of non-autoinducing tropodithetic acid (TDA) production from marine sponge *Pseudovibrio* species." Mar Drugs 12(12): 5960-5978.
- Hegde, M., Englert, D. L., Schrock, S., Cohn, W. B., Vogt, C., Wood, T. K., Manson, M. D. and Jayaraman, A. (2011). "Chemotaxis to the quorum-sensing signal AI-2 requires the Tsr chemoreceptor and the periplasmic LsrB AI-2-binding protein." J Bacteriol 193(3): 768-773.

- Hehemann, J. H., Arevalo, P., Datta, M. S., Yu, X. Q., Corzett, C. H., Henschel, A., Preheim, S. P., Timberlake, S., Alm, E. J. and Polz, M. F. (2016). "Adaptive radiation by waves of gene transfer leads to fine-scale resource partitioning in marine microbes." *Nat Commun* 7: 12860.
- Hemmi, A. and Jormalainen, V. (2004). "Geographic covariation of chemical quality of the host alga *Fucus vesiculosus* with fitness of the herbivorous isopod *Idotea baltica*." *Mar Biol* 145(4): 759-768.
- Herzberg, M., Kaye, I. K., Peti, W. and Wood, T. K. (2006). "YdgG (TqsA) controls biofilm formation in *Escherichia coli* K-12 through autoinducer 2 transport." *J Bacteriol* 188(2): 587-598.
- Hjelm, M., Bergh, O., Riaza, A., Nielsen, J., Melchiorsen, J., Jensen, S., Duncan, H., Ahrens, P., Birkbeck, H. and Gram, L. (2004). "Selection and identification of autochthonous potential probiotic bacteria from turbot larvae (*Scophthalmus maximus*) rearing units." *Syst Appl Microbiol* 27(3): 360-371.
- Hoang, T. T., Karkhoff-Schweizer, R. R., Kutchma, A. J. and Schweizer, H. P. (1998). "A broad-host-range Flp-FRT recombination system for site-specific excision of chromosomally-located DNA sequences: application for isolation of unmarked *Pseudomonas aeruginosa* mutants." *Gene* 212(1): 77-86.
- Hollants, J., Leliaert, F., De Clerck, O. and Willems, A. (2013). "What we can learn from sushi: a review on seaweed-bacterial associations." *FEMS Microbiol Ecol* 83(1): 1-16.
- Holmström, C., James, S., Egan, S. and Kjelleberg, S. (1996). "Inhibition of common fouling organisms by marine bacterial isolates with special reference to the role of pigmented bacteria." *Biofouling* 10(1-3): 251-259.
- Huang, Y. L., Ki, J. S., Lee, O. O. and Qian, P. Y. (2009). "Evidence for the dynamics of acyl homoserine lactone and AHL-producing bacteria during subtidal biofilm formation." *ISME J* 3(3): 296-304.
- Hudson, J., Gardiner, M., Deshpande, N. and Egan, S. (2018). "Transcriptional response of *Nautella italica* R11 towards its macroalgal host uncovers new mechanisms of host-pathogen interaction." *Mol Ecol* 27(8): 1820-1832.
- Huerta-Cepas, J., Forslund, K., Coelho, L. P., Szklarczyk, D., Jensen, L. J., von Mering, C. and Bork, P. (2017). "Fast genome-wide functional annotation through orthology assignment by eggNOG-mapper." *Mol Biol Evol* 34(8): 2115-2122.
- Huo, Y. Y., Li, Z. Y., You, H., Wang, C. S., Post, A. F., Oren, A. and Xu, X. W. (2014). "*Oceanicola antarcticus* sp. nov. and *Oceanicola flagellatus* sp. nov., moderately halophilic bacteria isolated from seawater." *Int J Syst Evol Microbiol* 64: 2975-2979.
- Imbs, T. I., P., K. N., Ermakova, S. P., Makarieva, T. N., Shevchenko, N. M. and Zvyagintseva, T. N. (2009). "Comparative study of chemical composition and antitumor activity of aqueous-ethanol extracts of brown algae *Laminaria cichorioides*, *Costaria costata*, and *Fucus evanescens*." *Russ J Mar Biol* 35(2): 164-170.
- Inoue, A., Nishiyama, R., Mochizuki, S. and Ojima, T. (2015). "Identification of a 4-deoxy-L-erythro-5-hexoseulose uronic acid reductase, FIRed, in an alginolitic bacterium *Flavobacterium* sp. strain UMI-01." *Mar Drugs* 13(1): 493-508.
- Jerković, I., Marijanovic, Z., Roje, M., Kus, P. M., Jokic, S. and Coz-Rakovac, R. (2018). "Phytochemical study of the headspace volatile organic compounds of fresh algae and seagrass from the Adriatic Sea (single point collection)." *PLoS One* 13(5): e0196462.
- Johnson, W. M., Soule, M. C. K. and Kujawinski, E. B. (2016). "Evidence for quorum sensing and differential metabolite production by a marine bacterium in response to DMSP." *ISME J* 10(9): 2304-2316.
- Joint, I., Tait, K., Callow, M. E., Callow, J. A., Milton, D., Williams, P. and Camara, M. (2002). "Cell-to-cell communication across the prokaryote-eukaryote boundary." *Science* 298(5596): 1207.
- Juhas, M., van der Meer, J. R., Gaillard, M., Harding, R. M., Hood, D. W. and Crook, D. W. (2009). "Genomic islands: tools of bacterial horizontal gene transfer and evolution." *FEMS Microbiol Rev* 33(2): 376-393.
- Junker, R. R. and Tholl, D. (2013). "Volatile organic compound mediated interactions at the plant-microbe interface." *J Chem Ecol* 39(7): 810-825.
- Kalhoefer, D., Thole, S., Voget, S., Lehmann, R., Liesegang, H., Wollher, A., Daniel, R., Simon, M. and Brinkhoff, T. (2011). "Comparative genome analysis and genome-guided physiological analysis of *Roseobacter litoralis*." *Bmc Genomics* 12: 324.
- Kalia, V. C., Wood, T. K. and Kumar, P. (2014). "Evolution of resistance to quorum-sensing inhibitors." *Microb Ecol* 68(1): 13-23.
- Karim, M., Zhao, W., Nelson, D. R., Rowley, D. and Gomez-Chiarri, M. (2013). "Probiotic strains for shellfish aquaculture: protection of Eastern Oyster, *Crassostrea virginica*, larvae and juveniles against bacterial challenge." *J Shell Res* 32(2): 401-408.
- Keshtacher-Liebson, E., Hadar, Y. and Chen, Y. (1995). "Oligotrophic bacteria enhance algal growth under iron-deficient conditions." *Appl Environ Microbiol* 61(6): 2439-2441.
- Kim, J. and Park, W. (2013). "Indole inhibits bacterial quorum sensing signal transmission by interfering with quorum sensing regulator folding." *Microbiology* 159(12): 2616-2625.
- Kisand, V., Røcker, D. and Simon, M. (2008). "Significant decomposition of riverine humic-rich DOC by marine but not estuarine bacteria assessed in sequential chemostat experiments." *Aquat Microb Ecol* 53(2): 151-160.
- Klindukh, M. P., Obluchinskaya, E. and Matishov, G. G. (2011). "Seasonal changes in the mannitol and proline contents of the brown alga *Fucus vesiculosus* L. on the Murman coast of the Barents Sea." *Dokl Biol Sci* 441: 373-376.
- Klotz, F., Brinkhoff, T., Freese, H. M., Wietz, M., Teske, A., Simon, M. and Giebel, H. A. (2018). "*Tritonibacter horizontalis* gen. nov., sp. nov., a member of the *Rhodobacteraceae*, isolated from the Deepwater Horizon oil spill." *Int J Syst Evol Microbiol* 68(3): 736-744.
- Kovach, M. E., Elzer, P. H., Hill, D. S., Robertson, G. T., Farris, M. A., Roop, R. M. and Peterson, K. M. (1995). "4 new derivatives of the broad-host-range cloning vector pBBR1MCS, carrying different antibiotic-resistance cassettes." *Gene* 166(1): 175-176.

- Kuchma, S. L. and O'Toole, G. A. (2000). "Surface-induced and biofilm-induced changes in gene expression." Curr Opin Biotechnol 11(5): 429-433.
- Labourel, A., Jam, M., Legentil, L., Sylla, B., Hehemann, J. H., Ferrieres, V., Czjzek, M. and Michel, G. (2015). "Structural and biochemical characterization of the laminarinase ZgLamCGH16 from *Zobellia galactanivorans* suggests preferred recognition of branched laminarin." Acta Crystallogr D Biol Crystallogr 71(Pt 2): 173-184.
- Lachnit, T., Meske, D., Wahl, M., Harder, T. and Schmitz, R. (2011). "Epibacterial community patterns on marine macroalgae are host-specific but temporally variable." Environ Microbiol 13(3): 655-665.
- Laganenka, L., Colin, R. and Sourjik, V. (2016). "Chemotaxis towards autoinducer 2 mediates autoaggregation in *Escherichia coli*" Nat Commun 7: 12984.
- Landa, M., Blain, S., Christaki, U., Monchy, S. and Obernosterer, I. (2016). "Shifts in bacterial community composition associated with increased carbon cycling in a mosaic of phytoplankton blooms." ISME J 10(1): 39-50.
- Lang, A. S., Westbye, A. B. and Beatty, J. T. (2017). "The distribution, evolution, and roles of gene transfer agents in prokaryotic genetic exchange." Annu Rev Virol 4: 87-104.
- Langmead, B. and Salzberg, S. L. (2012). "Fast gapped-read alignment with Bowtie 2." Nat Methods 9(4): 357-U354.
- Langmead, B. and Salzberg, S. L. (2012). "Fast gapped-read alignment with Bowtie 2." Nature methods 9(4): 357-359.
- Laub, M. T., Chen, S. L., Shapiro, L. and McAdams, H. H. (2002). "Genes directly controlled by CtrA, a master regulator of the *Caulobacter* cell cycle." Proc Natl Acad Sci USA 99(7): 4632-4637.
- Lee, J., Jayaraman, A. and Wood, T. K. (2007). "Indole is an inter-species biofilm signal mediated by SdiA." BMC Microbiology 7(1): 42.
- Legerski, R. J. and Robberson, D. L. (1985). "Analysis and optimization of recombinant DNA joining reactions." J Mol Biol 181(2): 297-312.
- Li, H., Handsaker, B., Wysoker, A., Fennell, T., Ruan, J., Homer, N., Marth, G., Abecasis, G., Durbin, R. and Proc, G. P. D. (2009). "The Sequence Alignment/Map format and SAMtools." Bioinformatics 25(16): 2078-2079.
- Li, L., Rock, J. L. and Nelson, D. R. (2008). "Identification and characterization of a repeat-in-toxin gene cluster in *Vibrio anguillarum*." Infect Immun 76(6): 2620-2632.
- Li, Y. H., Lau, P. C., Lee, J. H., Ellen, R. P. and Cvikovitch, D. G. (2001). "Natural genetic transformation of *Streptococcus mutans* growing in biofilms." J Bacteriol 183(3): 897-908.
- Linares, J. F., Gustafsson, I., Baquero, F. and Martinez, J. L. (2006). "Antibiotics as intermicrobial signaling agents instead of weapons." Proc Natl Acad Sci USA 103(51): 19484-19489.
- Lombard, V., Ramulu, H. G., Drula, E., Coutinho, P. M. and Henrissat, B. (2014). "The carbohydrate-active enzymes database (CAZy) in 2013." Nucleic Acids Res 42(1): 490-495.
- Long, R. A. and Azam, F. (2001). "Antagonistic interactions among marine pelagic bacteria." Appl Environ Microbiol 67(11): 4975-4983.
- Ludwig, W., Strunk, O., Westram, R., Richter, L., Meier, H., Yadhukumar, Buchner, A., Lai, T., Steppi, S., Jobb, G., Forster, W., Brettske, I., Gerber, S., Ginhart, A. W., Gross, O., Grumann, S., Hermann, S., Jost, R., Konig, A., Liss, T., Lussmann, R., May, M., Nonhoff, B., Reichel, B., Strehlow, R., Stamatakis, A., Stuckmann, N., Vilbig, A., Lenke, M., Ludwig, T., Bode, A. and Schleifer, K. H. (2004). "ARB: a software environment for sequence data." Nucleic Acids Res 32(4): 1363-1371.
- Lüning, K. (1979). "Growth strategies of three *Laminaria* species (*Phaeophyceae*) inhabiting different depth zones in the sublittoral region of Helgoland (North Sea)." Mar Ecol Prog Ser 1: 195-207.
- Luo, H. W. and Moran, M. A. (2014). "Evolutionary ecology of the marine *Roseobacter* clade." Microbiol Mol Biol Rev 78(4): 573-587.
- Lutz, C., Thomas, T., Steinberg, P., Kjelleberg, S. and Egan, S. (2016). "Effect of interspecific competition on trait variation in *Phaeobacter inhibens* biofilms." Environ Microbiol 18(5): 1635-1645.
- Mabeau, S. and Kloareg, B. (1987). "Isolation and analysis of the cell walls of brown algae - *Fucus spiralis*, *Fucus ceranoides*, *Fucus vesiculosus*, *Fucus serratus*, *Bifurcaria bifurcata* and *Laminaria digitata*." J Exp Bot 38(194): 1573-1580.
- Madsen, T. V. and Maberly, S. C. (1990). "A comparison of air and water as environments for photosynthesis by the intertidal alga *Fucus spiralis* (*Phaeophyta*)." J Phycol 26(1): 24-30.
- Martens, J. H., Barg, H., Warren, M. and Jahn, D. (2002). "Microbial production of vitamin B₁₂." Appl Microbiol Biot 58(3): 275-285.
- Martens, T., Gram, L., Grossart, H. P., Kessler, D., Muller, R., Simon, M., Wenzel, S. C. and Brinkhoff, T. (2007). "Bacteria of the *Roseobacter* clade show potential for secondary metabolite production." Microb Ecol 54(1): 31-42.
- Martens, T., Heidorn, T., Pukall, R., Simon, M., Tindall, B. J. and Brinkhoff, T. (2006). "Reclassification of *Roseobacter gallaeciensis* Ruiz-Ponte et al. 1998 as *Phaeobacter gallaeciensis* gen. nov., comb. nov., description of *Phaeobacter inhibens* sp nov., reclassification of *Ruegeria algicola* (Lafay et al. 1995) Uchino et al 1999 as *Marinovum algicola* gen. nov., comb. nov., and emended descriptions of the genera *Roseobacter*, *Ruegeria* and *Leisingera*." Int J Syst Evol Microbiol 56: 1293-1304.
- Martin, M. (2011). "Cutadapt removes adapter sequences from high-throughput sequencing reads." EMBnet journal 17: 10-12.
- McDougald, D. and Kjelleberg, S. (2006). Adaptive responses of vibrios. The Biology of Vibrios, American Society of Microbiology.

- Meier-Kolthoff, J. P., Auch, A. F., Klenk, H. P. and Goker, M. (2013). "Genome sequence-based species delimitation with confidence intervals and improved distance functions." *Bmc Bioinformatics* 14: 60.
- Meldau, D. G., Meldau, S., Hoang, L. H., Underberg, S., Wunsche, H. and Baldwin, I. T. (2013). "Dimethyl disulfide produced by the naturally associated bacterium *Bacillus* sp B55 promotes *Nicotiana attenuata* growth by enhancing sulfur nutrition." *Plant Cell* 25(7): 2731-2747.
- Mesibov, R., Ordal, G. W. and Adler, J. (1973). "Range of attractant concentrations for bacterial chemotaxis and threshold and size of response over this range - Weber Law and related phenomena." *J Gen Physiol* 62(2): 203-223.
- Messing, J. (1983). "New M13 Vectors for Cloning." *Method Enzymol* 101: 20-78.
- Michel, G., Tonon, T., Scornet, D., Cock, J. and Kloareg, B. (2010). "The cell wall polysaccharide metabolism of the brown alga *Ectocarpus siliculosus*. Insights into the evolution of extracellular matrix polysaccharides in Eukaryotes." *New Phytol* 188(1): 82-97.
- Miller, M. A., Pfeiffer, W. and Schwartz, T. (2010). Creating the CIPRES science gateway for inference of large phylogenetic trees. 2010 Gateway Computing Environments Workshop (GCE).
- Miller, T. R., Hnilicka, K., Dziedzic, A., Desplats, P. and Belas, R. (2004). "Chemotaxis of *Silicibacter* sp. strain TM1040 toward dinoflagellate products." *Appl Environ Microbiol* 70(8): 4692-4701.
- Moran, M. A., Belas, R., Schell, M. A., Gonzalez, J. M., Sun, F., Sun, S., Binder, B. J., Edmonds, J., Ye, W., Orcutt, B., Howard, E. C., Meile, C., Palefsky, W., Goesmann, A., Ren, Q., Paulsen, I., Ulrich, L. E., Thompson, L. S., Saunders, E. and Buchan, A. (2007). "Ecological genomics of marine Roseobacters." *Appl Environ Microbiol* 73(14): 4559-4569.
- Moran, M. A., Reisch Cr Fau - Kiene, R. P., Kiene Rp Fau - Whitman, W. B. and Whitman, W. B. (2012). "Genomic insights into bacterial DMSP transformations." *Ann Rev Mar, Sci*(1941-1405 (Print)).
- Moriya, Y., Itoh, M., Okuda, S., Yoshizawa, A. C. and Kanehisa, M. (2007). "KAAS: an automatic genome annotation and pathway reconstruction server." *Nucleic Acids Res* 35: 182-185.
- Mortazavi, A., Williams, B. A., McCue, K., Schaeffer, L. and Wold, B. (2008). "Mapping and quantifying mammalian transcriptomes by RNA-Seq." *Nature methods* 5(7): 621-628.
- Mueller, R. S., Beyhan, S., Saini, S., H Yildiz, F. and Bartlett, D. (2009). Indole acts as an extracellular cue regulating gene expression in *Vibrio cholerae*.
- Muyzer, G., de Waal, E. C. and Uitterlinden, A. G. (1993). "Profiling of complex microbial populations by denaturing gradient gel electrophoresis analysis of polymerase chain reaction-amplified genes coding for 16S rRNA." *Appl Environ Microbiol* 59(3): 695-700.
- Muyzer, G. and Smalla, K. (1998). "Application of denaturing gradient gel electrophoresis (DGGE) and temperature gradient gel electrophoresis (TGGE) in microbial ecology." *Antonie Van Leeuwenhoek* 73(1): 127-141.
- Muyzer, G., Teske, A., Wirsén, C. O. and Jannasch, H. W. (1995). "Phylogenetic-relationships of *Thiomicrospira* species and their identification in Deep Sea hydrothermal vent samples by denaturing gradient gel electrophoresis of 16S rDNA fragments." *Arch Microbiol* 164(3): 165-172.
- Na, S. I., Kim, Y. O., Yoon, S. H., Ha, S. M., Baek, I. and Chun, J. (2018). "UBCG: Up-to-date bacterial core gene set and pipeline for phylogenomic tree reconstruction." *J Microbiol* 56(4): 280-285.
- Nagy, K., Sipos, O., Valkai, S., Gombai, E., Hodula, O., Kerényi, A., Ormos, P. and Galajda, P. (2015). "Microfluidic study of the chemotactic response of *Escherichia coli* to amino acids, signaling molecules and secondary metabolites." *Biomicrofluidics* 9(4): 044105.
- Neuhaus, F. C. and Baddiley, J. (2003). "A continuum of anionic charge: structures and functions of D-alanyl-teichoic acids in gram-positive bacteria." *Microbiol Mol Biol Rev* 67(4): 686-723.
- Neumann, A., Patzelt, D., Wagner-Dobler, I. and Schulz, S. (2013). "Identification of new *N*-acylhomoserine lactone signalling compounds of *Dinoroseobacter shibae* DFL-12(T) by overexpression of luxI genes." *Chembiochem* 14(17): 2355-2361.
- Newton, R. J., Griffin, L. E., Bowles, K. M., Meile, C., Gifford, S., Givens, C. E., Howard, E. C., King, E., Oakley, C. A., Reisch, C. R., Rinta-Kanto, J. M., Sharma, S., Sun, S., Varaljay, V., Vila-Costa, M., Westrich, J. R. and Moran, M. A. (2010). "Genome characteristics of a generalist marine bacterial lineage." *ISME J* 4(6): 784-798.
- North, R. A., Horne, C. R., Davies, J. S., Remus, D. M., Muscroft-Taylor, A. C., Goyal, P., Wahlgren, W. Y., Ramaswamy, S., Friemann, R. and Dobson, R. C. J. (2018). "'Just a spoonful of sugar...': import of sialic acid across bacterial cell membranes." *Biophys Rev* 10(2): 219-227.
- Nykyri, J., Mattinen, L., Niemi, O., Adhikari, S., Koiv, V., Somervuo, P., Fang, X., Auvinen, P., Mae, A., Palva, E. T. and Pirhonen, M. (2013). "Role and regulation of the Flp/Tad pilus in the virulence of *Pectobacterium atrosepticum* SCRI1043 and *Pectobacterium wasabiae* SCC3193." *PloS One* 8(9): e73718.
- Ochiai, A., Yamasaki, M., Mikami, B., Hashimoto, W. and Murata, K. (2010). "Crystal structure of exotype alginate lyase Atu3025 from *Agrobacterium tumefaciens*." *J Biol Chem* 285(32): 24519-24528.
- Oliveira, N. M., Martinez-Garcia, E., Xavier, J., Durham, W. M., Kolter, R., Kim, W. and Foster, K. R. (2015). "Biofilm formation as a response to ecological competition." *PloS Biol* 13(7): e1002191.
- Palmer, R. J., Kazmerzak, K., Hansen, M. C. and Kolenbrander, P. E. (2001). "Mutualism versus independence: Strategies of mixed-species oral biofilms *in vitro* using saliva as the sole nutrient source." *Infect Immun* 69(9): 5794-5804.
- Pan, J. J., Solbiati, J. O., Ramamoorthy, G., Hillerich, B. S., Seidel, R. D., Cronan, J. E., Almo, S. C. and Poulter, C. D. (2015). "Biosynthesis of squalene from farnesyl diphosphate in bacteria: three steps catalyzed by three enzymes." *Acs Central Sci* 1(2): 77-82.

- Parks, D. H., Imelfort, M., Skennerton, C. T., Hugenholtz, P. and Tyson, G. W. (2015). "CheckM: assessing the quality of microbial genomes recovered from isolates, single cells, and metagenomes." Genome Res 25(7): 1043-1055.
- Patzelt, D., Michael, V., Pauker, O., Ebert, M., Tielen, P., Jahn, D., Tomasch, J., Petersen, J. and Wagner-Döbler, I. (2016). "Gene flow across genus barriers - conjugation of *Dinoroseobacter shibae*'s 191-kb killer plasmid into *Phaeobacter inhibens* and AHL-mediated expression of type IV secretion systems." Front Microbiol 7: 742.
- Patzelt, D., Wang, H., Buchholz, I., Rohde, M., Groebe, L., Pradella, S., Neumann, A., Schulz, S., Heyber, S., Münch, K., Münch, R., Jahn, D., Wagner-Döbler, I. and Tomasch, J. (2013). "You are what you talk: quorum sensing induces individual morphologies and cell division modes in *Dinoroseobacter shibae*." ISME J 7(12): 2274-2286.
- Paul, J. H. (2008). "Prophages in marine bacteria: dangerous molecular time bombs or the key to survival in the seas?" ISME J 2(6): 579-589.
- Penesyan, A., Breider, S., Schumann, P., Tindall, B. J., Egan, S. and Brinkhoff, T. (2013). "*Epibacterium ulvae* gen. nov., sp. nov., epibiotic bacteria isolated from the surface of a marine alga." Int J Syst Evol Microbiol 63(Pt 5): 1589-1596.
- Penesyan, A., Tebben, J., Lee, M., Thomas, T., Kjelleberg, S., Harder, T. and Egan, S. (2011). "Identification of the antibacterial compound produced by the marine epiphytic bacterium *Pseudovibrio* sp. D323 and related sponge-associated bacteria." Mar Drugs 9(8): 1391-1402.
- Percy, M. G. and Grundling, A. (2014). "Lipoteichoic acid synthesis and function in gram-positive bacteria." Annu Rev Microbiol 68: 81-100.
- Pereira, C. S., de Regt, A. K., Brito, P. H., Miller, S. T. and Xavier, K. B. (2009). "Identification of functional LsrB-like autoinducer-2 receptors." J Bacteriol 191(22): 6975-6987.
- Petersen, J., Frank, O., Goker, M. and Pradella, S. (2013). "Extrachromosomal, extraordinary and essential-the plasmids of the *Roseobacter* clade." Appl Microbiol Biot 97(7): 2805-2815.
- Petersen, J. and Wagner-Döbler, I. (2017). "Plasmid Transfer in the Ocean - A Case Study from the *Roseobacter* Group." Front Microbiol 8: 1350.
- Philippot, L., Raaijmakers, J. M., Lemanceau, P. and van der Putten, W. H. (2013). "Going back to the roots: the microbial ecology of the rhizosphere." Nat Rev Microbiol 11(11): 789-799.
- Piccoli, P. and Bottini, R. (2013). Terpene production by bacteria and its involvement in plant growth promotion, stress alleviation and yield increase. Molecular Microbial Ecology of the Rhizosphere. F. J. de Bruijn, John Wiley & Sons, Inc.: 335-343.
- Pinchuk, G. E., Ammons, C., Culley, D. E., Li, S. M. W., McLean, J. S., Romine, M. F., Neelson, K. H., Fredrickson, J. K. and Beliaev, A. S. (2008). "Utilization of DNA as a sole source of phosphorus, carbon, and energy by *Shewanella* spp.: ecological and physiological implications for dissimilatory metal reduction." Appl Environ Microbiol 74(4): 1198-1208.
- Planas, M., Perez-Lorenzo, M., Hjelm, M., Gram, L., Fiksdal, I. U., Bergh, O. and Pintado, J. (2006). "Probiotic effect in vivo of *Roseobacter* strain 27-4 against *Vibrio (Listonella) anguillarum* infections in turbot (*Scophthalmus maximus* L.) larvae." Aquaculture 255(1-4): 323-333.
- Porsby, C. H. and Gram, L. (2016). "*Phaeobacter inhibens* as biocontrol agent against *Vibrio vulnificus* in oyster models." Food Microbiol 57: 63-70.
- Porsby, C. H., Nielsen, K. F. and Gram, L. (2008). "*Phaeobacter* and *Ruegeria* species of the *Roseobacter* clade colonize separate niches in a Danish Turbot (*Scophthalmus maximus*)-rearing farm and antagonize *Vibrio anguillarum* under different growth conditions." Appl Environ Microbiol 74(23): 7356-7364.
- Porsby, C. H., Webber, M. A., Nielsen, K. F., Piddock, L. J. and Gram, L. (2011). "Resistance and tolerance to tropodithetic acid, an antimicrobial in aquaculture, is hard to select." Antimicrob Agents Chemother 55: 1332-1337.
- Powell, J. H. and Meeuse, B. J. D. (1964). "Laminarin in some *Phaeophyta* of the Pacific coast." Econ Bot 18(2): 164-166.
- Pujalte, M. J., Lucena, T., Ruvira, M. A., Arahál, D. R. and Macián, M. C. (2014). The Family *Rhodobacteraceae*. The Prokaryotes: Alphaproteobacteria and Betaproteobacteria. E. Rosenberg, E. F. DeLong, S. Lory, E. Stackebrandt and F. Thompson. Berlin, Heidelberg, Springer Berlin Heidelberg: 439-512.
- Quast, C., Priesse, E., Yilmaz, P., Gerken, J., Schweer, T., Yarza, P., Peplies, J. and Glöckner, F. (2012). "The SILVA ribosomal RNA gene database project: Improved data processing and web-based tools." Nucleic Acids Res 41: 590-596.
- Que, Y. A., Hazan, R., Strobel, B., Maura, D., He, J. X., Kesarwani, M., Panopoulos, P., Tsurumi, A., Giddey, M., Wilhelmy, J., Mindrinos, M. N. and Rahme, L. G. (2013). "A quorum sensing small volatile molecule promotes antibiotic tolerance in bacteria." PLoS One 8(12): 1-9.
- R Core Team (2018). "R: A language and environment for statistical computing." R Foundation for Statistical Computing, Vienna, Austria.
- Rader, B. A., Wreden, C., Hicks, K. G., Sweeney, E. G., Ottemann, K. M. and Guillemin, K. (2011). "*Helicobacter pylori* perceives the quorum-sensing molecule AI-2 as a chemorepellent via the chemoreceptor TlpB." Microbiol-Sgm 157: 2445-2455.
- Rao, D., Webb, J. S., Holmstrom, C., Case, R., Low, A., Steinberg, P. and Kjelleberg, S. (2007). "Low densities of epiphytic bacteria from the marine alga *Ulva australis* inhibit settlement of fouling organisms." Appl Environ Microbiol 73(24): 7844-7852.
- Rao, D., Webb, J. S. and Kjelleberg, S. (2005). "Competitive interactions in mixed-species biofilms containing the marine bacterium *Pseudoalteromonas tunicata*." Appl Environ Microbiol 71(4): 1729-1736.

- Rao, D., Webb, J. S. and Kjelleberg, S. (2006). "Microbial colonization and competition on the marine alga *Ulva australis*." *Appl Environ Microbiol* 72(8): 5547-5555.
- Raymond, K. N., Dertz, E. A. and Kim, S. S. (2003). "Enterobactin: An archetype for microbial iron transport." *Proc Natl Acad Sci USA* 100(7): 3584-3588.
- Reed, R. H., Davison, I. R., Chudek, J. A. and Foster, R. (1985). "The osmotic role of mannitol in the *Phaeophyta*: an appraisal." *Phycologia* 24(1): 35-47.
- Reisch, C. R., Moran, M. A. and Whitman, W. B. (2011). "Bacterial catabolism of dimethylsulfoniopropionate (DMSP)." *Front Microbiol* 2: 172.
- Riedel, T., Teshima, H., Petersen, J., Fiebig, A., Davenport, K., Daligault, H., Erkkila, T., Gu, W., Munk, C., Xu, Y., Chen, A., Pati, A., Ivanova, N., Goodwin, L. A., Chain, P., Detter, J. C., Rohde, M., Gronow, S., Kyrpides, N. C., Woyke, T., Goker, M., Brinkhoff, T. and Klenk, H. P. (2013). "Genome sequence of the *Leisingera aquimarinis* type strain (DSM 24565(T)), a member of the marine *Roseobacter* clade rich in extrachromosomal elements." *Stand Genomic Sci* 8(3): 389-402.
- Rink, B., Seeberger, S., Martens, T., Duerselen, C.-D., Simon, M. and Brinkhoff, T. (2007). "Effects of phytoplankton bloom in a coastal ecosystem on the composition of bacterial communities." *Aquat Microb Ecol* 48(1): 47-60.
- Robinson, M. D., McCarthy, D. J. and Smyth, G. K. (2010). "edgeR: a Bioconductor package for differential expression analysis of digital gene expression data." *Bioinformatics* 26(1): 139-140.
- Rocker, D., Brinkhoff, T., Gruner, N., Dogs, M. and Simon, M. (2012). "Composition of humic acid-degrading estuarine and marine bacterial communities." *FEMS Microbiol Ecol* 80(1): 45-63.
- Rodriguez-R, L. and Konstantinidis, K. (2014). "Bypassing cultivation to identify bacterial species." *Microbe Magazine* 9(3): 111-118.
- Rodriguez-R, L. and Konstantinidis, K. (2016). "The enveomics collection: a toolbox for specialized analyses of microbial genomes and metagenomes." *PeerJ Preprints* 4.
- Romero, D., Traxler, M. F., Lopez, D. and Kolter, R. (2011). "Antibiotics as signal molecules." *Chem Rev* 111(9): 5492-5505.
- Ruiz-Ponte, C., Cilia, V., Lambert, C. and Nicolas, J. L. (1998). "*Roseobacter gallaeciensis* sp. nov., a new marine bacterium isolated from rearings and collectors of the scallop *Pecten maximus*." *Int J Syst Bacteriol* 48: 537-542.
- Saha, M. and Wahl, M. (2013). "Seasonal variation in the antifouling defence of the temperate brown alga *Fucus vesiculosus*." *Biofouling* 29(6): 661-668.
- Sañudo-Wilhelmy, S. A., Gomez-Consarnau, L., Suffridge, C. and Webb, E. A. (2014). "The role of B vitamins in marine biogeochemistry." *Ann Rev Mar Sci* 6: 339-367.
- Schaefer, A. L., Taylor, T. A., Beatty, J. T. and Greenberg, E. P. (2002). "Long-chain acyl-homoserine lactone quorum-sensing regulation of *Rhodobacter capsulatus* gene transfer agent production." *J Bacteriol* 184(23): 6515-6521.
- Schaub, P., Yu, Q. J., Gemmecker, S., Poussin-Courmontagne, P., Mailliot, J., McEwen, A. G., Ghisla, S., Al-Babili, S., Cavarelli, J. and Beyer, P. (2012). "On the structure and function of the phytoene desaturase CRTI from *Pantoea ananatis*, a membrane-peripheral and FAD-dependent oxidase/isomerase." *PLoS One* 7(6): e39550.
- Schulz-Bohm, K., Martin-Sanchez, L. and Garbeva, P. (2017). "Microbial volatiles: small molecules with an important role in intra- and inter-kingdom interactions." *Front Microbiol* 8: 2484.
- Schulz, S., Fuhlendorff, J., Steidle, J. L. M., Collatz, J. and Franz, J. T. (2004). "Identification and biosynthesis of an aggregation pheromone of the storage mite *Chortoglyphus arcuatus*." *Chembiochem* 5(11): 1500-1507.
- Schwedt, A. (2011). "Physiology of a marine *Beggiatoa* strain and the accompanying organism *Pseudovibrio* sp. - a facultatively oligotrophic bacterium." *PhD Thesis, University of Bremen, Germany*.
- Seemann, T. (2014). "Prokka: rapid prokaryotic genome annotation." *Bioinformatics* 30(14): 2068-2069.
- Segev, E., Tellez, A., Vlamakis, H. and Kolter, R. (2015). "Morphological heterogeneity and attachment of *Phaeobacter inhibens*." *PLoS One* 10(11): e0141300.
- Segev, E., Wyche, T. P., Kim, K. H., Petersen, J., Ellebrandt, C., Vlamakis, H., Barteneva, N., Paulson, J. N., Chai, L., Clardy, J. and Kolter, R. (2016). "Dynamic metabolic exchange governs a marine algal-bacterial interaction." *eLife* 5: e17473.
- Selje, N., Simon, M. and Brinkhoff, T. (2004). "A newly discovered *Roseobacter* cluster in temperate and polar oceans." *Nature* 427(6973): 445-448.
- Seyedsayamdost, M., Case, R., Kolter, R. and Clardy, J. (2011). "The Jekyll-and-Hyde chemistry of *Phaeobacter gallaeciensis*." *Nat Chem* 3(4): 331-335.
- Seymour, J. R., Amin, S. A., Raina, J. B. and Stocker, R. (2017). "Zooming in on the phycosphere: the ecological interface for phytoplankton-bacteria relationships." *Nat Microbiol* 2(7): e17065.
- Seymour, J. R., Simo, R., Ahmed, T. and Stocker, R. (2010). "Chemoattraction to dimethylsulfoniopropionate throughout the marine microbial food web." *Science* 329(5989): 342-345.
- Shannon, C. E. (2001). "A mathematical theory of communication." *SIGMOBILE Mob. Comput. Commun. Rev.* 5(1): 3-55.
- Shin, S. H., Lim, Y., Lee, S. E., Yang, N. W. and Rhee, J. H. (2001). "CAS agar diffusion assay for the measurement of siderophores in biological fluids." *J Microbiol Methods* 44(1): 89-95.
- Silpe, J. E. and Bassler, B. L. (2019). "A host-produced quorum-sensing autoinducer controls a phage lysis-lysogeny decision." *Cell* 176(1-2): 268-280.

- Simon, M., Scheuner, C., Meier-Kolthoff, J. P., Brinkhoff, T., Wagner-Dobler, I., Ulbrich, M., Klenk, H.-P., Schomburg, D., Petersen, J. and Goker, M. (2017). "Phylogenomics of *Rhodobacteraceae* reveals evolutionary adaptation to marine and non-marine habitats." *ISME J* 11(6): 1483-1499.
- Singh, R. P. and Reddy, C. R. K. (2014). "Seaweed-microbial interactions: key functions of seaweed-associated bacteria." *FEMS Microbiol Ecol* 88(2): 213-230.
- Slightom, R. N. and Buchan, A. (2009). "Surface colonization by marine roseobacters: integrating genotype and phenotype." *Appl Environ Microbiol* 75(19): 6027-6037.
- Sonnenschein, E. C., Nielsen, K. F., D'Alvise, P., Porsby, C. H., Melchiorson, J., Heilmann, J., Kalatzis, P. G., Lopez-Perez, M., Bunk, B., Sproer, C., Middelboe, M. and Gram, L. (2017). "Global occurrence and heterogeneity of the *Roseobacter*-clade species *Ruegeria mobilis*." *ISME J* 11(2): 569-583.
- Soria-Dengg, S., Reissbrodt, R. and Horstmann, U. (2001). "Siderophores in marine, coastal waters and their relevance for iron uptake by phytoplankton: experiments with the diatom *Phaeodactylum tricorutum*." *Mar Ecol Prog Ser* 220: 73-82.
- Stackebrandt, E. and Goebel, B. M. (1994). "A place for DNA-DNA reassociation and 16S ribosomal RNA sequence analysis in the present species definition in bacteriology." *Int J Syst Bacteriol* 44(4): 846-849.
- Stamatakis, A. (2014). "RAxML version 8: a tool for phylogenetic analysis and post-analysis of large phylogenies." *Bioinformatics* 30(9): 1312-1313.
- Staufenberger, T., Thiel, V., Wiese, J. and Imhoff, J. F. (2008). "Phylogenetic analysis of bacteria associated with *Laminaria saccharina*." *FEMS Microbiol Ecol* 64(1): 65-77.
- Steinberg, P. D. (1988). "Effects of quantitative and qualitative variation in phenolic compounds on feeding in 3 species of marine invertebrate herbivores." *J Exp Mar Biol Ecol* 120(3): 221-237.
- Stocker, R. (2012). "Marine microbes see a sea of gradients." *Science* 338(6107): 628-633.
- Stratil, S. B., Neulinger, S. C., Knecht, H., Friedrichs, A. K. and Wahl, M. (2013). "Temperature-driven shifts in the epibiotic bacterial community composition of the brown macroalga *Fucus vesiculosus*." *Microbiology* 2(2): 338-349.
- Subramenium, G. A., Vijayakumar, K. and Pandian, S. K. (2015). "Limonene inhibits streptococcal biofilm formation by targeting surface-associated virulence factors." *J Med Microbiol* 64: 879-890.
- Suzuki, R. and Shimodaira, H. (2006). "Pvclust: an R package for assessing the uncertainty in hierarchical clustering." *Bioinformatics* 22(12): 1540-1542.
- Tang, L., Schramm, A., Neu, T. R., Revsbech, N. P. and Meyer, R. L. (2013). "Extracellular DNA in adhesion and biofilm formation of four environmental isolates: a quantitative study." *FEMS Microbiol Ecol* 86(3): 394-403.
- Tappin, A. D. and Millward, G. E. (2015). "The English Channel: contamination status of its transitional and coastal waters." *Mar Pollut Bull* 95(2): 529-550.
- Teeling, H., Fuchs, B. M., Becher, D., Klockow, C., Gardebrecht, A., Bennis, C. M., Kassabgy, M., Huang, S., Mann, A. J., Waldmann, J., Weber, M., Klindworth, A., Otto, A., Lange, J., Bernhardt, J., Reinsch, C., Hecker, M., Peplies, J., Bockelmann, F. D., Callies, U., Gerdts, G., Wichels, A., Wiltshire, K. H., Glockner, F. O., Schweder, T. and Amann, R. (2012). "Substrate-controlled succession of marine bacterioplankton populations induced by a phytoplankton bloom." *Science* 336(6081): 608-611.
- Theodore, T. S. and Calandra, G. B. (1981). "Streptolysin S activation by lipoteichoic acid." *Infect Immun* 33(1): 326-328.
- Thiel, V., Brinkhoff, T., Dickschat, J. S., Wickel, S., Grunenberg, J., Wagner-Dobler, I., Simon, M. and Schulz, S. (2010). "Identification and biosynthesis of tropone derivatives and sulfur volatiles produced by bacteria of the marine *Roseobacter* clade." *Org Biomol Chem* 8(1): 234-246.
- Thole, S., Kalhoefer, D., Voget, S., Berger, M., Engelhardt, T., Liesegang, H., Wollherr, A., Kjelleberg, S., Daniel, R., Simon, M., Thomas, T. and Brinkhoff, T. (2012). "*Phaeobacter gallaeciensis* genomes from globally opposite locations reveal high similarity of adaptation to surface life." *ISME J* 6(12): 2229-2244.
- Thomas, F., Bordron, P., Eveillard, D. and Michel, G. (2017). "Gene expression analysis of *Zobellia galactanivorans* during the degradation of algal polysaccharides reveals both substrate-specific and shared transcriptome-wide responses." *Front Microbiol* 8: 1808.
- Thomas, S., Holland, I. B. and Schmitt, L. (2014). "The Type 1 secretion pathway - The hemolysin system and beyond." *Bba-Mol Cell Res* 1843(8): 1629-1641.
- Tindall, B. J. (1990). "A comparative study of the lipid composition of *Halobacterium saccharovorum* from various sources." *Syst Appl Microbiol* 13(2): 128-130.
- Tindall, B. J. (1990). "Lipid composition of *Halobacterium lacusprofundi*." *Fems Microbiol Lett* 66(1-3): 199-202.
- Tomasch, J., Wang, H., Hall, A. T. K., Patzelt, D., Preusse, M., Petersen, J., Brinkmann, H., Bunk, B., Bhujji, S., Jarek, M., Geffers, R., Lang, A. S. and Wagner-Dobler, I. (2018). "Packaging of *Dinoroseobacter shibae* DNA into gene transfer agent particles is not random." *Genome Biol Evol* 10(1): 359-369.
- Torti, A., Lever, M. A. and Jorgensen, B. B. (2015). "Origin, dynamics, and implications of extracellular DNA pools in marine sediments." *Mar Genomics* 24(3): 185-196.
- Trautwein, K., Will, S. E., Hulsch, R., Maschmann, U., Wiegmann, K., Hensler, M., Michael, V., Ruppertsberg, H., Wunsch, D., Feenders, C., Neumann-Schaal, M., Kaltenhauser, S., Ulbrich, M., Schmidt-Hohagen, K., Blasius, B., Petersen, J., Schomburg, D. and Rabus, R. (2016). "Native plasmids restrict growth of *Phaeobacter inhibens* DSM 17395." *Environ Microbiol* 18(12): 4817-4829.
- Tsaihong, J. C. and Wennerstrom, D. E. (1983). "Effect of carrier molecules on production and properties of extracellular hemolysin produced by *Streptococcus agalactiae*." *Curr Microbiol* 9: 333-338.
- UniProt Consortium, T. (2018). "UniProt: the universal protein knowledgebase." *Nucleic Acids Res* 46(5): 2699-2699.

- Vasu, K. and Nagaraja, V. (2013). "Diverse functions of restriction-modification systems in addition to cellular defense." *Microbiol Mol Biol Rev* 77(1): 53-72.
- Venturi, V. (2006). "Regulation of quorum sensing in *Pseudomonas*." *FEMS Microbiol Rev* 30(2): 274-291.
- Vignaroli, C., Pasquaroli, S., Citterio, B., Di Cesare, A., Mangiaterra, G., Fattorini, D. and Biavasco, F. (2018). "Antibiotic and heavy metal resistance in enterococci from coastal marine sediment." *Environ Pollut* 237: 406-413.
- Voget, S., Wemheuer, B., Brinkhoff, T., Vollmers, J., Dietrich, S., Giebel, H. A., Beardsley, C., Sardemann, C., Bakenhus, I., Billerbeck, S., Daniel, R. and Simon, M. (2015). "Adaptation of an abundant *Roseobacter* RCA organism to pelagic systems revealed by genomic and transcriptomic analyses." *ISME J* 9(2): 371-384.
- Vorkapic, D., Pressler, K. and Schild, S. (2016). "Multifaceted roles of extracellular DNA in bacterial physiology." *Curr Genet* 62(1): 71-79.
- Wagner-Döbler, I., Ballhausen, B., Berger, M., Brinkhoff, T., Buchholz, I., Bunk, B., Cypionka, H., Daniel, R., Drepper, T., Gerdt, G., Hahnke, S., Han, C., Jahn, D., Kalhoefer, D., Kiss, H., Klenk, H. P., Kyrpides, N., Liebl, W., Liesegang, H., Meincke, L., Pati, A., Petersen, J., Piekarski, T., Pommerenke, C., Pradella, S., Pukall, R., Rabus, R., Stackebrandt, E., Thole, S., Thompson, L., Tielen, P., Tomasch, J., von Jan, M., Wanphrut, N., Wichels, A., Zech, H. and Simon, M. (2010). "The complete genome sequence of the algal symbiont *Dinoroseobacter shibae*: a hitchhiker's guide to life in the sea." *ISME J* 4(1): 61-77.
- Wagner-Döbler, I. and Biebl, H. (2006). "Environmental biology of the marine *Roseobacter* lineage." *Annu Rev Microbiol* 60: 255-280.
- Wagner-Döbler, I., Rheims, H., Felske, A., El-Ghezal, A., Flade-Schröder, D., Laatsch, H., Lang, S., Pukall, R. and Tindall, B. J. (2004). "*Oceanibulbus indolifex* gen. nov., sp. nov., a North Sea *alphaproteobacterium* that produces bioactive metabolites." *Int J Syst Evol Microbiol* 54(4): 1177-1184.
- Wahl, M., Goecke, F., Labes, A., Dobretsov, S. and Weinberger, F. (2012). "The second skin: ecological role of epibiotic biofilms on marine organisms." *Front Microbiol* 3: 292.
- Wang, H., Ziesche, L., Frank, O., Michael, V., Martin, M., Petersen, J., Schulz, S., Wagner-Döbler, I. and Tomasch, J. (2014). "The CtrA phosphorelay integrates differentiation and communication in the marine alphaproteobacterium *Dinoroseobacter shibae*." *Bmc Genomics* 15.
- Wang, R. R., Gallant, E. and Seyedsayamdost, M. R. (2016). "Investigation of the genetics and biochemistry of roseobactin production in the roseobacter clade bacterium *Phaeobacter inhibens*." *Mbio* 7(2).
- Wang, Y. D., Wang, H., Liang, W. L., Hay, A. J., Zhong, Z. T., Kan, B. and Zhu, J. (2013). "Quorum sensing regulatory cascades control *Vibrio fluvialis* pathogenesis." *J Bacteriol* 195(16): 3583-3589.
- Wang, Y. L. and Ruby, E. G. (2011). "The roles of NO in microbial symbioses." *Cell Microbiol* 13(4): 518-526.
- Waters, C. M. and Bassler, B. L. (2005). "Quorum sensing: cell-to-cell communication in bacteria." *Annu Rev Cell Dev Biol* 21: 319-346.
- Wayne, L. G., Brenner, D. J., Colwell, R. R., Grimont, P. A. D., Kandler, O., Krichevsky, M. I., Moore, L. H., Moore, W. E. C., Murray, R. G. E., Stackebrandt, E., Starr, M. P. and Truper, H. G. (1987). "Report of the ad-hoc-committee on reconciliation of approaches to bacterial systematics." *Int J Syst Bacteriol* 37(4): 463-464.
- Wei, J. R., Tsai, Y. H., Horng, Y. T., Soo, P. C., Hsieh, S. C., Hsueh, P. R., Horng, J. T., Williams, P. and Lai, H. C. (2006). "A mobile quorum-sensing system in *Serratia marcescens*." *J Bacteriol* 188(4): 1518-1525.
- Weinberger, F., Beltran, J., Correa, J. A., Lion, U., Pohnert, G., Kumar, N., Steinberg, P., Kloareg, B. and Potin, P. (2007). "Spore release in *Acrochaetium* sp. (*Rhodophyta*) is bacterially controlled." *J Phycol* 43(2): 235-241.
- Wemheuer, B., Gullert, S., Billerbeck, S., Giebel, H. A., Voget, S., Simon, M. and Daniel, R. (2014). "Impact of a phytoplankton bloom on the diversity of the active bacterial community in the southern North Sea as revealed by metatranscriptomic approaches." *FEMS Microbiol Ecol* 87(2): 378-389.
- Westbye, A. B., Beatty, J. T. and Lang, A. S. (2017). "Guaranteeing a captive audience: coordinated regulation of gene transfer agent (GTA) production and recipient capability by cellular regulators." *Curr Opin Microbiol* 38: 122-129.
- Whitehead, N. A., Barnard, A. M. L., Slater, H., Simpson, N. J. L. and Salmond, G. P. C. (2001). "Quorum-sensing in gram-negative bacteria." *FEMS Microbiol Rev* 25(4): 365-404.
- Wietz, M., Gram, L., Jørgensen, B. and Schramm, A. (2010). "Latitudinal patterns in the abundance of major marine bacterioplankton groups." *Aquat Microb Ecol* 61.
- Will, S. E., Neumann-Schaal, M., Heydorn, R. L., Bartling, P., Petersen, J. and Schomburg, D. (2017). "The limits to growth - energetic burden of the endogenous antibiotic tropodithietic acid in *Phaeobacter inhibens* DSM 17395." *PLoS One* 12(5): e0177295.
- Williams, S. G. and Manning, P. A. (1991). "Transcription of the *Vibrio cholerae* haemolysin gene, *hlyA*, and cloning of a positive regulatory locus, *hlyU*." *Mol Microbiol* 5(8): 2031-2038.
- Wilson, G. S., Raftos, D. A. and Nair, S. V. (2011). "Antimicrobial activity of surface attached marine bacteria in biofilms." *Microbiol Res* 166(6): 437-448.
- Wilson, M. Z., Wang, R. R., Gitai, Z. and Seyedsayamdost, M. R. (2016). "Mode of action and resistance studies unveil new roles for tropodithietic acid as an anticancer agent and the gamma-glutamyl cycle as a proton sink." *Proc Natl Acad Sci USA* 113(6): 1630-1635.
- Wirth, J. S. and Whitman, W. B. (2018). "Phylogenomic analyses of a clade within the *Roseobacter* group suggest taxonomic reassignments of species of the genera *Aestuariaivita*, *Citricella*, *Loktanella*, *Nautella*, *Pelagibaca*, *Ruegeria*, *Thalassobius*, *Thiobacimonas* and *Tropicibacter*, and the proposal of six novel genera." *Int J Syst Evol Microbiol*.

- Yan, L., Boyd, K. G. and Grant Burgess, J. (2002). "Surface attachment induced production of antimicrobial compounds by marine epiphytic bacteria using modified roller bottle cultivation." *Mar Biotechnol (NY)* 4(4): 356-366.
- Zan, J. D., Liu, Y., Fuqua, C. and Hill, R. T. (2014). "Acyl-homoserine lactone quorum sensing in the *Roseobacter* clade." *Int J Mol Sci* 15(1): 654-669.
- Zech, H., Thole, S., Schreiber, K., Kalhofer, D., Voget, S., Brinkhoff, T., Simon, M., Schomburg, D. and Rabus, R. (2009). "Growth phase-dependent global protein and metabolite profiles of *Phaeobacter gallaeciensis* strain DSM 17395, a member of the marine *Roseobacter*-clade." *Proteomics* 9(14): 3677-3697.
- Zech, H., Thole, S., Schreiber, K., Kalhöfer, D., Voget, S., Brinkhoff, T., Simon, M., Schomburg, D. and Rabus, R. (2009). "Growth phase-dependent global protein and metabolite profiles of *Phaeobacter gallaeciensis* strain DSM 17395, a member of the marine *Roseobacter* clade." *Proteomics* 9(14): 3677-3697.
- Zhang, H., Yohe, T., Huang, L., Entwistle, S., Wu, P., Yang, Z., Busk, P. K., Xu, Y. and Yin, Y. (2018). "dbCAN2: a meta server for automated carbohydrate-active enzyme annotation." *Nucleic Acids Res* 46(W1): 95-101.
- Zhang, Q. and Van, T. (2012). "Correlation of intracellular trehalose concentration with desiccation resistance of soil *Escherichia coli* populations." *Appl Environ Microbiol* 78(20): 7407-7413.
- Zheng, Q. A., Chen, C. A., Wang, Y. N. and Jiao, N. Z. (2010). "*Oceanicola nitratireducens* sp. nov., a marine alphaproteobacterium isolated from the South China Sea." *Int J Syst Evol Microbiol* 60: 1655-1659.
- Zhou, J., Bruns, M. A. and Tiedje, J. M. (1996). "DNA recovery from soils of diverse composition." *Appl Environ Microbiol* 62(2): 316-322.
- Zhu, Y., Thomas, F., Larocque, R., Li, N., Duffieux, D., Cladiere, L., Souchaud, F., Michel, G. and McBride, M. J. (2017). "Genetic analyses unravel the crucial role of a horizontally acquired alginate lyase for brown algal biomass degradation by *Zobellia galactanivorans*." *Environ Microbiol* 19(6): 2164-2181.
- Ziesche, L., Bruns, H., Dogs, M., Wolter, L., Mann, F., Wagner-Döbler, I., Brinkhoff, T. and Schulz, S. (2015). "Homoserine lactones, methyl oligohydroxybutyrates, and other extracellular metabolites of macroalgae-associated bacteria of the *Roseobacter* clade : identification and functions." *Chembiochem* 16(14): 2094-2107.
- Ziesche, L., Rinkel, J., Dickschat, J. S. and Schulz, S. (2018). "Acyl-group specificity of AHL synthases involved in quorum-sensing in *Roseobacter* group bacteria." *Beilstein J Org Chem* 14: 1309-1316.
- Ziesche, L., Wolter, L., Wang, H., Brinkhoff, T., Pohlner, M., Engelen, B., Wagner-Döbler, I. and Schulz, S. (2018). "An unprecedented medium-chain diunsaturated *N*-acylhomoserine lactone from marine *Roseobacter* group bacteria." *Mar Drugs* 17(1): 20.
- Zubia, M., Payri, C. and Deslandes, E. (2008). "Alginate, mannitol, phenolic compounds and biological activities of two range-extending brown algae, *Sargassum mangarevense* and *Turbinaria ornata* (*Phaeophyta: Fucales*), from Tahiti (French Polynesia)." *J Appl Phycol* 20(6): 1033-1043.

Danksagungen

An dieser Stelle möchte ich mich bei all den Menschen bedanken, die direkt oder indirekt zur Fertigstellung dieser Arbeit beigetragen haben.

Mein erster Dank gilt dabei Thorsten für die Bereitstellung dieses spannenden Projekts und für sein Vertrauen in mich. Die freundliche und unterstützende Art der Betreuung, und Ermutigungen in schwierigeren Zeiten, sowie das Engagement während des Endsprints sind dabei besonders hervorzuheben.

Herzlichen Dank auch an Tilmann Harder für die Erstellung des Zweitgutachtens, sowie Bert, dass er so spontan meine Anfrage, ob er dritter Prüfer sein möchte, angenommen hat.

Danke an Meinhard, dass ich so lange in seiner Gruppe arbeiten aber auch an den alljährlichen „Weihnachts“essen in der Schalotte teilnehmen durfte.

Mein Dank gilt außerdem allen Co-Autoren der gemeinsam veröffentlichten und noch zu veröffentlichen Studien für die stets gute Zusammenarbeit. Dabei besonders zu nennen sind: Jürgen für die großartige Unterstützung mit Rrr, Lisa für die chemischen Analysen und die vielen Telefonate und Anja für ihren unermüdlichen Einsatz am Sequenzierer.

Vielen Dank auch meinem Thesis Committee für die konstruktive Gespräche, die guten Denkanstöße und die angenehme Atmosphäre während dieser Treffen.

Einen großen Dank den Mitarbeitern aus den Arbeitsgruppen „Simon“ und „Cypionka“, die auch neben der Arbeit immer Zeit zum nicht nur wissenschaftlichen Austausch hatten und die mich -glücklicherweise- nie haben Kohlkönigin werden lassen ;-). Dabei gilt mein besonderes Dank auch den wissenschaftlichen Mitarbeitern, ohne deren Arbeit das Labor nicht so laufen würde. Vielen Dank!

Weiterhin danken möchte ich den Teilnehmer von SO248. Es war ein unvergessliches Erlebnis mit euch den Pazifik zu kreuzen, zwischen den Tagen zu stehen, die Uhr 24 Stunden zurück zu stellen, einen doppelten Dienstag zu erleben, ach und ja: zu arbeiten ;-).

Neben denjenigen Menschen, die mich vor allem während der Arbeitszeit begleitet haben, möchte ich auch meinen lieben Freunden danken, die mich immer mal kurz Abstand von der Arbeit haben nehmen lassen, sowie meinem Chor Bokaleta. Vielen Dank, dass ihr für mich da seid =)

Ein besonders großer Dank geht an meine Goldmami ;-), für Deine unermessliche Liebe und positive Energien. Danke dass du trotz der für Dich schwierigen Zeit immer guter Laune warst, immer für uns da bist und Dir deinen Humor bewahrt hast! Einen weiteren großes Dank in dem

Zusammenhang meinen Geschwistern, dass ihr in dieser Zeit mit mir zusammenhaltet. Ich liebe euch.

Als letztes möchte ich noch riesigen Dank an Matthias aussprechen, für Deine unermüdliche Geduld und Hilfe während der Endphase dieser Arbeit und für Deine Unterstützung dabei, mich immer wieder auf den Boden der Tatsachen zu holen. Ohne Dich hätte ich das hier nicht so geschafft und Ich freue mich schon sehr auf wieder entspanntere Zeiten => Tausend Dank und Küsse! Jeg elsker dig.

Curriculum vitae

Laura Amanda Wolter *16.11.1987 in Braunschweig, Germany

- | | |
|-------------------|---|
| Since 05/2019 | Postdoc at the University of Tsukuba, Japan. Laboratory of Prof. Dr. Ryo Miyazaki; National Institute of Advanced Industrial Science and Technology (AIST) |
| 01/2014 – 04/2019 | PhD student at the Carl von Ossietzky University of Oldenburg, Germany at the Institute for Chemistry and Biology of the Marine Environment (ICBM). Supervisor: apl. Prof. Dr. Thorsten Brinkhoff |
| 10/2013 | Internship at the Max Planck Institute for Biophysical Chemistry in Göttingen, Germany. Laboratory of Prof. Dr. Stefan Jacobs |
| 04/2011 – 09/2013 | M. Sc. Microbiology at the University of Oldenburg, Germany |
| 11/2010 – 02/2011 | Internship at the Fraunhofer EMB for Marine Biotechnology in Luebeck, Germany. Laboratory of Dr. Marina Gebert |
| 10/2007 – 09/2010 | B. Sc. Biotechnology at the Technical University of Braunschweig, Germany |

Erklärung

Hiermit versichere ich, dass ich diese Arbeit selbstständig verfasst und keine anderen, als die hier angegebenen Hilfsmittel und Quellen benutzt habe. Zudem versichere ich, dass diese Dissertation weder in ihrer Gesamtheit noch in Teilen einer anderen wissenschaftlichen Hochschule zur Begutachtung in einem Promotionsverfahren vorliegt oder vorgelegen hat. Die Leitlinien guter wissenschaftlicher Praxis der Carl von Ossietzky Universität Oldenburg wurden befolgt.

Oldenburg, 29.03.2019

Laura Amanda Wolter

Supplementary Material for Manuscript 1

Pseudooceanicola algae sp. nov., isolated from the marine macroalga *Fucus spiralis* shows genomic and physiological adaptations for an algal associated lifestyle

Supplementary methods

Marine broth (MB, Difco 2216) media modifications

(L⁻¹): 12.6 g MgCl₂*6H₂O and 2.38 g CaCl₂*2H₂O were included in the medium (compared to 8.8 g and 1.8 g in Difco 2216, respectively) and for trace elements 7 mg Na-Silicat*5H₂O and 21.2 mg boric acid were added per liter (compared to 4 and 2.2 mg, respectively).

Analysis of respiratory quinones, lipoquinones and cellular fatty acids

Respiratory quinones and lipoquinones were extracted from 100 mg freeze dried cells following the standard protocols by Tindall (Tindall 1990, Tindall 1990). Cellular fatty acids were extracted from growing culture on plate using the Sherlock MIS (MIDI Inc, Newark, USA) system as described (<https://www.dsmz.de/services/services-microorganisms/identification/analysis-of-cellular-fatty-acids.html>).

Reduction of nitrate and nitrite

After autoclaving, the medium was reduced by addition of ~1 mg sterile sodium sulfate (1 ml/L). The medium was placed into test tubes containing a small inverted glass tube, the headspace was flushed with N₂/CO₂ (80:20, v/v) and the tubes were sealed. Glucose as substrate and sodium nitrate or sodium nitrite were added to 5 mM. Cells were pre-cultured in MB to exponential phase and 2% (v/v) were added to the anaerobic medium. As control, only glucose was added without nitrate or nitrite and incubated at 20°C and 150 rpm shaking. Growth was monitored by analyzing change in OD₆₀₀.

Production of volatile organic compounds (VOCs) and acyl-homoserine lactones (AHLs)

Analysis of AHLs and VOCs was performed from 100 mL cultures, grown for three days. AHLs were extracted with Soxhlet precleaned Amberlite XAD-16, separated from the culture by filtration and extracted three times with CH₂Cl₂/water (10:1) (Neumann et al. 2013). Combined organic phases were dried with MgSO₄, solvent removed under reduced pressure and the extract dissolved in 50 µL CH₂Cl₂ and analyzed by GC/MS. For VOC analysis, headspace extraction by CLSA using active charcoal filters was performed as described earlier (Schulz et al. 2004). The active charcoal filter was extracted three times with 20 µL CH₂Cl₂ and analyzed by GC/MS. XAD and CLSA extracts were analyzed on an Agilent GC 7890A or B, connected to Agilent 5975C or 5977A mass-selective detectors, equipped with a HP-5 MS fused-silica capillary column (30 m x 0.25 mm i.d., 0.22 µm film; Hewlett-Packard), respectively. Conditions were as follows: carrier gas (He): 1.2 ml/min; injection volume: 1 mL; injector: 250°C; transfer line: 300°C, EI 70 eV. The gas chromatograph was programmed as follows: 50°C (5 min isothermal), increasing with 5°C min⁻¹ to 320°C, and operated in splitless mode. Gas chromatographic retention indices, RI, were determined from a homologous series of *n*-alkanes.

Supplementary Figures and Tables

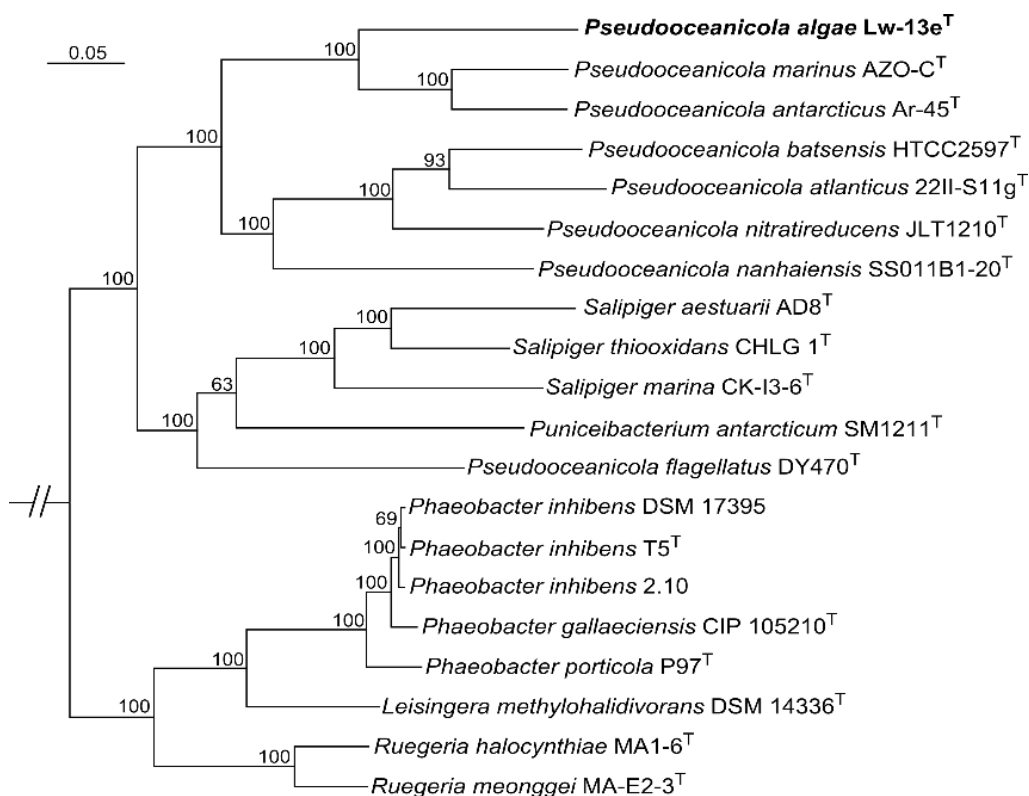


Fig. S1. Maximum-likelihood phylogeny using amino acid sequences of 20 random core genes automatically identified using BPGA. Support values (based on 1000 bootstrap replicates) are indicated. Phylogeny calculated with this method supports taxonomic relationship among *Pseudoceanicola* spp. obtained by UBCG (see Fig. 1B). *Roseobacter litoralis* (not shown) served as outgroup. Bar: 0.05 substitutions per nucleotide position.

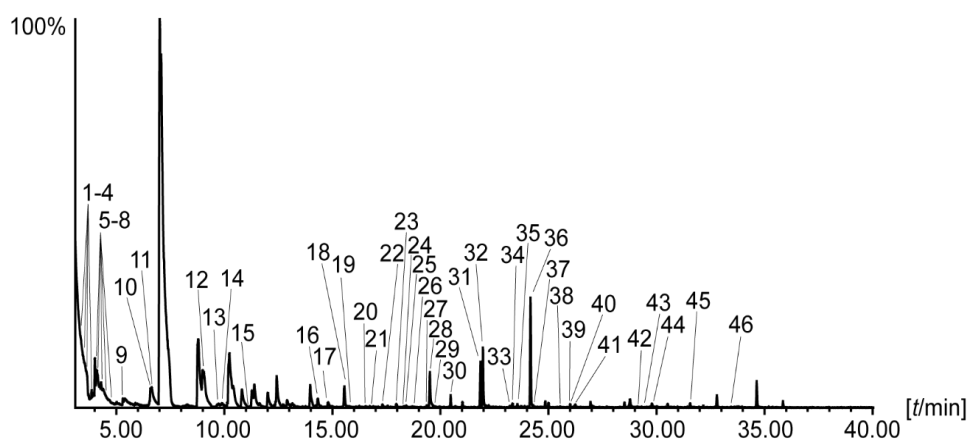


Fig. S2. Total ion chromatogram of GC/MS analysis of headspace extract of Lw-13e^T obtained by CLSA. Compound numbering refers to

Table S8. Non-assigned peaks are medium constituents.

Table S1: Genome statistics of Lw-13e^T and related taxa, including source of isolation, GenBank/NCBI accession numbers and numbers of core, accessory and unique genes.

Genome source	Taxon ID	Genome size (bp)	Total genes	Core genes (%)	Accessory genes (%)	Unique genes (%)	Core genes	Accessory genes	Unique genes
NCBI	QBBT00000000	4 067 555	3805	29.5	49.4	17.3	1123	1881	657
IMG	2721755848	4 232 532	3950	28.4	56.5	11.9	1123	2232	472
NCBI	CECT 7751	4 514 830	4109	27.3	56.9	12.9	1123	2340	530
IMG	2645727778	4 935 686	4628	24.3	56.0	13.3	1123	2590	616
IMG	2687453758	4 068 972	3850	29.2	55.5	11.2	1123	2136	432
IMG	638341139	4 437 668	4261	26.4	53.7	12.8	1123	2287	547
IMG	2558309102	4 659 730	4490	25.0	53.6	16.0	1123	2406	719
NCBI	PGTB00000000	5 235 220	5146						
IMG	2615840719	5 871 369	5575	20.1	53.3	20.2	1123	2974	1125
IMG	2615840712	4 658 697	4466	25.1	53.3	15.7	1123	2380	699
IMG	2615840707	5 611 602	5396	20.8	51.7	19.6	1123	2790	1059
IMG	2718217653	4 414 152	4194	26.8	47.9	19.9	1123	2007	834
NCBI	NZ_AWWI010001 21	5 546 830	4961	22.6	51.6	27.6	1123	2558	1371
IMG	2574179718	4 159 472	3897	28.8	65.1	3.1	1123	2538	119
IMG	2510065028	4 160 918	3723	30.2	64.1	3.0	1123	2387	111
IMG	2510065029	4 227 134	3875	29.0	63.7	3.6	1123	2470	139
IMG	2558309061	4 540 155	4359	25.8	62.1	8.4	1123	2706	367
IMG	2718218026	4 207 221	3948	28.4	61.7	5.7	1123	2437	225
IMG	2512564009	4 650 996	4527	24.8	50.9	18.0	1123	2305	817
NCBI	NZ_FWFP000000 00	4 543 070	4352	25.8	54.8	16.4	1123	2383	712
IMG	2693429872	4 243 668	4071	27.6	54.8	17.0	1123	2229	692
NCBI	CP002623	4 745 450	4397	25.5	46.5	24.6	1123	2045	1080

Table S2: Selected genes that correspond to traits discussed in the main text. Unique genes for Lw-13e^T are marked with a black box, accessory genes shared among different *Pseudoceanicola* with a grey box.

Transporter		
ABC transporter		
Psal_00560-00580		D-ribose or galactose/methyl galactoside import ABC transporter
Psal_02470-02490		aliphatic sulfonates import ABC transporter SsuABC-binding protein SsuB
Psal_18380-18400		inner membrane amino-acid ABC transporter
Psal_35210-35230		inner membrane amino-acid ABC transporter
Psal_15980-16030		dppABCDF dipeptide import
Tripartite tricarboxylate transporter family (TTT)		
Psal_15360-15380		TctABC transporter
Psal_15400	dctP_2	C4-dicarboxylate-binding periplasmic protein precursor
Psal_15410-15430		TctABC transporter
Psal_30530-30550		TctABC transporter
Tripartite ATP-independent periplasmic transporter (TRAP)		
Psal_15150	yaO_1	2,3-diketo-L-gulonate-binding periplasmic protein YiaO precursor
Psal_15160	siaT_14	sialic acid TRAP transporter permease protein SiaT
Psal_15520-15540		TRAP transporter
Psal_31060-31080		2,3-diketo-L-gulonate TRAP transporter YiaNMO
Psal_26970-26990		sialic acid TRAP transporter SiaPT
Psal_13280-13300		sialic acid TRAP transporter SiaPT
Psal_15230-15250		TRAP transporter
branched chain amino acids		
Psal_17050-17080		branched chain amino acid transport system livGFHM
Psal_08790-08830		branched chain amino acid transport system livGFHMK
Psal_33880	ribN	riboflavin transporter
Psal_37060	ribN	riboflavin transporter
Oligomeric alginate degradation		
Psal_29890	ugpC_6	sn-glycerol-3-phosphate import ATP-binding protein UgpC
Psal_29900	yteP	putative multiple-sugar transport system permease YteP
Psal_29910	ycjP_1	inner membrane ABC transporter permease protein YcjP
Psal_29920	yticQ	putative ABC transporter peptide-binding protein YtcQ
Psal_29930		alginate lyase PL15 family
Psal_29940	FabG	short chain dehydrogenase/reductase (SDR) family
Psal_29950	kdgF	cupin domain protein
Psal_29960	kdgK_2	2-dehydro-3-deoxygluconokinase
Multidrug resistance		
Psal_03920	emrB_1	multidrug export protein EmrB
Psal_37970	emrB_2	multidrug export protein EmrB
Psal_05140	macA_2	macrolide export protein MacA/MdtE
Psal_05150	mdtA_1	multidrug resistance protein MdtA precursor
Psal_31850	mdtA_2	multidrug resistance protein MdtA precursor
Psal_31850	mdtA_2	multidrug resistance protein MdtA precursor

Psal_05060	mdtB	multidrug resistance protein MdtB
Psal_16490	mdtK	multidrug resistance protein MdtK
Psal_05720	mdtE	multidrug resistance protein MdtE precursor
Psal_14750	mdtN	multidrug resistance protein MdtN
Psal_06080	mepA_1	multidrug export protein MepA
Psal_11270	bmr3	multidrug resistance protein 3
Psal_35110	ttgA	efflux pump periplasmic linker TtgA precursor
Psal_05730	mexB_1	multidrug resistance protein MexB
Psal_06990	mexB_2	multidrug resistance protein MexB
Psal_25450	emrE	multidrug transporter EmrE
Psal_03930	emrK	putative multidrug resistance protein EmrK
Psal_13910		multidrug export ATP-binding/permease protein
Psal_19550		multidrug resistance protein MdtH
Psal_29080		multidrug export ATP-binding/permease protein
Psal_29840		multidrug efflux protein
Psal_31870		multidrug export ATP-binding/permease protein
Psal_37620		multidrug export ATP-binding/permease protein
Psal_06810	bcr_1	bicyclomycin resistance protein
Psal_07430	bcr_2	bicyclomycin resistance protein
Psal_15820	bcr_3	bicyclomycin resistance protein
Psal_25490	bcr_4	bicyclomycin resistance protein
Psal_32040	bcr_5	bicyclomycin resistance protein
Psal_06830	vgb	virginiamycin B lyase

Reactive oxygen species

Psal_22750	ohrR_1	organic hydroperoxide resistance transcriptional regulator
Psal_22760	ohrB	organic hydroperoxide resistance protein OhrB
Psal_23420	ohrR_2	organic hydroperoxide resistance transcriptional regulator glyoxalase/bleomycin resistance protein/dioxygenase superfamily protein
Psal_12170		
Psal_31930	sodB	superoxide dismutase
Psal_10440	clpB	chaperone protein ClpB
Psal_04820	clpP	ATP-dependent Clp protease proteolytic subunit
Psal_37220	dnaK_2	chaperone protein DnaK
Psal_26730	katG1	catalase-peroxidase 1
Psal_30130	katE	catalase C
Psal_05720	arcA	multidrug resistance protein MdtE precursor
Psal_05730	arcB	multidrug resistance protein MexB
Psal_06980	acrA	multidrug efflux pump subunit AcrA precursor
Psal_03370	acrB_1	multidrug efflux pump subunit AcrB
Psal_35110	arcA	putative efflux pump periplasmic linker TtgA precursor
Psal_35120	acrB_2	multidrug efflux pump subunit AcrB

Aromatic hydrocarbons

Psal_05130	ttgB	toluene efflux pump membrane transporter TtgB
Psal_05740	ttgC	putative efflux pump outer membrane protein TtgC precursor
Psal_03380	ttgD	toluene efflux pump periplasmic linker protein TtgD precursor
Psal_31860	ttgE	toluene efflux pump membrane transporter TtgE

Heavy metal tolerance			
Psal_31310	copA_2	copper resistance protein A precursor	
Psal_31320	copB	copper resistance protein B precursor	
Psal_31330	copC	copper resistance protein C	
Psal_31340	copD	copper resistance protein D	
Psal_14200	arsC_1	arsenate reductase	
Psal_29740	arsC1	arsenate-mycothioli transferase ArsC1	
Psal_29770	arsB	arsenite resistance protein ArsB	
Psal_29780	arsC_2	arsenate reductase	
Psal_29790	arsH	NADPH-dependent FMN reductase ArsH	
Toxins			
Psal_13500	hlyA_1	hemolysin, chromosomal	
Psal_15700	prsE_1	type I secretion system membrane fusion protein PrsE	
Psal_15710	prsD_1	type I secretion system ATP-binding protein PrsD	
Psal_15720	hlyA_2	hemolysin, plasmid	
Psal_15730	ycaD_1	putative MFS-type transporter YcaD	
Psal_29410	cya	bifunctional hemolysin/adenylate cyclase precursor	
Psal_12420		entericidin B membrane lipoprotein	
Cell cycle control			
Psal_18710	ccrM	modification methylase ccrM	
Psal_12270	gcrA	GcrA cell cycle regulator	
Psal_20370	divL	sensor protein DivL	
Psal_25990	chpT	histidine phosphotransferase ChpT	
Psal_26390	cckA	blue-light-activated protein/cckA	
Psal_24690	cckA	blue-light activated sensor kinase cckA	
Psal_25000	ctrA	cell cycle response regulator CtrA	
Psal_07000	ctrA	cell cycle response regulator CtrA	
Psal_04820	clpP	ATP-dependent Clp protease proteolytic subunit	
Psal_36220	dnaA	chromosomal replication initiator protein DnaA	
Psal_04810	clpX	ATP-dependent Clp protease ATP-binding subunit ClpX	
Communication			
Psal_25610	luxR	transcriptional activator protein LuxR	
Psal_32700	luxR	bacterial regulatory proteins, luxR family	
PSAL_24590	lsrR	transcriptional regulator LsrR	
Psal_05100	luxQ	autoinducer 2 sensor kinase/phosphatase LuxQ	
Psal_27150	luxQ	autoinducer 2 sensor kinase/phosphatase LuxQ	
Psal_10000		purine-binding protein precursor	
Psal_10010	lsrA	autoinducer 2 import ATP-binding protein LsrA	
Psal_10020	putative lsrD	beta-methylgalactoside transporter inner membrane component	
Psal_10030	putative lsrC	branched-chain amino acid transport system / permease component	
Psal_15640	lsrD	autoinducer 2 import system permease protein LsrD	
Psal_15650	lsrC	autoinducer 2-binding protein LsrC precursor	
Psal_15660	rsbA	Ribose import ATP-binding protein RbsA	
Psal_15670	lsrB	autoinducer 2-binding protein LsrB precursor	

	Psal_32100	lsrC	autoinducer 2 import system permease protein LsrC
	Psal_32110	putative lsrD	branched-chain amino acid transport system / permease component
	Psal_32120	putative lsrA	ribose import ATP-binding protein RbsA
	Psal_07080	tqsA	AI-2 transport protein TqsA
	Psal_27420	tqsA	AI-2 transport protein TqsA
	Psal_07570		pheromone autoinducer 2 transporter
Motility			
	Psal_04630	fliM	flagellar motor switch protein FliM
	Psal_11940	motB	motility protein B
	Psal_22700	ylxH	flagellum site-determining protein YlxH
	Psal_33870	fliG	flagellar motor switch protein FliG
	Psal_34120		flagellin N-methylase
	Psal_35840	fliP	flagellar biosynthetic protein FliP precursor
	Psal_35850	fliN	flagellar motor switch protein FliN
	Psal_35860	fliH	flagellar biosynthesis protein FliH
	Psal_35870	fliF	flagellar M-ring protein
	Psal_35880	fliL	flagellar FliL protein
	Psal_35910	motA	motility protein A
	Psal_35930	flhA	flagellar biosynthesis protein FlhA
	Psal_35940	fliR	flagellar biosynthesis protein FliR
	Psal_35950	flhB	flagellar biosynthetic protein FlhB
	Psal_35980	flgH	flagellar L-ring protein precursor
	Psal_35990	flgA	flagellar basal body P-ring biosynthesis protein FlgA
	Psal_36000	flgG1	flagellar basal-body rod protein FlgG
	Psal_36010	flgG2	flagellar basal-body rod protein FlgG
	Psal_36020	fliQ	flagellar biosynthetic protein FliQ
	Psal_36030	fliE	flagellar hook-basal body protein FliE
	Psal_36040	flgC	flagellar basal-body rod protein FlgC
	Psal_36050	flgB	flagellar basal body rod protein FlgB
	Psal_36060	fliL	flagellum-specific ATP synthase
	Psal_36080	flbT	flagellar biosynthesis repressor FlbT
	Psal_36090	flaF	flagellar biosynthesis regulatory protein FlaF
	Psal_36100	fliC	flagellin
	Psal_36110	flgN	FlgN protein
	Psal_36130	fliK	flagellar hook-length control protein FliK
	Psal_36140	flgD	basal-body rod modification protein FlgD
	Psal_36590	flgI	flagellar P-ring protein precursor
	Psal_36600	flgL	flagellar hook-associated protein FlgL
	Psal_36610	flgK	flagellar hook-associated protein 1
	Psal_36620	flgE	flagellar hook protein FlgE
	Psal_36630	motB	motility protein B
	Psal_36670	flhA2	
Chemotaxis			
	Psal_10070	tsr_1	methyl-accepting Chemotaxis protein 1
	Psal_10670	mcp2_1	methyl-accepting Chemotaxis protein 2

Psal_13330	ctpH	methyl-accepting	Chemotaxis protein CtpH
Psal_17790	tsr_2	methyl-accepting	Chemotaxis protein I
Psal_25040	mcp2_2	methyl-accepting	Chemotaxis protein 2
Psal_26310	mcp4	methyl-accepting	Chemotaxis protein 4
Psal_27170	tar_2	methyl-accepting	Chemotaxis protein II
Psal_33130	trg	methyl-accepting	Chemotaxis protein III
Blue light proteins			
Psal_30140			blue-light-activated histidine kinase
Psal_30150	fixK_2		nitrogen fixation regulation protein FixK
Psal_05220			blue-light-activated protein
Psal_05230			response regulator receiver domain protein
Psal_10210	hssR		heme response regulator HssR
Psal_10220			blue-light-activated protein
Psal_10230	gmr_2		cyclic di-GMP phosphodiesterase Gmr
Psal_26340	mshB		1D-myo-inositol 2-acetamido-2-deoxy-alpha-D-glucopyranoside deacetylase
Psal_26350			hypothetical protein
Psal_26360			glycogen synthase
Psal_26370	wfgD		alpha-D-GlcNAc-diphosphoundecaprenol beta-1,3-glucosyltransferase WfgD
Psal_26380	bcsA		cellulose synthase catalytic subunit
Psal_26390			blue-light-activated protein/cckA

Table S3: Average amino acid identities (% AAI) between genomes analyzed in the present study; 1: *P. algae*, 2: *P. antarcticus*, 3: *P. marinus*, 4: *P. atlanticus*, 5: *P. nanhaensis*, 6: *P. batsensis* 7: *P. nitratireducens* 8: *P. lipolyticus* 9: *P. flagellatus* 10: *S. aestuarii* 11: *S. thiooxidans*, 12: *S. marina* 13: *P. antarcticum* 14: *P. inhibens T5* 15: *P. inhibens 2.10* 16: *P. inhibens DSM 17395*, 17: *P. porticola* 18: *P. gallaeciensis* 19: *L. methylohalidivorans* 20: *R. meonggei* 21: *R. halocynthiae*

	1	2	3	4	5	6	7	8	9	10	11	12	13	14	15	16	17	18	19	20	21		
1	100																						
2	70.4	100																					
3	70.1	79.2	100																				
4	66.2	67.2	66.7	100																			
5	66.2	67.4	66.7	71.2	100																		
6	65.3	66.0	66.3	77.6	70.5	100																	
7	65.3	66.4	66.4	74.9	68.4	77.1	100																
8	63.8	63.9	62.6	67.0	66.6	67.5	65.2	100															
9	62.4	62.9	63.1	64.1	64.1	64.3	64.7	65.4	100														
10	62.1	62.5	62.3	64.0	63.9	63.9	62.6	64.3	65.6	100													
11	62.5	63.5	63.2	64.5	64.1	64.3	63.0	65.1	65.8	76.3	100												
12	62.0	63.4	62.3	62.7	63.3	62.3	62.8	63.6	65.7	70.6	71.3	100											
13	61.4	62.2	62.0	63.4	63.9	62.9	62.6	63.4	66.9	66.3	66.2	66.0	100										
14	62.0	62.3	61.9	63.4	63.4	63.1	63.0	66.7	64.1	61.9	62.7	62.1	63.1	100									
15	61.9	62.2	62.0	63.0	63.2	62.8	63.1	66.6	64.3	62.2	62.6	62.4	63.0	98.6	100								
16	61.8	62.0	61.9	63.0	62.9	63.1	63.2	66.7	64.4	61.8	62.5	62.0	62.8	98.1	98.1	100							
17	61.5	62.1	61.8	62.8	62.6	62.5	62.8	66.4	63.9	62.8	62.0	62.3	62.4	89.7	89.8	89.8	100						
18	61.3	62.3	61.4	63.7	63.7	63.6	62.7	66.7	64.0	62.2	62.5	61.9	63.3	94.2	94.4	94.3	88.4	100					
19	61.9	62.2	62.1	62.7	63.1	62.8	63.1	66.5	64.7	62.5	63.0	62.5	62.4	74.8	75.2	74.9	74.4	74.4	100				
20	61.2	61.5	61.5	62.1	62.5	62.4	62.6	66.3	64.3	61.7	62.1	61.4	62.1	69.0	69.1	69.0	68.7	68.4	69.1	100			
21	61.0	61.3	61.3	62.1	62.1	61.8	62.6	66.2	64.4	61.8	62.0	61.4	61.9	68.9	68.8	69.2	68.6	68.4	69.2	81.1	100		

Table S4: Digital DNA-DNA hybridization (dDDH) values for the genome of strain Lw-13e^T compared to genomes of other *Pseudoceanicola* spp.

Reference genomes	Formula 1 DDH	Formula 2 DDH	Formula 3 DDH
<i>P. antarcticus</i>	16.2	24.8	16.3
<i>P. marinus</i>	18.8	20.4	18.3
<i>P. atlanticus</i>	14.8	22.8	15
<i>P. nanhaensis</i>	14.4	22.9	14.7
<i>P. nitratireducens</i>	15.2	22.6	15.3
<i>P. batsensis</i>	14.8	20.1	15
<i>S. aestuarii</i>	14.4	19.9	14.5
<i>S. thiooxidans</i>	14.6	19.9	14.8
<i>S. marina</i>	14.8	19.1	14.9
<i>P. flagellatus</i>	13.8	19	14.1
<i>P. antarcticum</i>	14	19.1	14.2
<i>R. litoralis</i>	12.9	19.3	13.3

Table S5: List of unique genes detected in Lw-13e^T. A complete list of all 13325 unique genes identified for all investigated genomes can be found in the digital supplementary material attached to the printed version of this dissertation.

locus tag	length	product	KEGG annotation	KEGG pathway	KEGG class
Psal_00010	228	hypothetical protein	NA	NA	NA
Psal_00020	440	hypothetical protein	NA	NA	NA
Psal_00030	540	hypothetical protein	NA	NA	NA
Psal_00040	128	hypothetical protein	NA	NA	NA
Psal_00050	79	hypothetical protein	NA	NA	NA
Psal_00060	185	hypothetical protein	NA	NA	NA
Psal_00100	53	hypothetical protein	NA	NA	NA
Psal_00150	110	hypothetical protein	NA	NA	NA
Psal_00230	86	hypothetical protein	NA	NA	NA
Psal_00350	283	putative 3-hydroxybutyryl-CoA dehydrogenase	NA	NA	NA
Psal_00360	159	hypothetical protein	NA	NA	NA
Psal_00370	115	hypothetical protein	NA	NA	NA
Psal_00380	80	hypothetical protein	NA	NA	NA
Psal_00390	89	hypothetical protein	NA	NA	NA
Psal_00410	222	hypothetical protein	NA	NA	NA
Psal_00420	269	Caffeine dehydrogenase subunit beta	NA	NA	NA
Psal_00430	168	4-hydroxybenzoyl-CoA reductase subunit gamma	coxS; aerobic carbon-monoxide dehydrogenase small subunit	Energy metabolism	Metabolism
Psal_00440	769	4-hydroxybenzoyl-CoA reductase subunit alpha	NA	NA	NA
Psal_00460	331	hypothetical protein	NA	NA	NA
Psal_00510	336	2-oxoglutarate-dependent ethylene/succinate-forming enzyme	NA	NA	NA
Psal_00530	230	putative HTH-type transcriptional regulator YdfH	NA	NA	NA
Psal_00540	330	2-oxoglutarate-dependent ethylene/succinate-forming enzyme	NA	NA	NA
Psal_00560	334	D-ribose-binding periplasmic protein precursor	rbsB; ribose transport system substrate-binding protein	Bacterial chemotaxis [PATH:ko02030]	Cell motility
Psal_00580	343	Ribose transport system permease protein RbsC	NA	NA	NA

Psal_00590	303	HTH-type transcriptional regulator CynR 2-oxoglutarate-dependent ethylene/succinate- forming enzyme	NA	NA	NA
Psal_00600	328		NA	NA	NA
Psal_00650	375	hypothetical protein	NA	NA	NA
Psal_00660	152	hypothetical protein	NA	NA	NA
Psal_00670	165	hypothetical protein	NA	NA	NA
Psal_00690	638	Papain family cysteine protease	NA	NA	NA
Psal_00700	1622	Peptidoglycan-binding protein ArfA	K16191, arfA; peptidoglycan-binding protein ArfA	Transporters [BR:ko02000]	Membrane transport
Psal_00720	176	hypothetical protein	NA	NA	NA
Psal_00730	253	hypothetical protein	NA	NA	NA
Psal_00750	325	hypothetical protein	NA	NA	NA
Psal_00760	491	hypothetical protein	NA	NA	NA
Psal_01140	256	Putative transmembrane protein (Alph_Pro_TM)	NA	NA	NA
Psal_01240	306	hypothetical protein	NA	NA	NA
Psal_01360	70	hypothetical protein	NA	NA	NA
Psal_01380	318	Phthiocerol synthesis polyketide synthase type I PpsC	NA	NA	NA
Psal_01420	153	Ion channel	NA	NA	NA
Psal_01790	600	RNA polymerase-associated protein RapA	NA	NA	NA
Psal_01800	125	hypothetical protein	NA	NA	NA
Psal_01810	586	hypothetical protein	NA	NA	NA
Psal_01820	1046	hypothetical protein	NA	NA	NA
Psal_01830	768	DNA-dependent helicase II	NA	NA	NA
Psal_01840	937	hypothetical protein	NA	NA	NA
Psal_01850	930	RNA polymerase-associated protein RapA	NA	NA	NA
Psal_02040	168	V4R domain protein	NA	NA	NA
Psal_02090	142	acyl-CoA thioesterase YbgC	NA	NA	NA
Psal_02140	125	putative acyl-CoA thioester hydrolase	NA	NA	NA
Psal_02180	141	Cupin domain protein	NA	NA	NA
Psal_02190	163	hypothetical protein	NA	NA	NA
Psal_02350	247	HTH-type transcriptional regulator YiaJ	NA	NA	NA

Psal_02360	592	hypothetical protein	NA	NA	NA
Psal_02370	248	hypothetical protein	NA	NA	NA
Psal_02400	276	Spermidine/putrescine transport system permease protein PotB	NA	NA	NA
Psal_02410	280	Trehalose transport system permease protein SugB	ABC.SP.P; putative spermidine/putrescine transport system permease protein dpkA, lhpD; delta1-piperideine-2-carboxylate reductase	Transporters [BR:ko02000]	Membrane transport
Psal_02440	337	(2R)-3-sulfolactate dehydrogenase (NADP(+))	K03710; GntR family transcriptional regulator	Lysine degradation [PATH:ko00310] Transcription factors [BR:ko03000]	Amino acid metabolism Transcription
Psal_02460	261	Putative L-lactate dehydrogenase operon regulatory protein			
Psal_02470	325	Putative aliphatic sulfonates-binding protein precursor	NA	NA	NA
Psal_02480	248	Aliphatic sulfonates import ATP-binding protein SsuB	ABC.SN.A; NitT/TauT family transport system ATP-binding protein tauC; taurine transport system permease protein	Transporters [BR:ko02000]	Membrane transport
Psal_02490	253	Putative aliphatic sulfonates transport permease protein SsuC		Transporters [BR:ko02000]	Membrane transport
Psal_02500	743	Arylsulfatase	E3.1.6.1, aslA; arylsulfatase	Sphingolipid metabolism [PATH:ko00600]	Lipid metabolism
Psal_02510	176	Ricin-type beta-trefoil lectin domain protein	NA	NA	NA
Psal_02520	214	hypothetical protein	NA	NA	NA
Psal_02640	82	hypothetical protein	NA	NA	NA
Psal_02770	317	Putative 2-aminoethylphosphonate-binding periplasmic protein precursor	afuA, fbpA; iron(III) transport system substrate-binding protein	Transporters [BR:ko02000]	Membrane transport
Psal_02780	563	Putative 2-aminoethylphosphonate transport system permease protein PhnV	NA	NA	NA
Psal_02790	328	Sulfate/thiosulfate import ATP-binding protein CysA	ABC.SP.A; putative spermidine/putrescine transport system ATP-binding protein	Transporters [BR:ko02000]	Membrane transport
Psal_02800	311	HTH-type transcriptional regulator GltC	NA	NA	NA
Psal_02810	173	Calcineurin-like phosphoesterase superfamily domain protein	NA	NA	NA
Psal_02820	337	hypothetical protein	NA	NA	NA

Psal_02850	219	hypothetical protein	NA	NA	NA
Psal_02860	189	hypothetical protein	NA	NA	NA
Psal_02870	319	hypothetical protein	NA	NA	NA
Psal_02880	246	hypothetical protein	NA	NA	NA
Psal_02890	319	hypothetical protein	NA	NA	NA
Psal_02900	54	hypothetical protein	NA	NA	NA
Psal_02920	677	Phage integrase family protein	NA	NA	NA
Psal_03000	223	Bacterial SH3 domain protein	NA	NA	NA
Psal_03040	114	hypothetical protein	NA	NA	NA
Psal_03200	299	hypothetical protein	NA	NA	NA
Psal_03460	130	Inner membrane protein YhaH	NA	NA	NA
Psal_03640	125	hypothetical protein	NA	NA	NA
Psal_03650	230	hypothetical protein	NA	NA	NA
Psal_03770	176	hypothetical protein	NA	NA	NA
Psal_03900	251	hypothetical protein	NA	NA	NA
Psal_03980	190	hypothetical protein	NA	NA	NA
Psal_04000	92	hypothetical protein	NA	NA	NA
Psal_04010	278	hypothetical protein	NA	NA	NA
Psal_04020	776	hypothetical protein	NA	NA	NA
Psal_04030	511	hypothetical protein	NA	NA	NA
Psal_04120	232	hypothetical protein	NA	NA	NA
Psal_04180	91	hypothetical protein	NA	NA	NA
Psal_04200	236	hypothetical protein	NA	NA	NA
Psal_04210	653	hypothetical protein	NA	NA	NA
Psal_04220	103	hypothetical protein	NA	NA	NA
Psal_04240	222	hypothetical protein	NA	NA	NA
Psal_04250	110	hypothetical protein	NA	NA	NA
Psal_04260	94	hypothetical protein	NA	NA	NA
Psal_04270	105	hypothetical protein	NA	NA	NA
Psal_04290	76	hypothetical protein	NA	NA	NA
Psal_04300	93	hypothetical protein	NA	NA	NA

Psal_04310	75	hypothetical protein	NA	NA	NA
Psal_04320	190	hypothetical protein	NA	NA	NA
Psal_04330	88	hypothetical protein	NA	NA	NA
Psal_04340	107	hypothetical protein	NA	NA	NA
Psal_04350	401	hypothetical protein	NA	NA	NA
Psal_04360	79	hypothetical protein	NA	NA	NA
Psal_04370	273	hypothetical protein	NA	NA	NA
Psal_04380	462	KAP family P-loop domain protein	NA	NA	NA
Psal_04390	137	hypothetical protein	NA	NA	NA
Psal_04400	231	hypothetical protein	NA	NA	NA
Psal_04420	262	hypothetical protein	NA	NA	NA
Psal_04430	214	hypothetical protein	NA	NA	NA
Psal_04440	265	hypothetical protein	NA	NA	NA
Psal_04450	307	hypothetical protein	NA	NA	NA
Psal_04460	252	hypothetical protein	NA	NA	NA
Psal_04470	238	hypothetical protein	NA	NA	NA
Psal_04480	259	Terminase-like family protein	NA	NA	NA
Psal_04490	196	hypothetical protein	NA	NA	NA
Psal_04500	131	hypothetical protein	NA	NA	NA
Psal_04510	204	hypothetical protein	NA	NA	NA
Psal_04520	114	hypothetical protein	NA	NA	NA
Psal_04530	320	hypothetical protein	NA	NA	NA
Psal_04540	792	hypothetical protein	NA	NA	NA
Psal_04550	78	Helix-turn-helix domain protein	NA	NA	NA
Psal_04560	398	integrase	NA	NA	NA
Psal_04580	291	hypothetical protein	NA	NA	NA
Psal_04850	111	dTDP-4-oxo-6-deoxy-D-allose reductase	NA	NA	NA
Psal_04940	330	Putative thiamine biosynthesis protein	ABC.SN.S; NitT/TauT family transport system substrate-binding protein	Transporters [BR:ko02000]	Membrane transport
Psal_04960	283	Putative aliphatic sulfonates transport permease protein SsuC	NA	NA	NA

Psal_04970	456	Isoxanthopterin deaminase	E3.5.4.32; 8-oxoguanine deaminase	Nucleotide metabolism	Metabolism
Psal_05050	110	hypothetical protein	NA	NA	NA
Psal_05080	308	UDP-Glc:alpha-D-GlcNAc-diphosphoundecaprenol beta-1,3-glucosyltransferase WfgD	NA	NA	NA
Psal_05090	102	hypothetical protein	NA	NA	NA
Psal_05120	279	HTH-type transcriptional repressor FabR	NA	NA	NA
Psal_05160	563	hypothetical protein	NA	NA	NA
Psal_05170	1044	Swarming motility protein SwrC	NA	NA	NA
Psal_05220	686	Blue-light-activated protein	NA	NA	NA
Psal_05230	140	Response regulator receiver domain protein	NA	NA	NA
Psal_05470	112	hypothetical protein	NA	NA	NA
Psal_05480	128	2-aminomuconate deaminase	NA	NA	NA
Psal_05490	291	CAAX amino terminal protease self- immunity	NA	NA	NA
Psal_05510	249	Pyrethroid hydrolase	NA	NA	NA
Psal_05540	70	hypothetical protein	NA	NA	NA
Psal_05710	193	Bacterial regulatory proteins, tetR family	NA	NA	NA
Psal_05760	225	Disulfide-bond oxidoreductase YfcG	yghU, yfcG; GSH-dependent disulfide-bond oxidoreductase	Amino acid metabolism	Metabolism
Psal_05780	300	HTH-type transcriptional regulator DmlR	NA	NA	NA
Psal_05790	68	hypothetical protein	NA	NA	NA
Psal_05810	303	hypothetical protein	NA	NA	NA
Psal_05860	208	transcriptional regulator BetI	NA	NA	NA
Psal_05870	310	Levodione reductase	NA	NA	NA
Psal_05880	88	hypothetical protein	NA	NA	NA
Psal_05890	108	hypothetical protein	NA	NA	NA
Psal_05930	122	YCII-related domain protein	NA	NA	NA
Psal_05940	427	RNA polymerase sigma factor	SIG3.2, rpoE; RNA polymerase sigma-70 factor, ECF subfamily	Transcription machinery [BR:ko03021]	Transcription
Psal_05950	259	hypothetical protein	NA	NA	NA
Psal_05960	154	hypothetical protein	NA	NA	NA
Psal_06070	1133	hypothetical protein	NA	NA	NA

Psal_06100	216	hypothetical protein	NA	NA	NA
Psal_06140	64	hypothetical protein	NA	NA	NA
Psal_06210	154	hypothetical protein	NA	NA	NA
Psal_06320	268	hypothetical protein	NA	NA	NA
Psal_06420	338	hypothetical protein	NA	NA	NA
Psal_06440	72	hypothetical protein	NA	NA	NA
Psal_06580	171	hypothetical protein	NA	NA	NA
Psal_06630	124	Cupin domain protein	NA	NA	NA
Psal_06730	448	Flavoheomprotein	NA	NA	NA
Psal_06750	39	hypothetical protein	NA	NA	NA
			bcr, tcaB; MFS transporter, DHA1 family, multidrug resistance protein	Transporters [BR:ko02000]	Membrane transport
Psal_06810	399	Bicyclomycin resistance protein			
Psal_06820	33	hypothetical protein	NA	NA	NA
Psal_06830	477	Virginiamycin B lyase	NA	NA	NA
			cysJ; sulfite reductase (NADPH) flavoprotein alpha-component	Sulfur metabolism [PATH:ko00920]	Energy metabolism
Psal_06840	450	Sulfite reductase flavoprotein alpha-component			
			apbE; FAD:protein FMN transferase	Metabolism of cofactors and vitamins	Metabolism
Psal_06850	303	Thiamine biosynthesis lipoprotein ApbE precursor			
Psal_06860	196	hypothetical protein	NA	NA	NA
Psal_06870	173	hypothetical protein	NA	NA	NA
Psal_06880	182	hypothetical protein	NA	NA	NA
Psal_07010	226	hypothetical protein	NA	NA	NA
Psal_07050	50	hypothetical protein	NA	NA	NA
Psal_07100	109	hypothetical protein	NA	NA	NA
Psal_07280	54	hypothetical protein	NA	NA	NA
			maa; maltose O-acetyltransferase	Others	Metabolism
Psal_07660	180	Maltose O-acetyltransferase			
			nudF; ADP-ribose pyrophosphatase	Purine metabolism [PATH:ko00230]	Nucleotide metabolism
Psal_07670	185	ADP-ribose pyrophosphatase			
Psal_07750	51	hypothetical protein	NA	NA	NA
Psal_07850	227	protein-L-isoaspartate O-methyltransferase	NA	NA	NA

Psal_07880	94	hypothetical protein	NA	NA	NA
Psal_07900	82	Helix-turn-helix domain protein	NA	NA	NA
Psal_07910	128	hypothetical protein	NA	NA	NA
Psal_07920	826	hypothetical protein	NA	NA	NA
Psal_07930	596	hypothetical protein	NA	NA	NA
Psal_07940	260	DpnII restriction endonuclease D12 class N6 adenine-specific DNA methyltransferase	NA	NA	NA
Psal_07950	336	site-specific tyrosine recombinase XerC	NA	NA	NA
Psal_08080	91	hypothetical protein	NA	NA	NA
Psal_08310	143	hypothetical protein	NA	NA	NA
Psal_08640	126	3-demethylubiquinone-9 3-methyltransferase	NA	NA	NA
Psal_08690	199	hypothetical protein	NA	NA	NA
Psal_08700	71	hypothetical protein	NA	NA	NA
Psal_08730	337	Alcohol dehydrogenase	NA	NA	NA
Psal_08740	313	Glycine betaine/carnitine transport binding protein GbuC precursor	proX; glycine betaine/proline transport system substrate-binding protein	ABC transporters [PATH:ko02010]	Membrane transport
Psal_08760	671	Glycine betaine transport system permease protein OpuAB	NA	NA	NA
Psal_08770	212	HTH-type transcriptional regulator BetI	betI; TetR/AcrR family transcriptional regulator, transcriptional repressor of bet genes	Transcription factors [BR:ko03000]	Transcription
Psal_08790	242	Lipopolysaccharide export system ATP-binding protein LptB	livG; branched-chain amino acid transport system ATP-binding protein	Transporters [BR:ko02000]	Membrane transport
Psal_08800	238	High-affinity branched-chain amino acid transport ATP-binding protein LivF	lptB; lipopolysaccharide export system ATP- binding protein	ABC transporters [PATH:ko02010]	Membrane transport
Psal_08810	289	High-affinity branched-chain amino acid transport system permease protein LivH	livH; branched-chain amino acid transport system permease protein	Quorum sensing [PATH:ko02024]	Cellular community - prokaryotes
Psal_08820	327	leucine/isoleucine/valine transporter permease subunit	livM; branched-chain amino acid transport	Transporters [BR:ko02000]	Membrane transport

			system permease protein		
Psal_08830	408	Leucine-, isoleucine-, valine-, threonine-, and alanine-binding protein precursor	NA	NA	NA
Psal_08840	270	HTH-type transcriptional regulator LutR	NA	NA	NA
Psal_08850	220	Protease synthase and sporulation protein PAI 2	NA	NA	NA
Psal_08860	306	Acetamidase/Formamidase family protein	NA	NA	NA
			hisC; histidinol-phosphate aminotransferase	Novobiocin biosynthesis [PATH:ko00401]	Biosynthesis of other secondary metabolites
Psal_08870	375	Histidinol-phosphate aminotransferase 2			
Psal_08880	341	Acetyl esterase	aes; acetyl esterase	Lipid metabolism	Metabolism
Psal_08890	550	Succinyl-diaminopimelate desuccinylase	NA	NA	NA
Psal_08900	99	hypothetical protein	NA	NA	NA
Psal_08910	202	hypothetical protein	NA	NA	NA
Psal_08920	455	hypothetical protein	NA	NA	NA
Psal_09180	153	hypothetical protein	NA	NA	NA
			ugpE; sn-glycerol 3-phosphate transport system permease protein	Transporters [BR:ko02000]	Membrane transport
Psal_09270	274	L-arabinose transport system permease protein AraQ			
			ugpA; sn-glycerol 3-phosphate transport system permease protein	Transporters [BR:ko02000]	Membrane transport
Psal_09280	289	sn-glycerol-3-phosphate transport system permease protein UgpA			
			ABC.MS.S; multiple sugar transport system substrate-binding protein	Transporters [BR:ko02000]	Membrane transport
Psal_09290	419	sn-glycerol-3-phosphate-binding periplasmic protein UgpB precursor			
Psal_09300	74	hypothetical protein	NA	NA	NA
			SLC5A2, SGLT2; solute carrier family 5 (sodium/glucose cotransporter), member 2	Exosome [BR:ko04147]	Transport and catabolism
Psal_09310	533	Sodium/glucose cotransporter			
Psal_09330	92	hypothetical protein	NA	NA	NA
Psal_09390	69	hypothetical protein	NA	NA	NA
Psal_09430	90	hypothetical protein	NA	NA	NA

Psal_09570	210	Ribonuclease T2 family protein	E3.1.27.1; ribonuclease T2	Transfer RNA biogenesis [BR:ko03016]	Translation
Psal_09660	164	hypothetical protein	NA	NA	NA
Psal_09710	80	hypothetical protein	NA	NA	NA
Psal_09810	160	DNA gyrase inhibitor	NA	NA	NA
Psal_09830	268	Putative 2-aminoethylphosphonate transport system permease protein PhnV	NA	NA	NA
Psal_09840	278	Putrescine transport system permease protein PotH	NA	NA	NA
Psal_09850	380	hypothetical protein	NA	NA	NA
Psal_09870	338	Catabolite control protein A	ascG; LacI family transcriptional regulator, asc operon repressor	Transcription factors [BR:ko03000]	Transcription
Psal_09880	172	RNA 2',3'-cyclic phosphodiesterase	NA	NA	NA
Psal_09890	509	Pyridoxine 4-oxidase	pno; pyridoxine 4-oxidase	Vitamin B6 metabolism [PATH:ko00750]	Metabolism of cofactors and vitamins
Psal_09900	237	Putative L-lactate dehydrogenase operon regulatory protein	NA	NA	NA
Psal_09910	394	Soluble hydrogenase 42 kDa subunit	ppaT; pyridoxamine---pyruvate transaminase	Vitamin B6 metabolism [PATH:ko00750]	Metabolism of cofactors and vitamins
Psal_09920	345	2,5-dihydropyridine 5,6-dioxygenase	NA	NA	NA
Psal_09930	172	Flavin-dependent monooxygenase, reductase subunit HsaB	hpaC; flavin reductase (NADH) K07120; uncharacterized protein	Tyrosine metabolism [PATH:ko00350]	Amino acid metabolism
Psal_09940	367	Putative ammonia monooxygenase	NA	Function unknown	Poorly characterized
Psal_09950	431	Glutamyl-tRNA(Gln) amidotransferase subunit A	NA	NA	NA
Psal_09970	133	SnoaL-like domain protein	NA	NA	NA
Psal_09980	497	4-nitrophenol 4-monooxygenase/4-nitrocatechol 2-monooxygenase, oxygenase component	NA	NA	NA
Psal_09990	156	hypothetical protein	NA	NA	NA
Psal_10000	345	Purine-binding protein precursor	ABC.SS.S; simple sugar transport system substrate-binding protein	Transporters [BR:ko02000]	Membrane transport
Psal_10010	527	Autoinducer 2 import ATP-binding protein LsrA	ABC.SS.A; simple sugar transport system ATP-binding protein	Transporters [BR:ko02000]	Membrane transport

Psal_10020	360	beta-methylgalactoside transporter inner membrane component	ABC.SS.P; simple sugar transport system permease protein	Transporters [BR:ko02000]	Membrane transport
Psal_10030	310	Branched-chain amino acid transport system / permease component	ABC.SS.P; simple sugar transport system permease protein	Transporters [BR:ko02000]	Membrane transport
Psal_10130	421	UDP-D-galactose:(glucosyl)lipopolysaccharide-1,6-D-galactosyltransferase	NA	NA	NA
Psal_10180	862	Calcium-dependent protease precursor	PCSK2; proprotein convertase subtilisin/kexin type 2	Peptidases [BR:ko01002]	Enzyme families
Psal_10190	539	hypothetical protein	NA	NA	NA
Psal_10210	120	Heme response regulator HssR	NA	NA	NA
Psal_10220	798	Blue-light-activated protein	NA	NA	NA
Psal_10290	125	hypothetical protein	NA	NA	NA
Psal_10330	66	Cyanate hydratase	NA	NA	NA
Psal_10390	215	putative transport protein HsrA	NA	NA	NA
Psal_10430	251	Transcriptional activator protein TraR	NA	NA	NA
Psal_10670	445	Methyl-accepting chemotaxis protein 2	NA	NA	NA
Psal_10700	133	hypothetical protein	NA	NA	NA
Psal_11150	381	hypothetical protein	NA	NA	NA
Psal_11480	282	hypothetical protein	NA	NA	NA
Psal_11640	304	Glyoxylate/hydroxypyruvate reductase B	serA, PHGDH; D-3-phosphoglycerate dehydrogenase / 2-oxoglutarate reductase	Glycine, serine and threonine metabolism [PATH:ko00260]	Amino acid metabolism
Psal_11650	231	HTH-type transcriptional regulator McbR	NA	NA	NA
Psal_11710	316	Pyrimidine-specific ribonucleoside hydrolase RihA	iunH; purine nucleosidase	Purine metabolism [PATH:ko00230]	Nucleotide metabolism
Psal_11720	429	hypothetical protein	K06954; uncharacterized protein	Function unknown	Poorly characterized
Psal_11730	288	All-trans-phytoene synthase	crtB; 15-cis-phytoene/all-trans-phytoene synthase	Carotenoid biosynthesis [PATH:ko00906]	Metabolism of terpenoids and polyketides
Psal_11740	286	15-cis-phytoene synthase	NA	NA	NA
Psal_11820	69	hypothetical protein	NA	NA	NA
Psal_11850	95	hypothetical protein	NA	NA	NA

Psal_11910	330	hypothetical protein	NA	NA	NA
Psal_12330	147	hypothetical protein	NA	NA	NA
Psal_12380	265	hypothetical protein	NA	NA	NA
Psal_12420	45	entericidin B membrane lipoprotein	NA	NA	NA
Psal_12430	98	hypothetical protein	NA	NA	NA
Psal_12450	124	hypothetical protein	NA	NA	NA
Psal_12510	139	hypothetical protein	NA	NA	NA
Psal_12610	286	Glycosyltransferase family 10 (fucosyltransferase)	NA	NA	NA
Psal_12620	297	hypothetical protein	NA	NA	NA
Psal_12700	214	hypothetical protein	NA	NA	NA
Psal_12820	253	3-oxoacyl- reductase FabG	NA	NA	NA
Psal_12870	525	tRNA modification GTPase MnmE	NA	NA	NA
Psal_12910	284	Glycine cleavage system transcriptional activator	NA	NA	NA
Psal_12920	454	putative FAD-linked oxidoreductase	NA	NA	NA
Psal_12930	297	Glycine cleavage system transcriptional activator	gcvA; LysR family transcriptional regulator, glycine cleavage system transcriptional activator	Transcription factors [BR:ko03000]	Transcription
Psal_13070	172	hypothetical protein	NA	NA	NA
Psal_13120	207	Response regulator protein TodT	ttrR; two-component system, LuxR family, response regulator TtrR	Two-component system [BR:ko02022]	Signal transduction
Psal_13130	122	Response regulator protein TmoT	NA	NA	NA
Psal_13160	316	HTH-type transcriptional regulator GltC	dhcR; LysR family transcriptional regulator, carnitine catabolism transcriptional activator	Transcription factors [BR:ko03000]	Transcription
Psal_13170	760	Caffeine dehydrogenase subunit alpha	coxL, cutL; aerobic carbon-monoxide dehydrogenase large subunit	Energy metabolism	Metabolism
Psal_13220	328	leucine/isoleucine/valine transporter permease subunit	NA	NA	NA
Psal_13250	296	Carboxylesterase NlhH	AFMID; arylformamidase	Tryptophan metabolism [PATH:ko00380]	Amino acid metabolism

Psal_13270	289	Carboxylesterase NlhH	PCME; prenylcysteine alpha-carboxyl methylesterase	Terpenoid backbone biosynthesis [PATH:ko00900]	Metabolism of terpenoids and polyketides
Psal_13280	429	Sialic acid TRAP transporter permease protein SiaT	NA	NA	NA
Psal_13290	172	Sialic acid TRAP transporter permease protein SiaT	NA	NA	NA
Psal_13300	332	Sialic acid-binding periplasmic protein SiaP precursor	NA	NA	NA
Psal_13310	239	HTH-type transcriptional repressor CsiR	csiR; GntR family transcriptional regulator, carbon starvation induced regulator	Transcription factors [BR:ko03000]	Transcription
Psal_13330	224	Methyl-accepting chemotaxis protein CtpH	NA	NA	NA
Psal_13340	117	Putative anti-sigma factor antagonist BtrV	NA	NA	NA
Psal_13350	598	Uric acid permease Puck	NA	NA	NA
Psal_13360	425	Serine/threonine-protein kinase BtrW	NA	NA	NA
Psal_13370	698	putative 3-hydroxyphenylpropionic transporter MhpT	NA	NA	NA
Psal_13380	351	ABC transporter substrate binding protein	ABC.X4.S; putative ABC transport system substrate-binding protein	Transporters [BR:ko02000]	Membrane transport
Psal_13390	219	hypothetical protein	NA	NA	NA
Psal_13400	588	Phosphoserine phosphatase RsbU	rsbU_P; phosphoserine phosphatase RsbU/P	Transcription machinery [BR:ko03021]	Transcription
Psal_13410	78	hypothetical protein	NA	NA	NA
Psal_13420	144	hypothetical protein	NA	NA	NA
Psal_13500	837	Hemolysin, chromosomal	NA	NA	NA
Psal_13510	125	hypothetical protein	NA	NA	NA
Psal_13610	193	hypothetical protein	NA	NA	NA
Psal_13640	182	Tetratricopeptide repeat protein	NA	NA	NA
Psal_13660	88	hypothetical protein	NA	NA	NA
Psal_13680	518	D-alanyl-D-alanine-carboxypeptidase/endopeptidase AmpH precursor	NA	NA	NA
Psal_13700	215	Uric acid degradation bifunctional protein	PRHOXNB, URAD; 2-oxo-4-hydroxy-4-carboxy-5-	Purine metabolism [PATH:ko00230]	Nucleotide metabolism

			ureidoimidazoline decarboxylase		
Psal_13880	258	Cephalosporin hydroxylase	NA	NA	NA
Psal_13940	324	2-dehydropantoate 2-reductase	NA	NA	NA
Psal_14160	54	hypothetical protein	NA	NA	NA
Psal_14310	126	Inner membrane transport protein YdhC	NA	NA	NA
Psal_14320	75	hypothetical protein	NA	NA	NA
Psal_14550	68	hypothetical protein	NA	NA	NA
Psal_14730	144	Transcriptional regulator SlyA	NA	NA	NA
Psal_15080	382	C4-dicarboxylate transporter/malic acid transport protein	NA	NA	NA
Psal_15100	389	hypothetical protein	NA	NA	NA
Psal_15110	190	hypothetical protein	NA	NA	NA
Psal_15120	340	Catabolite control protein A	lacI, galR; LacI family transcriptional regulator ugI; unsaturated chondroitin disaccharide hydrolase	Transcription factors [BR:ko03000] Glycan biosynthesis and metabolism	Transcription Metabolism
Psal_15130	401	Unsaturated glucuronyl hydrolase			
Psal_15150	337	2,3-diketo-L-gulonate-binding periplasmic protein YiaO precursor	NA	NA	NA
Psal_15160	637	Sialic acid TRAP transporter permease protein SiaT	NA	NA	NA
Psal_15170	622	hypothetical protein	NA	NA	NA
Psal_15190	260	hypothetical protein	NA	NA	NA
Psal_15200	100	hypothetical protein	NA	NA	NA
Psal_15210	342	hypothetical protein	NA	NA	NA
Psal_15220	369	Limonene 1,2-monooxygenase	NA	NA	NA
Psal_15230	438	Sialic acid TRAP transporter permease protein SiaT	NA	NA	NA
Psal_15240	174	Tripartite ATP-independent periplasmic transporters, DctQ component	NA	NA	NA
Psal_15250	359	Sialic acid-binding periplasmic protein SiaP precursor	NA	NA	NA
Psal_15260	263	hypothetical protein	NA	NA	NA
Psal_15270	218	Tetracycline repressor protein class H	NA	NA	NA
Psal_15280	140	Cupin domain protein	NA	NA	NA

Psal_15290	317	Ureidoglycolate dehydrogenase (NAD(+))	comC; L-2-hydroxycarboxylate dehydrogenase (NAD+)	Methane metabolism [PATH:ko00680] Transcription factors [BR:ko03000]	Energy metabolism
Psal_15300	269	HTH-type transcriptional regulator GmuR	ydhQ; GntR family transcriptional regulator hsaB; 3-hydroxy-9,10-secoandrosta-1,3,5(10)-triene-9,17-dione monooxygenase reductase component cynR; LysR family transcriptional regulator, cyn operon transcriptional activator	Transcription factors [BR:ko03000]	Transcription
Psal_15320	167	FMN reductase (NADH) NtaB		Steroid degradation [PATH:ko00984]	Xenobiotics biodegradation and metabolism
Psal_15330	320	HTH-type transcriptional regulator CynR		Transcription factors [BR:ko03000]	Transcription
Psal_15340	260	3-oxoadipate enol-lactonase 2	pcaD; 3-oxoadipate enol-lactonase K07088; uncharacterized protein	Benzoate degradation [PATH:ko00362]	Xenobiotics biodegradation and metabolism
Psal_15350	298	Membrane transport protein		Function unknown	Poorly characterized
Psal_15360	370	Tripartite tricarboxylate transporter family receptor	NA	NA	NA
Psal_15370	188	Tripartite tricarboxylate transporter TctB family protein	NA	NA	NA
Psal_15380	499	Tripartite tricarboxylate transporter TctA family protein	NA	NA	NA
Psal_15390	383	putative oxidoreductase YcjS	NA	NA	NA
Psal_15400	312	C4-dicarboxylate-binding periplasmic protein precursor	NA	NA	NA
Psal_15410	190	Tripartite tricarboxylate transporter TctB family protein	NA	NA	NA
Psal_15420	499	Tripartite tricarboxylate transporter TctA family protein	NA	NA	NA
Psal_15430	323	Tripartite tricarboxylate transporter family receptor	NA	NA	NA
Psal_15440	225	Putative L-lactate dehydrogenase operon regulatory protein	NA	NA	NA
Psal_15450	357	1,5-anhydro-D-fructose reductase	NA	NA	NA
Psal_15460	288	2-(hydroxymethyl)glutarate dehydrogenase	NA	NA	NA
Psal_15470	293	2-hydroxy-3-oxopropionate reductase	NA	NA	NA
Psal_15490	288	2-hydroxy-3-oxopropionate reductase	NA	NA	NA

Psal_15500	335	Quinone oxidoreductase 1	qor, CRYZ; NADPH2:quinone reductase	Energy metabolism	Metabolism
Psal_15510	101	hypothetical protein	NA	NA	NA
Psal_15520	461	Sialic acid TRAP transporter permease protein SiaT	NA	NA	NA
Psal_15530	166	Tripartite ATP-independent periplasmic transporters, DctQ component	NA	NA	NA
Psal_15540	354	Bacterial extracellular solute-binding protein, family 7	NA	NA	NA
Psal_15560	212	Glutathione S-transferase GstB	GST, gst; glutathione S- transferase	Hepatocellular carcinoma [PATH:ko05225]	Cancers
Psal_15570	337	Glucose--fructose oxidoreductase precursor	NA	NA	NA
Psal_15580	156	hypothetical protein	NA	NA	NA
Psal_15590	308	4-hydroxy-tetrahydrodipicolinate synthase	NA	NA	NA
Psal_15600	391	L-threonine 3-dehydrogenase	SORD, gutB; L-idoitol 2- dehydrogenase aldA; lactaldehyde dehydrogenase / glycolaldehyde dehydrogenase	Fructose and mannose metabolism [PATH:ko00051]	Carbohydrate metabolism
Psal_15630	493	Lactaldehyde dehydrogenase		Pyruvate metabolism [PATH:ko00620]	Carbohydrate metabolism
Psal_15680	711	Catabolite control protein A	NA	NA	NA
Psal_15690	224	L-fuculose phosphate aldolase	fucA; L-fuculose- phosphate aldolase	Fructose and mannose metabolism [PATH:ko00051]	Carbohydrate metabolism
Psal_15720	813	Hemolysin, plasmid	NA	NA	NA
Psal_15740	2235	hypothetical protein	NA	NA	NA
Psal_15750	121	two-component response regulator	NA	NA	NA
Psal_15760	1246	Sensor histidine kinase TmoS	resE; two-component system, OmpR family, sensor histidine kinase ResE	Protein kinases [BR:ko01001]	Enzyme families
Psal_15820	401	Bicyclomycin resistance protein	bcr, tcaB; MFS transporter, DHA1 family, multidrug resistance protein	Transporters [BR:ko02000]	Membrane transport
Psal_15840	74	hypothetical protein	NA	NA	NA

Psal_15890	214	Cation efflux family protein	NA	NA	NA
Psal_15900	141	Mercuric resistance operon regulatory protein	NA	NA	NA
Psal_15950	319	Isoaspartyl peptidase precursor	iaaA, ASRGL1; beta-aspartyl-peptidase (threonine type)	Peptidases [BR:ko01002]	Enzyme families
Psal_15970	358	hypothetical protein	NA	NA	NA
Psal_15980	530	putative D,D-dipeptide-binding periplasmic protein DdpA precursor	ABC.PE.S; peptide/nickel transport system substrate-binding protein K09703; uncharacterized protein	Quorum sensing [PATH:ko02024]	Cellular community - prokaryotes
Psal_15990	376	hypothetical protein	NA	Function unknown	Poorly characterized
Psal_16000	524	Acetophenone carboxylase gamma subunit	NA	NA	NA
Psal_16020	294	putative D,D-dipeptide transport system permease protein DdpC	ABC.PE.P1; peptide/nickel transport system permease protein ABC.PE.P; peptide/nickel transport system permease protein	Transporters [BR:ko02000]	Membrane transport
Psal_16030	342	putative D,D-dipeptide transport system permease protein DdpB	ABC.PE.P; peptide/nickel transport system permease protein	Quorum sensing [PATH:ko02024]	Cellular community - prokaryotes
Psal_16040	806	Transcriptional regulatory protein DevR (DosR)	NA	NA	NA
Psal_16070	135	RutC family protein YjgH	NA	NA	NA
Psal_16080	303	HTH-type transcriptional regulator DmlR	ttdR; LysR family transcriptional regulator, transcriptional activator for ttdABT operon	Transcription factors [BR:ko03000]	Transcription
Psal_16090	214	Bacterial regulatory proteins, gntR family	NA	NA	NA
Psal_16810	200	HTH-type transcriptional regulator AcrR	NA	NA	NA
Psal_17110	151	hypothetical protein	NA	NA	NA
Psal_17170	56	hypothetical protein	NA	NA	NA
Psal_17200	162	Guanine deaminase	NA	NA	NA
Psal_17210	91	hypothetical protein	NA	NA	NA
Psal_17220	546	hypothetical protein	NA	NA	NA
Psal_17230	647	Poly-beta-1,6-N-acetyl-D-glucosamine synthase	NA	NA	NA
Psal_17270	95	hypothetical protein	NA	NA	NA
Psal_17280	181	hypothetical protein	NA	NA	NA

Psal_17540	97	hypothetical protein	NA	NA	NA
Psal_17560	34	hypothetical protein	NA	NA	NA
Psal_17660	501	hypothetical protein	NA	NA	NA
Psal_18030	138	hypothetical protein	NA	NA	NA
Psal_18050	238	Glycosyltransferase family 25 (LPS biosynthesis protein)	NA	NA	NA
Psal_18080	150	hypothetical protein	NA	NA	NA
Psal_18110	416	hypothetical protein	NA	NA	NA
Psal_18320	233	HTH-type transcriptional regulator FrIR	NA	NA	NA
Psal_18380	271	Glutamine-binding periplasmic protein precursor	ABC.PA.S; polar amino acid transport system substrate-binding protein	Transporters [BR:ko02000]	Membrane transport
Psal_18390	217	Inner membrane amino-acid ABC transporter permease protein YecS	ABC.CYST.P; cystine transport system permease protein	Transporters [BR:ko02000]	Membrane transport
Psal_18400	219	Inner membrane amino-acid ABC transporter permease protein YecS	NA	NA	NA
Psal_18420	369	2-oxoglutarate-dependent ethylene/succinate-forming enzyme	NA	NA	NA
Psal_18430	359	spermidine/putrescine ABC transporter periplasmic substrate-binding protein	NA	NA	NA
Psal_18460	257	Putative 2-aminoethylphosphonate transport system permease protein PhnU	NA	NA	NA
Psal_18470	203	Peroxyureidoacrylate/ureidoacrylate amidohydrolase RutB	NA	NA	NA
Psal_18480	249	hypothetical protein	NA	NA	NA
Psal_18490	267	hydroxyacylglutathione hydrolase	NA	NA	NA
Psal_18500	749	DegT/DnrJ/EryC1/StrS aminotransferase family protein	NA	NA	NA
Psal_18510	353	Sulfotransferase domain protein	NA	NA	NA
Psal_18520	237	WbqC-like protein family protein	NA	NA	NA
Psal_18610	37	hypothetical protein	NA	NA	NA
Psal_18690	117	hypothetical protein	NA	NA	NA
Psal_19120	175	META domain protein	NA	NA	NA
Psal_19330	270	Putative monooxygenase YcnE	NA	NA	NA
Psal_19440	545	hypothetical protein	NA	NA	NA
Psal_19510	145	Cytochrome c-556	NA	NA	NA

Psal_19620	236	hypothetical protein	NA	NA	NA
Psal_19740	191	hypothetical protein	NA	NA	NA
Psal_20100	112	hypothetical protein	NA	NA	NA
Psal_20200	261	hypothetical protein	NA	NA	NA
Psal_20210	277	hypothetical protein	NA	NA	NA
			HSD17B8; 17beta-estradiol 17-dehydrogenase / 3alpha(17beta)-hydroxysteroid dehydrogenase (NAD+)	Steroid hormone biosynthesis [PATH:ko00140]	Lipid metabolism
Psal_20310	246	3-oxoacyl- reductase FabG			
Psal_20340	420	Gamma-glutamylputrescine oxidoreductase	NA	NA	NA
Psal_20360	266	Transcriptional regulator KdgR	NA	NA	NA
Psal_20550	259	MltA-interacting protein MipA	NA	NA	NA
			entA; 2,3-dihydro-2,3-dihydroxybenzoate dehydrogenase	Biosynthesis of siderophore group nonribosomal peptides [PATH:ko01053]	Metabolism of terpenoids and polyketides
Psal_20560	257	2,3-dihydro-2,3-dihydroxybenzoate dehydrogenase			
			entB, dhbB, vibB, mxcF; bifunctional isochorismate lyase / aryl carrier protein	Biosynthesis of siderophore group nonribosomal peptides [PATH:ko01053]	Metabolism of terpenoids and polyketides
Psal_20570	219	Isochorismatase			
			entC; isochorismate synthase	Ubiquinone and other terpenoid-quinone biosynthesis [PATH:ko00130]	Metabolism of cofactors and vitamins
Psal_20580	371	Isochorismate synthase EntC			
Psal_20590	314	Pyrimidine-specific ribonucleoside hydrolase RihA	NA	NA	NA
Psal_20600	298	HTH-type transcriptional regulator MurR	NA	NA	NA
Psal_20610	337	NMT1/THI5 like protein	NA	NA	NA
			ABC.SN.S; NitT/TauT family transport system substrate-binding protein	Transporters [BR:ko02000]	Membrane transport
Psal_20620	341	NMT1/THI5 like protein			
Psal_20630	465	Atrazine chlorohydrolase	NA	NA	NA
			Bicarbonate transport system permease protein		
Psal_20650	252	CmpB	NA	NA	NA

Psal_20660	254	Putative aliphatic sulfonates transport permease protein SsuC	NA bauB; beta-alanine degradation protein BauB	NA Amino acid metabolism	NA Metabolism
Psal_20670	96	hypothetical protein	NA	NA	NA
Psal_20680	192	hypothetical protein	NA	NA	NA
Psal_20690	185	Nucleoside 2-deoxyribosyltransferase	NA	NA	NA
Psal_20700	289	L-arabinolactonase	NA	NA	NA
Psal_20760	165	HTH-type transcriptional regulator SarZ	NA	NA	NA
Psal_21030	116	hypothetical protein	NA	NA	NA
Psal_21040	190	hypothetical protein	NA	NA	NA
Psal_21080	109	lysozyme inhibitor	NA	NA	NA
Psal_21100	195	hypothetical protein	NA	NA	NA
Psal_21140	47	hypothetical protein	NA	NA	NA
Psal_21220	120	hypothetical protein	NA	NA	NA
Psal_21630	145	hypothetical protein	NA	NA	NA
Psal_21700	86	hypothetical protein	NA	NA	NA
Psal_22040	243	NADH dehydrogenase subunit E	NA	NA	NA
Psal_22320	65	hypothetical protein	NA	NA	NA
Psal_22600	105	hypothetical protein	NA yihS; sulfoquinovose isomerase	NA Carbohydrate metabolism	NA Metabolism
Psal_22790	403	putative sugar isomerase YihS	NA	NA	NA
Psal_22830	179	hypothetical protein	NA	NA	NA
Psal_22930	130	hypothetical protein	NA	NA	NA
Psal_22970	34	hypothetical protein	NA	NA	NA
Psal_23050	264	Pyrroline-5-carboxylate reductase	NA	NA	NA
Psal_23070	214	HTH-type transcriptional repressor CsiR	NA	NA	NA
Psal_23320	208	hypothetical protein	NA	NA	NA
Psal_23490	211	hypothetical protein	NA	NA	NA
Psal_23760	79	hypothetical protein	NA	NA	NA
Psal_23770	47	hypothetical protein	NA	NA	NA
Psal_23780	173	hypothetical protein	NA	NA	NA
Psal_23790	119	hypothetical protein	NA	NA	NA

Psal_23820	71	hypothetical protein	NA	NA	NA
Psal_23950	239	hypothetical protein	NA	NA	NA
Psal_24160	225	hypothetical protein	NA	NA	NA
Psal_24210	207	Inner membrane protein Yabl	NA	NA	NA
Psal_24220	115	hypothetical protein	NA	NA	NA
Psal_24770	33	hypothetical protein	NA	NA	NA
Psal_25620	263	hypothetical protein	NA	NA	NA
Psal_25800	416	HTH-type transcriptional regulator GbpR	NA	NA	NA
Psal_25900	66	hypothetical protein	NA	NA	NA
Psal_25920	309	hypothetical protein	NA	NA	NA
Psal_26070	236	hypothetical protein	NA	NA	NA
Psal_26270	188	Yip1 domain protein	NA	NA	NA
Psal_26320	317	N-glycosyltransferase	NA	NA	NA
Psal_26390	973	Blue-light-activated protein	NA	NA	NA
Psal_26410	215	hypothetical protein	NA	NA	NA
Psal_26420	186	putative kinase inhibitor protein	NA	NA	NA
Psal_26430	325	hypothetical protein	NA	NA	NA
Psal_26450	165	Phage integrase family protein	NA	NA	NA
Psal_26460	474	Phage integrase family protein	NA	NA	NA
Psal_26510	637	hypothetical protein	NA	NA	NA
Psal_26540	59	hypothetical protein	NA	NA	NA
Psal_26580	157	hypothetical protein	NA	NA	NA
Psal_26960	305	HTH-type transcriptional regulator CynR	NA	NA	NA
Psal_26970	332	Sialic acid-binding periplasmic protein SiaP precursor	NA	NA	NA
Psal_26980	160	Sialic acid TRAP transporter permease protein SiaT	NA	NA	NA
Psal_26990	432	Sialic acid TRAP transporter permease protein SiaT	NA	NA	NA
Psal_27000	311	4-hydroxy-tetrahydrodipicolinate synthase	dapA; 4-hydroxy-tetrahydrodipicolinate synthase	Monobactam biosynthesis [PATH:ko00261] Phenylalanine metabolism	Biosynthesis of other secondary metabolites
Psal_27030	407	D-amino acid dehydrogenase small subunit	dadA; D-amino-acid dehydrogenase	[PATH:ko00360]	Amino acid metabolism

Psal_27040	253	META domain protein	K09914; putative lipoprotein	General function prediction only	Poorly characterized
Psal_27050	173	hypothetical protein	NA	NA	NA
Psal_27060	175	acid-resistance membrane protein	NA	NA	NA
Psal_27420	363	AI-2 transport protein TqsA	NA	NA	NA
Psal_27770	304	Glycosyl transferase family 8	NA	NA	NA
Psal_28000	392	Phytochrome-like protein cph1	cph1; two-component system, chemotaxis family, sensor kinase Cph1	Two-component system [PATH:ko02020]	Signal transduction
Psal_28010	529	Oligopeptide-binding protein AppA precursor	NA	NA	NA
Psal_28020	274	fructoselysine 3-epimerase	NA	NA	NA
Psal_28030	324	Nickel transport system permease protein NikB	NA	NA	NA
Psal_28040	292	Glutathione transport system permease protein GsiD	ABC.PE.P1; peptide/nickel transport system permease protein	Transporters [BR:ko02000]	Membrane transport
Psal_28050	551	Glutathione import ATP-binding protein GsiA	ABC.PE.A1; peptide/nickel transport system ATP-binding protein	Quorum sensing [PATH:ko02024]	Cellular community - prokaryotes
Psal_28070	1152	hypothetical protein	NA	NA	NA
Psal_28120	378	bifunctional tRNA (mnm(5)s(2)U34)-methyltransferase/FAD-dependent cmnm(5)s(2)U34 oxidoreductase	NA	NA	NA
Psal_28130	342	Glucose--fructose oxidoreductase precursor	NA	NA	NA
Psal_28150	277	Histidine-binding periplasmic protein precursor	ABC.PA.S; polar amino acid transport system substrate-binding protein kdgR; LacI family transcriptional regulator, kdg operon repressor	Transporters [BR:ko02000] Transcription factors [BR:ko03000]	Membrane transport Transcription
Psal_28160	353	HTH-type transcriptional regulator KdgR	NA	NA	NA
Psal_28340	118	hypothetical protein	NA	NA	NA
Psal_28490	137	hypothetical protein	NA	NA	NA
Psal_28580	279	hypothetical protein	NA	NA	NA
Psal_28700	202	putative HTH-type transcriptional regulator YttP	NA	NA	NA
Psal_28740	84	hypothetical protein	NA	NA	NA

Psal_28750	277	hypothetical protein	NA	NA	NA
Psal_28760	107	hypothetical protein	NA	NA	NA
Psal_28770	51	hypothetical protein	NA	NA	NA
Psal_28780	105	hypothetical protein	NA	NA	NA
Psal_28790	88	hypothetical protein	NA	NA	NA
Psal_28810	94	hypothetical protein	NA	NA	NA
Psal_28820	51	hypothetical protein	NA	NA	NA
Psal_28830	103	hypothetical protein	NA	NA	NA
Psal_28850	81	hypothetical protein	NA	NA	NA
Psal_28860	224	hypothetical protein	NA	NA	NA
Psal_28890	185	Phage terminase, small subunit	NA	NA	NA
Psal_28900	558	Phage Terminase	NA	NA	NA
Psal_28910	58	hypothetical protein	NA	NA	NA
Psal_28920	459	Phage portal protein	NA	NA	NA
Psal_28930	199	Caudovirus prohead protease	K06904; uncharacterized protein	Function unknown	Poorly characterized
Psal_28940	408	Phage capsid family protein	NA	NA	NA
Psal_28950	150	hypothetical protein	NA	NA	NA
Psal_28960	163	hypothetical protein	NA	NA	NA
Psal_28970	194	hypothetical protein	NA	NA	NA
Psal_28990	149	hypothetical protein	NA	NA	NA
Psal_29000	133	hypothetical protein	NA	NA	NA
Psal_29010	142	hypothetical protein	NA	NA	NA
Psal_29020	121	hypothetical protein	NA	NA	NA
Psal_29030	76	hypothetical protein	NA	NA	NA
Psal_29130	420	O-Antigen ligase	NA	NA	NA
Psal_29140	363	Acyltransferase family protein	NA	NA	NA
Psal_29150	364	Polysaccharide pyruvyl transferase	NA	NA	NA
Psal_29160	442	Polysaccharide biosynthesis protein	NA	NA	NA
Psal_29170	453	hypothetical protein	NA	NA	NA

Psal_29180	324	putative glycosyltransferase EpsJ	migA; alpha-1,6-rhamnosyltransferase	Glycosyltransferases [BR:ko01003]	Glycan biosynthesis and metabolism
Psal_29200	156	hypothetical protein	NA	NA	NA
Psal_29230	995	hypothetical protein	NA	NA	NA
Psal_29250	109	hypothetical protein	NA	NA	NA
Psal_29310	676	Putative tyrosine-protein kinase in cps region	NA	NA	NA
Psal_29410	1816	Bifunctional hemolysin/adenylate cyclase precursor	NA	NA	NA
Psal_29430	359	hypothetical protein	NA	NA	NA
Psal_29460	94	hypothetical protein	NA	NA	NA
Psal_29470	46	short chain dehydrogenase	NA	NA	NA
Psal_29480	321	HTH-type transcriptional regulator SyrM 1	NA	NA	NA
Psal_29490	458	putative D,D-dipeptide-binding periplasmic protein DdpA precursor	ABC.PE.S; peptide/nickel transport system substrate-binding protein	Quorum sensing [PATH:ko02024]	Cellular community - prokaryotes
Psal_29500	51	hypothetical protein	NA	NA	NA
Psal_29540	513	Heme-binding protein A precursor	NA	NA	NA
Psal_29590	477	8-oxoguanine deaminase	NA	NA	NA
Psal_29610	296	Acetate operon repressor	NA	NA	NA
Psal_29620	569	L-arabonate dehydratase	ilvD; dihydroxy-acid dehydratase	Pantothenate and CoA biosynthesis [PATH:ko00770]	Metabolism of cofactors and vitamins
Psal_29630	518	hypothetical protein	NA	NA	NA
Psal_29640	589	Aerobic respiration control sensor protein ArcB	arcB; two-component system, OmpR family, aerobic respiration control sensor histidine kinase ArcB	Two-component system [PATH:ko02020]	Signal transduction
Psal_29650	180	Heme NO binding protein	NA	NA	NA
Psal_29660	391	Phosphoserine phosphatase RsbP	NA	NA	NA
Psal_29680	137	serine-protein kinase RsbW	NA	NA	NA
Psal_29730	250	hypothetical protein	NA	NA	NA
Psal_29860	175	Tripartite ATP-independent periplasmic transporters, DctQ component	NA	NA	NA

Psal_29910	293	Inner membrane ABC transporter permease protein YcjP	IpIC; putative aldouronate transport system permease protein K17318, IpIA; putative aldouronate transport system substrate-binding protein	ABC transporters [PATH:ko02010]	Membrane transport
Psal_29920	532	Lipoprotein LipO precursor		ABC transporters [PATH:ko02010]	Membrane transport
Psal_29930	783	Heparinase II/III-like protein	NA	NA	NA
Psal_30010	332	Tripartite tricarboxylate transporter family receptor Tripartite tricarboxylate transporter TctB family protein	NA	NA	NA
Psal_30020	167		NA	NA	NA
Psal_30120	218	hypothetical protein	NA	NA	NA
Psal_30140	312	Blue-light-activated histidine kinase	NA	NA	NA
Psal_30240	162	2,3-diketo-L-gulonate TRAP transporter small permease protein YiaM	NA	NA	NA
Psal_30260	323	2,3-diketo-L-gulonate-binding periplasmic protein YiaO precursor	NA	NA	NA
Psal_30270	303	2-(hydroxymethyl)glutarate dehydrogenase	NA	NA	NA
Psal_30510	552	Ribulokinase	NA	NA	NA
Psal_30520	272	Gluconate 5-dehydrogenase	NA	NA	NA
Psal_30540	155	Tripartite tricarboxylate transporter TctB family protein	NA	NA	NA
Psal_30550	327	Tripartite tricarboxylate transporter family receptor	NA	NA	NA
Psal_30560	248	HTH-type transcriptional regulator LutR	NA	NA	NA
Psal_30570	219	4-hydroxy-4-methyl-2-oxoglutarate aldolase	NA	NA	NA
Psal_30580	1537	hypothetical protein	NA	NA	NA
Psal_30590	849	Exopolysaccharide glucosyl ketal-pyruvate-transferase	NA	NA	NA
Psal_30600	316	hypothetical protein	NA	NA	NA
Psal_30610	98	hypothetical protein	NA	NA	NA
Psal_30710	223	hypothetical protein	NA	NA	NA
Psal_30870	155	MarR family protein	NA	NA	NA
Psal_30880	391	hypothetical protein	NA	NA	NA
Psal_30950	74	hypothetical protein	NA	NA	NA

Psal_31060	415	Sialic acid TRAP transporter permease protein SiaT	yiaN; TRAP-type transport system large permease protein	Transporters [BR:ko02000]	Membrane transport
Psal_31070	180	2,3-diketo-L-gulonate TRAP transporter small permease protein YiaM	NA	NA	NA
Psal_31080	328	2,3-diketo-L-gulonate-binding periplasmic protein YiaO precursor	NA	NA	NA
Psal_31120	337	Thiosulfate-binding protein precursor	cysP, sbp; sulfate transport system substrate-binding protein	Sulfur metabolism [PATH:ko00920]	Energy metabolism
Psal_31180	266	Shikimate dehydrogenase	NA	NA	NA
Psal_31300	346	hypothetical protein	NA	NA	NA
Psal_31460	63	hypothetical protein	NA	NA	NA
Psal_31790	293	Secreted effector protein pipB2	NA	NA	NA
Psal_31980	135	hypothetical protein	NA	NA	NA
Psal_32060	81	hypothetical protein	NA	NA	NA
Psal_32070	228	N-carbamoylsarcosine amidase	NA	NA	NA
Psal_32080	129	Glyoxalase-like domain protein	NA	NA	NA
Psal_32090	327	2-oxoglutarate-dependent ethylene/succinate-forming enzyme	NA	NA	NA
Psal_32100	295	Autoinducer 2 import system permease protein LsrC	ABC.SS.P; simple sugar transport system permease protein	Transporters [BR:ko02000]	Membrane transport
Psal_32110	363	Branched-chain amino acid transport system / permease component	ABC.SS.P; simple sugar transport system permease protein	Transporters [BR:ko02000]	Membrane transport
Psal_32120	496	Ribose import ATP-binding protein RbsA	ABC.SS.A; simple sugar transport system ATP-binding protein	Transporters [BR:ko02000]	Membrane transport
Psal_32130	361	Purine-binding protein precursor	med; transcriptional activator of comK gene	Transcription factors [BR:ko03000]	Transcription
Psal_32150	276	putative oxidoreductase/MSMEI_2347	dkgA; 2,5-diketo-D-gluconate reductase A	Others	Metabolism
Psal_32220	270	hypothetical protein	NA	NA	NA
Psal_32530	756	Type IV pilus biogenesis	NA	NA	NA
Psal_32700	365	Bacterial regulatory proteins, luxR family	NA	NA	NA
Psal_32710	415	hypothetical protein	NA	NA	NA

Psal_32760	35	hypothetical protein	NA	NA	NA
Psal_32920	63	hypothetical protein	NA	NA	NA
Psal_33010	161	hypothetical protein	NA	NA	NA
Psal_33190	362	hypothetical protein	NA	NA	NA
Psal_33200	144	hypothetical protein	NA	NA	NA
Psal_33210	170	Amidohydrolase	K07045; uncharacterized protein	Function unknown	Poorly characterized
Psal_33220	108	hypothetical protein	NA	NA	NA
Psal_33300	125	Glutathione-dependent formaldehyde-activating enzyme	NA	NA	NA
Psal_33330	150	hypothetical protein	K06872; uncharacterized protein	Function unknown	Poorly characterized
Psal_33670	230	hypothetical protein	NA	NA	NA
Psal_33790	160	hypothetical protein	NA	NA	NA
Psal_34020	54	hypothetical protein	NA	NA	NA
Psal_34040	114	hypothetical protein	NA	NA	NA
Psal_34180	370	Zinc transport protein ZntB	NA	NA	NA
Psal_34380	54	hypothetical protein	NA	NA	NA
Psal_34450	210	HTH-type transcriptional repressor ComR	NA	NA	NA
Psal_34460	717	Dihydrolipoyl dehydrogenase	NA	NA	NA
Psal_34510	370	NADH dehydrogenase	NA	NA	NA
Psal_34530	84	hypothetical protein	NA	NA	NA
Psal_34540	235	RNA polymerase sigma factor YlaC	SIG3.2, rpoE; RNA polymerase sigma-70 factor, ECF subfamily	Transcription machinery [BR:ko03021] Glycine, serine and threonine metabolism [PATH:ko00260]	Transcription Amino acid metabolism
Psal_34900	315	Glyoxylate/hydroxypyruvate reductase B	HPR2; hydroxypyruvate reductase 2		
Psal_35100	243	HTH-type transcriptional regulator SrpR	NA	NA	NA
Psal_35210	268	Putative ABC transporter arginine-binding protein 2 precursor	ABC.PA.S; polar amino acid transport system substrate-binding protein	Transporters [BR:ko02000]	Membrane transport
Psal_35220	221	Inner membrane amino-acid ABC transporter permease protein YecS	ABC.PA.P; polar amino acid transport system permease protein	Transporters [BR:ko02000]	Membrane transport

Psal_35230	217	Inner membrane amino-acid ABC transporter permease protein YecS	ABC.PA.P; polar amino acid transport system permease protein	Transporters [BR:ko02000]	Membrane transport
Psal_35300	57	hypothetical protein	NA	NA	NA
Psal_35520	242	hypothetical protein	NA	NA	NA
Psal_36130	691	Flagellar hook-length control protein FliK	NA	NA	NA
Psal_36200	385	N-methyltryptophan oxidase	dauA; D-arginine dehydrogenase	D-Arginine and D-ornithine metabolism [PATH:ko00472]	Metabolism of other amino acids
Psal_36380	319	NMT1/THI5 like protein	NA	NA	NA
Psal_36440	277	Beta-barrel assembly-enhancing protease	NA	NA	NA
Psal_36940	320	Phosphotransferase enzyme family protein	NA	NA	NA
Psal_36980	304	Ferri-bacillibactin esterase BesA	K07017; uncharacterized protein	Function unknown	Poorly characterized
Psal_37280	503	hypothetical protein	NA	NA	NA
Psal_37300	731	Integrase core domain protein	NA	NA	NA
Psal_37340	71	hypothetical protein	NA	NA	NA
Psal_37350	961	Modification methylase BamHI	NA	NA	NA
Psal_37370	142	hypothetical protein	NA	NA	NA

Table S6: Species description of strain Lw-13e^T following the digital protologue protocol.

Date Created	2018-05-30 10:55:39
Date Updated	2019-01-22 11:56:18
USER	LAURA
TAXONUMBER (TXNR)	TA00551
AUTHORS (AUTE)	
FIRST SUBMISSION DATE	18 Sep 2018
TYPE OF DESCRIPTION (TYDE)	
FORMER TAXONUMBERS OF THE PROTOLOGUES SUBJECTED TO EMENDATION (FTXN)	
BASONYM (BASO)	
DATE OF THE EFFECTIVE PUBLICATION (EFPU)	
DATE OF VALID PUBLICATION (VAPU)	
SPECIES NAME (Give the binomial species name) (SPNA)	Pseudoceanicola algae
GENUS ETYMOLOGY (GETY)	
TYPE SPECIES OF THE GENUS (GENT)	
GENUS NAME (GENA)	Pseudoceanicola
SPECIFIC EPITHET (SPEP)	algae
SPECIES ETYMOLOGY (SPTY)	al'gae, L. gen. n. algae, of alga, seaweed; referring to the isolation source from algae
SUBSPECIES NAME (SSNA)	
SUBSPECIES ETYMOLOGY (SSTY)	
AUTHORS (AUTH)	Wolter LA, Wietz M, Ziesche L, Picard A, Breider S, Poehlein A, Daniel R, Schulz S, Brinkhoff T,
TITLE (TITL)	Pseudoceanicola algae sp. nov., isolated from the marine macroalga Fucus spiralis shows genomic and physiological adaptations for an algal associated lifestyle
JOURNAL (JOUR)	Systematic and Applied Microbiology
VOLUME & PAGES (VOLP)	
DOI (DOI)	
CORRESPONDING AUTHOR (COAU)	Thorsten Brinkhoff
E-MAIL OF THE CORRESPONDING AUTHOR (EMAU)	t.brinkhoff@icbm.de
SUBMITTER (SUBM)	LAURA WOLTER
E-MAIL OF THE SUBMITTER (EMSU)	laura.wolter@uni-oldenburg.de
YES	
NO	Checked
SUBMITTER (of the emendation) (SUBE)	
E-MAIL OF THE SUBMITTER (of the emendation) (EMSB)	
METAGENOME ACCESSION NUMBER (MECA)	
TITLE (TITE)	
JOURNAL (JOUE)	
MAG/SAG ACCESSION NUMBER [RefSeq] (GARE)	
VOLUME & PAGES (VOPE)	
DOI (DOIE)	
MAG/SAG ACCESSION NUMBER [other] (BINN)	

MODIFICATIONS TO THE ORIGINAL DESCRIPTION (EMEM)	
DESIGNATION OF THE TYPE STRAIN (TYPE)	Lw-13e
STRAIN COLLECTION NUMBERS (COLN)	DSM 29013 = LMG 30557
16S rRNA GENE ACCESSION NUMBER (16SR)	KM268063
ALTERNATIVE HOUSEKEEPING GENES:GENE [ACCESSION NUMBER] (HKGN)	
GENOME ACCESSION NUMBER [RefSeq] (GARE)	QBBT00000000
GENOME ACCESSION NUMBER [EMBL] (GAEM)	
GENOME STATUS (GSTA)	draft
GENOME SIZE (GSIZ)	4068
GC mol % (GGCM)	64.1
HOUR OF COLLECITON OF THE SAMPLE [Sharp hours] (HOCS)	
COUNTRY OF ORIGIN (COUN)	Germany
REGION OF ORIGIN (REGI)	Neuharlingersiel, North Sea coast
OTHER (COTH)	
DATE OF ISOLATION (DATI)	27 Jun 2013
DATE OF ISOLATION UNKNOWN (&lt; yyyy) (DATU)	
SOURCE OF ISOLATION (SOUR)	Surface of the marine macroalga Fucus spiralis
SAMPLING DATE (DATS)	27 Jun 2013
GEOGRAPHIC LOCATION (GEOL)	Neuharlingersiel
DNA EXTRACTION METHOD (DNAE)	
ASSEMBLY (ASEM)	
LATITUDE (LATI)	53°42'17.0"N
SEQUENCING TECHNOLOGY (SEQT)	
LONGITUDE (LONG)	7°42'16.1"E
BINNING SOFTWARE USED (BINS)	
DEPTH (DEPT)	
ASSEMBLY SOFTWARE USED (ASFT)	
ALTITUDE (ALTI)	
TEMPERATURE OF THE SAMPLE [In Celsius degrees] (TEMS)	
pH OF THE SAMPLE (PHSA)	
SALINITY OF THE SAMPLE [In percentage %] (SALS)	
yes	
no	Checked
LOWEST TEMPERATURE FOR GROWTH (TEML)	4
HIGHEST TEMPERATURE FOR GROWTH (TEMH)	34
TEMPERATURE OPTIMUM (TEMO)	20-28
LOWEST pH FOR GROWTH (PHLO)	5.5 (ASW+3% MB)
HIGHEST pH FOR GROWTH (PHHI)	9 (ASW+3% MB)
pH OPTIMUM (PHOP)	6.5 - 8
pH CATEGORY (PHCA)	neutrophile
LOWEST NaCl CONCENTRATION FOR GROWTH (SALL)	0.5 (ASW+3% MB)
HIGHEST NaCl CONCENTRATION FOR GROWTH (SALH)	17.5 (ASW+3% MB)
SALINITY OPTIMUM (SALO)	1-4

OTHER SALTS BESIDES NaCl TO BE REPORTED (SALW)	
SALINITY CATEGORY (SALC)	mild halophile (optimum 1-6 % NaCl)
RELATIONSHIP TO O₂ (OREL)	aerobe
TERMINAL ELECTRON ACCEPTOR (ELAC)	
ENERGY METABOLISM (EMET)	
BIOSAFETY LEVEL (BIOS)	1
HABITAT (HABT)	plant-associated environment (ENVO:01001001)
BIOTIC RELATIONSHIP (BIOR)	symbiotic
SYMBIOSIS WITH THE HOST (HOST)	
KNOWN PATHOGENICITY (PATH)	none
MISCELLANEOUS, EXTRAORDINARY FEATURES RELEVANT FOR THE DESCRIPTION (EXTR)	production of orange pigment heterogenic shape of cells, with propagation through binary fission and budding non-motile, despite genomic and microscopic evidence of flagella

Table S7: Fatty acid composition (%) of strain Lw 13e^T compared to related *Pseudoceanicola* type strains.

Fatty acid (%)	Lw-13e ^T	<i>P. antarcticus</i> Ar-45 ^T	<i>P. marinus</i> LMG 23705 ^T	<i>P. atlanticus</i> 22II-S11g ^T
Straight-chain:				
C _{12:0}	-	-	-	2.5
C _{16:0}	5	34	14.7	15.9
C _{18:0}	-	2.2	1	tr
Hydroxy:				
C _{10:0} 3-OH	-	-	tr	4.5
C _{12:0} 3-OH	tr	-	2.1	7.8
Unsaturated:				
11-methyl C _{18:1} ω _{7c}	2.8	4.6	6.6	10.5
C _{19:0} cyclo ω _{8c}	tr	33.1	24.6	-
Summed features:				
3 (C _{16:1} ω _{7c} , C _{16:1} ω _{6c} , C _{15:0} iso 2OH)	6.4	1.7	1	tr
8 (C _{18:1} ω _{6c} /ω _{7c})	84.4	21	49.1	54.7

-, not detected; tr, trace amounts (<1%).

Table S8: Volatile compounds (terpenes in bold) produced by strain Lw-13e^T based on total ion chromatogram from GC-MS analysis (Fig. S3).

Nr ^a	Volatile compounds (terpenes in bold)	RT [min]	RI ^b	RI [Lit][1]
1	1-pentanol	3.2	787	780
2	dimethyl disulfide	3.44	795	785
3	S-methyl propanethioate	3.72	804	806
4	3-hydroxypentan-2-one	3.86	809	800
5	2-hydroxypentan-3-one	4.1	817	817
6	butyl acetate	4.15	818	819
7	5-methylhexan-3-one	4.68	836	844
8	4-hydroxy-4-methyl-2-pentanone	4.96	845	847
9	unknown	5.39	859	
10	2-hydroxyhexan-3-one	6.58	899	900
11	3-hydroxyhexan-2-one	6.7	902	
12	dimethyl trisulfide	9.05	967	969
13	benzotrile	9.68	984	989
14	phenol	9.75	986	984
15	limonene	11.2	1027	1027
16	(methyldisulfanyl)-methylsulfanylmethane	14.32	1118	1110
17	3-hydroxy-4-methylbenzaldehyde	14.99	1139	
18	1-phenylpropan-1-one	15.62	1159	1164
19	unknown	15.79	1165	
20	2-butyl-3-methylpyrazine	16.54	1188	1193
21	2,6-dimethyl-3-(2-methylpropyl)pyrazine	16.76	1195	1194
22	unknown	17.13	1208	
23	3-phenylbutan-2-one	17.95	1238	1243
24	unknown	18.33	1252	1252
25	unknown pyrazine	18.42	1256	
26	ethyl 2-hydroxybenzoate	18.69	1265	1267
27	unknown	19.36	1290	
28	2-aminoacetophenone	19.51	1296	1299
29	2-isopentyl-3,6-dimethylpyrazine	19.67	1302	1308
30	4-methylquinazoline	20.67	1339	1332
31	dodecen-2-one	21.85	1383	
32	dodecen-2-ol	21.97	1387	
33	unknown S-compound	23.22	1437	
34	11-methyldodecen-3-one	23.34	1442	
35	11-methyldodecan-3-one	23.75	1458	
36	tridecen-3-one	24.17	1475	
37	tridecen-3-ol	24.29	1480	
38	unknown	25.55	1530	
39	unknown	26.01	1549	
40	methyltridecan-2-one	26.15	1554	
41	nerolidol	26.24	1558	1561
42	heptadecane	29.31	1699	1700
43	2-ethylhexyl benzoate	29.53	1709	
44	farnesol	29.8	1722	1721
45	2-ethylhexyl 2-hydroxybenzoate	31.56	1805	1805
46	nonadecane	33.45	1890	1900

^anumbering corresponds to peak numbers in the total ion chromatogram (Fig. S3).

^b Retention Index calculated from Retention time (RT)

[1] <http://webbook.nist.gov/chemistry/>

Supplementary Material for Manuscript 2

Rhodobacteraceae on the marine brown alga *Fucus spiralis* are abundant and show physiological adaptation to an epiphytic lifestyle

Supplementary Text S1

Materials and methods

454 pyrosequencing and pyrosequencing-derived dataset processing and analysis

For every sample, three 50 µL PCR approaches, each with 50 ng DNA as template, were performed using Phusion® High-Fidelity DNA Polymerase (Thermo Scientific, Wilmington, DE, USA). The primers 341F and 907RM (Muyzer et al. 1998) were used, amplifying a 566 bp long 16S rRNA gene fragment, including the hypervariable regions V3, V4 and V5. These primers were complemented with A and B adaptor, and the forward primer additionally contained one of the multiplex identifier (MID) sequences MID-132 – MID-153, according to the manufacturing protocol of “Technical Bulletin No. 005-2009” (Roche Applied Science, Mannheim, Germany). The final concentrations of a 50 µL PCR reaction were: 10 µL 5x Phusion GC buffer, 4 µL dNTPs (2.5 mM), 0.5 µL MgCl₂ (1.5 mM), 1 µL BSA (3 mg mL⁻¹), 1.5 µL 100% DMSO, 2.5 µL of each forward and reverse primer (10 pmol), 0.5 µL Phusion DNA polymerase and template DNA depending on the DNA concentration of the individual sample. Finally, molecular biology grade water (5-Prime GmbH, Hamburg, Germany) was added to a total volume of 50 µL. The conditions of the PCR were: 95 °C for 4 min, 30 cycles of 45 s denaturing at 95 °C, 1 min primer annealing at 58 °C, and 45 s extension at 72 °C, followed by a final extension step of 5 min at 72 °C. PCR products were checked on 1% agarose gels and DNA fragments of approximately 600 bp length, determined by using the Gene Ruler Express DNA Ladder (Thermo Fisher Scientific), were extracted from the agarose gel (NucleoSpin® Gel and PCR Clean-up, Macherey-Nagel). The purity and quantity of the DNA fragments were determined with a Nanodrop 2000c spectrophotometer (Thermo Fisher Scientific). The three PCR products of each sample generated in parallel were pooled and used for the downstream pyrosequencing step. Amplicon libraries were sequenced with a Roche 454 GS-FLX++ (Göttingen Genomics Laboratory, Göttingen, Germany) and deposited in the National Center for Biotechnology Information Sequence Read Archive under the accession number SRA198204.

After raw data extraction, reads shorter than 300 bp, possessing long homopolymer stretches (> 8 bp) or primer mismatches (> 5), were removed. Subsequently, sequences were denoised using Acacia (v1.53) (Bragg et al. 2012). Remaining primer sequences were truncated with cutadapt (Martin 2011). Afterwards, chimeric sequences were removed with UCHIME (denovo and reference) and the

SILVA SSU119NR database as the reference dataset (Edgar 2010, Quast et al. 2012). Processed sequences of all samples were combined, sorted by decreasing length, and clustered using the UCLUST algorithm (Edgar et al. 2011). The phylogenetic composition was determined with the QIIME assign_taxonomy.py script (Caporaso et al. 2010). For this purpose, a consensus sequence for each OTU was determined using USEARCH and classified by a BLAST alignment against the SILVA SSURef 119NR database. Sequences were classified with respect to the SILVA taxonomy of their best hit. Rarefaction curves, Shannon and Chao (Shannon 2001, Chao et al. 2002) indices were calculated as described by Wemheuer et al. (Wemheuer et al. 2014). In addition, the maximum number of OTUs (n_{max}) was estimated for each sample using the Michaelis-Menten-fit.

Sequencing and phylogenetic analysis of 16S rRNA genes

The 16S rRNA genes of the bacterial isolates were amplified and sequenced according to Brinkhoff and Muyzer (Brinkhoff et al. 1997). Sequencing reactions were performed by GATC Biotech (Constance, Germany). Sequences with a length of at least 1,000 bp were compared with those in GenBank using the BLAST analysis available on the National Center for Biotechnology Information (NCBI) server (www.ncbi.nlm.nih.gov). The 16S rRNA gene sequences of the isolates obtained in this study were deposited in GenBank under the accession numbers KC731427, KC731428, KJ786453 – KJ786461 and KM268054 – KM268074.

Phylogenetic trees with the 16S rRNA gene sequences obtained from the 454-based community analysis and the bacterial isolates were constructed using the ARB software package (www.arb-home.de) (Ludwig et al. 2004). Sequences of type strains (>1,300 bp) were used for construction of the backbone-tree using the neighbor-joining method with 1,500 replicates. Shorter sequences determined in this study were added afterwards by the parsimony-interactive method without using a filter. Sequences affiliated with the Marine Host-associated *Rhodobacteraceae* (MHR) cluster were determined by BLAST analysis of the 454 consensus operational taxonomic units (OTUs). Sequences with 16S rRNA gene similarity $\geq 96\%$ were added to the phylogenetic tree.

Growth experiments

Isolates were tested in triplicates for growth on substrates indicated for brown algae and *F. spiralis*, which were betaine, L-proline, D(+)-sucrose, taurine, D(+)-melibiose, D(+)-trehalose, D-mannitol, L-serine, D(+)-glucose, laminarin from *Laminaria digitata*, fucoidan from *Fucus vesiculosus*, D(+)-fucose (Powell et al. 1964, Graham et al. 1999, Hemmi et al. 2004, Imbs et al. 2009, Michel et al. 2010, Klindukh

et al. 2011) and the algal osmolyte sarcosine (Kalhoefer et al. 2011). Artificial seawater medium was prepared according to Zech et al. (Zech et al. 2009) and supplemented with a 5-fold concentrated vitamin solution (Balch et al. 1979). Substrates were added to a final concentration of 5 mM. Single isolates that did not show growth in this minimal medium were tested in the same medium supplemented with 0.01% yeast extract, according to Wagner-Döbler et al. (Wagner-Döbler et al. 2004). In this case, growth was compared to that on 0.01% yeast extract only. Growth was inspected daily by measuring the OD₆₀₀ (Spectronic® 70 Spectrophotometer, Bausch & Lomb) over a period of three weeks. Positive growth was defined as OD₆₀₀ ≥125% of the initial value, according to Rocker et al. (Rocker et al. 2012).

Screening for inhibitory effects

Isolates were tested for inhibitory activity against various marine bacteria affiliated to *Flavobacteriia*, *Alphaproteobacteria*, *Gammaproteobacteria* and *Actinobacteria*, as well as an axenic diatom culture of *Skeletonema costatum* CCMP 1332. Two strains of each bacterial class affiliated to different genera were used (Supplementary Table S2). Isolates tested for inhibitory activity were grown for two days in 5 mL of the following media: Marine Broth 2216, Marine Broth 2216 supplemented with 0.1% air dried pestled *F. spiralis*, Marine Broth 2216 containing a piece of autoclaved *F. spiralis*, and Marine Broth 2216 containing all *F. spiralis*-related substrates mentioned above at a final concentration of 2 mM of each substrate. Inhibition assays were performed as described by Brinkhoff et al. (Brinkhoff et al. 2004) with the following modification: Bacterial target strains were pre-cultured at 20 °C for two days with shaking in 20 mL Marine Broth 2216 and then a 200 µL volume of the target culture with an adjusted OD₆₀₀ of 0.2 was spread onto a Marine Broth 2216 agar plate.

Screening for siderophore production

Siderophore production was analysed by a Chrome Azurol S (CAS) assay with isolates grown on Marine Broth 2216 without iron (III) citrate. Siderophore production was determined according to Shin et al. (Shin et al. 2001). The agar plates were punched with 9-mm-diameter holes, which were filled with 200 µL stationary bacterial culture and incubated for three days at 20 °C in the dark. Marine Broth 2216 without iron (III) citrate, as well as water and *Roseobacter denitrificans* DSM 7001^T, were used as negative controls, whereas *Phaeobacter inhibens* DSM 16374^T and Marine Broth 2216 supplemented with 25 µL deferoxamine mesylate solution (2.5 mM) represented the positive control. Additionally, isolates were grown on iron (III) citrate-deficient Marine Broth 2216 agar plates to generate iron limiting conditions, and siderophore production was determined according to Thole et al. (Thole et al. 2012).

Screening for bacteriochlorophyll a and pufLM genes

Extraction of bacteriochlorophyll *a* (BChl *a*) was performed according to Giebel et al. (Giebel et al. 2013). Absorbance of the extracts was determined in the range of 650-1000 nm with a Beckmann DU 520 General Purpose UV/VIS Spectrophotometer. *Phaeobacter inhibens* DSM 16374^T was used as a negative control, and *Roseobacter denitrificans* DSM 7001^T as a positive control. Detection of genes coding for the subunits of the photosynthetic reaction centre complex (*pufL* and *pufM*) was carried out by using the primer set of Beja et al. (Beja et al. 2002).

Screening for vitamin B₁₂ biosynthesis

Due to the fact, that *F. spiralis* has a B₁₂-heterotrophy (Fries 1993), production of this vitamin by the isolated bacteria was tested. For detection of vitamin B₁₂ biosynthesis, isolates were grown in triplicate in artificial seawater medium, according to Zech et al. (Zech et al. 2009), supplemented with glucose (5 mM), yeast extract [0.01% (m/v)] and a 5-fold vitamin solution, according to Balch et al. (Balch et al. 1979), without cyanocobalamin (vitamin B₁₂), at 20 °C in the dark. Traces of vitamin B₁₂ in the medium derived from the yeast extract and the results for the isolates were normalized against the medium. In the late exponential growth phase, cells were removed by sterile filtration with a polyethersulfone filter (0.2 µm pore size, Sartorius Stedim Biotech GmbH, Göttingen, Germany). One millilitre of the filtrate was used for extraction and quantification of the complete vitamin B₁₂ content, according to the manufacturer's protocol for the VitaFast[®] Vitamin B₁₂ Kit (R-Biopharm AG, Darmstadt, Germany).

Results

454 statistics

Overall, 36,165 raw sequence reads were generated from three individual *F. spiralis* specimens (Supplementary Table S8). After denoising and removal of non-bacterial and chimeric sequences the average number of reads per sample was 9,035 with an average sequence length of 540 bp. Calculation of rarefaction curves showed an OTU coverage of approximately 95% at a 20% genetic divergence, indicating an almost complete elucidation of the bacterial community at the phylum level. For calculations considering the singletons at 3% and 1% genetic divergence, the OTU coverage was approximately 64% and 52%, respectively. The above-mentioned OTU coverages changed to 97%, 83% and 76% after discounting the singletons. Discounting singletons revealed much higher coverage rates but disregarded the rare community (Supplementary Fig. S5). Calculated Shannon indices ranged

from 7.49 to 4.94 (6.71 to 4.70), 6.34 to 4.23 (5.64 to 4.06) and 2.32 to 1.64 (2.19 to 1.58) at genetic distances of 1%, 3% and 20%, respectively, with and without singletons (in parentheses) (Supplementary Table S9).

Supplementary Figures and Tables

Fig. S1: Map showing the two sampling sites for *Fucus spiralis* (wave-breaker and harbour, each indicated by an asterisk) at the village of Neuharlingersiel, Germany. Light-grey: water; dark-grey: landmass.

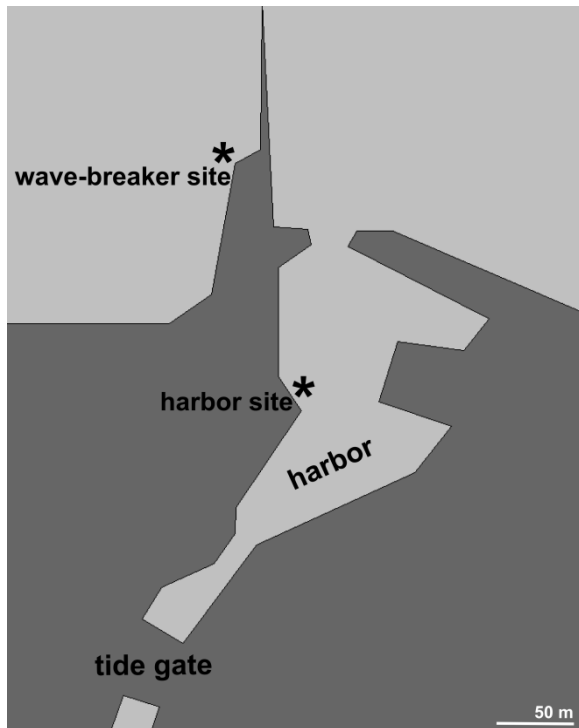


Fig. S2: Different parts of the thallus of *Fucus spiralis* investigated in this study.

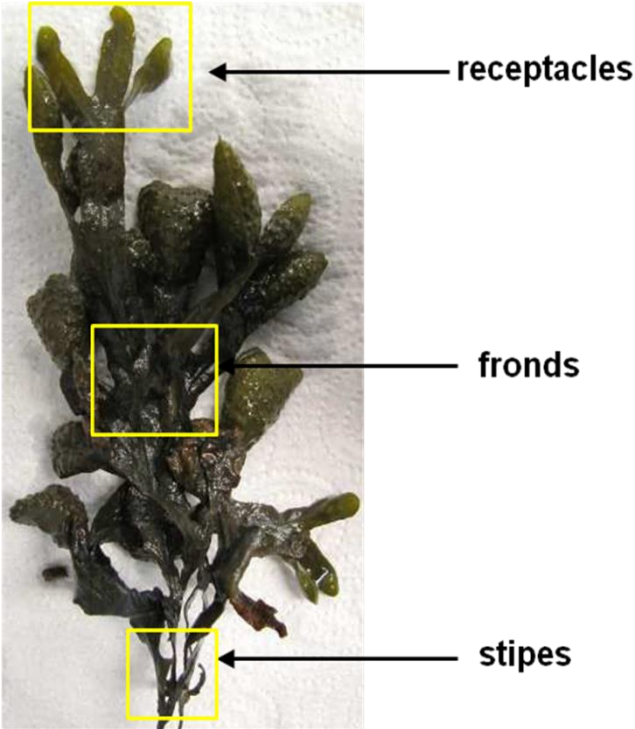
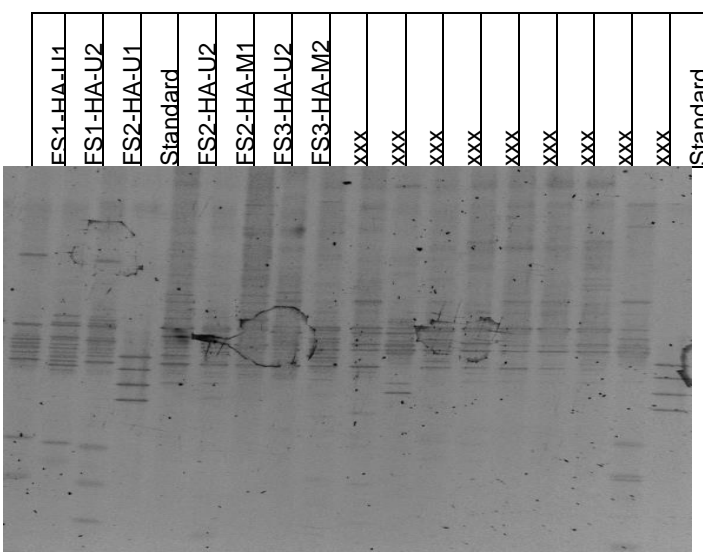
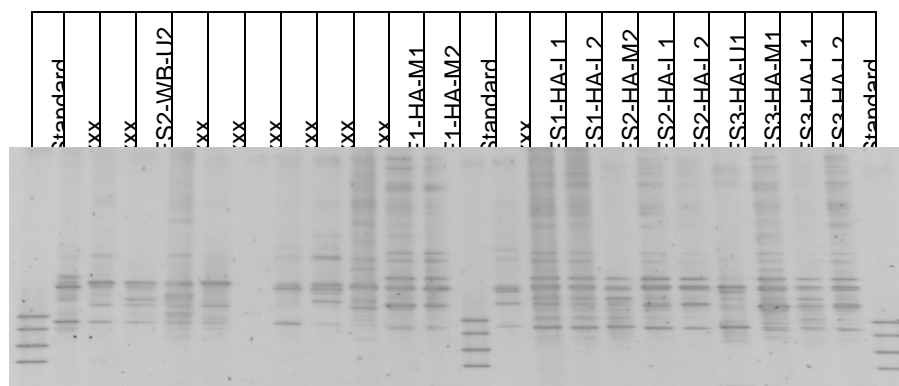
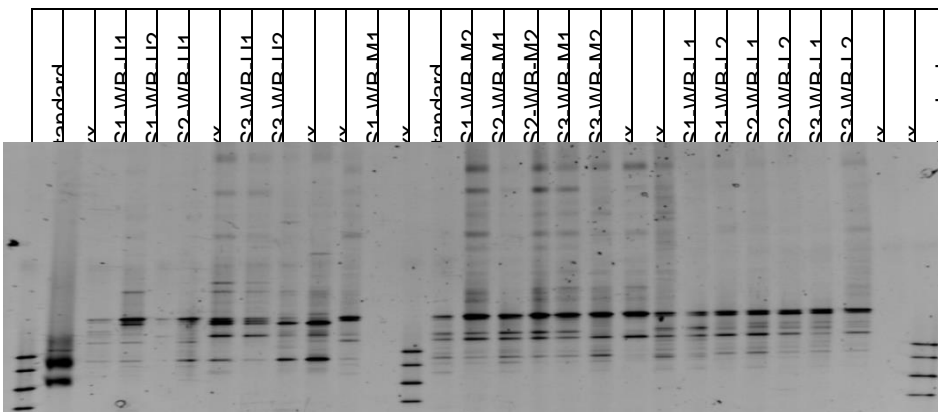
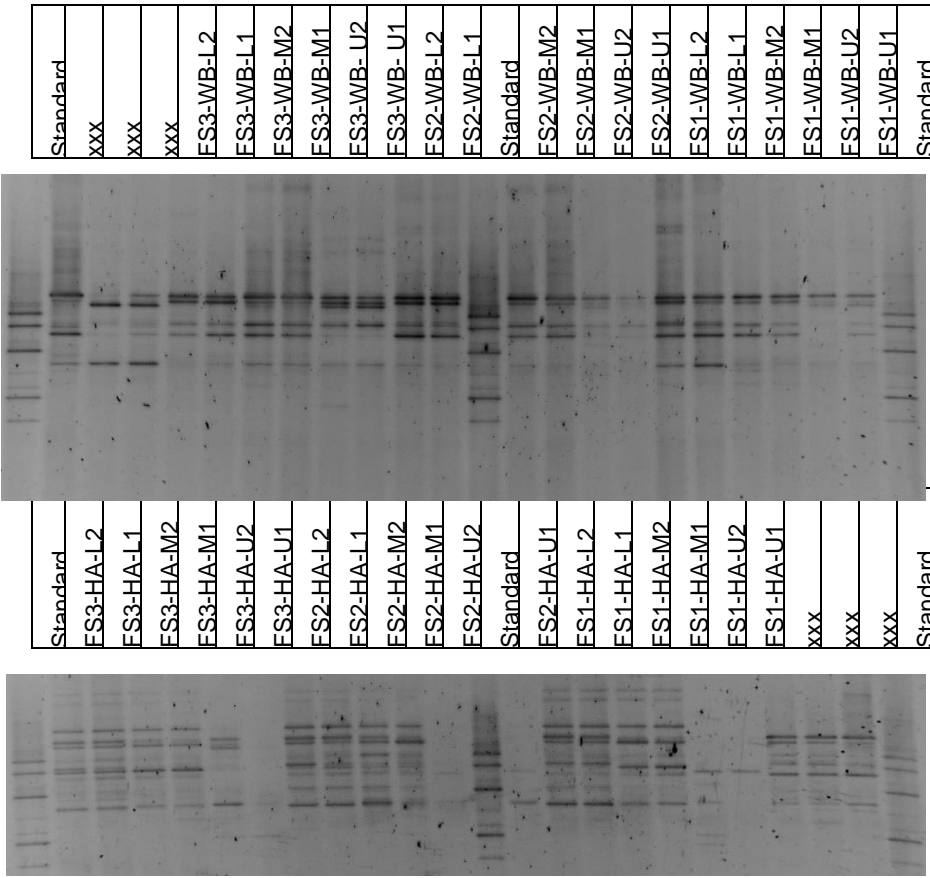


Figure S3: Images of DGGE banding patterns based on 16S rRNA gene amplicons obtained from DNA of *F. spiralis*-associated bacterial biofilms. Amplicons were generated with a universal bacterial primer system (A) and a *Rhodobacteraceae* (*Roseobacter*-group) specific primer system (B) from three specimens collected at two different sites on the coast off Neuharlingersiel, southern North Sea. Individual alga samples are indicated by the first position of the sample designation [*Fucus spiralis* = FS1/2/3] and the sample origin by the second position [i.e. WB = wave-breaker, HA = harbour (see Fig. S1)]. The third position indicates two parallel subsamples of different parts [U = upper part (receptacles); M = middle part (fronds); L = lower part (stipes)] of each individual alga. Lanes denoted by “xxx” are not part of this study or subsequent calculations. (C) Images of amplicons generated with the universal bacterial primer system of samples taken over a period of one year. Details concerning sampling and PCR are given in the section Experimental Procedures.

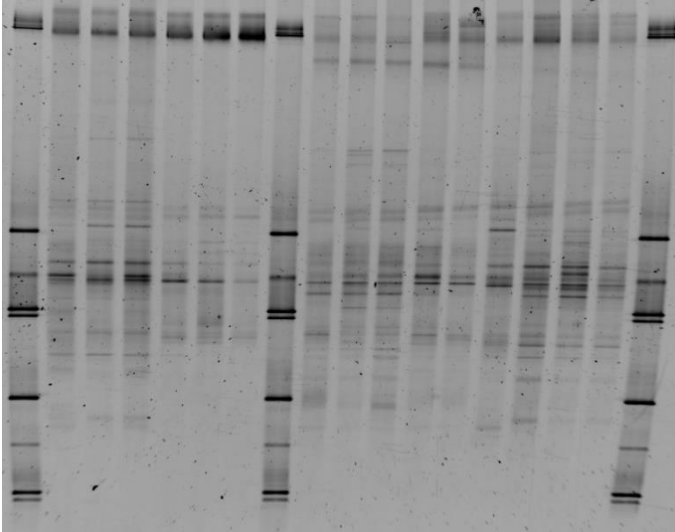
A



B

C

Standard
1 March '12
2 March '12
3 March '12
1 July '12
2 July '12
3 July '12
Standard
1 September '12
2 September '12
3 September '12
1 October '12
2 October '12
3 October '12
1 May '12
2 May '12
3 May '12
Standard



Standard
1 April '12
1 April '12
1 April '12
1 November '11
1 November '11
1 November '11
Standard
1 December '11
1 December '11
1 December '11
1 January '12
1 January '12
1 January '12
1 June '10 (<i>F. spiralis</i> I)
1 June '10 (<i>F. spiralis</i> II)
1 June '10 (<i>F. spiralis</i> III)
Standard

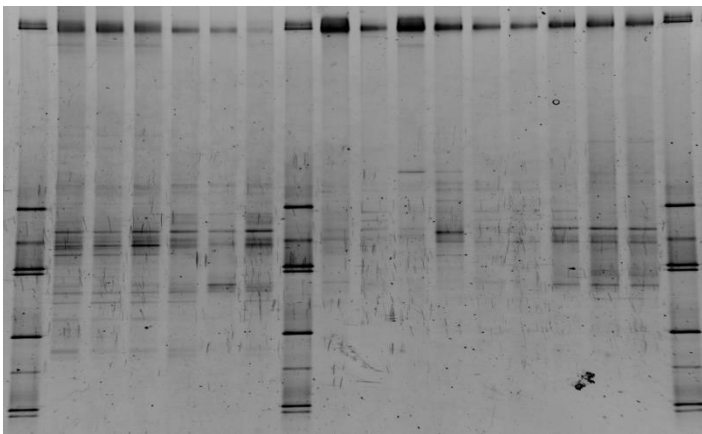


Fig. S4: Relative abundance (and mean) of bacterial phyla (A) and classes (B) present in the bacterial biofilms of three *F. spiralis* specimens. In (B), only taxa with a relative abundance of $\geq 1\%$ of the total bacterial community are shown. Taxa with lower abundance are combined within “other”.

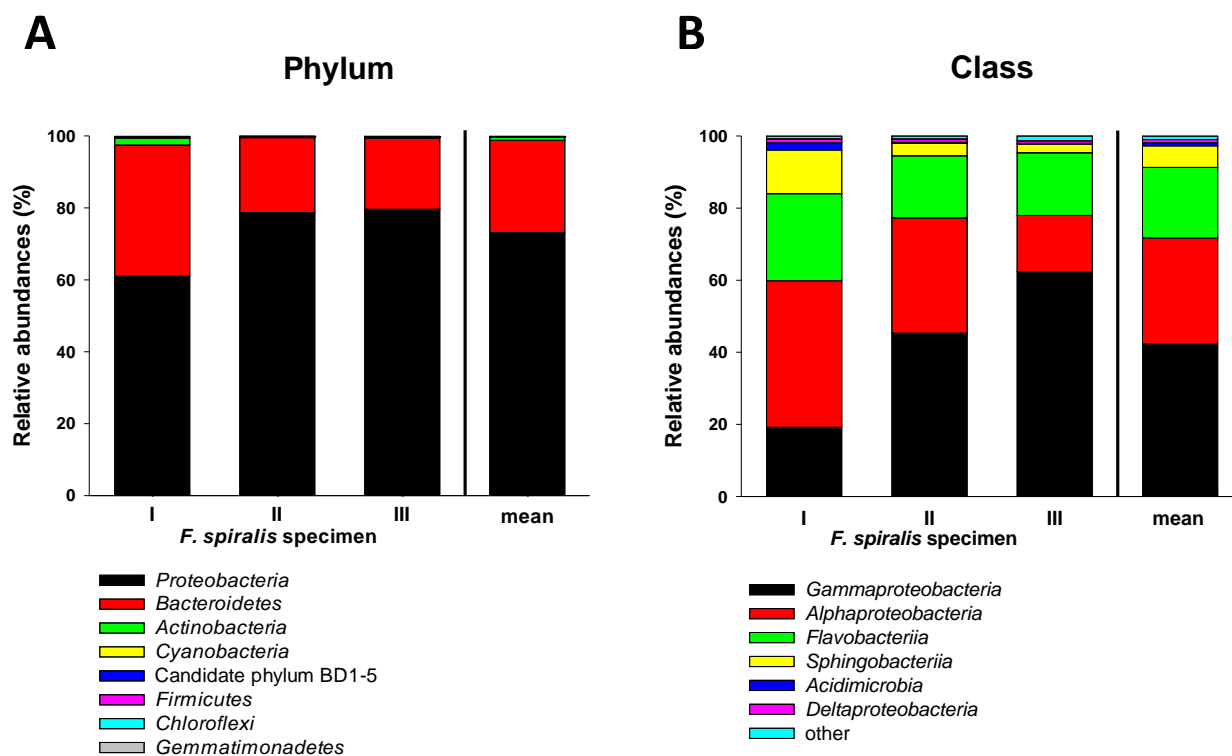


Fig. S5: Rarefaction curves calculated for the bacterial biofilms of the three individual *F. spiralis* samples studied at (A) 20%, (B) 3% and (C) 1% genetic distance with and without singletons. For details concerning sample preparation and treatment see Experimental Procedures or Supplementary Text S1.

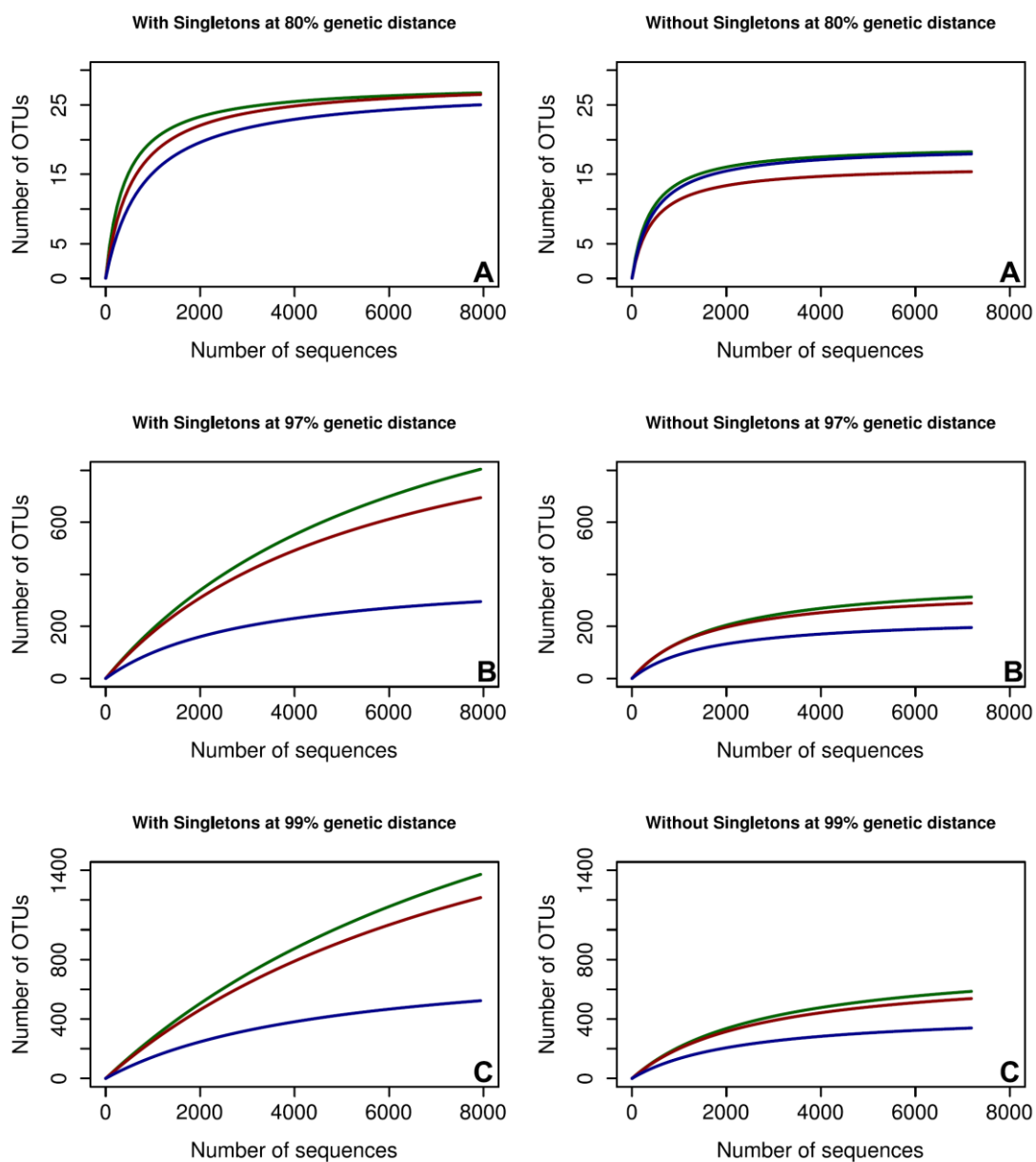


Table S1: Dates for the collection of *F. spiralis* at a tidal flat area of the southern North Sea, Germany (53°42'14" N, 07°42'13" E), physico-chemical parameters of the nearby hydrographic time series station Wadden Sea^a (data are represented by the mean value of each day), number of *F. spiralis* specimens that were taken in total at a wave-breaker and the nearby harbour, and number and use of specimens for isolation, DGGE and amplicon sequencing.

Date	Temperature (°C)		Salinity (psu)	No. of <i>F. spiralis</i> specimens			No. of specimens used for ^b		
	Air	Water		Total	Taken at the wave-breaker	Taken at the harbour	Isolation	DGGE	Amplicon sequencing
08.06.2010	15.88	15.62	30.67	3	3	0	3	3(w/m)	3(m)
09.11.2011	7.18	9.93	32.17	3	3	0	0	3(w/m)	0
19.12.2011	4.25	4.79	31.47	3	3	0	0	3(w/m)	0
18.01.2012	2.96	4.71	31.15	3	3	0	0	3(w/m)	0
06.03.2012	5.83	4.77	31.63	3	3	0	0	3(w/m)	0
24.04.2012	8.97	8.79	31.58	3	3	0	0	3(w/m)	0
22.05.2012	18.53	14.98	32.27	3	3	0	0	3(w/m)	0
26.06.2012	n.a.	n.a.	n.a.	6	3	3	0	3(w); 3(h)	0
30.07.2012 ^c	17.24	18.66	30.00	3	3	0	0	3(w/m)	0
06.09.2012	15.67	17.28	n.a.	3	3	0	0	3(w/m)	0
23.10.2012	12.29	12.48	n.a.	3	3	0	0	3(w/m)	0

^a <http://www.watt.icbm.de/16809.html>

^b Characteristics of the sample are given in brackets (w = wave-breaker; h = harbour site; m = merged sample)

^c No data from the time series station available. Therefore, data measured on 7th August 2012 are given. n.a. = not available

Table S2: Phylogenetic affiliation of bacterial strains used as target organisms for the inhibition assay.

Strain	Phylogenetic group		Accession no. of the 16S rRNA gene
	Class	Family	
TK	<i>Alphaproteobacteria</i>	<i>Phyllobacteriaceae</i>	AY177715
TL	<i>Alphaproteobacteria</i>	<i>Rhodobacteraceae</i>	AY177716
T8	<i>Gammaproteobacteria</i>	<i>Alteromonadaceae</i>	AY177718
T17	<i>Gammaproteobacteria</i>	<i>Oceanospirillaceae</i>	AY177720
T4	<i>Actinobacteria</i>	<i>Pseudonocardiaceae</i>	AY177725
T2	<i>Actinobacteria</i>	<i>Nocardioidaceae</i>	AY166703
BIA	<i>Flavobacteriia</i>	<i>Flavobacteriaceae</i>	AY177722
62.1	<i>Flavobacteriia</i>	<i>Flavobacteriaceae</i>	KM517579

Table S3: Relative abundance (% of all bacterial reads) of genera or equivalent clusters affiliated to the *Rhodobacteraceae* found in epibacterial biofilms of three *F. spiralis* specimens. The mean value and standard deviation are also given. n.d. = not detected/assigned reads.

Genus or cluster	<i>F. spiralis</i>			Mean	Standard deviation
	I	II	III		
Uncultured MHR Cluster	13.32	3.01	2.76	6.364	±4.919
<i>Sulfitobacter</i>	6.47	7.73	3.52	5.907	±1.767
<i>Loktanella</i>	5.21	8.75	2.81	5.588	±2.441
<i>Octadecabacter</i>	2.32	4.65	1.47	2.815	±1.344
<i>Roseobacter</i> sp. ANT9283 ^a	0.62	0.31	0.22	0.381	±0.17
<i>Roseobacter</i>	0.38	0.34	0.14	0.29	±0.105
<i>Shimia</i>	0.19	0.15	0.23	0.19	±0.035
<i>Litoreibacter</i>	0.33	0.12	0.08	0.178	±0.112
<i>Jannaschia</i>	0.16	0.26	0.06	0.158	±0.082
<i>Thalassobacter</i>	0.08	0.21	0.03	0.107	±0.072
<i>Rhodobacter</i>	0.09	0.18	n.d.	0.092	±0.046
<i>Roseobacter</i> clade NAC11-7 lineage	0.01	0.13	0.04	0.063	±0.053
<i>Planktotalea</i>	0.04	0.12	0.02	0.062	±0.044
<i>Tateyamarina</i>	0.08	0.04	n.d.	0.039	±0.022
<i>Roseovarius</i>	0.06	0.04	n.d.	0.032	±0.012
<i>Marinosulfonomonas</i>	0.03	0.04	n.d.	0.022	±0.003
<i>Rubellimicrobium</i>	0.02	0.04	n.d.	0.019	±0.008
<i>Celeribacter</i>	0.04	0.01	n.d.	0.018	±0.014
<i>Tropicimonas</i>	0.02	0.02	n.d.	0.015	±0.002
<i>Sagittula</i>	0.01	0.02	n.d.	0.012	±0.007
<i>Dinoroseobacter</i>	0.02	0.01	n.d.	0.011	±0.004
<i>Phaeobacter</i>	0.02	0.01	n.d.	0.011	±0.004
<i>Roseobacter</i> clade AS-21 lineage	0.02	0.01	n.d.	0.011	±0.004
<i>Thalassobius</i>	0.02	0.01	n.d.	0.011	±0.004
<i>Oceanicola</i>	n.d.	0.01	0.01	0.008	±0.001
<i>Albimonas</i>	n.d.	0.02	n.d.	0.008	±0.000
<i>Nereida</i>	0.01	0.01	n.d.	0.007	±0.001
<i>Pseudoruegeria</i>	0.01	0.01	n.d.	0.007	±0.001
<i>Maribius</i>	0.02	n.d.	n.d.	0.007	
<i>Pacificibacter</i>	n.d.	0.01	n.d.	0.004	
<i>Paracoccus</i>	n.d.	0.01	n.d.	0.004	
<i>Thalassococcus</i>	n.d.	0.01	n.d.	0.004	
<i>Wenxinia</i>	n.d.	0.01	n.d.	0.004	
<i>Citreicella</i>	0.01	n.d.	n.d.	0.003	
<i>Citreimonas</i>	0.01	n.d.	n.d.	0.003	
<i>Leisingera</i>	0.01	n.d.	n.d.	0.003	
<i>Maritimibacter</i>	0.01	n.d.	n.d.	0.003	
<i>Oceaniovalibus</i>	0.01	n.d.	n.d.	0.003	
<i>Palleronia</i>	0.01	n.d.	n.d.	0.003	
<i>Pelagicola</i>	0.01	n.d.	n.d.	0.003	
<i>Ponticoccus</i>	0.01	n.d.	n.d.	0.003	
<i>Profundibacterium</i>	0.01	n.d.	n.d.	0.003	
<i>Pseudorhodobacter</i>	0.01	n.d.	n.d.	0.003	
<i>Planktomarina</i> ^b	0.01	n.d.	n.d.	0.003	
Uncultured <i>Rhodobacteraceae</i>	0.9	1.05	0.24	0.729	±0.354

^a Manual correction of the *Roseobacter* cluster CHAB-1-5 to *Roseobacter* ANT9283 based on phylogenetic analysis and incorrect designations in the SILVA database.

^b Manual correction of the *Roseobacter* DC5-80-3 lineage (Buchan et al. 2005) to *Planktomarina* (Giebel et al. 2013).

Table S4: Percentages of genera present on *F. spiralis* and representing $\geq 1\%$ of the total bacterial community (genera affiliated to *Rhodobacteraceae* are shown in Table S3). Data are based on 454 analysis and are listed in decreasing percentage of the mean value.

Genus (family)	I	<i>F. spiralis</i> II	III	Mean	Standard deviation
<i>Halomonas</i> (<i>Halomonadaceae</i>)	3.73	15.68	39.14	19.52	± 18.02
<i>Shewanella</i> (<i>Shewanellaceae</i>)	1.04	6	14.89	7.31	± 7.02
<i>Granulosicoccus</i> (<i>Granulosicoccaceae</i>)	9.35	4.66	5.31	6.44	± 2.54
<i>Glaciecola</i> (<i>Alteromonadaceae</i>)	2.42	13.74	1.53	5.9	± 6.81
<i>Zobellia</i> (<i>Flavobacteriaceae</i>)	6.62	3.11	4.34	4.69	± 1.78
<i>Parvularcula</i> (<i>Parvularculaceae</i>)	5.80	1.55	1.34	2.9	± 2.52
<i>Nonlabens</i> (<i>Flavobacteriaceae</i>)	2.1	3.23	2.09	2.47	± 0.66
<i>Lewinella</i> (<i>Saprospiraceae</i>)	4.26	1.59	1.03	2.29	± 1.72
<i>Rubidimonas</i> (<i>Saprospiraceae</i>)	4.60	1.32	0.72	2.21	± 2.09
<i>Winogradskyella</i> (<i>Flavobacteriaceae</i>)	2.51	1.62	1.63	1.92	± 0.51
<i>Pibocella</i> (<i>Flavobacteriaceae</i>)	2.63	0.73	2.37	1.91	± 1.03
<i>Lacinutrix</i> (<i>Flavobacteriaceae</i>)	1.67	0.69	1.23	1.19	± 0.49
<i>Maribacter</i> (<i>Flavobacteriaceae</i>)	1.19	1.17	1.08	1.15	± 0.06

Table S5: Phylogenetic affiliation of isolates obtained in this study for which no physiological analyses were performed because of a 16S rRNA gene similarity to other strains of $\geq 99\%$.

Isolate	$\geq 99\%$ 16S rRNA similarity to isolate	Medium used for isolation ^a	Closest described relative ^b (Acc. No.)	16S rRNA similarity (%)
F13	D3	ASWF	<i>Loktanella salsilacus</i> (AJ440997)	100
Lw-26b	D3	MB	<i>Loktanella salsilacus</i> (AJ440997)	99
Lw-27b	D3	MB	<i>Loktanella salsilacus</i> (AJ440997)	100
MDLw-57	Lw-35	MB	<i>Dinoroseobacter shibae</i> (AJ534211)	99
MDLw-58	Lw-35	MB	<i>Dinoroseobacter shibae</i> (AJ534211)	99
Lw-41b	Lw-41a	MB	<i>Citreicella aestuarii</i> (FJ230833)	99
D12-1	D12-1.68	MB	<i>Roseovarius lutimaris</i> (JF714703)	99
D4_50	E8	MB	<i>Octadecabacter antarcticus</i> (U14583)	97
Lw-22	E8	MB	<i>Octadecabacter antarcticus</i> (U14583)	97

^a Medium abbreviation: ASWF = Artificial sea water supplemented with air dried *Fucus spiralis*; MB = Marine Broth Difco 2216.

^b Affiliation was identified by NCBI BLAST analysis (<http://blast.ncbi.nlm.nih.gov/Blast.cgi>).

Table S6: 16S rRNA genes of strains obtained in this study with similarities of $\geq 99\%$ and $\geq 97\%$ or $< 97\%$ compared to OTU consensus sequences derived from the 454 data set. Percentages of the genetic divergences between isolates and OTUs are shown in parenthesis. OTU consensus sequences representing more than 1% of the total epibacterial community are in bold.

Similarity	Isolate	Consensus OTU (genetic divergence % ^a)
$\geq 99\%$	<i>Sulfitobacter</i> sp. D4_47	OTU 471 (0.4); OTU 2439 (0.8); OTU 1020 (1)
	<i>Sulfitobacter</i> sp. B15_G2_red	OTU 471 (0.4); OTU 2439 (0.4); OTU 1020 (0.5); OTU 2149 (0.8)
	<i>Oceanibulbus</i> sp. E11	OTU 2439 (0.8); OTU 1020 (1)
	<i>Sulfitobacter</i> sp. E4-2.2	OTU 2439 (0.4); OTU 1020 (0.5); OTU 2149 (0.8)
	<i>Rhodobacteraceae</i> bacterium B14_27	OTU 1205 (0.4)
	<i>Litoreibacter</i> sp. F3	OTU 2093 (0.4)
	<i>Jannaschia</i> sp. B3	OTU 2237 (0.4)
$\geq 97\%$	<i>Sulfitobacter</i> sp. A12	OTU 471 (1.9); OTU 2439 (1.9); OTU 2149 (2.3); OTU 1020 (2.4); OTU 1693 (2.5); OTU 1205 (2.7); OTU 2635 (2.9); OTU 2782 (3)
	<i>Sulfitobacter</i> sp. B13	OTU 471 (1.7); OTU 2439 (1.7); OTU 1020 (1.7); OTU 2149 (2.1); OTU 1693 (2.3); OTU 2782 (2.9); OTU 1623 (2.9); OTU 1691 (3)
	<i>Roseobacter</i> sp. B14	OTU 2355 (1.1); OTU 2782 (1.5); OTU 471 (1.9); OTU 2439 (1.9); OTU 2149 (2.3); OTU 1623 (2.3); OTU 1020 (2.4); OTU 1693 (2.5); OTU 2635 (2.9); OTU 1691 (2.9); OTU 1721 (3)
	<i>Rhodobacteraceae</i> bacterium E13	OTU 2439 (1.4); OTU 2149 (1.7); OTU 1693 (1.7); OTU 1020 (1.7); OTU 471 (2.1); OTU 1205 (2.1); OTU 1623 (2.5); OTU 2355 (2.9)
	<i>Rhodobacteraceae</i> bacterium D17	OTU 471 (1.3); OTU 2439 (1.4); OTU 2149 (1.7); OTU 1020 (1.7); OTU 1693 (2.5); OTU 1691 (2.7); OTU 1721 (2.9); OTU 2355 (2.9); OTU 1072 (3)
	<i>Rhodobacteraceae</i> bacterium D4_55	OTU 2439 (1.7); OTU 1020 (1.7); OTU 2149 (2.1); OTU 471 (2.5); OTU 1623 (2.5); OTU 2355 (2.9)
	<i>Rhodobacteraceae</i> bacterium Lw-III1a	OTU 1623 (2.7)
	<i>Rhodobacteraceae</i> bacterium Lw-13e	OTU 2354 (2.3)
	<i>Octadecabacter</i> sp. E8	OTU 1068 (1.7); OTU 341 (1.7); OTU 1392 (2.7); OTU 295 (3); OTU 1511 (3)
	<i>Loktanella</i> sp. D3	OTU 565 (1.9); OTU 194 (1.9); OTU 2222 (2.8); OTU 1650 (3)
	<i>Loktanella</i> sp. D15_40	OTU 565 (2.4); OTU 194 (2.5)
	<i>Loktanella</i> sp. Lw-55a	OTU 565 (2.8); OTU 194 (2.9); OTU 2222 (3)
$< 97\%$	<i>Citreicella</i> sp. Lw-41a	OTU 2354 (5.5)
	<i>Roseovarius</i> sp. D12_1.68	OTU 1691 (3.4); OTU 130 (3.4)
	<i>Dinoroseobacter</i> sp. Lw-35	OTU 129 (3.3)
	<i>Paracoccus</i> sp. C13	OTU 565 (6.5)

^a Genetic divergence was determined by using the matrix calculator of the ARB software package according to Ludwig et al. (Ludwig et al. 2004).

Table S7: Detailed results of the physiological characterisation of the strains investigated in this study. n.a. = no data available

Strain	Antagonistic activity against °*				Siderophore production °#		Vitamin B ₁₂ synthesis °~	Bacteriochlorophyll a °§	
	T8	T17	TL	<i>Skeletonema costatum</i>	Overlay method	CAS diffusion agar		Spectrum	PCR <i>pufM</i> L
<i>Citricella</i> sp. Lw-41a				MB	(+)				
<i>Dinoroseobacter</i> sp. Lw-35						1	+	Bchl a	+
<i>Jannaschia</i> sp. B3						0.5	w		
<i>Litoreibacter</i> sp. F3					(+)	0.5	+		
<i>Loktanella</i> sp. D3						0.5			
<i>Loktanella</i> sp. D15_40						1	+		
<i>Loktanella</i> sp. Lw-55a						1	++	Bchl a	+
<i>Oceanibulbus</i> sp. E11					(+)		+		
<i>Octadecabacter</i> sp. E8					(+)	1	++		
<i>Paracoccus</i> sp. C13					+	3	+		
<i>Rhodobacteraceae</i> bacterium B14_27					(+)	0.5	+		
<i>Rhodobacteraceae</i> bacterium D4_55									
<i>Rhodobacteraceae</i> bacterium D17						1			
<i>Rhodobacteraceae</i> bacterium E13					(+)	0.5	+		+
<i>Rhodobacteraceae</i> bacterium Lw-III1a				MB	+	2		Bchl a	+
<i>Rhodobacteraceae</i> bacterium Lw-13e					+	3	w		
<i>Roseobacter</i> sp. B14			MB+F					Bchl a	+
<i>Roseovarius</i> sp. D12_1.68			MB+F	MB					
<i>Sulfitobacter</i> sp. A12							+		
<i>Sulfitobacter</i> sp. B13			MB+F		(+)		+		
<i>Sulfitobacter</i> sp. B15_G2_red							w	Bchl a	+
<i>Sulfitobacter</i> sp. D4_47						0.5	++		
<i>Sulfitobacter</i> sp. E4_2.2		MB+	MB+F				w		
<i>Phaeobacter inhibens</i> DSM 16374	n.a.	n.a.	n.a.	n.a.	+	3	n.a.		
<i>Roseobacter denitrificans</i> DSM 7001	n.a.	n.a.	n.a.	n.a.			n.a.	Bchl a	+
Deferroxamin (2.5 mM)	n.a.	n.a.	n.a.	n.a.	n.a.	9	n.a.	n.a.	n.a.

° Blank field indicates negative results.

* Inhibition is indicated by abbreviation of the medium in which the isolate was grown (MB = Marine Broth Difco 2216; MB+F = Marine Broth Difco 2216 amended by air dried *F. spiralis*; MB+A = Marine Broth Difco 2216 amended by a piece of *F. spiralis*; MB+ = Marine Broth Difco 2216 amended by *F. spiralis*-related substrates).

Overlay method [+]: clear orange red halo; (+): orange red halo close to the bacterial colony]; CAS diffusion agar [zone of colour change is given in millimetres].

~ Vitamin B₁₂ production was detected if the vitamin production was > consumption (++: > 30 ng; +: > 2 ng; w: > 0 ng).

§ Spectrum [Bchl a: peak at 770 nm]; *pufLM* PCR [+]: positive PCR product].

Table S8: Number of 16S rRNA gene sequences (reads) derived from 16S rRNA gene amplicon raw datasets before and after denoising and removal of non-bacterial or chimeric sequences.

Sample	Raw data	Finally processed data
	No. of sequences	No. of sequences
<i>Fucus spiralis</i> I	14,517	9,894
<i>Fucus spiralis</i> II	11,258	8,171
<i>Fucus spiralis</i> III	10,390	9,041
Sum	36,165	27,106

Table S9: Bacterial diversity and richness at 1%, 3% and 20% genetic distance with and without singletons. Coverage was determined based on observed cluster and max. cluster. To compare community structures, 7,936 (with singletons) and 7,237 (without singletons) randomly selected sequences from each sample were used for calculation.

Sample	Observed clusters						Max. clusters (n_{max})					
	1%		3%		20%		1%		3%		20%	
	singletons		singletons		singletons		singletons		singletons		singletons	
	with	without	with	without	with	without	with	without	with	without	with	without
<i>Fucus spiralis</i> I	1,397.3	593.5	819.4	318.9	26.7	18.8	3,219.76	808.67	1,470.64	392.56	28.03	19.25
<i>Fucus spiralis</i> II	1,244.0	545.0	715.0	293.0	27.0	16.0	2,687.22	731.97	1,192.52	351.39	28.1	16.0
<i>Fucus spiralis</i> III	540.0	347.6	305.5	201.0	26.0	18.0	826.02	441.97	406.933	238.14	28.03	19.17
Mean	1,060.4	495.4	613.3	271.0	26.6	17.6	2,244.3	660.9	1,023.4	327.4	28.1	18.1
SD ^a	457.2	130.2	271.6	62.0	0.5	1.4	1,256.8	193.4	551.7	80.0	0.0	1.9
CV ^b	0.43	0.26	0.44	0.23	0.02	0.08	0.56	0.29	0.54	0.24	0.00	0.10

	Coverage (%)						Shannon index (H')					
	1%		3%		20%		1%		3%		20%	
	singletons		singletons		singletons		singletons		singletons		singletons	
	with	without	with	without	with	without	with	without	with	without	with	without
<i>Fucus spiralis</i> I	43.40	73.39	55.72	81.24	95.27	97.65	7.49	6.71	6.34	5.64	2.32	2.19
<i>Fucus spiralis</i> II	46.29	74.46	59.96	83.38	96.08	99.98	7.09	6.39	6.02	5.41	1.99	1.97
<i>Fucus spiralis</i> III	65.37	78.65	75.07	84.41	92.75	93.91	4.94	4.70	4.23	4.06	1.64	1.58
Mean	-	-	-	-	-	-	6.51	5.93	5.53	5.04	1.98	1.91
SD ^a	-	-	-	-	-	-	1.37	1.08	1.14	0.85	0.34	0.31
CV ^b	-	-	-	-	-	-	0.21	0.18	0.21	0.17	0.17	0.16

^a Standard deviation

^b Coefficient of variation

Supplementary Material for Manuscript 3

Smalltalk in the ocean - signaling molecules and DNA elicit chemotactic and regulatory effects in surface-associated *Rhodobacteraceae*

Supplementary methods

Growth conditions

Bacteria were grown aerobically in chemotaxis medium (CM) in Erlenmeyer flasks with baffles (n = 3); Precultures of 10 mL were inoculated from plate (or glycerol stock for *Loktanella* sp. I 8.24; grown in test tubes) in CM for *Phaeobacter* or full marine broth (MB) for the other strains, modified after Difco 2216 [(L⁻¹): 12.6 g MgCl₂*6H₂O and 2.38 g CaCl₂*2H₂O were used instead of 8.8 g and 1.8 g, respectively; trace element solution (L⁻¹): 7 mg Na-Silicat*5H₂O and 21.2 mg boric acid were added compared to 4 and 2.2 mg, respectively]. Main cultures were inoculated with 5% (*Phaeobacter*) or 2% (other strains) (v/v) into 150 ml CM and incubated at 28°C, 100 rpm (20°C, 200 rpm for I 8.24) in Erlenmeyer flasks with baffles. Growth curves were analyzed by OD₆₀₀ measurements for 40 hours at regular time intervals of two or four hours and doubling times and time of mid-exponential growth phase analyzed (Fig. S1). Motility of all strains under test conditions was determined on soft agar (2.7 g/L) CM plates and by light microscopy in liquid CM.

Chemotaxis capillary test set-up

As chemotaxis chamber, a 150 mL cell culture flask (TPP 90150/1, Sigma Aldrich; Germany) was modified by drilling 16 holes (d = 4 mm) in the top side with 3 cm distance to each other (Fig. S2). The chemotaxis chamber was cleaned with 70% ethanol and distilled water and sterilized under UV light for 20 min. As capillaries, 10 µL filter tips (Starlab, No. S1121-3810; UK) were filled with 10 µL substance solution and carefully placed into the holes without pressure to exclude capillary forces disturbing the outcome. The open tip ends were immersed in the culture broth; filters excluded air pressure and contamination from the outside. The set-up was incubated for two hours, capillaries removed, and the outside rinsed with distilled water to remove attached bacteria before further analysis.

Chemotaxis-deficient mutant cheA::Tn5 and genetic complementation

CheA::Tn5 (Tm400) has an insertion mutation in the *cheA* gene (PGA1_262p02120; position 229,676) (Fig S1D). The mutant (provided by the DSMZ; Braunschweig, Germany) was produced using the EZ-Tn5™ Transposase kit (Epicentre, Illumina, WI, USA). Transposon insertion site was determined by specific PCR via transposon-specific primer P808 (5-GTTGATGCGAGTGATTTTGATGACGA-3) and *cheA*-specific primer cheAf (5-CACATTCTTTGAGGAGTGCG-3) to amplify, and transposon-specific primer P812 (5'-

ACCTACAACAAAGCTCTCATCAACC-3') and *cheA*-specific primer *cheAr* (5'-AGGATCATGGCAATCTTGCC-3') to sequence. For genetic complementation, the chemotaxis cluster (PGA1_262p02100-02149, including the promoter region) was blunt ended PCR amplified from chromosomal DNA of *P. inhibens* DSM 17395 using the specific primers *CheMotf* (5'-AATTTTCGACCTTACGAGAGG-3') and *CheMotr* (5'-AATTTTCGACCTTACGAGAGG-3') and Phusion polymerase (Thermo Fisher Scientific, Waltham, MA) and cloned into the *Eco*CR1 site of pBBR1-MCS5 (Gm^r) (GenBank No. U25061) (Kovach et al. 1995). The resulting plasmid was conjugated into electro-competent *cheA::Tn5* [grown in MB (28°C, 100 rpm) to logarithmic growth phase (OD₆₀₀ ~ 1.5), cooled down in ice-water mixture for 15 min, and centrifuged (10 min, 10,000 x g, 4°C). Cell pellet was washed twice with 50 mL and re-diluted in 0.2 mL cooled 10% (v/v) glycerol. For electroporation, 40 µL of electrocompetent cells were carefully mixed with 1 µL of ligated plasmid, transferred to cooled electroporation cuvette (0.2 cm gap) and electroporated with a pulse of 2.5 kV, 25 µF, 200 Ω. pulse 2.5 kV, 25 µF, 200 Ω]. Transformants were selected on gentamicin-containing (30 µg/mL) MB plates and successful complementation checked by PCR-amplified sequencing of the inserted chemotaxis gene sequence using the standard M13 primers (Messing 1983) at GATC (now Eurofins, Ebersberg, Germany). The genetically complemented strain was called *cheA::Tn5::cheA*.

Library preparation and RNA sequencing

Single-ended, strand specific cDNA libraries were prepared from rRNA depleted total RNA using Scriptseq v2 RNA-Seq Library Preparation Kit (Illumina) following the manufacturers protocol. For sequencing equal volume of libraries (12 PM) was multiplexed on a single lane. Sequencing was done on the HiSeq 2500 (Illumina) using TruSeq SBS Kit v3—HS (Illumina) for 50 cycles resulting in 50-bp reads. Image analysis and base calling were performed using the Illumina pipeline v1.8 (Illumina). The demultiplexed raw fastq-files were quality-controlled using the FASTQ-mcf suite (<https://github.com/ExpressionAnalysis/ea-utils>). Low quality bases (Phred-score<30) and identified Illumina adaptors were clipped from the sequences. Reads were mapped to reference genomes using bowtie2 (Langmead et al. 2012) with default parameters for single-end reads. Ambiguously mapping reads were randomly distributed between all regions to which they could be assigned. The resulting SAM-files were converted to indexed binary format and pile-up format using SAMtools (Li et al. 2009). Accession numbers of reference *P. inhibens* DSM 17395 genome: chromosome, 3.82 Mb [NC_018290.1]; pPGA1_262, 262 kb [NC_018291.1]; pPGA1_65, 65 kb [NC_018288.1]; pPGA1_78, 78 kb [NC_018287.1]. Functional gene annotations were done using eggNOG-mapper (Huerta-Cepas et al. 2017).

In vitro hemolysis test on blood agar plates

Cells were grown in MB to mid-exponential phase (20h, $OD_{600} \sim 1.5$) and either supplemented with 1 μM C14:1-HSL, 3OH-C10-HSL or left untreated incubated for 2h reflecting test conditions. Supernatant was harvested by centrifugation (10 min; 10,000 x g), sterile filtered and 50 μL filtrate inoculated in a pierced hole in Columbia blood agar plates (No. 146559; Merck Millipore, Germany). Occurrence of a yellow, clear ring around the well within one week was scored as β -hemolysis, clearing zones measured and statistical analysis performed using two-tailed Student's test, assuming unequal variances ($P < 0.001$).

TDA measurements

Lack of TDA production in CM was confirmed by chemical analysis to exclude interference of exogenously added with own-produced TDA under the test conditions. Therefore, filtered supernatants of 50 mL cell culture grown in CM following the chemotaxis test conditions were analyzed at BioViotika Naturstoffe GmbH (Göttingen, Germany). Samples were set to pH 3 using 2 M HCl, 20 mL supernatant extracted with 25 mL ethyl acetate, evaporated to dryness and re-dissolved in 1 mL acetonitrile. Analysis was conducted by high-performance liquid chromatography (HPLC) on a Celeno DAD II HPLC (Goebel Analytik, Hallertau, Germany), separated on a Nucleodur 100-5 C18 (250 mm x 3 mm) column using a water-acetonitrile gradient solvent system, with both solvents containing 20 mM formic acid. Using a flow of 0.5 mL/min, the gradient was started with 20% acetonitrile and increased to 100% acetonitrile within 25 min. TDA was determined using evaporative light scattering detector (ELSD) Sedex 85, following calibration with pure TDA.

*Inhibition test of TDA for *Loktanella* I 8.24*

Classical plate-based inhibition test was performed (Bauer et al. 1966), using 200 μL bacterial culture dispersed on MB agar (15 g/L) plate and 20 μL TDA in concentrations of 1, 10, 100 and 500 μM dissolved in DMSO, added on test flakes. Inhibition zones were examined daily for one week. DMSO and MB were used as controls.

Supplementary Figures and Tables

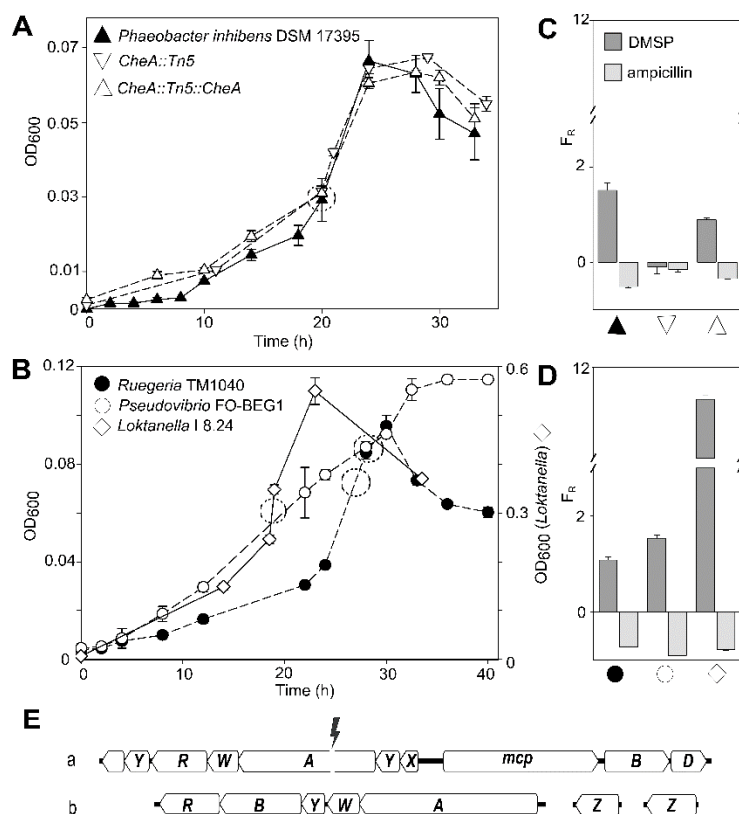


Figure S1: Confirmation of assay specificity and growth of *Rhodobacteraceae* analyzed in the present study. (A) Growth curves of wildtype *Phaeobacter inhibens* DSM 17395, chemotaxis-deficient mutant *cheA::Tn5* mutant and genetically complemented *cheA::Tn5::cheA*. (B) Growth curves for the other *Rhodobacteraceae* (*Pseudovibrio*, *Ruegeria*, *Loktanella*). OD₆₀₀ values for *Loktanella* growth (solid line) are shown on the right Y-axis. Dashed line dots represent the time at which chemotaxis tests were performed, corresponding to late mid-exponential growth of the cultures. (C & D) Chemotactic responses towards attractant (500 μM DMSP) and repellent (14 mM ampicillin), demonstrating that all bacteria but *cheA::Tn5* showed chemotaxis response. (E) Chemotaxis gene cluster of *Phaeobacter*, *Ruegeria* and *Loktanella* (*Roseobacter* relatives) (a) compared to more distantly related *Pseudovibrio* (*Rhodobacteraceae*) (b). Letters correspond to respective *Che* gene description and methyl-accepting proteins (*mcp*). The transposon insertion site in *cheA::Tn5* is depicted as flash.

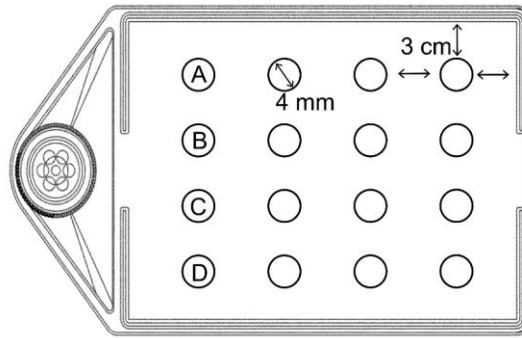


Fig. S2: Chemotaxis capillary chamber set-up.

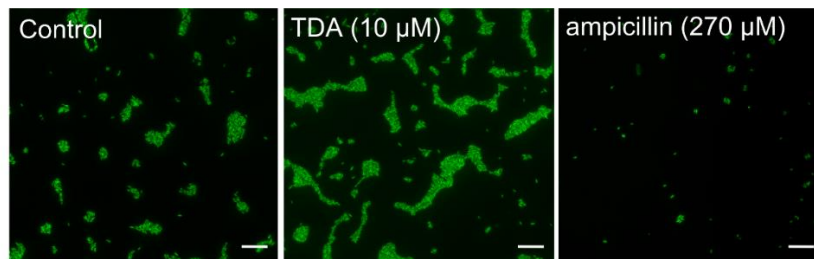


Fig. S3: Microscopic visualization of cells in chemotaxis capillaries after the test (2 h). Capillaries filled with TDA show massive aggregation compared to the medium control, supporting enhanced expression of attachment/biofilm genes, while capillaries containing ampicillin showed reduced cell numbers. In order to enumerate cell numbers correctly, samples were treated with EDTA to disrupt aggregates prior to counting.

Table S1: Genome characteristics, isolation source and genes involved in chemotaxis response and quorum sensing for *Rhodobacteraceae* analyzed in the present study.

Bacterial strain	Isolation source	AHLs	TDA	regulation of TDA production	<i>luxI</i>	<i>luxR</i>	<i>mcp</i>
<i>Phaeobacter inhibens</i> DSM 17395	Rearing of the scallop <i>Pecten maximus</i>	3OH-C10, C18:1, C16, C16:1	√	auto- and QS-regulated	2	7	12
<i>Ruegeria</i> sp. TM1040	Dinoflagellate <i>Pfisteria piscicida</i> CCMP1830 Close interaction with a <i>Beggiatoa</i> strain (sulfide-oxidizing, autotrophic bacterium), isolated from a coral (Florida)	-	√	autoregulation	-	10	19
<i>Pseudovibrio</i> sp. FO-BEG1	Macroalga <i>Sargassum muticum</i> (Galicia, NW Spain)	-	√	not auto- or QS-regulated	-	11	18
<i>Loktanella</i> sp. I8.24*		C14, C14:1	-	-	2	6	5

* for analysis the genome of closely related (99% 16S rRNA gene identity) *Yoonia tamlensis* DSM 26879 was used

Table S2: Overview of genes with specific regulation under different conditions on the transcriptome of *P. inhibens* DSM 17395. Values for in bold correspond to differentially expressed genes with absolute log₂-FC>2 and/or log₂-CPM higher than mean (>6).

Category	Locus Tag	Gene product	COG	COG description	COG Category	3OH C10	C14:1	C18:1	TDA	DMSP	DNA	Log ₂ - CPM
competence	PGA1_c 16950	competence protein DNA	COG0658	Predicted membrane metal-binding protein	General function prediction only	2.20	0.86	0.35	-0.93	-3.47	1.16	7.929
competence	PGA1_c 15260	recombination/re pair protein RecA	COG0468	RecA/RadA recombinase	Replication, recombination and repair	2.27	-0.62	-0.07	-0.27	-1.94	0.35	10.923
Signal transduction	PGA1_c 02470	serine protein kinase PrkA	COG2766	Putative Ser protein kinase	Signal transduction mechanisms	2.06	0.33	0.19	-3.61	-4.05	0.09	13.700
Signal transduction	PGA1_c 02480	hypothetical protein	COG2718	Uncharacterized conserved protein	Function unknown	2.34	0.84	0.39	-2.77	-3.47	0.13	12.310
Signal transduction	PGA1_c 02490	SpoVR family protein	COG2719	Uncharacterized conserved protein	Function unknown	2.26	0.97	0.54	-2.67	-3.26	-0.12	11.435
Signal transduction	PGA1_c 16940	repressor LexA	COG1974	SOS-response transcriptional repressors (RecA-mediated autopeptidases)	Signal transduction mechanisms	0.59	-0.09	-0.45	-0.31	-2.37	-0.14	9.495
Signal transduction	PGA1_c 14360	DNA-binding response regulator CtrA	COG0745	Response regulators consisting of a CheY-like receiver domain and a winged-helix DNA-binding domain	Multiple classes	1.42	-0.27	-0.06	-3.07	-1.85	0.06	12.995
Motility	PGA1_c 23640	flagellar protein methyl-accepting			Motility	2.20	0.96	0.67	-2.00	-1.00	1.49	10.342
Motility	PGA1_c 24960	chemotaxis protein	COG0840	Methyl-accepting chemotaxis protein	Chemotaxis	2.14	0.15	0.14	-3.19	-2.26	0.56	13.399
Motility	PGA1_c 35560	chemotaxis protein MotB	COG1360	Flagellar motor protein	Chemotaxis	1.47	0.93	0.48	-2.25	-1.28	1.06	10.397
Motility	PGA1_c 35570	flagellar hook protein FlgE	COG1749	Flagellar hook protein FlgE	Cell motility	1.79	0.34	0.18	-2.20	-1.31	0.62	11.713
Motility	PGA1_c 35580	flagellar hook-associated protein FlgK	COG1256	Flagellar hook-associated protein	Cell motility	1.89	0.47	0.26	-2.18	-1.28	0.48	10.658
Motility	PGA1_c 35590	flagellar hook protein FlgL	COG1344	Flagellin and related hook-associated proteins	Cell motility	1.54	0.28	0.22	-2.42	-0.99	-0.03	10.756
Motility	PGA1_c 35600	flagellar P-ring protein FlgI	COG1706	Flagellar basal-body P-ring protein	Cell motility	1.47	0.42	0.11	-2.00	-1.45	0.25	10.765
Motility	PGA1_c 35610	flagellar biosynthetic protein FlIP	COG1338	Flagellar biosynthesis pathway, component FlIP	Multiple classes	1.46	0.30	0.06	-2.52	-1.71	-0.10	8.771
Motility	PGA1_c 35620	hypothetical protein	COG1886	Flagellar motor switch/type III secretory pathway protein	Multiple classes	1.48	-0.11	-0.23	-2.95	-2.13	-0.57	10.067

Motility	PGA1_c 35630	hypothetical protein				1.63	0.02	-0.09	-2.98	-1.88	-0.22	10.267
Motility	PGA1_c 35640	flagellar M-ring protein FliF	COG1766	Flagellar biosynthesis/type III secretory pathway lipoprotein	Multiple classes	1.71	-0.06	0.00	-3.44	-1.67	0.14	11.766
Motility	PGA1_c 35650	flagellar basal body protein FliL	COG1580	Flagellar basal body-associated protein	Cell motility	1.70	0.06	0.11	-3.68	-1.58	0.32	11.605
Motility	PGA1_c 35660	hypothetical protein				1.83	0.17	0.08	-3.11	-1.97	0.14	10.222
Motility	PGA1_c 35670	hypothetical protein	COG3334	Uncharacterized conserved protein	Function unknown	1.88	0.07	0.11	-3.13	-1.94	0.09	10.438
Motility	PGA1_c 35680	flagellar motor stator protein MotA	COG1291	Flagellar motor component	Cell motility	2.06	0.42	0.30	-2.56	-2.04	0.34	11.001
Motility	PGA1_c 35690	hypothetical protein				1.87	0.47	0.23	-2.38	-2.12	0.03	11.441
Motility	PGA1_c 35700	tail length tape measure protein flagellar				2.13	0.30	0.24	-3.28	-2.35	0.78	9.052
Motility	PGA1_c 35710	biosynthesis protein FlhA flagellar	COG1298	Flagellar biosynthesis pathway, component FlhA	Multiple classes	1.83	0.12	0.03	-3.15	-2.20	-0.35	10.829
Motility	PGA1_c 35720	biosynthesis protein FliR flagellar	COG1684	Flagellar biosynthesis pathway, component FliR	Multiple classes	1.42	0.12	-0.03	-2.87	-1.72	-0.09	8.202
Motility	PGA1_c 35730	biosynthesis protein FlhB	COG1377	Flagellar biosynthesis pathway, component FlhB	Multiple classes	1.39	0.03	-0.03	-2.92	-1.54	-0.08	9.641
Motility	PGA1_c 35740	hypothetical protein				1.61	0.18	0.12	-2.72	-1.20	0.20	8.708
Motility	PGA1_c 35750	flagellar basal body-associated protein FliL				1.49	0.04	-0.04	-2.81	-1.84	0.00	9.280
Motility	PGA1_c 35760	flagellar L-ring protein FlgH flagella basal body P-ring	COG2063	Flagellar basal body L-ring protein	Cell motility	1.47	0.11	-0.01	-2.53	-1.80	-0.27	10.218
Motility	PGA1_c 35770	formation protein FlgA flagellar basal	COG1261	Flagellar basal body P-ring biosynthesis protein	Multiple classes	1.81	0.26	0.12	-2.73	-1.63	-0.12	7.651
Motility	PGA1_c 35780	body rod protein FlgG flagellar basal	COG4786	Flagellar basal body rod protein	Cell motility	1.81	0.19	-0.07	-2.83	-1.94	-0.48	8.994
Motility	PGA1_c 35790	body rod protein FlgF	COG4786	Flagellar basal body rod protein	Cell motility	1.88	0.01	-0.05	-3.30	-1.73	-0.33	9.891

Motility	PGA1_c 35800	flagellar biosynthesis protein FliQ flagellar hook- basal body	COG1987	Flagellar biosynthesis pathway, component FliQ	Multiple classes	1.80	0.02	0.05	-2.83	-1.39	0.49	8.534
Motility	PGA1_c 35810	protein FliE flagellar basal body rod protein	COG1677	Flagellar hook-basal body protein	Multiple classes	2.02	0.18	0.19	-2.68	-1.37	0.49	8.257
Motility	PGA1_c 35820	FlgC flagellar biosynthesis	COG1558	Flagellar basal body rod protein	Cell motility	2.02	-0.09	0.35	-3.22	-1.13	1.01	9.113
Motility	PGA1_c 35830	protein FlgB Flii/YscN family	COG1815	Flagellar basal body protein	Cell motility	2.07	0.26	0.40	-3.14	-1.04	0.93	7.918
Motility	PGA1_c 35840	ATPase flagellar biosynthesis	COG1157	Flagellar biosynthesis/type III secretory pathway ATPase	Multiple classes	1.64	0.10	0.17	-1.80	-1.49	0.85	8.931
Motility	PGA1_c 35850	repressor FliB flagellar biosynthesis	COG5443	Flagellar biosynthesis regulator FliB	Cell motility	1.59	0.50	0.15	-3.00	-1.96	0.08	10.427
Motility	PGA1_c 35860	regulatory protein FlaF	COG5442	Flagellar biosynthesis regulator FlaF	Cell motility	1.59	0.48	0.22	-3.30	-1.75	0.10	10.783
Motility	PGA1_c 35870	flagellin	COG1344	Flagellin and related hook- associated proteins	Cell motility	1.53	0.51	0.26	-2.37	-1.32	0.49	14.074
Motility	PGA1_c 35880	FlgN-like protein flagellar protein				2.19	0.06	0.09	-4.51	-2.49	0.18	10.479
Motility	PGA1_c 35890	FlgJ flagellar hook-length control				2.09	0.02	0.02	-4.93	-2.32	0.22	9.710
Motility	PGA1_c 35900	protein FliK flagellar basal body rod				2.39	0.51	0.33	-2.33	-1.74	0.74	11.348
Motility	PGA1_c 35910	modification protein FlgD	COG1843	Flagellar hook capping protein	Cell motility	2.17	0.48	0.22	-2.22	-2.19	0.09	9.708
GTA	PGA1_c 17700	hypothetical protein			GTA	2.31	0.43	0.38	0.49	-2.22	0.64	2.328
GTA	PGA1_c 17710	hypothetical protein			GTA	2.34	0.16	0.13	-0.05	-1.65	0.98	6.140
GTA	PGA1_c 17720	peptidase hypothetical	COG0791	Cell wall-associated hydrolases (invasion-associated proteins)	GTA	2.53	-0.33	0.12	-0.71	-1.45	0.29	2.134
GTA	PGA1_c 17730	protein Uncharacterized conserved	COG5449	protein	GTA	2.74	0.06	0.37	-0.31	-1.96	0.91	4.195

GTA	PGA1_c 17740	glycoside hydrolase family 24	COG5448	Uncharacterized conserved protein	GTA	2.61	-0.45	0.19	-0.59	-1.81	0.89	4.474
GTA	PGA1_c 17750	tail protein	COG5281	Phage-related minor tail protein	GTA	2.81	-0.38	0.33	-0.88	-1.94	1.16	4.211
GTA	PGA1_c 17760	hypothetical protein			GTA	2.39	-0.70	0.16	-1.47	-2.22	0.85	3.415
GTA	PGA1_c 17770	hypothetical protein			GTA	2.70	-0.85	0.35	-1.56	-2.11	0.85	3.978
GTA	PGA1_c 17780	tail protein	COG5437	Predicted secreted protein	GTA	2.75	-0.41	0.34	-1.41	-2.24	1.03	4.624
GTA	PGA1_c 17790	DUF3168 domain- containing protein			GTA	2.48	-0.87	0.03	-1.00	-2.25	0.47	3.887
GTA	PGA1_c 17800	head-tail adaptor protein	COG5614	Bacteriophage head-tail adaptor	GTA	2.56	-1.16	-0.01	-0.58	-2.05	0.51	3.473
GTA	PGA1_c 17810	hypothetical protein			GTA	2.43	-0.94	-0.04	-0.71	-2.64	0.75	4.493
GTA	PGA1_c 17820	phage major capsid protein	COG4653	Predicted phage phi-C31 gp36 major capsid-like protein	Mobilome, prophages, transposons	2.40	-1.12	-0.08	-2.30	-1.92	0.66	7.671
GTA	PGA1_c 17830	peptidase U35	COG3740	Phage head maturation protease	Mobilome, prophages, transposons	2.55	-0.98	-0.01	-2.36	-2.03	0.44	5.206
GTA	PGA1_c 17840	hypothetical protein			Mobilome, prophages, transposons	2.29	-0.93	-0.07	-2.91	-2.02	0.63	4.359
GTA	PGA1_c 17850	portal protein	COG4695	Phage-related protein	Mobilome, prophages, transposons	2.48	-0.64	0.05	-2.39	-1.97	0.95	4.352
GTA	PGA1_c 17860	ATP-binding protein	COG5323	Uncharacterized conserved protein	GTA	2.32	0.88	0.59	1.52	-2.05	0.47	1.736
GTA	PGA1_c 17870	hypothetical protein			GTA	2.55	1.13	0.91	1.74	-1.94	0.85	1.940
Attachment/B iofilm	PGA1_c 19090	host attachment protein			hypothetical gene	1.18	0.93	0.71	7.91	-2.46	0.33	10.435
Attachment/B iofilm	PGA1_c 19100	hypothetical protein			hypothetical gene	1.48	0.89	0.81	8.56	-2.03	0.74	10.203
Attachment/B iofilm	PGA1_c 19730	YqaE/Pmp3 family membrane protein	COG0401	Uncharacterized homolog of Blt101	Stress response/potential membrane modulator	1.38	1.05	0.37	9.53	-2.50	0.71	10.107
Attachment/B iofilm	PGA1_c 19740	hypothetical protein				0.90	0.62	0.36	8.43	-0.96	0.66	9.761

Attachment/Biofilm	PGA1_c10960	membrane protein			Cell wall/membrane/envelope biogenesis	0.62	0.61	0.29	5.81	-1.14	0.49	8.408
Attachment/Biofilm	PGA1_c30550	membrane protein				0.83	0.46	0.36	5.53	-0.89	1.18	6.643
Attachment/Biofilm	PGA1_c02400	MFS transporter YihY/virulence factor BrkB family protein	COG1295	Predicted membrane protein	Carbohydrate transport and metabolism	0.70	0.53	0.10	4.13	-0.82	1.00	5.961
Attachment/Biofilm	PGA1_c02370	protein			Function unknown	1.12	0.89	0.36	5.44	-1.74	0.81	5.637
Attachment/Biofilm	PGA1_c11450	prokaryotic membrane lipoprotein lipid attachment site profile			cell wall Replication, recombination and repair	1.45	0.97	0.93	5.08	-4.12	0.07	7.396
Attachment/Biofilm	PGA1_c27020	phage holin family protein			General function prediction only	1.06	1.08	0.70	4.99	-3.24	0.64	5.764
Attachment/Biofilm	PGA1_c26950	exopolysaccharide biosynthesis protein ExoD			Intracellular trafficking, secretion, and vesicular transport	0.39	0.54	0.38	3.62	-1.30	0.66	3.206
Tad Pilus	PGA1_c08700	hypothetical protein	COG4961	Flp pilus assembly protein TadG	Intracellular trafficking, secretion, and vesicular transport	0.96	1.59	0.22	-1.71	-1.29	0.40	9.966
Tad Pilus	PGA1_c08710	pilus biosynthesis protein TadE	COG4961	Flp pilus assembly protein TadG	Intracellular trafficking, secretion, and vesicular transport	0.92	1.59	0.16	-1.68	-1.07	0.64	8.684
Tad Pilus	PGA1_c08720	hypothetical protein	COG4961	Flp pilus assembly protein TadG	Intracellular trafficking, secretion, and vesicular transport	0.90	1.54	0.34	-1.82	-0.88	1.07	11.512
Tad Pilus	PGA1_c06090	pilus assembly protein TadC	COG2064	Flp pilus assembly protein TadC	Multiple classes	0.82	1.36	0.14	-1.87	-1.27	-0.05	8.313
Tad Pilus	PGA1_c06100	pilus assembly protein TadB	COG4965	Flp pilus assembly protein TadB	Intracellular trafficking, secretion, and vesicular transport	1.05	1.45	0.24	-2.04	-1.32	0.16	8.354
Tad Pilus	PGA1_c06110	hypothetical protein	COG4962	Flp pilus assembly protein, ATPase CpaF	Intracellular trafficking, secretion, and vesicular transport	0.83	1.32	0.21	-2.36	-1.25	0.18	9.506
Tad Pilus	PGA1_c06120	pilus assembly protein CpaE	COG4963	Flp pilus assembly protein, ATPase CpaE	Intracellular trafficking, secretion, and vesicular transport	0.70	1.15	0.20	-2.61	-1.25	0.52	9.941

Tad Pilus	PGA1_c 06150	Flp pilus assembly protein CpaB	COG3745	Flp pilus assembly protein CpaB	and vesicular transport Intracellular trafficking, secretion, and vesicular transport	0.73	1.69	0.39	-1.35	-0.57	0.55	9.490
Tad Pilus	PGA1_c 06170	hypothetical protein				0.13	1.53	0.22	-2.45	-1.00	0.04	10.744
T1RMS	PGA1_c 30680	M48 family peptidase restriction			Defense mechanisms	-0.11	-0.09	-0.56	-2.59	-1.18	-0.68	7.957
T1RMS	PGA1_c 30690	endonuclease subunit R restriction			Defense mechanisms	-0.16	-0.19	-0.62	-1.99	-1.12	-0.86	9.313
T1RMS	PGA1_c 30700	endonuclease subunit S SAM-dependent DNA	COG0732	Restriction endonuclease S subunits	Defense mechanisms	-0.68	-0.50	-0.72	-2.22	-1.14	-1.01	7.206
T1RMS	PGA1_c 30710	methyltransferase M	COG0286	Type I restriction-modification system methyltransferase subunit	Defense mechanisms	-0.74	-0.64	-0.72	-1.77	-1.20	-1.28	8.298
T1RMS	PGA1_c 30720	hypothetical protein			Defense mechanisms	-0.56	-0.44	-0.29	-1.68	-1.13	-0.50	4.706
T1RMS	PGA1_c 30730	transcriptional regulator	COG1396	Predicted transcriptional regulators	Defense mechanisms	-0.76	-0.67	-0.28	-2.58	-0.81	-0.86	6.661
Terpenoid biosynthesis	PGA1_c 32010	isopentenyl-diphosphate Delta- isomerase			Secondary metabolites biosynthesis, transport and catabolism	-0.21	0.05	0.96	2.84	4.15	0.95	4.925
Terpenoid biosynthesis	PGA1_c 32020	2-polyprenyl-6- methoxyphenol hydroxylase and related FAD- dependent oxidoreductases	COG0654	2-polyprenyl-6-methoxyphenol hydroxylase and related FAD- dependent oxidoreductases	Secondary metabolites biosynthesis, transport and catabolism	-1.14	-0.78	0.16	2.37	3.16	0.00	5.668
Terpenoid biosynthesis	PGA1_c 32030	glycerol kinase	COG0554	Glycerol kinase	Secondary metabolites biosynthesis, transport and catabolism	-0.52	-0.02	0.28	1.38	0.74	-0.07	6.188
Terpenoid biosynthesis	PGA1_c 32040	pantoate--beta- alanine ligase	COG0414	Panthothenate synthetase	Secondary metabolites biosynthesis,	-0.96	-0.55	0.25	2.21	3.33	-0.11	6.888

Terpenoid biosynthesis	PGA1_c 32050	3-methyl-2-oxobutanoate hydroxymethyltransferase		Pantothenate biosynthesis	transport and catabolism Secondary metabolites biosynthesis, transport and catabolism	-0.27	-0.15	0.38	2.38	3.24	0.10	5.325
Siderophore import	PGA1_7 8p00360	ABC transporter ATP-binding protein			Inorganic ion transport and metabolism	0.56	0.55	0.00	3.00	1.47	0.18	1.429
Siderophore import	PGA1_7 8p00370	iron ABC transporter permease			Inorganic ion transport and metabolism	0.38	0.56	-0.29	2.07	1.00	0.52	2.458
Siderophore import	PGA1_7 8p00380	iron ABC transporter permease			Inorganic ion transport and metabolism	0.78	0.77	0.39	2.09	0.64	0.68	3.022
Siderophore import	PGA1_7 8p00390	iron ABC transporter substrate-binding protein			Inorganic ion transport and metabolism	0.34	0.40	0.85	3.07	2.76	0.75	3.609
Osmoprotection/General stress response	PGA1_c 02340	small mechanosensitive ion channel protein MscS	COG0668	Small-conductance mechanosensitive channel	Cell wall/membrane/envelope biogenesis	1.58	0.94	0.71	5.91	-1.93	1.16	5.046
Osmoprotection/General stress response	PGA1_c 02350	transporter (formate/nitrite transporter family protein)	COG2116	Formate/nitrite family of transporters	Inorganic ion transport and metabolism	1.38	0.90	0.58	5.91	-2.82	0.40	3.953
Osmoprotection/General stress response	PGA1_c 02360	glutathione reductase	COG1249	Pyruvate/2-oxoglutarate dehydrogenase complex, dihydrolipoamide dehydrogenase (E3) component, and related enzymes	Energy production and conversion	0.87	0.53	0.29	4.33	-1.32	0.88	3.613
Osmoprotection/General stress response	PGA1_c 07450	NAD(P)-dependent oxidoreductase	COG0451	Nucleoside-diphosphate-sugar epimerases	Multiple classes	1.27	0.81	0.74	4.11	-1.81	0.27	4.375
Osmoprotection/General stress response	PGA1_c 07460	glutathione S-transferase	COG0625	Glutathione S-transferase	Posttranslational modification, protein turnover, chaperones	1.34	0.49	0.81	5.68	-1.61	0.96	4.890

Osmoprotectin/General stress response	PGA1_c 29220	mechanosensitive ion channel protein MscS	COG0668	Small-conductance mechanosensitive channel	Cell wall/membrane/envelope biogenesis	1.45	1.19	0.93	5.54	-3.09	0.84	4.995
General stress response	PGA1_c 26990	general stress protein			General function prediction only	0.87	0.61	0.24	2.90	-2.52	0.49	7.975
General stress response	PGA1_c 27000	general stress protein CsbD			Function unknown	0.76	0.41	0.30	3.55	-3.07	0.08	8.098
General stress response	PGA1_c 27100	DNA starvation/stationary phase protection protein	COG0783	DNA-binding ferritin-like protein (oxidative damage protectant)	Inorganic ion transport and metabolism	1.72	1.54	1.16	5.82	-1.60	1.65	4.620
General stress response	PGA1_c 07120	universal stress protein			General stress response	-0.24	-0.34	-0.70	-0.51	-3.81	-1.16	7.966
hemolysin, RTX toxin	PGA1_2 62p01140	hypothetical protein			NA	1.85	-0.19	-0.35	-2.96	-2.68	-0.02	11.805
hemolysin, RTX toxin	PGA1_6 5p00020	HlyD family type I secretion periplasmic adaptor subunit			T1SS	0.81	5.88	0.35	1.28	-1.02	2.13	5.477
hemolysin, RTX toxin	PGA1_6 5p00030	type I secretion system permease/ATPase			T1SS	0.62	5.95	0.63	1.10	-1.48	1.82	5.545
hemolysin, RTX toxin	PGA1_6 5p00040	hemolysin-like protein			T1SS	1.01	6.35	0.95	0.22	-1.37	2.38	9.438
hemolysin, RTX toxin	PGA1_6 5p00050	hypothetical protein			T1SS	-0.08	5.62	0.20	-0.95	-1.27	2.05	7.600
hemolysin, RTX toxin	PGA1_6 5p00060	LuxR family transcriptional regulator			T1SS	0.44	5.77	0.43	-0.45	-1.19	2.39	7.000
hemolysin, RTX toxin	PGA1_6 5p00260	metallopeptidase	COG2931	RTX toxins and related Ca ²⁺ -binding proteins	Secondary metabolites biosynthesis, transport and catabolism	1.78	0.25	-0.03	-2.93	-2.98	0.27	9.537
hemolysin, RTX toxin	PGA1_6 5p00270	hypothetical protein	and related Ca ²⁺ -binding proteins	Secondary metabolites biosynthesis, transport and catabolism	hemolysin, RTX toxin	2.67	2.32	0.88	-1.56	-2.06	2.18	9.000

hemolysin, RTX toxin	PGA1_c 07100	hypothetical protein	COG2931	RTX toxins and related Ca2+binding proteins	Secondary metabolites biosynthesis, transport and catabolism	1.06	0.98	0.22	-2.17	-1.08	0.49	9.031
hemolysin, RTX toxin	PGA1_c 10270	hemolysin hemolysin-tyoe calcium-binding repeat-containing protein	RTX toxins and related Ca2+binding proteins	Secondary metabolites biosynthesis, transport and catabolism	Secondary metabolites biosynthesis, transport and catabolism	-0.32	0.81	-0.17	-2.89	-0.83	0.11	7.632
hemolysin, RTX toxin	PGA1_c 21610	hypothetical protein	RTX toxins and related Ca2+binding proteins	Secondary metabolites biosynthesis, transport and catabolism	hemolysin, RTX toxin	3.07	0.28	0.15	-1.48	-1.55	1.57	5.900
hemolysin, RTX toxin	PGA1_c 26130	hypothetical protein	RTX toxins and related Ca2+binding proteins	Secondary metabolites biosynthesis, transport and catabolism	hemolysin, RTX toxin	-1.08	-4.14	-4.39	-1.03	-0.17	-0.97	5.400
hemolysin, RTX toxin	PGA1_c 26140	hemolysin	RTX toxins and related Ca2+binding proteins	Secondary metabolites biosynthesis, transport and catabolism	hemolysin, RTX toxin	-1.03	-4.51	-4.37	-1.40	-0.27	-0.75	9.875
hemolysin, RTX toxin	PGA1_c 32970	hypothetical protein			Secondary metabolites biosynthesis, transport and catabolism	1.74	0.72	0.44	-2.40	-1.38	0.92	10.847
hemolysin, RTX toxin	PGA1_c 36250	metallopeptidase			Secondary metabolites biosynthesis, transport and catabolism	0.54	0.82	0.08	-3.43	-1.26	0.21	10.400
TDA biosynthesis	PGA1_2 62p009 70	tdaB beta-aryl ether-cleaving enzyme		Glutathione S-transferase	Posttranslational modification, protein turnover, chaperones	-1.01	-1.07	-0.51	-2.97	1.26	-0.65	8.102
TDA biosynthesis	PGA1_2 62p009 80	tda A LysR family transcriptional regulator		Transcriptional regulator	Transcription	-1.01	-1.07	-0.36	-2.15	0.95	-0.46	8.429
Nitrogen metabolism	PGA1_2 62p011 70	NnrS family protein	COG3213	Uncharacterized protein involved in response to NO	Inorganic ion transport and metabolism	-3.62	-3.75	0.74	-4.24	-0.26	-2.12	1.346
Nitrogen metabolism	PGA1_2 62p012 00	protein norD	COG4548	Nitric oxide reductase activation protein	Inorganic ion transport and metabolism	-4.02	-4.43	0.92	-4.75	0.10	-2.71	2.911

Nitrogen metabolism	PGA1_2 62p012 10	CbbQ/NirQ/NorQ /GpvN family protein	COG0714	MoxR-like ATPases	General function prediction only	-3.80	-4.07	1.08	-4.03	0.24	-2.68	3.953
Nitrogen metabolism	PGA1_2 62p012 20	nitric oxide reductase	COG3256	Nitric oxide reductase large subunit	Inorganic ion transport and metabolism	-3.56	-3.90	1.03	-3.72	0.22	-2.78	3.981
Nitrogen metabolism	PGA1_2 62p012 30	cytochrome c				-4.10	-4.56	1.34	-4.43	0.59	-2.68	11.276
Nitrogen metabolism	PGA1_2 62p012 60	nitrite reductase%2C copper-containing nitrogen	COG2132	Putative multicopper oxidases	Secondary metabolites biosynthesis, transport and catabolism	-1.91	-2.70	0.90	-3.42	0.07	-1.86	7.011
Nitrogen metabolism	PGA1_c 18710	regulatory protein P-II 1	COG0347	Nitrogen regulatory protein PII	Amino acid metabolism	-2.70	-2.30	1.44	-0.42	4.66	-1.25	8.203
Nitrogen metabolism	PGA1_c 18720	type I glutamate-- ammonia ligase	COG0174	Glutamine synthetase	Amino acid transport and metabolism	-3.86	-3.49	0.52	-1.02	2.24	-3.07	10.070
Nitrogen metabolism	PGA1_c 29400	P-II family nitrogen regulator	COG0347	Nitrogen regulatory protein PII	Amino acid transport and metabolism	-4.17	-5.01	0.37	-4.12	0.67	-3.42	5.046
Nitrogen metabolism	PGA1_c 29410	ammonium transporter	COG0004	Ammonia permease	Amino acid transport	-2.75	-2.85	0.02	-1.96	-0.25	-2.30	4.715
Nitrogen metabolism	PGA1_c 29420	aromatic amino acid aminotransferase	COG1448	Aspartate/tyrosine/aromatic aminotransferase	Amino acid metabolism	-2.07	-1.41	-0.51	1.76	2.93	-0.89	7.366
Nitrogen metabolism	PGA1_c 36090	dihydropyrimidin e dehydrogenase subunit A	COG0493	NADPH-dependent glutamate synthase beta chain and related oxidoreductases	Amino acid metabolism	-0.91	-1.07	0.48	3.50	4.21	0.67	7.182
Nitrogen metabolism	PGA1_c 36100	glutamate synthase subunit alpha	COG0069	Glutamate synthase domain 2	Amino acid metabolism	-2.72	-2.91	0.30	1.12	1.67	-2.41	10.173
Purin metabolism	PGA1_c 12940	adenylate kinase	COG0563	Adenylate kinase and related kinases	Nucleotide metabolism	-2.68	-2.27	-0.80	2.19	1.78	-2.26	7.473
Nitrogen metabolism	PGA1_c 09550	glutaminase	COG2066	Glutaminase	Amino acid metabolism	1.13	0.82	0.80	3.06	0.84	1.68	4.449
Nitrogen metabolism	PGA1_c 17060	glutamate racemase			Cell wall/membrane/enve lope biogenesis	-0.08	0.15	0.83	2.04	3.12	1.31	6.603
Nitrogen metabolism	PGA1_c 08740	glutamate dehydrogenase	COG0334	Glutamate dehydrogenase/leucine dehydrogenase	Amino acid metabolism	0.86	-0.02	0.02	-2.04	-2.32	0.43	10.376

Amino Acid Transport	PGA1_c 12630	ABC transporter ATP-binding protein	COG0410	ABC-type branched-chain amino acid transport systems, ATPase component	branched chain amino acid transport	-5.75	-6.15	-0.76	0.58	0.39	-5.65	8.564
Amino Acid Transport	PGA1_c 12640	ABC transporter ATP-binding protein	COG0411	ABC-type branched-chain amino acid transport systems, ATPase component	branched chain amino acid transport	-5.86	-6.46	-0.65	0.57	0.95	-5.65	10.304
Amino Acid Transport	PGA1_c 12650	branched-chain amino acid ABC transporter permease	COG4177	ABC-type branched-chain amino acid transport system, permease component	branched chain amino acid transport	-5.20	-5.73	-0.63	1.06	1.41	-4.92	9.763
Amino Acid Transport	PGA1_c 12660	branched-chain amino acid ABC transporter permease	COG0559	Branched-chain amino acid ABC-type transport system, permease components	branched chain amino acid transport	-4.99	-5.38	-0.68	1.77	2.40	-4.93	9.684
Amino Acid Transport	PGA1_c 12670	branched-chain amino acid ABC transporter substrate-binding protein	COG0683	ABC-type branched-chain amino acid transport systems, periplasmic component	branched chain amino acid transport	-4.84	-4.05	-1.52	0.67	0.81	-5.16	11.798
Lipoteichoic acids	PGA1_c 13580	secretion protein	COG1566	Multidrug resistance efflux pump	Cell wall/membrane/envelope biogenesis	-1.31	1.63	0.19	-3.83	-0.71	-3.87	9.680
Lipoteichoic acids	PGA1_c 13590	ABC transporter ATP-binding protein			Cell wall/membrane/envelope biogenesis	-0.93	1.98	0.12	-3.18	-0.84	-4.32	10.208
Lipoteichoic acids	PGA1_c 13600	ABC transporter permease			Cell wall/membrane/envelope biogenesis	-0.92	1.93	0.11	-2.62	-0.79	-4.76	11.548
Lipoteichoic acids	PGA1_c 13610	ABC transporter permease			Cell wall/membrane/envelope biogenesis	-0.62	2.15	0.24	-1.41	-0.76	-4.26	9.612
Lipoteichoic acids	PGA1_c 13630	hypothetical protein			Cell wall/membrane/envelope biogenesis	-2.08	1.33	0.90	-1.73	0.78	-3.40	8.953
Lipoteichoic acids	PGA1_c 13640	hypothetical protein			Cell wall/membrane/envelope biogenesis	-1.99	1.57	0.47	-1.50	0.19	-4.23	7.709
Lipoteichoic acids	PGA1_c 13650	hypothetical protein			Cell wall/membrane/envelope biogenesis	-1.94	1.71	0.49	-1.38	0.18	-4.08	8.651
Lipoteichoic acids	PGA1_c 13660	hypothetical protein			Cell wall/membrane/envelope biogenesis	-2.05	1.56	0.53	-1.35	0.34	-4.81	8.586

Lipoteichoic acids	PGA1_c 13670	hypothetical protein	COG0534	Na ⁺ -driven multidrug efflux pump	Cell wall/membrane/envelope biogenesis	-1.69	1.72	0.39	-0.73	0.18	-4.39	8.503
Lipoteichoic acids	PGA1_c 13680	alpha/beta hydrolase	COG1506	Dipeptidyl aminopeptidases/acylaminoacyl-peptidases	Cell wall/membrane/envelope biogenesis	-1.49	1.52	0.10	-0.03	-0.05	-4.76	7.124
Lipoteichoic acids	PGA1_c 13690	hypothetical protein			Cell wall/membrane/envelope biogenesis	-1.10	1.49	0.09	-0.09	-0.11	-4.84	7.955
Lipoteichoic acids	PGA1_c 13700	hypothetical protein			Cell wall/membrane/envelope biogenesis	-0.84	1.48	0.03	0.61	-0.24	-4.58	7.155
Lipoteichoic acids	PGA1_c 13710	diaminopimelate decarboxylase			Cell wall/membrane/envelope biogenesis	-0.69	1.59	-0.12	0.59	-0.72	-4.78	10.183
Lipoteichoic acids	PGA1_c 13720	hypothetical protein			Cell wall/membrane/envelope biogenesis	-0.79	1.73	-0.19	0.76	-0.64	-4.87	8.409
Lipoteichoic acids	PGA1_c 13730	hypothetical protein			Cell wall/membrane/envelope biogenesis	-0.68	1.74	0.00	0.42	-0.53	-4.80	8.390
Lipoteichoic acids	PGA1_c 13740	long-chain-fatty-acid--CoA ligase			Cell wall/membrane/envelope biogenesis	-0.78	1.76	-0.20	0.24	-0.74	-5.19	8.626
Lipoteichoic acids	PGA1_c 13750	phosphopantetheine-binding protein			Cell wall/membrane/envelope biogenesis	-0.94	1.67	-0.41	0.55	-0.96	-5.26	7.576
Lipoteichoic acids	PGA1_c 13760	D-alanine--poly(phosphoribitol) ligase			Cell wall/membrane/envelope biogenesis	-0.68	2.05	-0.17	0.87	-0.67	-4.64	8.680
Lipoteichoic acids	PGA1_c 13770	cytochrome P450			Cell wall/membrane/envelope biogenesis	-0.69	1.86	-0.25	0.70	-0.91	-5.32	9.560
Lipoteichoic acids	PGA1_c 13780	D-alanine--poly(phosphoribitol) ligase			Cell wall/membrane/envelope biogenesis	-0.76	1.99	-0.22	0.85	-1.01	-5.08	9.227
Lipoteichoic acids	PGA1_c 13790	hypothetical protein			Cell wall/membrane/envelope biogenesis	-0.58	2.12	-0.05	1.03	-0.85	-4.76	9.037
Lipoteichoic acids	PGA1_c 13800	alkanesulfonate monooxygenase			Cell wall/membrane/envelope biogenesis	-0.46	2.01	-0.14	0.96	-1.00	-4.60	9.894

Lipoteichoic acids	PGA1_c 13810	acyl-CoA dehydrogenase 4'-		Cell wall/membrane/enve lope biogenesis	-0.40	1.74	-0.23	0.84	-0.86	-4.17	9.530
Lipoteichoic acids	PGA1_c 13820	phosphopantethe nyl transferase		Cell wall/membrane/enve lope biogenesis	-0.41	2.01	-0.22	1.78	-0.89	-4.16	6.105
Lipoteichoic acids	PGA1_c 13830	hypothetical protein		Cell wall/membrane/enve lope biogenesis	-1.53	1.61	0.35	-1.64	-0.92	-4.62	9.057
T4SS	PGA1_c 22820	transglycosylase	COG0741	Soluble lytic murein transglycosylase and related regulatory proteins (some contain LysM/invasin domains)	1.07	0.36	0.74	1.73	-2.01	-0.23	3.414
T4SS	PGA1_c 22830	type IV secretion system protein VirB2		Cell wall/membrane/enve lope biogenesis Intracellular trafficking, secretion, and vesicular transport	0.89	0.17	-0.09	1.25	-1.89	-0.16	0.708
T4SS	PGA1_c 22840	type IV secretion protein VirB3		Intracellular trafficking, secretion, and vesicular transport	0.61	0.22	-0.42	0.81	-2.15	0.21	1.636
T4SS	PGA1_c 22850	type IV secretion system protein B4		Intracellular trafficking, secretion, and vesicular transport	0.27	0.15	-0.40	-0.08	-1.63	-0.39	4.156
T4SS	PGA1_c 22870	lytic transglycosylase		Intracellular trafficking, secretion, and vesicular transport	0.59	0.30	-0.27	-0.65	-1.21	-0.10	3.451
T4SS	PGA1_c 22880	conjugal transfer protein TraF		Intracellular trafficking, secretion, and vesicular transport	0.61	0.63	-0.11	-0.68	-1.22	-0.08	3.610
T4SS	PGA1_c 22890	type IV secretion system protein VirB8		Intracellular trafficking, secretion, and vesicular transport	0.54	0.04	-0.29	-1.50	-1.49	-0.63	2.437
T4SS	PGA1_c 22900	conjugal transfer protein TrbG	COG3504	Type IV secretory pathway, VirB9 components	1.20	1.04	0.26	-0.85	-1.09	-0.57	2.464
T4SS	PGA1_c 22910	conjugal transfer protein		Intracellular trafficking, secretion,	0.62	0.62	0.05	-0.99	-1.54	-0.42	3.814

T4SS	PGA1_c 22920	type IV secretion system protein VirB11			and vesicular transport Intracellular trafficking, secretion, and vesicular transport	0.43	0.41	0.01	-1.04	-1.18	-0.75	4.451
T4SS	PGA1_c 22940	type IV secretion system protein VirB6			and vesicular transport Intracellular trafficking, secretion, and vesicular transport	0.24	0.40	-0.36	-0.20	-1.15	-0.48	2.926
T4SS	PGA1_c 22980	protein VirD2			and vesicular transport	0.36	0.19	-0.16	0.53	-1.34	0.22	4.782
DMSP conversion to Methanethiol	PGA1_2 62p015 40	enoyl-CoA hydratase			Lipid transport and metabolism	0.19	0.33	0.08	0.70	5.20	0.21	7.967
DMSP conversion to Methanethiol	PGA1_2 62p015 50	acyl-CoA dehydrogenase	COG1960	Acyl-CoA dehydrogenases	Lipid transport and metabolism	0.77	0.71	0.45	1.33	5.49	0.79	8.017
DMSP conversion to Methanethiol	PGA1_2 62p018 30	dimethylsulfonypropionate demethylase			Lipid transport and metabolism	-0.30	-0.27	-0.27	-1.09	5.47	0.16	8.359
DMSP conversion to Methanethiol	PGA1_2 62p018 40	acyl-CoA synthetase			Lipid transport and metabolism	-0.07	-0.34	-0.29	0.04	6.44	0.08	7.973
DMSP conversion to Methanethiol	PGA1_2 62p018 50	enoyl-CoA hydratase			Lipid transport and metabolism	0.06	-0.12	-0.37	-0.16	7.23	0.09	7.546
DMSP conversion to Methanethiol	PGA1_2 62p018 60	acyl-CoA dehydrogenase			Lipid transport and metabolism	0.61	0.29	0.36	0.61	7.24	0.59	7.792
DMSP conversion to Methanethiol	PGA1_c 22710	acyl-CoA dehydrogenase			Lipid transport and metabolism	0.43	0.38	-0.08	1.82	5.99	0.45	4.587
Energy production	PGA1_c 00700	ATP synthase F0 subunit I	COG5336	ATPase	Function unknown	-1.51	-1.15	0.66	2.31	4.07	-0.03	7.743
Energy production	PGA1_c 00710	ATP synthase subunit A	COG0356	ATPase	Energy production and conversion	-2.37	-1.55	0.48	1.47	3.55	-0.73	8.573
Energy production	PGA1_c 00720	ATP synthase subunit C		ATPase		-3.40	-2.60	-0.58	0.37	2.21	-2.33	9.291

Energy production	PGA1_c 00730	FOF1 ATP synthase subunit B'	COG0711	ATPase	Energy production and conversion	-2.87	-1.97	-0.30	0.97	2.66	-2.34	8.551
Energy production	PGA1_c 00740	FOF1 ATP synthase subunit B	COG0711	ATPase	Energy production and conversion	-2.65	-1.94	-0.43	0.48	2.26	-2.14	8.082
Energy production	PGA1_c 25080	FOF1 ATP synthase subunit epsilon	COG0355	ATPase	Energy production and conversion	-2.72	-1.58	-0.36	0.82	2.05	-2.26	8.480
Energy production	PGA1_c 25090	ATP synthase subunit beta	COG0055	ATPase	Energy production and conversion	-2.36	-1.29	-0.03	1.44	2.47	-2.11	10.053
Energy production	PGA1_c 25100	FOF1 ATP synthase subunit gamma	COG0224	ATPase	Energy production and conversion	-1.79	-0.94	0.25	1.69	3.15	-1.54	9.412
Energy production	PGA1_c 25110	ATP synthase subunit alpha	COG0056	ATPase	Energy production and conversion	-1.31	-0.75	0.49	1.90	3.34	-0.07	9.341
Energy production	PGA1_c 25120	FOF1 ATP synthase subunit delta	COG0712	ATPase	Energy production and conversion	-1.05	-0.69	1.01	1.88	4.35	0.74	8.202
Energy production	PGA1_c 33980	cytochrome c	COG2857	Cytochrome c1	Cytochrome c	-1.61	-1.18	-0.08	1.51	2.31	-1.69	9.628
Energy production	PGA1_c 33990	cytochrome b ubiquinol-cytochrome c reductase iron-sulfur subunit	COG1290	Cytochrome b subunit of the bc complex	Cytochrome c	-1.30	-0.85	0.21	1.97	2.74	-0.69	9.008
Energy production	PGA1_c 34000	FOF1 ATP synthase subunit delta	COG0723	Rieske Fe-S protein	Cytochrome c	-1.01	-0.75	0.56	2.24	3.57	-0.08	8.926
Translation, Ribosomal structure	PGA1_c 01320	elongation factor Tu	COG0050	GTPases - translation elongation factors	transcription factor	-2.71	-1.61	-0.12	1.15	2.18	-1.86	9.921
Translation, Ribosomal structure	PGA1_c 01380	50S ribosomal protein L11	COG0080	Ribosomal protein L11	Ribosome	-1.85	-1.43	0.34	1.46	2.93	-0.84	8.297
Translation, Ribosomal structure	PGA1_c 01400	50S ribosomal protein L1 rplA	COG0081	Ribosomal protein L1	Ribosome	-2.10	-1.36	0.21	1.45	2.67	-1.13	6.874
Translation, Ribosomal structure	PGA1_c 01410	50S ribosomal protein L10 rplJ	COG0244	Ribosomal protein L10	Ribosome	-2.95	-2.16	-0.27	0.06	2.66	-1.54	11.178
Translation, Ribosomal structure	PGA1_c 01420	50S ribosomal protein L7/L12 rplL	COG0222	Ribosomal protein L7/L12	Ribosome	-2.63	-1.95	-0.20	-0.21	2.48	-1.58	11.206

Translation, Ribosomal structure	PGA1_c 01490	30S ribosomal protein S12 rpsL	COG0048	Ribosomal protein S12	Ribosome	-1.61	-0.77	1.21	0.49	4.15	-0.56	9.104
Translation, Ribosomal structure	PGA1_c 01500	30S ribosomal protein S7 rpsG	COG0049	Ribosomal protein S7	Ribosome	-1.82	-0.78	1.00	1.23	3.74	-0.62	9.139
Translation, Ribosomal structure	PGA1_c 01510	elongation factor G	COG0480	Translation elongation factors (GTPases)	transcription factor	-2.28	-1.24	0.42	1.04	2.89	-1.57	11.130
Translation, Ribosomal structure	PGA1_c 01520	elongation factor Tu	COG0050	GTPases - translation elongation factors	transcription factor	-2.88	-1.78	-0.07	0.64	2.05	-2.23	10.758
Translation, Ribosomal structure	PGA1_c 01560	50S ribosomal protein L4 rplD	COG0088	Ribosomal protein L4	Ribosome	-2.12	-0.90	0.27	0.97	2.39	-1.28	9.670
Translation, Ribosomal structure	PGA1_c 01590	50S ribosomal protein L2 rplB	COG0090	Ribosomal protein L2	Ribosome	-1.11	-0.41	0.68	0.73	3.01	-0.29	10.222
Translation, Ribosomal structure	PGA1_c 01600	30S ribosomal protein S19 rpsS	COG0185	Ribosomal protein S19	Ribosome	-1.54	-0.77	0.39	0.79	2.82	-1.03	9.517
Translation, Ribosomal structure	PGA1_c 01610	50S ribosomal protein L22 rplV	COG0091	Ribosomal protein L22	Ribosome	-1.42	-0.56	0.47	1.01	2.65	-0.71	9.099
Translation, Ribosomal structure	PGA1_c 01620	30S ribosomal protein S3 rpsC	COG0092	Ribosomal protein S3	Ribosome	-1.79	-0.75	0.25	0.94	2.33	-1.71	9.262
Translation, Ribosomal structure	PGA1_c 01630	50S ribosomal protein L16 rplP	COG0197	Ribosomal protein L16/L10E	Ribosome	-2.13	-0.79	0.08	0.25	1.90	-1.83	6.701
Translation, Ribosomal structure	PGA1_c 01680	50S ribosomal protein L29 rpmC	COG0255	Ribosomal protein L29	Ribosome	-1.55	-0.73	1.11	0.29	3.87	-0.08	7.526
Translation, Ribosomal structure	PGA1_c 01690	30S ribosomal protein S17 rpsQ	COG0186	Ribosomal protein S17	Ribosome	-1.98	-0.96	0.68	0.44	3.15	-0.39	9.227
Translation, Ribosomal structure	PGA1_c 01700	50S ribosomal protein L14 rplN	COG0093	Ribosomal protein L14	Ribosome	-1.98	-1.03	0.83	1.10	3.48	-0.80	8.959
Translation, Ribosomal structure	PGA1_c 01710	50S ribosomal protein L24 rplX	COG0198	Ribosomal protein L24	Ribosome	-1.99	-0.95	0.72	1.27	3.08	-0.64	7.949

Translation, Ribosomal structure	PGA1_c 01720	50S ribosomal protein L5 rplE	COG0094	Ribosomal protein L5	Ribosome	-2.19	-1.19	0.58	0.86	2.81	-1.31	10.321
Translation, Ribosomal structure	PGA1_c 01730	30S ribosomal protein S14 rpsN	COG0199	Ribosomal protein S14	Ribosome	-2.47	-1.15	0.49	0.72	2.51	-1.44	8.609
Translation, Ribosomal structure	PGA1_c 01740	30S ribosomal protein S8 rpsH	COG0096	Ribosomal protein S8	Ribosome	-2.40	-1.15	0.38	0.71	2.36	-1.53	7.591
Translation, Ribosomal structure	PGA1_c 01750	50S ribosomal protein L6 rplF	COG0097	Ribosomal protein L6P/L9E	Ribosome	-2.67	-1.46	0.18	0.29	2.08	-1.81	8.925
Translation, Ribosomal structure	PGA1_c 01760	50S ribosomal protein L18 rplR	COG0256	Ribosomal protein L18	Ribosome	-2.72	-1.60	0.22	0.25	2.21	-1.91	8.149
Translation, Ribosomal structure	PGA1_c 01770	30S ribosomal protein S5 rpsE	COG0098	Ribosomal protein S5	Ribosome	-3.11	-2.18	0.00	0.26	2.08	-2.51	9.748
Translation, Ribosomal structure	PGA1_c 01780	50S ribosomal protein L30 rpmD	COG1841	Ribosomal protein L30/L7E	Ribosome	-3.18	-2.23	-0.29	0.05	1.51	-2.98	6.116
Translation, Ribosomal structure	PGA1_c 01880	30S ribosomal protein S13 rpsM	COG0099	Ribosomal protein S13	Ribosome	-1.25	-0.61	1.12	2.61	3.97	0.16	8.981
Translation, Ribosomal structure	PGA1_c 01890	30S ribosomal protein S11 rpsK	COG0100	Ribosomal protein S11	Ribosome	-1.24	-0.45	1.08	2.21	3.77	0.11	7.940
Translation, Ribosomal structure	PGA1_c 01910	50S ribosomal protein L17 rplQ	COG0203	Ribosomal protein L17	Ribosome	-2.98	-2.06	-0.52	0.50	2.11	-2.83	8.429
Translation, Ribosomal structure	PGA1_c 04900	aminoacyl-tRNA hydrolase			tRNA (processing)	-0.03	-0.06	1.12	2.52	3.55	1.29	4.263
Translation, Ribosomal structure	PGA1_c 04910	50S ribosomal protein L25 rplY	COG1825	Ribosomal protein L25 (general stress protein Ctc)	Ribosome	-2.05	-1.06	0.34	1.10	2.32	-0.55	7.825
Translation, Ribosomal structure	PGA1_c 07010	phenylalanine-- tRNA ligase subunit alpha	COG0016	Phenylalanyl-tRNA synthetase alpha subunit	tRNA (processing)	-0.90	-0.55	0.82	2.33	3.51	0.53	6.325
Translation, Ribosomal structure	PGA1_c 14510	50S ribosomal protein L13 rplM	COG0102	Ribosomal protein L13	Ribosome	-1.25	-1.01	1.51	2.10	4.93	0.61	9.244

Translation, Ribosomal structure	PGA1_c 14520	30S ribosomal protein S9 rpsI	COG0103	Ribosomal protein S9	Ribosome	-1.40	-1.01	0.89	1.46	3.91	-0.21	5.212
Translation, Ribosomal structure	PGA1_c 15570	30S ribosomal protein S2 rpsB	COG0052	Ribosomal protein S2	Ribosome	-2.16	-1.18	0.24	1.88	3.26	-1.10	7.728
Translation, Ribosomal structure	PGA1_c 15580	elongation factor Ts tsf	COG0264	Translation elongation factor Ts	transcription factor	-2.37	-1.33	0.25	1.57	3.11	-1.38	7.915
Translation, Ribosomal structure	PGA1_c 18090	30S ribosomal protein S6 rplO	COG0360	Ribosomal protein S6	Ribosome	-2.64	-1.79	0.52	0.91	3.05	-1.14	8.066
Translation, Ribosomal structure	PGA1_c 18100	30S ribosomal protein S18	COG0238	Ribosomal protein S18		-1.81	-1.48	0.47	0.95	2.63	-0.98	7.679
Translation, Ribosomal structure	PGA1_c 18110	50S ribosomal protein L9	COG0359	Ribosomal protein L9		-1.74	-1.45	0.25	0.62	2.27	-1.10	8.385
Translation, Ribosomal structure	PGA1_c 21940	50S ribosomal protein L33 rpmG			Ribosome	0.05	-0.21	0.85	0.95	3.05	1.10	6.978
Translation, Ribosomal structure	PGA1_c 24170	50S ribosomal protein L28 rpmB	COG0227	Ribosomal protein L28	Ribosome	-0.60	-0.22	0.82	1.26	3.14	0.84	7.206
Translation, Ribosomal structure	PGA1_c 24530	aspartate--tRNA ligase	COG0173	Aspartyl-tRNA synthetase	tRNA (processing)	-1.31	-0.60	0.69	1.66	3.04	0.34	7.981
Translation, Ribosomal structure	PGA1_c 24920	molecular chaperone GroEL	COG0459	Chaperonin GroEL (HSP60 family)	Chaperonin	-2.86	-2.66	-1.36	1.10	1.72	-0.30	11.755
Translation, Ribosomal structure	PGA1_c 24930	molecular chaperone GroES	COG0234	Co-chaperonin GroES (HSP10)	Chaperonin	-3.01	-2.75	-0.75	1.23	2.76	0.19	9.410
Translation, Ribosomal structure	PGA1_c 25280	30S ribosomal protein S4 rpsD	COG0522	Ribosomal protein S4 and related proteins	Ribosome	-1.67	-0.67	0.91	3.01	3.74	0.21	6.539
Translation, Ribosomal structure	PGA1_c 32500	50S ribosomal protein L36 rpmJ			Ribosome	-1.17	-0.42	0.93	-1.28	3.78	0.34	6.006
Translation, Ribosomal structure	PGA1_c 36510	30S ribosomal protein S20 rpsT	COG0268	Ribosomal protein S20	Ribosome	-1.64	-0.31	1.06	0.96	4.04	0.61	6.490

Amino acid transport	PGA1_c 32610	branched-chain amino acid ABC transporter permease ABC transporter		branched chain AA	-0.57	0.37	0.15	-3.23	-4.34	-1.70	10.057
Amino acid transport	PGA1_c 32620	ATP-binding protein		branched chain AA	-0.30	0.18	0.14	-3.84	-4.42	-2.13	9.868
Amino acid transport	PGA1_c 32630	long-chain fatty acid--CoA ligase		branched chain AA	0.28	0.18	0.17	-3.41	-4.24	0.10	11.265
Carbohydrate transport	PGA1_c 07780	C4-dicarboxylate ABC transporter	COG1638	TRAP-type C4-dicarboxylate transport system, periplasmic component	2.13	2.22	1.79	-1.35	-3.13	1.57	7.698
Carbohydrate transport	PGA1_c 07770	TRAP transporter permease DctQ	COG3090	TRAP-type C4-dicarboxylate transport system, small permease component	2.25	2.77	1.93	0.11	-3.07	1.48	3.987
Carbohydrate transport	PGA1_c 07760	C4-dicarboxylate ABC transporter carbohydrate ABC transporter	COG1593	TRAP-type C4-dicarboxylate transport system, large permease component	2.49	3.13	2.22	-0.23	-2.09	0.69	4.519
Carbohydrate transport	PGA1_7 8p0016 0	substrate-binding protein	COG1653	ABC-type sugar transport system, periplasmic component	-1.29	-1.07	-0.61	-3.93	-2.55	0.41	8.269
Carbohydrate transport	PGA1_7 8p0017 0	sugar ABC transporter permease	COG1175	ABC-type sugar transport systems, permease components	-0.95	-0.73	-0.28	-3.45	-2.31	0.23	6.591
Carbohydrate transport	PGA1_7 8p0018 0	sugar ABC transporter permease ABC transporter	COG0395	ABC-type sugar transport system, permease component	-1.02	-0.55	-0.29	-3.37	-2.11	-0.87	5.972
Carbohydrate transport	PGA1_c 27320	ATP-binding protein sugar ABC transporter	COG3839	ABC-type sugar transport systems, ATPase components	1.77	1.33	0.92	-0.63	-3.27	1.53	7.312
Carbohydrate transport	PGA1_c 27330	substrate-binding protein sugar ABC transporter	COG1653	ABC-type sugar transport system, periplasmic component	1.66	1.55	0.75	-1.10	-3.71	0.58	7.834
Carbohydrate transport	PGA1_c 27340	permease carbohydrate ABC transporter	COG1175	ABC-type sugar transport systems, permease components	2.07	1.82	0.92	-0.61	-3.44	0.37	6.418
Carbohydrate transport	PGA1_c 27350	permease	COG0395	ABC-type sugar transport system, permease component	1.72	1.62	0.86	-1.03	-3.19	0.17	6.274
Purin metabolism	PGA1_c 10770	stationary phase survival protein SurE		General function prediction only	-0.36	-0.03	0.46	1.66	3.00	0.37	7.136

Purin metabolism	PGA1_c 13260	phosphoribosylformylglycinamide cyclo-ligase		Nucleotide metabolism	0.38	0.27	0.44	1.92	1.98	0.63	5.837
Purin metabolism	PGA1_c 13270	phosphoribosylglycinamide formyltransferase PurN		Nucleotide metabolism	-0.41	0.00	0.78	2.28	2.70	0.69	5.673
Purin metabolism	PGA1_c 13400	phosphoribosylaminimidazole succinocarboxamide synthase	COG0152	Nucleotide metabolism	-0.59	-0.35	1.02	2.17	3.74	1.19	7.275
Purin metabolism	PGA1_c 14610	GMP synthase (glutamine- hydrolyzing)		Nucleotide metabolism	-0.62	-0.14	0.99	2.43	3.99	1.04	7.828
Purin metabolism	PGA1_c 15220	IMP dehydrogenase	COG0516	Nucleotide metabolism	-1.10	-0.61	0.27	1.75	2.78	0.26	6.604
Purin metabolism	PGA1_c 17120	phosphoribosylformylglycinamide synthase II	COG0046	Nucleotide metabolism	-0.71	-0.04	0.98	2.73	3.12	0.74	7.695
Purin metabolism	PGA1_c 18780	adenylosuccinate lyase		Nucleotide metabolism	-0.42	-0.26	0.92	3.62	3.60	0.48	7.390
Purin metabolism	PGA1_c 23610	phosphoribosylamine--glycine ligase PurM		Nucleotide metabolism	-0.67	-0.14	0.80	2.07	2.73	0.71	5.246
Purin metabolism	PGA1_c 23820	adenylosuccinate synthase		Nucleotide metabolism	-0.58	-0.31	0.92	2.82	3.09	0.76	8.038
Purin metabolism	PGA1_c 24860	5-(carboxyamino)imidazole ribose-phosphate		Nucleotide metabolism	0.28	0.50	0.82	2.28	2.11	1.14	4.524
Purin metabolism	PGA1_c 25050	pyrophosphokinase		Multiple classes	-0.34	0.03	1.01	1.98	2.75	0.67	5.467
Glycolysis	PGA1_c 23910	class I fructose-bisphosphate aldolase		Carbohydrate metabolism	-0.24	-0.23	0.39	3.62	2.68	0.54	5.228
Glycolysis	PGA1_c 17250	type I glyceraldehyde-3-phosphate dehydrogenase		Carbohydrate metabolism	0.09	0.04	0.36	6.35	4.82	0.15	5.955
Protein transport	PGA1_c 00630	signal recognition particle protein preprotein		Protein transport	-0.44	-0.11	1.07	2.07	2.58	1.47	7.812
Protein transport	PGA1_c 01360	translocase subunit SecE preprotein		Protein transport	0.23	0.58	1.06	2.64	1.89	1.58	6.015
Protein transport	PGA1_c 01860	translocase subunit SecY membrane	COG0201	Preprotein translocase subunit SecY	-0.80	-0.32	0.42	1.05	1.97	0.33	8.701
Protein transport	PGA1_c 02090	protein insertase YidC		Protein transport	-0.52	-0.34	0.90	1.93	3.08	0.82	8.363
Protein transport	PGA1_c 10700	prohead protease	COG1826	Sec-independent protein secretion pathway components	-2.02	-1.62	-0.39	-0.64	2.80	-0.81	7.079

Protein transport	PGA1_c 10710	twin-arginine translocase subunit TatB preprotein	COG1826	Sec-independent protein secretion pathway components	Protein transport	-1.71	-1.28	-0.48	-0.03	2.36	-0.53	6.855
Protein transport	PGA1_c 10720	translocase subunit TatC protein	COG0805	Sec-independent protein secretion pathway component	Protein transport	-1.70	-1.07	-0.63	0.07	1.88	-0.80	6.598
Protein transport	PGA1_c 18910	translocase subunit SecF protein	COG0341	Preprotein translocase subunit SecF	Protein transport	-1.12	-0.39	0.13	0.22	1.53	-0.29	6.332
Protein transport	PGA1_c 18920	translocase subunit SecD preprotein	COG0342	Preprotein translocase subunit SecD	Protein transport	-1.42	-0.49	0.39	0.20	1.98	0.53	7.621
Protein transport	PGA1_c 18930	translocase subunit YajC preprotein	COG1862	Preprotein translocase subunit YajC	Protein transport	-1.93	-1.16	0.51	-0.97	2.41	0.81	6.040
Protein transport	PGA1_c 23890	translocase subunit SecG preprotein			Protein transport	-0.19	0.01	1.26	2.57	3.59	1.40	4.272
Protein transport	PGA1_c 34580	translocase subunit SecA			Protein transport	-0.46	0.10	0.66	0.53	2.00	0.94	9.446
Glutamine metabolism	PGA1_c 06670	carbamoyl phosphate synthase small subunit carbamoyl phosphate			Amino acid metabolism	-0.36	0.08	1.25	2.60	3.29	1.59	7.048
Glutamine metabolism	PGA1_c 24560	synthase large subunit phosphoribosyl-ATP diphosphatase	COG0458	Glutamine to carbamoyl-P	Amino acid metabolism	-1.29	-0.55	0.51	2.52	3.03	0.13	7.606
histidine biosynthesis	PGA1_c 09230	imidazole glycerol phosphate synthase cyclase subunit			Amino acid metabolism	-0.69	-0.59	-0.26	2.55	3.08	0.11	3.044
histidine biosynthesis	PGA1_c 09240	imidazole glycerol phosphate synthase cyclase subunit			Amino acid metabolism	-1.12	-0.77	0.22	2.69	3.65	0.19	4.051
histidine biosynthesis	PGA1_c 09320	imidazole glycerol phosphate synthase subunit HisH			Amino acid metabolism	-0.23	0.50	0.71	2.20	2.78	0.56	4.535
histidine biosynthesis	PGA1_c 09330	imidazoleglycerol-phosphate dehydratase			Amino acid metabolism	0.00	0.56	0.93	2.14	3.38	0.70	4.650
histidine biosynthesis	PGA1_c 25240	histidinol-phosphate transaminase ATP phosphoribosyltransferase catalytic subunit HisG	COG0040	ATP phosphoribosyltransferase	Amino acid metabolism	-0.35	-0.03	0.57	2.49	2.27	0.79	6.284
histidine biosynthesis	PGA1_c 29870	ATP phosphoribosyltransferase catalytic subunit HisG	COG0040	ATP phosphoribosyltransferase	Amino acid metabolism	-1.72	-1.00	0.03	1.50	2.34	-1.25	6.658

histidine biosynthesis	PGA1_c 29880	ATP phosphoribosyltransferase regulatory subunit	COG3705	ATP phosphoribosyltransferase involved in histidine biosynthesis	Amino acid metabolism	-1.04	-0.52	0.33	2.16	2.83	-0.03	6.205
histidine degradation	PGA1_c 36320	urocanate hydratase	COG2987	Urocanate hydratase	Amino acid metabolism	2.12	1.73	0.52	-0.25	-1.62	1.73	5.502
histidine degradation	PGA1_c 36330	N-formylglutamate deformylase	COG3741	N-formylglutamate amidohydrolase	Amino acid metabolism	2.71	1.82	0.80	-0.43	-1.61	2.13	4.681
histidine degradation	PGA1_c 36340	histidine ammonia-lyase	COG2986	Histidine ammonia-lyase	Amino acid metabolism	2.60	1.51	0.68	0.59	-1.89	2.81	6.032
histidine degradation	PGA1_c 36350	imidazolonepropionase	COG1228	Imidazolonepropionase and related amidohydrolases	Amino acid metabolism	2.35	1.55	0.59	1.33	-1.75	3.14	5.258
Arginine degradation to putrescine	PGA1_c 16370	arginase	COG0010	Arginase/agnmatinase/formimionoglutamate hydrolase, arginase family	Amino acid metabolism	3.51	1.96	2.39	-0.42	-1.11	2.98	6.064
Arginine degradation to putrescine	PGA1_c 16380	hypothetical protein	COG4874	Uncharacterized protein conserved in bacteria containing a penta-in-type domain	Function unknown	2.86	1.43	1.82	-1.30	-1.20	2.37	6.447
Arginine degradation to putrescine	PGA1_c 16390	ornithine cyclodeaminase	COG2423	Predicted ornithine cyclodeaminase, mu-crystallin homolog	Amino acid metabolism	3.00	1.48	1.75	-1.07	-1.38	2.14	6.898
Arginine degradation to putrescine	PGA1_c 11650	ornithine decarboxylase	COG0019	Diaminopimelate decarboxylase	Amino acid metabolism	3.38	2.44	2.68	-0.49	-3.96	1.67	9.522
Spermidine/Spermine biosynthesis from Putrescine	PGA1_c 14470	spermidine synthase			Amino acid metabolism	-0.52	-0.08	1.50	3.34	4.94	1.13	4.776
Spermidine/Spermine biosynthesis from Putrescine	PGA1_c 14480	S-adenosylmethionine decarboxylase proenzyme			Amino acid metabolism	-0.70	0.20	1.70	3.18	5.12	1.47	6.312
Pyruvate metabolism	PGA1_c 17550	pyruvate dehydrogenase (acetyl-transferring) E1 component subunit alpha	COG1071	Pyruvate/2-oxoglutarate dehydrogenase complex, dehydrogenase (E1) component, eukaryotic type, alpha subunit	Carbohydrate metabolism	-0.62	-0.53	-0.16	-2.25	-1.90	-0.47	9.367

Pyruvat metabolism	PGA1_c 17560	pyruvate dehydrogenase complex E1 component subunit beta	COG0022	Pyruvate/2-oxoglutarate dehydrogenase complex, dehydrogenase (E1) component, eukaryotic type, beta subunit	Carbohydrate metabolism	-0.63	-0.62	-0.37	-2.41	-2.22	-0.87	10.033
Pyruvat metabolism	PGA1_c 17570	pyruvate dehydrogenase complex dihydrolipoamide acetyltransferase	COG0508	Pyruvate/2-oxoglutarate dehydrogenase complex, dihydrolipoamide acyltransferase (E2) component, and related enzymes	Carbohydrate metabolism	-0.61	-0.46	-0.46	-2.33	-2.34	-1.12	9.010
Pyrimidin metabolism	PGA1_c 03060	aspartate carbamoyltransferase			Nucleotide metabolism	-0.53	-0.25	0.59	2.07	2.26	0.43	4.665
Pyrimidin metabolism	PGA1_c 10770	stationary phase survival protein SurE			General function prediction only	-0.36	-0.03	0.46	1.66	3.00	0.37	7.136
Pyrimidin metabolism	PGA1_c 10900	orotate phosphoribosyltransferase	COG0461	Orotate phosphoribosyltransferase	Nucleotide metabolism	-1.03	-0.37	0.25	1.36	2.88	0.07	4.954
Pyrimidin metabolism	PGA1_c 10910	dihydroorotate dehydrogenase			Nucleotide metabolism	0.11	0.56	0.85	2.17	2.57	0.76	5.020
Pyrimidin metabolism	PGA1_c 12150	(quinone)			Nucleotide metabolism	-0.61	-0.32	0.71	1.69	2.56	0.68	4.832
Pyrimidin metabolism	PGA1_c 32450	orotidine-5'-phosphate decarboxylase			Nucleotide metabolism	-0.40	-0.34	0.97	2.61	2.61	0.49	3.686

Table S3 with the complete transcriptomic data including 2747 genes for *Phaeobacter inhibens* DSM 17395 can be found in the digital supplementary material attached to the printed version of this dissertation.

Supplementary Material for Manuscript 4

Different AHL-based quorum sensing systems in *Phaeobacter inhibens* T5^T regulate distinct traits for host-association or horizontal gene transfer

Supplementary methods

Transformation of E. coli

E. coli was grown in 100 mL Luria-Bertani (LB) (L⁻¹: 5 g yeast extract, 10 g tryptone, 10 g sodium chloride) at 37°C, 100 rpm to OD₆₀₀ ~ 0.6 (logarithmic growth), cooled down in ice water mixture for 15 min, and centrifuged (10 min, 10,000 x g, 4°C). Cell pellet was washed twice with 50 ml and finally re-diluted in 0.2 ml cooled 10% (v/v) glycerol. Aliquots of 40 µl were stored at -80°C until further use. For transformation, 40 µl portions of the cells were carefully mixed with 1 µl of ligation approach and transferred to cooled electroporation cuvette (0.2 cm gap) and electroporated by applying a pulse of 2.5 kV, 25 µF, 200 Ω. 1 ml LB were directly added, incubated at 37°C, 2 h, 100 rpm and plated onto antibiotic selective plates in several dilutions for mutant isolation incubated at 37°C at least 48 h.

Conjugation of P. inhibens and E. coli ST18

For conjugation, ST18, transformed with the pEX18 phin1 1 Km, pEX18 phin1 2 Gm or pEX18 phin1 3 Km plasmid, serving as donor strain, was grown to logarithmic phase (3 h, 37°C, 100 rpm, OD ~ 0.6) in LB supplemented with 50 µg/mL 5-aminolevulinic acid (ALA) and the respective antibiotic (Gm 30 µg/mL; Km 80 µg/mL). *P. inhibens* T5 wild type cells (recipient) were grown to stationary growth phase (20 h, 28°C, 100 rpm, OD ~ 4) in MB. For conjugation, liquid cultures were mixed in 1:4 and 1:5 proportions (donor:recipient), centrifuged (5 min, 9,000 x g), supernatant discarded and the pellet resuspended in rest of liquid and dropped on a very dry ½ MB+ALA plate, incubated 24 h at 25°C. Afterwards pellet was scraped from plate, resuspended in PBS buffer, diluted in several steps (10⁰ – 10⁻²) and plated for antibiotic selection on ½ MB plates containing the respective antibiotic, incubated at 25°C until colonies are visible. Successful conjugation was checked by restriction digestion analysis and sequencing as specified above.

TDA measurements

TDA production was measured for mutants and the wild type. Filtered supernatants of 50 mL culture grown in MB (28°C, 100 rpm) until late exponential phase (20 h, OD₆₀₀ ~4) were analyzed at BioViotika Naturstoffe GmbH (Göttingen, Germany). Samples were set to pH 3 using 2 M HCl, 20 mL supernatant extracted with 25 mL ethyl acetate, evaporated to dryness and re-dissolved in 1 mL acetonitrile. Analysis was conducted by high-performance liquid chromatography (HPLC) on a Celeno DAD II HPLC (Goebel Analytik, Hallertau, Germany), separated on a Nucleodur 100 5 C18 (250 mm x 3 mm) column using a water-acetonitrile gradient solvent system, with both solvents containing 20 mM formic acid. Using a flow of 0.5 mL/min, the gradient was started

with 20% acetonitrile and increased to 100% acetonitrile within 25 min. TDA was determined using evaporative light scattering detector (ELSD) Sedex 85, following calibration with pure TDA.

RNA isolation, sequencing and analysis

Harvested cells were resuspended in 800 μ l RLT buffer (RNeasy Mini Kit, Qiagen) with β -Mercaptoethanol (10 μ l/ml) and cell lysis was performed using a laboratory ball mill. Subsequently 400 μ l RLT buffer (RNeasy Mini Kit Qiagen) with β -Mercaptoethanol (10 μ l/ml) and 1200 μ l 96% [v/v] ethanol was added. For RNA isolation, the RNeasy Mini Kit (Qiagen) was used as recommended by the manufacturer, but instead of RW1 buffer RWT buffer (Qiagen) was used in order to additionally isolate RNAs \leq 200 nucleotides. To determine the RNA integrity number (RIN) the isolated RNA was run on an Agilent Bioanalyzer 2100 using an Agilent RNA 6000 Nano Kit as recommended (Agilent Technologies, Waldbronn, Germany). Remaining genomic DNA was digested with TURBO DNase (Invitrogen, ThermoFischer Scientific, Paisley, United Kingdom). The Ribo-Zero magnetic kit (Epicentre Biotechnologies, Madison, WI, USA) was used to reduce the amount of rRNA-derived sequences. Strand-specific cDNA libraries were constructed with a NEBNext Ultra II directional RNA library preparation kit for Illumina (New England BioLabs, Frankfurt am Main, Germany) and sequenced with the HiSeq4000 instrument (Illumina Inc., San Diego, CA, USA) using the HiSeq 3000/4000 SR Cluster Kit for cluster generation and the HiSeq 3000/4000 SBS Kit (50 cycles) for sequencing in the single-end mode running 1x 50 cycles. For quality filtering and removing of remaining adaptor sequences, Trimmomatic-0.32 (Bolger et al. 2014) and a cutoff phred-33 score of 15 were used. The mapping of the remaining sequences was performed with the Bowtie2 program (Langmead et al. 2012) using the implemented end-to-end mode, which requires that the entire read aligns from one end to the other. First, remaining paired end reads were mapped against a database consisting of tRNA and rRNA sequences of *P. inhibens* T5 and unaligned reads were subsequently mapped against the genome. Differential expression analyses were performed with the BaySeq program (Mortazavi et al. 2008). Genes with absolute \log_2 -fold change >1 , a likelihood value of ≥ 0.9 , and an adjusted *P* value of ≤ 0.05 (corrected by the false discovery rate [FDR] based on the Benjamini-Hochberg procedure) were considered differentially expressed.

Supplementary Figures and Tables

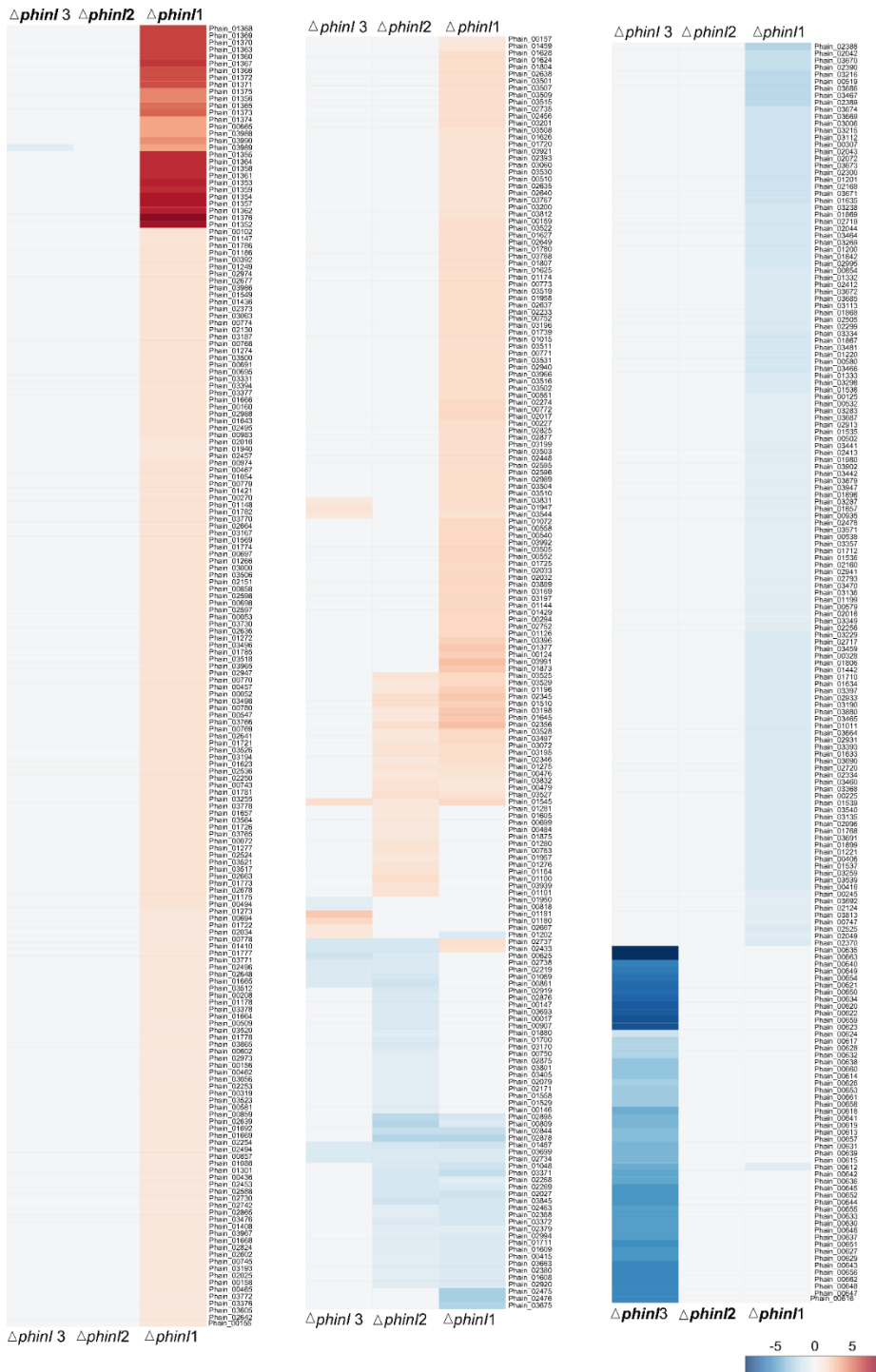


Fig. S1: Complete heatmap for *phin1::Km*, *phin2::Gm* and *phin3::Km* compared to wild type expression level, including locus tags of regulated genes.

Table S1: Overview of genes with specific regulation in the transcriptome of *P. inhibens* T5 mutant strains vs. wild type. Values in bold correspond to differentially expressed genes with absolute log2-FC>1 and/or log2-CPM higher than mean (>5.5).

COG Category	Group	Locus Tag	Contig	Gene product	<i>phin1::Km_I</i> og2-FC	<i>phin2::Gm_I</i> og2-FC	<i>phin3::Kn_I</i> og2-FC	log2-CPM
M		Phain_00156	Chromosome	UDP-glucose 4-epimerase	1.05	0.40	-0.07	3.357
M		Phain_00158	Chromosome	CDP-6-deoxy-D-xylo-4-hexulose-3-dehydrase	1.01	0.13	0.07	4.406
M		Phain_00159	Chromosome	GDPmannose 4,6-dehydratase	1.48	0.44	0.05	0.264
M		Phain_00457	Chromosome	Sugar transferase involved in LPS biosynthesis (colanic, teichoic acid)	1.30	0.36	-0.33	5.712
M		Phain_00462	Chromosome	Glycosyltransferase involved in cell wall bisynthesis	1.05	0.20	-0.28	5.857
M		Phain_00470	Chromosome	polymer biosynthesis protein, WecB/TagA/CpsF family	0.55	0.03	-0.14	6.159
M		Phain_00691	Chromosome	small conductance mechanosensitive channel	1.18	0.18	-0.12	4.745
M		Phain_00692	Chromosome	large conductance mechanosensitive channel	0.81	0.54	0.18	5.503
MD		Phain_00939	Chromosome	cell division protein FtsI (penicillin-binding protein 3)	0.66	0.29	-0.04	10.455
M		Phain_00940	Chromosome	UDP-N-acetylmuramoylalananyl-D-glutamate--2,6-diaminopimelate ligase	0.93	0.15	-0.22	9.188
M		Phain_00941	Chromosome	UDP-N-acetylmuramoyl-tripeptide--D-alanyl-D-alanine ligase	0.89	0.12	-0.24	7.895
M		Phain_00942	Chromosome	Phospho-N-acetylmuramoyl-pentapeptide-transferase	0.93	0.15	0.01	6.797
M		Phain_00949	Chromosome	UDP-N-acetylglucosamine--N-acetylmuramyl-(pentapeptide) pyrophosphoryl-undecaprenol N-acetylglucosamine transferase	0.87	0.22	0.15	7.645
M		Phain_00950	Chromosome	UDP-N-acetylmuramate--L-alanine ligase	0.86	0.42	0.22	8.347
M		Phain_01065	Chromosome	Murein DD-endopeptidase MepM and murein hydrolase activator NlpD, contain LysM domain	0.78	0.15	0.07	7.500
M		Phain_01144	Chromosome	dTDP-4-amino-4,6-dideoxygalactose transaminase	1.91	-0.36	-0.04	4.064
M		Phain_01352	Chromosome	RND family efflux transporter, MFP subunit	7.49	-0.35	-0.23	7.319
M		Phain_01353	Chromosome	putative ABC transport system ATP-binding protein	6.80	-0.42	-0.13	9.184
M		Phain_01354	Chromosome	putative ABC transport system permease protein	7.14	-0.13	-0.09	9.481
M		Phain_01355	Chromosome	putative ABC transport system permease protein	6.59	-0.11	-0.07	9.344
M		Phain_01356	Chromosome	3-Oxoacyl-[acyl-carrier-protein (ACP)] synthase III C terminal	4.48	-0.49	-0.19	5.031
M		Phain_01357	Chromosome	acyl carrier protein	7.07	0.29	0.06	5.259
M		Phain_01358	Chromosome	hypothetical protein	6.61	-0.03	-0.11	6.773
M		Phain_01359	Chromosome	hypothetical protein	6.72	-0.22	0.27	5.701
M		Phain_01360	Chromosome	Na+-driven multidrug efflux pump	5.99	-0.45	0.13	6.812
M		Phain_01361	Chromosome	Alpha/beta hydrolase family protein	6.47	-0.45	-0.31	6.842
M		Phain_01362	Chromosome	3-oxoacyl-[acyl-carrier-protein] synthase-3	6.98	0.05	0.10	6.294
M		Phain_01363	Chromosome	hypothetical protein	6.04	-0.15	-0.06	4.805
M		Phain_01364	Chromosome	diaminopimelate decarboxylase	6.57	0.02	0.02	8.770
M		Phain_01365	Chromosome	hypothetical protein	4.84	0.19	0.34	7.531
M		Phain_01366	Chromosome	3-oxoacyl-[acyl-carrier-protein] synthase-3	5.88	-0.22	-0.22	6.256
M		Phain_01367	Chromosome	amino acid adenylation domain-containing protein	6.24	0.09	-0.14	6.925
M		Phain_01368	Chromosome	acyl carrier protein	6.11	0.23	-0.06	4.960
M		Phain_01369	Chromosome	D-alanine--poly(phosphoribitol) ligase subunit 1	6.10	0.10	0.16	7.470
M		Phain_01370	Chromosome	Cytochrome P450	6.07	0.06	0.00	7.040

M	Phain_01371	Chromosome	D-alanine--poly(phosphoribitol) ligase subunit 1	5.63	0.02	-0.05	7.494
M	Phain_01372	Chromosome	RND family efflux transporter, MFP subunit	5.71	0.13	0.04	7.662
M	Phain_01373	Chromosome	putative ABC transport system ATP-binding protein	5.66	0.15	0.05	7.373
M	Phain_01374	Chromosome	putative ABC transport system permease protein	5.60	0.17	0.06	7.312
M	Phain_01375	Chromosome	putative ABC transport system permease protein	5.55	0.19	0.07	5.713
M	Phain_01376	Chromosome	3-Oxoacyl-[acyl-carrier-protein (ACP)] synthase III C terminal	5.49	0.22	0.07	7.891
M	Phain_01377	Chromosome	acyl carrier protein	5.43	0.24	0.08	6.443
M	Phain_01645	Chromosome	Outer membrane protein beta-barrel domain-containing protein	2.41	1.11	0.66	4.707
M	Phain_01703	Chromosome	glutamate racemase	0.61	-0.09	-0.06	6.276
M	Phain_01752	Chromosome	Murein DD-endopeptidase MepM and murein hydrolase activator NlpD, contain LysM domain	0.68	0.09	-0.07	6.226
M	Phain_01806	Chromosome	Outer membrane protein (porin)	-1.24	0.18	0.02	11.396
M	Phain_01873	Chromosome	mannose-1-phosphate guanylyltransferase / mannose-6-phosphate isomerase	2.45	0.34	0.31	5.824
M	Phain_02147	Chromosome	Choline-glycine betaine transporter	0.80	0.47	0.98	5.168
M	Phain_02253	Chromosome	Putative peptidoglycan binding domain-containing protein	1.06	-0.07	-0.11	5.189
MG	Phain_02326	Chromosome	capsular polysaccharide transport system ATP-binding protein	0.67	0.23	-0.13	5.092
M	Phain_02327	Chromosome	capsular polysaccharide transport system permease protein	0.53	0.12	-0.16	8.067
M	Phain_02328	Chromosome	2-dehydro-3-deoxyphosphooctonate aldolase (KDO 8-P synthase)	0.56	0.10	-0.06	6.681
M	Phain_02369	Chromosome	Prolipoprotein diacylglycerol transferase	-0.93	-0.58	-0.03	6.724
M	Phain_02413	Chromosome	Peptidase family M23	-1.03	-0.24	-0.31	8.741
M	Phain_02490	Chromosome	D-alanyl-D-alanine carboxypeptidase / D-alanyl-D-alanine-endopeptidase (penicillin-binding protein 4)	0.65	0.06	-0.16	7.654
MR	Phain_02558	Chromosome	nucleoside-binding protein, ABC transporter substrate-binding protein	0.60	0.30	0.04	7.113
M	Phain_02565	Chromosome	Small-conductance mechanosensitive channel	0.66	0.33	-0.38	10.750
M	Phain_02656	Chromosome	dolichol-phosphate mannosyltransferase	0.94	0.38	-0.16	6.309
M	Phain_02664	Chromosome	N-acetylmuramic acid 6-phosphate etherase	1.23	0.50	-0.41	3.197
M	Phain_02691	Chromosome	nucleoside-binding protein	0.63	0.23	-0.23	7.102
M	Phain_02800	Chromosome	small conductance mechanosensitive channel	0.78	0.81	-0.07	10.485
M	Phain_02813	Chromosome	phospholipid-binding lipoprotein MlaA	-0.67	-0.65	0.06	9.342
M	Phain_03237	Chromosome	Glycosyltransferase involved in LPS biosynthesis, GR25 family	-0.39	-0.46	-0.06	5.836
M	Phain_03266	Chromosome	Outer membrane lipoprotein-sorting protein	-0.83	-0.55	0.16	8.828
M	Phain_03286	Chromosome	3-deoxy-D-manno-octulosonic-acid transferase	-0.95	-0.55	-0.47	5.682
M	Phain_03287	Chromosome	lipid-A-disaccharide kinase	-1.04	-0.52	-0.40	4.852
M	Phain_03357	Chromosome	Nucleoside-diphosphate-sugar epimerase	-1.07	-0.75	0.06	6.886
M	Phain_03461	Chromosome	membrane-bound lytic murein transglycosylase A	-0.89	-0.56	0.06	8.419
M	Phain_03510	Chromosome	Soluble lytic murein transglycosylase	1.56	0.58	-0.05	4.022
M	Phain_03538	Chromosome	lipopolysaccharide export system ATP-binding protein	-0.67	-0.46	-0.48	6.982
M	Phain_03539	Chromosome	lipopolysaccharide export system protein LptA	-1.13	-0.69	-0.27	6.531
M	Phain_03540	Chromosome	lipopolysaccharide export system protein LptC	-1.16	-0.76	-0.28	8.525
MG	Phain_03541	Chromosome	arabinose-5-phosphate isomerase	-0.87	-0.64	0.05	8.963
MDP	Phain_03726	227kb	dissimilatory nitrite reductase (NO-forming), copper type apoprotein	0.86	0.32	0.70	8.870

M		Phain_03744	227kb	Choline-glycine betaine transporter	0.73	0.52	0.30	4.309
M		Phain_03785	227kb	UDP-N-acetyl-D-galactosamine dehydrogenase	-0.57	-0.70	0.08	7.682
M		Phain_03890	78kb	Outer membrane scaffolding protein for murein synthesis, MipA/OmpV family	0.71	-0.20	-0.25	4.420
MV		Phain_03891	78kb	membrane fusion protein, multidrug efflux system	-0.68	-0.22	-0.46	6.751
M		Phain_03947	69kb	UDP-glucuronate 4-epimerase	-1.04	-0.90	0.31	6.888
M		Phain_03950	69kb	capsular polysaccharide transport system permease protein	0.63	-0.03	-0.03	7.342
MG		Phain_03951	69kb	capsular polysaccharide transport system ATP-binding protein	0.53	-0.12	0.01	4.973
NT	MCP	Phain_00446	Chromosome	methyl-accepting chemotaxis protein	0.73	0.17	0.14	4.419
N		Phain_00743	Chromosome	aerotaxis receptor	1.29	0.70	0.22	6.135
NT	MCP	Phain_01174	Chromosome	methyl-accepting chemotaxis sensory transducer with Pas/Pac sensor	1.50	0.25	0.58	6.617
N		Phain_01266	Chromosome	Type III flagellar switch regulator (C-ring) FliN C-term	1.24	0.48	0.19	6.093
NT	MCP	Phain_01807	Chromosome	methyl-accepting chemotaxis protein	1.46	0.65	0.14	4.169
N		Phain_01819	Chromosome	flagellar motor switch protein FliG	0.74	0.26	-0.07	6.934
NT	MCP	Phain_02393	Chromosome	methyl-accepting chemotaxis protein	1.37	0.55	0.25	7.124
NT	MCP	Phain_02448	Chromosome	methyl-accepting chemotaxis protein	1.59	0.76	0.29	6.066
N	chemotaxis	Phain_03496	Chromosome	chemotaxis protein MotB	1.32	0.98	0.41	5.221
N	flagella	Phain_03497	Chromosome	flagellar hook protein FlgE	1.70	1.05	0.43	5.034
N		Phain_03498	Chromosome	flagellar hook-associated protein 1 FlgK	1.34	0.47	0.22	4.900
N		Phain_03499	Chromosome	flagellar hook-associated protein 3 FlgL	0.93	0.28	0.27	4.908
N		Phain_03500	Chromosome	flagellar P-ring protein precursor FlgI	1.18	0.49	0.36	5.645
N		Phain_03501	Chromosome	flagellar biosynthetic protein FliP	1.43	0.32	0.17	4.734
N		Phain_03502	Chromosome	flagellar motor switch protein FliN/FliY	1.64	0.45	0.26	3.029
N		Phain_03503	Chromosome	flagellar assembly protein FliH	1.60	0.38	-0.09	3.783
NU		Phain_03504	Chromosome	flagellar M-ring protein FliF	1.56	0.62	0.07	5.870
N		Phain_03505	Chromosome	flagellar FliL protein	1.86	0.95	0.15	4.325
N		Phain_03507	Chromosome	Flagellar motility protein MotE, a chaperone for MotC folding	1.43	0.47	0.09	4.640
N		Phain_03508	Chromosome	chemotaxis protein MotA	1.40	0.52	0.31	4.752
NU		Phain_03511	Chromosome	flagellar biosynthesis protein FlhA	1.52	0.39	0.01	4.805
N		Phain_03512	Chromosome	flagellar biosynthetic protein FliR	1.08	0.25	-0.16	3.880
NU		Phain_03513	Chromosome	flagellar biosynthetic protein FlhB	0.95	0.19	0.05	4.764
N		Phain_03515	Chromosome	Flagellar basal body-associated protein FliL	1.42	0.65	0.35	4.291
N		Phain_03516	Chromosome	flagellar L-ring protein precursor FlgH	1.64	0.65	0.51	4.970
N		Phain_03517	Chromosome	flagella basal body P-ring formation protein FlgA	1.26	0.28	0.27	4.576
N		Phain_03518	Chromosome	flagellar basal-body rod protein FlgG	1.32	0.49	0.40	4.657
N		Phain_03519	Chromosome	flagellar basal-body rod protein FlgF	1.48	0.60	0.15	3.848
N		Phain_03520	Chromosome	flagellar biosynthetic protein FliQ	1.10	0.47	-0.02	2.426
N		Phain_03521	Chromosome	flagellar hook-basal body complex protein FliE	1.26	0.55	-0.04	2.564
N		Phain_03522	Chromosome	flagellar basal-body rod protein FlgC	1.48	0.55	0.35	2.209
N		Phain_03523	Chromosome	flagellar basal-body rod protein FlgB	1.06	0.49	0.07	2.979
N	flagella	Phain_03525	Chromosome	flagellar protein FliB	1.88	1.14	0.60	5.082
N		Phain_03526	Chromosome	flagellar protein FlaF	1.34	0.92	0.37	4.595

N	flagella	Phain_03527	Chromosome	flagellin	1.31	1.53	0.98	9.373
N	flagella	Phain_03528	Chromosome	FlgN protein	1.77	1.10	0.27	3.483
N	flagella	Phain_03529	Chromosome	Rod binding protein (flagellar rod)	1.92	1.09	0.48	1.740
N		Phain_03530	Chromosome	hook-length control protein FlhK	1.36	0.40	-0.07	6.480
N		Phain_03531	Chromosome	flagellar basal-body rod modification protein FlgD	1.65	0.66	0.23	4.624
NT	MCP	Phain_03606	227kb	Methyl-accepting chemotaxis protein	0.82	0.15	0.07	6.015
NT		Phain_03627	227kb	methyl-accepting chemotaxis sensory transducer with Cache sensor	0.79	0.37	0.40	6.812
NT	chemotaxis	Phain_03764	227kb	two-component system, chemotaxis family, response regulator CheY	0.87	0.37	0.22	5.279
NT	chemotaxis	Phain_03765	227kb	chemotaxis protein methyltransferase CheR	1.28	0.70	0.55	5.409
NT	chemotaxis	Phain_03766	227kb	purine-binding chemotaxis protein CheW	1.33	0.76	0.46	4.537
NT	chemotaxis	Phain_03767	227kb	two-component system, chemotaxis family, sensor kinase CheA	1.39	0.63	0.27	7.516
NT	chemotaxis	Phain_03770	227kb	methyl-accepting chemotaxis protein	1.23	0.66	0.34	4.858
NT	chemotaxis	Phain_03771	227kb	two-component system, chemotaxis family, response regulator CheB	1.08	0.56	0.17	4.243
NT	chemotaxis	Phain_03772	227kb	chemotaxis protein CheD	1.02	0.50	0.12	4.901
S	GTA	Phain_01769	Chromosome	hypothetical protein	0.83	-0.08	-0.25	3.658
X	GTA	Phain_01770	Chromosome	Putative phage tail protein	0.80	0.06	-0.05	6.521
X	GTA	Phain_01771	Chromosome	putative phage cell wall peptidase, NlpC/P60 family	0.97	0.08	-0.01	2.691
X	GTA	Phain_01772	Chromosome	phage conserved hypothetical protein BR0599	0.67	0.11	0.00	3.602
S	GTA	Phain_01773	Chromosome	TIGR02217 family protein	1.25	0.62	0.48	3.009
X	GTA	Phain_01774	Chromosome	phage tail tape measure protein, lambda family	1.22	0.39	0.37	3.171
X	GTA	Phain_01775	Chromosome	phage conserved hypothetical protein	0.91	0.13	0.02	3.137
X	GTA	Phain_01776	Chromosome	Phage tail tube protein, GTA-gp10	0.78	0.28	0.06	3.335
S	GTA	Phain_01777	Chromosome	phage major tail protein, TP901-1 family	1.09	0.48	0.28	3.520
S	GTA	Phain_01778	Chromosome	Protein of unknown function (DUF3168)	1.10	0.29	0.07	1.995
X	GTA	Phain_01779	Chromosome	head-tail adaptor	0.96	0.06	0.00	2.446
X	GTA	Phain_01780	Chromosome	phage conserved hypothetical protein, phiE125 gp8 family	1.47	0.14	-0.02	3.599
X	GTA	Phain_01781	Chromosome	phage major capsid protein, HK97 family	1.29	0.48	0.22	5.530
X	GTA	Phain_01782	Chromosome	hypothetical protein	1.23	-0.03	-0.31	3.892
S	GTA	Phain_01783	Chromosome	hypothetical protein	0.89	0.21	-0.11	1.646
X	GTA	Phain_01784	Chromosome	phage portal protein, HK97 family	1.00	0.25	-0.19	3.966
X	GTA	Phain_01785	Chromosome	Large terminase phage packaging protein	1.33	0.22	0.18	3.865
S	GTA	Phain_01786	Chromosome	hypothetical protein	1.16	0.13	0.13	0.663
Q	hemolysin	Phain_00693	Chromosome	Ca2+-binding protein, RTX toxin-related	0.94	0.18	0.15	5.550
Q	hemolysin	Phain_01804	Chromosome	Hemolysin-type calcium-binding repeat-containing protein	1.44	0.28	-0.03	6.577
Q	hemolysin	Phain_02476	Chromosome	Ca2+-binding protein, RTX toxin-related /hemolysin (PGA1_c26140)	-2.84	-0.01	-0.22	9.215
Q	hemolysin	Phain_02947	Chromosome	Ca2+-binding protein, RTX toxin-related	1.30	0.53	0.31	5.645
V	hemolysin	Phain_03966	69kb	type I secretion C-terminal target domain (VC_A0849 subclass)	1.66	0.75	0.49	4.332
Q	hemolysin	Phain_03967	69kb	serralysin	1.00	0.54	-0.08	7.987
Q	hemolysin	Phain_03564	Chromosome	Hemolysin-type calcium-binding repeat-containing protein	1.28	0.62	0.13	6.483
Q	T1SS	Phain_03988	69kb	regulatory protein, luxR family	3.48	-0.65	-0.95	5.668
Q	T1SS	Phain_03989	69kb	hypothetical protein	3.46	-0.83	-1.05	5.068

	hemolysin/T								
Q	1SS	Phain_03990	69kb	Hemolysin-type calcium-binding repeat-containing protein	3.95	-0.51	-0.46	9.087	
Q	T1SS	Phain_03991	69kb	type I secretion system ABC transporter, PrtD family	2.76	-0.76	-0.59	6.963	
V	T1SS	Phain_03992	69kb	membrane fusion protein, epimerase transport system	1.81	-0.26	-0.19	6.943	
M	paa	Phain_03669	227kb	Nucleoside-diphosphate-sugar epimerase	-1.93	0.69	-0.08	8.550	
Q	paa	Phain_03670	227kb	paaZ oxepin-CoA hydrolase / 3-oxo-5,6-dehydrosuberyl-CoA semialdehyde dehydrogenase	-2.06	0.75	-0.10	11.781	
Q	tda	Phain_03671	227kb	tdaF phosphopantothenoilcysteine decarboxylase / phosphopantothenate--cysteine ligase	-1.77	0.64	-0.08	10.418	
S	paa	Phain_03672	227kb	hypothetical protein	-1.36	0.30	0.07	5.231	
S	paa	Phain_03673	227kb	hypothetical protein	-1.71	0.34	-0.39	9.046	
S	paa	Phain_03674	227kb	hypothetical protein	-1.90	0.59	-0.12	11.735	
G	paa	Phain_03675	227kb	Di- and tricarboxylate transporter	-2.75	0.69	-0.09	8.518	
P	tdaR3	Phain_03681	227kb	cation transport protein ChaC (tdaR3)	-0.57	0.69	0.28	11.035	
A	tdaR2	Phain_03682	227kb	Peptidase family M23 (tdaR2)	-0.72	0.72	0.24	11.712	
S	tdaR1	Phain_03683	227kb	hypothetical protein (tdaR1)	-0.86	0.71	0.09	11.138	
I	tda	Phain_03684	227kb	Acyl-CoA dehydrogenase (tdaE)	-0.96	0.88	-0.12	12.572	
I	tda	Phain_03685	227kb	acyl-CoA thioester hydrolase (tdaD)	-1.36	0.99	-0.08	10.968	
S	tda	Phain_03686	227kb	hypothetical protein / prephenate dehydratase (tdaC)	-2.26	0.73	-0.11	10.291	
O	tda	Phain_03687	227kb	Glutathione S-transferase / beta-aryl ether-cleaving enzyme (tdaB)	-1.01	0.83	-0.09	7.287	
X	Prophage	Phain_00612	Chromosome	hypothetical protein	-1.11	-0.67	-4.48	0.058	
X	Prophage	Phain_00613	Chromosome	hypothetical protein	-0.52	-0.07	-3.84	-0.198	
X	Prophage	Phain_00614	Chromosome	hypothetical protein	-0.30	-0.05	-3.42	-0.479	
X	Prophage	Phain_00615	Chromosome	hypothetical protein	0.41	0.36	-3.94	0.246	
L	Prophage	Phain_00616	Chromosome	DNA polymerase-3 subunit beta	0.17	-0.09	-5.82	1.733	
X	Prophage	Phain_00617	Chromosome	hypothetical protein	0.15	-0.47	-2.58	-1.056	
X	Prophage	Phain_00618	Chromosome	hypothetical protein	0.43	-0.70	-4.25	0.259	
X	Prophage	Phain_00619	Chromosome	hypothetical protein	0.93	0.00	-4.20	0.552	
X	Prophage	Phain_00620	Chromosome	hypothetical protein	-0.10	-0.30	-7.38	3.105	
T	Prophage	Phain_00621	Chromosome	N-acyl-L-homoserine lactone synthetase	-0.08	-0.22	-6.88	2.631	
X	Prophage	Phain_00622	Chromosome	Autoinducer binding domain-containing protein	0.34	0.14	-7.50	4.478	
X	Prophage	Phain_00623	Chromosome	hypothetical protein	0.01	0.03	-7.64	3.482	
X	Prophage	Phain_00624	Chromosome	hypothetical protein	-0.29	0.35	-1.87	-1.411	
X	Prophage	Phain_00625	Chromosome	hypothetical protein	0.35	-1.14	-1.87	-1.514	
X	Prophage	Phain_00626	Chromosome	hypothetical protein	0.11	0.36	-3.06	-0.550	
X	Prophage	Phain_00627	Chromosome	hypothetical protein	-0.09	-0.25	-5.24	1.063	
X	Prophage	Phain_00628	Chromosome	hypothetical protein	-0.79	-0.66	-2.66	-1.233	
X	Prophage	Phain_00629	Chromosome	Uncharacterized conserved protein, UPF0335 family	0.02	-0.07	-5.31	1.216	
X	Prophage	Phain_00630	Chromosome	Protein of unknown function (DUF1064)	0.35	-0.26	-4.91	0.906	
X	Prophage	Phain_00631	Chromosome	hypothetical protein	0.34	0.06	-4.03	0.207	
X	Prophage	Phain_00632	Chromosome	hypothetical protein	-0.42	0.14	-2.74	-0.940	
JO	Prophage	Phain_00633	Chromosome	Protein N-acetyltransferase, RimJ/RimL family	0.74	-0.02	-4.98	1.184	

X	Prophage	Phain_00634	Chromosome	hypothetical protein	0.32	-0.17	-7.31	4.403
L	Prophage	Phain_00635	Chromosome	Superfamily I DNA and RNA helicases	0.20	-0.12	-8.98	6.564
X	Prophage	Phain_00636	Chromosome	hypothetical protein	0.21	-0.94	-4.64	0.469
M	Prophage	Phain_00637	Chromosome	Phage-related lysozyme (muramidase), GH24 family	0.45	-0.19	-4.92	0.969
X	Prophage	Phain_00638	Chromosome	hypothetical protein	0.44	0.08	-3.50	-0.192
X	Prophage	Phain_00639	Chromosome	Phage DNA packaging protein, Nu1 subunit of terminase	0.65	0.28	-3.94	0.297
X	Prophage	Phain_00640	Chromosome	Phage terminase, large subunit GpA	0.35	-0.25	-6.09	2.408
X	Prophage	Phain_00641	Chromosome	hypothetical protein	0.58	-0.51	-4.17	0.278
X	Prophage	Phain_00642	Chromosome	phage portal protein, lambda family phage prohead protease, HK97 family/phage major capsid protein, HK97 family, TIGR01554	0.54	-0.19	-4.58	1.075
X	Prophage	Phain_00643	Chromosome	hypothetical protein	0.13	-0.32	-5.64	1.489
X	Prophage	Phain_00644	Chromosome	hypothetical protein	-0.23	-0.03	-5.09	0.957
X	Prophage	Phain_00645	Chromosome	ATP-binding sugar transporter	-0.50	-0.58	-5.10	0.740
X	Prophage	Phain_00646	Chromosome	hypothetical protein	0.30	-0.46	-4.92	0.850
X	Prophage	Phain_00647	Chromosome	hypothetical protein	0.39	0.00	-5.81	1.826
X	Prophage	Phain_00648	Chromosome	phage baseplate assembly protein V	0.54	0.14	-5.80	1.917
X	Prophage	Phain_00649	Chromosome	hypothetical protein	0.66	-0.19	-6.29	2.330
X	Prophage	Phain_00650	Chromosome	Phage-related baseplate assembly protein	0.12	-0.10	-6.90	2.758
X	Prophage	Phain_00651	Chromosome	phage tail protein, P2 protein I family	-0.06	-0.58	-5.43	1.164
X	Prophage	Phain_00652	Chromosome	Phage tail-collar fibre protein	-0.63	-0.81	-5.09	0.644
X	Prophage	Phain_00653	Chromosome	hypothetical protein	-0.24	-0.12	-3.12	-0.711
X	Prophage	Phain_00654	Chromosome	hypothetical protein	0.08	-0.43	-6.58	2.343
X	Prophage	Phain_00655	Chromosome	hypothetical protein	-0.13	-0.64	-4.97	1.089
X	Prophage	Phain_00656	Chromosome	hypothetical protein	-0.18	-0.22	-5.85	1.624
X	Prophage	Phain_00657	Chromosome	hypothetical protein	-0.37	-0.55	-3.87	-0.263
X	Prophage	Phain_00658	Chromosome	Phage tail assembly chaperone protein, E, or 41 or 14	0.14	0.04	-3.25	-0.149
X	Prophage	Phain_00659	Chromosome	Phage-related protein	0.15	-0.42	-7.62	3.375
X	Prophage	Phain_00660	Chromosome	hypothetical protein	0.17	-0.91	-3.42	-0.545
X	Prophage	Phain_00661	Chromosome	P2-like prophage tail protein X	-0.28	-0.16	-3.22	-0.659
X	Prophage	Phain_00662	Chromosome	hypothetical protein	-0.33	-0.51	-5.86	1.891
XL	Prophage	Phain_00663	Chromosome	Integrase	0.51	0.08	-8.99	5.428
X	Phage- related	Phain_01181	Chromosome	hypothetical protein	-0.77	-0.14	2.33	3.717
X	Phage- related	Phain_01180	Chromosome	phage shock protein A (PspA) family protein	-0.18	-0.15	1.85	4.507

Table S2 with the complete transcriptomic data including 3977 genes for the *Phaeobacter inhibens* T5 mutants can be found in the digital supplementary material attached to the printed version of this dissertation.

Table S3: Strains and plasmids used in this study. Amp^r, ampicillin resistance; Km^r, kanamycin resistance; Gm^r, gentamicin resistance. In bold and underlined are the respective restriction sites for the specified enzymes. DSMZ, German Collection of Microorganisms and Cell Cultures, Braunschweig, Germany.

Strain/plasmid	Relevant genotype, phenotype and/or characteristics	Source
Strains		
<i>Phaeobacter inhibens</i>		
T5	Wild-type strain	DSMZ
<i>phin1::Km</i>	T5 <i>phin1::Km</i> ; Km ^r	This study
<i>phin3::Km</i>	T5 <i>phin3::Km</i> ; Km ^r	This study
<i>Escherichia coli</i>		
DH5α	F ⁻ endA1 glnV44 thi-1 recA1 relA1 gyrA96 deoR nupG φ80dlacZΔM15 Δ(lacZYA-argF)U169 hsdR17(rK ⁻ m _K ⁺) λ ⁻	(Hanahan 1983)
ST18	Δ <i>hemA</i> (defective in tetrapyrrole biosynthesis). Needs 5-aminolevulinic acid to grow	DSMZ (22074)
Plasmids		
pBBR1MCS-2	Broad-host-range vector; Source of kanamycin resistance cassette; Km ^r	(Kovach et al. 1995)
pBBR1MCS-5	Broad-host-range vector; Source of gentamicin resistance cassette; Gm ^r	(Kovach et al. 1995)
pEX18Ap (AF004910)	Cloning vector; Amp ^r	(Hoang et al. 1998)
pEX18 <i>phin1</i>	PCR product <i>phin1</i> f <i>phin1</i> r cloned into EcoICRI site of pEX18Ap; Amp ^r	This study
pEX18 <i>phin1</i> Km	PCR product Km BspEI f Km BspEI r cloned into BspEI site of pEX18Ap <i>phin1</i> ; Amp ^r Km ^r	This study
pEX18 <i>phin2</i>	PCR product <i>phin2</i> f <i>phin2</i> r cloned into EcoICRI site of pEX18Ap; Amp ^r	This study
pEX18 <i>phin2</i> Gm*	PCR product Gm MfeI f Gm MfeI r cloned into MfeI site of pEX18Ap <i>phin2</i> ; Amp ^r Gm ^r	This study
pEX18 <i>phin3</i>	PCR product <i>phin3</i> f <i>phin3</i> r cloned into EcoICRI site of pEX18Ap; Amp ^r	This study
pEX18 <i>phin3</i> Km	PCR product Km KasI f Km KasI r cloned into KasI site of pEX18Ap <i>phin3</i> ; Amp ^r Km ^r	This study

Table S4: Primer used for mutant construction in this study

Primer	Name	Sequence (5' - 3')
	phin1 f	TAT GTC CGT TCT TGT TCA GG
	phin1 r	CGT TTC TTG CGG TGT TTC AT
	phin2 f	GCG ATG AGC CAT GAA ATT CG
	phin2 r	TGA TGA TCA TCG ACA ATG GC
	phin3 f	TTG TAG GGG CAG TCA GG
	phin3 r	GTC TCA TTA TCG CCC TTT GC
	Km BspEI F	GTA <u>CCT CCG GAT</u> AGC TGT TTC C
	Km BspEI r	GTA <u>CAT CCG GAT</u> CAG CTA CTG G
	Gm MfeI f	TAC <u>CAA TTG</u> AAC GGA TGA AGG
	Gm MfeI r	TAC <u>CAA TTG</u> GAC AAT TTA CCG
	Km KasI f	GTA <u>CGG CGC CTA</u> GCT GTT TCC
	Km KasI r	GTA <u>CGG CGC CTC</u> AGC TAC TGG
	Test phin1 f	ACA ATC TGA CCT TCG ATG TGC
	Test phin1 r	TCA GGC TTT TCA ATC TTC ACG
	Test phin2 f	CAT TCT CTT GCT GGG AGC
	Test phin2 r	GGA AAT CGC CCC TAT CCT
	Test phin3 f	CAT TGA AAC GGG GCT TCT GG
	Test phin3 r	TGC CCT CAA TCC ACT TCA CC

Homoserine Lactones, Methyl Oligohydroxybutyrates, and Other Extracellular Metabolites of Macroalgae-Associated Bacteria of the *Roseobacter* Clade: Identification and Functions

Lisa Ziesche,^[a] Hilke Bruns,^[a] Marco Dogs,^[b] Laura Wolter,^[b] Florian Mann,^[a] Irene Wagner-Döbler,^[c] Thorsten Brinkhoff,^[b] and Stefan Schulz^{*,[a]}

Twenty-four strains of marine *Roseobacter* clade bacteria were isolated from macroalgae and investigated for the production of quorum-sensing autoinducers, *N*-acylhomoserine lactones (AHLs). GC/MS analysis of the extracellular metabolites allowed us to evaluate the release of other small molecules as well. Nineteen strains produced AHLs, ranging from 3-OH-C10:0-HSL (homoserine lactone) to (2*E*,11*Z*)-C18:2-HSL, but no specific phylogenetic or ecological pattern of individual AHL occurrence was observed when cluster analysis was performed.

Other identified compounds included indole, tropone, methyl esters of oligomers of 3-hydroxybutyric acid, and various amides, such as *N*-9-hexadecenoylalanine methyl ester (9-C16:1-NAME), a structural analogue of AHLs. Several compounds were tested for their antibacterial and anti-algal activity on marine isolates likely to occur in the habitat of the macroalgae. Both AHLs and 9-C16:1-NAME showed high anti-algal activity against *Skeletonema costatum*, whereas their antibacterial activity was low.

Introduction

Bacteria of the Rhodobacteraceae, and especially of an intensively studied subgroup of this family, the *Roseobacter* clade (roseobacters), are important members of the marine microbial community. They occur in a wide variety of habitats and often constitute a large percentage of the bacterial community. How they can achieve this competitive success is unclear, but one aspect might be the extracellular metabolites they produce.^[1–3]

One microhabitat where roseobacters are frequently found is the surfaces of marine macroalgae.^[4] Macroalgae are under constant pressure of being overgrown by other organisms in the oceans; therefore, they need to have means to avoid hazardous formation of microorganismic settlement or biofilm formation.^[5] On macroalgae, roseobacters are implicated in symbiotic interactions with the host, such as production of vitamins^[6] or antibiotics^[2,7,8] that are potentially useful to inhibit growth of other micro- or macroorganisms (e.g., see ref. [5]). *Phaeobacter inhibens* 2.10 (former *Roseobacter* sp. 2.10) has been shown to be advantageous to its macroalgal host, *Ulva*

australis, by reducing growth of fouling microorganisms,^[9] probably promoted by the release of the antibiotic tropodithetic acid (**10**).

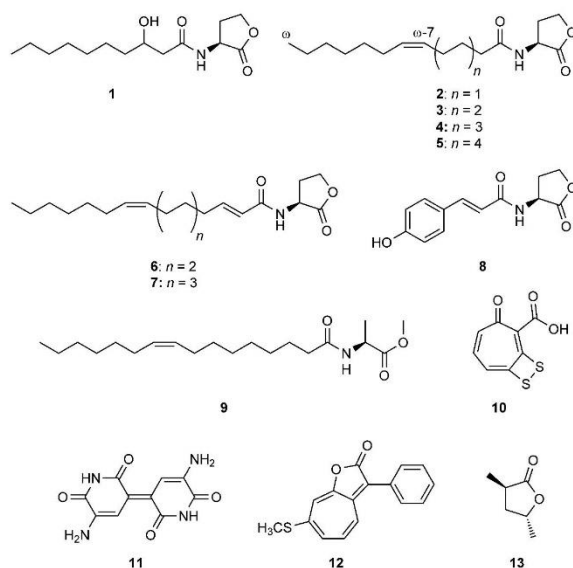
Roseobacters are well known for their production of *N*-acylhomoserine lactones (AHLs) that serve as quorum-sensing signals.^[10,11] Quorum sensing uses cell density to regulate several physiological traits of roseobacters, such as antibiotic production in *P. inhibens*,^[12] motility and biofilm formation in *Ruegeria* HLH11,^[13] and cell differentiation in *Dinoroseobacter shibae*.^[14] AHLs have been detected in many *Roseobacter* strains. In the 57 genomes of roseobacters published to date, 49 (87%) carry *luxI* homologues, a gene responsible for AHL biosynthesis.^[11] By using reporter strains, several studies have shown that *Roseobacter* strains from different habitats, like marine snow^[15] or marine sponges,^[16,17] produce AHLs. More specific chemical analysis led to the identification of *N*-3-hydroxydecanoylhomoserine lactone (3-OH-C10:0-HSL, **1**, Scheme 1) in *Phaeobacter* sp. 27-4.^[18] AHLs were also identified in 22 *Roseobacter* strains originating from dinoflagellate cultures (DFL), picoplankton (PIC), water column samples (HEL), laminaria surfaces (LM), and the hypersaline Ekho Lake in Antarctica (EL).^[19] The DFL strains of *D. shibae* (C18:1-HSL, C18:2-HSL) and *Roseovarius mucosus* (7-C14:1-HSL, C16:1-HSL, C18:1-HSL) contained long chain AHLs, whereas no AHLs were found in two *Sulfitobacter* strains, despite a positive sensor response. In strain *D. shibae* DFL 12, AHLs were identified as (11*Z*)-C18:1-HSL (**5**) and (2*E*,11*Z*)-C18:2-HSL (**7**).^[20] The eight EL strains of *Roseovarius tolerans* all produced C14:0-HSL and C14:1-HSL, and in some cases, 3-oxo-C14:1-HSL, C16:0-HSL, and C16:1-HSL. Three HEL strains of *Jannaschia helgolandensis* contained 7-C14:1-HSL (**3**), C16:1-HSL,

[a] L. Ziesche, H. Bruns, F. Mann, Prof. S. Schulz
Institute of Organic Chemistry, Technische Universität Braunschweig
Hagenring 30, 38106 Braunschweig (Germany)
E-mail: stefan.schulz@tu-bs.de

[b] M. Dogs, L. Wolter, Prof. Dr. T. Brinkhoff
Institute for Chemistry and Biology of the Marine Environment
University of Oldenburg
Carl von Ossietzky Straße 9-11, 26111 Oldenburg (Germany)

[c] Prof. I. Wagner-Döbler
Helmholtz Centre for Infection Research
Inhoffenstraße 7, 38124 Braunschweig (Germany)

Supporting information for this article is available on the WWW under <http://dx.doi.org/10.1002/cbic.201500189>.



Scheme 1. *N*-Acylhomoserine lactones (AHLs, 1–8), *N*-acylalanine methyl esters (9, a NAME) and other bioactive compounds as the antibiotic tropodithietic acid (TDA, 10), indigoidine (11), an algicidal roseobactin (12), and an antialgal lactone (13), all produced by bacteria of the *Roseobacter* clade.

and (2*E*,9*Z*)-C16:2-HSL (6),^[21] whereas *Oceanibulbus indolifex* HEL 76 released only 9-C16:1-HSL (4). Another bacterium isolated from the surface of the macroalga *Laminaria*, *Staleyia gutiformis* LM 09, produced C16:0-HSL, C16:1-HSL, and C16:2-HSL. Six *Sulfitobacter* PIC strains showed no AHLs despite positive sensor response, similar to five *Ahrensia* (as *Hoflea*) DFL strains and two *D. shibae* DFL strains. The type strain *Roseobacter denitrificans* DSM 7001^T contained only C8:0-HSL, whereas *P. inhibens* T5 from other sources released R3-OH-C10:0-HSL (1)^[21] and C18:1-HSL. The odd-numbered AHLs—C13:0-HSL, C15:0-HSL, C15:1-HSL, and C15:2-HSL—were trace constituents accompanying, in some cases, the major AHLs.^[19] The unusual *p*-coumaroylhomoserine lactone **8** was produced by *Ruegeria* (*Silicibacter*) *pomeroyi* DSS-3 when *p*-coumaric acid was present, such as in degrading algal blooms.^[22] In *R. tolerans* EL 164, but not in other roseobacters, AHL **3** was accompanied by recently discovered *N*-acylalanine methyl esters (NAMEs), with the major compound being (*Z*)-*N*-hexadec-9-enoylalanine methyl ester (9, [9*Z*]-C16:1-NAME). Although structurally closely related to AHLs, NAMEs do not inhibit or stimulate AHL biosensors.^[23] In this work, we show that these compounds have antialgal properties.

Several other secondary metabolites are also released by roseobacters. These include the antibiotic tropodithietic acid (TDA, 10), produced by several *Phaeobacter* strains,^[7,2] *Ruegeria* (*Silicibacter*) *sp.*,^[24] *Ruegeria mobilis*,^[25] as well as *Pseudovibrio* strains isolated from macroalgae.^[26] *Phaeobacter* strains show

potential for suppressing pathogens in fish farming, likely through the action of 10.^[27] Indigoidine (11) is produced by *Phaeobacter* *sp.* strain Y4I and inhibits growth of other bacteria.^[28] Tropone (38) and related compounds have been identified in volatiles of *P. inhibens*.^[29] Tropone is a shunt product of TDA biosynthesis.^[29,30] In the presence of *p*-coumaric acid^[8] and also other cinnamic acid derivatives,^[31] roseobactins that inhibit algal growth (e.g., 12) are released by *Phaeobacter gallaeciensis* BS107. The bacterium thus switches from a mutualistic symbiotic lifestyle to a parasitic one during algal blooms.^[8] Several diketopiperazines and indole derivatives have been reported from *O. indolifex* HEL-45^T^[32] but some of these seem to be derived from the medium.^[21] Various roseobacters also release volatiles, often containing sulfur compounds, derived from algal dimethylsulfoniopropionate (DMSP)^[33] as well as other compounds, such as lactones and pyrazines.^[34] Some of the latter (e.g., lactone 13, produced by *R. pomeroyi*) showed inhibitory effects at high concentrations against freshwater algae.^[35] Compared to the Actinobacteria or Cyanobacteria, the number of known secondary metabolites is quite small for the *Roseobacter* clade, but certainly not fully explored yet.^[36] Roseobacters seem to lack the large genetic diversity of biosynthetic genes for secondary metabolite production found in those groups. Nevertheless, the compounds discussed so far play important roles in the ecology of roseobacters (Scheme 1).

In our ongoing studies of the ecology of the roseobacters, we became interested in their mutualistic interactions with macroalgae mediated by secondary metabolites. In the current work, we investigated whether AHLs of roseobacters growing on macroalgae surfaces have a similar structure or whether their structural diversity is independent of the ecological niche they inhabit.

The GC/MS method used also allowed the identification of other small secondary metabolites released by the roseobacters. Several compounds not previously known from roseobacters were identified as AHLs, amides, and 3-hydroxybutyrate oligomers. Some of the identified and synthesized compounds were tested for antibacterial and antialgal activity on marine microorganisms likely to occur in the natural habitat of the algae-associated roseobacters. Interestingly, especially strong antialgal activity against the diatom *Skeletonema costatum* CCMP 1332 was observed for AHLs and NAMEs.

Results

Of the 26 Rhodobacteraceae strains analyzed in this work, 25 were obtained from the surface of macroalgae of the genera *Bifurcaria*, *Cystoseira*, *Enteromorpha*, *Fucus*, *Gracilaria*, *Sargassum*, and *Ulva* (Table 1). The exception was *P. gallaeciensis* CIP 105210, which was previously isolated from the scallop *Pecten maximus*.^[37] The phylogenetic relationships of the bacterial strains were analyzed based on their 16S rRNA gene

Table 1. New bacterial isolates, their closest described relatives, the respective similarity of their 16S rRNA genes, and the marine macroalgae from which the new strains were obtained.

Strain	Closest described relative	16S rRNA gene similarity (%)	Strain origin/host	3-OH-C1000-HSL	3-OH-C121-HSL	3-Ox-C160-HSL	C14:1-HSL	C14:2-HSL	C16:1-HSL	C16:2-HSL	3-Ox-C16:0-HSL	C17:1-HSL	C18:1-HSL	2,11-C18:2-HSL
B3	<i>Jannaschia donghaensis</i> DSW-17	98	<i>Fucus spiralis</i> ^(a)											
F4	<i>J. helgolandensis</i> Hel 10	99	<i>Gracilaria verrucosa</i> ^(a)											
E6	<i>J. helgolandensis</i> Hel 10	97	<i>Enteromorpha</i> sp. ^(b)											
F3	<i>Litoreaibacter albidus</i> JCM 16493	100	<i>F. spiralis</i> ^(a)											
II 4.36	<i>L. koreensis</i> GA2-M3	96	<i>Cystoseira baccata</i> ^(b)	xxx (5)										
A2	<i>Loktanella salsilacus</i> CIP 108322	98	<i>Ulva lactuca</i> ^(a)											
F13	<i>L. salsilacus</i> CIP 108322	100	<i>F. spiralis</i> ^(a)											
F14	<i>L. salsilacus</i> CIP 108322	99	<i>Enteromorpha</i> sp. ^(b)	xx										
IV 6.39	<i>Loktanella tamilensis</i> SSW-35	99	<i>Cystoseira baccata</i> ^(b)				x	xx (7)						
I 8.24	<i>L. tamilensis</i> SSW-35	99	<i>Sargassum muticum</i> ^(b)				x	xxx (7)						
E8	<i>Octadecabacter antarcticus</i> 307	97	<i>F. spiralis</i> ^(a)	xx (5)										
C13	<i>Paracoccus zeaxanthinifaciens</i> R-1512	98	<i>F. spiralis</i> ^(a)					xxx (9)						
I 8.25	<i>P. gallaeciensis</i> BS107	98	<i>Sargassum muticum</i> ^(b)				x							
I 8.30	<i>Roseovarius aestuarii</i> SMK-122	99	<i>Sargassum muticum</i> ^(b)				x	xxx (7)						
III 2.4	<i>R. aestuarii</i> SMK-122	98	<i>Bifurcaria bifurcata</i> ^(a)				x	xxx (7)						
D12-1	<i>Roseovarius lutimaris</i> 112	99	<i>F. spiralis</i> ^(a)											
I 8.10	<i>Ruegeria atlantica</i> 1480	99	<i>Fucus vesiculosus</i> ^(b)					xx (9)						
I 9.31	<i>R. atlantica</i> 1480	99	<i>Gracilaria multipartita</i> ^(b)					xxx (7)						
IV 8.38	<i>Ruegeria scottomalliae</i> CCIUG 55858	98	<i>Cystoseira baccata</i> ^(b)											
E4-1	<i>Sulfitobacter dubius</i> ATCC BAA-320	99	<i>U. lactuca</i> ^(a)											
B2-1	<i>Sulfitobacter guttiformis</i> EL-38	99	<i>Gracilaria verrucosa</i> ^(a)											
B13	<i>Sulfitobacter mediterraneus</i> CH-B427	99	<i>F. spiralis</i> ^(a)											
D17	<i>S. mediterraneus</i> CH-B427	97	<i>F. spiralis</i> ^(a)											
E4-2.2	<i>S. mediterraneus</i> CH-B427	98	<i>F. spiralis</i> ^(a)											

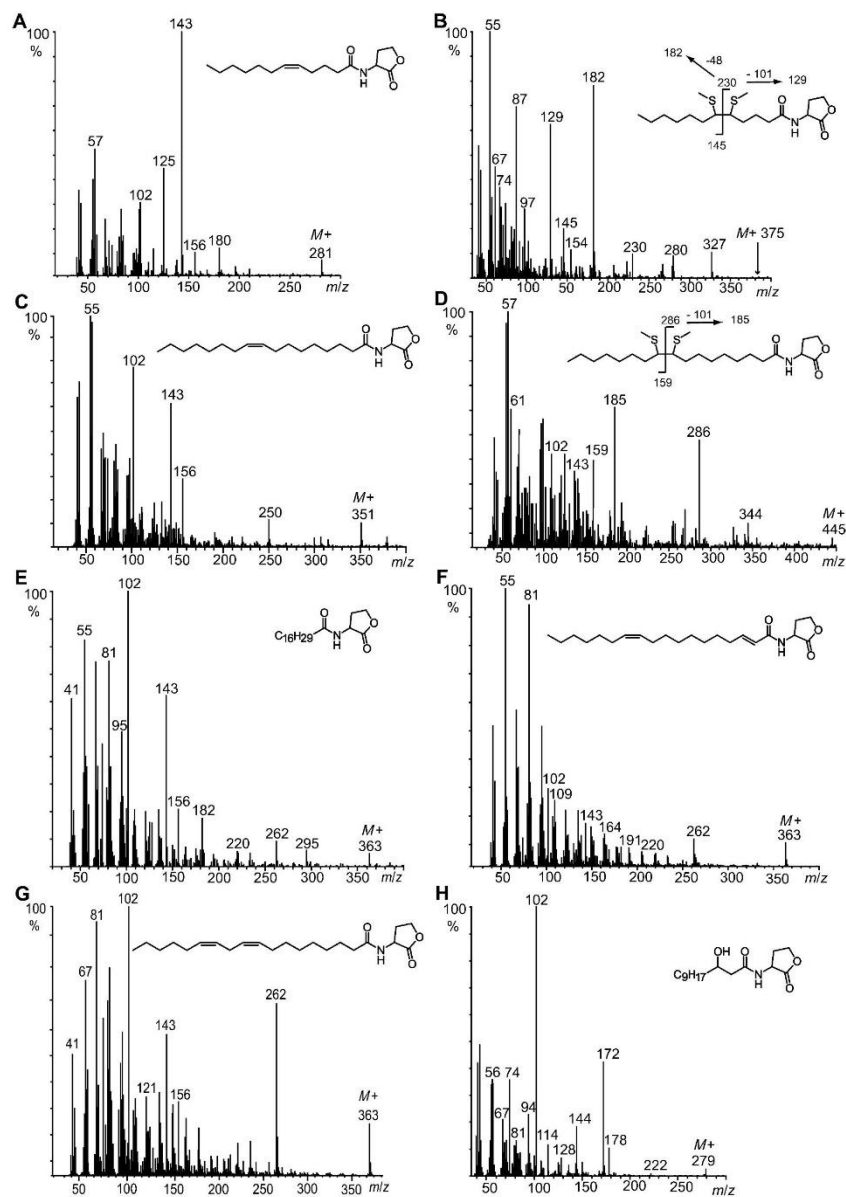


Figure 1. Mass spectra of various *N*-acylhomoserine lactones and their respective dimethyl disulfide adducts for the determination of double bond positions. A) 5-C12:1-HSL; B) DMDS adduct of 5-C12:1-HSL; C) 9-C17:1-HSL; D) DMDS adduct of 9-C17:1-HSL; E) C18:2-HSL; F) (2*E*,11*Z*)-C18:2-HSL; G) (9*Z*,12*Z*)-C18:2-HSL; H) 3-OH-C12:1-HSL.

sequences and are depicted in Figure S1 in the Supporting Information. Only one of the new isolates, *Paracoccus* sp. C13, did not belong to the *Roseobacter* clade. The majority of the strains were affiliated with the genera *Loktanella* (six strains),

Sulfitobacter (four strains), *Jannaschia* (three strains), and *Roseovarius* (three strains; Figure S1). As no clear affiliations to validated genera were found for the two strains E13 and D17, these organisms might be representatives of new genera.

All strains were grown as liquid culture in marine broth medium MB 2216. As we have described earlier, AHLs can be obtained from the liquid phase by extraction with pre-cleaned XAD-16 resin and can then be identified by GC/MS.^[19,20] These extracts usually contain large amounts of medium constituents, such as diketopiperazines that were initially present in the medium or were formed during the autoclaving process. Nevertheless, careful analysis of the extracts by GC/MS revealed the presence of several other components besides AHL produced by the bacteria. Although the extracts could be separated further into different fractions that could be analyzed independently, this would introduce inevitably more impurities and probably discrimination against or in favor of certain compounds. Therefore, we opted to try to analyze as many compounds as possible from the original extract obtained after XAD treatment. The analysis by GC/MS was, in this case, favorable compared to HPLC/MS methods because of the higher sensitivity, more informative mass spectra, and easier identification procedure of the former method. The results will be discussed in detail below in three parts.

N-Acylhomoserine lactones

AHLs were identified according to our published GC/MS procedure.^[19–21] Liquid culture contained XAD-16 resin that was extracted for analysis. In 19 of the 26 strains, AHLs were detected, carrying saturated, unsaturated, or sometimes oxygenated acyl chains ranging from C₁₀ to C₁₈ (Table 1).

Major compounds from many strains were monounsaturated AHLs; saturated AHLs occurred only as minor additional compounds. When the quantity of an unsaturated AHL in an extract was sufficiently large, the position of the double bond was determined by addition of dimethyl disulfide (DMDS) to the extract and analysis by GC/MS as reported previously.^[19–21] In four strains, 12:1-HSL was detected. The ions *m/z* 145 and 230 of the DMDS derivative and the subsequent fragments obtained by loss of CH₂SH (*m/z* 97, 182) or the HSL ring (*m/z* 129) indicated that the double bond was located at C-5 (Figure 1), presumably in *Z* configuration. All known unsaturated AHLs with a mid-chain double bond, as well as the majority of their respective precursor fatty acids, have this configuration.^[38] The most widespread AHL was tetradecenylhomoserine lactone (14:1-HSL), which was present in seven strains and usually accompanied by smaller amounts of the saturated analogue, 14:0-HSL. DMDS analysis revealed that these strains produced *N*-7-tetradecenylhomoserine lactone (7-14:1-HSL). Four strains produced 16:1-HSL, in which in three cases, the position of the double bond was located at C-9. This double bond position was also found in 9-17:1-HSL of strain E13, deduced from the characteristic ions of the DMDS derivative at *m/z* 286, 185, and 131 (Figure 1). The compound showed an unbranched chain, as can be seen from its GC retention index (*I*) of 2876, in congruence with those of 7-C16:1-HSL (*I* = 2769) and 9-C18:1-HSL (*I* = 2965).^[21] Five strains released C18:1-HSL. The double bond positions could not be determined because of the low quantities of compound present. *Phaeobacter* 18.25 produced (2*E*,11*Z*)-18:2-HSL (7), the major AHL of *D. shibae*,^[20] accompa-

nied by minor amounts of two C18:2-HSL isomers. Their shorter GC retention times and the higher intensities of the ions *m/z* 102 and 143 compared to those of (2*E*,11*Z*)-18:2-HSL indicated that these C18:2 HSL isomers contained two non-conjugated double bonds in their chains. A model compound, (9*Z*,12*Z*)-C18:2-HSL, synthesized from commercially available linoleic acid, showed a similar mass spectrum (Figure 1) and a similar retention index, confirming our assumptions. Determination of the double bond locations in the two minor C18:2-HSLs was not possible because of the low amounts produced. Structures like 8,11-C18:2-HSL and/or 11,14-C18:2-HSL seem likely because of their similarity to the known monounsaturated HSL, but confirmation awaits synthetic proof.

Few oxygenated HSLs were present, such as 3-OH-C10:0-HSL, which occurred in three strains, and 3-oxo-C16:0-HSL in

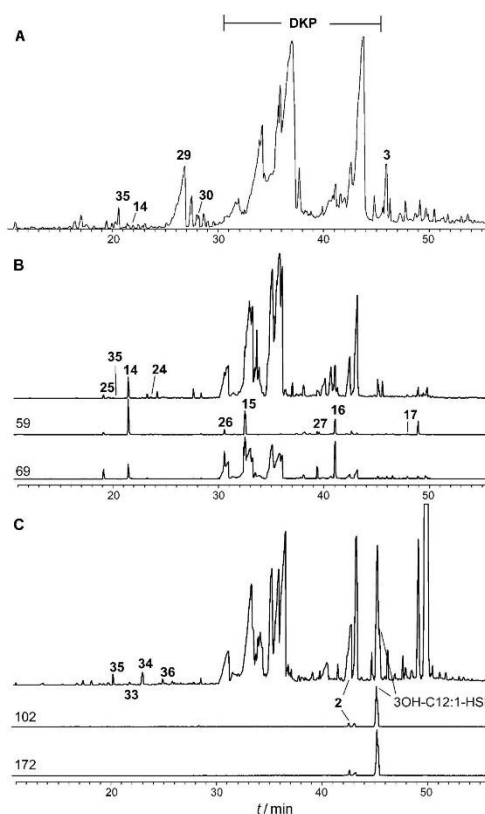


Figure 2. Total ion chromatograms (GC/MS) of A) *Roseovarius* sp. III 2.4. DKP: region of elution of diketopiperazines originating from the medium. B) *Loktanelia* sp. F13. Ion traces *m/z* 59 and 69 were used to locate PHB oligomers. C) *Loktanelia* sp. F14. Ion traces *m/z* 102 and 172 are characteristic for 3-hydroxyalkanoly-HSL. Peaks not assigned are compounds originating from the medium or are contaminants.

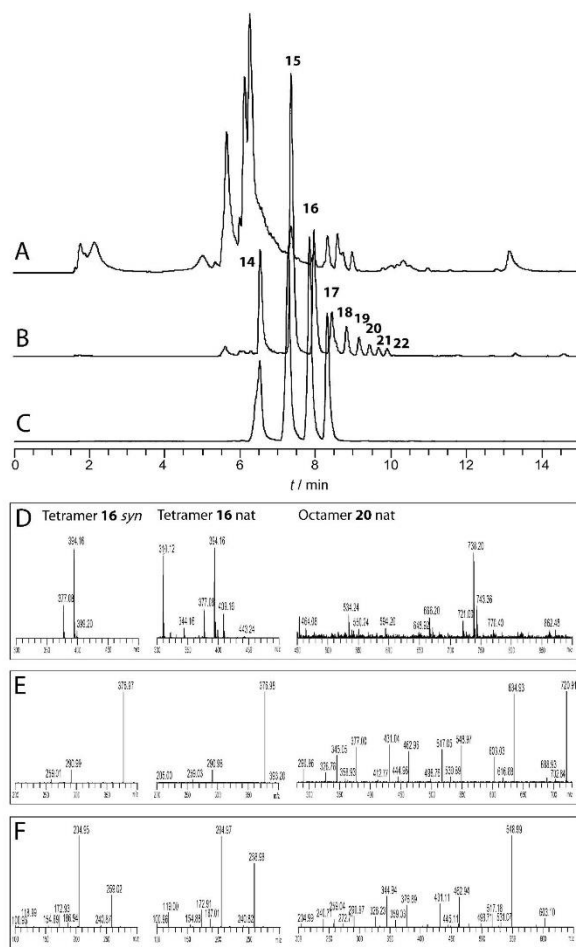


Figure 3. ESI-HPLC/MS/MS analysis of an extract of *Jannaschia* sp. E6. A) TIC of natural extract; B) trace of the $[M+NH_4]^+$ ions of the oligomers 14–23; C) trace of the $[M+NH_4]^+$ ions of synthetic compounds 14–17; D) ESI-MS² of natural tetramer 16, synthetic tetramer 16, and natural oligomer 19; E) ESI-MS² of the $[M+NH_4]^+$ ions; F) ESI-MS³ of the m/z 259 or m/z 635 ions.

Phaeobacter sp. 18.25. *Loktanella* sp. F14 produced 3-OH-C12:1-HSL. Its mass spectrum (Figure 1) showed the characteristic fragmentation of 3-hydroxyalkanoyl-HSL: ions m/z 74, 102, and 172. The small molecular ion at m/z 297 and the prominent ions m/z 279 (M-H₂O) and 178 (M-H₂O-HSL) indicated an additional double bond in the chain. Assuming the general rules found so far for the location and configuration of natural AHLs, this compound was tentatively identified as (Z)-N-3-hydroxydodec-5-enoylhomoserine lactone, a compound not reported previously from any other bacterium, because it carries

the double bond at position ω–7, as do almost all known monounsaturated AHLs.

Other compounds

Other extracellular metabolites can be analyzed by HPLC/MS or, with some restrictions, by GC/MS. Volatile non-polar compounds are preferably analyzed by headspace analytical methods, as reported earlier,^[29] but certain compounds, especially those with an N–H or O–H, are sometimes not detected because of their high water solubility.^[39] HPLC/MS is problematic for the analysis of low amounts of unknown metabolites because no machine-independent spectral databases exist, and structural information on the ESI spectra is scarce. We therefore chose to look into the data of the AHL GC/MS analyses to identify other metabolites produced by roseobacters and to evaluate their biological relevance. The advantage of this approach was high sensitivity and separation power, as well as the information-rich EI mass spectra. In contrast, a serious drawback was the large amount of diketopiperazines originating from the medium, which could not be avoided (Figure 2). Restrictions also applied for polar compounds that could not be analyzed and were not adsorbed on the XAD-16 resin. Nevertheless, various metabolites were detected in the analysis.

Closely related to AHLs is N-9-hexadecenoylaniline methyl ester (9-C16:1-NAME), produced by *Loktanella* sp. II 4.36 and *Roseovarius* sp. D12-1 (Table 1). The corresponding DMDS derivative^[23] revealed the location of the double bond at C-9. *Roseobacter* clade bacteria are also known to store poly-3-hydroxybutyrate (PHB). PHB was recently found in *Planktomarina temperata*,^[40] and the physiological pathway of PHB production was detected previously in some other organisms of the *Roseobacter* clade.^[32,41] In 12 extracts, oligomeric methyl esters of 3-hydroxybutyrate (14–17, Figure 3) were present and were especially abundant in *Loktanella* sp. F13 (Table 2, Scheme 2). Although the monomer was not found, methyl di-, tri-, tetra-, and penta(3-hydroxybutyrate) were detected. These compounds were occasionally accompanied by the terminal butenyl derivatives 25–27, formed by water elimination, and by pentanoate ester 24. The methyl ester function was not an artifact of the workup, because no methanol was used in the procedure. The identities of the products were confirmed by partial methanolysis of PHB.^[42] Higher oligomers than the pentamer were too large to be detected by GC/MS. Therefore, ESI-HPLC/MSⁿ analysis of *Jannaschia* sp. E6 and *Loktanella* sp. F13 was performed (Figure 3). All hydroxybutyrates identified by GC/MS could also be detected by this method. In addition, oligomers up to decamer 23 were detected by HPLC/MS/MS. Their identities were confirmed by the characteristic mass spectra of the oligomers. Under ESI conditions in positive

Table 2. Compounds identified in addition to AHLs in the various Rhodobacteraceae strains.

Strain	9	1	2	3	4	24	25	26	27	28	29	30	31	32	33	34	35	36	37	38	39	
I 8.30		x				x	x				xxx	xx	x				x					
I 9.31		xx				x	x				xxx						x					
IV 6.39		x									xxx	x	x				x					
I 8.25														x	x	xx	x	x	x			
III 2.4		x									xxx	x					x					
II 4.36	xx (9)	x															x			x		
I 8.10		x									xxx	x					x					
IV 8.38																	x					
I 8.24		x									xx	x					x					
CIP105210		x				x								x			x				xx	x
A2		x								x						x	x	x				
B13		x															x					
B2-1		x															x					
B3		x								x						xx	x	x				
C13																	x					
D17																x	x					
D12-1	xx (9)																					
E8																x	x			x		
E4-1		x				x										x	x					
E6		xx	x	x	x	x	x	x									x	x				
E4-2.2														x			x					x
E13														x		x	x			x		
F13		xx	xx	x	x	x	x	x	x								x					
F4																						
F14										x					x	x	x	x				
F3		x								x						x	xxx	x				

Strain assignments can be found in Table 1. Relative amounts are given: xxx: intensity > 20%, xx: 1–20%, X: < 1% of highest peak in the total ion chromatogram. (9): double bond at C-9.

mode, intense $[M+NH_4]^+$ ions were formed. The MS/MS fragmentation of these adducts showed characteristic mass spectra as shown in Figure 3, allowing unambiguous identification. Oligomers **14–17** were identified by comparison of retention times and mass spectra for the synthetic and natural samples with fragmentation up to MS^3 . As shown for tetramer **C** with m/z 394 ($[M+NH_4]^+$), the first fragmentation furnished $[M+H]^+$ ion m/z 377 and ion m/z 291, corresponding to loss of NH_3 and ester bond cleavage, respectively. The m/z 291 ion was formed by loss of an oligomer unit (86 amu) from the hydroxy end of the tetramer. Upon further fragmentation (MS^3), m/z 291 lost one and two oligomer units (m/z 205 and 119), as well as methanol (m/z 259 and 173). The ions m/z 241, 187, 155, and 101 corresponded to loss of water from m/z 259, 205, 173, and 119. The retention times and mass spectra of the synthetic and natural samples of **14–17** were in very good accordance.

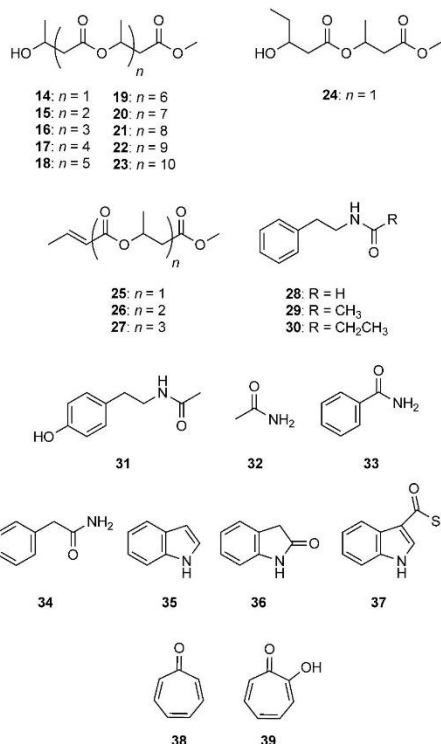
The larger oligomers **18–23** show mass spectra following the fragmentation pattern described (Figure 3). Octamer **20**, with m/z 738 ($[M+NH_4]^+$), formed $[M+H]^+$ at m/z 721 upon MS^2 . The ester cleavage ion series m/z 635, 549, 463, 377, and 291 was accompanied by a series with additional loss of methanol: m/z 689, 603, 517, 431, and 345. Most of these ions were accompanied by smaller ions (m/z 703, 617, 531, 499, 445, 413, 359, and 327), due to elimination of water. Further fragmentation of m/z 635 (MS^3) mostly yielded ions already described from MS^2 fragmentation, as well as m/z 205 and 291 and m/z 273 and 241, due to loss of water. Identical mass spectra were

obtained when the $[M+H]^+$ ions were used instead of the $[M+NH_4]^+$ ions.

The apparent question of whether free acids are also secreted by the bacteria remains to be answered. Although there were expected ions present in the HPLC/MS analysis in low intensity, they did not produce good spectra in MS/MS mode. Derivatization of the XAD extracts with $[D_2]$ diazomethane, obtained from $[D_3]$ methylamine,^[43,44] did not yield deuterated methyl esters. Therefore, the free acids were either not released or, because of their high content of free hydroxy and acid groups, were too polar to be adsorbed on the XAD resin used.

Another group of compounds frequently found were small amides (Table 2). Large amounts of *N*-(2-phenylethyl)acetamide (**29**) were produced by strains *Roseovarius* sp. I 8.30, *Ruegeria* sp. I 9.31 and I 8.10, *Loktanella* sp. IV 6.39 and I 8.24, and *Roseovarius* sp. III 2.4. The related homologues **28** and **30** occurred occasionally, as did *N*-(2-(4-hydroxyphenyl)ethyl)acetamide (**31**). Additionally, 2-phenylacetamide (**34**) was often produced, whereas acetamide (**32**) and benzamide (**33**) occurred more rarely.

Almost all strains produced indole (**35**), a known signaling compound in several bacteria.^{[45][46][47]} Large amounts were emitted especially by strain *Litoreibacter* sp. F3, which also contains the oxidized indolin-2-one (**36**), and *Phaeobacter* sp. I 8.25. *S*-Methyl 1*H*-indole-3-carbothioate (**37**) was identified earlier in *O. indolifex*, together with 1*H*-indole-3-carbalde-



Scheme 2. Compounds released by *Roseobacter* clade bacteria investigated in this study.

hyde.^[32] The latter compound was present in all strains investigated, but also in control samples of the medium without inoculation. Obviously, it was not produced by the roseobacters.

Tropone (**38**) and tropolone (**39**) are shunt products of TDA (**10**) biosynthesis,^[29,30] common to several strains of the *Roseobacter* clade.^[12,30] Besides the already known occurrence in *P. gallaeciensis* CIP 105210, tropone was also found in *Phaeobacter* sp. I 8.25 and *Loktanella koreensis* II 4.36.

Bioassay results

Some of the compounds produced by the roseobacters were tested for their inhibitory activity against marine microorganisms. Four marine bacterial strains belonging to different classes, *Pseudonocardiaceae* bacterium T4 (Actinobacteria), *Phyllobacteriaceae* bacterium TK (α -Proteobacteria), *Oceanospirillaceae* bacterium T17 (γ -Proteobacteria), and *Maribacter* sp. 62-1 (Flavobacteria), as well as the bloom-forming, coastal microalgae *S. costatum*, were tested in agar diffusion assays. The highly potent antibiotic TDA was used for comparison. The results are shown in Table 3. Most compounds did not show any antibacterial activity, with the exception of (9Z)-C16:1-NAME (**9**) and (7Z)-C14:1-HSL (**2**), which were active in the low nanomolar range against *Maribacter*. These two compounds also inhibited growth of the algae *S. costatum* at similar concentrations (Table 3). Low anti-algal activity was recorded for indole **35** and phenylethylacetamide **29**, as well as tropone **38**. The antibiotic TDA (**10**) was used as a reference compound and showed higher activity both against bacteria and against algae than did the other compounds tested.

Discussion

Several of the AHLs identified in this study have not been previously detected in roseobacters. These include 5-C12:1-HSL (**2**) and 3-OH-C12:1. The rare 9-C17:1-HSL of *Sulfitobacter* sp. D13 is, to the best of our knowledge, the first example of an AHL with an odd number of carbon atoms in the chain being the major AHL produced by a bacterium. *Phaeobacter* sp. I 8.25 is the first strain outside the genus *Dinoroseobacter* able to produce C18:2-HSL **7** and also produced the shortest known dienioic AHL, C14:2-HSL. Predominant AHLs used by roseobact-

Table 3. Agar diffusion assays with different bacteria and the algae *S. costatum*.

	Pseudonocardiaceae bacterium T4			Phyllobacteriaceae bacterium TK			Oceanospirillaceae bacterium T17			<i>Maribacter</i> sp. 62-1			<i>S. costatum</i> CCMP 1332			MIC nmol
	1 μ g	10 μ g	100 μ g	1 μ g	10 μ g	100 μ g	1 μ g	10 μ g	100 μ g	1 μ g	10 μ g	100 μ g	1 μ g	10 μ g	100 μ g	
(9Z)-C16:1-NAME (9)	0	0	0	0	0	0	0	0	0	0	1	2	0	2	6	2.9/8.7
2-phenylacetamide (34)	0	0	0	0	0	0	0	0	0	0	0	0	0	0	0	–
methyl di(3-hydroxybutyrate) (14)	0	0	0	0	0	0	0	0	0	0	0	0	0	0	0	–
indole (35)	0	0	0	0	0	0	0	0	0	0	0	0	0	0	1	>85
N-(2-phenylethyl)acetamide (29)	0	0	0	0	0	0	0	0	0	0	0	0	0	0	1	>61
N-(2-phenylethyl)formamide (28)	0	0	0	0	0	0	0	0	0	0	0	0	0	0	0	–
tropone (38)	0	0	0	0	0	0	0	0	0	0	0	0	0	0	2	>94
(7Z)-C14:1-AHL (3)	0	0	0	0	0	0	0	0	0	0	2	4	0	2	5	3.2/6.5
TDA (2 μ g, 10)	4			5			3–4			10			6–7			<0.5
solvent CH ₂ Cl ₂	0			0			0			0			0			–

The width of the inhibition zone after application of different amounts of a test substance is given in mm, and the minimal inhibitory concentration (MIC) was calculated from these data.

ers have a long, monounsaturated acyl chain. In almost all bacteria investigated thus far, the double bond is located at position $\omega-7$,^[38] regardless of the chain length. Although modifications include variations in chain length, addition or absence of a double bond, and oxidative modification at C-3, the overall structural diversity of the AHLs seems limited. For comparison, many more structural modifications are observed in signaling compounds of higher organisms, such as in the restricted group of type 1 lepidopteran sex pheromones, and lead to species-specific responses.^[48] In a bacterial community, it is likely that many different strains or species react to a specific AHL, although the physiological reactions can certainly be different.

We therefore asked whether macroalgal-associated *Roseobacter* bacteria show specific occurrence of certain AHLs, different from those of other sources. The data from Table 1 and

data we obtained previously from the analysis of roseobacters originating from a free water column, microalgae, the hypersaline Ekho Lake in Antarctica, and laminaria surfaces^[19] were used in a cluster analysis, based on the occurrence or absence of individual AHLs in the strains (Figure 4). Although strains that were phylogenetically very closely related clustered together, no clustering of macroalgae-associated strains was observed. It was also evident that very closely related strains use similar AHLs, as exemplified by *Dinoroseobacter*, *Jannaschia*, and *Roseovarius*. On the other hand, it could also be seen that, on the 16S gene level, very closely related strains could produce different AHLs. One such example is the *P. inhibens* strains T5 and DSM17395, which share 99% 16S gene identity, but strain T5 produces one additional AHL (C18:1-HSL) not detected in the other strain. Another example includes two isolates analyzed in this study, *Sulfitobacter* sp. E4-1 and E4-2.2, which share 99% identity on the 16S gene level but produce different AHLs (Table 1 and Figure 4). However,

clustering showed that phylogenetically diverse strains like *Ruegeria*, *Roseovarius*, and *Loktanella* (Figure S1) can use very similar AHLs. Picoplankton strains are less likely to produce AHLs, although only *Sulfitobacter* has been analyzed in detail.^[19]

In inhibition assays, we used bacteria and an alga, representing ecologically important groups potentially co-occurring on macroalgae together with roseobacters, to evaluate the functions of the identified compounds. AHL **3** was a major compound of many strains investigated here. Such widespread AHLs might be used in bacterial crosstalk between different roseobacters and other bacterial strains living on the same host. The antibacterial activity observed against *Maribacter* sp. 62-1 was not without precedence, as antibacterial effects of AHLs have been reported before, albeit not on marine bacteria.^[49] The antialgal activity against the dinoflagellate *S. costatum*, a coastal species occurring in algal blooms, might be of ecological relevance. *S. costatum* was used in this study due to the feasibility of inhibition tests with this organism and growth under axenic conditions to avoid indirect influence from associated bacteria. To investigate the ecological relevance of the antialgal activity in more detail, however, tests with biofilm-forming algae would be desirable. In a symbiotic relationship with their hosts, roseobacters might, for example, diminish attachment of detrimental microorganisms or resource competitors. TDA (**10**) showed higher activities compared to **3**, but its occurrence within the *Roseobacter* clade is much more restricted than that of AHLs. The antialgal activities of AHLs have not been reported before, and AHLs other than **3** will likely have similar effects. Roseobacters are reported to produce antialgal compounds, and the described roseobactericides inhibit growth of various microalgae.^[8,31] Although these inhibitory activities are exhibited by bacterial AHLs, microalgae as well as macroalgae are able to inhibit

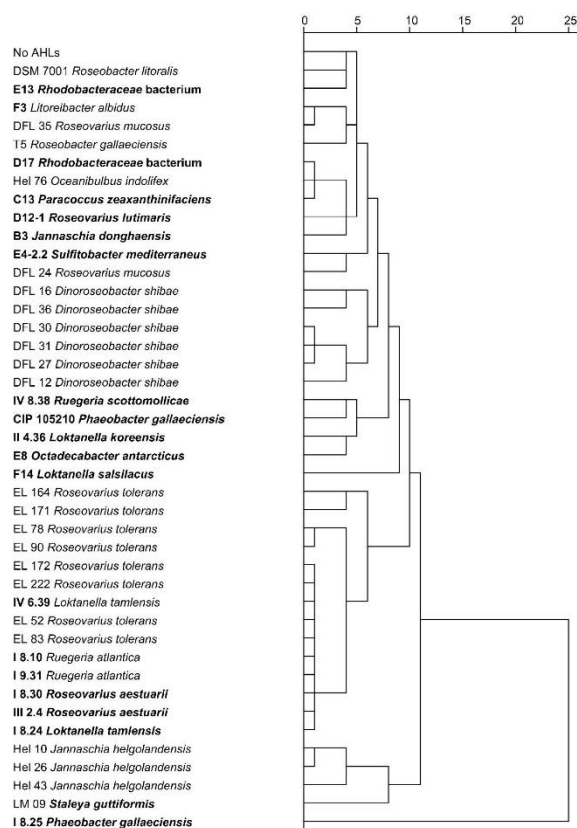


Figure 4. Hierarchical cluster analysis of the presence or absence of individual AHLs of different organisms of the *Roseobacter* clade. Data obtained in this work (bold) and in previous studies were considered.^[19,20] The origin of the other samples can be derived from their letter codes: dinoflagellate cultures (DFL), picoplankton (PIC), water column sample (HEL), laminaria surfaces (LM), hypersaline Ekho Lake in Antarctica (EL).

AHL synthesis in different ways. Quorum-sensing systems can be inhibited by destabilization of protein–ligand binding at the *LuxR* binding site, by interference from compounds mimicking bacterial signaling, or by deactivation of AHLs by degradation processes. Also, secondary metabolites produced by different plants and algae like *p*-coumaric acid, salicylic acid, and vanillin could act as quorum-sensing inhibitors.^[50]

The amide (9*Z*)-C16:1-NAME (**9**) is the major metabolite of the alanine amide esters produced by *R. tolerans* EL 164^[23] and several other *Roseovarius* strains (H. Bruns, S. Schulz, unpublished). Here, compound **9** was identified in *Roseovarius* sp. D12-1 but also for the first time in another genus, *Loktanella*, although there is no close phylogenetic association between the two genera (Figure S1). NAME **9** showed high antialgal and antimicrobial activity, similar to that of AHL **3**, but it was not active in quorum-sensing activation or suppression.^[23] NAMES could therefore be more widespread within the roseobacters than previously thought and might play a role in their algal associations. No biosynthetic genes for their production or perception are currently known.

Amides **28–31** have been reported from other bacteria.^[51,52] The major amide **29**, produced in large amounts by some roseobacters, showed weak antialgal activity. Antialgal activity of these amides against freshwater *Chlorella* algae have been reported before, but no antibacterial activity was observed, similar to our results.^[51,52] Phenylacetamide (**34**) has been reported from the sponge *Halicondria* and has antifungal activity.^[53]

The presence of tropone (**38**) can be regarded as indicator of TDA biosynthesis (see above). Although production of TDA has been proven for *P. gallaeciensis*, *Phaeobacter*, *Ruegeria*, and *Pseudovibrio*,^[3,27,54] it was not reported to occur in *Loktanella* or *Sulfotobacter* spp.^[50] It might be that the full TDA biosynthetic pathway is not operational in these strains or that the TDA production rate is very low. A detailed genomic analysis should reveal the presence of the genes for TDA production in these strains. *Loktanella* sp. II 4.36 is the only known *Roseobacter* strain that contains all three compound classes: AHLs, NAMES, and tropone. Tropone shows weak antialgal activity. Moderate antibacterial activity has been reported,^[55] but no effect was observed on the marine strains used here.

Indole (**35**), present in almost all investigated strains, is well known as a bacterial metabolite, especially from *Escherichia coli*,^[56] although it is also released by several other bacteria.^[57] Extracellular indole serves as a signal.^[58] It has been implicated in regulating gene expression in *Vibrio cholerae*,^[46] biofilm formation,^[47] virulence,^[59,60] spore maturation,^[61,62] and bacterial persistence. Recently, it has been shown that indole negatively affects AHL-regulated bacterial phenotypes by inhibiting regulator folding.^[63] This effect leads to quorum-sensing inhibition by indole.

Similar to plants, many algae respond to auxin, indole-3-acetic acid, with increased growth.^[64] In plants, root-associated bacteria produce indole that is imported by the plant and modifies the auxin response,^[65] a scenario also possible for macroalgae. Indole produced by roseobacters is therefore likely involved in modulating biofilms on algae surfaces, especially in cases where high levels of indole are released, as by

Litoreibacter sp. F3. The indole derivative **37** was previously identified in *O. indolifex*.^[32]

PHB serves as an energy source for many bacteria,^[66,67] and production of PHB was previously described for various roseobacters.^[40,41] Several bacteria can use extracellular enzymes to degrade PHB, either to the monomer or the dimer.^[68] Because no PHB source was present in the medium, the PHB oligomers of roseobacters have varying chain lengths, and their derivatives must originate from the bacteria. This release has not been reported previously except with *Sphingomonas*, which produces the tetramer that acts as a growth promoter for *Fraxetia*.^[69] Oligomers usually occur as free acids, not as methyl esters, as are found in the roseobacters. Oligomers of considerably larger size can act as ion channels for Ca²⁺ transport in *E. coli*,^[67,70] but no ion specificity seems to occur.^[71] It might be possible that either the oligomers identified or larger ones not identifiable by the methods used here are involved in regulation of cation exchange in roseobacters, although the chelating activity of oligomers of the size discussed here might not be strong enough.

The current study shows that the diversity of small compounds released by roseobacters is greater than previously thought. Variations in these metabolites were found not only within a group, as for the AHLs, but also in the occurrence of the other compounds. Several of the identified compounds might be involved in signaling processes. Antialgal activity has thus far only been reported for roseobactericides and with low activity for lactones such as **13**; both compound classes occur only in a few specific *Roseobacter* strains. Here, we found additional antialgal activity in AHLs, NAMES, and TDA, with much more widespread occurrence within the roseobacters. How the macroalgae cope with this activity is not clear, but potential mechanisms in roseobacters have been observed. Roseobactericides are only produced when an external cue, coumaric acid, is present, as in algal blooms.^[8] In phytoplankton-associated *Silicibacter* sp. TM1040, coumaric acid induces the production of a motility inducer.^[72] This example shows that roseobacters can respond to small molecule signals other than AHLs with a distinct physiological response. The wide array of compounds detectable in the vicinity of the bacteria might play important roles in shaping algae–bacteria and bacteria–bacteria interactions. To fully understand this picture, identification of the extracellular bacterial inventory is a prerequisite.

Conclusions

In summary, a large proportion of algae-associated roseobacters produce a wide variety of AHLs. These AHLs, the structurally related NAMES, and TDA showed antialgal activity. Several other small compounds were also released and might play additional roles in algae–*Roseobacter* interactions, such as indole, methyl 3-hydroxybutyrate oligomers, tropone, or *N*-(2-phenylethyl)acetamide, the functions of which need to be delineated in the future.

Table 4. Phylogenetic affiliation of bacterial strains used as target strains for inhibition assays.

Strain	Phylogenetic group (class)	Accession no. of the 16S rRNA gene
Pseudonocardiaceae bacterium T4	Actinobacteria	AY177725
Phyllobacteriaceae bacterium TK	α -Proteobacteria	AY177715
Oceanospirillaceae bacterium T17	γ -Proteobacteria	AY177720
<i>Maribacter</i> sp. 62-1	Flavobacteria	KM517579

Experimental Section

Bacterial strains investigated: *P. gallaeciensis* CIP 105210^[37,73] was isolated from the scallop *Pecten maximus* and obtained from the Collection de l'Institut Pasteur, Paris, France. Further strains analyzed in this study were isolated from the surface of different marine macroalgae collected on the 8th June, 2010 at tidal flat areas at the German Wadden Sea (53°42'14" N, 07°42'13" E), and from 8th to 11th November 2010 at three sampling sites in Galicia, Spain (42°33'59" N, 8°53'25" W; 42°41'41.40" N, 9°1'57.10" W; 43°06'43" N, 9°13'10" W). For details about the algal host of each strain, see Table 4. After sampling, parts of the algae were washed three times with sterile filtered and autoclaved seawater to remove non-attached bacteria and particles and then spread out on a marine agar plates (Difco). Plates were then incubated for two weeks at 25 °C in the dark. Single colonies were selected and transferred at least three times until considered pure.

Strains affiliated with the *Roseobacter* clade were identified by screening with clade-specific PCR,^[74,75] which also detects some other members of the *Rhodobacteraceae*. Subsequently, sequencing and analysis of 16S rRNA genes were used to determine the phylogenetic positions of the isolates. Amplification and sequencing of the 16S rRNA genes were performed according to the methods of Brinkhoff and Muyzer.^[75] Sequences of at least 650 bp were determined and compared to those in GenBank by using BLAST analysis on the National Center for Biotechnology Information (NCBI) server (blast.ncbi.nlm.nih.gov). A phylogenetic tree was calculated by using the ARB software package.^[76] Sequences of type strains (> 1300 bp) were used for construction of the backbone tree by the neighbor joining method. Shorter sequences of bacterial strains analyzed in this study were added afterwards by parsimony interactive. The 16S rRNA gene sequences obtained in this study were deposited at GenBank under the accession numbers KC731428, KJ786453–KJ786472, KJ862835–KJ862837, KM065450, and KP723466–KP723472.

Inhibition assay: Compounds were tested for inhibitory activity against various marine bacteria (Table 1), as well as an axenic diatom culture of *S. costatum* CCMP 1332. The compounds were diluted in CH₂Cl₂ and tested in quantities of 1, 10, and 100 μ g. Inhibition assays were performed as described by Brinkhoff et al.^[7] with slight modifications. Bacterial target strains were precultured at 20 °C for two days with shaking in Marine Broth 2216 (20 mL, Difco). In each case, the target culture (200 μ L) with an adjusted OD₆₀₀ of 0.2 was spread on a Marine Agar 2216 plate. Compounds dissolved in CH₂Cl₂ were spotted on filter paper (6 mm diameter, Carl Roth, Karlsruhe), and after evaporation of the CH₂Cl₂, the filter disks were transferred onto the agar plate. The antibiotic TDA was used as positive control, and a filter disk treated with CH₂Cl₂ and

an untreated filter disk were used as negative controls. Inhibition assays were carried out at least in duplicate. Inhibition zones were determined by the distances between the filter disk and the bacterial lawn of the target organism. Minimal inhibitory concentrations (MICs) were determined by plotting the various inhibition zone data (y-axis) against a logarithmic scale of the concentration (x-axis), with the intersection point of the interpolated straight line on the x-axis giving the MIC.

XAD extracts: The bacterial cultures (100 mL) were grown for three days in marine broth medium containing precleaned Amberlite XAD-16 (2 g). The adsorbent was separated from the culture by filtration and extracted three times with CH₂Cl₂/water (10:1). The combined organic phases were dried with MgSO₄, and the solvent was removed under reduced pressure. The extract was redissolved in CH₂Cl₂ (50 μ L) and analyzed by GC/MS.

Cluster analysis: To test whether the production of AHLs was linked to the relation of the bacterial strains in the phylogenetic tree, relatedness was estimated by using the multivariate Euclidian distance method with the qualitative occurrence or absence of all found AHLs, excluding trace occurrence of AHLs with odd-numbered acyl chains.^[77,78] The multivariate Euclidian distance was calculated with the program IBM SPSS Statistics 22.

General conditions: PHB pellets and other chemicals were obtained from Sigma-Aldrich or from Acros Organics and were used without further purification. Solvents were purified by distillation and dried according to standard procedures. Moisture- and/or oxygen-sensitive reactions were carried out under nitrogen atmosphere in vacuum-heated flasks with dried solvents. Thin-layer chromatography (SiO₂, TLC) was performed on 0.20 mm Macherey-Nagel silica gel plates (Polygram SIL G/UV254), and column chromatography was performed with Merck silica gel 60 (0.040–0.063 mm) by using standard flash chromatographic methods. NMR spectra were recorded on Bruker DRX-400 (400 MHz), AV III-400 (400 MHz), or AV II-600 (600 MHz) spectrometers and were referenced against TMS (δ = 0.00 ppm) for ¹H NMR and CHCl₃ (δ = 77.01 ppm) for ¹³C NMR experiments. Infrared spectra were recorded on a Bruker Tensor 27ATR spectrometer. UV spectra were recorded on a Varian Cary 100 Bio spectrometer. GC/MS analyses were carried out on an Agilent GC 7890A system connected to a 5975C mass-selective detector (Agilent) fitted with a HP-5 MS fused-silica capillary column (30 m \times 0.25 mm i.d., 0.22 μ m film; Hewlett-Packard). Conditions were as follows: carrier gas (He): 1.2 mL min⁻¹; injection volume: 1 μ L; injector: 250 °C; transfer line: 300 °C. The gas chromatograph was programmed as follows: 50 °C (5 min isothermal), increased at 5 °C min⁻¹ to 320 °C, and operated in splitless mode for XAD extracts and in split mode (20:1) for synthetic compounds. Gas chromatographic retention indices, *I*, were determined from a homologous series of *n*-alkanes. The identification of compounds was performed by comparison of mass spectra and retention times with those of reference compounds. HPLC/MS analyses were carried out on a Thermo Fisher Accela LC System connected to an electrospray LTQ XL mass spectrometer (Thermo Scientific) fitted with a RP-C18 column (150 mm length \times 2.1 mm diameter, Agilent), operated in ESI positive mode. All solvents used were of LCMS grade. The compounds or extracts analyzed were dissolved in acetonitrile, and a volume of 10 μ L was injected. Compounds were eluted starting with a gradient of 92.5% solvent A (water), 2.5% solvent B (acetonitrile), and 5% solvent C (2% formic acid in MeOH/water 1:1) for 1.5 min. The gradient was changed to 2.5% A, 92.5% B, and 5% C over 6.5 min and then held for 7 min.

Polyhydroxybutyrate cleavage: The cleavage of polyhydroxybutyrate (PHB, 10 g) was carried out according to the procedure of Seebach.^[42,79] After 7 h of reflux, about half of the PHB was cleaved. After workup of the supernatant, the crude product was submitted to column chromatography. Gradient elution (pentane/EtOAc=4:1, 3:1, 2:1, 1:1) furnished, in order of elution: methyl 3-hydroxypentanoate (derived from a minor PHB polymer constituent), methyl 3-hydroxybutanoate, methyl 3-(3-hydroxybutyryloxy)pentanoate, methyl 3-(3-hydroxybutyryloxy)butanoate (**14**, dimer), methyl 3-(3-hydroxybutyryloxy)butyryloxy butanoate (**15**, trimer), methyl 3-(3-(3-hydroxybutyryloxy)butyryloxy)butyryloxy butanoate (**16**, tetramer), and the respective pentamer (**17**). Hexa- and heptamers occurred in small amounts as byproducts of **17**.

Methyl 3-hydroxypentanoate: 0.15 g, 1.13 mmol (1.5%); $R_f=0.64$ (pentane/EtOAc, 1:1); l : 957; $^1\text{H NMR}$ (400 MHz, CDCl_3): $\delta=3.97\text{--}3.90$ (m, 7H; CH), 3.72 (s, 3H; OCH_3), 2.90 (brs, 1H; OH), 2.53 (ddd, $J=3.2, 6.4$ Hz, 1H; CHH), 2.42 (dd, $J=9.0, 16.4$ Hz, 1H; CHH), 0.97 (t, $J=7.4$ Hz, 3H; CH_3); $^{13}\text{C NMR}$ (100 MHz, CDCl_3): $\delta=173.5$ (C=O), 69.3 (HOCH), 51.7 (OCH_3), 40.7 (CH_2), 29.4 (COCH_2), 9.8 (CH_3); MS (70 eV, EI): m/z (%): 132 (<1) [M^-]; 114 (5) [$\text{M}-\text{H}_2\text{O}]^-$; 103 (96), 74 (66), 71 (92), 61 (44), 59 (56), 43 (100).

Methyl 3-hydroxybutanoate: 1.96 g, 16.59 mmol (19.6%); $R_f=0.54$ (pentane/EtOAc, 1:1); l : 851; $^1\text{H NMR}$ (400 MHz, CDCl_3): $\delta=4.21$ (sext, $J=6.3$ Hz, 1H, CH), 3.71 (s, 3H, OCH_3), 3.25 (brs, 1H, OH), 2.48–2.46 (m, 2H, COCH_2), 1.23 (d, $J=6.3$ Hz, 3H, CH_3); $^{13}\text{C NMR}$ (100 MHz, CDCl_3): $\delta=173.0$ (C=O), 64.1 (HOCH), 51.5 (OCH_3), 42.6 (COCH_2), 22.4 (CH_3); MS (70 eV, EI): m/z (%): 118 (<1) [M^+]; 103 (33) [$\text{M}-\text{CH}_3$] $^+$; 87 (27), 74 (74), 71 (40), 61 (17), 59 (18), 45 (56), 43 (100).

Methyl 3-(3-hydroxybutyryloxy)pentanoate (24**):** 0.06 g, 0.28 mmol (0.6%); $R_f=0.58$ (pentane/EtOAc, 1:1); l : 1432; $^1\text{H NMR}$ (400 MHz, CDCl_3): $\delta=^1\text{H NMR}$ (400 MHz, CDCl_3): $\delta=5.25\text{--}5.19$ (m, 7H, OCH), 4.24–4.16 (m, 7H, OHCH), 3.68 (s, 3H, OCH_3), 3.10 (brs, 1H, OH), 2.58 (dd, $J=6.4, 2.0$ Hz, 2H, CH_2), 2.44 (dq, $J=15.8, 6.1$ Hz, 2H, CH_2), 1.70–1.63 (m, 3H, COCH_2CH_2), 1.23 (d, $J=6.3$ Hz, 3H, CH_3), 0.95–0.91 (m, 3H, CH_3); $^{13}\text{C NMR}$ (100 MHz, CDCl_3): $\delta=172.2$ (C=O), 171.0 (C=O), 71.9 (CH), 64.5 (HOCH), 51.8 (OCH_3), 43.2 (CH_2), 38.5 (CH_2), 27.0 (CH_2), 22.4 (OHCHCH $_3$), 9.4 (CH_3); MS (70 eV, EI): m/z (%): 218 (<1) [M^+]; 203 (6) [$\text{M}-\text{CH}_3$] $^+$; 174 (9), 131 (18), 115 (100), 103 (58), 87 (53), 83 (76), 73 (42), 55 (42), 43 (55).

Dimer **14:** 0.66 g, 3.23 mmol (6.6%); $R_f=0.52$ (pentane/EtOAc, 1:1); l : 1351; $^1\text{H NMR}$ (400 MHz, CDCl_3): $\delta=5.32$ (sext, $J=6.4$ Hz, 1H, OCH), 4.23–4.11 (m, 7H, OHCH), 3.69 (s, 3H, OCH_3), 3.13 (brs, 1H, OH), 2.60 (qdd, $J=15.6, 6.5, 1.5$ Hz, 2H, CH_2), 2.48–2.37 (m, 2H, CH_2), 1.32 (dd, $J=6.4, 1.5$ Hz, 3H, CH_3), 1.22 (dd, $J=6.2, 1.6$ Hz, 3H, HOCHCH $_3$); $^{13}\text{C NMR}$ (100 MHz, CDCl_3): $\delta=171.9$ (C=O), 170.7 (C=O), 67.5 (CH), 64.3 (HOCH), 51.8 (OCH_3), 43.2 (CH_2), 40.4 (CH_2), 22.4 (HOCHCH $_3$), 19.8 (CH_3); MS (70 eV, EI): m/z (%): 204 (<1) [M^+]; 189 (7) [$\text{M}-\text{CH}_3$] $^+$; 160 (12), 128 (24), 119 (20), 101 (90), 87 (57), 69 (66), 59 (100), 43 (60).

Trimer **15:** 0.41 g, 1.41 mmol (4.1%); $R_f=0.52$ (pentane/EtOAc, 1:1); l : 1822; $^1\text{H NMR}$ (400 MHz, CDCl_3): $\delta=5.35\text{--}5.24$ (m, 2H, 2CH), 4.23–4.15 (m, 7H, OHCH), 3.69 (s, 3H, OCH_3), 3.10 (brs, 1H, OH), 2.67–2.58 (m, 2H, CH_2), 2.54–2.47 (m, 2H, CH_2), 2.44–2.37 (m, 2H, CH_2), 1.31 (dd, $J=6.1, 0.8$ Hz, 3H, CH_3), 1.30 (dd, $J=6.3, 0.8$ Hz, 3H, CH_3), 1.21 (dd, $J=6.3, 0.8$ Hz, 3H, CH_3); $^{13}\text{C NMR}$ (100 MHz, CDCl_3): $\delta=171.9$ (C=O), 170.5 (C=O), 169.4 (C=O), 67.8 (CH), 67.5 (CH), 64.3 (HOCH), 51.7 (OCH_3), 43.2 (CH_2), 40.8 (CH_2), 40.4 (CH_2), 22.4 (HOCHCH $_3$), 19.8 (CH_3), 19.7 (CH_3); MS (70 eV, EI): m/z (%): 290 (<1) [M^-]; 275 (<1) [$\text{M}-\text{CH}_3$] $^-$; 205 (8), 173 (11), 155 (20), 128 (23), 119 (16), 101 (66), 87 (42), 69 (100), 59 (55), 43 (34).

Tetramer **16:** 0.32 g, 0.85 mmol (3.2%); $R_f=0.51$ (pentane/EtOAc, 1:1); l : 2270; $^1\text{H NMR}$ (400 MHz, CDCl_3): $\delta=5.35\text{--}5.23$ (m, 3H, 3CH), 4.23–4.14 (m, 7H, OHCH), 3.68 (s, 3H, OCH_3), 3.08 (d, $J=3.6$ Hz, 1H, OH), 2.68–2.36 (m, 6H, 3 CH_2), 1.31 (d, $J=6.2$ Hz, 3H, CH_3), 1.29 (d, $J=6.0$ Hz, 3H, CH_3), 1.28 (d, $J=6.2$ Hz, 3H, CH_3), 1.22 (dd, $J=6.3, 0.7$ Hz, 3H, CH_3); $^{13}\text{C NMR}$ (100 MHz, CDCl_3): $\delta=172.0$ (C=O), 170.5 (C=O), 169.4 (C=O), 169.2 (C=O), 67.73 (CH), 67.68 (CH), 67.5 (CH), 64.3 (HOCH), 51.7 (OCH_3), 43.2 (CH_2), 40.83 (CH_2), 40.79 (CH_2), 40.4 (CH_2), 22.5 (HOCHCH $_3$), 19.85 (CH_3), 19.78 (CH_3), 19.7 (CH_3); MS (70 eV, EI): m/z (%): 376 (<1) [M^+]; 291 (3), 243 (2), 205 (5), 173 (13), 155 (39), 128 (11), 119 (7), 101 (36), 87 (30), 69 (100), 59 (29), 43 (21).

Pentamer **17:** 0.25 g, 0.54 mmol (2.5%); $R_f=0.50$ (pentane/EtOAc, 1:1); l : 2705; $^1\text{H NMR}$ (400 MHz, CDCl_3): $\delta=5.35\text{--}5.22$ (m, 4H, 4CH), 4.23–4.11 (m, 7H, OHCH), 3.68 (s, 3H, OCH_3), 3.12 (d, $J=3.8$ Hz, 1H, OH), 2.68–2.58 (m, 4H, 2 CH_2), 2.54–2.36 (m, 6H, 3 CH_2), 1.31 (d, $J=6.1$ Hz, 3H, CH_3), 1.29 (d, $J=6.2$ Hz, 3H, CH_3), 1.28 (d, $J=6.3$ Hz, 3H, CH_3), 1.27 (d, $J=6.3$ Hz, 3H, CH_3), 1.23 (d, $J=6.3$ Hz, 3H, CH_3); $^{13}\text{C NMR}$ (100 MHz, CDCl_3): $\delta=171.9$ (C=O), 170.5 (C=O), 169.3 (C=O), 169.2 (C=O), 169.1 (C=O), 67.7 (CH), 67.63 (CH), 67.58 (CH), 67.4 (CH), 64.3 (HOCH), 51.7 (OCH_3), 43.2 (CH_2), 40.8 (CH_2), 40.74 (CH_2), 40.72 (CH_2), 40.4 (CH_2), 22.5 (HOCHCH $_3$), 19.8 (CH_3), 19.73 (CH_3), 19.68 (CH_3), 19.6 (CH_3); MS (70 eV, EI): m/z (%): 462 (<1) [M^+]; 291 (<1), 241 (2), 205 (2), 187 (4), 173 (9), 155 (32), 128 (4), 101 (21), 87 (19), 69 (100), 59 (20), 43 (17).

Synthesis of (9Z,12Z)-N-(octadeca-9,12-dienoyl)-L-homoserine lactone: L-Homoserine lactone hydrobromide (0.64 g, 3.5 mmol) was dissolved in CH_2Cl_2 . Triethylamine (0.36 g, 3.5 mmol) was added to the solution, followed by the addition of linoleic acid (1 g, 3.5 mmol) and 1-ethyl-3-(3-dimethylaminopropyl)carbodiimide hydrochloride (0.68 g, 3.5 mmol). The reaction mixture was stirred for 12 h at room temperature, and the solvent was evaporated. The residue was extracted with EtOAc (3 \times 50 mL). The combined organic phases were washed with H_2O , saturated NaHCO_3 solution, and brine, dried with MgSO_4 , and concentrated. The crude product was purified by flash column chromatography to obtain (9Z,12Z)-N-(octadeca-9,12-dienoyl)-L-homoserine lactone (0.84 g, 2.3 mmol, 65%) as a white solid; $R_f=0.38$ (pentane/EtOAc, 1:1); $^1\text{H NMR}$ (400 MHz, CDCl_3): $\delta=6.24$ (d, $J=5.8$ Hz, NH), 5.42–5.29 (m, 4H, CH=CH), 4.58 (ddd, $J=6.1, 8.6, 11.6$ Hz, NCH), 4.46 (t, $J=9.1$ Hz, OCH $_2$), 4.29 (ddd, $J=6.1, 9.4, 11.4$ Hz, OCH $_2$), 2.86–2.81 (m, 1H, NCHCH $_2$), 2.78 (t, $J=6.8$ Hz, CH=CHCH $_2$ CH=CH), 2.35–2.23 (m, NOCCH $_2$), 2.18–2.09 (m, NCHCH $_2$), 2.05 (q, $J=6.8$ Hz, 2 $\text{CH}_2\text{CH}=\text{CHCH}_2\text{CH}_2$), 1.63 (quint, $J=7.3$ Hz, 2H, COCH_2CH_2), 1.40–1.24 (m, 7 CH_2), 0.89 ppm (t, $J=7.1$ Hz, CH_3); $^{13}\text{C NMR}$ (100 MHz, CDCl_3): $\delta=175.6$ (CO $_2$), 173.7 (CON), 130.2 (CH), 130.0 (CH), 128.1 (CH), 127.9 (CH), 66.1 (CH_2), 49.3 (CH), 36.2 (CH_2), 31.5 (CH_2), 30.6 (CH_2), 29.6 (CH_2), 29.3 (CH_2), 29.2 (CH_2), 29.2 (CH_2), 29.1 (CH_2), 27.2 (CH_2), 27.2 (CH_2), 25.6 (CH_2), 25.4 (CH_2), 22.6 (CH_2), 14.1 (CH_3).

Acknowledgements

We thank Martin Stürminger for technical assistance. This study was funded by the Deutsche Forschungsgemeinschaft through the Transregional Collaborative Research Centre "Roseobacter" (SFB/TRR 51).

Keywords: quorum sensing • antialgal activity • autoinducer • macroalgae • polyhydroxybutyrate

- [1] T. Martens, L. Gram, H.-P. Grossart, D. Kessler, R. Müller, M. Simon, S. Wenzel, T. Brinkhoff, *Microb. Ecol.* **2007**, *54*, 31–42.
- [2] J. B. Bruhn, L. Gram, R. Belas, *Appl. Environ. Microbiol.* **2007**, *73*, 442–450.
- [3] S. Thole, D. Kalhoefer, S. Voget, M. Berger, T. Engelhardt, H. Liesegang, A. Wollherr, S. Kjelleberg, R. Daniel, M. Simon, T. Thomas, T. Brinkhoff, *ISME J.* **2012**, *6*, 2229–2244.
- [4] A. Buchan, J. M. Gonzalez, M. A. Moran, *Appl. Environ. Microbiol.* **2005**, *71*, 5665–5677.
- [5] S. Egan, N. D. Fernandes, V. Kumar, M. Gardiner, T. Thomas, *Environ. Microbiol.* **2014**, *16*, 925–938.
- [6] I. Wagner-Döbler, B. Ballhausen, M. Berger, T. Brinkhoff, I. Buchholz, B. Bunk, H. Cypionka, R. Daniel, T. Drepper, G. Gerds, S. Hahnke, C. Han, D. Jahn, D. Kalhoefer, H. Kiss, H.-P. Klenk, N. Kyrpides, W. Liebl, H. Liesegang, L. Meincke, A. Pati, J. Petersen, T. Piekarski, C. Pommerenke, S. Pradella, R. Pukall, R. Rabus, E. Stackebrandt, S. Thole, L. Thompson, P. Tielen, J. Tomasch, M. von Jan, N. Wanphrut, A. Wichels, H. Zech, M. Simon, *ISME J.* **2010**, *4*, 61–77.
- [7] T. Brinkhoff, G. Bach, T. Heidorn, L. Liang, A. Schlingloff, M. Simon, *Appl. Environ. Microbiol.* **2004**, *70*, 2560–2565.
- [8] M. R. Seyedsayamdost, R. J. Case, R. Kolter, J. Clardy, *Nat. Chem.* **2011**, *3*, 331–335.
- [9] D. Rao, J. S. Webb, C. Holmström, R. Case, A. Low, P. Steinberg, S. Kjelleberg, *Appl. Environ. Microbiol.* **2007**, *73*, 7844–7852.
- [10] W. N. Cude, A. Buchan, *Front. Microbiol.* **2013**, *4*, 336.
- [11] J. Zan, Y. Liu, C. Fuqua, R. Hill, *Int. J. Mol. Sci.* **2014**, *15*, 654–669.
- [12] M. Berger, A. Neumann, S. Schulz, M. Simon, T. Brinkhoff, *J. Bacteriol.* **2011**, *193*, 6576–6585.
- [13] J. Zan, E. M. Cicirelli, N. M. Mohamed, H. Sibhatu, S. Kroll, O. Choi, C. L. Uhlson, C. L. Wysoczinski, R. C. Murphy, M. E. A. Churchill, R. T. Hill, C. Fuqua, *Mol. Microbiol.* **2012**, *85*, 916–933.
- [14] D. Patzelt, H. Wang, I. Buchholz, M. Rohde, L. Gröbe, S. Pradella, A. Neumann, S. Schulz, S. Heyber, K. Münch, R. Münch, D. Jahn, I. Wagner-Döbler, J. Tomasch, *ISME J.* **2013**, *7*, 2274–2286.
- [15] L. Gram, H.-P. Grossart, A. Schlingloff, T. Kiorboe, *Appl. Environ. Microbiol.* **2002**, *68*, 4111–4116.
- [16] M. W. Taylor, P. J. Schupp, H. J. Baillie, T. S. Charlton, R. de Nys, S. Kjelleberg, P. D. Steinberg, *Appl. Environ. Microbiol.* **2004**, *70*, 4387–4389.
- [17] N. M. Mohamed, E. M. Cicirelli, J. Kan, F. Chen, C. Fuqua, R. T. Hill, *Environ. Microbiol.* **2008**, *10*, 75–86.
- [18] J. B. Bruhn, K. F. Nielsen, M. Hjelm, M. Hansen, J. Bresciani, S. Schulz, L. Gram, *Appl. Environ. Microbiol.* **2005**, *71*, 7263–7270.
- [19] I. Wagner-Döbler, V. Thiel, L. Eberl, M. Allgaier, A. Bodor, S. Meyer, S. Ebner, A. Hennig, R. Pukall, S. Schulz, *ChemBioChem* **2005**, *6*, 2195–2206.
- [20] A. Neumann, D. Patzelt, I. Wagner-Döbler, S. Schulz, *ChemBioChem* **2013**, *14*, 2355–2361.
- [21] V. Thiel, B. Kunze, P. Verma, I. Wagner-Döbler, S. Schulz, *ChemBioChem* **2009**, *10*, 1861–1868.
- [22] A. L. Schaefer, E. P. Greenberg, C. M. Oliver, Y. Oda, J. J. Huang, G. Bittan-Banin, C. M. Peres, S. Schmidt, K. Juhaszova, J. R. Sufrin, C. S. Harwood, *Nature* **2008**, *454*, 595–599.
- [23] H. Bruns, V. Thiel, S. Voget, D. Patzelt, R. Daniel, I. Wagner-Döbler, S. Schulz, *Chem. Biodiversity* **2013**, *10*, 1559–1573.
- [24] H. Geng, J. B. Bruhn, K. F. Nielsen, L. Gram, R. Belas, *Appl. Environ. Microbiol.* **2008**, *74*, 1535–1545.
- [25] P. W. D'Alvise, O. Magdenoska, J. Melchiorson, K. F. Nielsen, L. Gram, *Environ. Microbiol.* **2014**, *16*, 1252–1266.
- [26] A. Penesyan, J. Tebben, M. Lee, T. Thomas, S. Kjelleberg, T. Harder, S. Egan, *Mar. Drugs* **2011**, *9*, 1391–1402.
- [27] C. H. Porsby, K. F. Nielsen, L. Gram, *Appl. Environ. Microbiol.* **2008**, *74*, 7356–7364.
- [28] W. N. Cude, J. Mooney, A. A. Tavanaei, M. K. Hadden, A. M. Frank, C. A. Gulvik, A. L. May, A. Buchan, *Appl. Environ. Microbiol.* **2012**, *78*, 4771–4780.
- [29] V. Thiel, T. Brinkhoff, J. S. Dickschat, S. Wickel, J. Grunenberg, I. Wagner-Döbler, M. Simon, S. Schulz, *Org. Biomol. Chem.* **2010**, *8*, 234–246.
- [30] N. L. Brock, A. Nikolay, J. S. Dickschat, *Chem. Commun.* **2014**, *50*, 5487–5489.
- [31] M. R. Seyedsayamdost, G. Carr, R. Kolter, J. Clardy, *J. Am. Chem. Soc.* **2011**, *133*, 18343–18349.
- [32] I. Wagner-Döbler, H. Rheims, A. Felske, A. El-Ghezal, D. Flade-Schröder, H. Laatsch, S. Lang, R. Pukall, B. J. Tindall, *Int. J. Syst. Evol. Microbiol.* **2004**, *54*, 1177–1184.
- [33] J. S. Dickschat, C. Zell, N. L. Brock, *ChemBioChem* **2010**, *11*, 417–425.
- [34] J. S. Dickschat, I. Wagner-Döbler, S. Schulz, *J. Chem. Ecol.* **2005**, *31*, 925–947.
- [35] R. Riclea, J. Gleitzmann, H. Bruns, C. Junker, B. Schulz, J. S. Dickschat, *Beilstein J. Org. Chem.* **2012**, *8*, 941–950.
- [36] T. Brinkhoff, H.-A. Giebel, M. Simon, *Arch. Microbiol.* **2008**, *189*, 531–539.
- [37] C. Ruiz-Ponte, J. F. Samain, J. L. Sanchez, J. L. Nicolas, *Mar. Biotechnol.* **1999**, *1*, 52–59.
- [38] J. S. Dickschat, *Nat. Prod. Rep.* **2010**, *27*, 343–369.
- [39] U. Groenhagen, M. Maczka, J. S. Dickschat, S. Schulz, *Beilstein J. Org. Chem.* **2014**, *10*, 1421–1432.
- [40] H.-A. Giebel, D. Kalhoefer, R. Gahl-Janssen, Y.-J. Choo, K. Lee, J.-C. Cho, B. J. Tindall, E. Rhiel, C. Beardsley, Ö. O. Aydogmus, S. Voget, R. Daniel, M. Simon, T. Brinkhoff, *Int. J. Syst. Evol. Microbiol.* **2013**, *63*, 4207–4217.
- [41] J.-C. Cho, S. J. Giovannoni, *Int. J. Syst. Evol. Microbiol.* **2004**, *54*, 1129–1136.
- [42] D. Seebach, M. Züger, *Helv. Chim. Acta* **1982**, *65*, 495–503.
- [43] J. A. Moore, D. E. Reed, *Org. Synth.* **1961**, *41*, 16.
- [44] F. Arndt, *Org. Synth.* **1935**, *15*, 3.
- [45] K. Benkendorf, J. B. Bremner, A. R. Davis, *Molecules* **2001**, *6*, 70–78.
- [46] R. S. Mueller, S. Beyhan, S. G. Saini, F. H. Yildiz, D. H. Bartlett, *J. Bacteriol.* **2009**, *191*, 3504–3516.
- [47] J. Lee, A. Jayaraman, T. K. Wood, *BMC Microbiol.* **2007**, *7*, 42.
- [48] T. Ando, S. I. Inomata, M. Yamamoto in *Top. Curr. Chem. Vol. 239* (Ed.: S. Schulz), Springer, Berlin **2004**.
- [49] A. M. Pomini, A. J. Marsaioli, *J. Nat. Prod.* **2008**, *71*, 1032–1036.
- [50] V. C. Kalia, *Biotechnol. Adv.* **2013**, *31*, 224–245.
- [51] R. P. Maskey, P. N. Asolkar, E. Kapaun, I. Wagner-Döbler, H. Laatsch, *J. Antibiot.* **2002**, *55*, 643–649.
- [52] K. Böröczky, H. Laatsch, I. Wagner-Döbler, K. Stritzke, S. Schulz, *Chem. Biodiversity* **2006**, *3*, 622–634.
- [53] H.-y. Li, S. Matsunaga, N. Fusetani, *Comp. Biochem. Physiol. Part B* **1994**, *107*, 261–264.
- [54] L. Gram, J. Melchiorson, J. B. Bruhn, *Mar. Biotechnol.* **2010**, *12*, 439–451.
- [55] T. J. Trust, K. H. Bartlett, *Antimicrob. Agents Chemother.* **1975**, *8*, 381–383.
- [56] D. D. Woods, *Biochem. J.* **1935**, *29*, 640–648.
- [57] S. Schulz, J. S. Dickschat, *Nat. Prod. Rep.* **2007**, *24*, 814–842.
- [58] J.-H. Lee, J. Lee, *FEMS Microbiol. Rev.* **2010**, *34*, 426–444.
- [59] J. Lee, C. Attila, L. G. Suat, J. D. Cirillo, T. K. Wood, *J. Microb. Biotechnol.* **2009**, *2*, 75–90.
- [60] E. Nikaido, E. Giraud, S. Baucheron, S. Yamasaki, A. Wiedemann, K. Okamoto, T. Takagi, A. Yamaguchi, A. Cloeckaert, K. Nishino, *Gut Pathog.* **2012**, *4*, 5.
- [61] Y.-G. Kim, J.-H. Lee, M. Cho, J. Lee, *BMC Microbiol.* **2011**, *11*, 119.
- [62] N. M. Vega, K. R. Allison, A. S. Khalil, J. J. Collins, *Nat. Chem. Biol.* **2012**, *8*, 431–433.
- [63] J. Kim, W. Park, *Microbiology* **2013**, *159*, 2616–2625.
- [64] C. E. Bagwell, M. Piskorska, T. Soule, A. Petelos, C. M. Yeager, *Appl. Biochem. Biotechnol.* **2014**, *173*, 1977–1984.
- [65] A. Bailly, U. Groenhagen, S. Schulz, M. Geisler, L. Eberl, L. Weisskopf, *Plant J.* **2014**, *80*, 758–771.
- [66] H. M. Müller, D. Seebach, *Angew. Chem.* **1993**, *105*, 483–509.
- [67] R. N. Reusch, *Chem. Biodiversity* **2012**, *9*, 2343–2366.
- [68] T. M. Scherer, R. C. Fuller, S. Goodwin, R. W. Lenz, *Biomacromolecules* **2000**, *1*, 577–583.
- [69] N. Ogita, Y. Hashidoko, S. H. Limin, S. Tahara, *Biosci. Biotechnol. Biochem.* **2006**, *70*, 2325–2329.
- [70] S. Das, U. D. Lengweiler, D. Seebach, R. N. Reusch, *Proc. Natl. Acad. Sci. USA* **1997**, *94*, 9075–9079.
- [71] D. Seebach, A. Brunner, H. M. Büger, R. N. Reusch, L. L. Bramble, *Helv. Chim. Acta* **1996**, *79*, 507–517.
- [72] P. Sule, R. Belas, *J. Bacteriol.* **2013**, *195*, 637–646.
- [73] T. Martens, T. Heidorn, R. Pukall, M. Simon, B. J. Tindall, T. Brinkhoff, *Int. J. Syst. Evol. Microbiol.* **2006**, *56*, 1293–1304.
- [74] B. Rink, S. Seeberger, T. Martens, C.-D. Duerksen, M. Simon, T. Brinkhoff, *Aquat. Microb. Ecol.* **2007**, *48*, 47–60.

- [75] T. Brinkhoff, G. Muyzer, *Appl. Microbiol. Biotechnol.* **1997**, *63*, 3789–3796.
- [76] W. Ludwig, O. Strunk, R. Westram, L. Richter, H. Meier, Yadhukumar, A. Buchner, T. Lai, S. Steppi, G. Jobb, W. Förster, I. Brettske, S. Gerber, A. W. Ginhart, O. Gross, S. Grumann, S. Hermann, R. Jost, A. König, T. Liss, R. Lüßmann, M. May, B. Nonhoff, B. Reichel, R. Strehlow, A. Stamatakis, N. Stuckmann, A. Vilbig, M. Lenke, T. Ludwig, A. Bode, K. Schleifer, *Nucleic Acids Res.* **2004**, *32*, 1363–1371.
- [77] A. A. Khan, S.-J. Kim, D. D. Paine, C. E. Cerniglia, *Int. J. Syst. Evol. Microbiol.* **2002**, *52*, 1997–2002.
- [78] K. M. M. da Silva, M. d. F. Agra, D. Y. A. C. dos Santos, A. F. M. de Oliveira, *Biochem. Sys. Ecol.* **2012**, *44*, 48–52.
- [79] D. Seebach, M. F. Züger, *Tetrahedron Lett.* **1984**, *25*, 2747–2750.

Manuscript received: April 13, 2015

Accepted article published: July 25, 2015

Final article published: ■ ■ ■ ■, 0000

Supplementary Material for Manuscript 5

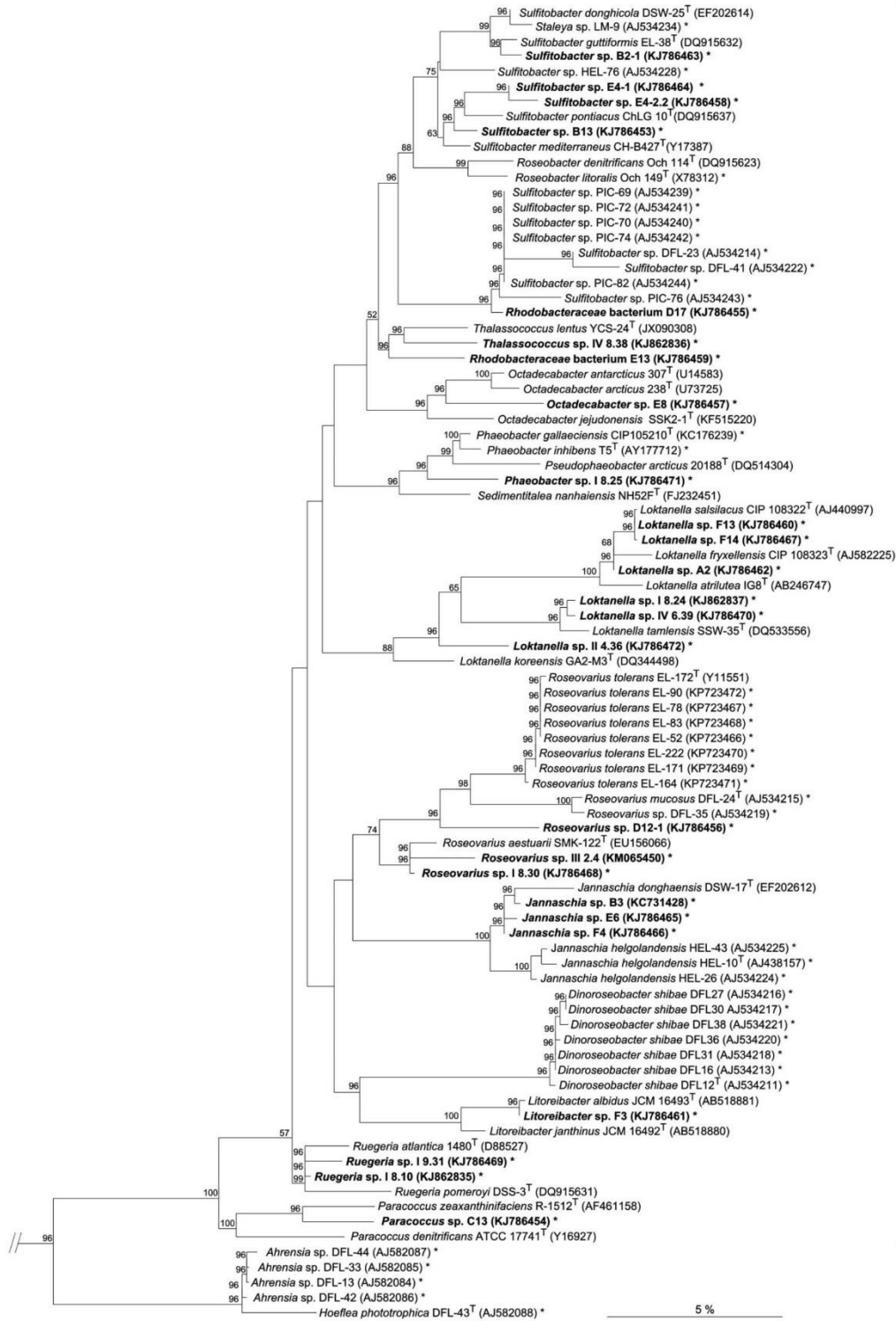


Figure S1. Phylogenetic tree of the *Rhodobacteraceae* based on 16S rRNA gene sequence similarity showing affiliation of the bacterial strains investigated in this (bold letters) and previous studies.^{[19][20]} The *Roseobacter* group to which the majority of strains belongs to is indicated. Sequences of type strains (>1300 bp, indicated by a ^T) were used for construction of the backbone-tree applying the neighbor joining method. Only bootstrap values $\geq 50\%$ derived from 1000 replicates are shown. Shorter sequences of bacterial strains analyzed in this study were added afterwards using parsimony interactive. Asterisks indicate organisms tested for AHL production, and new isolates obtained from macroalgae and investigated in this study are labeled in bold face. Selected sequences of the γ -*Proteobacteria* were used as outgroup (not shown). The scale bar indicates 5 % sequence divergence.



Article

An Unprecedented Medium-Chain Diunsaturated *N*-acylhomoserine Lactone from Marine *Roseobacter* Group Bacteria

Lisa Ziesche ¹, Laura Wolter ², Hui Wang ³, Thorsten Brinkhoff ², Marion Pohlner ², Bert Engelen ², Irene Wagner-Döbler ³ and Stefan Schulz ^{1,*}

¹ Institute of Organic Chemistry, Technische Universität Braunschweig, Hagenring 30, 38106 Braunschweig, Germany; l.ziesche@tu-braunschweig.de

² Institute for Chemistry and Biology of the Marine Environment, University of Oldenburg, Carl-von-Ossietzky-Straße 9-11, 26111 Oldenburg, Germany; laura.wolter@uni-oldenburg.de (L.W.); thorsten.brinkhoff@icbm.de (T.B.); marion.pohlner@uni-oldenburg.de (M.P.); bert.engelen@uni-oldenburg.de (B.E.)

³ Helmholtz Centre for Infection Research, Department of Medical Microbiology, Group Microbial Communication, Inhoffenstr. 7, 38124 Braunschweig, Germany; Hui.Wang@helmholtz-hzi.de (H.W.); Irene.Wagner-Doebler@helmholtz-hzi.de (I.W.-D.)

* Correspondence: stefan.schulz@tu-braunschweig.de; Tel.: +49-531-391-5272

Received: 7 December 2018; Accepted: 21 December 2018; Published: 31 December 2018



Abstract: *N*-acylhomoserine lactones (AHLs), bacterial signaling compounds involved in quorum-sensing, are a structurally diverse group of compounds. We describe here the identification, synthesis, occurrence and biological activity of a new AHL, *N*-((2*E*,5*Z*)-2,5-dodecadienoyl)homoserine lactone (**11**) and its isomer *N*-((3*E*,5*Z*)-3,5-dodecadienoyl)homoserine lactone (**13**), occurring in several *Roseobacter* group bacteria (Rhodobacteraceae). The analysis of 26 strains revealed the presence of **11** and **13** in six of them originating from the surface of the macroalgae *Fucus spiralis* or sediments from the North Sea. In addition, 18 other AHLs were detected in 12 strains. Compound identification was performed by GC/MS. Mass spectral analysis revealed a diunsaturated C₁₂ homoserine lactone as structural element of the new AHL. Synthesis of three likely candidate compounds, **11**, **13** and *N*-((2*E*,4*E*)-2,4-dodecadienoyl)homoserine lactone (**5**), revealed the former to be the natural AHLs. Bioactivity test with quorum-sensing reporter strains showed high activity of all three compounds. Therefore, the configuration and stereochemistry of the double bonds in the acyl chain seemed to be unimportant for the activity, although the chains have largely different shapes, solely the chain length determining activity. In combination with previous results with other *Roseobacter* group bacteria, we could show that there is wide variance between AHL composition within the strains. Furthermore, no association of certain AHLs with different habitats like macroalgal surfaces or sediment could be detected.

Keywords: quorum-sensing; structure elucidation; Rhodobacteraceae; autoinducers; bacterial signaling; Heck coupling; mass spectrometry; gas chromatography; sediment; AHL

1. Introduction

N-acylhomoserine lactones (AHLs) are well known signalling compounds used by Gram-negative bacteria for quorum-sensing (QS)-driven cell-to-cell communication. QS is a cell density-dependant mechanism to regulate physiological traits like antibiotic production, cell differentiation or biofilm formation [1–7]. AHLs constitute a γ -lactone ring and an acyl side chain that is usually even-numbered and unbranched, ranging in chain length from C₄–C₁₈ [3]. The stereochemistry of the lactone ring

is S. Functional groups like hydroxy- or carbonyl-group can be present at C-3 of the acyl chain. The double bond of unsaturated AHLs is Z-configured and in the position ω -7, with few exceptions [3]. An additional double bond can occur at C-2 in E-configuration, a feature especially occurring in AHLs produced by marine *Roseobacter* group bacteria (Rhodobacteraceae). Roseobacters are abundant in the ocean, occurring in diverse habitats [8], e. g. in open waters, shore environments, sediments, attached to biotic and abiotic surfaces as well as in symbiosis with higher organisms like algae [9–11]. AHLs of this bacterial group have saturated, unsaturated and sometimes oxygenated acyl chains, ranging in length between C₈ and C₁₈ [12] with the exception of aromatic *p*-coumaroylhomoserine lactone produced by *Ruegeria pomeroyi* DSS-3 [13]. They are involved in various biological traits [14], e.g., in the production of the antibiotic tropodithietic acid in *Phaeobacter inhibens* [5] or cell differentiation in *Dinoroseobacter shibae* [4].

In a broader program, we currently look into the inventory of AHLs occurring in *Roseobacter* group bacteria. A non-targeted analytical approach was developed using extraction of AHLs from bacterial cultures by XAD-16 adsorption, solvent extraction, and direct analysis by GC/MS. This approach combines high-sensitivity with unbiased analysis and allows structural proposals to be made basing on the information rich EI-mass spectra obtained. We could successfully use this approach to identify several previously unknown AHLs [12,15,16] as well as related *N*-acylalanine methyl esters (NAMEs) [17,18]. We have previously analyzed AHLs from roseobacters isolated from macroalgae surfaces and found a high proportion of strains producing AHLs in various mixtures [12]. A specific AHL signature of macroalgae associated strains was not observed. In an extension of this study we investigated 16 strains obtained from one location of samples of the algae *Fucus spiralis*, collected from a single location (Neuharlingersiel, German Wadden Sea), nine strains from Norwegian trench sediments [19] and one sea water strain from the German/Danish coast to test for the occurrence of specific AHL signatures. During this investigation we detected two previously unreported AHLs, their identification, synthesis, and biological activities being reported.

2. Results

2.1. Occurrence of *N*-acylhomoserine Lactones in *Roseobacter* Group Bacteria of *Fucus Spiralis* and the Eastern North Sea

Sixteen roseobacters originating from *Fucus spiralis* from the German Wadden Sea and 10 strains from the eastern North Sea were cultivated in marine broth and analyzed for the presence of AHLs by GC/MS as described previously [12,20]. AHLs were detected in eight of the isolates from *F. spiralis* (50%) and three of the sediment strains (33%) as well as in the open water strain (Table 1). The highest numbers of individual compounds were detected on the extracts obtained from *Octadecabacter* sp. (Lw-22) and *Loktanella* sp. (D15 (40)), 12 and 13 AHLs being detected, exhibiting a distinct qualitative profile. The sediment strain *Phaeobacter* sp. (SK040) contained nine different AHLs, while the other sediment strains SK013 and SK032 had only one or two AHLs, comparable to the water column strain. The AHL composition of other strains varied between single compounds and mixtures (Table 1).

Octadecenoylhomoserine lactone (C18:1-HSL) and C16:1-HSL were the most common compounds, produced by six of the 12 bacteria. *Roseovarius* sp. D12-1.68 displayed a unique profile due to the presence of C12:0 as major AHL with a relatively short chain length compared to most other major AHLs of roseobacters [12,15,21]. *Dinoroseobacter shibae* MDLw-58 produced three different isomers of the C18:2-HSL, consistent with previous observations of closely related strains [20]. While the major component was 2*E*,11*Z*-C18:2-HSL, the location and configuration of the double bonds in the other two isomers remains unknown. Other diunsaturated AHLs with shorter chain lengths, rarely observed in strains taxonomically distant from roseobacters, occurred as well. These include C16:2-HSL in *Huaishuia* sp. SK032, C14:2-HSL in *Octadecabacter* sp. Lw-22 and several strains containing C12:2-HSL. Because this AHL was not previously reported and due to its abundant occurrence in the investigated strains, we determined its structure of this new AHL, as reported in Section 2.2. Less abundant were

the oxygenated AHLs, 3-OH-C10- and 3-OH-C14-HSL. The only odd numbered AHLs were C15:0-HSL, C15:1-HSL and C17:1-HSL which occurred as minor components in several strains.

Table 1. AHL production of *Roseobacter* group isolates from *Fucus spiralis* (German Wadden Sea) and sediments as well as open waters (Eastern North Sea) ^a.

Strain	Genus Affiliation	C12:0	C12:1	C12:2 (11)	C12:2 (13)	3-OH-C10	3-OH-C14	C14:0	C14:1	C14:2	C15:0	C15:1	C16:0	C16:1	C16:2	C17:1	C18:0	C18:1	C18:2	C18:2	C18:2
<i>Fucus Spiralis</i>																					
D12-1.68	<i>Roseovarius</i> sp.	94.4							1.3			4.3									
D3	<i>Loktanella</i> sp.			15.7	2.4	21.2	60.7														
Lw-22	<i>Octadecabacter</i> sp.	6.6	3.7	0.7				4.6	72.7	4.3	1.2	1.9	0.9	0.6			1.1	1.8			
D4 (50)	<i>Octadecabacter</i> sp.	8.3	25.8	4.4									1.1	0.7							59.8
Lw-26b	<i>Loktanella</i> sp.						100														
D15 (40)	<i>Loktanella</i> sp.	3.9	5.9	1.2	0.9	18.4	2.3	58.6			0.5	0.8	0.6	6.1			0.5	0.3			
Lw-55a	<i>Loktanella</i> sp.																				100
MDLw-58	<i>Dinoroseobacter</i> sp.																	5.4	3.9	2.5	88.2
Sediment																					
SK013	<i>Shimia</i> sp.																				100
SK032	<i>Huaishuia</i> sp.												81.7	18.3							
SK040	<i>Phaeobacter</i> sp.	5.8	3.7	1.4	7.3	4.4							4.8	64.9	3.5		4.1				
Water Column																					
SK038	<i>Sulfitobacter</i> sp.													100							

^a relative amounts of AHLs for each strain in %. No AHLs detected in *Puniceibacterium* sp. Lw-III1a, *Sulfitobacter* sp. B15 G2, *Pseudoceanicola* sp. Lw-13e, *Roseobacter* sp. B14, *Loktanella* sp. SK033, *Phaeobacter* sp. N051, *Sulfitobacter* sp. B14 27, A12, D4 55, SK012, *Citricella* sp. Lw-41a, *Roseovarius pelophilus* G511, *Tateyamaria pelophila* SAM4, *Pseudoruegeria* sp. SK021.

2.2. Identification and Synthesis of New Diunsaturated N-acylhomoserine Lactones from the *Roseobacter* Group

During these analyses two compounds, **A** as the major component and **B** in lower concentration, were detected in five of the strains, whose mass spectra showed similarity to those of other AHLs. The spectra of **A** (Figure 1b) and **B** (Supplementary Figure S1) were very similar, although the quality of the spectra was often low due to overlapping peaks from other compounds. To elucidate their structure, analysis of mass spectral data and total synthesis were performed.

Electron impact mass spectra of AHLs have a typical fragmentation pattern shown in Figure 1a. AHLs are characterized by the fragment ions m/z 102, 143 and a small $[M]^+$ [15,22]. The ion m/z 102 is formed by α -cleavage of the homoserine lactone unit and transfer of two hydrogens, while McLafferty-rearrangement forms the ion m/z 143. The intensity of m/z 102 is higher in monounsaturated compared to diunsaturated AHLs and the intensities of m/z 102 and 143 decrease with the acyl chain length [15]. Cleavage of the homoserine moiety explains the ion $[M-101]^+$, m/z 264, in the spectrum of (*Z*)-11-octadecenylhomoserine lactone (Z11-C18:1-HSL, Figure 1a).

Compound **A** and **B** showed both ions m/z 102 and 143 and a putative $[M]^+$ at m/z 279, indicating to be C12:2-homoserine lactones (C12:2-HSL). Additional ions at m/z 94 and 107, untypical for AHLs, were present in high intensity. The gas chromatographic retention index of **A** was 2422 and that of **B** 2388. High resolution ESI-MS of **A** delivered an ion at m/z 280.19071 $[M + H]^+$, consistent with the formula $C_{16}H_{26}NO_3$ (calc. 280.19072) required for an diunsaturated AHL. The homoserine lactone unit is indicated by the ion m/z 102.05496 ($C_4H_8NO_2$) and the acyl chain by the ion m/z 179.14314 ($C_{12}H_{19}O$) in the ESI spectrum [18]. The location of the double bonds could not be determined with dimethyl disulfide derivatization [12,20] because of the low concentration of the compound. Nevertheless, the usual ω -7 position of double bonds in AHLs and the previous detection of Z5-C12:1-HSL in roseobacters [12] suggested **A** to be 2*E*,5*Z*-C12:2-HSL, because the second double-bond in all known natural AHLs is located at C-2 with *E*-configuration. The close proximity of the double bonds might also favor a double bond shift into conjugation during biosynthesis with concomitant double bond isomerization, leading to 2*E*,4*E*-C12:2-HSL. Furthermore, deconjugation is a known process known to occur during formation of α,β -unsaturated amides under basic conditions, leading potentially to 3*E*,5*Z*-C12:2-HSL [23,24]. Therefore, we decided to synthesize all three compounds to reveal insight

into the MS and GC behavior of the isomers and also allowing to perform bioassays to investigate whether slight changes in double bond location and geometry have an influence on the activity in AHL reporter assays.

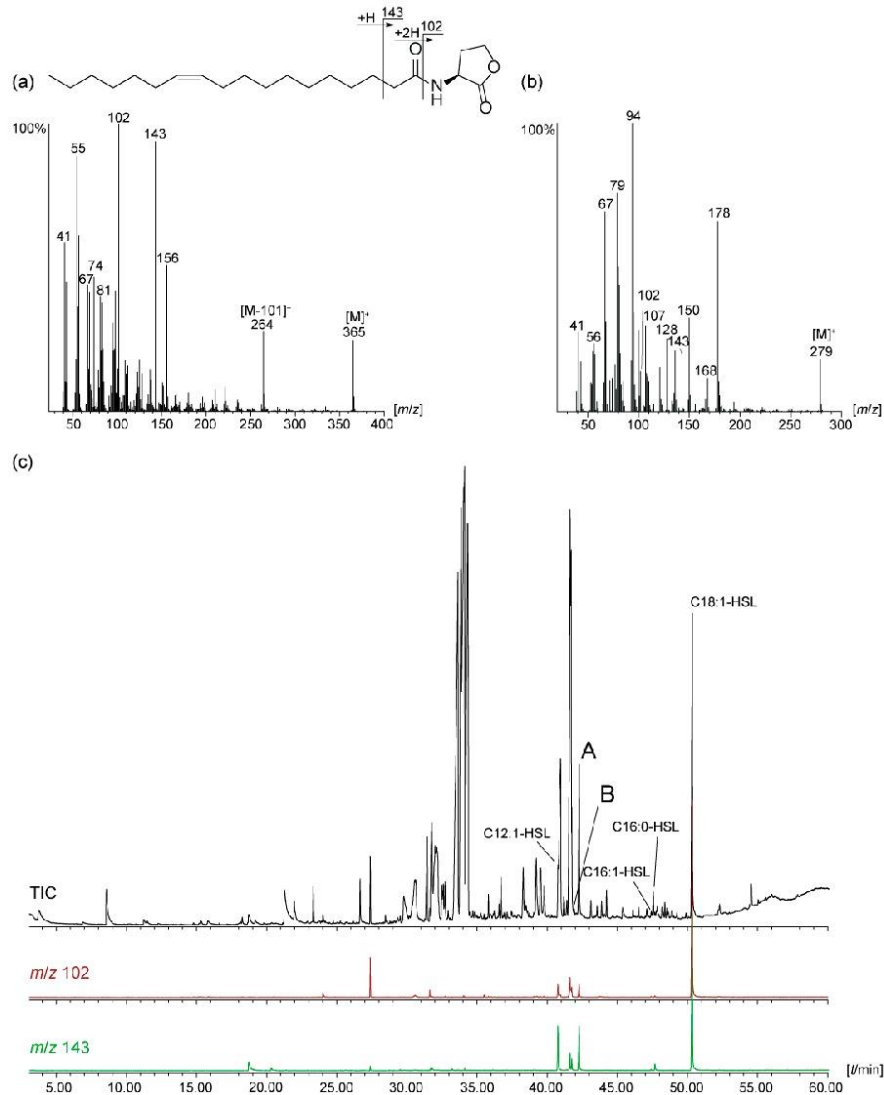
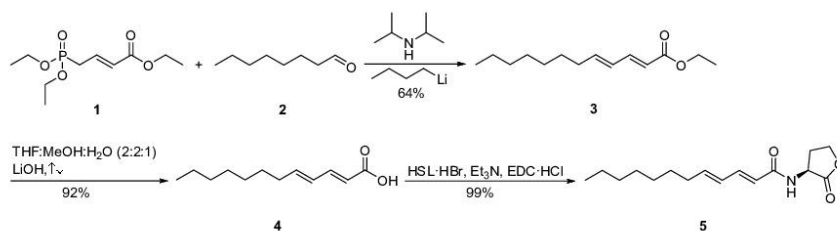


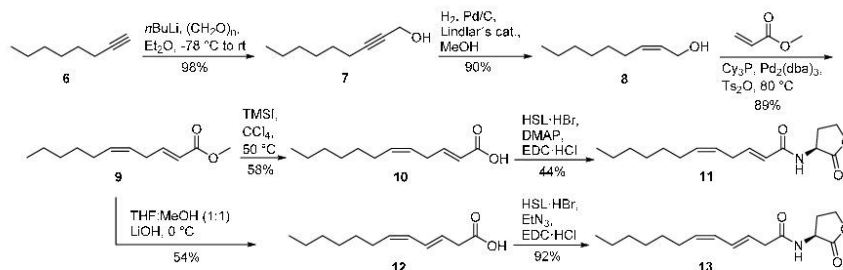
Figure 1. (a) Mass spectrum and fragmentation pattern of *N*-((*Z*)-11-octadecenyl)homoserine lactone (Z11-C18:1-HSL); (b) mass spectrum of the unknown AHL A; (c) total ion chromatogram of the natural extract of *Octadecabacter* D4 (50) and characteristic ion traces *m/z* 102 and 143, indicating potential presence of AHLs.

The synthesis of 2*E*,4*E*-C12:2-HSL (**5**) started with a homologous Horner-Wadsworth-Emmons reaction of triethyl (*E*)-4-phosphonocrotonate (**1**) with octanal (**2**) to furnish ethyl (2*E*,4*E*)-2,4-dodecadienoate (**3**) (Scheme 1). After saponification with lithium hydroxide, **4** was coupled with L-homoserine lactone hydrobromide (HSL·HBr) in the presence of *N*-(3-dimethylaminopropyl)-*N'*-ethylcarbodiimide hydrochloride (EDC·HCl) and triethylamine, yielding the desired AHL *N*-((2*E*,4*E*)-2,4-dodecadienyl)homoserine lactone (**5**).



Scheme 1. Synthesis of *N*-((2*E*,4*E*)-2,4-dodecadienyl)homoserine lactone (2*E*,4*E*-C12:2-HSL, **5**). L-homoserine lactone hydrobromide (HSL·HBr), *N*-(3-dimethylaminopropyl)-*N'*-ethylcarbodiimide hydrochloride (EDC·HCl).

The isomers 2*E*,5*Z*-C12:2-HSL (**11**) and 3*E*,5*Z*-C12:2-HSL (**13**) were synthesized from octyne (**6**) (Scheme 2). The addition of paraformaldehyde furnished non-2-yn-1-ol (**7**). The allylic alcohol (*Z*)-non-2-en-1-ol (**8**) was obtained after hydrogenation with Lindlar's catalysts. A Heck reaction according to Tsukuda et al. [25] using methyl acrylate instead of butyl acrylate yielded in excellent yield the desired diastereomerically pure methyl (2*E*,5*Z*)-2,5-dodecadienoate (**9**) that was saponified with lithium hydroxide. The basic conditions lead to a rearrangement of the double bond from C-2 to C-3, forming acid **12**. This acid was coupled with HSL·HBr in the presence of EDC·HCl and triethylamine to form *N*-((3*E*,5*Z*)-3,5-dodecadienyl)homoserine lactone (**13**). The saponification of ester **9** can also be performed under milder conditions, thus preventing the rearrangement. First, ester **9** was transesterified to the trimethylsilyl ester (TMSI) in CCl₄. Aqueous hydrolysis delivers acid **10** without rearrangement [26]. Finally, acid **10** was coupled with HSL·HBr in the presence of EDC·HCl and *p*-dimethylaminopyridine (DMAP) to furnish *N*-((2*E*,5*Z*)-2,5-dodecadienyl)homoserine lactone (**11**). The isomerization of the double bond, leading again to **13**, can also be induced by the use of triethylamine in this step instead of the weaker base DMAP [24]. AHL **11** is not stable for prolonged storage under room temperature, leading to the isomerized compound **13** and other stereoisomers.



Scheme 2. Synthesis of *N*-((2*E*,5*Z*)-2,5-dodecadienyl)homoserine lactone (2*E*,5*Z*-C12:2-HSL, **11**) and *N*-((3*E*,5*Z*)-3,5-dodecadienyl)homoserine lactone (3*E*,5*Z*-C12:2-HSL, **13**). Tricyclohexylphosphine (C₇₅P), tris(dibenzylideneacetone)dipalladium (Pd₂(dba)₃), L-homoserine lactone hydrobromide (HSL·HBr), *N*-(3-dimethylaminopropyl)-*N'*-ethylcarbodiimide hydrochloride (EDC·HCl), *p*-dimethylaminopyridine (DMAP).

Comparison of both mass spectra (Figure 2) and gas chromatographic retention indices of the synthesized AHLs with those of the natural compounds indicated the unknown major AHL **A** to be *2E,5Z-C12:2-HSL (11)*, while the minor component **B** is its rearrangement product, *3E,5Z-C12:2-HSL (13)*. The mass spectrum of **5** differs from those of **11** and **13**, showing an ion at m/z 180 instead of m/z 178. The ions m/z 94, 102, 107 and 143 are present, but the intensity of these fragment ions is different to those of the natural compounds, as is the retention index of 2510. HR-MS data showed that the ions m/z 107 and 94, not observed in high intensity in other diunsaturated AHLs with longer acyl chains, are composed of C_8H_{11} and C_6H_6O , respectively. They seem to be formed by acyl cleavage followed by allylic chain cleavage with or without previous elimination of water.

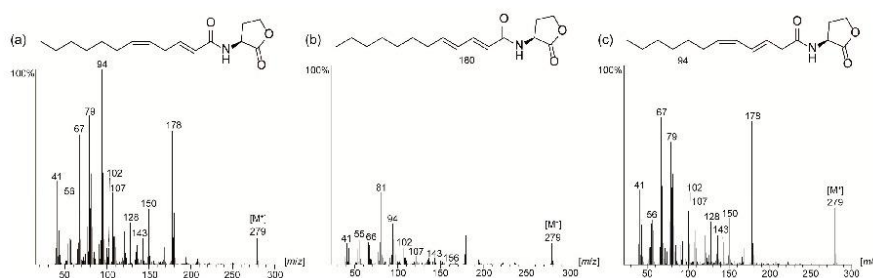


Figure 2. Mass spectra of synthetic AHLs: (a) *2E,5Z-C12:2-HSL (11)*; (b) *2E,4E-C12:2-HSL (5)*; (c) *3E,5Z-C12:2-HSL (13)*.

2.3. Activity of *N*-acylhomoserine Lactones in AHL Reporter Assays

The three C12:2-HSLs **5**, **11**, and **13** as well as *2E,11Z-C18:2-HSL*, a major AHL of the *Roseobacter* group model strain *Dinoroseobacter shibae* DFL12 [4,20] were tested for quorum sensing activity with two sensor strains (Table 2). *Escherichia coli* MT102 (pJBA132) [27] responds primarily to short chain AHLs while *Pseudomonas putida* F117 (pRK-C12) [28] prefers long chain AHLs. Both strains do not produce AHLs but are able to respond to them through the expression of a LuxR-controlled promoter fused to a gene coding for an easily detectable output signal, fluorescence [15]. In addition, C6:0-, C8:0- and 3-oxo-C8:0-HSL for *E.coli* MT102 and Z9-C16:1-, 3-oxo-C8:0- and 3-oxo-C12:0-HSL for *P. putida* F117 were tested as references. The maximum fold induction with sensor strain *E.coli* MT102 was low for all target AHLs, **5**, **11**, **13** as well as *2E,11Z-C18:2-HSL*, but C6 and C8-HSLs showed activity as expected.

Table 2. Activity of synthetic AHLs in quorum sensing experiments with the sensor strains *E.coli* MT102 (pJBA132) and *P. putida* F117 (pRK-C12). Maximum fold induction.

AHL ^a	MT102	F117
<i>2E,4E-C12:2 (5)</i>	1.00 ± 0.01	81.22 ± 1.26
<i>2E,5Z-C12:2 (11)</i>	1.01 ± 0.01	78.03 ± 2.05
<i>3E,5Z-C12:2 (13)</i>	1.03 ± 0	73.64 ± 2.34
<i>2E,11Z-C18:2</i>	1.02 ± 0.01	1.32 ± 0.04
3-oxo-C8:0	13.41 ± 0.49	30.46 ± 2.79
C6:0	17.09 ± 1.04	
C8:0	10.24 ± 0.55	
3-oxo-C12:0		77.75 ± 2.51
Z9-C16:1		72.37 ± 2.47

^a The final concentration of each tested compound was 10 μ M.

In contrast, sensor *P. putida* F117, most sensitive to C12:0-HSL [16], showed high induction upon exposure to AHLs **5**, **11**, and **13**, as well as 3-oxo-C12:0-HSL and Z9-C16:1-HSL, a lower activity for 3-oxo-C8:0-HSL being noted. The almost identical values exhibited by the four C12 compounds evidence a certain degree of selectivity dependent on chain length, but the reporter strain is insensitive to position and configuration of the double bonds, as well as presence or absence of a 3-oxo functional group.

3. Discussion

The unknown AHL **A** was identified to be 2*E*,5*Z*-C12:2-HSL (**11**). This new AHL is the smallest AHL with two double-bonds identified so far and occurs in several roseobacters. The minor 3*E*,5*Z*-C12:2-HSL (**13**) seems to be a rearrangement product of **11**. Although we cannot exclude that the process took place during work-up, the observed chemical instability of **11** may point to the formation of **13** as a bacterial metabolic product. Different roseobacters are able to produce a bishomologous series of diunsaturated AHLs with double-bonds at C-2 and the ω -7 position [12,15,16,20]. AHL **11** extends this series to a shorter C₁₂ chain length. It is also within the preferred chain-length of major AHLs of roseobacters that ranges from C₁₂ to C₁₈, with the exception of 3-OH-C10-AHL. Although we analyzed many roseobacters for AHL presence using GC/MS as well as HPLC/MS methods, we never found evidence for the presence of *p*-coumaroyl-HSL reported from *Ruegeria pomeroyi* DSS-3 [13] in any of these strains.

Although the AHLs **5**, **11** and **13** have the same chain length, the shape of the side chain differs. The two (*E*)-configured double bonds of 2*E*,4*E*-C12:2-HSL lead to a straight aliphatic chain, while the (*Z*)-configured double-bonds in 2*E*,5*Z*-C12:2-HSL and 3*E*,5*Z*-C12:2-HSL induce a bend in the chain. 3-oxo-C12:0-HSL even has a bend chain due to H-bonding towards the amide carbonyl group [29]. Obviously, there is no influence of the chain configuration on the activity of the reporter strain. Therefore, the configuration of the side chain does not seem to be recognized by the receptor, although the chain-length obviously is. Whether this is also true for the cognate receptors in the roseobacters is unknown. Nevertheless, the (2*E*)-double bond is not common in fatty acids of roseobacters [30] and thus the prominent occurrence of this structural motif and of diunsaturated AHLs in general indicate the importance of the double bonds for their function as signaling compounds of these bacteria.

No general association of specific AHLs or their mixtures with certain habitats was observed. This includes strains originating from the same host organism as *F. spiralis* reported here, but also strains from the sediment or the water phase [12,15]. In general, surface-associated strains seem to produce AHLs more often under laboratory conditions compared to those obtained from sediments or the water column.

4. Materials and Methods

4.1. General Experimental Procedures

General conditions: Chemicals were obtained from Sigma-Aldrich (Taufkirchen, Germany), Carl Roth (Karlsruhe, Germany) or from Acros Organics (Schwerte, Germany) and were used without further purification. Solvents were purified by distillation and dried according to standard procedures. Moisture- and/or oxygen-sensitive reactions were carried out under a nitrogen atmosphere in vacuum-heated flasks with dried solvents. Thin-layer chromatography (SiO₂, TLC) was performed on 0.20 mm Macherey-Nagel silica gel plates (Polygram SIL G/UV254), and column chromatography was performed with Merck silica gel 60 (0.040–0.063 mm) by using standard flash chromatographic methods. NMR spectra were recorded on DRX-400 (400 MHz), AV III-400 (400 MHz) or AV II-600 (600 MHz) spectrometers (Bruker: Bremen, Germany), and were referenced against TMS (δ = 0.00 ppm), CDCl₃ (δ = 7.26 ppm) for ¹H-NMR and CDCl₃ (δ = 77.01 ppm) for ¹³C-NMR experiments. GC/MS analyses of extracts were carried out on an GC 7890A gas chromatograph connected to a 5975C mass-selective detector (Agilent; Waldbronn, Germany). Synthetic samples were analyzed on an HP

GC 6890 system connected to an HP 5973 mass selective detector fitted with a HP-5 MS fused-silica capillary column (30 m × 0.25 mm i.d., 0.22 µm film; (Agilent; Waldbronn, Germany). Conditions were as follows: carrier gas (He): 1.2 mL min⁻¹; injection volume: 1 mL; injector: 250 °C; transfer line: 300 °C, EI 70 eV. The gas chromatograph was programmed as follows: 50 °C (5 min isothermal), increasing with 5 °C min⁻¹ to 320 °C, and operated in splitless mode for XAD extracts and 50 °C (5 min isothermal), increasing with 10 °C min⁻¹ to 320 °C in split mode (20:1) for synthetic compounds. Gas chromatographic retention indices, *I*, were determined from a homologous series of *n*-alkanes. Acids were transformed into volatile trimethylsilyl esters with *N*-methyl-*N*-(trimethylsilyl)trifluoroacetamide (MSTFA) for analysis by GC/MS [31]. HRMS analyses were carried out on a Thermo Fisher linear iontrap (Thermo Fisher: Bremen, Germany) coupled with an LTQ-Orbitrap mass spectrometer (Thermo Fisher: Bremen, Germany) using ESI positive mode. ESI measurements were performed by direct infusion mode using a custom-made micro-spray device mounted on a Proxeon nano-spray ion source. All solvents used were of LC/MS grade.

4.2. Strains and Culture Conditions

The bacterial strains were collected at various occasions in the North Sea [19]. Information on bacterial strains investigated is shown in Table 3.

Table 3. Bacterial isolates with GenBank accession number, genus affiliation and origin.

Strain	GenBank Acc No (16S)	Genus Affiliation	Strain Origin/Host	Location
Lw-III1a	KM268064	<i>Puniceibacterium</i> sp.	<i>Fucus spiralis</i>	Neuharlingersiel
B15 G2	KM268068	<i>Sulfitobacter</i> sp.	<i>Fucus spiralis</i>	Neuharlingersiel
Lw-13e	KM268063	<i>Pseudoceanicola</i> sp.	<i>Fucus spiralis</i>	Neuharlingersiel
D12-1.68	KM268065	<i>Roseovarius</i> sp.	<i>Fucus spiralis</i>	Neuharlingersiel
B14	KM268066	<i>Roseobacter</i> sp.	<i>Fucus spiralis</i>	Neuharlingersiel
B14 27	KM268072	<i>Sulfitobacter</i> sp.	<i>Fucus spiralis</i>	Neuharlingersiel
A12	KM268070	<i>Sulfitobacter</i> sp.	<i>Fucus spiralis</i>	Neuharlingersiel
D3	KC731427	<i>Loktanella</i> sp.	<i>Fucus spiralis</i>	Neuharlingersiel
D4 55	KM268071	<i>Sulfitobacter</i> sp.	<i>Fucus spiralis</i>	Neuharlingersiel
Lw-22	KM268073	<i>Octadecabacter</i> sp.	<i>Fucus spiralis</i>	Neuharlingersiel
D4 50	KM268074	<i>Octadecabacter</i> sp.	<i>Fucus spiralis</i>	Neuharlingersiel
Lw-26b	KM268054	<i>Loktanella</i> sp.	<i>Fucus spiralis</i>	Neuharlingersiel
D15 40	KM268056	<i>Loktanella</i> sp.	<i>Fucus spiralis</i>	Neuharlingersiel
Lw-55a	KM268057	<i>Loktanella</i> sp.	<i>Fucus spiralis</i>	Neuharlingersiel
MDLw-58	KM268059	<i>Dinoroseobacter</i> sp.	<i>Fucus spiralis</i>	Neuharlingersiel
Lw-41a	KM268061	<i>Citricella</i> sp.	<i>Fucus spiralis</i>	Neuharlingersiel
N051	AJ968647	<i>Phaeobacter</i> sp.	German North Sea Coast	Tidal-flat sediment
G5II	AJ968650	<i>Roseovarius pelophilus</i>	German North Sea Coast	Tidal-flat sediment
SAM4	AJ968651	<i>Tateyamaria pelophila</i> ^a	German North Sea Coast	Tidal-flat sediment
SK012	HG423260	<i>Sulfitobacter</i> sp.	Danish North Sea	sediment
SK013	LAJH0000000	<i>Shiimia</i> sp. ^b	Norwegian North Sea	sediment
SK021	HG423263	<i>Pseudoruegeria</i> sp. ^b	Norwegian North Sea	sediment
SK032	HG423269	<i>Huainhuia</i> sp.	German North Sea	sediment
SK033	HG423270	<i>Loktanella</i> sp.	Norwegian North Sea	sediment
SK040	HG423272	<i>Phaeobacter</i> sp.	Danish North Sea	sediment
SK038	HG423271	<i>Sulfitobacter</i> sp.	German North Sea	seawater

^a [32]; ^b [33,34].

4.3. Bacteria Cultivation and XAD Extraction

Bacterial strains were inoculated from marine broth (MB) medium agar plates into a preculture (50 mL, MB medium) and were cultivated for one to three days at 20/28 °C and 160 rpm. Bacterial cultures (100 mL) were grown from precultures for three to five days in MB medium at 20/28 °C and 160 rpm containing Amberlite XAD-16 (2 g). The XAD-16 resin was cleaned using Soxhlet extraction with acetonitrile, methanol and finally diethyl ether. The adsorbent was separated from the culture by filtration and extracted three times with CH₂Cl₂/H₂O (10:1). The combined organic phases were

dried with MgSO_4 , and the solvent was removed under reduced pressure. The extract was dissolved in CH_2Cl_2 (50 μL) and analyzed by GC/MS [20].

4.4. AHL Reporter Assays

The sensor strain *Pseudomonas putida* pRK-C12 [27] was inoculated from plates into a preculture which was grown on LB medium (20 mL with 20 mg/mL gentamycin) at 30 °C with shaking (160 rpm) overnight. The next day fresh medium was added, and the culture was grown on a shaking platform for 1–2 h until an OD620 value of 1.0 was reached. For the test, LB medium (99 μL) and 1 μL of the test compound (final concentration 10 μM , stock solution 1 mg/mL in dichloromethane) were pipetted into 96-well microtiter plates, and the sensor strain (100 μL) was added. Microtiter plates were incubated at 30 °C and shaken. Fluorescence was determined in a Victor 1420 Multilabel Counter (Perkin Elmer; Rodgau, Germany) at an excitation wavelength of 485 nm and a detection wavelength of 535 nm every 60 min for the first 6 h, and finally after 24 h of incubation. The OD620 value was also measured. Dichloromethane was used as negative control, and synthetic 3-oxo-C12:0-HSL was used as positive control. Fold induction of fluorescence was calculated by dividing the specific fluorescence (gfp535/OD620) of the test sample by the specific fluorescence of the negative control. Mean and standard deviation of three biological replicas after 6 h were determined, because fluorescence decreased slightly in the 24 h time point. The sensor strain *Escherichia coli* MT102 [29] was used as described [15] and the highest values obtained after 24 h in this case are reported in Table 2.

4.5. Synthetic Procedures

4.5.1. L-Homoserine Lactone Hydrobromide

A solution of bromoacetic acid (5.12 g, 36.9 mmol) and L-methionine (5.00 g, 33.5 mmol) in $\text{H}_2\text{O}/2$ -propanol/AcOH (5:5:2, 48.3 mL) was heated to reflux for 8 h. The solvent of the cooled mixture was evaporated. The orange solid was dissolved in dioxane/HCl (2:1, 20.1 mL), heated 10 min at 50 °C and stirred for 5 h at room temperature. The reaction mixture was placed in a fridge over night to evoke precipitation. L-Homoserine lactone hydrobromide was obtained by filtration and washed with cold isopropanol (3.19 g, 17.5 mmol, 52%) [35].

$^1\text{H-NMR}$ (400 MHz, DMSO-d_6): δ = 4.44 (t, J = 8.8 Hz, 1H), 4.36–4.25 (m, 2H), 2.60–2.51 (m, 1H), 2.42–2.31 (m, 1H); $^{13}\text{C-NMR}$ (100 MHz, DMSO-d_6): δ = 173.4, 66.3, 47.8, 27.0; MS (70 eV, EI): m/z (%): 43 (100), 57 (90.5), 56 (62.4), 42 (40.1), 44 (16.0), 41 (8.3), 101 (5.0) [M^+], 54 (4.8), 39 (4.3), 73 (4.0).

4.5.2. Ethyl (2E,4E)-2,4-Dodecadienoate (3)

N,N-Diisopropylamine (1.64 mL, 11.7 mmol) was dissolved in THF (25 mL) and cooled to -78 °C. *n*-Butyl lithium in hexane (1.6 M, 4.88 mL, 7.8 mmol) was added slowly to the mixture. The solution was stirred for 10 min at -78 °C, followed by 15 min at 0 °C. (*E*)-Triethyl-4-phosphonocrotonate (1, 1.30 mL, 5.8 mmol) was added slowly at -78 °C under stirring and after 15 min octanal (2, 0.61 mL, 3.9 mmol) was added at the same temperature, again stirring continued for 15 min. The reaction mixture was allowed to warm up to room temperature and stirred for 2.5 h. Sat. NH_4Cl solution was added and the mixture was extracted three times with ethyl acetate. The combined organic phases were dried with MgSO_4 , filtered and the solvent was evaporated in *vacuo*. The crude product was purified by flash chromatography on silica [pentane/EtOAc (30:1)] to receive the desired product as a clear oil (280 mg, 1.25 mmol, 64%) [36].

R_f = 0.4 (pentane/EtOAc 30:1); $^1\text{H-NMR}$ (400 MHz, CDCl_3): δ = 7.29–7.22 (m, 1H), 6.20–6.08 (m, 2H), 5.78 (d, J = 15.4 Hz, 1H), 4.19 (q, J = 7.2 Hz, 2H), 2.16 (q, J = 7.0 Hz, 2H), 1.43 (quin, J = 7.3 Hz, 2H), 1.32–1.24 (m, 11H), 0.88 (t, J = 7.1 Hz, 3H); $^{13}\text{C-NMR}$ (100 MHz, CDCl_3): δ = 167.3, 145.1, 144.8, 128.3, 119.1, 60.1, 33.0, 31.8, 29.1, 29.1, 28.7, 22.6, 14.3, 14.1; MS (70 eV, EI): m/z (%): 125 (100), 97 (58.4), 81 (51.7), 67 (39.6), 179 (34.9), 98 (30.6), 79 (30.5), 95 (25.3), 127 (22.8), 99 (22.4), 224 (21.0) [M^+].

4.5.3. (2E,4E)-2,4-Dodecadienoic Acid (4)

Lithium hydroxide (106.8 mg, 4.46 mmol) was added to a stirred solution of ester 3 (50 mg, 0.22 mmol) in THF/MeOH/H₂O (2:2:1) and stirred for 12 h under reflux. The mixture was acidified with 2 M sulfuric acid and extracted three times with dichloromethane. The combined organic phases were dried with Na₂SO₄, filtered and concentrated in *vacuo* to get the desired product after purification by flash chromatography on silica [pentane/EtOAc (2:1)] as a white solid (39.9 mg, 0.20 mmol, 92%).

R_f = 0.3 (pentane/EtOAc 2:1); ¹H-NMR (400 MHz, CDCl₃): δ = 7.35 (dd, *J* = 15.3, 10.0 Hz, 1H), 6.24–6.16 (m, 2H), 5.78 (d, *J* = 15.3 Hz, 1H), 2.18 (q, *J* = 7.3 Hz, 2H), 1.43 (quin, *J* = 7.3 Hz, 2H), 1.33–1.20 (m, 8H), 0.88 (t, *J* = 7.0 Hz, 3H); ¹³C-NMR (100 MHz, CDCl₃): δ = 172.8, 147.5, 146.3, 128.2, 118.2, 33.1, 31.8, 29.1, 29.1, 28.6, 22.6, 14.1; MS (70 eV, EI, trimethylsilyl ester): *m/z* (%): 169 (100), 253 (64.0), 73 (31.9), 155 (30.1), 170 (20.5), 75 (17.5), 254 (15.7), 268 (13.8) [M⁺], 81 (13.4), 171 (9.2).

4.5.4. N-((2E,4E)-2,4-Dodecadienyl)homoserine Lactone (5)

L-Homoserine lactone hydrobromide (53 mg, 0.29 mmol) was dissolved in dry dichloromethane. Triethylamine (0.04 mL, 0.29 mmol) was added to the solution, followed by the addition of acid 4 (57 mg, 2.29 mmol) and EDC·HCl (56 mg, 0.29 mmol). The reaction mixture was stirred for 12 h at room temperature and washed with H₂O, sat. NaHCO₃ solution, and brine. The organic layers were extracted three times with dichloromethane, dried with Na₂SO₄, filtered and concentrated. The crude product was purified by flash chromatography on silica [pentane/EtOAc (1:1)] to obtain pure AHL 5 (80.6 mg, 0.28 mmol, 99%).

R_f = 0.3 (pentane/EtOAc 1:1); ¹H-NMR (600 MHz, CDCl₃): δ = 7.23 (dd, *J* = 15.0, 9.7 Hz, 1H), 6.25 (br s, 1H), 6.17–6.08 (m, 2H), 5.81 (d, *J* = 15.1 Hz, 1H), 4.66 (ddd, *J* = 11.6, 8.6, 6.0 Hz, 1H), 4.48 (td, *J* = 9.0, 1.1 Hz, 1H), 4.31 (ddd, *J* = 11.3, 9.3, 5.9 Hz, 1H), 2.87 (dddd, *J* = 12.5, 8.5, 5.9, 1.2 Hz, 1H), 2.22–2.18 (m, 1H), 2.15 (q, *J* = 7.0 Hz, 2H), 1.41 (quin, *J* = 7.0 Hz, 2H), 1.33–1.26 (m, 8H), 0.88 (t, *J* = 7.2 Hz, 3H); ¹³C-NMR (150 MHz, CDCl₃): δ = 175.5, 166.6, 144.4, 142.7, 127.8, 119.9, 66.0, 49.2, 32.8, 31.5, 30.4, 28.9, 28.9, 28.5, 22.4, 14.0 (Supplementary Figure S4); HRMS (ESI+) *m/z*: 302.1728 [M + Na]⁺, calculated for C₁₆H₂₅NO₃Na 302.1727 [M + Na]⁺.

4.5.5. Non-2-yn-1-ol (7)

n-Butyl lithium in hexane (1.6 M, 31.25 mL, 50 mmol) was added at −78 °C to a stirred solution of 1-octyne (6, 5 g, 45 mmol) in dry diethyl ether and stirred for 30 min. Paraformaldehyde (2.77 g, 90 mmol) was added and the mixture was allowed to warm up to room temperature. Sat. NH₄Cl solution was added, the phases were separated and extracted three times with diethyl ether. The combined organic phases were washed with brine, dried with Na₂SO₄, filtered and the solvent was evaporated. The crude product was purified by flash chromatography on silica [pentane/EtOAc (7:1)] to furnish the desired product as a clear oil (6.2 g, 40 mmol, 98%) [37].

R_f = 0.4 (pentane/EtOAc 7:1); ¹H-NMR (400 MHz, CDCl₃): δ = 4.25 (dt, *J* = 5.8, 2.1 Hz, 2H), 2.21 (tt, *J* = 7.1, 2.2 Hz, 2H), 1.51 (quin, *J* = 7.3 Hz, 2H), 1.41–1.24 (m, 6H), 0.89 (t, *J* = 6.8 Hz, 3H); ¹³C-NMR (100 MHz, CDCl₃): δ = 86.7, 78.3, 51.4, 31.3, 28.6, 28.5, 22.5, 18.7, 14.0; MS (70 eV, EI): *m/z* (%): 67 (100), 55 (97.2), 41 (95.0), 93 (73.4), 70 (72.5), 39 (68.8), 43 (64.0), 69 (58.0), 79 (57.4), 83 (56.5), 122 (10.0) [M⁺·H₂O].

4.5.6. Non-2-en-1-ol (8)

Lindlar's catalyst (50 mg) was added to a solution of ynol 7 (500 mg, 3.57 mmol) and methanol (10 mL). The mixture was stirred for 20 min at room temperature under a H₂ atmosphere. The catalyst was filtered through a short pad of silica and the solvent was evaporated. The product was received after purification by flash chromatography on silica [pentane/EtOAc (10:1)] as a colorless oil (454 mg, 3.19 mmol, 90%).

R_f = 0.3 (pentane/EtOAc 10:1); ¹H-NMR (400 MHz, CDCl₃): δ = 5.63–5.51 (m, 2H), 4.2 (d, *J* = 6.0 Hz, 2H), 2.07 (q, *J* = 6.7 Hz, 2H), 1.40–1.23 (m, 8H), 0.88 (t, *J* = 7.0 Hz, 3H); ¹³C-NMR (100 MHz, CDCl₃):

δ = 133.3, 128.3, 58.6, 31.7, 29.6, 28.9, 27.4, 22.6, 14.1; MS (70 eV, EI): m/z (%): 57 (100), 41 (69.6), 55 (50.7), 43 (49.0), 54 (41.0), 67 (39.4), 82 (38.7), 81 (36.0), 68 (34.6), 95 (33.7), 124 (22.7) [$M^+ - H_2O$], 142 (0.3) [M^+].

4.5.7. Methyl (2E,5Z)-2,5-Dodecadienoate (9)

The allylic alcohol **8** (454 mg, 3.19 mmol) was added to a mixture of tris(dibenzylideneacetone) dipalladium (83 mg, 0.08 mmol), tricyclohexylphosphine (45 mg, 0.16 mmol) and *p*-toluenesulfonic anhydride (1.25 g, 3.8 mmol) in methyl acrylate (16 mL) and stirred for 12 h at 80 °C in a special high-pressure vial under argon. The catalyst was filtered through a short silica column and washed with diethyl ether. The solvent was evaporated in *vacuo* and the crude product was purified by flash chromatography on silica [pentane/EtOAc (30:1)] to the desired product (599.7 mg, 2.85 mmol, 89%) [25].

R_f = 0.4 (pentane/EtOAc 30:1); 1H -NMR (400 MHz, $CDCl_3$): δ = 6.97 (dt, J = 15.7, 6.4 Hz, 1H), 5.82 (dt, J = 15.7, 1.8 Hz, 1H), 5.56–5.34 (m, 2H), 3.73 (s, 3H), 2.88 (dd, J = 6.9, 6.3 Hz, 2H), 2.01 (q, J = 6.6 Hz, 2H), 1.38–1.26 (m, 8H), 0.88 (t, J = 7.1 Hz, 3H); ^{13}C -NMR (100 MHz, $CDCl_3$): δ = 167.1, 148.1, 133.8, 124.9, 121.1, 51.4, 35.1, 32.6, 31.7, 29.3, 28.8, 22.6, 14.1; MS (70 eV, EI): m/z (%): 79 (100), 111 (90.3), 81 (70.2), 67 (63.6), 41 (60.0), 210 (52.8) [M^+], 55 (50.0), 95 (47.4), 80 (47.3), 100 (45.9).

4.5.8. (2E,5Z)-2,5-Dodecadienoic Acid (10)

Trimethylsilyl iodide (0.038 mL, 0.268 mmol) was added to a stirred solution of ester **9** (30 mg, 0.134 mmol) in 0.5 mL CCl_4 and warmed to 50 °C for one hour. The mixture was washed with sat. NH_4Cl solution followed by sat. sodium thiosulfate solution and extracted three times with dichloromethane. The combined organic phases were dried with $MgSO_4$, filtered and concentrated in *vacuo* to get the desired product after purification by flash chromatography on silica [pentane/ Et_2O (5:1)] as a white solid (15 mg, 0.077 mmol, 58%).

R_f = 0.2 (pentane/ Et_2O 5:1); 1H -NMR (400 MHz, $CDCl_3$): δ = 7.08–7.01 (m, 1H), 5.81 (d, J = 15.6 Hz, 1H), 5.42–5.26 (m, 2H), 2.94 (dd, J = 6.9, 6.3 Hz, 2H), 2.01 (q, J = 6.9 Hz, 2H), 1.35–1.24 (m, 8H), 0.81 (t, J = 7.0 Hz, 3H); ^{13}C -NMR (100 MHz, $CDCl_3$): δ = 172.8, 148.8, 133.4, 124.4, 121.5, 33.0, 28.9, 28.8, 28.7, 27.8, 22.6, 14.0; MS (70 eV, EI, trimethylsilyl ester): m/z (%): 169 (100), 253 (42.4), 73 (40.2), 155 (21.9), 75 (19.9), 170 (15.1), 81 (13.5), 254 (8.8), 43 (8.7), 268 (8.0) [M^+].

4.5.9. N-((2E,5Z)-2,5-Dodecadienyl)homoserine Lactone (11)

L-Homoserine lactone hydrobromide (22 mg, 0.1224 mmol) was dissolved in dry dichloromethane, followed by the addition of *p*-dimethylaminopyridine (DMAP) (15 mg, 0.1224 mmol) and acid **10** (24 mg, 0.1224 mmol). EDC·HCl (23.5 mg, 0.1224 mmol) was added at 0 °C, the solution was stirred for 5 min at 0 °C and for 12 h at room temperature. The reaction mixture was washed one time with H_2O , sat. $NaHCO_3$ solution and brine. The organic layers were extracted three times with dichloromethane, dried with Na_2SO_4 , filtered and the solvent was evaporated. The crude product was purified by flash chromatography on silica [pentane/EtOAc (1:1)] to the desired AHL (15 mg, 0.054 mmol, 44%).

R_f = 0.2 (pentane/EtOAc 1:1); 1H -NMR (600 MHz, $CDCl_3$): δ = 6.91 (dt, J = 15.4, 6.4 Hz, 1H), 6.06 (br s, 1H), 5.83 (dt, J = 15.3, 1.7 Hz, 1H), 5.53–5.36 (m, 2H), 4.62 (ddd, J = 11.6, 8.6, 5.6 Hz, 1H), 4.50–4.47 (m, 1H), 4.33–4.28 (m, 1H), 2.92–2.87 (m, 3H), 2.20–2.12 (m, 1H), 2.01 (q, J = 7.0 Hz, 2H), 1.39–1.25 (m, 8H), 0.88 (t, J = 7.0 Hz, 3H); ^{13}C -NMR (150 MHz, $CDCl_3$): δ = 175.5, 166.3, 145.1, 133.8, 125.0, 122.5, 66.2, 49.4, 34.9, 32.6, 31.7, 30.7, 29.3, 28.9, 22.6, 14.1 (Supplementary Figure S2); HRMS (ESI+) m/z : 280.1909 [$M + H$] $^+$, calculated for $C_{16}H_{26}NO_3$ 280.1907 [$M + H$] $^+$; 302.1729 [$M + Na$] $^+$, calculated for $C_{16}H_{25}NO_3Na$ 302.1727 [$M + Na$] $^+$.

4.5.10. (3E,5Z)-3,5-Dodecadienoic Acid (12)

Lithium hydroxide (0.238 mL, 1.5 M) was added to a stirred solution of ester **9** (50 mg, 0.238 mmol) in THF/MeOH (1:1) and stirred for 3 h at 0 °C. The mixture was acidified with 1 M HCl and extracted three times with dichloromethane. The combined organic phases were dried with Na_2SO_4 , filtered and

concentrated in *vacuo* to get the desired product after purification by flash chromatography on silica [pentane/EtOAc (5:1)] as a white solid (25 mg, 0.128 mmol, 54%).

$R_f = 0.2$ (pentane/EtOAc 5:1); $^1\text{H-NMR}$ (400 MHz, CDCl_3): $\delta = 6.19\text{--}5.98$ (m, 2H), 5.72 (dt, $J = 15.1$, 7.1 Hz, 1H), 5.39 (dt, $J = 10.8$, 7.6 Hz, 1H), 3.10 (d, $J = 7.2$ Hz, 2H), 2.09 (q, $J = 7.6$, 7.2 Hz, 2H), 1.43–1.26 (m, 8H), 0.86 (t, $J = 6.9$ Hz, 3H); $^{13}\text{C-NMR}$ (100 MHz, CDCl_3): $\delta = 178.2$, 135.4, 134.7, 129.3, 121.3, 37.7, 31.7, 29.2, 28.9, 27.8, 22.6, 14.1; MS (70 eV, EI, trimethylsilyl ester): m/z (%): 73 (100), 75 (23.5), 253 (15.2), 74 (14.4), 268 (12.2) $[\text{M}^+]$, 79 (10.9), 150 (10.9), 41 (6.4), 67 (6.4), 224 (6.4).

4.5.11. *N*-(3*E*,5*Z*)-3,5-Dodecadienyl)homoserine Lactone (**13**)

L-Homoserine lactone hydrobromide (21.8 mg, 0.12 mmol) was dissolved in dry dichloromethane. Triethylamine (0.02 mL, 0.12 mmol) was added to the solution, followed by the addition of acid **12** (24.4 mg, 0.12 mmol) and EDC·HCl (23 mg, 0.12 mmol). The reaction mixture was stirred for 12 h at room temperature and washed successively with H_2O , sat. NaHCO_3 solution and brine. The organic layers were extracted three times with dichloromethane, dried with Na_2SO_4 , filtered and the solvent was evaporated. The crude product was purified by flash chromatography on silica [pentane/EtOAc (1:1)] to obtain the desired AHL **13** (32 mg, 0.115 mmol, 92%).

$R_f = 0.2$ (pentane/EtOAc 1:1); $^1\text{H-NMR}$ (400 MHz, CDCl_3): $\delta = 6.34$ (br s, 1H), 6.12–5.93 (m, 2H), 5.66–5.51 (m, 2H), 4.51 (ddd, $J = 11.5$, 8.5, 6.5 Hz, 1H), 4.41–4.36 (m, 1H), 4.2 (ddd, $J = 11.0$, 9.3, 6.0 Hz, 1H), 3.00 (d, $J = 7.3$ Hz, 2H), 2.74–2.68 (m, 1H), 2.15–2.04 (m, 1H), 2.00 (q, $J = 7.2$ Hz, 2H), 1.32–1.20 (m, 8H), 0.81 (t, $J = 7.0$ Hz, 3H); $^{13}\text{C-NMR}$ (100 MHz, CDCl_3): $\delta = 175.4$, 171.6, 135.8, 135.7, 129.2, 122.0, 66.0, 49.2, 39.9, 32.6, 31.7, 30.1, 29.1, 28.8, 22.5, 14.0 (Supplementary Figure S3); HRMS (ESI1/z: 280.1909 $[\text{M} + \text{H}]^+$, calculated for $\text{C}_{16}\text{H}_{26}\text{NO}_3$ 280.1907 $[\text{M} + \text{H}]^+$; 302.1729 $[\text{M} + \text{Na}]^+$, calculated for $\text{C}_{16}\text{H}_{25}\text{NO}_3\text{Na}$ 302.1727 $[\text{M} + \text{Na}]^+$.

Supplementary Materials: The following are available online at <http://www.mdpi.com/1660-3397/17/1/20/s1>, Figure S1: Mass spectrum of natural compound **B**. Figure S2: $^1\text{H-NMR}$ and $^{13}\text{C-NMR}$ spectrum of 2*E*,5*Z*-C12:2-HSL (**11**). Figure S3: $^1\text{H-NMR}$ and $^{13}\text{C-NMR}$ spectrum of 3*E*,5*Z*-C12:2-HSL (**13**). Figure S4: $^1\text{H-NMR}$ and $^{13}\text{C-NMR}$ spectrum of 2*E*,4*E*-C12:2-HSL (**5**).

Author Contributions: Conceptualization, L.Z. and S.S.; Data curation, L.Z.; Methodology, L.Z.; Validation, S.S. and I.W.-D.; Investigation, L.Z. and H.W.; Resources, S.S., L.W., M.P., T.B., B.E. and I.W.-D.; Writing-Original Draft Preparation, L.Z.; Writing-Review & Editing, S.S.; Visualization, S.S.; Supervision, S.S.; Project Administration, S.S.; Funding Acquisition, S.S.

Funding: This research was funded by The Deutsche Forschungsgemeinschaft (DFG) in the framework of TRR/SFB 51 “Roseobacter”.

Acknowledgments: We thank the DFG for funding in the framework of TRR/SFB 51 “Roseobacter”.

Conflicts of Interest: The authors declare no conflict of interest. The funders had no role in the design of the study; in the collection, analyses, or interpretation of data; in the writing of the manuscript, and in the decision to publish the results.

References

- Zan, J.; Liu, Y.; Fuqua, C.; Hill, R. Acyl-homoserine Lactone Quorum Sensing in the *Roseobacter* Clade. *Int. J. Mol. Sci.* **2014**, *15*, 654–669. [[CrossRef](#)] [[PubMed](#)]
- Buchan, A.; Mitchell, A.; Nathan Cude, N.W.; Campagna, S. Acyl-homoserine Lactone-Based Quorum Sensing in Members of the Marine Bacterial *Roseobacter* Clade: Complex Cell-to-Cell Communication Controls Multiple Physiologies. In *Stress and Environmental Regulation of Gene Expression and Adaptation in Bacteria*; de Bruijn, F.J., Ed.; Wiley Blackwell: Hoboken, NJ, USA; pp. 225–233.
- Schulz, S.; Hötling, S. The use of the lactone motif in chemical communication. *Nat. Prod. Rep.* **2015**, *32*, 1042–1066. [[CrossRef](#)] [[PubMed](#)]
- Patzelt, D.; Wang, H.; Buchholz, I.; Rohde, M.; Gröbe, L.; Pradella, S.; Neumann, A.; Schulz, S.; Heyber, S.; Münch, K.; et al. You are what you talk: Quorum sensing induces individual morphologies and cell division modes in *Dinoroseobacter shibae*. *ISME J.* **2013**, *7*, 2274–2286. [[CrossRef](#)] [[PubMed](#)]

5. Berger, M.; Neumann, A.; Schulz, S.; Simon, M.; Brinkhoff, T. Tropodithietic acid production in *Phaeobacter gallaeciensis* is regulated by *N*-acyl homoserine lactone-mediated quorum sensing. *J. Bacteriol.* **2011**, *193*, 6576–6585. [[CrossRef](#)] [[PubMed](#)]
6. Wang, H.; Ziesche, L.; Frank, O.; Michael, V.; Martin, M.; Petersen, J.; Schulz, S.; Wagner-Döbler, I.; Tomasch, J. The CtrA phosphorelay integrates differentiation and communication in the marine alphaproteobacterium *Dinoroseobacter shibae*. *BMC Genomics* **2014**, *15*, 130. [[CrossRef](#)] [[PubMed](#)]
7. Dickschat, J.S. Quorum sensing and bacterial biofilms. *Nat. Prod. Rep.* **2010**, *27*, 343–369. [[CrossRef](#)] [[PubMed](#)]
8. Giebel, H.-A.; Kalhoefer, D.; Lemke, A.; Thole, S.; Gahl-Janssen, R.; Simon, M.; Brinkhoff, T. Distribution of *Roseobacter* RCA and SAR11 lineages in the North Sea and characteristics of an abundant RCA isolate. *ISME J.* **2011**, *5*, 8–19. [[CrossRef](#)]
9. Freese, H.M.; Methner, A.; Overmann, J. Adaptation of Surface-Associated Bacteria to the Open Ocean. *Front. Microbiol.* **2017**, *8*, 1659. [[CrossRef](#)]
10. Buchan, A.; Gonzalez, J.M.; Moran, M.A. Overview of the Marine Roseobacter Lineage. *Appl. Environ. Microbiol.* **2005**, *71*, 5665–5677. [[CrossRef](#)]
11. Brinkhoff, T.; Giebel, H.-A.; Simon, M. Diversity, ecology, and genomics of the Roseobacter clade: A short overview. *Arch. Microbiol.* **2008**, *189*, 531–539. [[CrossRef](#)]
12. Ziesche, L.; Bruns, H.; Dogs, M.; Wolter, L.; Mann, F.; Wagner-Döbler, I.; Brinkhoff, T.; Schulz, S. Homoserine Lactones, Methyl Oligohydroxybutyrates, and Other Extracellular Metabolites of Macroalgae-Associated Bacteria of the *Roseobacter* Clade: Identification and Functions. *ChemBioChem* **2015**, *16*, 2094–2107. [[CrossRef](#)] [[PubMed](#)]
13. Schaefer, A.L.; Greenberg, E.P.; Oliver, C.M.; Oda, Y.; Huang, J.J.; Bittan-Banin, G.; Peres, C.M.; Schmidt, S.; Juhaszova, K.; Sufrin, J.R.; et al. A new class of homoserine lactone quorum-sensing signals. *Nature* **2008**, *454*, 595–599. [[CrossRef](#)] [[PubMed](#)]
14. Cude, W.N.; Buchan, A. Acyl-homoserine lactone-based quorum sensing in the *Roseobacter* clade: Complex cell-to-cell communication controls multiple physiologies. *Front. Microbiol.* **2013**, *4*, 336. [[CrossRef](#)] [[PubMed](#)]
15. Wagner-Döbler, I.; Thiel, V.; Eberl, L.; Allgaier, M.; Bodor, A.; Meyer, S.; Ebner, S.; Hennig, A.; Pukall, R.; Schulz, S. Discovery of complex mixtures of novel long-chain quorum sensing signals in free-living and host-associated marine Alphaproteobacteria. *ChemBioChem* **2005**, *6*, 2195–2206. [[CrossRef](#)] [[PubMed](#)]
16. Thiel, V.; Kunze, B.; Verma, P.; Wagner-Döbler, I.; Schulz, S. New Structural Variants of Homoserine Lactones in Bacteria. *ChemBioChem* **2009**, *10*, 1861–1868. [[CrossRef](#)]
17. Bruns, H.; Thiel, V.; Voget, S.; Patzelt, D.; Daniel, R.; Wagner-Döbler, I.; Schulz, S. *N*-acylated alanine methyl esters (NAMEs) from *Roseovarius tolerans*, structural analogs of quorum-sensing autoinducers, *N*-acylhomoserine lactones. *Chem. Biodivers.* **2013**, *10*, 1559–1573. [[CrossRef](#)]
18. Bruns, H.; Herrmann, J.; Müller, R.; Wang, H.; Wagner Döbler, I.; Schulz, S. Oxygenated *N*-Acyl Alanine Methyl Esters (NAMEs) from the Marine Bacterium *Roseovarius tolerans* EL-164. *J. Nat. Prod.* **2018**, *81*, 131–139. [[CrossRef](#)]
19. Kanukollu, S.; Wemheuer, B.; Herber, J.; Billerbeck, S.; Lucas, J.; Daniel, R.; Simon, M.; Cypionka, H.; Engelen, B. Distinct compositions of free-living, particle-associated and benthic communities of the *Roseobacter* group in the North Sea. *FEMS Microbiol. Ecol.* **2016**, *92*, fiv145. [[CrossRef](#)]
20. Neumann, A.; Patzelt, D.; Wagner-Döbler, I.; Schulz, S. Identification of new *N*-acylhomoserine lactone signalling compounds of *Dinoroseobacter shibae* DFL-12^T by overexpression of *luxI* genes. *ChemBioChem* **2013**, *14*, 2355–2361. [[CrossRef](#)]
21. Doberva, M.; Stien, D.; Sorres, J.; Hue, N.; Sanchez-Ferandin, S.; Eparvier, V.; Ferandin, Y.; Lebaron, P.; Lami, R. Large Diversity and Original Structures of Acyl-homoserine Lactones in Strain MOLA 401, a Marine Rhodobacteraceae Bacterium. *Front. Microbiol.* **2017**, *8*, 1152. [[CrossRef](#)]
22. Camara, M.; Daykin, M.; Chhabra, S.R. Detection, purification, and synthesis of *N*-acylhomoserine lactone quorum sensing signal molecules. *Meth. Microbiol.* **1998**, *27*, 319–330.
23. Majewski, M.; Green, J.R.; Snieckus, V. Stereoselective deprotonation of α,β -unsaturated amides. *Tetrahedron Lett.* **1986**, *27*, 531–534. [[CrossRef](#)]
24. Theodorou, V.; Gogou, M.; Philippidou, M.; Ragoussis, V.; Paraskevopoulos, G.; Skobridis, K. Synthesis of β,γ -unsaturated primary amides from α,β -unsaturated acids and investigation of the mechanism. *Tetrahedron* **2011**, *67*, 5630–5634. [[CrossRef](#)]

25. Tsukada, N.; Sato, T.; Inoue, Y. Palladium-catalyzed allylic alkenylation of allylic alcohols with *n*-butyl acrylate. *Chem. Commun.* **2003**, *19*, 2404–2405. [[CrossRef](#)]
26. Jung, M.F.; Lyster, M.A. Quantitative dealkylation of alkyl esters via treatment with trimethylsilyl iodide. A new method for ester hydrolysis. *J. Am. Chem. Soc.* **1977**, *99*, 968–969. [[CrossRef](#)]
27. Riedel, K.; Hentzer, M.; Geisenberger, O.; Huber, B.; Steidle, A.; Wu, H.; Hoiby, N.; Givskov, M.; Molin, S.; Eberl, L. *N*-Acylhomoserine-lactone-mediated communication between *Pseudomonas aeruginosa* and *Burkholderia cepacia* in mixed biofilms. *Microbiology* **2001**, *147*, 3249–3262. [[CrossRef](#)] [[PubMed](#)]
28. Steidle, A.; Allesen-Holm, M.; Riedel, K.; Berg, G.; Givskov, M.; Molin, S.; Eberl, L. Identification and characterization of an *N*-acylhomoserine lactone-dependent quorum-sensing system in *Pseudomonas putida* strain IsoF. *Appl. Environ. Microbiol.* **2002**, *68*, 6371–6382. [[CrossRef](#)]
29. Crowe, D.; Nicholson, A.; Fleming, A.; Carey, E.; Sánchez-Sanz, G.; Kelleher, F. Conformational studies of Gram-negative bacterial quorum sensing 3-oxo *N*-acyl homoserine lactone molecules. *Bioorg. Med. Chem.* **2017**, *25*, 4285–4296. [[CrossRef](#)]
30. Ziesche, L.; Rinkel, J.; Dickschat, J.S.; Schulz, S. Acyl-group specificity of AHL synthases involved in quorum-sensing in *Roseobacter* group bacteria. *Beilstein J. Org. Chem.* **2018**, *14*, 1309–1316. [[CrossRef](#)]
31. Schulz, S. Composition of the silk lipids of the spider *Nephila clavipes*. *Lipids* **2001**, *36*, 637–647. [[CrossRef](#)]
32. Sass, H.; Köpke, B.; Rütters, H.; Feuerlein, T.; Dröge, S.; Cypionka, H.; Engelen, B. *Tateyamaria pelophila* sp. nov., a facultatively anaerobic alphaproteobacterium isolated from tidal-flat sediment, and emended descriptions of the genus *Tateyamaria* and of *Tateyamaria omphalii*. *Int. J. Syst. Evol. Microbiol.* **2010**, *60*, 1770–1777. [[CrossRef](#)] [[PubMed](#)]
33. Kanukollu, S.; Voget, S.; Pohlner, M.; Vandieken, V.; Petersen, J.; Kyrpides, N.C.; Woyke, T.; Shapiro, N.; Göker, M.; Klenk, H.-P.; et al. Genome sequence of *Shimia* str. SK013, a representative of the *Roseobacter* group isolated from marine sediment. *Stand. Genom. Sci.* **2016**, *11*, 25. [[CrossRef](#)] [[PubMed](#)]
34. Pohlner, M.; Degenhardt, J.; von Hoyningen-Huene Avril, J.E.; Wemheuer, B.; Erlmann, N.; Schmetzer, B.; Badewien, T.H.; Engelen, B. The Biogeographical Distribution of Benthic *Roseobacter* Group Members along a Pacific Transect Is Structured by Nutrient Availability within the Sediments and Primary Production in Different Oceanic Provinces. *Front. Microbiol.* **2017**, *8*, 2550. [[CrossRef](#)] [[PubMed](#)]
35. Angle, S.R.; Henry, R.M. Studies toward the Synthesis of (+)-Palustrine. *J. Org. Chem.* **1998**, *63*, 7490–7497. [[CrossRef](#)] [[PubMed](#)]
36. Clerc, J.; Li, N.; Krahn, D.; Groll, M.; Bachmann, A.S.; Florea, B.I.; Overkleeft, H.S.; Kaiser, M. The natural product hybrid of Syringolin A and Glidobactin A synergizes proteasome inhibition potency with subsite selectivity. *Chem. Commun.* **2011**, *47*, 385–387. [[CrossRef](#)]
37. Kleinbeck, F.; Toste, F.D. Gold (I)-catalyzed enantioselective ring expansion of allenylcyclopropanols. *J. Am. Chem. Soc.* **2009**, *131*, 9178–9179. [[CrossRef](#)]



© 2018 by the authors. Licensee MDPI, Basel, Switzerland. This article is an open access article distributed under the terms and conditions of the Creative Commons Attribution (CC BY) license (<http://creativecommons.org/licenses/by/4.0/>).

Supplementary Materials

An Unprecedented Medium-Chain Diunsaturated *N*-acylhomoserine Lactone from Marine *Roseobacter* Group Bacteria

Lisa Ziesche ¹, Laura Wolter ², Hui Wang ³, Thorsten Brinkhoff ², Marion Pohlner ², Bert Engelen ², Irene Wagner-Döbler ³ and Stefan Schulz ^{1,*}

¹ Institute of Organic Chemistry, Technische Universität Braunschweig, Hagenring 30, 38106 Braunschweig, Germany; l.ziesche@tu-braunschweig.de (L.Z.)

² Institute for Chemistry and Biology of the Marine Environment, University of Oldenburg, Carl-von-Ossietzky-Straße 9-11, 26111 Oldenburg, Germany; laura.wolter@uni-oldenburg.de (L.W.); thorsten.brinkhoff@icbm.de (T.B.); marion.pohlner@uni-oldenburg.de (M.P.); bert.engelen@uni-oldenburg.de (B.E.)

³ Helmholtz Centre for Infection Research, Department of Medical Microbiology, Group Microbial Communication, Inhoffenstr. 7, 38124 Braunschweig, Germany; Hui.Wang@helmholtz-hzi.de (H.W.); Irene.Wagner-Doebler@helmholtz-hzi.de (I.W.-D.)

* Correspondence: stefan.schulz@tu-braunschweig.de; Tel.: +49-531-391-5272

NMR and Mass Spectra

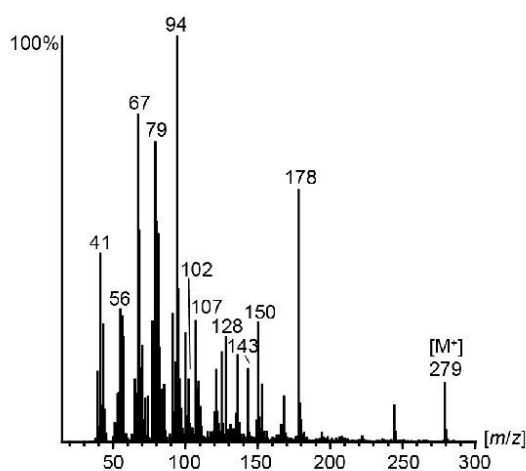


Figure S1. Mass spectrum of natural compound B.

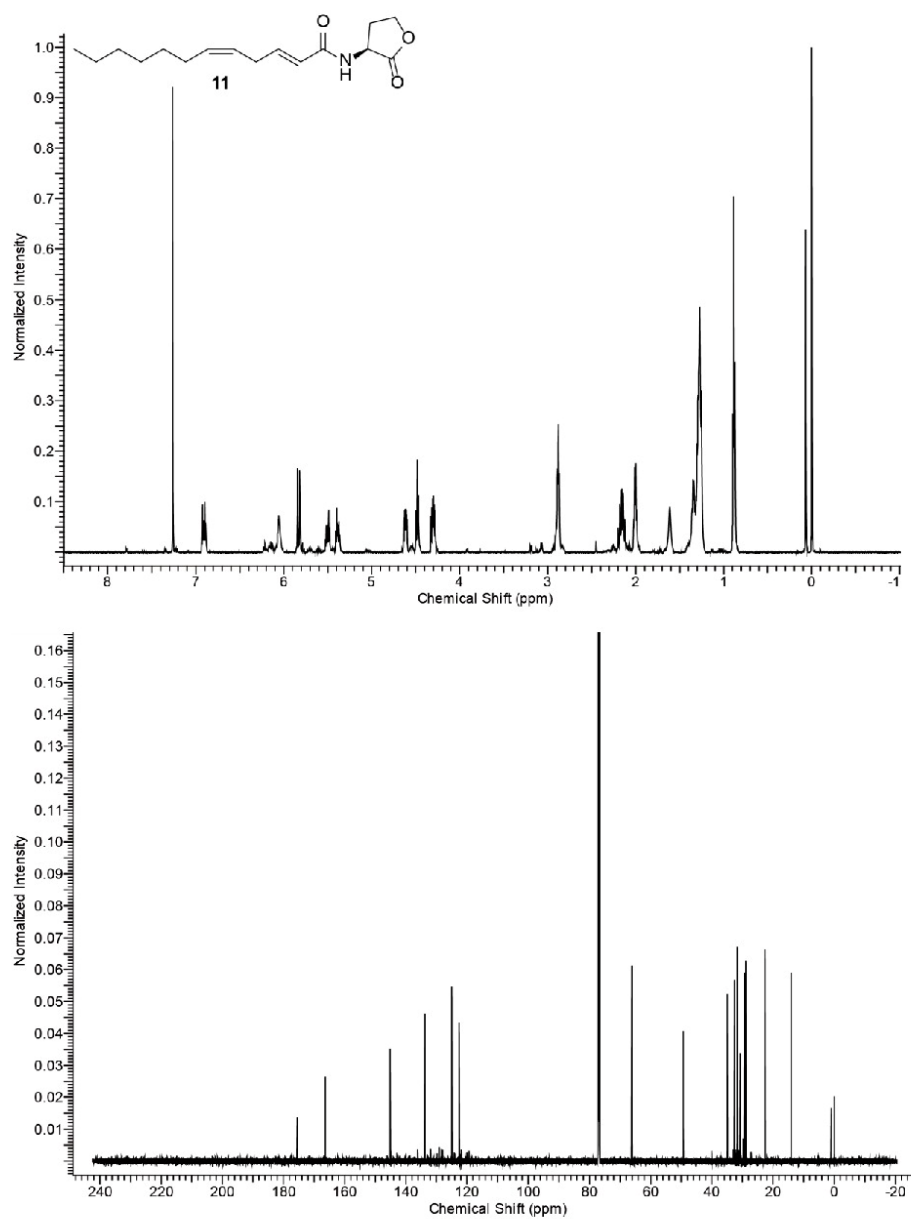


Figure S2. ¹H-NMR and ¹³C-NMR spectrum of *N*-((2*E*,5*Z*)-2,5-dodecadienyl)homoserine lactone (2*E*,5*Z*-C12:2-HSL, **11**).

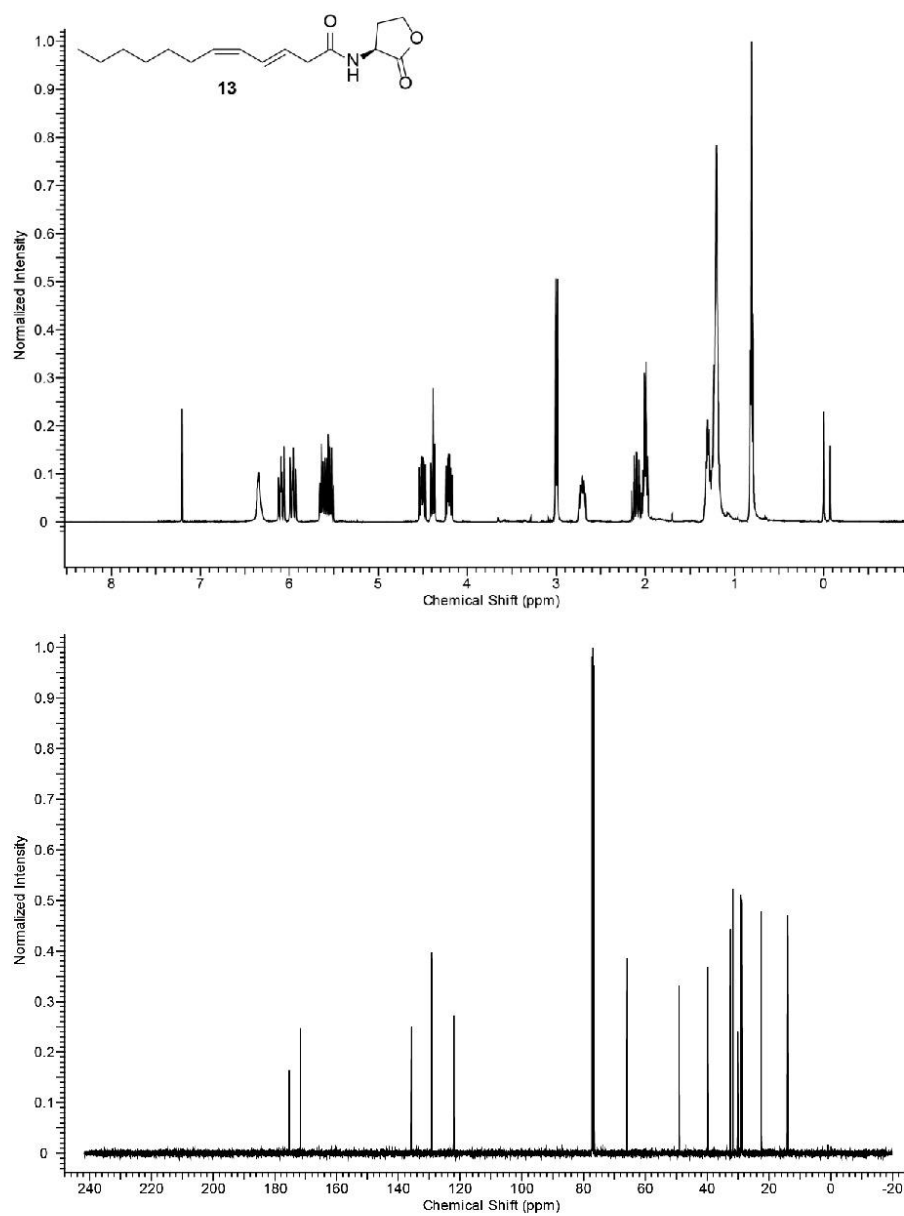


Figure S3. ¹H-NMR and ¹³C-NMR spectrum of *N*-((3*E*,5*Z*)-3,5-dodecadienyl)homoserine lactone (3*E*,5*Z*-C12:2-HSL, 13).

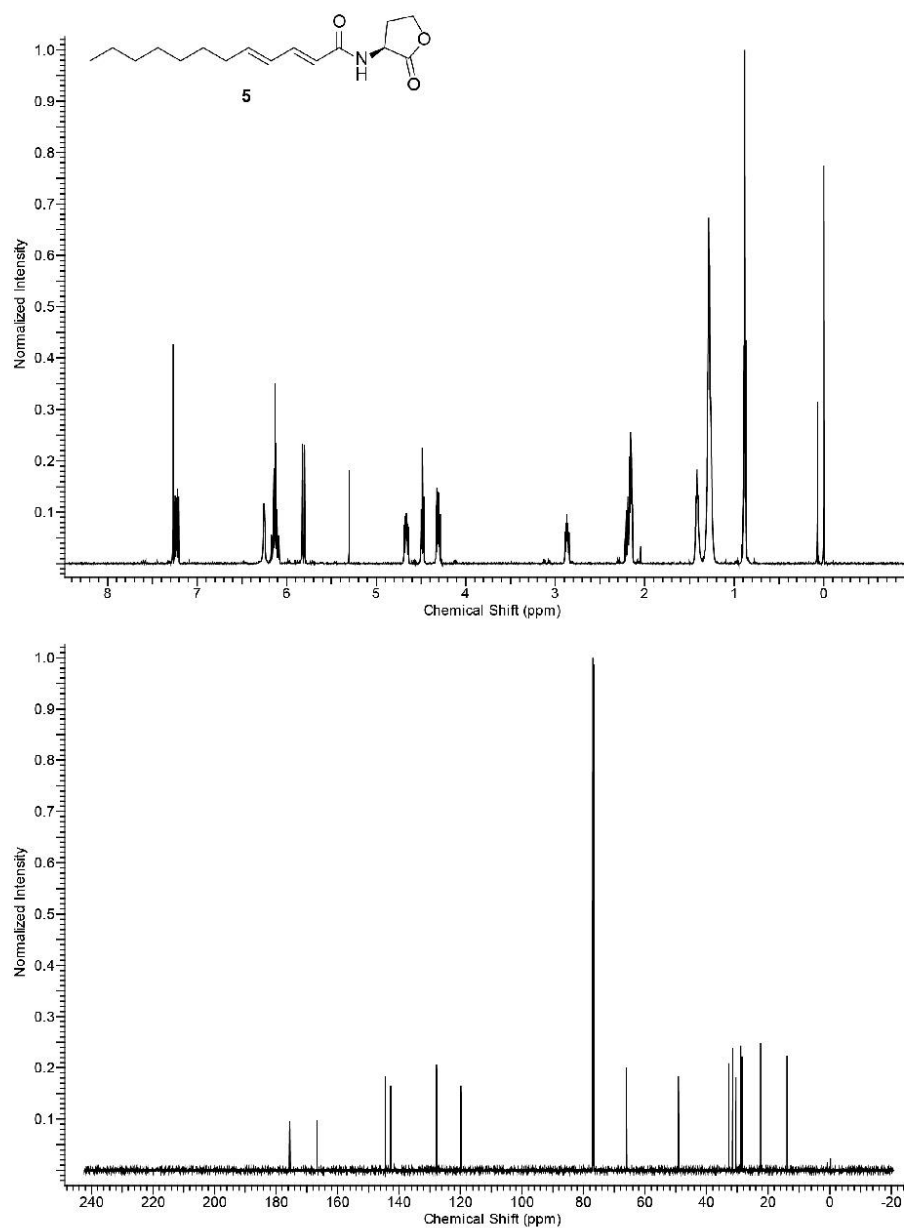


Figure S4. ¹H-NMR and ¹³C-NMR spectrum of *N*-((2*E*,4*E*)-2,4-dodecadienyl)homoserine lactone (2*E*,4*E*-C12:2-HSL, **5**).



***N*-Acylated amino acid methyl esters from marine *Roseobacter* group bacteria**

Hilke Bruns^{1,§}, Lisa Ziesche^{1,§}, Nargis Khakin Taniwal¹, Laura Wolter², Thorsten Brinkhoff², Jennifer Herrmann³, Rolf Müller³ and Stefan Schulz^{*1}

Full Research Paper

Open Access

Address:

¹Institute of Organic Chemistry, Technische Universität Braunschweig, Hagenring 30, 38106 Braunschweig, Germany, ²Institute for Chemistry and Biology of the Marine Environment, University of Oldenburg, Carl-von-Ossietzky-Straße 9–11, 26111 Oldenburg, Germany and ³Helmholtz Institute for Pharmaceutical Research Saarland (HIPS), Helmholtz Center for Infection Research (HZI), Saarland University, Campus E8.1, 66123 Saarbrücken, Germany

Email:

Stefan Schulz* - stefan.schulz@tu-braunschweig.de

* Corresponding author

§ Both authors added equally to this work and are therefore both first authors.

Keywords:

amino acid derivatives; 2-aminobutyric acid; homoserine lactones; natural products; quorum sensing

Beilstein J. Org. Chem. **2018**, *14*, 2964–2973.
doi:10.3762/bjoc.14.276

Received: 13 September 2018

Accepted: 15 November 2018

Published: 03 December 2018

Associate Editor: J. S. Dickschat

© 2018 Bruns et al.; licensee Beilstein-Institut.
License and terms: see end of document.

Abstract

Bacteria of the *Roseobacter* group (Rhodobacteraceae) are important members of many marine ecosystems. Similar to other Gram-negative bacteria many roseobacters produce *N*-acylhomoserine lactones (AHLs) for communication by quorum sensing systems. AHLs regulate different traits like cell differentiation or antibiotic production. Related *N*-acylalanine methyl esters (NAMEs) have been reported as well, but so far only from *Roseovarius tolerans* EL-164. While screening various roseobacters isolated from macroalgae we encountered four strains, *Roseovarius* sp. D12_1.68, *Loktanella* sp. F13, F14 and D3 that produced new derivatives and analogs of NAMEs, namely *N*-acyl-2-aminobutyric acid methyl esters (NABME), *N*-acylglycine methyl esters (NAGME), *N*-acylvaline methyl esters (NAVME), as well as for the first time a methyl-branched NAME, *N*-(13-methyltetradecanoyl)alanine methyl ester. These compounds were detected by GC–MS analysis, and structural proposals were derived from the mass spectra and by derivatization. Verification of compound structures was performed by synthesis. NABMEs, NAVMEs and NAGMEs are produced in low amounts only, making mass spectrometry the method of choice for their detection. The analysis of both EI and ESI mass spectra revealed fragmentation patterns helpful for the detection of similar compounds derived from other amino acids. Some of these compounds showed antimicrobial activity. The structural similarity of *N*-acylated amino acid methyl esters and similar lipophilicity to AHLs might indicate a yet unknown function as signalling compounds in the ecology of these bacteria, although their singular occurrence is in strong contrast to the common occurrence of AHLs. Obviously the structural motif is not restricted to *Roseovarius* spp. and occurs also in other genera.

2964

Introduction

The identification and structural elucidation of naturally occurring compounds traditionally requires isolation and NMR investigation as key method to detect novel compounds and new structural classes. Although the advent of NMR spectrometers with high frequencies and cryoprobes with small diameters enables experiments to be performed in the μg scale with pure compound, the isolation of the pure material from complex samples as well as the access to the expensive equipment still pose a considerable challenge to find new compounds. The ongoing quest for new structures also increasingly addresses minor components, requiring larger amounts of the producing organism, not always readily accessible, to isolate a targeted compound [1–3].

An alternative methodology can avoid the laborious isolation procedure. Direct analysis by mass-spectrometric methods of natural materials, e.g., extracts, may give enough information to infer the structure of an unknown compound that is finally proven by synthesis and comparison with natural material. The use of GC/EI-MS is especially advantageous because such mass spectra often reveal key structural features. Furthermore, the availability of large cross-platform databases useful for dereplication allows focussing on new compounds.

We are interested in natural compounds from *Roseobacter* group bacteria, an abundant class of marine bacteria occurring in diverse habitats with a broad metabolic potential [4–7]. Especially attached-living roseobacters produce diverse secondary metabolites, e.g., *N*-acylhomoserine lactones (AHLs) that the bacteria use for communication by quorum sensing [8–10]. AHLs are extensively investigated because of the broad knowledge on their biosynthesis, the underlying gene organization, as well as their function in many bacteria [11–13]. In the *Roseobacter* group, AHLs are involved, e.g., in antibiotic production [9] or cell differentiation [10]. Although many other bacterial signalling compounds must exist, only few of them have been characterized so far [14–18]. Such signalling compounds as well as many other unknown metabolites often occur in small amounts, which renders trace detecting methods like GC/MS a suitable approach for their detection and structure elucidation, provided their polarity falls into the analytical window of the method.

A wide variety of AHLs, e.g., widespread (*Z*)-*N*-(tetradec-7-enyl)homoserine lactone (**1**, Z7-C-14:1-AHL, Figure 1), have been identified in roseobacters by these methods [19–22]. A related group of compounds occurring in *Roseovarius* only, are *N*-acylalanine methyl esters (NAMEs), e.g., (*Z*)-*N*-(hexadec-9-enyl)alanine methyl ester (**2**, Z9-C16:1-NAME), the major NAME produced by *Roseovarius tolerans* EL 164 [23]. Al-

though NAMEs are structurally similar to AHLs by an acyl chain linked to an amino acid derivative via an amide bond, they do not activate AHL receptors in roseobacters [21]. Instead, they show moderate antialgal activity [21]. In contrast to AHLs, the acyl chain can also be terminally oxidized [24]. During our analyses of different *Roseobacter* isolates, we encountered several compounds, which mass spectra show similarities to known NAMEs. These compounds proved to be either new NAMEs or constitute new classes of acylated amino acid methyl esters, derived from valine (NAVME), glycine (NAGME), or 2-aminobutyric acid (NABME). The identification of these compounds will be discussed based on the outlined approach including GC/MS analysis, interpretation of mass spectra, and verification by synthesis.

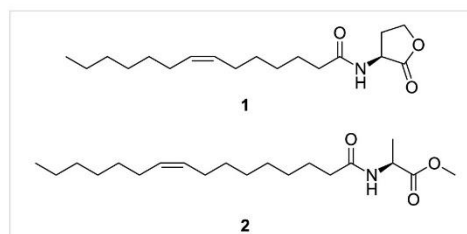


Figure 1: *N*-Acylhomoserine lactones **1** (Z7-C14:1-AHL) and *N*-acylalanine methyl esters **2** (Z9-C16:1-NAME) occurring in *Roseobacter* group bacteria.

Results and Discussion

The secondary metabolites released by liquid cultures of various roseobacters were collected by extraction via Amberlite XAD-16 resin and analysed by GC/MS. Four of these strains, *Roseovarius* sp. D12_1.68 and *Loktanella* sp. F13, F14 and D3, contained low amounts of compounds with similar mass spectra to those of NAMEs [23].

Roseovarius sp. D12_1.68

The investigation of an extract by GC/MS (Figure 2) revealed the presence of several NAMEs and AHLs due to their characteristic ions at m/z 104, 145, and 158 and m/z 102, 143, and 156, respectively [21,23]. Some of these compounds, **E** and **L** in Figure 2, were readily identified by their mass spectra and gas chromatographic retention indices I_{nat} as known AHLs, containing saturated C_{12} and C_{14} acyl chains (Table 1).

Similarly, compounds **C**, **F**, **H**, **I**, and **M** were identified as the already known C14:0-, C15:0-, 9-C16:1-, C16:0-, and 9-C17:1-NAMEs. Compounds **A**, **B**, and **O** proved to be not previously reported C13:0-, C14:1- and C18:1-NAMEs, assignable by their mass spectra and gas chromatographic retention indices. These

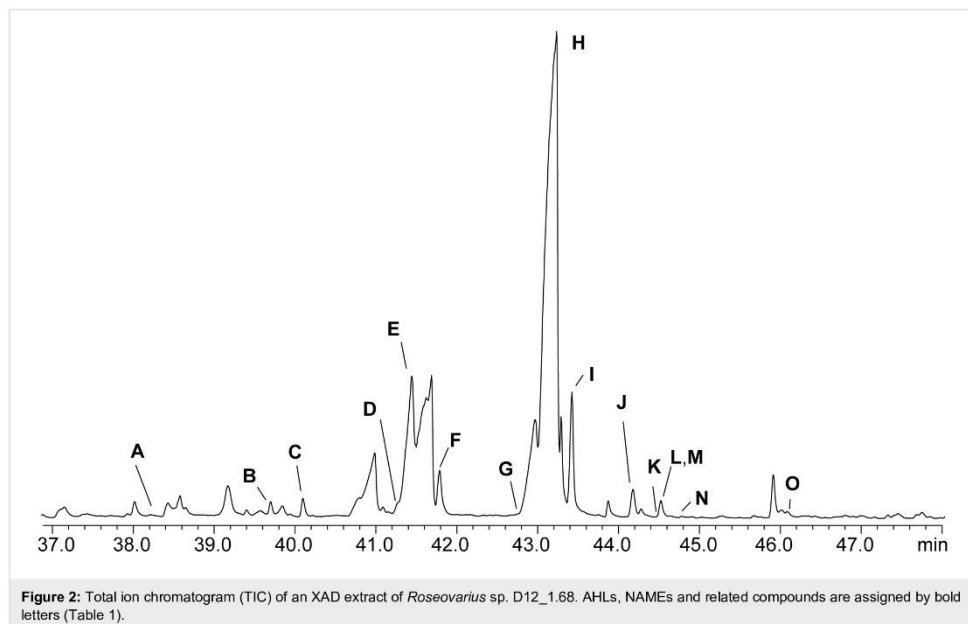


Table 1: Composition of the extracellular metabolites of *Roseovarius* sp. D12_1.68. [M]⁺, *m/z*: molecular and characteristic ions in EI mass spectrum. *t*_{nat}: gas chromatographic retention index of natural compounds. HRMS: HR-mass spectral data of [M + H]⁺ obtained by HPLC/HR-ESI⁺-MS.

peak	compound	[M] ⁺	<i>m/z</i>	<i>t</i> _{nat}	HRMS [M + H] ⁺
A	C13:0-NAME	299	104, 145, 158	2181	
B	C14:1-NAME	311	104, 145, 158	2265	C ₁₈ H ₃₄ NO ₃
C	C14:0-NAME	313	104, 145, 158	2289	C ₁₈ H ₃₆ NO ₃
D	<i>iso</i> -C15:0-NAME	327	104, 145, 158	2354	C ₁₉ H ₃₈ NO ₃
E	C12:0-AHL	283	102, 143, 156	2367	
F	C15:0-NAME	327	104, 145, 158	2392	C ₁₉ H ₃₈ NO ₃
G	C16:1-NAME	339	104, 145, 158	2457	C ₂₀ H ₃₈ NO ₃
H	Z9-C16:1-NAME	339	104, 145, 158	2473	C ₂₀ H ₃₈ NO ₃
I	C16:0-NAME	341	104, 145, 158	2497	C ₂₀ H ₄₀ NO ₃
J	9-C16:1-NABME	353	118, 159, 172	2548	C ₂₁ H ₄₀ NO ₃
K	C16:0-NABME	355	118, 159, 172	2569	C ₂₁ H ₄₂ NO ₃
L	C14:0-AHL	311	102, 143, 156	2570	
M	9-C17:1-NAME	353	104, 145, 158	2570	C ₂₁ H ₄₀ NO ₃
N	9-C16:1-NAVME	367	132, 173, 181	2588	C ₂₂ H ₄₂ NO ₃
O	11-C18:1-NAME	367	104, 145, 158	2677	C ₂₂ H ₄₂ NO ₃

conclusions were supported by HRMS data obtained by HPLC/MS (Table 1). Localization of the double bond was established via DMDS derivatization as described previously [23]. Due to the low amounts no double bond position could be established for C14:1-NAME, while the double bond of C18:1 NAME was located at C-11. Similar as in AHLs, the double

bond location in unsaturated NAMEs seems to be fixed at the ω-7 position [8,25].

Compound **D** (C₁₉H₃₇NO₃) showed a mass spectrum identical to C15:0-NAME, albeit the retention index deviated by 38 units. A methyl branch at *iso*- or *anteiso*-position seemed

likely. Therefore, the theoretical retention index I_c were calculated for methyl branched C15:0-NAMES using an empirical model established in our work group [26] that had successfully been used for the detection of methyl branched AHLs [27]. The retention indices were calculated using the formula

$$I_c = N + FG(n) + Me_i$$

with N indicating the number of n carbons in the chain times hundred, FG as the functional group increment depending on and Me_i as an increment for the methyl branching in different positions. The increments for Me_i are known [26]. The functional group increment was calculated to be $836 + 4 \cdot n$ using the retention indices of C14:0, C15:0, and C16:0-NAME. Therefore, the calculated retention index for *iso*-C15:0 and *anteiso*-C15:0-NAME are $I_c = 2352$ and $I_c = 2365$, respectively, while all other methyl branch locations had a lower value. The close similarity of $I_{nat} = 2354$ and $I_c = 2352$ suggested the methyl branch to be located in the *iso*-position. Consequently, *iso*-C15:0-NAME (**6**) was synthesized as shown in Scheme 1 to verify the structural proposal.

11-Bromoundecan-1-ol (**3**) was converted into the alcohol 13-methyltetradecan-1-ol (**4**) with isobutylmagnesium bromide under Li_2CuCl_4 catalysis according to Mori et al. [28]. After Jones oxidation, 13-methyltetradecanoic acid (**5**) was coupled with L-alanine methyl ester hydrochloride to deliver the desired product **6**. The mass spectra and retention indices of the natural and synthetic samples were identical, proving the proposed structure (Figure 3). This compound is the first natural NAME featuring a methyl branched acyl chain.

Compound **G** showed a mass spectrum identical to C16:1-NAME and a retention index with $I = 2457$, eluting earlier than compound **H**, Z9-C16:1-NAME with $I = 2473$. The low amount of the material produced excluded further structural characteri-

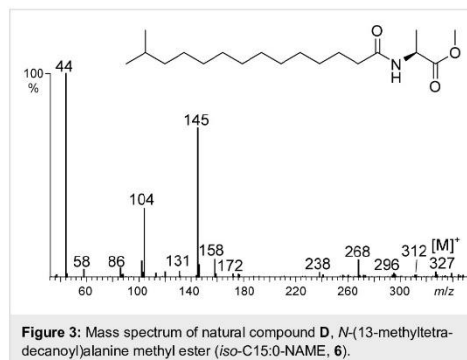
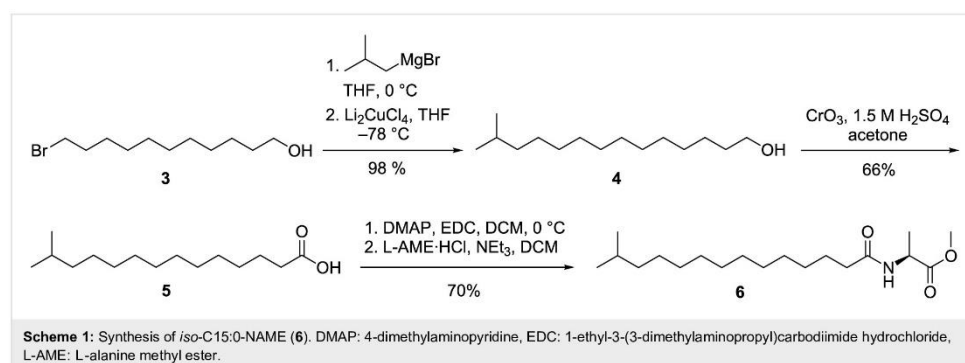


Figure 3: Mass spectrum of natural compound **D**, *N*-(13-methyltetradecanoyl)alanine methyl ester (*iso*-C15:0-NAME, **6**).

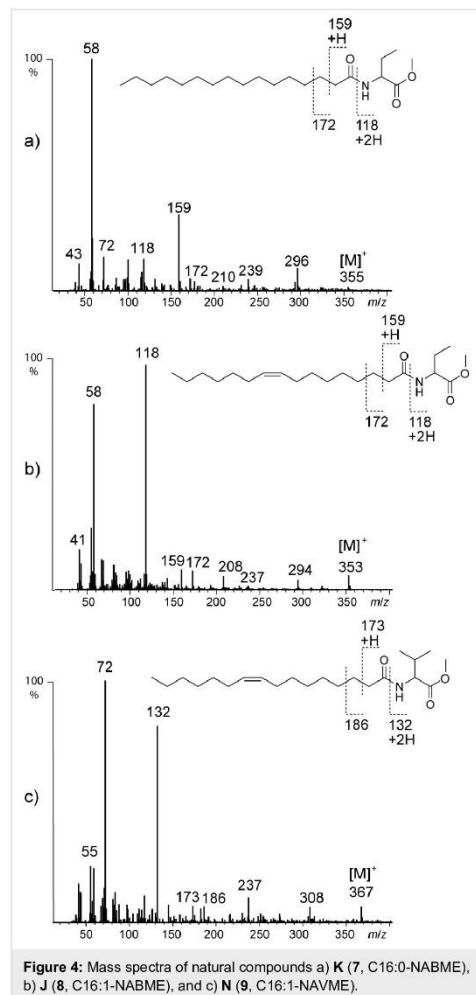
zation of the compound that could either be methyl-branched in the acyl chain or might show a different double bond position or configuration.

The remaining three compounds **J**, **K**, and **N** with the molecular composition $C_{21}H_{42}NO_3$, $C_{21}H_{40}NO_3$, and $C_{22}H_{42}NO_3$ determined by HRMS showed related mass spectra with a characteristic mass shift compared to NAMES. Ions m/z 44, 104, 145, and 158 were shifted, however, to m/z 58, 118, 159, and 172 in the spectra of **J** and **K** (Figure 4a,b).

These ions can be explained by an additional CH_2 group in the alanine part, leading to a 2-aminobutyric acid fragment in these compounds. The later eluting compound **K** with a molecular ion at m/z 355 was therefore proposed to be *N*-(hexadecanoyl)-2-aminobutyric acid methyl ester (**7**), while the earlier eluting **J** with m/z 353 compound was likely *N*-[(*Z*)-hexadec-9-enoyl]-2-aminobutyric acid methyl ester (**8**). The double bond position was determined by DMDS derivatization. The structures of both **K** and **J** were verified by synthesis according to Scheme 2. Palmitoleic acid was synthesized in g-scale by standard proce-



Scheme 1: Synthesis of *iso*-C15:0-NAME (**6**). DMAP: 4-dimethylaminopyridine, EDC: 1-ethyl-3-(3-dimethylaminopropyl)carbodiimide hydrochloride, L-AME: L-alanine methyl ester.



dures as shown in the Supporting Information File 1, Scheme S1. This acid and palmitic acid were converted into the respective chlorides and standard acylation delivered 2-aminobutyric acid derivatives **7** and **8** (Scheme 2) that proved to be identical with the natural products. The absolute configuration of the amino acid could not be determined due to the low amount of material present. Nevertheless, because NAMES showed the common L-configuration [23], this configuration also seems likely for the other amino acid derivatives reported here. We suggest the term NABME (*N*-acylated 2-aminobutyric acid methyl esters) for the new compounds that can thus be assigned as C16:0-NABME (**7**) and Z9-C16:1-NABME (**8**).

Compound **N** showed a mass spectrum (Figure 4c) featuring characteristic ions at m/z 72, 132, and 173, indicating a further carbon in the amino acid part. Together with the molecular ion at m/z 367 ($C_{22}H_{41}NO_3$) the data indicate the presence of valine in the compound. DMDS derivatization proved the unknown compound to also carry a double bond at C-9 of the alkenoyl chain. The proposed structure *N*-[(*Z*)-hexadec-9-enoyl]valine methyl ester (**9**) was proven by synthesis starting from valine methyl ester as described (Scheme 2). The gas chromatographic retention indices of the synthetic material and the natural compound matched perfectly. We propose to call the *N*-acylated valine methyl ester **9** Z9-C16:1-NAVME.

The extract of *Roseovarius* sp. D12_1.68 was also investigated by HPLC/ESI⁺-MS to detect more polar compounds compared to GC. The NAMES, NABMEs and NAVMEs reported here were detected by MS² analyses based on their characteristic fragmentation (see below). The only oxygenated derivative present was 16OH-C16:1-NAME, which has been described before from *Roseovarius tolerans* EL-164 [24].

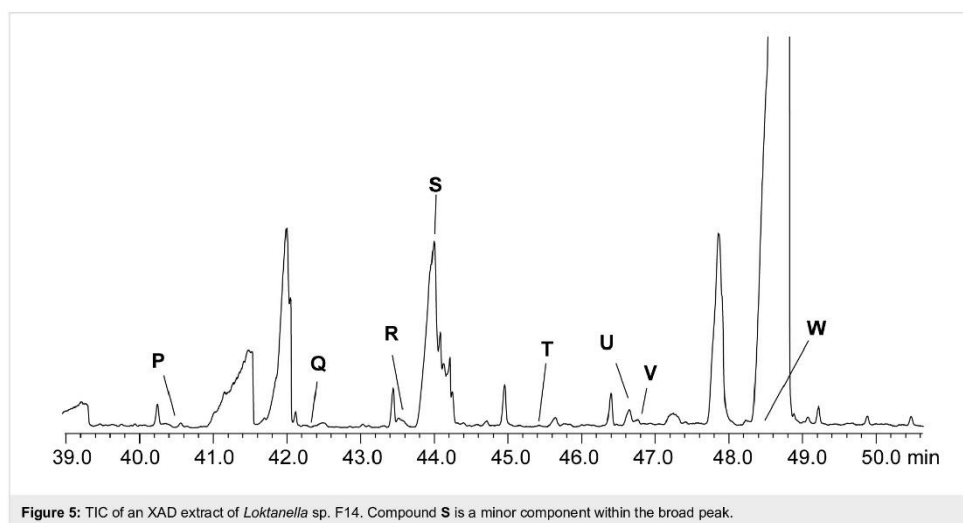
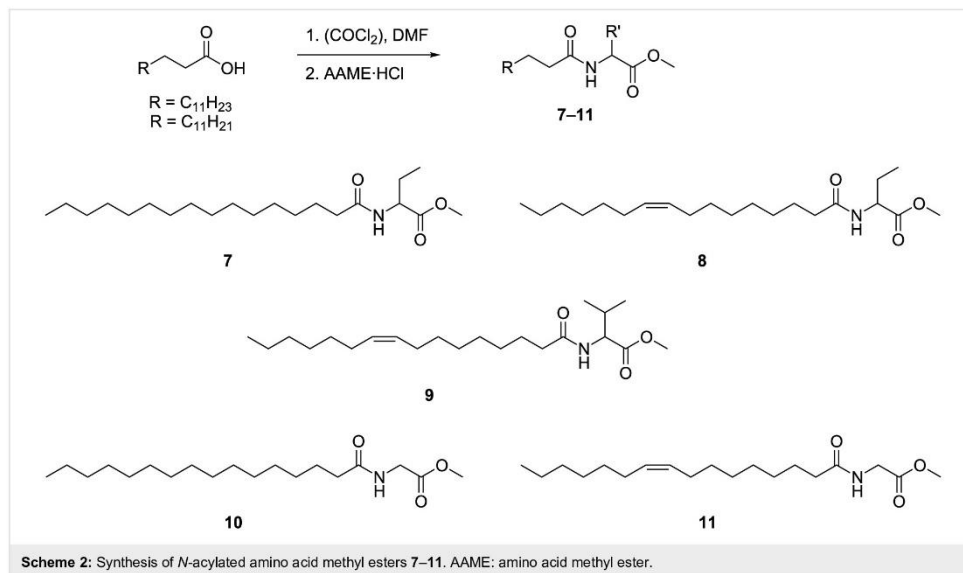
Loktanelia sp. D3, F13 and F14

Investigation of extracts of the three isolates F14, F13, and D3 by GC-MS indicated the presence of compounds whose mass spectra were again similar to those of NAMES (Figure 5). The spectra show characteristic ions at m/z 90, 131, and 144 (Figure 6), a loss of one methylene group compared to ions m/z 104, 145, and 158 of NAMES. The lack of an analogous ion to m/z 44 (m/z 30 is outside the mass range of the spectrometer used) pointed this time to glycine as the core amino acid.

Molecular formulas were obtained via HPLC/HRMS measurements and supported the *N*-acylglycine methyl ester (NAGME) structure proposed for these compounds.

Saturated and unsaturated NAGMEs can be distinguished by the intensity of the ions m/z 90 and 131. Similar to NAMES saturated NAGMEs show a high intensity of m/z 131 whereas unsaturated NAGMEs show higher intensity of m/z 90 (Figure 6). The low amounts available did not allow to determine the position of the double bond in unsaturated NAGMEs. Nevertheless, the predominance of the (*Z*)-9-hexadecenoyl side chain in all NAME family compounds suggested compound **R** to be *N*-[(*Z*)-hexadec-9-enoyl]glycine methyl ester (**11**, Z9-C16:1-NAGME), while **S** is its saturated analogue. Therefore, both compounds were synthesized as described before from glycine methyl ester and the respective acid (Scheme 2) and their identity confirmed. The other components **P**, **Q** and **T–W** were also NAGMEs.

Their chain length was established using EI mass spectra and the gas chromatographic retention indices I_{nat} of the com-

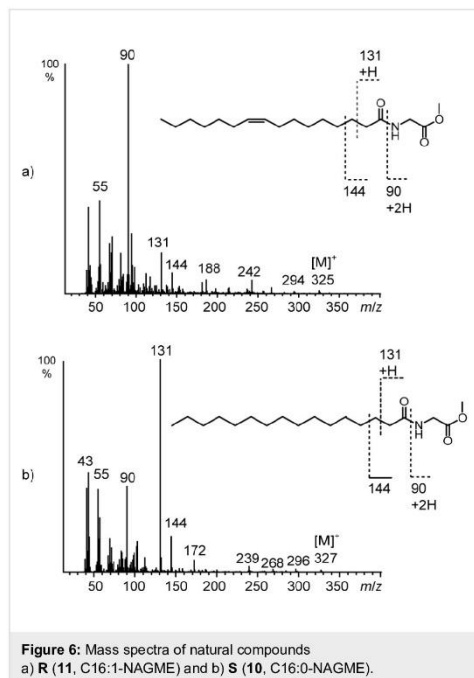


compounds (Table 2). Overall, six saturated and unsaturated compounds with a chain length between C₁₄ and C₁₉ were detected. The roughly 100 retention index units between the members of this homologous series indicated that the acyl chains are unbranched. Additionally, two unsaturated glycine derivatives were present, 9-C16:1-NAGME (**11**) and C18:1-NAGME (Table 2).

Analysis by HPLC/MS revealed no additional NAGME. Furthermore, no NAMES, NABMEs, or NAVMEs were observed in the three strains.

Mass spectrometry

The analysis of the mass spectra of NAMES, NABMEs, NAVMEs, and NAGMEs revealed the typical fragmentation of



N-acylated amino acid methyl esters under both EI (Figure 7) and ESI ionization (Figure 8). Detailed structural information can be obtained by EI-MS. A dominant peak in the mass spectrum is the McLafferty rearrangement ion **y**, if the acyl chain is saturated. Together with prominent ion **w** [$\text{NH}-\text{CH}_2-\text{R}$]⁺, often the base peak, and **x** it defines the amino acid, while **z** is usually of low abundance. Formation of **x** requires transfer of two H atoms to this fragment. In compounds carrying an unsaturated acyl chain the intensity of **y** is reduced, and **x** increases in inten-

sity. In addition to these features, the molecular ion is visible, as is the loss of the carbomethoxy group [$\text{M} - 59$]⁺.

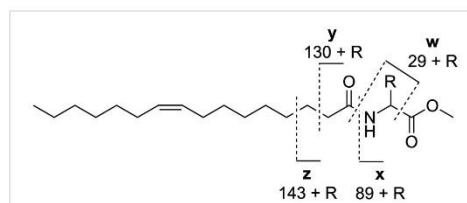


Figure 7: EI mass spectrometric fragmentation of *N*-acylated amino acid derivatives. The ions **w–z** allow identification of the respective amino acid residue.

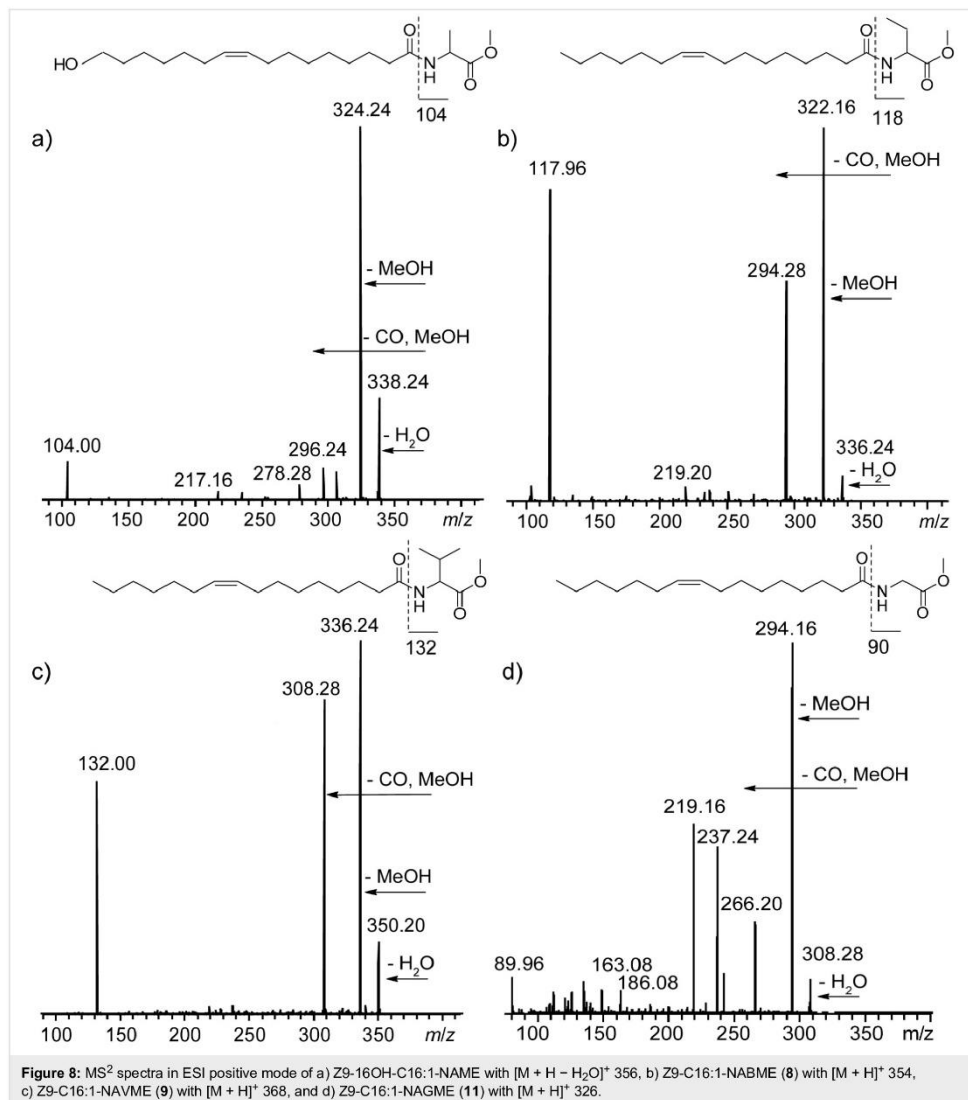
The MS² spectrum of the [$\text{M} + \text{H}$]⁺-ion obtained in ESI positive mode shows loss of water, an intense ion due to loss of methanol, and loss of the carbomethoxy group [24]. Often the amino acid ion can also be observed. These features indicate the presence of an amino acid methyl ester.

Biological activity

Several of the synthesized compounds were tested in a broader screening program for their antimicrobial activity (Table 3). While the valine derivative **9** was virtually inactive, the other compounds showed some activity. Glycine compound **11** showed good activity against the Gram-positive bacteria *Bacillus subtilis*, *Staphylococcus aureus*, and *Micrococcus luteus*, and against the filamentous fungus *Mucor hiemalis*. In addition, **11** displayed moderate active on *Mycobacterium smegmatis* and the efflux-deficient *Escherichia coli* TolC strain. The 2-aminobutyric acid derivative **7** was active against *M. hiemalis*, *M. luteus* and *S. aureus*, while the unsaturated analogue **8** was mainly active against *E. coli* TolC, and it was the only compound that showed moderate cytotoxicity on a human cancer cell line.

Table 2: NAGMEs produced by *Loktanelia* related isolates F14, F13 and D3. *I_{nat}*: gas chromatographic retention index on a HP-5 phase; [M]⁺: molecular mass; *m/z*: characteristic ions in EI mass spectra.

peak	compound	<i>I_{nat}</i>	[M] ⁺	<i>m/z</i>	<i>Loktanelia</i> isolate		
					F14	F13	D3
P	C14:0-NAGME	2312	299	131 > 90	x	x	
Q	C15:0-NAGME	2415	313	131 > 90	x	x	
R	C16:1-NAGME	2495	325	90 < 131	x	x	
S	C16:0-NAGME	2515	327	131 > 90	x	x	x
T	C17:0-NAGME	2618	341	131 > 90		x	
U	C18:1-NAGME	2702	353	90 < 131	x	x	
V	C18:0-NAGME	2720	355	131 > 90	x	x	
W	C19:0-NAGME	2832	369	131 > 90	x		



The close similarity of NAMES, NAVMEs, and NAGMEs to AHLs might indicate a function as signalling compounds, although experiments with NAMES and AHL reporter assays did not reveal any activity on the LuxR type receptors for AHLs in bacteria [23,24]. Other potential functions are antimicrobial or cytotoxic activity of the tested derivatives. *Roseovarius* sp. D12_1.68 showed antimicrobial activity against a Rhodobacteraceae sp. TL and antialgal activity against *Skeletonema*

costatum while *Loktanella* sp. D3 showed no antagonistic activity [29]. This observation fits well with the detection of antimicrobial or cytotoxic NAVME 9 and NABMEs 7 and 8 only in *Roseovarius* sp. D12_1.68.

Bacteria are known to produce acylated amino acids, although the number reported so far is small, including tyrosine, tryptophan, arginine, or phenylalanine [30-32]. They all carry long

Table 3: Antimicrobial activity (minimum inhibitory concentration, MIC, in µg/mL) and cytotoxicity (minimum inhibitory concentration, MIC, in µg/mL) of selected NAVME, NABME and NAGME derivatives. Minimal inhibitory concentration and IC₅₀ values for cytotoxicity in µg/mL.

strain	11	9	8	7
<i>Chromobacterium violaceum</i> DSM-30191	>128	>128	nd	>128
<i>Escherichia coli</i> DSM-1116	>128	>128	nd	>128
<i>Escherichia coli</i> (ToC-deficient)	128	>128	16	>128
<i>Pseudomonas aeruginosa</i> PA14	>128	>128	nd	>128
<i>Bacillus subtilis</i> DSM-10	4–8	>128	>128	>128
<i>Micrococcus luteus</i> DSM-1790	4	>128	64–128	16
<i>Staphylococcus aureus</i> Newman	16	>128	nd	8–16
<i>Mycobacterium smegmatis</i> mc ² 155	64	>128	nd	>128
<i>Mucor hiemalis</i> DSM-2656	8–16	>128	nd	32
<i>Pichia anomala</i> DSM-6766	>128	>128	nd	>128
<i>Candida albicans</i> DSM-1665	>128	>128	nd	>128
cytotoxicity				
HCT-116 (human colon carcinoma)	>67	>67	15.8	>67

chain saturated or unsaturated acyl chains similar to those reported here. Recently, derivatives of the hydrophobic amino acids valine, leucine and isoleucine were also reported [33]. These compounds are produced by a family of acyl amino acid synthases structurally related to AHL synthases, further suggesting a function as bacterial signalling compounds [34]. In contrast to the reported compounds carrying a free acid group, all derivatives reported here are native methyl esters because no methanol was used during sample preparation

Conclusion

We have identified here new classes of acylated amino acid derivatives including previously unknown glycine and 2-aminobutyric acid derived compounds. The combination of GC/MS, HPLC/MS, retention indices and synthesis proved to be especially suited to structurally identify minor components of complex extracellular metabolite mixtures. The reported compounds are specific for *Roseobacter* group bacteria of the genera *Roseovarius* and *Loktanella*, in contrast to broadly distributed AHLs. Although their function as signalling compounds is not proven, the occurrence of 2-aminobutyric acid might indicate some similarity to homoscrine in AHLs because both are non-proteinogenic amino acids. This similarity might also be functional, because the structures of NAMEs, NABMEs, NAGMEs and NAVMEs are similar to other bacterial signalling compounds, often carrying a lipophilic side chain and a medium polar core structure [8,16]. Nevertheless, the ecological function of NAMEs and its derivatives could also be antagonistic activity against concurrent biofilm microorganisms, suggested by the bioactivity of some of the compounds as observed in this study and the antimicrobial and antialgal activity of the producing organism [29].

Supporting Information

Supporting Information File 1

Experimental synthetic procedures, biological tests and NMR spectra.

[<https://www.beilstein-journals.org/bjoc/content/supplementary/1860-5397-14-276-S1.pdf>]

Acknowledgements

We thank the Deutsche Forschungsgemeinschaft (DFG) for supporting our work through the Transregional Collaborative Research Center “Roseobacter” (SFB TRR 51/3)

ORCID® iDs

Laura Wolter - <https://orcid.org/0000-0002-1238-2232>

Thorsten Brinkhoff - <https://orcid.org/0000-0003-3917-6882>

Rolf Müller - <https://orcid.org/0000-0002-1042-5665>

Stefan Schulz - <https://orcid.org/0000-0002-4810-324X>

References

- Hüttel, S.; Testolin, G.; Herrmann, J.; Planke, T.; Gille, F.; Moreno, M.; Stadler, M.; Brönstrup, M.; Kirschning, A.; Müller, R. *Angew. Chem., Int. Ed.* **2017**, *56*, 12760–12764. doi:10.1002/anie.201705913
- Cociancich, S.; Pesic, A.; Petras, D.; Uhlmann, S.; Kretz, J.; Schubert, V.; Vieweg, L.; Duplan, S.; Marguerettaz, M.; Noëll, J.; Pieretti, I.; Hügelland, M.; Kemper, S.; Mainz, A.; Rott, P.; Royer, M.; Süßmuth, R. D. *Nat. Chem. Biol.* **2015**, *11*, 195–197. doi:10.1038/nchembio.1734

3. Ling, L. L.; Schneider, T.; Peoples, A. J.; Spoering, A. L.; Engels, I.; Conlon, B. P.; Mueller, A.; Schäberle, T. F.; Hughes, D. E.; Epstein, S.; Jones, M.; Lazarides, L.; Steadman, V. A.; Cohen, D. R.; Felix, C. R.; Fetterman, K. A.; Millett, W. P.; Nitti, A. G.; Zullo, A. M.; Chen, C.; Lewis, K. *Nature* **2015**, *517*, 455–459. doi:10.1038/nature14098
4. Giebel, H.-A.; Kalhoefer, D.; Lemke, A.; Thole, S.; Gahl-Janssen, R.; Simon, M.; Brinkhoff, T. *ISME J.* **2011**, *5*, 8–19. doi:10.1038/ismej.2010.87
5. Freese, H. M.; Methner, A.; Overmann, J. *Front. Microbiol.* **2017**, *8*, 1659. doi:10.3389/fmicb.2017.01659
6. Brinkhoff, T.; Giebel, H.-A.; Simon, M. *Arch. Microbiol.* **2008**, *189*, 531–539. doi:10.1007/s00203-008-0353-y
7. Buchan, A.; Gonzalez, J. M.; Moran, M. A. *Appl. Environ. Microbiol.* **2005**, *71*, 5665–5677. doi:10.1128/aem.71.10.5665-5677.2005
8. Schulz, S.; Hötling, S. *Nat. Prod. Rep.* **2015**, *32*, 1042–1066. doi:10.1039/c5np00006h
9. Berger, M.; Neumann, A.; Schulz, S.; Simon, M.; Brinkhoff, T. *J. Bacteriol.* **2011**, *193*, 6576–6585. doi:10.1128/jb.05818-11
10. Patzelt, D.; Wang, H.; Buchholz, I.; Rohde, M.; Gröbe, L.; Pradella, S.; Neumann, A.; Schulz, S.; Heyber, S.; Münch, K.; Münch, R.; Jahn, D.; Wagner-Döbler, I.; Tomasch, J. *ISME J.* **2013**, *7*, 2274–2286. doi:10.1038/ismej.2013.107
11. Winans, S. C.; Bassler, B. L., Eds. *Chemical communication among bacteria*; ASM Press: Washington, DC, 2008. doi:10.1128/9781555815578
12. Dickschat, J. S. *Nat. Prod. Rep.* **2010**, *27*, 343–369. doi:10.1039/b804469b
13. Papenfort, K.; Bassler, B. L. *Nat. Rev. Microbiol.* **2016**, *14*, 576–588. doi:10.1038/nrmicro.2016.89
14. Higgins, D. A.; Pomianek, M. E.; Kraml, C. M.; Taylor, R. K.; Semmelhack, M. F.; Bassler, B. L. *Nature* **2007**, *450*, 883–886. doi:10.1038/nature06284
15. Thiel, V.; Vilchez, R.; Sztajer, H.; Wagner-Döbler, I.; Schulz, S. *ChemBioChem* **2009**, *10*, 479–485. doi:10.1002/cbic.200800606
16. Brachmann, A. O.; Brameyer, S.; Kresovic, D.; Hitkova, I.; Kopp, Y.; Manske, C.; Schubert, K.; Bode, H. B.; Heermann, R. *Nat. Chem. Biol.* **2013**, *9*, 573–578. doi:10.1038/nchembio.1295
17. Chen, X.; Schauder, S.; Potier, N.; Van Dorsselaer, A.; Pelczar, I.; Bassler, B. L.; Hughson, F. M. *Nature* **2002**, *415*, 545–549. doi:10.1038/415545a
18. Papenfort, K.; Silpe, J. E.; Schramma, K. R.; Cong, J.-P.; Seyedsayamdost, M. R.; Bassler, B. L. *Nat. Chem. Biol.* **2017**, *13*, 551–557. doi:10.1038/nchembio.2336
19. Wagner-Döbler, I.; Thiel, V.; Eberl, L.; Allgaier, M.; Bodor, A.; Meyer, S.; Ebner, S.; Hennig, A.; Pukall, R.; Schulz, S. *ChemBioChem* **2005**, *6*, 2195–2206. doi:10.1002/cbic.200500189
20. Neumann, A.; Patzelt, D.; Wagner-Döbler, I.; Schulz, S. *ChemBioChem* **2013**, *14*, 2355–2361. doi:10.1002/cbic.201300424
21. Ziesche, L.; Bruns, H.; Dogs, M.; Wolter, L.; Mann, F.; Wagner-Döbler, I.; Brinkhoff, T.; Schulz, S. *ChemBioChem* **2015**, *16*, 2094–2107. doi:10.1002/cbic.201500189
22. Schaefer, A. L.; Greenberg, E. P.; Oliver, C. M.; Oda, Y.; Huang, J. J.; Bittan-Banin, G.; Peres, C. M.; Schmidt, S.; Juhaszova, K.; Sufin, J. R.; Harwood, C. S. *Nature* **2008**, *454*, 595–599. doi:10.1038/nature07088
23. Bruns, H.; Thiel, V.; Voget, S.; Patzelt, D.; Daniel, R.; Wagner-Döbler, I.; Schulz, S. *Chem. Biodiversity* **2013**, *10*, 1559–1573. doi:10.1002/cbdv.201300210
24. Bruns, H.; Herrmann, J.; Müller, R.; Wang, H.; Wagner Döbler, I.; Schulz, S. *J. Nat. Prod.* **2018**, *81*, 131–139. doi:10.1021/acs.jnatprod.7b00757
25. Ziesche, L.; Rinkel, J.; Dickschat, J. S.; Schulz, S. *Beilstein J. Org. Chem.* **2018**, *14*, 1309–1316. doi:10.3762/bjoc.14.112
26. Schulz, S. *Lipids* **2001**, *36*, 637–647. doi:10.1007/s11745-001-0768-7
27. Thiel, V.; Kunze, B.; Verma, P.; Wagner-Döbler, I.; Schulz, S. *ChemBioChem* **2009**, *10*, 1861–1868. doi:10.1002/cbic.200900126
28. Takikawa, H.; Nozawa, D.; Kayo, A.; Muto, S.-e.; Mori, K. *J. Chem. Soc., Perkin Trans. 1* **1999**, 2467–2477. doi:10.1039/a904258j
29. Dogs, M.; Wemheuer, B.; Wolter, L.; Bergen, N.; Daniel, R.; Simon, M.; Brinkhoff, T. *Syst. Appl. Microbiol.* **2017**, *40*, 370–382. doi:10.1016/j.syapm.2017.05.006
30. Brady, S. F.; Clardy, J. *J. Am. Chem. Soc.* **2000**, *122*, 12903–12904. doi:10.1021/ja002990u
31. Brady, S. F.; Chao, C. J.; Clardy, J. *Appl. Environ. Microbiol.* **2004**, *70*, 6865–6870. doi:10.1128/aem.70.11.6865-6870.2004
32. Brady, S. F.; Clardy, J. *Org. Lett.* **2005**, *7*, 3613–3616. doi:10.1021/ol0509585
33. Guo, H.; Rischer, M.; Sperfeld, M.; Weigel, C.; Menzel, K. D.; Clardy, J.; Beemelmans, C. *Bioorg. Med. Chem.* **2017**, *25*, 6088–6097. doi:10.1016/j.bmc.2017.06.053
34. Van Wagoner, R. M.; Clardy, J. *Structure* **2006**, *14*, 1425–1435. doi:10.1016/j.str.2006.07.005

License and Terms

This is an Open Access article under the terms of the Creative Commons Attribution License (<http://creativecommons.org/licenses/by/4.0>). Please note that the reuse, redistribution and reproduction in particular requires that the authors and source are credited.

The license is subject to the *Beilstein Journal of Organic Chemistry* terms and conditions: (<https://www.beilstein-journals.org/bjoc>)

The definitive version of this article is the electronic one which can be found at:
doi:10.3762/bjoc.14.276



Supporting Information

for

***N*-Acylated amino acid methyl esters from marine *Roseobacter* group bacteria**

Hilke Bruns, Lisa Ziesche, Nargis Khakin Taniwal, Laura Wolter, Thorsten Brinkhoff,
Jennifer Herrmann, Rolf Müller and Stefan Schulz

Beilstein J. Org. Chem. **2018**, *14*, 2964–2973. doi:10.3762/bjoc.14.276

Experimental synthetic procedures, biological tests and NMR spectra

License and Terms: This is a supporting information file under the terms of the Creative Commons Attribution License (<http://creativecommons.org/licenses/by/4.0>). Please note that the reuse, redistribution and reproduction in particular requires that the authors and source are credited.
The license is subject to the *Beilstein Journal of Organic Chemistry* terms and conditions: (<https://www.beilstein-journals.org/bjoc>)

Contents

Experimental	S3
Synthetic procedures	S6
NMR spectra	S20
References	S26

Experimental

General. IR Spectra: Bruker Tensor 27 ATR spectrometer. UV Spectra: Varian Cary 100 Bio spectrometer. NMR Spectra: Bruker DRX-400 (400 MHz), AV III-400 (400 MHz), or AV II-600 (600 MHz) spectrometers; referenced to TMS (δ 0.00 ppm) for ^1H NMR and CDCl_3 (δ 77.01 ppm) for ^{13}C NMR, chemical shifts are in ppm, coupling constants J in Hz. LC–MS: Only LC–MS grade eluents were used. LC–MS data were acquired on a Thermo Fischer Accela equipped with pump, autosampler, and PDA detector, connected to a LTQ XL from Thermo Fischer. The measurements were carried out in ESI positive mode. The temperature of the ion source was 40 °C and the capillary temperature was 275 °C. The sheath gas flow was 15 mL/min and auxiliary gas 10 mL/min. MS^2 analyses were carried out in CID mode with a normalized collision energy of 35%. The activation Q was 0.250 and Activation time 30 ms. Spectra were evaluated with Thermo Xcalibur 2.2 software. GC–MS: HP6890 GC system connected to a HP5973 Mass Selective Detector fitted with a BPX-5 fused silica cap. column (25 m, 0.22 mm i.d., 0.25 mm film, SGE Inc., Melbourne, Australia); conditions: inlet pressure 97.0 kPa, He 45.5 mL/min; injection volume 1 μL ; injector 250 °C, transfer line 300 °C, electron energy 70 eV. The GC was programmed as follows: 50 °C (5 min isotherm), increasing at 10 °C/min to 320 °C, and operated in split mode (35:1), carrier gas (He) 1.2 mL/min. GC–MS analyses of XAD extracts and of the synthesized compounds: Agilent GC 7890A system connected to a 5975C mass-selective detector (Agilent) fitted with a HP-5 MS fused silica capillary column (30 m, 0.25 mm i. d., 0.22 mm film, Hewlett-Packard, Wilmington, USA), conditions: inlet pressure 67.5 kPa, He 24.2 mL/min, injection volume 1 μL , injector 250 °C, transfer line 300 °C, electron energy 70 eV. The GC was programmed as follows: 50 °C (5 min isothermal), increasing at 5 °C/min to

320 °C, and operated in splitless mode, carrier gas (He) 1.2 mL/min. Gas chromatographic retention indices (*I*) were determined from a homologous series of *n*-alkanes (C₈–C₃₃).

Chemicals were purchased from Sigma Aldrich Chemie GmbH (Steinheim, Germany) or from Acros Organics (Geel, Belgium), and used without further purification. Solvents were purified by distillation and dried according to standard procedures. Moisture- and/or oxygen-sensitive reactions were carried out under N₂ in vacuum-heated flasks with dried solvents. Amberlite XAD-16 was purified before by washing with 30 mL methanol and 3 × 30 mL distilled water. TLC: 0.20 mm Macherey-Nagel silica gel plates (Polygram SIL G/UV254). Column chromatography (CC): Merck silica gel 60 (0.040–0.063 mm) using standard flash chromatographic methods.

Strains, culture conditions, and extraction. *Roseovarius* sp. D12_1.68 (KM268065) and *Loktanella* sp. F13 (KJ786460) and D3 (KC731427) were isolated during the analysis of the epibacterial community associated with *Fucus spiralis* from a tidal flat area of the southern North Sea in Germany, collected from a rocky site in summer 2010. *Loktanella* sp. F14 was isolated from a marine green alga *Ulva* sp. on the same date and location. In a similar manner as described in [S1], precultures were routinely grown in marine broth medium (MB, Carl Roth, Karlsruhe, Germany) in Erlenmeyer flasks at 28 °C on a rotary shaker at 160 rpm. Erlenmeyer flasks (500 mL) containing 100 mL of MB were inoculated with 2% preculture, and 2% of Amberlite XAD-16 was added. After growth of culture (3–5 days), the resin was filtered off and extracted with 3 × 10 mL of CH₂Cl₂/H₂O 2:1 (v/v) mixture. The two phases were separated, the organic phase was dried (MgSO₄), and the solvent was evaporated under reduced pressure. The extract was concentrated at 60 °C under N₂

to a volume of ca. 500 μ L. For HPLC analysis, 400 μ L of an extract was evaporated to dryness and dissolved in 300 μ L of MeCN.

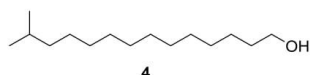
LC–MS of XAD extracts. The dried extract was dissolved in MeCN/H₂O 1:1 and filtered prior to analysis. An Agilent Eclipse Plus C18 column (3.5 μ m, 2.1 \times 150 mm) was used with a flow of 250 μ L/min and an injection volume of 10 μ L. The method used was 92.5% H₂O (B), 2.5% MeCN (C) and 5% MeCN containing 2% formic acid (D) from 0–1.5 min, 2.5% B, 92.5% C, 5% D from 8–15 min and reequilibration from 17–22 min to 92.5% B, 2.5% C and 5% D.

Bioassays. All compounds were dissolved in DMSO and their minimum inhibitory concentrations (MIC) were tested in standard microbroth dilution assays as described earlier [S2]. Cultures of *Bacillus subtilis* DSM-10, *Staphylococcus aureus* Newman, *Micrococcus luteus* DSM-1790, *Escherichia coli* DSM-1116, TolC-deficient *E. coli*, *Chromobacterium violaceum* DSM-30191, *Pseudomonas aeruginosa* PA14, *Mycobacterium smegmatis* mc²155, *Mucor hiemalis* DSM-2656, *Pichia anomala* DSM-6766, *Candida albicans* DSM-1665 in mid-log phase were diluted to achieve a final inoculum of ca. 5×10^5 – 5×10^6 cfu/mL in Mueller-Hinton broth (1.75% casein hydrolysate, 0.2% beef infusion, 0.15% starch; pH 7.4; used for all bacteria, except *M. smegmatis*), M7H9 medium (Difco™ Middlebrook 7H9 broth supplemented with BBL™ Middlebrook ADC enrichment and 2 mL/L glycerol; used for *M. smegmatis*) or Myc medium (1% phytone peptone, 1% glucose, 50 mM HEPES, pH 7.0; used for yeasts and fungi). Serial dilutions of samples were prepared from DMSO stock solutions in sterile 96-well plates, the cell suspension was added, and microorganisms were grown for 16–48 h at their optimal growth temperature at either

30 °C or 37 °C. Given MIC values are the lowest concentration of antibiotic at which there was no visible growth.

Synthetic procedures

13-Methyltetradecan-1-ol (**4**)



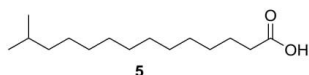
The reaction was carried out under dry conditions. A small layer of dry THF was placed on magnesium chips (0.90 g, 36.82 mmol, 3.7 equiv), a small portion of pure 1-bromo-2-methylpropane (4.01 mL, 5.05 g, 36.82 mmol, 3.7 equiv) was added and the mixture slightly heated [S3]. When the ether started to boil the remaining 1-bromo-2-methylpropane, dissolved in dry THF (15 mL), was added slowly. The mixture started to boil and after 30 min of reflux the solution was allowed to cool to room temperature. In another flask 1-bromoundecan-1-ol (**3**, 2.50 g, 9.95 mmol, 1 equiv) in dry THF (20 mL) was cooled with ice and the previously prepared isobutylmagnesium bromide solution was added slowly. The mixture was cooled to -78 °C and Li_2CuCl_4 solution (0.1 M in THF, 1.49 mL, 0.015 equiv) was added. The mixture was allowed to warm to room temperature and stirred for 5 h. The mixture was again cooled with an ice bath and hydrolyzed with 2 M HCl until the precipitate dissolved. After separation of the phases and extraction of the water phase with diethyl ether (3 × 60 mL) the combined organic layers were washed with saturated NaCl solution (50 mL) and distilled water (30 mL). The organic layers were dried with MgSO_4 , the solvent was evaporated under reduced pressure and the residue was subjected to column chromatography which yielded compound **4** (2.22 g, 9.72 mmol, 98%) as a white solid.

GC (HP-5MS): $I = 1739$;

TLC [Pentane/diethyl ether (1:1)]: $R_f = 0.30$;

$^1\text{H-NMR}$ (CDCl_3 , 400 MHz) $\delta = 3.64$ (t, $J = 6.6$ Hz, CH_2OH , 2H), 1.60-1.53 (m, 2H), 1.53 (non, $J = 6.7$ Hz, 1 H), 1.36-1.22 (m, 18H), 1.17 -1.12 (m, 2H), 0.86 (d, $J = 6.6$ Hz, 6 H) ppm; $^{13}\text{C-NMR}$ (CDCl_3 , 100 MHz): $\delta = 63.1$ (CH_2OH), 39.1 (CH_2), 32.8 (CH_2), 29.9 (CH_2), 29.7 (CH_2), 29.7 (CH_2), 29.7 (CH_2), 29.6 (CH_2), 29.6 (CH_2), 29.4 (CH_2), 28.0 (CH), 27.4 (CH_2), 25.7 (CH_2), 22.6 (2 x CH_3) ppm; MS (70 eV, EI): m/z (%) = 228 (<1, $[\text{M}]^+$), 210 (5, $[\text{M}-\text{H}_2\text{O}]^+$), 182 (26), 154 (31), 125 (24), 111 (56), 97 (77), 83 (90), 69 (100), 55 (87), 43 (66); IR (ATR): $1/\lambda = 3346$ (w, br), 2921 (s), 2852 (s), 1466 (m), 1366 (w), 1054 (m), 720 (m), 605 (w), 580 (w) cm^{-1}

13-Methyltetradecanoic acid (**5**)

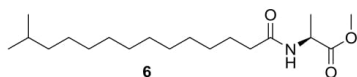


Alcohol **4** (1.20 g, 5.25 mmol, 1 equiv) was dissolved in acetone (70 mL, HPLC grade) and cooled with ice. A solution of CrO_3 (2.10 g, 21.02 mmol, 4 equiv) in H_2SO_4 (1.5 M, 31.5 mL) was prepared and slowly added to the alcohol solution so that the temperature did not rise above 5–10°C. The solution was allowed to warm to room temperature, washed with sat. NaCl solution (100 mL) and extracted with diethyl ether (3 x 50 mL). The combined organic phases were washed with sat. NaCl solution, dried with MgSO_4 and the solvent was evaporated under reduced pressure [S4,S5]. After column chromatography compound **5** (0.84 g, 3.47 mmol, 66%) was obtained as a white solid.

TLC [Pentane/diethyl ether containing 1 % acetic acid (6:1)]: $R_f = 0.29$;

$^1\text{H-NMR}$ (CDCl_3 , 400 MHz) δ = 2.35 (t, J = 7.5 Hz, 2 H, CH_2COOH), 1.63 (q, J = 7.5 Hz, 2 H, $\text{CH}_2\text{CH}_2\text{COOH}$), 1.51 (non, J = 6.6 Hz, 1 H), 1.35-1.21 (m, 16H), 1.17-1.12 (m, 2H), 0.86 (d, J = 6.6 Hz, 6 H) ppm; $^{13}\text{C-NMR}$ (CDCl_3 , 100 MHz): δ = 180.1 (C=O), 39.1 (CH_2), 34.1 (CH_2), 29.9 (CH_2), 29.7 (CH_2), 29.7 (CH_2), 29.6 (CH_2), 29.4 (CH_2), 29.2 (CH_2), 29.1 (CH_2), 28.0 (CH), 27.4 (CH_2), 24.7 (CH_2), 22.7 (2 x CH_3) ppm; IR (ATR): $1/\lambda$ = 2954 (m), 2916 (s), 2849 (s), 1694 (s), 1470 (m), 1430 (m), 1408 (m), 1381 (w), 1362 (w), 1304 (m), 1286 (m), 1263 (m), 1237 (m), 1213 (m), 1191 (m), 1098 (w), 934 (m, br), 773 (w), 719 (m), 683 (m), 544 (m) cm^{-1} ; UV/VIS (CH_2Cl_2): λ_{max} (log ϵ) = 222 (2.05), 224 (2.25), 230 (2.25) nm.

***N*-(13-Methyltetradecanoyl)alanine methyl ester (6, iso-15:0-NAME)**



In a similar manner as described in [S1], acid **5** (0.20 g, 0.83 mmol, 1 equiv) was dissolved in abs. CH_2Cl_2 (10 mL) under a N_2 atmosphere. After addition of 4-(*N,N*-dimethylamino)pyridine (DMAP, 0.10 g, 0.83 mmol, 1 equiv), 1-ethyl-3-(3-dimethylaminopropyl)carbodiimide (EDC, 0.19 mL, 1.07 mmol, 1.3 equiv) was added at 0 °C and the solution was stirred for 1 h at 0 °C. The resulting mixture was allowed to warm to room temperature and stirred for an additional hour. A solution of L-alanine methyl ester hydrochloride (0.15 g, 1.07 mmol, 1.3 equiv) in abs. CH_2Cl_2 (10 mL) was prepared and triethylamine (0.15 mL, 1.07 mmol, 1.3 equiv) was added. This solution was added dropwise to the solution of **5** and stirred over night at room temperature. The solution was washed with 1 M HCl (10 mL), NaHCO_3 (10 mL) and H_2O (10 mL), the phases were separated and the organic phase dried with MgSO_4 .

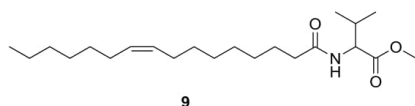
[S6,S7]. Product **6** (0.19 g, 0.58 mmol, 70%) was obtained after column chromatography as a white solid (pentane/ethyl acetate 2:1).

GC (HP-5MS): $t = 2353$;

TLC [Pentane/diethyl ether (2:1)]: $R_f = 0.39$;

$^1\text{H-NMR}$ (CDCl_3 , 300 MHz): $\delta = 6.03$ (d, $J = 6.6$ Hz, 1 H, NH), 4.61 (q, $J = 7.3$ Hz, 1 H), 3.75 (s, 3 H), 2.21 (t, $J = 7.8$ Hz, 2 H), 1.65-1.58 (m, 2H, $\text{CH}_2\text{CH}_2\text{C}=\text{O}$), 1.51 (non, 1H, $J = 6.5$ Hz, CH), 1.40 (d, 3H, $J = 7.1$ Hz, CHCH_3); 1.29-1.20 (m, 16H, 8 x CH_2), 1.18-1.12 (m, 2H, CH_2), 0.86 (d, 6H, $J = 6.6$ Hz, 3 x CH_2) ppm; $^{13}\text{C-NMR}$ (CDCl_3 , 75 MHz): $\delta = 173.7$ (NHC=O), 172.6 (C=O), 52.4 (OCH_3), 47.8 (CH), 39.0 ($\text{CH}_2\text{C}=\text{O}$), 36.6 (CH_2), 29.9 (CH_2), 29.7 (CH_2), 29.6 (CH_2), 29.6 (CH_2), 29.5 (CH_2), 29.3 (CH_2), 29.2 (CH_2), 27.9 (CH), 27.4 (CH_2), 25.6 (CH_2), 22.6 (2 x CH_3), 18.6 (CH_2CH_3) ppm; MS (70 eV, EI): m/z (%) = 327 (3, $[\text{M}]^+$), 296 (2), 268 (12), 158 (12), 145 (93), 104 (28), 86 (7), 69 (9), 55 (17), 44 (100).

Methyl (*Z*)-*N*-hexadec-9-enoylvalinate (**9**)



Dimethylformamide (1 drop) was added to a solution of palmitoleic acid (**S7**) (0.100 g, 0.393 mmol, 1 equiv) in CH_2Cl_2 (2 mL). Oxalyl chloride (0.074 g, 0.586 mmol, 1.5 equiv) in CH_2Cl_2 (1 mL) was added dropwise to the solution at 0 °C. The resulting solution was left to stir at room temperature for 3 h until gas formation ended and the solvent was removed. A mixture of valine methyl ester hydrochloride (0.066 g, 0.393 mmol, 1 equiv), CH_2Cl_2 (0.65 mL) and water (0.65 mL) was prepared. K_2CO_3 (0.163 g, 1.179 mmol, 3 equiv) was added to the resulting solution at 0 °C. The mixture was stirred at 0 °C for 5 min before the freshly synthesized (*Z*)-hexadec-9-enoyl chloride

in CH₂Cl₂ (0.65 mL) was added. After stirring at room temperature for 16 h the mixture was extracted with CH₂Cl₂ (3 × 10 mL), dried with MgSO₄, and concentrated in vacuo. Flash column chromatography (pentane/diethyl ether 1:1) provided the pure compound **9** as colorless oil (0.120 g, 0.326 mmol, 83%).

TLC [Pentane/diethyl ether (1:1)]: $R_f = 0.31$;

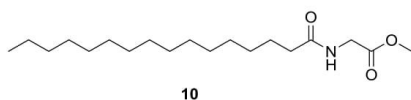
¹H-NMR (CDCl₃, 300 MHz): δ (ppm) = 6.00 (d, $J = 8.7$ Hz, 1 H), 5.35 (m, 2 H), 4.59 (dd, $J = 8.8$ Hz, $J = 5.0$ Hz, 1 H), 3.74 (s, 3 H), 2.23 (t, 2 H), 1.94-2.20 (m, 3 H), 1.64 (m, 2 H), 1.31 (s, 24 H), 0.92 (m, 9 H);

¹³C-NMR (CDCl₃, 100 MHz): δ (ppm) = 173.0 (NHC=O), 172.7 (C=O), 130.0 (CH), 129.7 (CH), 56.7 (CH), 52.0 (CH₃), 36.6 (CH₂), 31.7 (CH₂), 31.2 (CH), 29.7 (CH₂), 29.7 (CH₂), 29.3 (CH₂), 29.2 (CH₂), 29.1 (CH₂), 28.9 (CH₂), 27.2 (CH₂), 27.1 (CH₂), 25.6 (CH₂), 22.6 (CH₂), 18.9 (CH₃), 17.8 (CH₃), 14.0 (CH₃);

IR (diamond-ATR): $\tilde{\nu} = 3302$ (w, br) cm⁻¹, 3003 (w), 2957 (m), 2925 (m), 2854 (m), 1745 (m), 1648 (s), 1535 (m), 1463 (w), 1436 (w), 1373 (w), 1309 (w), 1262 (w), 1203 (m), 1153 (m), 1118 (w), 1023 (w), 1004 (w), 919 (w), 730 (m).

EI-MS (70 eV): m/z (%) = 367 (5) [M⁺], 308 (8), 292 (2), 254 (4), 237 (3), 206 (2), 186 (7), 173 (6), 154 (3), 132 (100), 114 (6), 98 (6), 88 (7), 72 (93), 67 (10), 55 (23), 41 (10), 39 (2).

Methyl *N*-hexadecanoylglycinate (**10**)



Compound **10** was prepared according to the procedure for **9** from palmitic acid (1.38 g, 5.37 mmol) glycine methyl ester hydrochloride (0.67 g, 5.37 mmol) as a white crystalline solid (1.48 g, 4.52 mmol, 84%).

S10

TLC [Acetonitrile]: $R_f = 0.38$;

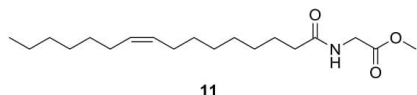
$^1\text{H-NMR}$ (CDCl_3 , 300 MHz, TMS): δ (ppm) = 5.99 (br. s, 1 H), 4.05 (d, $J = 5.1$ Hz, 2 H), 3.77 (s, 3 H), 2.24 (m, 2 H), 1.57 (m, 2 H), 1.17 (m, 24 H), 0.81 (m, 3 H);

$^{13}\text{C-NMR}$ (CDCl_3 , 100 MHz, TMS): δ (ppm) = 172.9 (NHC=O), 170.3 (C=O), 51.9 (CH_3), 410.8 (CH_2), 36.0 ($\text{CH}_2\text{C=O}$), 31.6 (CH_2), 29.3 (CH_2), 29.3 (CH_2), 29.2 (CH_2), 29.2 (CH_2), 29.1 (CH_2), 28.9 (CH_2), 28.8 (CH_2), 28.6 (CH_2), 25.2 (CH_2), 22.3 (CH_2), 13.7 (CH_3);

IR (diamond-ATR): $\tilde{\nu} = 3302$ (w) cm^{-1} , 2957 (w), 2918 (s), 2849 (m), 1738 (m), 1639 (s), 1545 (m), 1460 (w), 1435 (m), 1375 (m), 1270 (w), 1214 (s), 1181 (m), 1124 (w), 1084 (w), 1044 (w), 991 (w), 890 (w), 872 (w), 718 (m), 678 (m), 607 (w);

EI-MS (70 eV): m/z (%) = 327 (2) [M^+], 239 (6), 167 (4), 149 (11), 144 (20), 132 (9), 131 (100), 112 (8), 103 (11), 99 (9), 90 (28), 89 (5), 69 (7), 57 (9), 55 (12), 43 (11), 41 (8).

Methyl (Z)-N-hexadec-9-enoylglycinate (**11**)



Compound **11** was prepared according to the procedure for **9** from palmitoleic acid (**S7**, 0.250 g, 0.98 mmol) and glycine methyl ester hydrochloride (0.123 g, 0.98 mmol, 1 equiv) as colorless oil (0.246 g, 0.76 mmol, 77%).

TLC [Pentane/diethyl ether (1:2)]: $R_f = 0.33$;

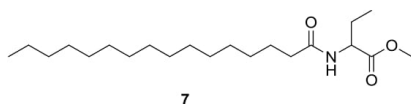
$^1\text{H-NMR}$ (CDCl_3 , 300 MHz, TMS): δ (ppm) = 6.13 (br. s, 1 H), 5.34 (m, 2 H), 4.05 (d, $J = 5.2$ Hz, 2 H), 3.76 (s, 3 H), 2.24 (m, 2 H), 2.01 (m, 4 H), 1.63 (dd, $J = 14.6$ Hz, $J = 7.2$ Hz, 2 H), 1.30 (m, 16 H), 0.88 (dd, $J = 9.3$ Hz, $J = 4.2$ Hz, 3 H);

^{13}C -NMR (CDCl_3 , 100 MHz, TMS): δ (ppm) = 173.3 (NHC=O), 170.5 (C=O), 129.9 (CH), 129.7 (CH), 52.2 (CH_3), 41.1 (CH_2), 36.3 (CH_2), 31.7 (CH_2), 29.7 (CH_2), 29.6 (CH_2), 29.2 (CH_2), 29.1 (CH_2), 29.0 (CH_2), 28.9 (CH_2), 27.1 (CH_2), 27.0 (CH_2), 25.5 (CH_2), 22.6 (CH_2), 14.0 (CH_2);

IR (diamond-ATR): $\tilde{\nu}$ = 3301 (w, br) cm^{-1} , 3076 (w), 3004 (w), 2924 (m), 2854 (m), 1756 (m), 1652 (m), 1539 (m), 1460 (w), 1437 (w), 1370 (w), 1203 (s), 1180 (m), 1036 (w), 987 (w), 846 (w), 722 (m), 706 (m), 561 (w);

EI-MS (70 eV): m/z (%) = 325 (3) [M^+], 294 (3), 266 (4), 237 (2), 236 (3), 206 (3), 198 (3), 143 (12), 131 (26), 112 (6), 98 (11), 95 (9), 90 (100), 81 (11), 69 (10), 55 (18), 41 (9).

Methyl *N*-hexadecanoyl-2-aminobutyrate (**7**)



Compound **7** was prepared according to the procedure for **9** from palmitic acid (0.497 g, 1.94 mmol) and L-2-aminobutyric acid methyl ester hydrochloride (0.200 g, 1.94 mmol) as colorless oil (0.590 g, 1.66 mmol, 86%) which crystallized on standing.

TLC [Pentane/diethyl ether (1:1)]: R_f = 0.28;

^1H -NMR (CDCl_3 , 300 MHz, TMS): δ (ppm) = 6.03 (d, J = 7.7 Hz, 1 H, NH), 4.60 (ddd, J = 7.9 Hz, J = 6.7 Hz, J = 5.5 Hz, 1 H, CH), 3.74 (s, 3 H, OCH_3), 2.20 (t, 2H, CH_3CO), 1.83-1.94 (m, 2 H, CH_2), 1.58-1.76 (m, 2 H, CH_2), 1.25 (s, 24 H, CH_2), 0.90 (q, J = 7.2 Hz, 6 H, CH_3);

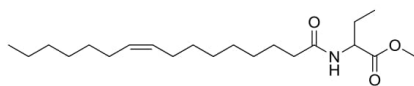
^{13}C -NMR (CDCl_3 , 100 MHz, TMS): δ (ppm) = 173.1 (NHC=O), 172.8 (C=O), 53.0 (CH), 52.2 (CH_3), 36.6 (CH_2), 31.9 (CH_3), 29.65 (CH_2), 29.61 (CH_2), 29.57 (CH),

29.45 (CH₂), 29.32 (CH₂), 29.30 (CH₂), 29.21 (CH₂), 25.65 (CH₂), 25.63 (CH₂), 24.85 (CH₂), 22.65 (CH₂), 14.1 (CH₃), 9.4 (CH₃);

IR (diamond-ATR): $\tilde{\nu}$ = 3305 (w) cm⁻¹, 3076 (w), 2960 (m), 2917 (s), 2849 (m), 1741 (s), 1646 (s), 1548 (m), 1461 (w), 1435 (w), 1383 (w), 1313 (w), 1263 (3), 1246 (m), 1211 (m), 1152 (w), 1098 (w), 1070 (w), 1006 (m), 956 (w), 698 (m);

EI-MS (70 eV): *m/z* (%) = 355 (8) [M]⁺, 324 (4), 312 (1), 296 (33), 256 (7), 239 (4), 228 (2), 214 (2), 196 (4), 182 (2), 172 (14), 159 (65), 140 (8), 131 (8), 118 (21), 100 (19), 83 (7), 69 (10), 58 (100), 43 (22).

Methyl (Z)-hexadec-9-enoyl-2-aminobutyrate (**8**)



Compound **8** was prepared according to the procedure for **9** from palmitoleic acid (**S7**, 0.984 g, 3.79 mmol) and L-2-aminobutyric acid methyl ester hydrochloride (0.400 g, 3.88 mmol) as yellowish oil (0.955 g, 2.70 mmol, 70%).

TLC [Pentane/diethyl ether (1.5:1)]: *R_f* = 0.27;

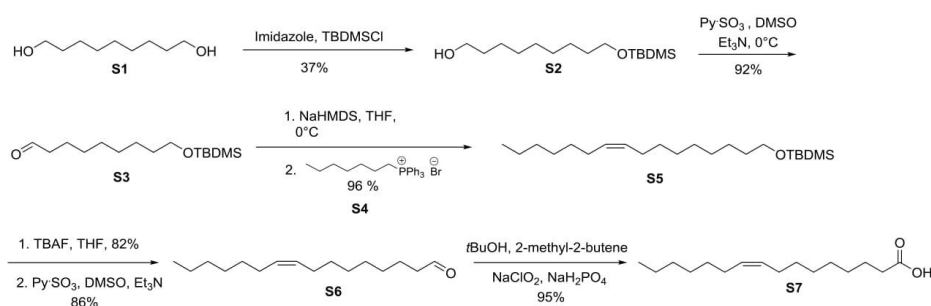
¹H-NMR (CDCl₃, 300 MHz, TMS): δ (ppm) = 5.99 (d, *J* = 7.1 Hz, 1 H, NH), 5.34 (m, 2 H), 4.6 (m, 1 H), 3.7 (s, 3 H), 2.23 (m, 2 H), 1.92-2.30 (m, 4 H), 1.58-1.79 (m, 4 H), 1.24-1.38 (m, 16 H), 0.90 (m, 6 H);

¹³C-NMR (CDCl₃, 100 MHz, TMS): δ (ppm) = 172.7 (NHC=O), 172.4 (C=O), 129.5 (CH), 129.3 (CH), 52.6 (CH), 51.8 (CH₃), 36.2 (CH₂), 31.3 (CH₂), 29.3 (CH₂), 29.2 (CH₂), 28.8 (CH₂), 28.8 (CH₂), 28.7 (CH₂), 28.5 (CH₂), 26.8 (CH₂), 26.7 (CH₂), 25.2 (CH₂), 25.2 (CH₂), 22.2 (CH₂), 13.6 (CH₃), 9.0 (CH₃);

IR (diamond-ATR): $\tilde{\nu}$ = 3298 (w, br) cm^{-1} , 3063 (w), 2926 (m), 2855 (m), 1743 (s), 1649 (s), 1536 (m), 1459 (m), 1438 (w), 1374 (w), 1295 (w), 1255 (m), 1203 (s), 1155 (m), 988 (w), 725 (w), 680 (w);

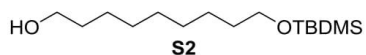
EI-MS (70 eV): m/z (%) = 353 (16) $[\text{M}]^+$, 322 (3), 310 (1), 294 (12), 264 (2), 254 (2), 236 (4), 226 (4), 214 (2), 193 (2), 186 (1), 172 (16), 159 (16), 140 (6), 131 (3), 118 (100), 100 (8), 95 (7), 81 (10), 69 (12), 58 (57), 41 (11).

Synthesis of palmitoleic acid (S7)



Scheme S1: Synthesis of palmitoleic acid in g-scale [S8].

9-((*tert*-Butyldimethylsilyloxy)nonan-1-ol (S2)



In a similar manner as described in [S1], a solution of 1,9-nonandiol (S1, 8.013 g, 50 mmol, 1 equiv) in dry DCM (450 mL) imidazole (4.425 g, 65 mmol, 1.3 equiv) was added at 0 °C and stirred for 15 min, followed by addition of TBDMSCl (9.796 g, 65 mmol, 1.3 equiv) in portions. The solution was poured into H₂O after stirring at rt for 2.5 days, and extracted with ethyl acetate (3 × 100 mL). The combined organic phases were washed with brine, dried with Na₂SO₄, filtered, and concentrated in

vacuo. Chromatographic separation on silica with pentane/EtOAc (5:1) gave **S2** (5.050 g, 18.4 mmol, 37%).

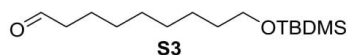
TLC [Pentane/ethyl acetate (2:1)]: $R_f = 0.33$;

$^1\text{H-NMR}$ (CDCl_3 , 300 MHz): δ (ppm) = 4.1 (t, 1 H), 3.62 (td, $J = 6.6$ Hz, $J = 13.2$ Hz, 4 H), 1.53 (m, 4 H), 1.32 (m, 10 H), 0.89 (s, 9 H), -0.052 (s, 6 H);

$^{13}\text{C-NMR}$ (CDCl_3 , 100 MHz): δ (ppm) = 63.4 (CH_2OH), 63.1 (CH_2), 32.9 (CH_2), 32.9 (CH_2), 29.6 (CH_2), 29.4 (2 C, CH_2), 26.0 (3 C, CH_3), 25.8 (CH_2), 25.8 (CH_2), 18.4 (C_q), -5.2 (2 C, CH_3);

EI-MS (70 eV): m/z (%) = 217 (2), 199 (3), 115 (10), 105 (37), 101 (12), 99 (6), 93 (17), 89 (10), 83 (66), 75 (80), 73 (25), 69 (100), 55 (57), 41 (20).

9-(*tert*-Butyldimethylsilyloxy)nonanal (**S3**)



In a similar manner as described in [S1], a solution of $\text{SO}_3\cdot\text{py}$ (8.7 g, 54.6 mmol, 3 equiv) in DMSO (56 mL) was added dropwise to a solution of **S2** (5.00 g, 18.2 mmol, 1 equiv) and Et_3N (30.4 g, 300 mmol, 16.5 equiv) in dry DCM (162 mL) at 0°C under argon. The resulting mixture was allowed to stir at rt for 2.5 h until the reaction was completed. The reaction was quenched with H_2O , extracted with DCM (3×100 mL), washed with brine (3×60 mL), dried with MgSO_4 , and concentrated in vacuo to afford the crude product. Flash column chromatography (pentane/ Et_2O (19:1)) gave the pure title compound **S3** as clear oil (4.836 g, 17.7 mmol, 92%).

TLC [Pentane/diethyl ether (19:1)]: $R_f = 0.31$;

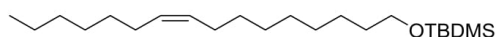
$^1\text{H-NMR}$ (CDCl_3 , 300 MHz): δ (ppm) = 9.76 (t, CHO, 1 H), 3.59 (t, $J = 4.8$ Hz, 2 H), 2.42 (dt, $J = 1.9$ Hz, $J = 7.3$ Hz, 2 H), 1.57 (m, 4 H), 1.30 (s, 8 H), 0.89 (m, 9 H), 0.046 (s, 6 H);

^{13}C -NMR (CDCl_3 , 100 MHz): δ (ppm) = 202.9 (CHO), 63.2 (CH_2), 43.9 (CH_2), 32.8 (CH_2), 29.4 (CH_2), 29.3 (CH_2), 29.2 (CH_2), 29.1 (CH_2), 26.0 (3 C, CH_3), 22.1 (CH_2), 18.4 (CH_2), -5.3 (2 C, CH_3);

IR (diamond-ATR): $\tilde{\nu}$ = 2929 (m) cm^{-1} , 2856 (m), 2712 (w), 1727 (m), 1466 (w), 1388 (w), 1361 (w), 1253 (w), 1095 (m), 1006 (w), 938 (w), 833 (s), 774 (s), 713 (w), 662 (w);

EI-MS (70 eV): m/z (%) = 215 (9), 131 (30), 123 (6), 115 (6), 105 (24), 101 (9), 89 (11), 81 (75), 75 (100), 73 (22), 67 (33), 55 (16), 41 (10).

(Z)-tert-Butyl(hexadec-9-en-1-yloxy)dimethylsilane (S5)



S5

NaHMDS (1.0 M in THF, 38.51 mL, 38.51 mmol, 2.1 equiv) was added dropwise to a stirred solution of the hexyl triphenylphosphonium bromide **S4** (8.50 g, 19.26 mmol, 1.05 equiv) in THF (68 mL) at 0 °C. The reaction mixture was stirred at rt for 45 min. The bright orange solution was recooled to -78 °C before **S3** (5 g, 18.34 mmol, 1 equiv) was added. After stirring for 1 h at -78 °C, the mixture was allowed to warm to rt and poured into ice-cooled pentane. Ph_3PO was filtered off and two third of the solvent was evaporated under reduced pressure. The mixture was adsorbed on SiO_2 and purification of the crude residue by column chromatography (pentane/ Et_2O (80:1)) gave **S5** (6.56 g, 18.49 mmol, 96%) as clear, colorless oil.

TLC [Pentane/diethyl ether (80:1)]: R_f = 0.33;

^1H -NMR (CDCl_3 , 300 MHz): δ (ppm) = 5.35 (m, 2 H), 3.59 (t, 2 H), 2.01 (m, 4 H), 1.52 (m, 2 H), 1.28 (m, 18 H), 0.89 (m, 12 H), 0.046 (s, 6 H);

^{13}C -NMR (CDCl_3 , 100 MHz): δ (ppm) = 129.9 (CH), 129.9 (CH), 63.3 (CH_2), 32.9 (CH_2), 31.8 (CH_2), 29.8 (2 C, CH_2), 29.5 (CH_2), 29.4 (CH_2), 29.3 (CH_2), 29.0 (CH_2),

S16

27.2 (CH₂), 27.2 (CH₂), 26.0 (3 C, CH₃), 25.8 (CH₂), 22.7 (CH₂), 18.4 (C-*t*Bu), 14.1 (CH₃), -5.3 (2 C, CH₃);

IR (Diamond-ATR): $\tilde{\nu}$ = 3005 (w) cm⁻¹, 2925 (m), 2855 (m), 1464 (w), 1386 (w), 1253 (w), 1098 (m), 1006 (w), 834 (s), 774 (m), 723 (w), 661 (w), 542 (w);

EI-MS (70 eV): *m/z* (%) = 339 (3), 299 (11), 298 (37), 297 (100), 269 (34), 115 (10), 109 (15), 101 (12), 95 (21), 89 (19), 75 (91), 67 (13), 55 (19), 41 (13).

(*Z*)-Hexadec-9-en-1-ol



Aldehyde **S5** (7.15 g, 20.15 mmol, 1 equiv) was added to a THF solution (76 mL) of TBAF (1 M in THF, 48.38 mL, 48.38 mmol, 2.4 equiv) at 0 °C. The resulting mixture was stirred at 0 °C for 5 min and at rt for 3 h until the reaction was completed. The solution was quenched with H₂O, extracted with Et₂O (3 × 50 mL), washed with brine, dried with Na₂SO₄ and concentrated under reduced pressure. The residue was purified by flash chromatography (pentane/ethyl acetate (5:1)) affording (*Z*)-hexadec-9-en-1-ol (3.96 g, 16.44 mmol, 82%) as clear, colorless oil.

TLC [Pentane/ethyl acetate (5:1)]: *R_f* = 0.36;

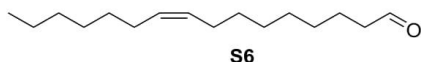
¹H-NMR (CDCl₃, 300 MHz): δ (ppm) = 6.34 (m, 2 H), 3.63 (t, 2 H), 2.02 (m, 4 H), 1.56 (m, 2 H), 1.29 (m, 18 H), 0.88 (t, 3 H);

¹³C-NMR (CDCl₃, 100 MHz): δ (ppm) = 129.9 (CH), 129.8 (CH), 63.0 (CH₂), 32.8 (CH₂), 31.8 (CH₂), 29.7 (CH₂), 29.5 (CH₂), 29.4 (CH₂), 29.2 (CH₂), 29.0 (CH₂), 27.2 (CH₂), 27.2 (CH₂), 25.7 (CH₂), 22.6 (CH₂), 14.1 (CH₃);

IR (diamond-ATR): $\tilde{\nu}$ = 3328 (br, w) cm⁻¹, 3005 (w), 2923 (s), 2854 (m), 1462 (w), 1378 (w), 1055 (w), 883 (w), 722 (w);

EI-MS (70 eV): m/z (%) = 222 (17), 138 (12), 123 (24), 109 (44), 96 (83), 82 (100), 67 (76), 55 (88), 41 (52).

(Z)-Hexadec-9-enal (S6)



The oxidation was performed as described for **S3** from (Z)-hexadec-9-en-1-ol (4.11 g, 17.09 mmol) to afford by flash column chromatography (pentane/Et₂O (19:1)) the pure **S6** as clear oil (3.48 g, 14.62 mmol, 86%).

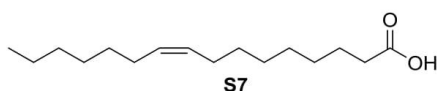
TLC [Pentane/diethyl ether (19:1)]: R_f = 0.32;

¹H-NMR (CDCl₃, 300 MHz): δ (ppm) = 9.68 (t, J = 1.88 Hz, 1 H), 5.25 (m, 2 H), 2.34 (td, 2 H), 1.92 (m, 4 H), 1.53 (m, 2 H), 1.22 (m, 16 H), 0.82 (t, 3 H);

¹³C-NMR (CDCl₃, 100 MHz): δ (ppm) = 202.9 (CHO), 130.0 (CH), 129.7 (CH), 43.9 (CH₂), 31.7 (CH₂), 29.7 (CH₂), 29.6 (CH₂), 29.2 (CH₂), 29.1 (CH₂), 29.0 (CH₂), 29.0 (CH₂), 27.2 (CH₂), 25.6 (CH₂), 22.6 (CH₂), 22.0 (CH₂), 14.1 (CH₃);

EI-MS (70 eV): m/z (%) = 238 (3) [M⁺], 220 (9), 163 (3), 149 (6), 138 (7), 135 (17), 121 (30), 111 (29), 98 (55), 81 (63), 69 (73), 55 (100), 41 (71), 39 (14).

(Z)-Hexadec-9-enoic acid (S7)



A solution of NaClO₂ (9.26 g, 102 mmol, 7 equiv) and NaH₂PO₄·H₂O (18.12 g, 132 mmol, 9 equiv) in H₂O (120 mL) was added dropwise into a mixture of aldehyde **S6** (3.48 g, 14.6 mmol, 1 equiv) and 2-methyl-2-butene (60 mL) in *t*-BuOH/THF (359 mL and 298 mL, respectively). The resulting mixture was stirred at rt until the reaction was completed. The reaction was quenched with brine and extracted with DCM. The

S18

organic phase was washed with brine (3 × 150 mL), dried with MgSO₄, and concentrated in vacuo to afford the crude product. Flash column chromatography (pentane/ethyl acetate (10:1)) gave the pure title compound **S7** as clear colorless oil (3.53 g, 13.9 mmol, 95%).

TLC [Pentane/ethyl acetate (10:1)]: $R_f = 0.37$;

¹H-NMR (CDCl₃, 300 MHz): δ (ppm) = 6.13 (br.s, 1 H), 5.25 (m, 2 H), 2.24 (t, $J = 7.50$ Hz, 2 H), 1.91 (m, 4 H), 1.41 (m, 2 H), 1.19 (m, 16 H), 0.88 (t, 3 H);

¹³C-NMR (CDCl₃, 100 MHz): δ (ppm) = 179.5 (C=O), 130.0 (CH), 129.7 (CH), 31.8 (CH₂), 29.7 (CH₂), 29.7 (CH₂), 29.1 (CH₂), 29.0 (CH₂), 29.0 (CH₂), 29.0 (CH₂), 27.2 (CH₂), 27.1 (CH₂), 25.6 (CH₂), 24.7 (CH₂), 22.6 (CH₂), 14.1 (CH₃);

EI-MS (70 eV) of trimethylsilyl ester: m/z (%) = 326 (7) [M⁺], 311 (100), 236 (9), 199 (10), 194 (16), 185 (10), 152 (11), 145 (32), 129 (72), 117 (76), 96 (19), 81 (17), 75 (68), 55 (28), 41 (17).

NMR spectra

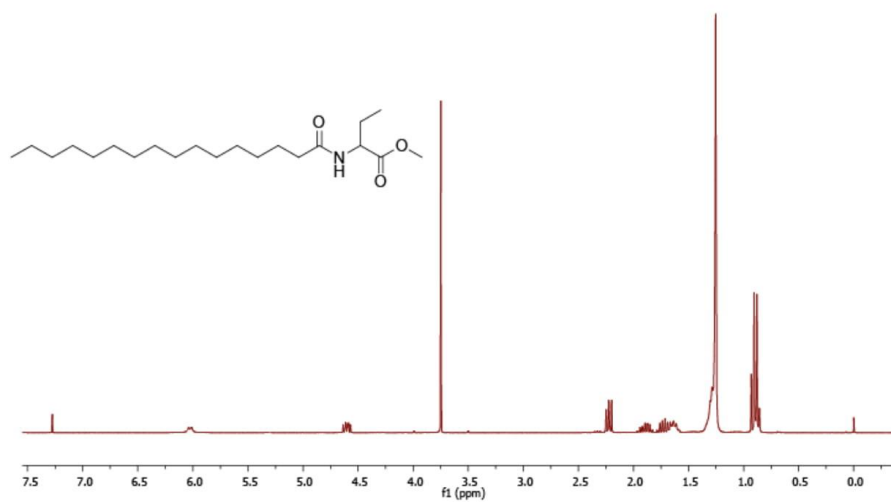


Figure S1: ¹H NMR spectrum of 7 (400 MHz, CDCl₃).

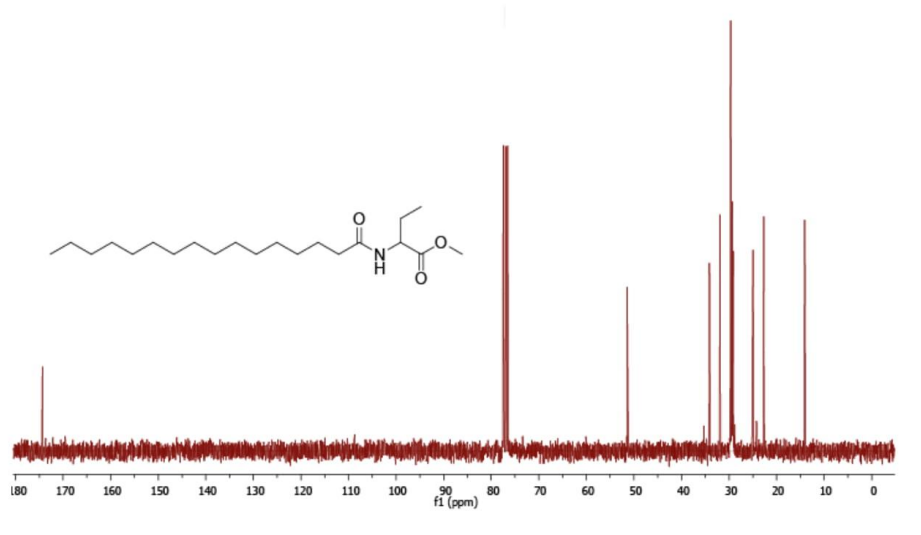


Figure S2: ¹³C NMR spectrum of 7 (100 MHz, CDCl₃).
S20

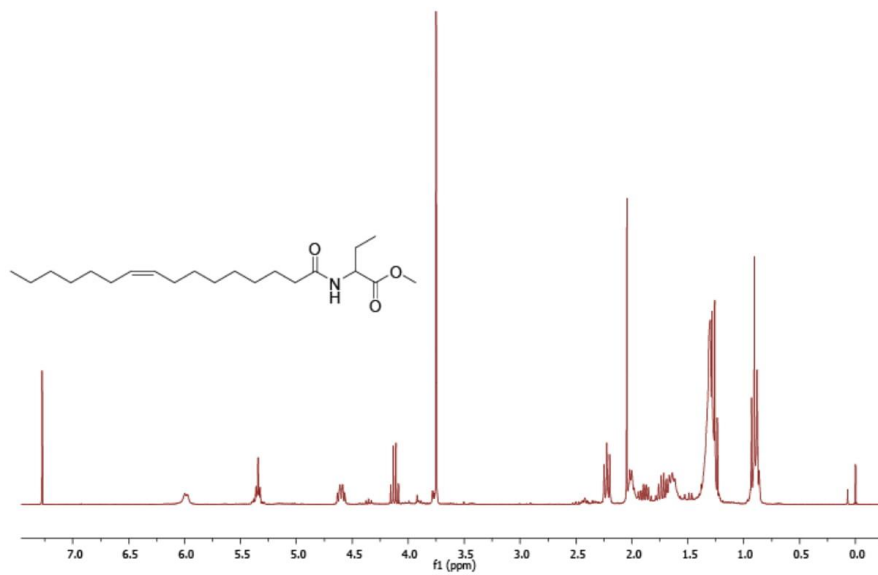


Figure S3: ¹H NMR spectrum of **8** (400 MHz, CDCl₃).

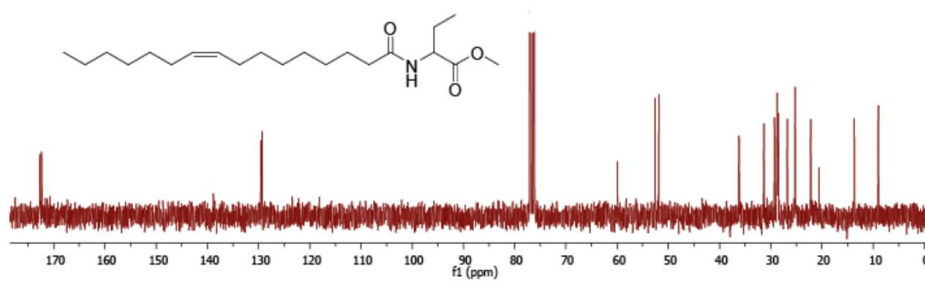


Figure S4: ¹³C NMR spectrum of **8** (100 MHz, CDCl₃).

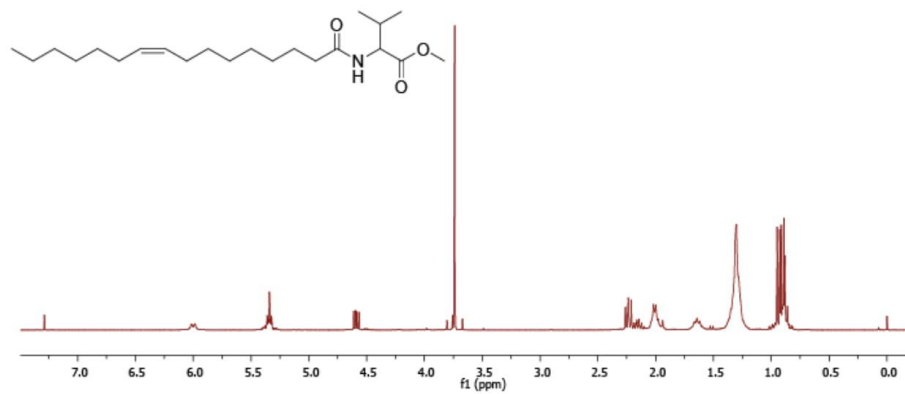


Figure S5: ^1H NMR spectrum of **9** (400 MHz, CDCl_3).

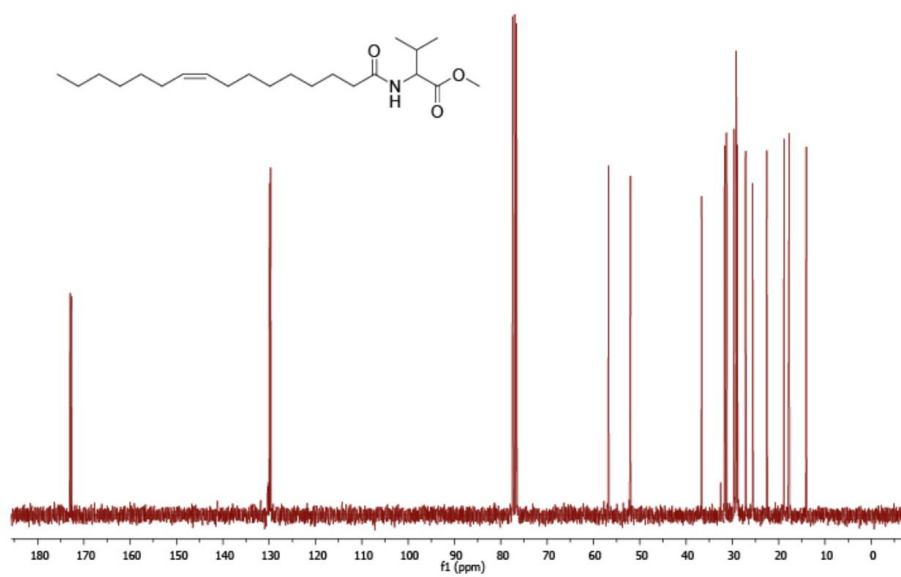


Figure S6: ^{13}C NMR spectrum of **9** (100 MHz, CDCl_3).

S22

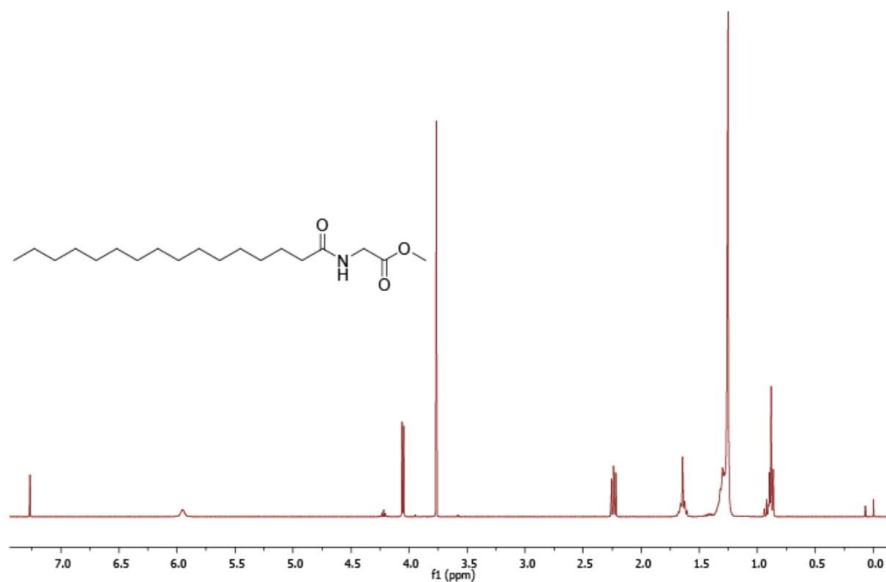


Figure S7: ^1H NMR spectrum of **10** (400 MHz, CDCl_3).

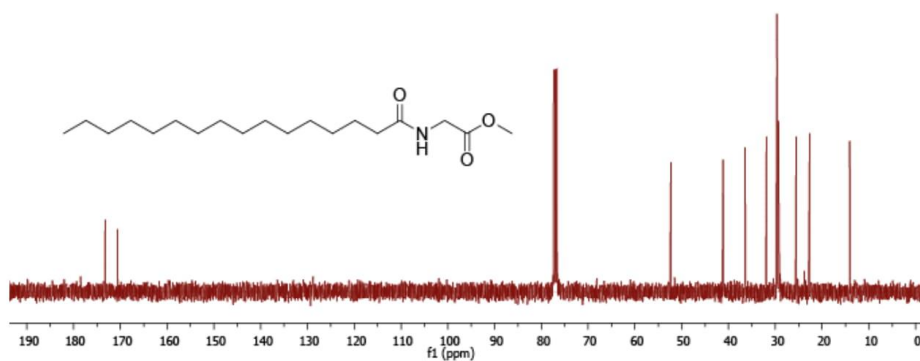


Figure S8: ^{13}C NMR spectrum of **10** (100 MHz, CDCl_3).

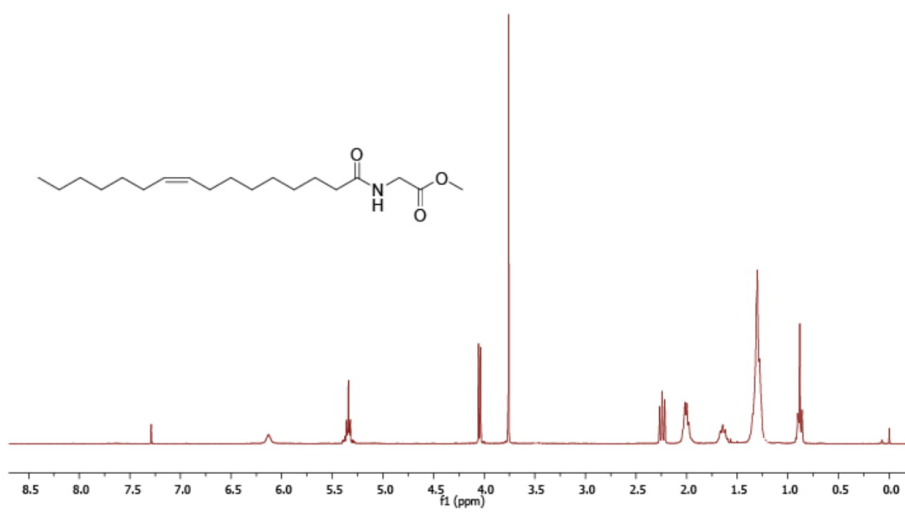


Figure S9: ^1H NMR spectrum of **11** (400 MHz, CDCl_3).

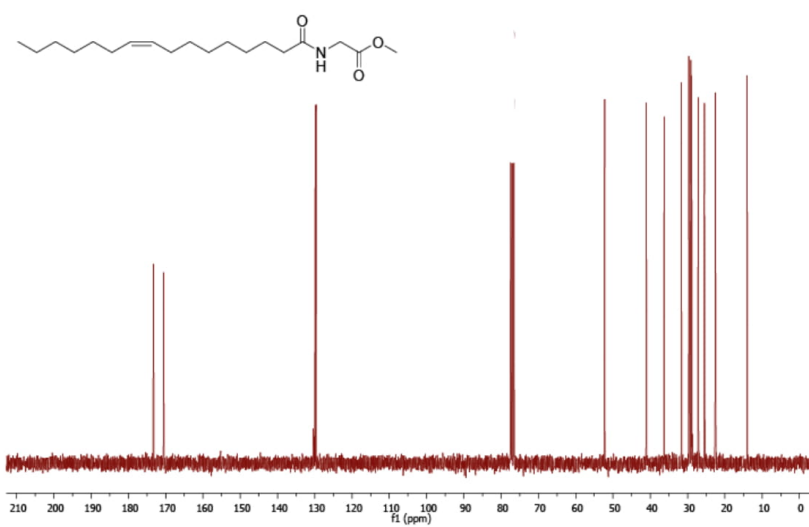


Figure S10: ^{13}C NMR spectrum of **11** (100 MHz, CDCl_3).

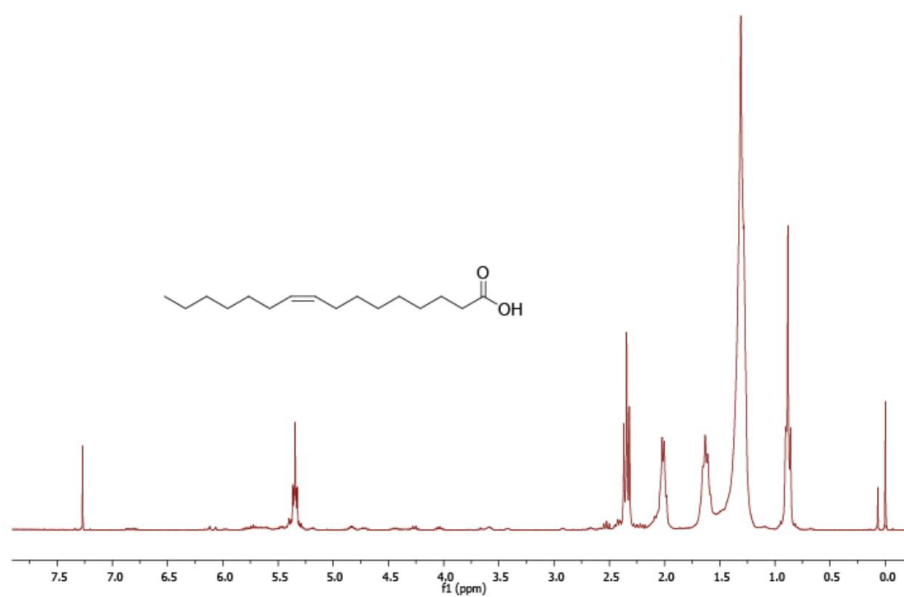


Figure S11: ¹H NMR spectrum of **S7** (400 MHz, CDCl₃).

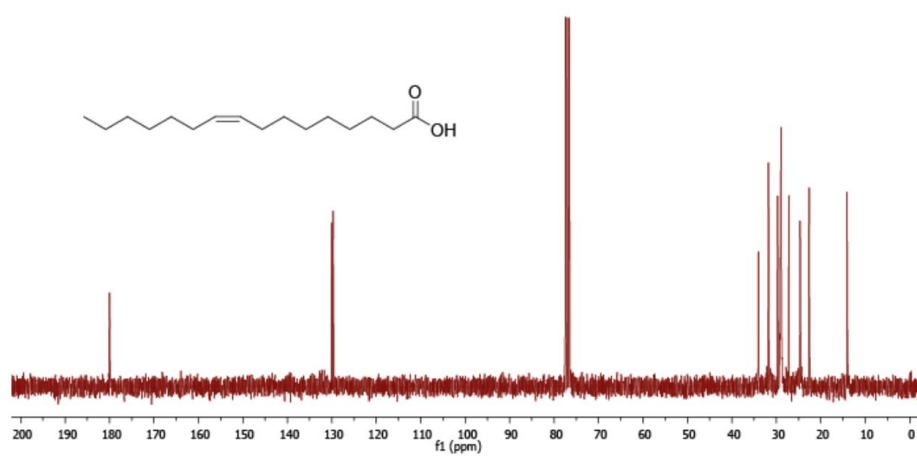


Figure S12: ¹³C NMR spectrum of **S7** (100 MHz, CDCl₃).

References

- S1. Bruns, H.; Herrmann, J.; Müller, R.; Wang, H.; Wagner Döbler, I.; Schulz, S. *J. Nat. Prod.* **2018**, *81*, 131–139. doi:10.1021/acs.jnatprod.7b00757
- S2. Montes Vidal, D.; Rymon-Lipinski, A.-L. von; Ravella, S.; Groenhagen, U.; Herrmann, J.; Zaburannyi, N.; Zarbin, P. H. G.; Varadarajan, A. R.; Ahrens, C. H.; Weisskopf, L.; Müller, R.; Schulz, S. *Angew. Chem. Int. Ed.* **2017**, *56*, 4342–4346. doi:10.1002/anie.201611940
- S3. Takikawa, H.; Nozawa, D.; Kayo, A.; Muto, S.-e.; Mori, K. *J. Chem. Soc., Perkin Trans. 1* **1999**, 2467–2477. doi:10.1039/A904258J
- S4. Millar, J. G.; Oehlschlager, A. C.; Won, J. W. *J. Org. Chem.* **1983**, *48*, 4404–4407.
- S5. Bowden, K.; Heilbron, I. M.; Jones, E. H.; Weedon, B. C. L. *J. Chem. Soc.* **1946**, 39.
- S6. Patel, J.; Hoyt, J. C.; Parry, R. J. *Tetrahedron* **1998**, *54*, 15927–15936. doi:10.1016/S0040-4020(98)01002-3
- S7. Camarero, J. A.; Hackel, B. J.; Yoreo, J. J. de; Mitchell, A. R. *J. Org. Chem.* **2004**, *69*, 4145–4151. doi:10.1021/jo040140h
- S8. Bruns, H.; Thiel, V.; Voget, S.; Patzelt, D.; Daniel, R.; Wagner-Döbler, I.; Schulz, S. *Chem. Biodiversity* **2013**, *10*, 1559–1573. doi:10.1002/cbdv.201300210